EMERGING
INFECTIOUS DISEASES®

Parasitology

EMERGING INFECTIOUS DISEASES

EDITOR-IN-CHIEF
D. Peter Drotman

EMERGING INFECTIOUS DISEASES®

On the Cover

Synopses

p. 1337

p. 1413

Research

p. 1425

p. 1446

EMERGING INFECTIOUS DISEASES®

August 2016

Letters

p. 1499

p. 1516

Books and Media

About the Cover

Online Report

Toward Developing a Preventive MERS-CoV Vaccine
http://dx.doi.org/10.3201/eid2208.160229

Co-infections in Visceral Pentastomiasis, Democratic Republic of the Congo

Dennis Tappe, Mihály Sulyok, Therese Riu, Lajos Rózsa, Imre Bodó, Christoph Schoen, Birgit Muntau, Gergely Babocsay, Richard Hardi

Snakeborne *Armillifer* pentastomiasis is an emerging human parasitic infection in rural tropical areas where snake meat is eaten. After a series of severe ocular *A. grandis* larval infections and anecdotal abdominal infection in Sankuru District, Democratic Republic of the Congo, during 2014–2015, we systematically investigated possible pentastomid etiology in patients who underwent surgery in the region. Histologic and molecular analyses by established pentastomid 18S rDNA- and newly developed *Armillifer*-specific cytochrome oxidase PCRs revealed larval pentastomid lesions in 3.7% of patients. Some persons had *A. armillatus* and *A. grandis* co-infections. Another pentastomid larva, *Raillietiella* sp., was molecularly detected in 1 patient who had concomitant *A. grandis* and *A. armillatus* infection. The PCRs used were suitable for detecting pentastomid species even in highly necrotic tissues. Phylogenetic analyses of *Armillifer* cytochrome oxidase genes detected multiple local strains.

S nakeborne pentastomiasis, a parasitic zoonotic disease in rural tropical areas where snake meat is eaten (*1,2*), is caused by a unique group of crustacean-related parasites (*3,4*). Adult *Armillifer* pentastomids inhabit the respiratory tract of large snakes (final hosts), where they sexually reproduce, resulting in shedding of infective ova into the environment by snake feces or respiratory secretions (*5,6*). In natural intermediate hosts (rodents and small monkeys), and accidentally humans, larvae hatch in the gastrointestinal tract after ingestion of pentastomid eggs, leading to dissemination and, eventually, to encapsulation of the vermiform larvae in internal organs (most often abdominal or peritoneal organs [visceral pentastomiasis (*1*)]) or in the eye (ocular pentastomiasis (*7,8*)]). Visceral pentastomiasis is often asymptomatic and an incidental finding during surgery or autopsy, and pentastomid larvae occasionally might be seen on radiologic films (*1*). However, fatal cases caused by heavy infections have been described (*9*).

Human infections are caused mainly by larvae of *A. armillatus,* which is distributed in West and Central Africa (*1*). *A. grandis*, which has drawn recent attention because of heavily symptomatic ocular infections (*7,8*), is prevalent in Central Africa (*1*). Two other species, *A. moniliformis* and *A. akgistrodontis*, are found in Asia (*1,10,11*).

Armillifer infection in humans is diagnosed by parasitologic examination of excised complete larvae or by histologic and radiologic investigations (*1*). Genus and species are determined by counting the body annulations of completely recovered specimens, but radiology and histology enable only limited conclusions about genus and species, respectively. In most cases, *A. armillatus* has been assumed to be the etiologic agent (*12*). Molecular tools recently have been used successfully in human infections for species discrimination in immigrants from tropical areas (*2*) and local populations in Africa (*8,12*). The main risk factors for human pentastomiasis caused by snakeborne parasites are handling and eating snake products (*1,3*). No effective chemotherapeutic antiparasitic treatment has been established (*1*).

In the Sankuru District, Democratic Republic of the Congo (DRC), severe ocular infections caused by *A. grandis* recently have surfaced (*7,8*). The same species also was molecularly found in the region in an asymptomatic abdominal infection (*12*), indicating a widespread problem in this remote area. We therefore conducted a cross-sectional observational study of patients undergoing abdominal surgery to investigate in detail the etiology of abdominal cystic lesions for the presence of pentastomid larvae in the district by histology and immunohistologic and molecular methods. In addition, we surveyed local markets for pentastomid-infested snakes.

Patients and Methods

Patients and Study Location

During December 1, 2014–March 31, 2015, we investigated cystic or fibrous lesions found incidentally during abdominal surgery from patients at the Hospital of Kole, Kole, Sankuru District, DRC. The medical center serves an area of 9,840 km² of mainly tropical rain forest. Most patients come from the Kutshu, Hindu, and Tétéla tribes, which inhabit a 200-km area around the hospital. Patients of both sexes >18 years of age were enrolled after providing written consent; oral consent was obtained from some because of illiteracy. The ethics committee of the St. Raphael Ophthalmological Center (Mbuji Mayi, DRC) approved the study (no. COR/CE/1-7/15). Samples excised from visceral surfaces or from the peritoneal cavity were fixed in 90% ethanol and transferred to the Bernhard Nocht Institute for Tropical Medicine (Hamburg, Germany) for histologic and molecular analysis for a presumptive pentastomid etiology.

We also surveyed local markets in the Kole area (3°27′37.24″N, 22°26′33.13″E) for snake meat. Large snakes offered by private hunters were analyzed directly for adult pentastomid infection of respiratory tissues. Pentastomids were extracted by using forceps and placed in 100% ethanol for later parasitologic and molecular examination.

Tissue Analysis for Pentastomid Etiology

The ethanol-fixed tissue specimens were directly processed for PCRs targeting the nuclear pentastomid 18S rRNA gene (3,8) and the mitochondrial *Armillifer* cytochrome oxidase (*cox*) subunit I gene by newly designed PCRs (forward primer Arm-F 5′-AGCAATAATAGGAGGATTC-GGGA-3′ and reverse primer Arm-R 5′-GGATGGTTG-TAATRAAGTTGATTGAGC-3′) or were transferred to formalin and embedded in paraffin for histologic and immunohistochemical analyses, later also followed by PCR. For PCR of the ethanol-fixed specimens, soft cysts were treated with proteinase K, and calcified cysts were completely ground before digestion. DNA was extracted by using the DNeasy Blood & Tissue kit (QIAGEN, Hilden, Germany). PCRs from the formalin refixed and embedded specimens were conducted after proteinase K digestion and DNA extraction by using the QIAamp DNA FFPE Tissue kit (QIAGEN) from either 5-µm tissue sections or the whole paraffin block. The pentastomid 18S rDNA-PCRs were performed as previously described (3,8). For the *Armillifer cox* PCRs, 40 cycles with denaturation at 94°C for 40 s, annealing at 55°C for 40 s, and elongation at 72°C for 60 s were run. Positive PCR products (430 and 288 bp, respectively) were visualized by gel electrophoresis followed by sequencing and BLAST analysis (http://www.ncbi.nlm.nih.gov/blast).

Histologic examinations were conducted from hematoxylin and eosin and periodic acid-Schiff stained tissue sections. Immunochistochemical analyses for CD3 (rabbit monoclonal IgG, 1:400; Epitomics-Abcam, Cambridge, UK); CD20 (mouse monoclonal IgG, 1:150; Dako, Hamburg, Germany); and TFG-β (rabbit polyclonal IgG, 1:100; DCS, Hamburg, Germany) were performed according to the manufacturers' instructions by using the 2-component AEC-2 detection chromogen kit (DCS; for CD3 and CD20) or the horseradish peroxidase/DAB supervision2 kit (DCS [for TGF-β]) for visualization after antigen retrieval with boiling in citric acid (pH 6.0) for 2–3 min. A light hematoxylin counterstain was used.

Phylogenetic Analyses of Larval and Adult Pentastomids

We used the *cox* sequences of the respective pentastomid specimens recovered from patients and local snakes for a multiple sequence alignment with MUSCLE software (http://www.ebi.ac.uk/Tools/msa/muscle/). Poorly aligned and divergent positions were removed by using Gblocks with the following parameter settings: –t = d, –b1 = 14, –b2 = 14, –b3 = 8, –b4 = 5, –b5 = h. The final alignment consisted of 286 of the original 1,527 positions from 26 sequences. We used MEGA6 (http://www.megasoftware.net/) for subsequent substitution model estimation and for phylogenetic tree reconstruction.

Results

From 188 patients seen during the study period, we identified 7 (3.7%, of whom 4 were female) with incidental visceral fibrotic lesions, cystic lesions, or both (Table). Age (not determined for 4 patients) ranged from 35 to 42 years. All patients had undergone surgery for non–pentastomid-related conditions. A total of 23 lesions (1–6 individual cysts per patient) were resected. Multiple lesions (2 to 6) were resected in 5 (2.7%) of the 188 participants (Figure 1). All 7 patients with cystic lesions had pentastomid larvae as the underlying cause, as identified by pentastomid 18S rDNA PCR, *Armillifer cox* PCR, or both. In all but 3 lesions, at least 1 PCR was positive and gave a pentastomid sequencing result directly from the ethanol fixed specimens or from the formalin-fixed, paraffin-embedded tissue (tissue slice or whole block). In 2 of these 3 lesions, ovarial tissue was detected by histology (patient 6, cysts 2 and 3); in 1 necrotic pentastomid lesion, no positive PCR result was obtained (patient 1, cyst 4) (Table).

Pentastomids identified after sequencing (98%–100% homology) were *A. armillatus* larvae in 10 (43%) of 23 lesions, *A. grandis* larvae in 9 (39%), and *Raillietiella* sp. larva in 1 (0.04%). The *Raillietiella* sequence obtained was identical to 2 unspecified *Raillietiella* sp. GenBank entries (accession nos. EU370434 and AY744887). In total, we

Table. Patient characteristics and sequencing results of pentastomid 18S rDNA and *Armillifer*-specific cytochrome oxidase gene PCRs, Sankuru District, Democratic Republic of the Congo, 2014–2015*

Patient no.	Age, y/sex	Type of surgery	Location of pentastomid cyst	Sequencing result		Histology
				Pentastomid 18S rDNA-gene, 430 bp	*Armillifer* cytochrome oxidase subunit I-gene, 288 bp	
1†	NA/M	Laparotomy	Peritoneum	Cyst 1: *A. grandis*	*A. grandis*	Not done
				Cyst 2: negative	*A. armillatus*	Not done
				Cyst 3: *Raillietiella* sp.‡	Negative‡	Necrotic pentastomid
				Cyst 4: negative§	Negative§	Necrotic pentastomid
2†	35/F	Laparotomy	Peritoneum	Cyst 1: *A. grandis*	*A. grandis*	Not done
				Cyst 2: *A. armillatus*	*A. armillatus*	Not done
				Cyst 3: negative‡	*A. grandis*‡	Necrotic pentastomid
				Cyst 4: negative‡	*A. grandis*‡	Total necrosis
				Cyst 5: negative‡	*A. grandis*‡	Necrotic pentastomid
				Cyst 6: negative‡	*A. grandis*‡	Total necrosis
3†	NA/M	Laparotomy	Peritoneum	Cyst 1: *A. grandis*	*A. grandis*	Not done
				Cyst 2: *A. armillatus*	*A. armillatus*	Not done.
				Cyst 3: *A. grandis*	Negative	Not done
				Cyst 4: negative§	*A. grandis*§	Total necrosis
				Cyst 5: negative§	*A. armillatus*§	Total necrosis
				Cyst 6: negative‡	*A. armillatus*§	Total necrosis
4	NA/M	Hernioplasty	Peritoneum	Cyst 1: *A. armillatus*	*A. armillatus*	Not done
5	NA/F	Cesarean section	Omentum	Cyst 1: *A. armillatus*	*A. armillatus*	Not done
				Cyst 2: *A. armillatus*‡	*A. armillatus*‡	Necrotic pentastomid
6	36/F	Laparotomy, appendectomy	Left ovary	Cyst 1: *A. armillatus*	*A. armillatus*	Not done
				Cyst 2: not done	Not done	Ovarian cyst
				Cyst 3: not done	Not done	Ovarian cyst
7	42/F	Laparotomy, appendectomy	Omentum	Cyst 1: *A. armillatus*	*A. armillatus*	Not done

*NA, not available; negative, PCR negative or no positive sequence result.
†Co-infected.
‡PCRs performed from paraffin block tissue slices.
§Repeat PCRs performed from whole paraffin block, after PCRs from block slices were negative. Tissue materials from patient 1 (cysts 1, 2), patient 3 (cyst 3), and patient 7 (cyst 1) were ground, as the tissue was too hard to cut into pieces for PCR.

detected *A. armillatus* in all 7 patients. Co-infections with *A. armillatus* and *A. grandis* larvae were identified in 3 (43%) patients (patients 1–3); patient 1 had a triple pentastomid species infection, including a *Raillietiella* sp. larva.

Histology was performed from 12 cysts (including the 2 diagnosed as ovarian cysts) resected from 5 patients. Necrotic pentastomids were identified in 5 cysts, from a total of 3 patients, and the decay-refractory shed exuvia surrounded by fibrosis was found (Figure 2, panels A, B). In 4 of these 5 necrotic pentastomid cysts, PCR and sequencing results were positive, even from tissue slices. We found total necrosis of histologically unknown etiology in an additional 5 cysts from 2 patients; in all of them, we obtained positive pentastomid PCR and sequencing results (Table).

Immunohistochemical analysis showed B cells and T cells clustering locally at the fibrous capsule of necrotic pentastomid lesions (Figure 2, panel C). Immunostaining for TGF-β showed a slight expression of TGF-β in fibrous tissue surrounding the larvae (Figure 2, panel D).

Examination of 4 large snakes (2 Gaboon vipers [*Bitis gabonica*], 1 rhinoceros viper [*B. nasicornis*], and 1 African rock python [*Python sebae*]) offered for consumption at markets near Kole during the study period showed pentastomid infections of the trachea and lungs and the mesenteric membrane. *A. grandis* was detected morphologically and molecularly (99%–100% sequence homology) in the

2 Gaboon vipers (8 and 10 parasites, respectively) and in the rhinoceros viper (10 parasites). The python harbored 6 adult *Raillietiella* sp. as identified by PCR (identical to the 2 unspecified *Raillietiella* sp. sequences in GenBank) (Figure 3).

Phylogenetic analyses based on *cox* results obtained from patients' samples and snake specimens showed sequence variations within the *A. grandis* and the *A. armillatus* branch, indicating the presence of multiple local parasite strains. The *Armillifer* sequences found in 1 patient did not all cluster directly together, suggesting multiple infection events or ingestion of multiple pentastomid species or strains at the same time. Some sequences from patients' larval *Armillifer* parasites were highly similar to sequences from adult *Armillifer* parasites found in snakes (Figure 4). The *Raillietiella* sp. 18S rDNA sequence from the patient showed 100% nt identity with the sequence from the snake's *Raillietiella*.

Discussion

After reports of heavily symptomatic eye infections (7,8) and incidentally found asymptomatic abdominal infections (12) with pentastomids in the remote tropical and forested Sankuru District of DRC, we conducted a short-term systematic study that sheds light on visceral pentastomiasis as an emerging infectious disease in this area. The previously
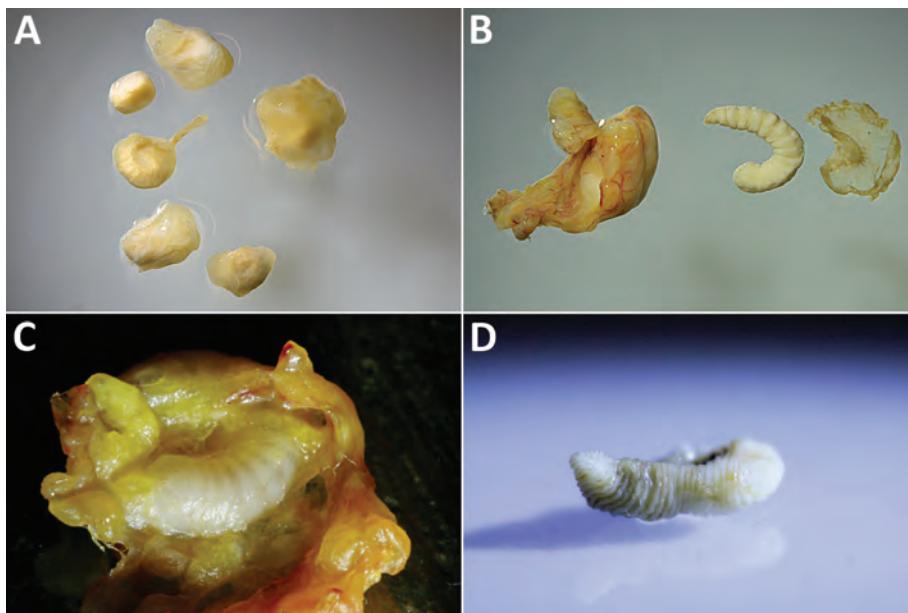
Figure 1. Resected cystic pentastomid lesions extracted from patients during abdominal surgery, Sankuru District, Democratic Republic of the Congo, 2014–2015. A) Six abdominal cysts resected from patient 3, who was found to be co-infected: 3 cysts each were *Armillifer grandis* and *A. armillatus* larvae, as determined by PCR. B) One of 2 resected *A. armillatus* cysts from patient 5. The fibrous capsule, the larva itself, and the parasite's exuvia are shown. The larva has 20 annulations, morphologically consistent with the molecular result of *A. armillatus*. C) Resected and opened cyst from patient 5. The *A. armillatus* larva (as determined by PCR) is still embedded in its capsule. D) *A. grandis* larva from patient 2 with >25 annulations.

described series of ocular infections with *A. grandis* larvae in the region was believed to indicate a local problem (*8*) because ophthalmologic infections are severely symptomatic, whereas visceral (abdominal) cases usually go unnoticed (*1*). The prevalence of visceral pentastomiasis we detected was not totally surprising because an earlier report of 2 patients had suggested that emerging situation (*12*). However, multispecies pentastomid co-infections as described here were not anticipated.

In this investigation, co-infection was detected molecularly by application of established pentastomid 18S rDNA PCRs and the newly developed *Armillifer*-specific *cox* PCRs. Positive PCR results were obtained from all but 1 resected pentastomid lesions, even from necrotic pentastomid cysts and necrotic lesions of histologically unidentifiable etiology. By histologic examination only, determining the pentastomid species, even in nonnecrotic lesions, is nearly impossible and would rely on counting the body annulations in arbitrary section planes. Molecular tools, as shown in this investigation, can facilitate diagnosis and are able to determine the causative organism to the species level, even in necrotic or calcified tissue samples.

We detected *A. armillatus* and *A. grandis* in roughly similar frequencies in the cysts we tested (43.5% and 39.1%, respectively). Whether the co-infections in 3 patients represent superinfections or simultaneous infection events remains unclear. The finding of highly similar sequences of *A. grandis* from local snakes and patients underscores local transmission, although the snake *A. armillatus* sequence was more divergent from patient *A. armillatus* sequences. *A. armillatus* is geographically more widely distributed; its preferred final hosts are mainly

pythons (*1,3,13*), whereas vipers are usually the hosts for the more geographically restricted *A. grandis* (*1*). We did not find co-infected snakes, but co-infections occur in reptile hosts as well (*14*).

Our finding of a third pentastomid species responsible for a human infection, *Raillietiella*, was completely unexpected. Earlier work in 1954 proposed that *R. hemidactyli*, a pentastomid using lizards as final hosts and coprophageous insects, such as cockroaches, as intermediate hosts, might cause a dermatologic condition similar to creeping eruption in Vietnam (*15*). The authors described the syndrome in 3 patients who had eaten live lizards, similar to a report from 1952 (*16*). However, *Raillietiella* was not proven as the causative agent in the reported disease (and human infection with this parasite in general) because the parasite (adult or larval) was not found in the skin; speculation was based on the finding of local lizards harboring this parasite (*15*). This investigation confirms that *Raillietiella* can cause human infection, similar to *Armillifer* parasites. We also showed that snake meat consumption might factor into transmission of this pentastomid parasite because a *Raillietiella* sp. was found in a local snake in the district with identical 18S rDNA sequences to those from the human infection. In contrast, the consumption of lizards, a reptile host in which *Raillietiella* is common, is not a habit in this region.

In the human host, encapsulated pentastomid larvae can live for a few years, after which they calcify (which might be seen as C-shaped calcifications on radiology films [*1*]). Dying larvae are thought to release antigens, provoking an immune reaction (*1*). We detected an accumulation of B cells and T cells around the disintegrating

Figure 2. Histologic and immunohistochemical analyses of resected pentastomid lesions from patients in Sankuru District, Democratic Republic of the Congo, 2014–2015. A) Typical necrotic pentastomid lesion from patient 5. Internal structures of the larvae are decayed; only the directly surrounding exuvia following the annulated body of the parasite and the fibrous capsule are visible. This organism has been molecular identified as *A. armillatus*. Periodic acid Schiff stain; original magnification ×2.5. B) Necrotic pentastomid lesion from patient 1, with a similar appearance. This organism has been molecularly identified as *Raillietiella* sp. Hematoxylin and eosin stain; original magnification ×2.5. C) Immunohistochemical staining of B cells (blue) and T cells (brown) surrounding the *A. armillatus* lesion from patient 5. The lymphocytes cluster locally adjacent to the lesion. Mouse monoclonal anti-CD20 and rabbit monoclonal anti-CD3 stain with hematoxylin counterstain; original magnification ×2.5. D) Immunohistochemical staining for TGF-β (brown) around an *A. armillatus* larva of patient 5. Immunoreactivity is seen surrounding the lesion and nonspecifically within the parasite larva itself. Rabbit polyclonal IgG with hematoxylin counterstain; original magnification ×2.5.
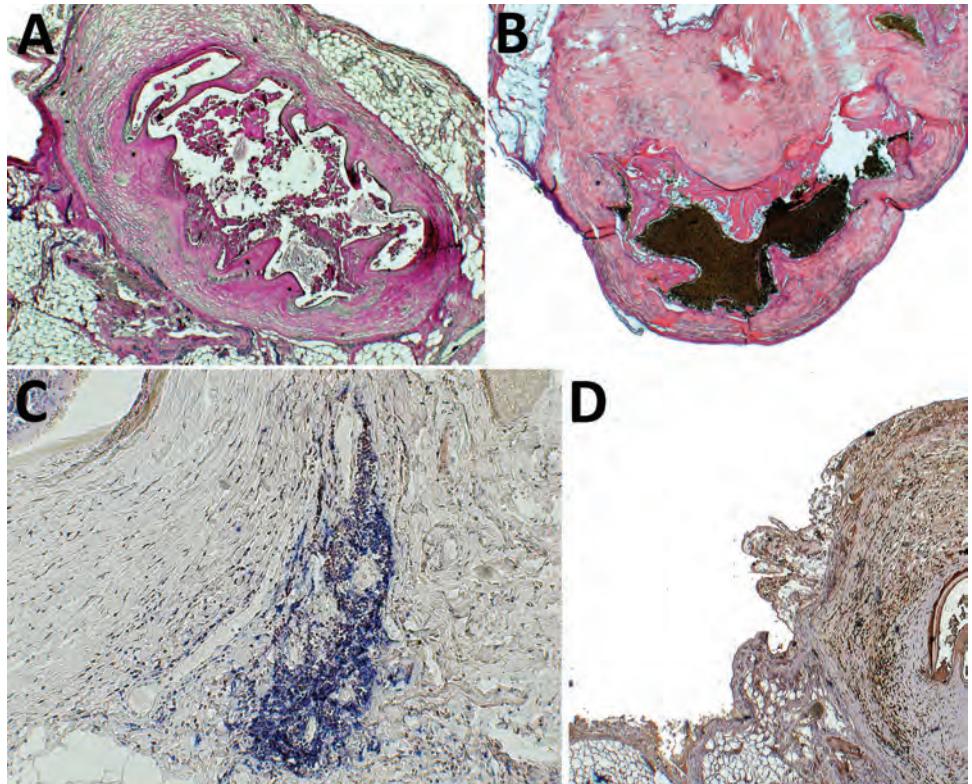
pentastomid lesions. TGF-β, a fibrosis-inducing cytokine, was expressed in the fibrous capsule surrounding the parasite lesion. Because patients sometimes harbor hundreds of larvae without overt clinical symptoms (*1*), the host–parasite interface and possibly locally produced host cytokines or factors released by living pentastomids deserve future research attention. A local or systemic immunosuppression induced by secretion of soluble factors by pentastomid larvae might be possible.

The patients in our study regularly ate snake meat, as is the habit in this region. At local markets, we found adult *A. grandis* and *A. armillatus* parasites in snake meat on several occasions and once adult *Raillietiella* parasites. The presence of adult pentastomids in snakes is well known to the local population. The local residents believe that *Armillifer* pentastomids are internal structures of snakes, "spiral springs," that help in the serpent's locomotion. Residents are unaware of the infective nature of these structures and,

Figure 3. Adult *Armillifer* and *Raillietiella* parasites found in snakes at local markets in Kole, Sankuru District, Democratic Republic of the Congo, 2014–2015. A) Adult *A. grandis* in respiratory tract of a local rhinoceros viper (*Bitis nasicornis*). B) Adult *A. armillatus* in the lung of an African rock python (*Python sebae*) found in 2014, for comparison. Note the different annulation also between the adult stage of *A. grandis* and *A. armillatus*. C) Adult *Raillietiella* pentastomid in the lung of an African rock python. The rostral end of the parasite with central mouth and 2 pairs of perioral hooklets is shown.
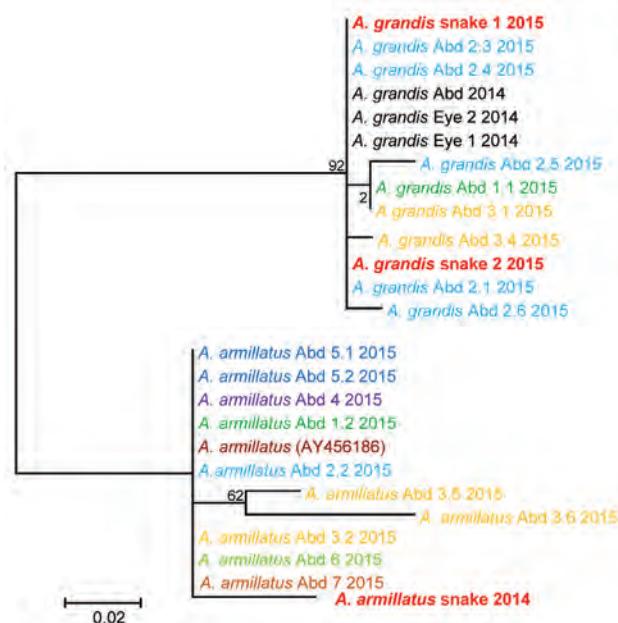
Figure 4. Molecular phylogenetic analysis of *Armillifer* spp. sequences obtained from humans and snakes in Sankuru District, Democratic Republic of the Congo, 2014–2015. Parasite cytochrome oxidase subunit I gene sequences from abdominal (Abd) surgery patient specimens (larval parasites) and from snake meats for sale at local markets (adult parasites) are shown. Human cases are numbered according to the patient and cyst numbers shown in the Table. Sequences obtained from the same patient share the same color. A GenBank reference sequence (*A. armillatus* AY456186) is included, as are sequences from the human abdominal and eye infections from the same region of the Democratic Republic of the Congo investigated in 2014 (*8,12*). The evolutionary history was inferred by using the maximum-likelihood method based on the Hasegawa-Kishino-Yano model. The tree with the highest log likelihood (−646.8057) is shown. The percentage of trees in which the associated taxa clustered together is shown next to the branches. Initial tree(s) for the heuristic search were obtained automatically by applying neighbor-joining and BioNJ algorithms to a matrix of pairwise distances estimated using the maximum composite likelihood approach, and then selecting the topology with superior log likelihood value. Codon positions included were 1st+2nd+3rd+Noncoding. *A. grandis* and *A. armillatus* sequences form their own respective branches. Scale bar indicates number of substitutions per site.

during consumption of undercooked snake meat, spit out adult parasites. This habit seems highly risky, leading to ingestion of pentastomid ova released during chewing. Simple hygiene instructions, such as removal of any parasites visible in slaughtered serpents, hand washing after handling snake meat, and proper cooking of snake meat, is likely to reduce the risk.

Our study also draws attention to the medical consequences of increasing bushmeat consumption in the Congo basin (*17*). Extensive deforestation and reduced availability of birds and mammals have resulted in consumption of snake and other reptile meat (*8*). Although these phenomena are not limited to Sankuru District, the geographic extent and incidence of snakeborne pentastomiasis as an emerging infectious disease is likely to increase. Currently, only scarce and outdated information exists about the prevalence of human pentastomiasis: radiology studies in the Congo region in the 1950s (<1% prevalence [*18*]), in Nigeria in the 1990s (1.4% [*19*]), a serosurvey in Côte d'Ivoire in the 1980s (4.2% [*20*]); and autopsy studies in the Congo region in the 1910s and 1930s (12%–22.5% [*21,22*]), in Cameroon in the 1910s (7.8%–12.6% [*23,24*]), Nigeria in the 1960s (33% [*25*]), and in indigenous people in Malaysia in the 1960s (45.4% [*26*]).

In summary, we undertook a surgery-based study of patients in a region where snake meat consumption is widely practiced to investigate etiology of abdominal cystic lesions for the presence of pentastomid larvae. Seroprevalence studies using crude parasite antigens (ELISA and immunoblot [*3*]) in the affected region will follow. Our findings indicate that the rate of visceral pentastomiasis as an incidental finding during surgery indicates endemicity, most likely fueled by consumption of bushmeat and animal exploitation.

References

1. Tappe D, Büttner DW. Diagnosis of human visceral pentastomiasis. PLoS Negl Trop Dis. 2009;3:e320. http://dx.doi.org/10.1371/journal.pntd.0000320
2. Tappe D, Haeupler A, Schäfer H, Racz P, Cramer JP, Poppert S. *Armillifer armillatus* pentastomiasis in African immigrant, Germany. Emerg Infect Dis. 2013;19:507–8. http://dx.doi.org/ 10.3201/eid1903.121508
3. Tappe D, Meyer M, Oesterlein A, Jaye A, Frosch M, Schoen C, et al. Transmission of *Armillifer armillatus* ova at snake farm, The Gambia, West Africa. Emerg Infect Dis. 2011;17:251–4. http://dx.doi.org/10.3201/eid1702.101118
4. Lavrov DV, Brown WM, Boore JL. Phylogenetic position of the Pentastomida and (pan)crustacean relationships. Proc Biol Sci. 2004;271:537–44. http://dx.doi.org/10.1098/rspb.2003.2631
5. Riley J. The biology of pentastomids. Adv Parasitol. 1986;25:45–128. http://dx.doi.org/10.1016/S0065-308X(08)60342-5
6. Paré JA. An overview of pentastomiasis in reptiles and other vertebrates. J Exot Pet Med. 2008;17:285–94 http://dx.doi.org/10.1053/j.jepm.2008.07.005.
7. Hardi R, Sulyok M, Rózsa L, Bodó I. A man with unilateral ocular pain and blindness. Clin Infect Dis. 2013;57:418, 469–70. http://dx.doi.org/10.1093/cid/cit316

8. Sulyok M, Rózsa L, Bodó I, Tappe D, Hardi R. Ocular pentastomiasis in the Democratic Republic of the Congo. PLoS Negl Trop Dis. 2014;8:e3041. http://dx.doi.org/10.1371/journal.pntd.0003041

9. Lavarde V, Fornes P. Lethal infection due to *Armillifer armillatus* (Porocephalida): a snake-related parasitic disease. Clin Infect Dis. 1999;29:1346–7. http://dx.doi.org/10.1086/313460

10. Latif B, Omar E, Heo CC, Othman N, Tappe D. Human pentastomiasis caused by *Armillifer moniliformis* in Malaysian Borneo. Am J Trop Med Hyg. 2011;85:878–81. http://dx.doi.org/10.4269/ajtmh.2011.11-0404

11. Chen SH, Liu Q, Zhang YN, Chen JX, Li H, Chen Y, et al. Multi-host model-based identification of *Armillifer agkistrodontis* (Pentastomida), a new zoonotic parasite from China. PLoS Negl Trop Dis. 2010;4:e647. http://dx.doi.org/10.1371/journal.pntd.0000647

12. Tappe D, Sulyok M, Rózsa L, Muntau B, Haeupler A, Bodó I, et al. Molecular diagnosis of abdominal *Armillifer grandis* pentastomiasis in the Democratic Republic of Congo. J Clin Microbiol. 2015;53:2362–4. http://dx.doi.org/10.1128/JCM.00336-15

13. De Meneghi D. Pentastomes (Pentastomida, *Armillifer armillatus* Wyman, 1848) in snakes from Zambia. Parassitologia. 1999; 41:573–4.

14. Kelehear C, Spratt DM, O'Meally D, Shine R. Pentastomids of wild snakes in the Australian tropics. Int J Parasitol Parasites Wildl. 2013;3:20–31. http://dx.doi.org/10.1016/j.ijppaw.2013.12.003

15. Dollfus RP, Canet J. [Pentastomide; *Raillietiella* (*Heymonsia*) *hemidactylia* M. L. Hett 1934; supposed susceptibility of parasiting man after the therapeutic ingestion of living lizards] [in French]. Bull Soc Pathol Exot Filiales. 1954;47:401–8.

16. Soulange, Lesnard, Brygoo. Un cas de parasitose erratique cuntanée. Med Trop (Mars). 1952;1 (Jan–Feb):12.

17. Fa JE, Currie D, Meeuwig J. Bushmeat and food security in the Congo Basin: linkages between wildlife and people's future. Environ Conserv. 2003;30:71–8 http://dx.doi.org/10.1017/S0376892903000067.

18. Woithelet G. Porocéphalose et radiologie. Med Trop (Mars). 1956;16:379–85.

19. Nzeh DA, Akinlemibola JK, Nzeh GC. Incidence of *Armillifer armillatus* (pentastome) calcification in the abdomen. Cent Afr J Med. 1996;42:29–31.

20. Nozais JP, Cagnard V, Doucet J. Pentastomosis. A serological study of 193 Ivorians [in French]. Med Trop (Mars). 1982;42:497–9.

21. Mouchet R. Note on *Porocephalus moniliformis* [in French]. Bull Soc Pathol Exot. 1914;7:497–501.

22. Pales M, Pouderoux M. The anatomo-pathologic lesions of pneumonias in A.E.F. [in French]. Bull Soc Pathol Exot. 1934;27:45–55.

23. Seiffert H. Further findings of *Porocephalus moniliformis* in Cameroon [in German]. Arch Schiffs u Tropenhyg. 1910;14:506–14.

24. Schäffer H. About the occurence of *Porocephalus moniliformis* in Cameroon [in German]. Arch Schiffs u Tropenhyg. 1912;16:109–13.

25. Smith JA, Oladiran B, Lagundoye SB, Lawson EAL, Francis TI. Pentastomiasis and malignancy. Ann Trop Med Parasitol. 1975; 69:503–12, http://dx.doi.org/10.1080/00034983.1975.11687039

26. Prathap K, Lau KS, Bolton JM. Pentastomiasis: a common finding at autopsy among Malaysian aborigines. Am J Trop Med Hyg. 1969;18:20–7.

Address for correspondence: Dennis Tappe, Bernhard Nocht Institute for Tropical Medicine, Bernhard-Nocht-Str. 74, 20359 Hamburg, Germany; email: tappe@bnitm.de

Sign up for the EID journal on Twitter and get the most current information about Emerging Infectious Diseases.

@CDC_EIDjournal

Multistate US Outbreak of Rapidly Growing Mycobacterial Infections Associated with Medical Tourism to the Dominican Republic, 2013–2014[1]

**David Schnabel, Douglas H. Esposito, Joanna Gaines, Alison Ridpath,
M. Anita Barry, Katherine A. Feldman, Jocelyn Mullins, Rachel Burns, Nina Ahmad,
Edith N. Nyangoma, Duc B. Nguyen, Joseph F. Perz, Heather A. Moulton-Meissner,
Bette J. Jensen, Ying Lin, Leah Posivak-Khouly, Nisha Jani, Oliver W. Morgan,
Gary W. Brunette, P. Scott Pritchard, Adena H. Greenbaum, Susan M. Rhee, David Blythe,
Mark Sotir, and the RGM Outbreak Investigation Team[2]**

During 2013, the Maryland Department of Health and Mental Hygiene in Baltimore, MD, USA, received report of 2 Maryland residents whose surgical sites were infected with rapidly growing mycobacteria after cosmetic procedures at a clinic (clinic A) in the Dominican Republic. A multistate investigation was initiated; a probable case was defined as a surgical site infection unresponsive to therapy in a patient who had undergone cosmetic surgery in the Dominican Republic. We identified 21 case-patients in 6 states who had surgery in 1 of 5 Dominican Republic clinics; 13 (62%) had surgery at clinic A. Isolates from 12 (92%) of those patients were culture-positive for *Mycobacterium abscessus* complex. Of 9 clinic A case-patients with available data, all required therapeutic surgical intervention, 8 (92%) were hospitalized, and 7 (78%) required ≥3 months of antibacterial drug therapy. Healthcare providers should consider infection with rapidly growing mycobacteria in patients who have surgical site infections unresponsive to standard treatment.

Author affiliations: Centers for Disease Control and Prevention, Atlanta, Georgia, USA (D. Schnabel, D.H. Esposito, J. Gaines, A. Ridpath, J. Mullins, N. Ahmad, E.N. Nyangoma, D.B. Nguyen, J.F. Perz, H.A. Moulton-Meissner, B.J. Jensen, O.W. Morgan, G.W. Brunette, M. Sotir); Maryland Department of Health and Mental Hygiene, Baltimore, Maryland, USA (D. Schnabel, K.A. Feldman, D. Blythe); New York City Department of Health and Mental Hygiene, New York, New York, USA (A. Ridpath, Y. Lin); Boston Public Health Commission, Boston, Massachusetts, USA (M.A. Barry); Connecticut Department of Public Health, Hartford, Connecticut, USA (J. Mullins); Massachusetts Department of Public Health, Boston (R. Burns); New York State Department of Health, Albany, New York (N. Ahmad); Montgomery County Health Department, Norristown, Pennsylvania, USA (L. Posivak-Khouly); Newark Department of Child and Family Well-Being, Newark, New Jersey, USA (N. Jani); Florida Department of Health, Tallahassee, Florida, USA (P.S. Pritchard); Johns Hopkins Hospital, Baltimore (A.H. Greenbaum); Johns Hopkins Bayview Medical Center, Baltimore (S.M. Rhee)

DOI: http://dx.doi.org/10.3201/eid2208.151938

Infections with rapidly growing mycobacteria (RGM), which include the species *Mycobacterium abscessus*, *M. chelonae* and *M. fortuitum*, are difficult to diagnose (*1,2*) and treat (*3,4*). RGMs primarily cause pulmonary or cutaneous infections (*5*). Although symptoms vary and can be nonspecific, the classic cutaneous symptoms include painful nodules that develop into persistent, discharging abscesses (*2,4,6,7*). Systemic symptoms (e.g., fever) are often absent (*2,4*). Certain RGMs, including those in the *M. abscessus* complex, are notoriously resistant to most antibacterial drug classes (*5*). Surgical debridement or removal of foreign bodies (e.g., implants) is usually a necessary adjunct to antibacterial therapy (*1,4*). Infections are prolonged; median symptom duration is reported as 3–12 months (*4,8*).

RGMs, similar to other nontuberculous mycobacteria, are ubiquitous environmental organisms reported worldwide (*5*) and are most frequently detected in nonsterile water sources, including natural waters and engineered water systems (*9*). Infections by these organisms acquired in healthcare settings are most often associated with breeched sterile technique and exposure to nonsterile water (*4,10*).

Outbreaks in these settings have been reported (*11,12*) and include those associated with cosmetic surgeries performed in the United States (*13*) and internationally (*14*). RGM infections acquired by medical tourists, who are persons who travel to another country specifically to receive healthcare (*15*), have been reported (*6,16–18*). Nevertheless, scope, impact, and character of medical tourism and its public health significance are not well defined (*15,19,20*).

On August 23, 2013, a physician in Maryland, USA, reported to the Maryland Department of Health and Mental Hygiene *M. abscessus* complex–positive surgical site infections in 2 women who had undergone cosmetic surgery the previous month at a private surgical clinic in the Dominican Republic. These women disclosed that they had an acquaintance in Massachusetts with "similar problems" after a procedure at the same clinic. Concerned that additional unrecognized cases might exist, Department of Health staff consulted with multiple state and local health departments in collaboration with the US Centers for Disease Control and Prevention (CDC) and initiated an investigation. Investigation objectives were to determine outbreak scope of RGM surgical site infections among medical tourists who traveled to the Dominican Republic for procedures, identify epidemiologic links among patients, and mitigate outbreak effect.

Methods

Epidemiologic Investigation

This outbreak investigation was determined to be a public health response. Therefore, review by institutional review board was not required. All patients gave informed consent.

After identification of the first 2 patients, measures were taken by the RGM Outbreak Investigation team, which consisted of state and local health departments and the CDC, to locate additional patients who had RGM infections that were associated with cosmetic surgery undergone in the Dominican Republic. Health alerts selective for clinicians, especially those serving Dominican communities, were disseminated through Epi-X (http://www.cdc. gov/epix), a secure notification network for public health professionals; the Emerging Infections Network (http://ein. idsociety.org/), a secure notification network for clinicians; the American Society of Plastic Surgeons (http://www. plasticsurgery.org/); and local public health networks. In addition, health messages encouraging clinicians and patients to report possible RGM infections to local public health authorities were distributed through mainstream and social media outlets. A probable case-patient was defined as a US resident who had a cosmetic surgery procedure in the Dominican Republic during March 2013–February 2014 and a diagnosed soft tissue infection unresponsive to standard antibacterial drug therapy. A confirmed case was defined as a probable case with a culture positive for RGM.

Patients were interviewed verbally by state or local public health authority personnel, who used a standard questionnaire that was designed by the RGM Outbreak Investigation Team to elucidate common exposures or experiences, characterize clinical symptoms and disease courses, and estimate the associated financial burdens. Interviews were conducted in Spanish or English at the patient's request. A standard medical chart abstraction form was used to review available US medical records to obtain medical histories and document medical and surgical interventions that included antibacterial drugs, clinical encounters, and disease courses. All identified surgical clinics in the Dominican Republic were geolocated by using street addresses to assess for geographic clustering (Google Earth, Mountain View, CA, USA; and ArcGIS, Environmental Systems Research Institute, Redlands, CA, USA). Data from questionnaires and medical chart abstraction forms were entered into a spreadsheet and analyzed. CDC reported findings to the Dominican Republic Ministry of Health (MOH) throughout the investigation.

Laboratory Analysis

Patient wound culture isolates from clinical and public health laboratories were submitted to CDC for organism confirmation and for pulsed-field gel electrophoresis (PFGE) testing. In addition to submitting isolates, the New York City Public Health Laboratory staff analyzed all isolates from New York, NY, USA, by PFGE and sent corresponding PFGE band patterns to CDC for comparison.

Isolates were first subcultured onto Middlebrook and Cohn 7H10 Agar (Fisher Scientific, Pittsburgh, PA, USA) and were checked for purity after 7 days of incubation at 30°C. Molecular typing was performed by using PFGE. Molecular chromosomal DNA was prepared as described previously (*21*). Genetic relatedness of the isolates was analyzed by using BioNumerics software (Applied Maths, Austin, TX, USA). PFGE pattern similarity was based on Dice coefficients, and a dendrogram was built by using the unweighted pair group method (Figure 1). The Tenover criteria (*22*) were used to interpret comparison of the patient isolate PFGE patterns; patterns were classified as indistinguishable (100% similarity), closely related (1–3 band difference), possibly related (4–6 band difference), or unrelated (>7 band difference). Use of 16s rRNA and rpoB gene sequencing of representative isolates (on the basis of PFGE patterns) confirmed species of isolates (*23–25*).

Results

Patient Characteristics

In 6 states, 21 patients (18 confirmed and 3 probable) were identified: New York, 11; Massachusetts, 4; Connecticut, 2; Maryland, 2; New Jersey, 1; and Pennsylvania, 1. Core
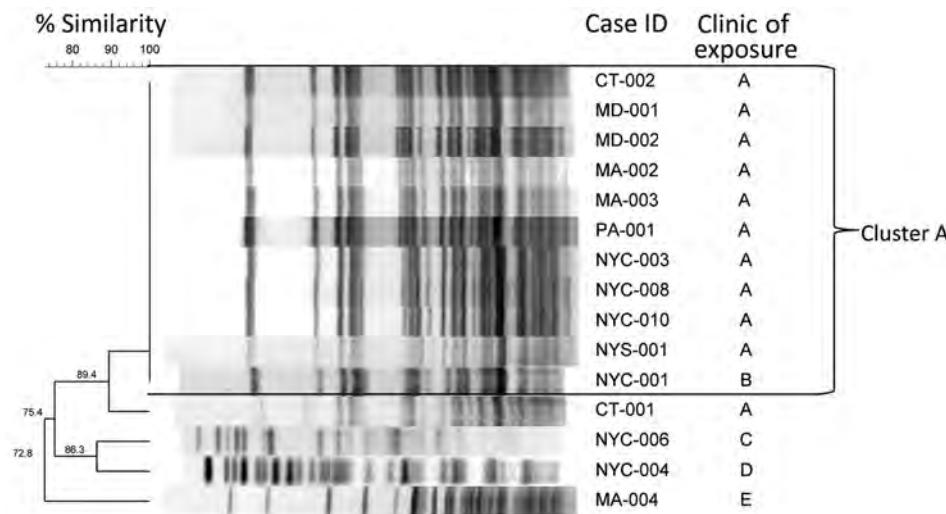
Figure 1. Dendrogram of rapidly growing mycobacteria in surgical site infections among patients in the US associated with medical tourism to the Dominican Republic, 2013–2014. Patients were exposed in 5 known clinics and 1 unknown clinic (data not shown). Pulsed-field gel electrophoresis band patterns for available *Mycobacterium abscessus* complex isolates were restricted with the AseI enzyme and run at 3 and 20 seconds for 20 hours. Isolates with indistinguishable band patterns are labelled cluster A. Case ID indicates US location and patient case number. ID, identification; NYC, New York City; NYS, state of New York.

demographic information was available for all 21 patients, 18 (86%) patients provided questionnaire information, and 3 (14%) declined to be interviewed. Median age of the 21 patients was 40 years (range 18–59 years); all were female (Table 1). Of those for whom data were available (n = 20), all reported US residency for a median of 25 years (range 9–44 years); 15 (75%) patients were born in the Dominican Republic, 2 in the United States, and 1 each in Brazil, Puerto Rico, and Jamaica. Residency and country of origin information were unknown for 1 patient.

Of the 21 case-patients, 13 (62%) learned of the Dominican Republic clinic where they had surgery through friends or family, 7 (33%) through the Internet, and 1 through a television advertisement. None had previously had cosmetic surgery performed in the Dominican Republic. Of the 16 who reported, cost affected the decision of 15 (94%) to undergo procedures in the Dominican Republic: "a lot" for 9 (56%); "somewhat" for 3 (19%); and "a little" for 1 (6%).

Of the 21 case-patients, 13 (62%) underwent surgical procedures at clinic A (Table 1); no common clinic was identified for the remaining 8, although data were missing for 1. No geographic clustering of clinics was observed. All procedures occurred during March 21–November 12, 2013 (Figure 2); 10 (85%) of clinic A patients reported procedures during July and August. Fifteen (71%) case-patients underwent liposuction; less frequent procedures included abdominoplasties, buttocks augmentations, breast augmentations, and breast reduction (Table 1). Eighteen (86%) case-patients had >1 procedure performed.

Postsurgery and Prediagnosis

All 21 case-patients remained in the Dominican Republic after their surgeries for a median duration of 18 days (range 10–80 days); 14 (67%) stayed with friends or relatives,

and the remainder stayed in hotels or guest houses. Of 17 for whom data were available, all had ≥1 postsurgery follow-up visits at the clinic where their surgery was performed. All but 1 (94%) case-patient reported having a dressing change; 9 of 15 (60%) reported that clinic staff did not wear gloves during a follow-up visit. None of the patients reported observing the use of tap water for wound care or reuse of wound care supplies by clinic staff. For 10 (48%) case-patients who provided their own wound care, none reported using saline, syringes, tap water, or multiuse alcohol while in the Dominican Republic. Seven (33%) case-patients reported bathing in the Dominican Republic; of these, 5 (71%) only sponge-bathed to minimize water exposure to the wounds. All denied swimming in the Dominican Republic. No postsurgical epidemiologic links among patients were described. Patients also were interviewed about their wound care and possible exposures after return to the United States; no common exposures were identified.

Laboratory Testing

Of the 18 confirmed RGM infections, 16 (89%) were of the *M. abscessus* complex and 2 (11%) were *M. fortuitum*. Surgical site specimens from all 12 (92%) confirmed clinic A patients grew *M. abscessus* complex; specimens from 1 clinic A patient did not grow RGMs, and the patient's status was classified as a probable case. *M. abscessus* complex isolates from 15 patients were analyzed by using PFGE (Figure 1); 11 (73%) were from clinic A and 4 from clinics B, C, D, and E (Figure 2). Overall, 11 (73%) of 15 isolates had indistinguishable PFGE patterns. Of the 11 clinic A isolates tested, 10 (91%) matched by PFGE. The clinic A patient whose isolate did not match the primary PFGE cluster pattern reported a procedure date 3 weeks earlier than all other clinic A patients (Figure 2). One isolate from

a patient whose procedure was not performed at clinic A (NYC-001 in Figure 1) matched the PFGE cluster associated with the clinic A infections.

Clinical Courses and Treatment

Medical chart abstractions were completed for 9 (69%) of 13 clinic A patients and 1 (12%) of 8 non–clinic A patients; we report data from the 9 available clinic A patients' charts. Illness onset was a median 24 days (range 1–60 days) after the surgical procedure (Table 2). Among 9 patients for whom we had data, care was sought a median 38 days (range 23–142 days) after the procedure. For 5 of the 9 patients for whom we had data and for whom RGM culture was positive, time to RGM laboratory confirmation was a median of 79 days (range 20–111 days) after the initial US medical encounter.

Wound-related signs and symptoms were reported more frequently than systemic signs and symptoms: >80% of case-patients reported swelling, pain, clear fluid drainage, and scarring, but only 45% exhibited systemic symptoms such as chills, malaise, and fever (Table 2). Of 9 (92%) clinic A patients for whom data were available, 8 were hospitalized in the United States; 5 (55%) were hospitalized on ≥2 occasions (Table 2). All of the 9 underwent ≥1 therapeutic surgical procedure; 5 (55%) required ≥3 separate procedures (range 1–11 procedures). Procedures included incision and drainage, debridement, implant removal, ultrasound-guided drainage, and insertions of peripherally inserted central catheters. Of the 9 patients, 7 (78%) required courses of antibacterial drugs >3 months duration, and 7 (78%) were prescribed ≥5 different classes of antibacterial drugs. A change in antibacterial drug treatment regimens was required for 7 (78%) patients. Of 5 patients' susceptibility data, all associated infections exhibited resistance or intermediate resistance to most classes of antibacterial drugs tested. Of 13 clinic A patients, 12 (92%) were contacted an average of 9 months after their surgeries (1 patient was lost to follow-up); only 1 (8%) patient reported full recovery when contacted.

Financial Burden

Financial burdens associated with therapeutic care were examined for 18 (86%) of the 21 confirmed and probable case-patients; 3 (14%) patients did not provide information. Of the 18 who responded, 13 (62%) used medical insurance to pay for treatment of infection in the United States; 3 (14%) paid cash; and 2 (10%) answered "don't know." Four (19%) patients reported that their insurer had declined to cover certain costs; 10 (48%) reported that their illness had caused financial problems; and 2 reported that the financial burden was not limited to direct medical costs but that indirect costs (e.g., the inability to work) compounded their financial difficulties.

Discussion

We identified 21 cases of RGM surgical site infections in 6 US states among medical tourists to the Dominican Republic. Thirteen of the patients underwent procedures at a single clinic, clinic A; most were infected by the same strain of *M. abscessus* complex, potentially from a single, unidentified point source. Most of the procedures at clinic A occurred within a 2-month period. Similar to a previously reported outbreak among "lipotourists," who had traveled to the Dominican Republic to have liposuction during 2003 (*16,17*), the clinic A cluster in this investigation occurred during what might represent a baseline of unrelated cosmetic surgery–associated RGM infections. This baseline might reflect sporadic or systematic failures in hygienic practices at certain surgical centers.

RGM infection is not a nationally notifiable disease in the United States or Dominican Republic. Therefore, cases described here might represent a limited proportion of those that actually occurred. Cases were dispersed throughout 6 states in the United States and were only identified after active case-finding was initiated, catalyzed by recognition of the initial 2-case cluster by an astute clinician. Health alerts to clinicians and the public

Table 1. Characteristics of 21 patients in multistate US outbreak of RGM infections after medical tourism to the Dominican Republic, 2013–2014*

Characteristic	Value
Demographics	
Female sex	21 (100)
Median age, y (range)	40 (18–59)
United States resident	20 (95)
Birth country	
Dominican Republic	15 (71)
United States	2 (10)
Other	3 (14)
Missing	1 (5)
US residency,† median y (range)	25 (9–44)
Clinical background, n = 15	
Surgical history	
Previous cosmetic surgeries in Dominican Republic	0 (0)
Any previous cosmetic surgeries	2 (13)
None	8 (53)
Dominican Republic surgical history	
Surgical clinic	
Clinic A	13 (62)
Clinics B, C, D, E	7 (33)
Unknown clinic	1 (5)
Most common procedures‡	
Liposuction	15 (71)
Abdominoplasty	12 (57)
Buttocks augmentation	8 (38)
Breast augmentation	6 (29)
Breast reduction	4 (19)
Median no. procedures received (range)	2 (1–6)

*Values are no. (%) except as indicated. Residency data are missing for 1 patient. RGM, rapidly growing mycobacteria.
†Among 15 case-patients whose charts were abstracted.
‡>1 answer possible per patient.
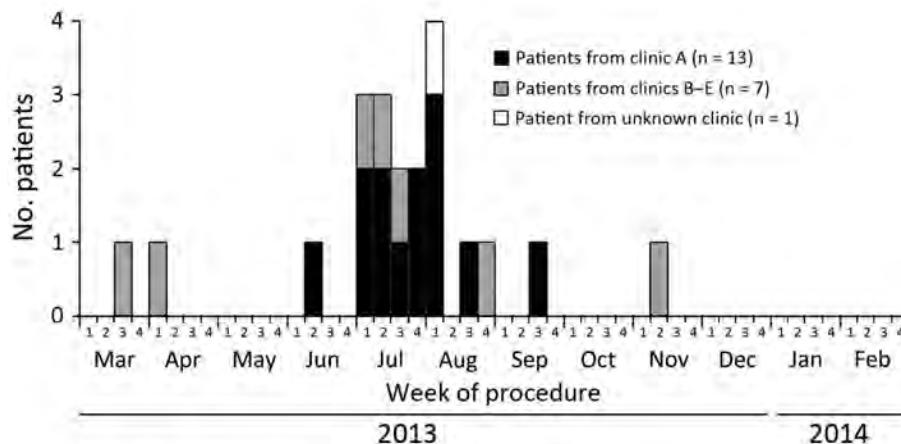
Figure 2. Number of case-patients in the United States who were infected in surgical sites with rapidly growing mycobacteria associated with medical tourism to the Dominican Republic, by procedure week, March 2013–February 2014 (N = 21). Weeks are defined uniformly as week 1, days 1–7 of the month; week 2, days 8–15; week 3, days 16–23; week 4, days 24–28/30/31. Pulsed-field electrophoresis pattern of the *Mycobacterium abscessus* isolate from the clinic A case-patient diagnosed during week 2 of June 2003 differed from those of remaining clinic A case-patients who were infected with *M. abscessus*.

associated with the investigation facilitated identification and treatment of some RGM patients.

This RGM outbreak illustrates potential risks for medical tourists. Little systematically collected data is available about the scope of and risks for medical tourism (*20*). Industry estimates regarding the number of US residents who travel abroad for medical services vary widely, from 75,000 to 750,000/year (*26,27*). In 2010, travel of an estimated 4 million medical tourists worldwide/year was reported by the Institute of Medicine, now known as Health and Medicine Division, of the US National Academy of Sciences (Washington, DC, USA) (*28*). Despite this discrepancy in estimated numbers, most reports indicate that the frequency of medical tourist activities and subsequent public health effects will likely increase in the future because of ease of travel, increased marketing and communications, and anticipated cost savings (*15,26,29,30*).

Cost previously has been reported to be the primary driver of medical tourism decisions (*31*) and was the case among our patients: 88% noted that cost affected their decision to undergo surgery in Dominican Republic. Studies have reported a cost savings of ≈28%–88%, depending on destination and services (*32–34*). However, among patients in this investigation, cost was not the only factor and possibly not the most important factor. Most patients had friends or family in the Dominican Republic or were originally from the Dominican Republic and learned of the Dominican Republic surgical clinic through word-of-mouth from friends or family; these factors might have played an important role in their decision making.

Both the American Medical Association and American College of Surgeons recommend that prospective medical tourists use internationally accredited facilities (*35*). During our investigation, we were unable to identify any Dominican Republic surgical centers accredited by an internationally recognized accrediting organization. However, standards vary between accrediting organizations, and no

published evidence is available that shows improved outcomes are associated with accreditation internationally (*35*). Although accreditation might offer guidance to consumers (*15*), expansion of medical tourism should spur international organizations to understand what aspects of accreditation methods improve patient outcomes and to uniformly apply these across settings. Outbreak activity has also prompted calls to strengthen infection control and safety standards for cosmetic surgery centers in United States (*36*). In addition to enhanced oversight, improved outcome surveillance related to medical tourism and better information about the scope, costs, and safety of the industry are needed to establish guidance for healthcare consumers, payers, healthcare providers, and policy makers (*15,19,20,32*).

The clinical courses of clinic A patients exhibited symptoms, diagnostic delays, and treatment difficulties typical of *M. abscessus* complex infections (*4*). Signs and symptoms among patients were largely cutaneous and localized, but severe in nature, and most case-patients exhibited painful, nonhealing soft-tissue infections; systemic signs and symptoms were less prominent. The 24-day incubation period after surgery for clinic A patients is comparable with that described by previous studies (*10,17*). Some patients might have delayed seeking care because of the localized nature and from mild to moderate severity of initial symptoms (*2*). Even after seeking care, some patients experienced a substantial delay in diagnosis. As described in the literature, initial cultures in RGM infections frequently demonstrate no pathogenic organism growth, and clinicians might only consider RGMS after a wound infection fails to respond to typical postsurgical therapeutic interventions (*4*).

Although RGMs grow well on routine bacterial culture media, clinical specimens frequently fail to exhibit growth after empirical use of common antibacterial drug therapy, particularly when swab specimens are collected instead of body fluids or tissue (*4*). To minimize diagnostic delays,

Table 2. Clinical course and therapeutic interventions for patients in multistate US outbreak of RGM infections acquired by medical tourists who underwent procedures in clinic A in the Dominican Republic, 2013–2014*

Characteristics	Value
Time from clinic A surgical procedure	
Median days to illness onset, n = 13	24 (1–60)
Median days to seek care†	38 (23–142)
Median days to RGM diagnosis‡	138 (52–183)
Time course from initial US clinic visit	
Median days to RGM diagnosis§	79 (20–111)
Signs and symptoms,¶ n = 11	
Systemic	
Chills	6 (55)
Malaise	5 (45)
Fever	5 (45)
Localized	
Swelling	10 (91)
Pain	10 (91)
Clear fluid discharge	9 (82)
Scarring	9 (82)
Redness	7 (64)
Warmth	7 (64)
Pus collection	5 (45)
Patient medical history, n = 9#	
No. days hospitalized for RGM infection	8 (92)
1	3 (33)
2–3	3 (33)
>3	2 (22)
No. therapeutic surgical procedures	
1–2	4 (44)
3–5	3 (33)
>5	2 (22)
Types of therapeutic surgical procedures**	
Debridements	6 (67)
Drainage procedures	5 (56)
PICC line	3 (33)
Ultrasound guided aspiration	3 (33)
Implant removal	2 (22)
Abdominal washouts	2 (22)
Missing data	0 (0)
No. antibacterial drug classes used per patient	
<3	0 (0)
4–5	2 (22)
>5	7 (78)
Duration of antibacterial drug therapy, mo	
<1	0 (0)
>1–≤3	2 (22)
>3	5 (56)
Unknown duration	2 (22)
Changed antibacterial drugs	
Yes	7 (78)
No	2 (22)

*Values are no. (%) except as indicated. PICC, peripheral inserted central catheters; RGM, rapidly growing mycobacteria.
†10 of 13 (77%) with available data.
‡6 of 13 (46%) with available data.
§5 of 13 (38%) with available data.
¶Signs and symptoms reported at a frequency <19% include skin stretching, fluctuance, bleeding from breast (site of surgical procedure), ulcerations, back pain, itching, body aches, and blisters and painful and red nodules that gradually enlarged and dehisced.
#Medical charts assessed for only 9 of 13 clinic A patients.
**≥1 answer possible per patient.

especially when encountering surgical site infections among medical tourists, clinicians should consider RGMs, collect adequate specimens, and communicate this suspicion to ensure correct laboratory testing is performed (*1,8*).

RGMs are notoriously antimicrobial drug resistant and difficult to treat (*37,38*). The isolates from patients in this investigation were resistant to multiple classes of antibacterial drugs and required protracted and complex antibacterial drug combinations and courses. Surgical interventions are frequently necessary adjuncts to antibacterial drug therapy (*1,4,39*). Multiple clinic A patients required ≥2 hospitalizations and multiple surgical procedures. Considering the 6–12-month duration of a typical *M. abscessus* complex disease course (*4*), our finding that only 1 clinic A patient was known to have fully recovered by the close of our investigation was expected.

Because RGMs are ubiquitous environmental contaminants, site inspections to identify inadequate infection control practices (e.g., reuse of equipment or inadequate cleaning and disinfection procedures) and to test water sources are crucial in discovering the point source of an outbreak (*10,11*). However, although environmental reservoirs usually serve as a primary source for RGMs, how these organisms are introduced into the patient is often difficult to determine. The tendency of RGMs to cause soft tissue infection in immunocompetent adults after surgical procedures is not understood (*8*). Whereas specific virulence factors among RGMs might predispose the patient to dermal and subdermal infection, such infections could also reflect the propensity of RGMs to form biofilms and relative resistance to disinfectants and surgical antibacterial drug prophylaxis, combined with lapses in infection control (*8–11*).

CDC provided epidemiologic information identifying the involved surgical clinics, clinic practices, and patient activities in the Dominican Republic to the Dominican Republic MOH. On the basis of this information, the Dominican Republic MOH performed site visits to certain identified clinics, including clinic A. Although detailed inspection findings were unavailable, and its current status is unknown, the Dominican Republic MOH reported that clinic A was closed after their site visit.

In summary, our investigation identified a cluster of RGMs associated with surgery at clinic A and additional cases associated with other cosmetic surgery clinics in the Dominican Republic. RGM infection remains a potential risk for medical tourism, and clinicians should consider RGMs early, especially among medical tourists. As this investigation demonstrates, treatment of persons with RGM infections is often prolonged and resource-intensive. Patient burdens were not limited to the financial cost of healthcare but also included a loss of ability to work and decreased quality of life during treatment. The extensive number of hospitalizations, drugs, and corrective surgeries required by patients in this study illustrates the considerable burden of illness to individual patients and the healthcare system (*40*). Understanding the role of medical tourism in disease risk and increasing patient protections in this context will require an ongoing effort by the international public health

and medical communities. Clinicians and public health officials, particularly those serving communities with connections to immigrants from medical tourism destinations, should be vigilant and consider RGM infections in the differential diagnosis for persons who have wound infections after surgery in these destinations.

Acknowledgments

References

1. Atkins BL, Gottlieb T. Skin and soft tissue infections caused by nontuberculous mycobacteria. Curr Opin Infect Dis. 2014;27: 137–45. http://dx.doi.org/10.1097/QCO.0000000000000041
2. Regnier S, Cambau E, Meningaud JP, Guihot A, Deforges L, Carbonne A, et al. Clinical management of rapidly growing mycobacterial cutaneous infections in patients after mesotherapy. Clin Infect Dis. 2009;49:1358–64. http://dx.doi.org/10.1086/606050
3. Bastian S, Veziris N, Roux AL, Brossier F, Gaillard JL, Jarlier V, et al. Assessment of clarithromycin susceptibility in strains belonging to the Mycobacterium abscessus group by erm(41) and rrl sequencing. Antimicrob Agents Chemother. 2011;55:775–81. http://dx.doi.org/10.1128/AAC.00861-10
4. Griffith DE, Aksamit T, Brown-Elliott BA, Catanzaro A, Daley C, Gordin F, et al.; ATS Mycobacterial Diseases Subcommittee; American Thoracic Society; Infectious Disease Society of America. An official ATS/IDSA statement: diagnosis, treatment, and prevention of nontuberculous mycobacterial diseases. Am J Respir Crit Care Med. 2007;175:367–416. Erratum in: Am J Respir Crit Care Med. 2007;175:744–5.
5. Brown-Elliott BA, Wallace RJ Jr. Clinical and taxonomic status of pathogenic nonpigmented or late-pigmenting rapidly growing mycobacteria. Clin Microbiol Rev. 2002;15:716–46. http://dx.doi.org/10.1128/CMR.15.4.716-746.2002
6. Zosso C, Lienhard R, Siegrist HH, Malinverni R, Clerc O. Post liposuction infections by rapidly growing mycobacteria. Infect Dis. 2015;47:69–72. http://dx.doi.org/10.3109/00365548.2014.968865.
7. Uslan DZ, Kowalski TJ, Wengenack NL, Virk A, Wilson JW. Skin and soft tissue infections due to rapidly growing mycobacteria: comparison of clinical features, treatment, and susceptibility. Arch Dermatol. 2006;142:1287–92. http://dx.doi.org/10.1001/archderm.142.10.1287.
8. Kothavade RJ, Dhurat RS, Mishra SN, Kothavade UR. Clinical and laboratory aspects of the diagnosis and management of cutaneous and subcutaneous infections caused by rapidly growing mycobacteria. Eur J Clin Microbiol Infect Dis. 2013;32:161–88. http://dx.doi.org/10.1007/s10096-012-1766-8.
9. Falkinham JO III. Surrounded by mycobacteria: nontuberculous mycobacteria in the human environment. J Appl Microbiol. 2009; 107:356–67. http://dx.doi.org/10.1111/j.1365-2672.2009.04161.x
10. Meyers H, Brown-Elliott BA, Moore D, Curry J, Truong C, Zhang Y, et al. An outbreak of Mycobacterium chelonae infection following liposuction. Clin Infect Dis. 2002;34:1500–7. http://dx.doi.org/10.1086/340399
11. Tiwari TS, Ray B, Jost KC Jr, Rathod MK, Zhang Y, Brown-Elliott BA, et al. Forty years of disinfectant failure: outbreak of postinjection Mycobacterium abscessus infection caused by contamination of benzalkonium chloride. Clin Infect Dis. 2003;36:954–62. http://dx.doi.org/10.1086/368192
12. Phillips MS, von Reyn CF. Nosocomial infections due to nontuberculous mycobacteria. Clin Infect Dis. 2001;33:1363–74. http://dx.doi.org/10.1086/323126
13. Toy BR, Frank PJ. Outbreak of Mycobacterium abscessus infection after soft tissue augmentation. Dermatol Surg. 2003;29:971–3.
14. Centers for Disease Control and Prevention (CDC). Rapidly growing mycobacterial infection following liposuction and liposculpture—Caracas, Venezuela, 1996–1998. MMWR Morb Mortal Wkly Rep. 1998;47:1065–7.
15. Chen LH, Wilson ME. The globalization of healthcare: implications of medical tourism for the infectious disease clinician. Clin Infect Dis. 2013;57:1752–9. http://dx.doi.org/10.1093/cid/cit540
16. Centers for Disease Control and Prevention. Nontuberculous mycobacterial infections after cosmetic surgery—Santo Domingo, Dominican Republic, 2003–2004. MMWR Morb Mortal Wkly Rep. 2004;53:509.
17. Furuya EY, Paez A, Srinivasan A, Cooksey R, Augenbraun M, Baron M, et al. Outbreak of Mycobacterium abscessus wound infections among "lipotourists" from the United States who underwent abdominoplasty in the Dominican Republic. Clin Infect Dis. 2008;46:1181–8. http://dx.doi.org/10.1086/529191
18. Maurer F, Castelberg C, von Braun A, Wolfensberger A, Bloemberg G, Bottger E, et al. Postsurgical wound infections due to rapidly growing mycobacteria in Swiss medical tourists following cosmetic surgery in Latin America between 2012 and 2014. Euro Surveill. 2014;19:20905. http://dx.doi.org/10.2807/1560-7917.ES2014.19.37.20905
19. Hall CM, James M. Medical tourism: emerging biosecurity and nosocomial issues. Tourism Review. 2011;66:118–26 http://dx.doi.org/10.1108/16605371111127288.

20. Talbot EA, Chen LH, Sanford C, McCarthy A, Leder K; Research Committee of International Society of Travel Medicine. Travel medicine research priorities: establishing an evidence base. J Travel Med. 2010;17:410–5. http://dx.doi.org/10.1111/j.1708-8305.2010.00466.x

21. Wallace RJ Jr, Zhang Y, Brown BA, Fraser V, Mazurek GH, Maloney S. DNA large restriction fragment patterns of sporadic and epidemic nosocomial strains of *Mycobacterium chelonae* and *Mycobacterium abscessus*. J Clin Microbiol. 1993;31:2697–701.

22. Tenover FC, Arbeit RD, Goering RV, Mickelsen PA, Murray BE, Persing DH, et al. Interpreting chromosomal DNA restriction patterns produced by pulsed-field gel electrophoresis: criteria for bacterial strain typing. J Clin Microbiol. 1995;33:2233–9.

23. Rogall T, Wolters J, Flohr T, Böttger EC. Towards a phylogeny and definition of species at the molecular level within the genus *Mycobacterium.* Int J Syst Bacteriol. 1990;40:323–30. http://dx.doi.org/10.1099/00207713-40-4-323

24. Adékambi T, Colson P, Drancourt M. rpoB-based identification of nonpigmented and late-pigmenting rapidly growing mycobacteria. J Clin Microbiol. 2003;41:5699–708. http://dx.doi.org/10.1128/JCM.41.12.5699-5708.2003

25. Adékambi T, Drancourt M. Dissection of phylogenetic relation-ships among 19 rapidly growing *Mycobacterium* species by 16S rRNA, hsp65, sodA, recA and rpoB gene sequencing. Int J Syst Evol Microbiol. 2004;54:2095–105. http://dx.doi.org/10.1099/ijs.0.63094-0

26. Keckley PH, Underwood HR. Medical tourism: update and implications. Report no: 9112. Washington: Deloitte Center for Health Solutions; 2009 [cited 2015 May 15]. http://www.deloitte.com/assets/Dcom-UnitedStates/Local%20assets/documents/us_chs_medicaltourism_111209_web.pdf

27. The McKinsey Quarterly. Key findings from the McKinsey report on medical tourism. 2008 Nov 28 [cited 2015 May 15]. http://www.allaboutmedicaltourism.com/2008/11/the-mckinsey-quarterly-has-published-a-key-study-on-medical-tourism-here-which-has-provided-a-much-lower-set-of-projecti.html

28. Relman DA, Choffnes ER, Mack A. Infectious disease movement in a borderless world: workshop summary. Washington (DC): National Academies Press; 2010. http://dx.doi.org/10.17226/12758

29. Milstein A, Smith M. America's new refugees—seeking affordable surgery offshore. N Engl J Med. 2006;355:1637–40. http://dx.doi.org/10.1056/NEJMp068190

30. Nassab R, Hamnett N, Nelson K, Kaur S, Greensill B, Dhital S, et al. Cosmetic tourism: public opinion and analysis of information and content available on the Internet. Aesthet Surg J. 2010;30:465–9. http://dx.doi.org/10.1177/1090820X10374104

31. Weisz G. Historical reflections on medical travel. Anthropol Med. 2011;18:137–44. http://dx.doi.org/10.1080/13648470.2010.525880

32. Lunt N, Smith R, Exworthy M, Green ST, Horsfall D, Mannion R. Medical tourism: treatments, markets and health system implications: a scoping review. Commissioned Report. Paris: OECD, Directorate for Employment Labour and Social Affairs; 2011 [cited 2015 May 15]. http://search.oecd.org/els/health-systems/48723982.pdf

33. Smith RD, Chanda R, Tangcharoensathien V. Trade in health-related services. Lancet. 2009;373:593–601. http://dx.doi.org/10.1016/S0140-6736(08)61778-X

34. Kumar S, Breuing R, Chahal R. Globalization of health care delivery in the United States through medical tourism. J Health Commun. 2012;17:177–98. http://dx.doi.org/10.1080/10810730.2011.585699

35. Centers for Disease Control and Prevention: CDC health information for international travel 2016. New York: Oxford University Press; 2015.

36. Morgan DJ, Harris AD. The gap in patient protection for outpatient cosmetic surgery. JAMA Intern Med. 2014;174:1142–3. http://dx.doi.org/10.1001/jamainternmed.2014.441

37. Nessar R, Cambau E, Reyrat JM, Murray A, Gicquel B. *Mycobacterium abscessus*: a new antibiotic nightmare. J Antimicrob Chemother. 2012;67:810–8. http://dx.doi.org/10.1093/jac/dkr578

38. Petrini B. *Mycobacterium abscessus*: an emerging rapid-growing potential pathogen. APMIS. 2006;114:319–28. http://dx.doi.org/10.1111/j.1600-0463.2006.apm_390.x

39. Engdahl R, Cohen L, Pouch S, Rohde C. Management of *Mycobacterium abscessus* post abdominoplasty. Aesthetic Plast Surg. 2014;38:1138–42. http://dx.doi.org/10.1007/s00266-014-0410-7

40. Helble M. The movement of patients across borders: challenges and opportunities for public health. Bull World Health Organ. 2011;89:68–72. http://dx.doi.org/10.2471/BLT.10.076612

Address for correspondence: David Schnabel, Centers for Disease Control and Prevention, UNIT 8900, Box 360 DPO, AE 09831, USA; email: DSchnabel@cdc.gov

Probable Rabies Virus Transmission through Organ Transplantation, China, 2015

Hang Zhou,[1] Wuyang Zhu,[1] Jun Zeng,[1] Jianfeng He,[1] Kai Liu, Yu Li, Shuwu Zhou, Di Mu,
Kechun Zhang, Pengcheng Yu, Zhijian Li, Meng Zhang, Xueqiong Chen, Chun Guo, Hongjie Yu

During July 2015, physicians at a hospital in Beijing, China, diagnosed rabies in 2 patients who had each received a kidney from a common organ donor who had died from acute progressive encephalitis of unknown cause. The patients had rabies incubation periods of 42 and 48 days. Altered mental status developed in both patients and progressively worsened to deep coma within 80 days after transplantation; both patients died. Two other transplant recipients received corneas but remained well after receiving timely rabies prophylaxis. An effective regulatory system for testing donors should be implemented to decrease the occurrence of donor-derived infectious diseases. In addition, health education should be improved to enhance public awareness of transplant-associated infectious diseases. Transplant recipients and other persons with exposure to organs or tissues from donors with rabies must be provided consistent health monitoring and follow-up, including rabies postexposure prophylaxis; any remaining organs and tissues must be quarantined and not transplanted.

In July 2015, physicians at a hospital in Beijing, China, diagnosed rabies in 2 recipients of kidneys from a common organ donor. The donor's corneas were transplanted into 2 other patients. Rabies virus transmission via nonbite exposures is rare. Thus, the Chinese Center for Disease Control and Prevention (China CDC) initiated an investigation to determine if the virus was transmitted through organ transplantation and to identify and prevent rabies in other transplant recipients and persons who may have been exposed to potentially infectious material.

Methods

We reviewed medical records for the donor and recipients to determine if the kidney recipients acquired rabies virus through the transplanted organs and to identify other potentially infected recipients of transplants from the same donor. We also interviewed family members of the donor and the deceased kidney recipients.

We used reverse transcription PCR (RT-PCR) targeting the rabies virus nucleoprotein gene (1) to extract and amplify RNA from saliva, urine, and sputum samples from kidney transplant recipients. We collected serum samples from the 2 cornea transplant recipients on postexposure prophylaxis (PEP) days 0, 1, 5, 8, 15, and 32. To determine whether an adequate adaptive immune response was produced after vaccination, we measured rabies virus–neutralizing antibody levels in samples by using the rapid fluorescent focus inhibition test (2); titers ≥0.5 IU/mL were considered to provide an adequate level of protection according to World Health Organization standards (2).

Results

Organ Donor

The donor was a 6-year-old boy who lived in Guangxi Province, an area of China that had the highest number of cumulative reported rabies cases during 2004–2014. During that period, ≈10 rabies cases were reported almost every year in the northeastern part of Guangxi, where the boy resided. On May 13, 2015, the boy had a fever (temperature not recorded) and refused to eat, drink, or sleep (Figure). On May 15th, the boy was sent to a county hospital because

Author affiliations: Division of Infectious Disease, Key Laboratory of Surveillance and Early-Warning on Infectious Disease, Chinese Center for Disease Control and Prevention, Beijing, China (H. Zhou, Y. Li, D. Mu, C. Guo, H. Yu); State Key Laboratory of Infectious Disease Prevention and Control, National Institute for Viral Disease Control and Prevention, Chinese Center for Disease Control and Prevention, Beijing (W. Zhu, P. Yu); Collaborative Innovation Center for Diagnosis and Treatment of Infectious Diseases, Hangzhou, China (W. Zhu, P. Yu); Guangxi Provincial Center for Disease Control and Prevention, Nanning, China (J. Zeng, S. Zhou); Guangdong Provincial Center for Disease Control and Prevention, Guangzhou, China (J. He, M. Zhang); Xiaogan Prefecture Center for Disease Control and prevention, Xiaogan, China (K. Liu); Longhua District Center for Disease Control and Prevention, Shenzhen, China (K. Zhang); Hezhou Prefecture Center for Disease Control and prevention, Hezhou, China (Z. Li, X. Chen): Fudan University School of Public Health, Key Laboratory of Public Health Safety, Ministry of Education, Shanghai, China (H. Yu)

DOI: http://dx.doi.org/10.3201/eid2208.151993

Figure. Clinical course of a transplant donor, 2 recipients of kidneys, and 2 recipients of corneas in investigation of probable transplant-associated transmission of rabies virus, China, 2015. RT-PCR, reverse transcription PCR.

the fever and symptoms had not resolved and he showed additional symptoms of extreme irritability, screaming, and slurred speech. The boy refused a physical examination, including measurement of his body temperature. The doctor administered infusion therapy with vitamins B and C, aspirin/glycine , and diazepam, but symptoms persisted.

On May 16, the boy showed signs of dysphagia and hypersalivation and was moved to another county-level hospital. Doctors presumptively treated the boy with intravenous ribavirin for a possible viral infection, but the boy's condition continued to deteriorate. Later that day, he was admitted to a prefecture-level hospital with a diagnosis of possible viral encephalitis. Chest and head computed tomography scan images showed pulmonary infection and slightly decreased density of the bilateral temporal lobes. The boy had a leukocyte count of 15.7×10^9 cells/L (reference range $5–12 \times 10^9$ cells/L). Cerebral spinal fluid test results showed an opening pressure of 60 drops/min, a transparent and colorless fluid, a protein level of 265.0 mg/L, and a glucose level of 4.70 mmol/L, indicating the probability of viral encephalitis. The boy's neurologic condition continued to decline, progressing to coma with progressive loss of all physiologic and pathologic reflexes. On May 26, the boy died, and his kidneys and corneas were collected

for transplantation; no other organs or tissues were used for transplantation. The boy's remains were cremated. Before he died, testing was done for HIV, hepatitis B, and syphilis, according to the organ donation law in China; all test results were negative. No autopsy was performed, and no specimens were retained for later testing.

The epidemiologic investigation revealed that the child's family kept dogs for many years, and the child had had frequent contact with the dogs. However, the boy lived with his elderly grandmother in a different city than that where his parents lived and worked, and the grandmother did not recall any animal bites on the child. In addition, the boy had no travel history, except to attend nursery school, and no pets were kept at the school. The boy had no history of rabies prophylaxis.

Transplant Recipients

Patient 1 was a 55-year-old man who lived in Hebei Province, China. Because of uremia, he received a kidney allograft transplant on May 27, 2015, in Beijing. Patient 1 had an uncomplicated postoperative course and was discharged home on June 15. During 2 postoperative outpatient visits, he was noted to have a normal recovery. However, on July 8, 42 days after receiving the kidney

transplant, he had mild abdominal distension and low-grade fever, and on July 9, limb weakness developed (Figure). He was hospitalized on July 10 for evaluation of fever, fatigue, and worsening muscle soreness. On July 17, he showed symptoms of dysphagia, hearing loss, and incoherent speech and was transferred to the intensive care unit (ICU) and intubated. On July 24, based on the presence of fever, muscle spasms after external stimulation, laryngeal spasms, and muscle atrophy, doctors diagnosed the patient with suspected rabies and transferred him to the infectious disease ICU. On July 28, the diagnosis was confirmed based on rabies-positive RT-PCR results. Patient 1 died on August 23, 46 days after onset of posttransplantion symptoms. Family members reported he had no pets, and they gave no history of animal bites or scratches or of rabies prophylaxis for the patient.

Patient 2 was a 43-year-old man from Liaoning Province, China. On May 27, 2015, he received a kidney allograft transplant in the same hospital and for the same reason (uremia) as patient 1. Patient 2 had an unremarkable postoperative course. He was seen twice as an outpatient and had no unusual findings. On July 14, 48 days after receiving the transplant, he had low back pain, a low-grade fever, and increasing general weakness and leg pain (Figure). He was readmitted to the hospital on July 18 for evaluation of fever and back pain; his speech became incoherent, and he had intermittent fever. On July 21, he had a high fever, anxiety, and paranoia, and on July 22, he had shortness of breath and dysphagia and refused to drink liquids. On July 23, doctors transferred him to an ICU, where seizures subsequently developed. On July 24, the patient was diagnosed with suspected rabies based on the clinical symptoms and was transferred to the infectious disease ICU. On July 28, the diagnosis was confirmed based on rabies-positive RT-PCR results. Patient 2 died on August 17, 34 days after onset of posttransplantation symptoms. Family members reported he had no pets, and they gave no history of animal bites or scratches or of rabies prophylaxis for the patient.

Patient 3 was a 42-year-old man from Guangdong Province, China. The patient had corneal leukoplakia and underwent right eye penetrating keratoplasty and anterior chamber plasty on June 1, 2015. He was discharged on June 12.

Patient 4 was a 62-year-old man from Guangdong Province. He underwent a right eye cornea transplant replacement on June 1 in the same hospital as patient 3. The procedure was done to treat a corneal graft rejection; the operation was successful.

Patients 3 and 4 had no history of chronic disease, bloodborne infection, trauma, blood transfusion, or rabies prophylaxis. They did not have pets and gave no history of animal bites or scratches. After discharge, the patients underwent weekly examinations the first month and monthly examination for the next 2 years. As of February 2, 2016, both had self-reported good health and no discomfort. Corneas were not explanted. Both patients received full rabies PEP beginning on August 5, 2015, immediately following confirmation of corneal transplantation from the donor from Guangxi.

The rabies incubation period for patients 1 and 2 were 42 and 48 days, respectively. Signs and symptoms of altered mental status developed in both patients and progressively worsened to deep coma within 80 days after transplantation (Figure).

We included 290 persons in the epidemiologic investigation of donor and transplant recipient contacts, including family members and healthcare workers in the hospitals. Of the 290 contacts, 233 received PEP. The 57 other evaluated persons did not need PEP because they had not had close contact with the patients or virus.

Laboratory Findings

Patients 1 and 2

Saliva, urine, and sputum samples from patient 1 and saliva and urine samples from patient 2 were positive for rabies virus nucleic acid. Thus, according to diagnostic criteria in China (3), both kidney recipients were laboratory-confirmed to be positive for rabies.

Patients 3 and 4

Twelve serum samples were collected from the 2 corneal transplant patients. Baseline rabies virus–neutralizing antibody titers on day 0 of PEP were 0.07 IU/mL and 0.02 IU/mL for patients 3 and 4, respectively. However, on PEP day 15, titers were 133.24 IU/mL and 154.78 IU/mL for patients 3 and 4, respectively; on PEP day 32, titers were 168.61 IU/mL and 110.95 IU/mL for patients 3 and 4, respectively. These levels indicate sufficient protection against rabies, according to World Health Organization guidelines (2).

Discussion

Based on these findings, we conclude that rabies in the 2 kidney transplant recipients probably resulted from rabies virus transmitted from the common organ donor. Our findings show that the donor was probably exposed to dogs at home and had symptoms typical of rabies, that neither kidney recipient had a history of exposure to animals with suspected rabies, and that both recipients had posttransplant symptoms of rabies and were PCR-positive for the virus. Further confirmation could not be done because the donor, who was diagnosed with infectious encephalitis, was cremated after organs and tissues were collected for transplantation, and no clinical specimens were kept by the

hospital. Thus, we could not confirm rabies in the donor by laboratory methods.

The rabies incubation periods for patients 1 and 2 were 42 and 48 days, respectively, after receiving the kidney transplants, and for both patients, the period from symptom onset to death was >1 month. Similar to findings from previous reports in the transplantation literature, the rabies incubation periods for the 2 kidney recipients were relatively shorter than those for persons infected via the bite route; the long survival periods may also be related to the route of virus transmission (4). Rabies did not develop in the cornea recipients before they received PEP, possibly indicating that the virus load in these recipients was lower than that for the kidney recipients (4,5). We cannot know if rabies would have developed in the 2 cornea transplant recipients if they had not been administered PEP in a timely manner. Rabies also did not develop in other cornea transplant recipients who received timely postexposure rabies PEP or who had transplanted corneas removed (6,7).

Our study had several limitations. No donor specimens were preserved, an in-depth gene sequencing analysis between donor and recipients could not be conducted, and sequence analyses and a comparison of amplicons from PCR of kidney patients' saliva were not conducted. In addition, we collected only saliva, urine, and sputum samples from the kidney transplant recipients; cerebrospinal fluid or central nervous system tissues would have been better samples for the laboratory confirmation of rabies.

Rabies has been a notifiable disease in China since 1949. Since then, the highest number of rabies-associated human deaths (>7,000) was reported in 1981 (8). The annual incidence has shown a continuous downward trend from 2007 (9). However, rabies is believed to be underreported in China because most cases occur in remote rural areas, patients may not be seen by a clinician before death, the proportion of laboratory-confirmed cases is relatively low compared with other causes of illness, and confirmatory laboratory diagnoses is lacking for some cases of infectious encephalitis (10). To achieve the goal of rabies elimination, the China CDC is working with the national agricultural departments to improve the national rabies surveillance system, increase testing of suspected human cases of rabies, enhance surveillance and testing of dogs that attack humans, and improve monitoring of rabies PEP clinics.

Based on a regulation issued by the China Ministry of Health in 2006, organs or tissues from HIV-infected or AIDS patients, hepatitis B virus carriers, and persons with other bloodborne diseases, syphilis, or malignant tumors cannot be used for transplantation (11). Rabies was not specifically mentioned in the regulation, so it is a challenge to have donors screened for rabies. In some remote or rural areas in China, it is difficult to definitively diagnose the cause of infectious encephalitis, and rabies cases with atypical symptoms might be misdiagnosed. Given that laboratory diagnosis of rabies can only be conducted at prefecture-level and above China CDC laboratories, it is difficult to provide a definitive diagnosis of suspected rabies cases within the short window of time for organ transplantations. Therefore, to reduce infections transmitted from organ donors, we recommend development and implementation of standard questionnaires or tables for use in interviewing relatives of persons who died from infectious encephalitis to identify any rabies exposure history and associated symptoms. Implementation of this questionnaire would prompt regional CDCs to collect specimens from potential donors in time for testing. Cerebrospinal fluid, saliva, and skin biopsies are generally considered as critical samples for antemortem human rabies testing, and brain tissue is considered critical for postmortem confirmation. If time does not permit testing, the presence of infectious encephalitis symptoms in the donor should lead to a determination that organs and tissues are not suitable for transplantation, especially in regions with a high incidence of rabies.

One reason that the rabies cluster reported here was detected is that the 2 kidney recipients were hospitalized in the same facility. If only 1 rabies case is diagnosed in a transplant recipient at a facility, it might be difficult to identify the organ donor as the infectious source.

Other infectious pathogens can also be transmitted during transplantation (12–15), and the cause of encephalitis among solid organ transplant recipients can be multifactorial. Other infectious agents associated with encephalitis, including West Nile virus, lymphocytic choriomeningitis virus, and *Balamuthia mandrillaris* amebae, have been reported in clusters of solid organ transplant recipients (16). The occurrence of donor-derived infectious diseases in transplant recipients can be decreased by strengthening donor assessment and evaluation and by implementing an effective regulatory system for testing donors. In addition, health education should be improved to enhance public awareness of possible transplant-associated infectious diseases. If it is determined that organs or tissues from a donor with rabies have been transplanted, the transplant recipients and other exposed persons who are at risk must receive consistent health monitoring and follow-up, including rabies PEP, and any remaining organs and tissues must be quarantined and not transplanted.

Dr. Zhou is an associate research scientist in the Division of Infectious Disease, Chinese Center for Disease Control and Prevention, Beijing, China. Her research focuses on the epidemiology, transmission dynamics, and surveillance of zoonotic and vectorborne diseases, such as rabies, brucellosis and dengue.

References

1. Warner CK, Zaki SR, Shieh WJ, Whitfield SG, Smith JS, Orciari LA, et al. Laboratory investigation of human deaths from vampire bat rabies in Peru. Am J Trop Med Hyg. 1999;60:502–7.
2. World Health Organization. WHO expert consultation on rabies. Second report [cited 2015 Sep 15]. http://apps.who.int/iris/bitstream/10665/85346/1/9789240690943_eng.pdf
3. Ministry of Health of the People's Republic of China. Diagnostic criteria for human rabies (WS 281–2008) [in Chinese] [cited 2010 Jan 18]. http://www.nhfpc.gov.cn/zhuzhan/tgggao/lists.shtml
4. Vora NM, Basavaraju SV, Feldman KA, Paddock CD, Orciari L, Gitterman S, et al. Raccoon rabies virus variant transmission through solid organ transplantation. JAMA. 2013;310:398–407. http://dx.doi.org/10.1001/jama.2013.7986
5. Vetter JM, Frisch L, Drosten C, Ross RS, Roggendorf M, Wolters B, et al. Survival after transplantation of corneas from a rabies-infected donor. Cornea. 2011;30:241–4. http://dx.doi.org/10.1097/ICO.0b013e3181e4572a
6. Jackson AC. Rabies. 3rd ed. New York: Academic Press; 2013. p. 270–1.
7. Bronnert J, Wilde H, Tepsumethanon V, Lumlertdacha B, Hemachudha T. Organ transplantations and rabies transmission. J Travel Med. 2007;14:177–80. http://dx.doi.org/10.1111/j.1708-8305.2006.00095.x
8. Hu R, Tang Q, Tang J, Fooks AR. Rabies in China: an update. Vector Borne Zoonotic Dis. 2009;9:1–12. http://dx.doi.org/10.1089/vbz.2008.0046
9. Yao HW, Yang Y, Liu K, Li XL, Zuo SQ, Sun RX, et al. The spatiotemporal expansion of human rabies and its probable explanation in mainland China, 2004–2013. PLoS Negl Trop Dis. 2015;9:e0003502. http://dx.doi.org/10.1371/journal.pntd.0003502
10. Yin W, Dong J, Tu C, Edwards J, Guo F, Zhou H, et al. Challenges and needs for China to eliminate rabies. Infect Dis Poverty. 2013;2:23. http://dx.doi.org/10.1186/2049-9957-2-23
11. Ministry of Health of the People's Republic of China. Interim regulation on the administration of clinical application of human organ transplant technology [in Chinese] [cited 2015 Aug 7]. 2006. http://www.nhfpc.gov.cn/yzygj/s3585u/200804/b6e-135abbdba4372b111015571f903dc.shtml
12. Razonable RR. Rare, unusual, and less common virus infections after organ transplantation. Curr Opin Organ Transplant. 2011;16:580–7. http://dx.doi.org/10.1097/MOT.0b013e32834cdaf2
13. Schafer IJ, Miller R, Ströher U, Knust B, Nichol ST, Rollin PE, et al. Notes from the field: a cluster of lymphocytic choriomeningitis virus infections transmitted through organ transplantation—Iowa, 2013. MMWR Morb Mortal Wkly Rep. 2014;63:249.
14. Nagai S, Mangus RS, Anderson E, Ekser B, Kubal CA, Fridell JA, et al. Cytomegalovirus infection after intestinal/multivisceral transplantation: a single center experience with 210 cases. Transplantation. 2016 [cited 2015 Nov 18]. Epub 2015 Aug 5. http://dx.doi.org/10.1097/TP.0000000000000832
15. Fischer SA, Graham MB, Kuehnert MJ, Kotton CN, Srinivasan A, Marty FM, et al. Transmission of lymphocytic choriomeningitis virus by organ transplantation. N Engl J Med. 2006;354:2235–49. http://dx.doi.org/10.1056/NEJMoa053240
16. Basavaraju SV, Kuehnert MJ, Zaki SR, Sejvar JJ. Encephalitis caused by pathogens transmitted through organ transplants, United States, 2002–2013. Emerg Infect Dis. 2014;20:1443–51. http://dx.doi.org/10.3201/eid2009.131332

Address for correspondence: Hongjie Yu, School of Public Health, Fudan University, Key Laboratory of Public Health Safety, Ministry of Education, Xuhui District, Shanghai 200032, China; email: cfetpyhj@vip.sina.com

Virulence and Evolution of West Nile Virus, Australia, 1960–2012

Natalie A. Prow,[1,2] Judith H. Edmonds,[2] David T. Williams, Yin X. Setoh, Helle Bielefeldt-Ohmann, Willy W. Suen, Jody Hobson-Peters, Andrew F. van den Hurk, Alyssa T. Pyke, Sonja Hall-Mendelin, Judith A. Northill, Cheryl A. Johansen, David Warrilow, Jianning Wang, Peter D. Kirkland, Stephen Doggett, Christy C. Andrade,[3] Aaron C. Brault, Alexander A. Khromykh,[4] Roy A. Hall[4]

Worldwide, West Nile virus (WNV) causes encephalitis in humans, horses, and birds. The Kunjin strain of WNV (WNV$_{KUN}$) is endemic to northern Australia, but infections are usually asymptomatic. In 2011, an unprecedented outbreak of equine encephalitis occurred in southeastern Australia; most of the ≈900 reported cases were attributed to a newly emerged WNV$_{KUN}$ strain. To investigate the origins of this virus, we performed genetic analysis and in vitro and in vivo studies of 13 WNV$_{KUN}$ isolates collected from different regions of Australia during 1960–2012. Although no disease was recorded for 1984, 2000, or 2012, isolates collected during those years (from Victoria, Queensland, and New South Wales, respectively) exhibited levels of virulence in mice similar to that of the 2011 outbreak strain. Thus, virulent strains of WNV$_{KUN}$ have circulated in Australia for ≥30 years, and the first extensive outbreak of equine disease in Australia probably resulted from a combination of specific ecologic and epidemiologic conditions.

West Nile virus (WNV) is a mosquito-transmitted flavivirus that causes encephalitis. Outbreaks of potentially fatal neurologic syndromes have occurred in Europe and Africa (1); recently, however, strains of WNV have caused large outbreaks of encephalitis in humans and horses in the Americas and Australia (2,3). The Kunjin strain of WNV (WNV$_{KUN}$) is indigenous to Australia and historically has caused only relatively mild, nonfatal disease in humans and horses. However, in 2011, a large unprecedented outbreak of encephalitis in horses, involving ≈900 reported cases, occurred in southeastern Australia; a high proportion of cases were attributed to the emergence of a virulent strain of WNV$_{KUN}$ (3,4). WNV$_{KUN}$ has been shown to be enzootic to northern Australia and to have episodic activity in southern regions thought to be associated with periods of heavy rainfall (5). However, the epidemiology of WNV$_{KUN}$ seems to have changed over the past decade; virus activity has been detected in the absence of prior flooding and in areas where it was previously not detected (4).

Studies comparing the virulence of various WNV strains in mouse models have identified several motifs, residing in both structural and nonstructural genes as well as in the 5′ and 3′ untranslated regions (UTRs). These motifs were associated with enhanced viral invasion of the central nervous system and onset of neurologic disease (5–11).

To identify potential markers of virulence of WNV$_{KUN}$ in Australia, we investigated evolutionary mechanisms behind the emergence of virulent strain(s) by using established mouse models to compare the neuroinvasive properties of WNV$_{KUN}$ isolates collected from different regions of Australia during 1960–2012. To investigate known markers of WNV virulence, we conducted comparative analyses of viral genome sequences.

Author affiliations: The University of Queensland, St. Lucia, Queensland, Australia (N.A. Prow, J.H. Edmonds, Y.X. Setoh, H. Bielefeldt-Ohmann, W.W. Suen, J. Hobson-Peters, A.A. Khromykh, R.A. Hall); CSIRO Australian Animal Health Laboratory, Geelong, Victoria, Australia (D.T. Williams, J. Wang); The University of Queensland, Gatton, Queensland, Australia (H. Bielefeldt-Ohmann, W.W. Suen); Department of Health, Brisbane, Queensland, Australia (A.F. van den Hurk, A.T. Pyke, S. Hall-Mendelin, J.A. Northill, D. Warrilow); The University of Western Australia, Nedlands, Western Australia, Australia (C.A. Johansen); Elizabeth Macarthur Agriculture Institute, Menangle, New South Wales, Australia (P.D. Kirkland); University of Sydney and Pathology West–ICPMR, Westmead, New South Wales, Australia (S. Doggett); University of California, Davis, California, USA (C.C. Andrade, A.C. Brault); Centers for Disease Control and Prevention, Fort Collins, Colorado, USA (C.C. Andrade, A.C. Brault)

[1]Current affiliation: QIMR Berghofer Medical Research Institute, Herston, Queensland, Australia.

[2]These authors contributed equally to the major technical aspects of the work.

[3]Current affiliation: Willamette University, Salem, Oregon, USA.

[4]These authors served as joint senior authors.

Methods

Cell Culture, Virus Production, and Titration

We used 13 WNV$_{KUN}$ strains isolated during 1960–2012 (Table 1) and African green monkey kidney (Vero) and *Aedes albopictus* mosquito (C6/36) cells, cultured as previously described (*3*). The 1960 prototype WNV$_{KUN}$ strain (WNV$_{KUN1960}$) was used as the attenuated reference virus and was either an unknown passage of the original isolate (WNV$_{MRM16}$) or derived from an infectious clone of a plaque-purified virus (WNV$_{MRM61C}$) (*12,13*). These isolates were previously shown to be phenotypically identical (*13,14*). WNV strain NY99-4132 was obtained from the US Centers for Disease Control and Prevention (Fort Collins, CO, USA) and used as a virulent control. Virus stocks and methods for determination of infectious titers have been described (*3*).

Antigenic Analysis

We compared reactivity of WNV$_{KUN}$ isolates with a panel of monoclonal antibodies (mAbs) with that of reference strains WNV$_{KUN1960}$ and WNV$_{NY99.}$ To do so, we used a fixed-cell ELISA, as previously described (*3,5,15*).

Virus Replication Kinetics

We performed growth kinetics analysis by infecting Vero and C6/36 cells at a multiplicity of infection of 1 at 37°C (Vero) or 28°C (C6/36) with WNV$_{KUN}$. Culture supernatants were harvested at 0, 24, 48, and 72 h after infection (Vero) and 0, 24, 48, 72, 96, and 120 h after infection (C6/36) and titrated (*3*). Statistical significance from 3 independent experiments was determined by using 2-way analysis of variance following log transformation (*16*). Mean virus titers were compared between viruses by using the Tukey method for pairwise multiple comparisons (GraphPad Prism, version 6.0; GraphPad Software Inc., San Diego, CA, USA).

Virulence in Mice

Performance of all animal procedures was approved by The University of Queensland Animal Ethics Committee. To determine virus virulence in mice, we intraperitoneally inoculated 20 Swiss white outbred CD-1 mice (weanlings [18–19 days of age] and young adults [28 days of age]) with a range of doses (0.1–10,000 PFU) of each WNV strain (Table 1) (*3*). The significance of clinical differences between groups was calculated by Kaplan-Meier analysis and analyzed by log-rank test where noted (GraphPad Prism, version 6.0). A virus strain was designated as virulent if survival times for mice infected with this strain (both age groups) differed significantly from those of mice infected with the attenuated reference strain WNV$_{KUN1960}$. All virus strains that did not meet this criterion for virulence were designated as attenuated.

Full-length Genome Sequencing

We sequenced 9 WNV$_{KUN}$ genomes (online Technical Appendix Table 1, http://wwwnc.cdc.gov/EID/article/22/8/15-1719-Techapp1.pdf) by using random primer sequencing on extracts of C6/36 cell cultures (*17*). Viral RNA was extracted by using a MagMAX-96 Viral RNA Isolation Kit (Ambion, Waltham, MA, USA) according to the manufacturer's instructions. cDNA synthesis and random PCR amplification were conducted according to previously described methods (*18*), and resultant PCR amplicons were used for sequencing library preparation. DNA libraries were prepared by using a Nextera XT DNA Sample Preparation Kit (Illumina, San Diego, CA, USA) according to the manufacturer's protocols. Paired-end sequencing of 150-bp fragments was performed by using a MiSeq Reagent Kit V2 (300 cycles) and MiSeq Sequencing System (Illumina). Sequencing data were analyzed by using CLC Genomics Workbench version 6.5.0 (http://www.clcbio.com). The sequence data were trimmed by

Table 1. WNV$_{KUN}$ strains used during study of virulence and evolution of WNV, Australia, 1960–2012*

Isolate	Year collected	Location	Source	Passage history
MRM16/MRM61C†	1960	Mitchell River Mission, Queensland	Mosquito‡	Unknown
Boort	1984	Victoria	Horse spinal cord	Unknown
K2499	1984	Kimberley region, Western Australia	Mosquito‡	2× C6/36; 1× PSEK
Hu6774	1991	New South Wales	Human	Unknown
K6453	1991	Kimberley region, Western Australia	Mosquito‡	2× C6/36; 1× PSEK
SH183	1991	Victoria	Chicken	Unknown
Gu0631	2000	Gulf of Carpentaria, Queensland	Mosquito‡	3× C6/36
Gu1009	2000	Gulf of Carpentaria, Queensland	Mosquito‡	3× C6/36
K68967	2009	Kimberley region, Western Australia	Mosquito‡	3× C6/36
P9974	2009	Pilbara region, Western Australia	Mosquito‡	3× C6/36
NSW2011	2011	New South Wales	Horse brain	2× C6/36; 1 Vero
K74015	2011	Kimberley region, Western Australia	Mosquito‡	3× C6/36
NSW2012	2012	New South Wales	Mosquito‡	3× C6/36

*C6/36, from *Aedes albopictus* mosquitoes; PSEK, porcine squamous equine kidney cells; WNV, West Nile virus; WNV$_{KUN}$, Kunjin strain of WNV.
†Prototype strain.
‡*Culex annulirostris*.

using quality scores specified in CLC Genomics Workbench before performing read-mapping analysis. The genome sequences were assembled by read mapping against the reference WNV$_{KUN}$ strain genome (GenBank accession no. JX276662) with use of default parameters in the mapping algorithm. Where gaps in the genome sequence or low coverage (<10 reads/site) were observed, conventional Sanger sequencing was performed to complete or verify the sequence. Oligonucleotide primers sequences designed for these purposes are available upon request to A.A.K or R.A.H.

Bioinformatics Analysis

We used MUSCLE, as implemented in MEGA6 (19), to align complete open reading frame (ORF) (10,320 nt) and partial (402 nt) envelope (E) gene nucleotide sequences of the newly sequenced WNV$_{KUN}$ strains, together with those available for 6 other WNV$_{KUN}$ strains and selected WNV isolates, representing different lineages. We estimated maximum-likelihood phylogenetic trees by using PhyML version 3.0 (20) and by using substitution models and rates among sites selected with JModelTest version 2.1.5 (21). We tested reliability of the inferred trees by using the bootstrap method with 1,000 replicates. All trees were rooted with analogous ORF sequences from Murray Valley encephalitis virus (GenBank accession no. NC000943) and Japanese encephalitis virus (GenBank accession no. EF571853) and visualized by using FigTree version 1.4.0 (http://tree.bio.ed.ac.uk/software/figtree/). Pairwise distances were determined at the nucleotide and amino acid levels by using the p-distance model in MEGA6.

Results

WNV$_{KUN}$ Strains

A panel of previously characterized mAbs (5,15,22–24) was used to antigenically type 13 WNV$_{KUN}$ strains. The binding profiles of these mAbs confirmed that all WNV$_{KUN}$ isolates closely resembled the prototype WNV$_{KUN1960}$ strain, including strong recognition by mAb 10A1, known to be specific for WNV$_{KUN}$ strains (Table 2) (2,24). Only WNV$_{KUN}$ strains isolated before 2000 were recognized by mAb 5H1, which binds a linear epitope in the αA3 motif (residues 39–53) in the methyltransferase domain of nonstructural (NS) protein 5 (15). Lack of 5H1 binding was associated with a substitution at residue 49 (Ile-Val) in αA3 (Table 3); this finding was consistent with previous mutagenesis study findings that a substitution of Ile to Ala at this residue was associated with abolition of 5H1 binding (26).

Glycosylated E Proteins

All analyzed WNV$_{KUN}$ isolates collected after 1960 contain glycosylated E proteins. The sequence analysis of the E gene of WNV$_{KUN}$ isolates revealed the presence of a conserved potential N-linked glycosylation site at residue 154 in all but the prototype WNV$_{KUN1960}$ isolate (Table 3). To confirm that this site was indeed glycosylated on the viral E protein, each virus was assessed for recognition in ELISA by mAbs 17D7 and 3.101C (Table 2), which specifically recognize glycosylated and unglycosylated WNV$_{KUN}$ E proteins, respectively (5,23). The results supported the predictions from our sequencing data; all WNV$_{KUN}$ strains except the prototype WNV$_{KUN1960}$ strain were recognized by mAb 17D7 but not by 3.101C.

Table 2. Binding patterns of monoclonal antibodies to WNV strains in ELISA*

Strain	Year of isolation	Panflavivirus, 4G2, anti-env	Pan-WNV, 2B2, anti-env	WNV$_{KUN}$-specific 10A1, anti-env	5D4, anti-NS5	5H1, anti-NS5	Glycosylated E, 17D7	Unglycosylated E, 3.101C	MVEV-specific, 10C6
WNV$_{KUN}$†									
KUN1960	1960	+	+	+	+	+	–	+	–
Boort	1984	+	+	+	+	+	+	–	–
K2499	1984	+	+	+	+	+	+	–	–
SH183	1991	+	+	+	+	+	+	–	–
K6453	1991	+	+	+	+	+	+	–	–
Hu6774	1991	+	+	+	+	+	+	–	–
Gu0631	2000	+	+	+	+	+	+	–	–
Gu1009	2000	+	+	+	+	+	+	–	–
K68967	2009	+	+	+	+	–	+	–	–
P9974	2009	+	+	+	+	–	+	–	–
NSW2011	2011	+	+	+	+	–	+	–	–
K74015	2011	+	+	+	+	–	+	–	–
NSW2012	2012	+	+	+	+	–	+	–	–
Reference									
WNV$_{NY99}$	1999	+	+	–	+	–	+	–	–
MVEV$_{1–51}$	1951	+	–	–	–	–	–	–	+

*Binding of a monoclonal antibody was designated as positive if the optical density was at least double the optical density of the negative control (mock-infected C6/36 cells). E, envelope protein; MVEV, Murray Valley encephalitis virus; NS5, nonstructural protein 5; WNV, West Nile virus; WNV$_{KUN}$, Kunjin strain of WNV; +, positive; –, negative.
†WNV$_{KUN}$ strains collected during 1960–2012, Australia.

Table 3. Amino acid sequences in the West Nile virus genome*

WNV strain	Year of isolation	prM, residue 22/72†	E protein, residues 154–156‡	NS3, residue 249§	NS5, residue 653¶	NS5, residue 49	3′ UTR residues 64–71
			Putative virulence determinant				
NY99	1999	Val/Ser	Asn-Tyr-Ser (NYS)	Pro	Phe	Val	Present
KUN1960	1960	Ile/Leu	Asn-Tyr-Phe (NYF)	Ala	Ser	Ile	Present
Boort	1984	Ile/Leu	Asn-Tyr-Ser (NYS)	Ala	Phe	Ile	Present
K2499	1984	Ile/Leu	Asn-Tyr-Ser (NYS)	Ala	Phe	Ile	Present
K6453	1991	Ile/Leu	Asn-Tyr-Ser (NYS)	Ala	Phe	Ile	Present
Hu6774	1991	Ile/Leu	Asn-Tyr-Ser (NYS)	Ala	Phe	Ile	Present
Gu0631	2000	Ile/Leu	Asn-Tyr-Ser (NYS)	Ala	Phe	Ile	Present
Gu1009	2000	Ile/Leu	Asn-Tyr-Ser (NYS)	Ala	Phe	Ile	Absent
K68967	2009	Ile/Leu	Asn-Tyr-Ser (NYS)	Ala	Phe	Val	Absent
P9974	2009	Ile/Leu	Asn-Tyr-Ser (NYS)	Ala	Phe	Val	Absent
NSW2011	2011	Ile/Leu	Asn-Tyr-Ser (NYS)	Ala	Phe	Val	Absent
K74015	2011	Ile/Leu	Asn-Tyr-Ser (NYS)	Ala	Phe	Val	Absent
NSW2012	2012	Ile/Leu	Asn-Tyr-Ser (NYS)	Ala	Phe	Val	Absent

*E, envelope; NS, nonstructural; prM, premembrane; UTR, untranslated region.
†(*11*).
‡(*7*).
§(*25*).
¶(*10*).

Growth Kinetics and Plaque Morphology of WNV$_{KUN}$ Strains

Infection of Vero cells at 24 h postinfection demonstrated that WNV$_{KUN1960}$, WNV$_{K2499}$, WNV$_{K6453}$, and WNV$_{K68967}$ isolates yielded significantly lower titers than did WNV$_{NY99}$ (p<0.05) (Figure 1, panel A). However, by 48 h postinfection, similar titers were reached for all WNV isolates except WNV$_{KUN1960}$.

A similar trend was observed in C6/36 cells, in which viral titers of WNV$_{KUN1960}$, WNV$_{K2499}$, WNV$_{K68967}$, and WNV$_{GU1009}$ were significantly lower than those for WNV$_{NY99}$, WNV$_{NSW2011}$, and WNV$_{Boort}$ at 48 h after infection (p<0.05) and titers for WNV$_{K6453}$, WNV$_{K74015}$, and WNV$_{GU0631}$ were intermediate. By 96 h after infection, the titers of all WNV isolates except WNV$_{KUN1960}$ were similar.

In terms of plaque morphology of WNV$_{KUN}$ strains, in Vero cells, WNV$_{NSW2011}$ and WNV$_{K74015}$ produced large plaques (average size 4.3 ± 0.63 and 4.3 ± 0.77 mm, respectively), a size similar to those produced by the WNV$_{NY99}$ strain (average size 4.8 ± 0.45 mm). The prototype virus, WNV$_{KUN1960}$, produced very small plaques (average size

2.7 ± 0.47 mm), which differed significantly from those of all other viruses tested during this study (p<0.0001). The remaining isolates produced intermediate-sized plaques (average size 3.5–3.9 ± 0.45–0.84 mm) (Figure 2) (*5*). Plaques formed by WNV$_{K6453}$, WNV$_{K74015}$, WNV$_{Gu1009}$, and WNV$_{Gu0631}$ were less well defined than those formed by WNV$_{NY99}$, WNV$_{NSW2011}$, WNV$_{K2499}$, and WNV$_{Boort}$.

Virulence of WNV$_{KUN}$ Strains in Mice

We previously demonstrated that differentiation between virulent and attenuated strains of WNV can be detected in weanling and young adult mice (*3,27*). In this study, we found that in addition to WNV$_{NSW2011}$, 3 other WNV$_{KUN}$ isolates (WNV$_{Boort}$, WNV$_{Gu0631}$, WNV$_{NSW2012}$) were neuroinvasive in both mouse models (Figure 3; online Technical Appendix Table 2). The WNV$_{Boort}$ strain, obtained from the spinal cord of a symptomatic horse during a small outbreak of equine disease in southeastern Australia in 1984, was neuroinvasive in young adult mice (40% mortality rate at 1,000 PFU); this finding did not statistically differ in this respect from that for WNV$_{NSW2011}$ (p = 0.3218)
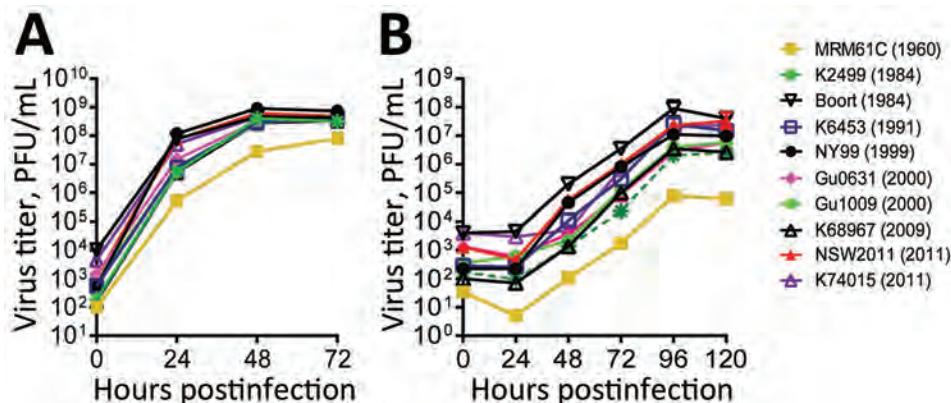
Figure 1. Growth kinetics of West Nile virus strains isolated in Australia, 1960–2012, in Vero (A) and C6/36 (B) cells. Cells were infected with a multiplicity of infection of 1, and the virus titers in the supernatants were determined by plaque assay on Vero cells.
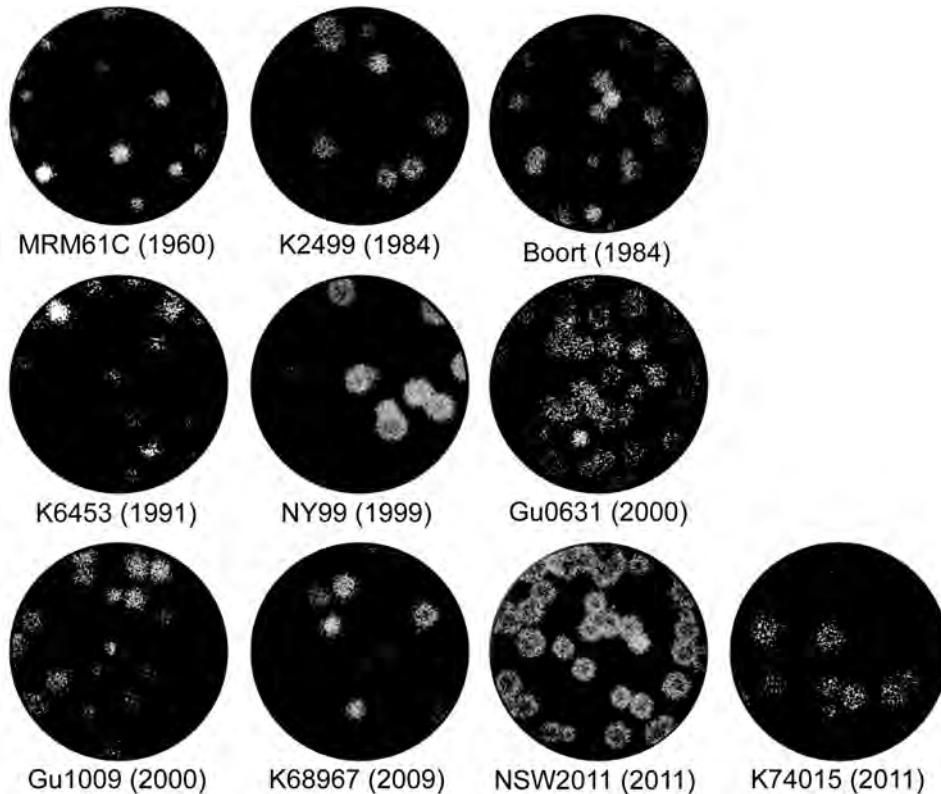
Figure 2. Plaque morphology of representative West Nile virus strains isolated in Australia, 1960–2012. Virus was allowed to adsorb to monolayers of Vero cells for 2 h at 37°C. The cells were then overlaid with Dulbecco Modified Eagle Medium containing 0.5% low melting point agarose and 2% fetal bovine serum. Four days after infection, the cells were fixed with 4% formaldehyde solution and stained with 0.2% crystal violet.

(Figure 3). Two other isolates obtained from mosquitoes, 1 from the Gulf of Carpentaria in 2000 (WNV$_{Gu0631}$) and 1 from southeastern Australia in 2012 (WNV$_{NSW2012}$), also exhibited levels of neuroinvasive properties in young adult mice similar to those caused by WNV$_{NSW2011}$ (Figure 3). In weanling mice, the virulence of WNV$_{Boort}$, WNV$_{Gu0631}$, and WNV$_{NSW2012}$ was also similar to that of WNV$_{NSW2011}$; mortality rates, 50% lethal dose, or time to death did not differ significantly (Table 4). Of note, WNV$_{Gu1009}$ isolated at the same time and from the same region as WNV$_{GU0631}$ was significantly less virulent in young adult mice (Figure 3; online Technical Appendix Table 2). The remaining isolates were relatively attenuated in both young adult (Figure 3) and weanling (online Technical Appendix Table 2) mice and did not differ significantly from the attenuated prototype WNV$_{KUN1960}$ strain (p>0.05).

Sequence of Viral Genomes

We sequenced WNV$_{KUN}$ isolates to analyze their relationship to the prototype WNV$_{KUN}$ strains from 1960 (WNV$_{MRM16}$, WNV$_{MRM61C}$); the 2011 outbreak strains (WNV$_{NSW2011}$, WNV$_{SA2011}$, WNV$_{V11-03}$, and WNV$_{V11-07}$); and exotic strains of WNV known to be virulent in humans and horses (WNV$_{NY99}$) or representing different WNV lineages. Phylogenetic analysis of the ORF sequences demonstrated that the WNV$_{KUN}$ strains form a single genetically homogeneous clade within lineage 1 (Figure 4), as previously

recognized (*24*); nucleotide and amino acid identities between strains were 96.1%–99.4% and 98.5%–100%, respectively. As expected, the most recent isolates, including the 2011 outbreak strain, were the most divergent, and the early prototype strains (WNV$_{MRM61C}$ and WNV$_{MRM16}$) occupied the basal lineage of this clade. Recent strains isolated in 2011 and 2012 from southeastern Australian states clustered together and shared high levels of nucleotide (98.6%–100%) and amino acid (99.6%–100%) identities, indicating transmission of a genetically homogeneous virus population during this period. These strains were either virulent for horses or shown in this study to be virulent in mice (Figure 3; online Technical Appendix Table 2). No other association between phylogenetic relationships and virulence was found; other virulent strains clustered closely and interspersed with the attenuated strains identified in this study. An expanded phylogenetic analysis that used 45 partial E gene sequences (402 nt) and a larger range of reference WNV$_{KUN}$ strains showed a similar pattern of relationships (online Technical Appendix Figure).

Of note is the very close relationship (99.9% aa identity) between a virulent 2011 strain isolated from a horse and an isolate obtained from *Culex annulirostris* mosquitoes trapped in New South Wales, Australia, in 2012 (WNV$_{NSW2012}$). Only 3 nonconservative changes were identified between WNV$_{NSW2011}$ and WNV$_{NSW2012}$, located in NS1 (Lys33Arg), NS3 (Phe509Leu), and NS4A
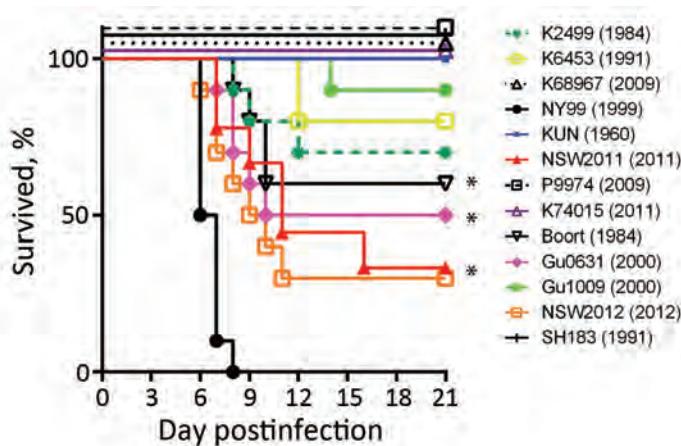
Figure 3. Survival curves for young adult (28-day-old) Swiss outbred mice after intraperitoneal infection with 1,000 PFU of West Nile virus (WNV) strains isolated in Australia, 1960–2012. Groups of 10 mice were infected with each virus. The mice were monitored for 21 days after infection for signs of encephalitis and then euthanized. WNV$_{NY99}$ and WNV$_{NSW2011}$ with previously demonstrated virulence were included as controls. The significance of clinical differences between groups was calculated by Kaplan-Meier analysis and analyzed by log-rank test. Significantly increased virulence over that of WNV$_{KUN1960}$ is indicated by an asterisk (*): WNV$_{Boort}$ (p = 0.0295), WNV$_{Gu0631}$ (p = 0.0115), and WNV$_{NSW2012}$ (p = 0.0011). No significant differences were observed between WNV$_{Boort}$, WNV$_{Gu0631}$, and WNV$_{NSW2012}$ compared with WNV$_{NSW2011}$ (p>0.05).

(Phe92Leu). These results suggest that the virulent strain either had persisted in New South Wales after the end of the 2011 outbreak or had been reintroduced to the area.

Analyses of predicted gene products from the complete ORF sequence of each WNV$_{KUN}$ isolate revealed that, in addition to the glycosylation site at residues 154–156 in the E protein, all strains isolated after 1960 contained a Phe residue at position 653 in the NS5 protein, which has previously been shown to play a role in resistance to antiviral activity of interferon-α/β (10) (Table 3). In contrast, WNV$_{KUN1960}$ contained a Ser residue at position 653 in NS5 (3,5,24,28). The Pro residue at position 249 in the NS3 protein, previously shown to be present in WNV strains and associated with increased virulence in birds of some species (25), was not present in any of the WNV$_{KUN}$ isolates, which all contained an Ala residue at this position (Table 3).

In addition to an Ile→Val substitution at position 49 in NS5 of WNV$_{KUN}$ isolates collected after 2009, analysis of more contemporary WNV$_{KUN}$ isolates also revealed a consistent 8-nt deletion in the 3′ UTR, just downstream from the ORF stop codon. This deletion was identified in WNV$_{Gu1009}$ and all isolates collected after 2000. In contrast, this deletion was not present in isolates collected before 2000 (Table 3) or in another isolate from Gulf of Carpentaria collected in 2000 (WNV$_{Gu0631}$). We suggest that these 2 features (Ile→Val 49 residue in NS5 and an 8-nt deletion in the 3′ UTR) can be considered as potential evolutionary markers.

In addition to the genetic variability described above, sequence analysis between virulent and attenuated WNV$_{KUN}$ strains identified other nucleotide differences between isolates, located throughout the viral genome. These differences result in amino acid substitutions (Table 4) and may contribute to observed phenotypic differences.

We also sequenced WNV$_{KUN}$ viral RNA extracted directly from mosquito saliva expectorated onto sugar-soaked nucleic acid preservation cards placed in mosquito traps in Darwin, Northern Territory, in 2012 (WNV$_{NT2012}$)

(29,30). When partial sequences from E, NS5, and the 3′ UTR from this RNA were aligned, we observed a high level (99.7%) of identity with the WNV$_{KUN1960}$ strains, indicating that viruses genetically homologous to the prototype virus are still circulating in some regions of Australia (online Technical Appendix Figure). Closer analysis revealed a lack of E glycosylation, similar to that found in the prototype strain. However, Phe was identified at position 653 of NS5, similar to that found in recent isolates.

Discussion

Historically, WNV$_{KUN}$ has been associated with only mild disease in humans and rare cases of disease in horses, consistent with data from mouse virulence studies that revealed a relatively attenuated phenotype (3,8,27). Thus, the emergence of an equid-virulent strain of WNV$_{KUN}$, responsible for ≈900 cases of encephalitis in horses in southeastern Australia, was unprecedented.

Although most WNV$_{KUN}$ isolates examined in this study exhibited an attenuated phenotype, similar to that of the prototype WNV$_{KUN1960}$, we identified an additional 3 strains with neuroinvasive properties in mice similar to those reported for WNV$_{NSW2011}$ (3). The first, WNV$_{Boort}$, was isolated from the spinal cord of a horse with nonsuppurative encephalomyelitis and severe neurologic symptoms in northern Victoria in 1984 (31). At that time, 53 animals in the same area were clinically affected. However, a high incidence of Ross River virus–specific antibody in these animals implicated that virus rather than WNV$_{KUN}$ as the primary etiologic agent (31). Our results are also supported by another recent study showing virulence of WNV$_{Boort}$ in 18–19-day-old mice (32).

The second virulent strain identified in this study, WNV$_{Gu0631}$, was isolated from *Cx. annulirostris* mosquitoes collected from Normanton, Gulf of Carpentaria, in April 2000. Of note, this virus was isolated in the absence of any reported disease outbreak, as part of a survey for the presence of Japanese encephalitis virus in northern Queensland

Table 4. Comparison of amino acid sequences between virulent and attenuated West Nile virus strains*

Gene and amino acid position in polyprotein (corresponding protein)	Virulent strains		Attenuated Kunjin strains						
	NY99	Boort, NSW2011, NSW2012, Gu0631	KUN1960	K68967	K2499	K6453	K74015	Hu6774	Gu1009
C									
86 (86)	Lys	Lys	Arg	Lys	Lys	Lys	Lys	Lys	Lys
114 (114)	Met	Ile (Boort), Thr (NSW2011, NSW2012, Gu0631)	Met	Thr	Thr	Thr	Met	Thr	Thr
prM									
143 (20)	Thr	Ala	Thr	Ala	Ala	Ala	Ala	Ala	Ala
158 (35)	Ile	Thr	Ile	Thr	Thr	Thr	Thr	Thr	Thr
279 (156)	Val	Thr	Ala	Thr	Thr	Thr	Thr	Thr	Thr
E									
413 (123)	Thr	Thr	Ala	Thr	Thr	Thr	Thr	Thr	Thr
446 (156)	Ser	Ser	Phe	Ser	Ser	Ser	Ser	Ser	Ser
600 (310)	Lys	Arg	Thr	Arg	Arg	Arg	Arg	Arg	Arg
773 (483)	Leu	Phe	Leu	Phe	Phe	Phe	Leu	Phe	Phe
790 (500)	His	His	Tyr	His	His	His	His	His	His
NS1									
1081 (290)	Ser	Asn	Ser	Asn	Asn	Asn	Ser	Asn	Asn
NS2A									
1255 (112)	Val	Val	Ala	Val	Val	Val	Val	Val	Val
1272 (129)	Ile	Ile	Met	Ile	Ile	Ile	Ile	Ile	Ile
1366 (223)	Ile	Ile	Val	Ile	Ile	Ile	Ile	Ile	Ile
NS3									
1520 (146)	Lys	Lys	Arg	Lys	Lys	Lys	Lys	Lys	Lys
1970 (586)	Asn	Ser	Asn	Ser	Ser	Ser	Asn	Ser	Ser
NS4A									
2179 (55)	Ala	Thr	Ala	Thr	Thr	Thr	Thr	Thr	Ala
NS4B									
2296 (23)	Val	Ile	Thr	Ile	Ile	Ile	Ile	Ile	Ile
2324 (51)	Val	Phe	Val	Phe	Phe	Phe	Val	Phe	Phe
2368 (95)	Ala	Ser	Ala	Ser	Ser	Ser	Ser	Ser	Ser
2450 (177)	Met	Ile	Met	Ile	Ile	Ile	Ile	Ile	Ile
2518 (245)	Ile	Ile	Val	Ile	Ile	Ile	Ile	Ile	Ile
NS5									
2629 (101)	Arg	Lys	Arg	Lys	Lys	Lys	Arg	Lys	Lys
3088 (560)	Asp	Asn	Asp	Asn	Asn	Asn	Asp	Asn	Asn

*C, capsid; E, envelope; NS, nonstructural; prM, premembrane.

(33). The second Gulf of Carpentaria isolate, WNV$_{Gu1009}$, was also collected in April 2000, from the town of Karumba, which is ≈30 km from Normanton. However, WNV$_{GU1009}$ is genetically distinct and attenuated to the same degree as the prototype WNV$_{KUN1960}$ in 28-day-old mice (Figure 4). These observations demonstrated that virulent WNV$_{KUN}$ strains might co-circulate with attenuated strains in some regions of Australia. Furthermore, the circulation of neuroinvasive strains may often appear in the absence of disease outbreaks. This suggestion is consistent with our finding that WNV$_{NSW2012}$ was genetically almost identical to the WNV$_{NSW2011}$ and exhibited similar levels of neuroinvasiveness in mice. However, no cases of disease in equids were associated with WNV$_{KUN}$ infection during the 2012 season (3,4,34). This lack of cases suggests that the persistence of virulent strains in southeastern Australia is not the sole determinant for initiating disease outbreaks and that specific climatic and ecologic conditions, perhaps influencing mosquito populations and viral transmission, are also required.

A similar scenario occurred in North America, where an unusually high number of cases in humans (5,387),

most in Texas, USA, were reported in 2012. However, sequence analysis of WNV isolates from 2012 revealed that the strains circulating in Texas were virulent and attenuated, and no specific virulence determinants responsible for the increase in cases could be identified (35). Instead, other factors, including temperature and changes in mosquito or bird populations, were speculated to have contributed to the magnitude of the 2012 outbreak (36).

To identify a phylogenetic association with virulence and to identify potential virulence determinants encoded in the genome of WNV$_{KUN}$ strains, we also performed full-length sequencing of the ORF of several of the viruses studied. Although recent virulent strains were phylogenetically closely related, no other association between phylogenetic grouping and virulence phenotype was found (Figure 4; online Technical Appendix Figure). One notable change in the genome that was clearly associated with the temporal distribution of these viruses was a highly conserved 8-base deletion in the 3′ UTR, just downstream of the ORF stop codon. Isolates from samples collected after 2000, including the virulent WNV$_{NSW2011}$ and attenuated
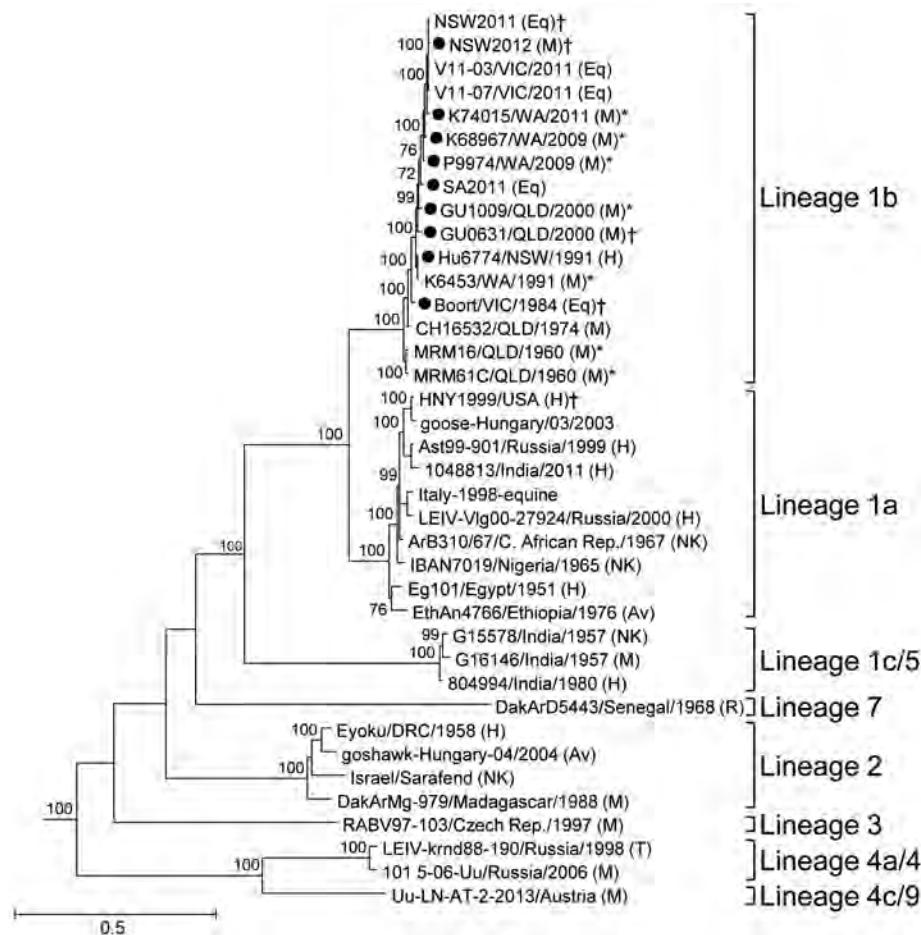
Figure 4. Maximum-likelihood phylogenetic tree estimated by using nucleotide sequences of the complete open reading frame (ORF) of genomes of West Nile virus (WNV) strains isolated in Australia, 1960–2012 (black circles), compared with representative strains from different lineages and clades. The tree was estimated by using a general time-reversible model of nucleotide substitution with a gamma distribution and invariant sites. Bootstrap values are shown on the nodes and are expressed as a percentage of 1,000 replicates; only values >70% are shown. Horizontal branch lengths indicate genetic distance. The tree was rooted with the ORF sequences of Murray Valley encephalitis virus and Japanese encephalitis virus; however, these branches have been removed to improve resolution. Strains that were assessed as having an attenuated virulence phenotype are indicated by a single asterisk (*), and virulent strains are indicated by a dagger (†). The state of origin for WNV_KUN strains is shown as follows: NSW, New South Wales; QLD, Queensland; SA, South Australia; VIC, Victoria; WA, Western Australia. Virus sources are indicated in parentheses next to virus identity, as follows: Av, avian; Eq, equine; H, human; M, mosquito; NK, not known; R, rodent; T, tick. Scale bar indicates nucleotide substitutions per site.

strains, invariably contained this deletion. This finding suggests that the deletion is an evolutionary marker but is not directly associated with virulence. This finding is also consistent with our observation that the neuroinvasive 2000 Gulf of Carpentaria isolate, WNV_Gu0631, did not have this deletion but that the co-circulating attenuated isolate, WNV_Gu1009, collected from the same region at the same time, did have this deletion.

An additional evolutionary change was observed in the a-A3 motif of the methyltransferase domain of the NS5 protein. Isolates obtained before 2009, including the prototype WNV_KUN1960, contained a conserved Ile residue at position 49. However, all isolates collected after 2009 displayed an Ile→Val substitution at this position. Coincidentally, this substitution abolished the binding of a mAb (5H1) that recognizes a linear epitope comprising the a-A3 peptide (15).

Initial comparisons between the virulent isolate WNV_NSW2011 from a horse and the attenuated prototype WNV_KUN1960 revealed that several previously identified WNV virulence markers were detected in the former but not in the latter isolate (3). These markers included the conserved N-linked glycosylation of the E protein (7) and the Phe residue at position 653 in the NS5 protein, associated with resistance to antiviral activity of interferon a/b (8). Although these initial observations suggested the involvement of these motifs in the enhanced neuroinvasive properties of the isolate collected from a horse in 2011, our study revealed that, with the exception of WNV_KUN1960, all strains examined contain both of these markers, regardless of virulence phenotype in mouse models. Thus, it seems that, although these motifs contribute to virulence in mice, they are not likely to be solely responsible for enhancing the neuroinvasive properties of some WNV_KUN strains and, hence, not likely to be markers of evolving virulence in recent isolates of WNV_KUN.

Additional markers of WNV virulence identified in WNV strains from North America were not detected in any of the WNV_KUN isolates. This finding is consistent with our repeated observations that even the equid-virulent

$WNV_{NSW2011}$ is substantially less neuroinvasive than WNV_{NY99} in young adult mice (*3*). These motifs may include Val 22 and Ser 72 residues in the premembrane, which enhance mouse neuroinvasiveness when introduced into the prototype $WNV_{KUN1960}$ (*11*), and the Pro residue at position 249 in NS3, which is associated with enhanced virulence in birds (*25*). The absence of the latter motif in all WNV_{KUN} strains is also consistent with the perceived lack of illness and death among birds in Australia, notably during the 2011 outbreak among equids. Some isolates included in this study (including $WNV_{KUN1960}$, WNV_{SH183}, WNV_{Boort}, and WNV_{Hu6774}) have an unknown passage history. Extensive passage through cells is known to occasionally lead to passage-adapted mutations, and care should be taken when interpreting sequencing data from these virus strains.

WNV_{KUN} is thought to be endemic to the tropical areas of northern Australia, suggesting that virulent viruses emerging in southeastern Australia probably originate from northern Australia. However, WNV_{KUN} recently isolated from mosquitoes in northern Australia, including the 2011 Kimberley isolate WNV_{K74015}, were more attenuated than $WNV_{NSW2011}$. This finding suggests a different explanation for the evolution of virulent WNV_{KUN} viruses, which may be associated with the adaption of WNV_{KUN} to different hosts (avian and terrestrial) or different vector species in temperate regions. In this context, virulence in equids may be just a coincidental outcome of the constraints placed on virus fitness in different geographic locations (*35–37*).

Overall, our results show that virulent strains of WNV_{KUN} have been circulating in Australia for $\geq$30 years and that the first extensive outbreak of disease among horses in Australia in 2011 probably resulted from a combination of ecologic and epidemiologic conditions rather than the emergence of a novel, more virulent strain. Further studies evaluating viral fitness of West Nile virus quasispecies in terms of population-dependent host–virus interactions, are warranted.

Acknowledgments

Dr. Prow is a postdoctoral research fellow at the QIMR Berghofer Medical Research Institute and is engaged in research to characterize the pathogenesis and virulence of WNV strains in murine models. She also has a special interest in understanding the neuroinvasive properties of neurotrophic flaviviruses.

References

1. Murgue B, Zeller H, Deubel V. The ecology and epidemiology of West Nile virus in Africa, Europe and Asia. Curr Top Microbiol Immunol. 2002;267:195–221. http://dx.doi.org/10.1007/978-3-642-59403-8_10

2. Lanciotti RS, Roehrig JT, Deubel V, Smith J, Parker M, Steele K, et al. Origin of the West Nile virus responsible for an outbreak of encephalitis in the northeastern United States. Science. 1999;286:2333–7. http://dx.doi.org/10.1126/science.286.5448.2333

3. Frost MJ, Zhang J, Edmonds JH, Prow NA, Gu X, Davis R, et al. Characterization of virulent West Nile virus Kunjin strain, Australia, 2011. Emerg Infect Dis. 2012;18:792–800. http://dx.doi.org/10.3201/eid1805.111720

4. Roche SE, Wicks R, Garner MG, East IJ, Paskin R, Moloney BJ, et al. Descriptive overview of the 2011 epidemic of arboviral disease in horses in Australia. Aust Vet J. 2013;91:5–13. http://dx.doi.org/10.1111/avj.12018

5. Adams SC, Broom AK, Sammels LM, Hartnett AC, Howard MJ, Coelen RJ, et al. Glycosylation and antigenic variation among Kunjin virus isolates. Virology. 1995;206:49–56. http://dx.doi.org/10.1016/S0042-6822(95)80018-2

6. Audsley M, Edmonds JH, Liu W, Mokhonov V, Mokhonova E, Melian EB, et al. Virulence determinants between New York 99 and Kunjin strains of West Nile virus. Virology. 2011;414:63–73. http://dx.doi.org/10.1016/j.virol.2011.03.008

7. Beasley DW, Whiteman MC, Zhang S, Huang CY, Schneider BS, Smith DR, et al. Envelope protein glycosylation status influences mouse neuroinvasion phenotype of genetic lineage 1 West Nile virus strains. J Virol. 2005;79:8339–47. http://dx.doi.org/10.1128/JVI.79.13.8339-8347.2005

8. Daffis S, Lazear HM, Liu WJ, Audsley M, Engle M, Khromykh AA, et al. The naturally attenuated Kunjin strain of West Nile virus shows enhanced sensitivity to the host type I interferon response. J Virol. 2011;85:5664–8.

9. Keller BC, Fredericksen BL, Samuel MA, Mock RE, Mason PW, Diamond MS, et al. Resistance to alpha/beta interferon is a determinant of West Nile virus replication fitness and virulence. J Virol. 2006;80:9424–34. http://dx.doi.org/10.1128/JVI.00768-06

10. Laurent-Rolle M, Boer EF, Lubick KJ, Wolfinbarger JB, Carmody AB, Rockx B, et al. The NS5 protein of the virulent West Nile virus NY99 strain is a potent antagonist of type I interferon-mediated JAK-STAT signaling. J Virol. 2010;84:3503–15. http://dx.doi.org/10.1128/JVI.01161-09

11. Setoh YX, Prow NA, Hobson-Peters J, Lobigs M, Young PR, Khromykh AA, et al. Identification of residues in West Nile virus pre-membrane protein that influence viral particle secretion and virulence. J Gen Virol. 2012;93:1965–75. http://dx.doi.org/10.1099/vir.0.044453-0

12. Doherty RL, Carley JG. Studies of arthropod-borne virus infections in Queensland. II. Serological investigations of antibodies to dengue and Murray Valley encephalitis in eastern Queensland. Aust J Exp Biol Med Sci. 1960;38:427–39. http://dx.doi.org/10.1038/icb.1960.46

13. Khromykh AA, Kenney MT, Westaway EG. Trans-complementation of flavivirus RNA polymerase gene NS5 by using Kunjin virus replicon–expressing BHK cells. J Virol. 1998;72:7270–9.

14. Westaway EG. Assessment and application of a cell line from pig kidney for plaque assay and neutralization tests with twelve group B arboviruses. Am J Epidemiol. 1966;84:439–56.

15. Hall RA, Tan SE, Selisko B, Slade R, Hobson-Peters J, Canard B, et al. Monoclonal antibodies to the West Nile virus NS5 protein map to linear and conformational epitopes in the methyltransferase and polymerase domains. J Gen Virol. 2009;90:2912–22. http://dx.doi.org/10.1099/vir.0.013805-0

16. Wang GP, Bushman FD. A statistical method for comparing viral growth curves. J Virol Methods. 2006;135:118–23. http://dx.doi.org/10.1016/j.jviromet.2006.02.008

17. Warrilow D, Hall-Mendelin S, Hobson-Peters J, Prow NA, Allcock R, Hall RA. Complete coding sequences of three members of the Kokobera group of flaviviruses. Genome Announc. 2014; 2:pii:e00890-14. http://dx.doi.org/10.1128/genomeA.00890-14

18. Palacios G, Quan PL, Jabado OJ, Conlan S, Hirschberg DL, Liu Y, et al. Panmicrobial oligonucleotide array for diagnosis of infectious diseases. Emerg Infect Dis. 2007;13:73–81. http://dx.doi.org/10.3201/eid1301.060837

19. Tamura K, Stecher G, Peterson D, Filipski A, Kumar S. MEGA6: Molecular Evolutionary Genetics Analysis version 6.0. Mol Biol Evol. 2013;30:2725–9. http://dx.doi.org/10.1093/molbev/mst197

20. Guindon S, Gascuel O. A simple, fast, and accurate algorithm to estimate large phylogenies by maximum likelihood. Syst Biol. 2003;52:696–704. http://dx.doi.org/10.1080/10635150390235520

21. Darriba D, Taboada GL, Doallo R, Posada D. jModelTest 2: more models, new heuristics and parallel computing. Nat Methods. 2012;9:772. http://dx.doi.org/10.1038/nmeth.2109

22. Hall RA, Kay BH, Burgess GW, Clancy P, Fanning ID. Epitope analysis of the envelope and non-structural glycoproteins of Murray Valley encephalitis virus. J Gen Virol. 1990;71:2923–30. http://dx.doi.org/10.1099/0022-1317-71-12-2923

23. Hobson-Peters J, Toye P, Sanchez MD, Bossart KN, Wang LF, Clark DC, et al. A glycosylated peptide in the West Nile virus envelope protein is immunogenic during equine infection. J Gen Virol. 2008;89:3063–72. http://dx.doi.org/10.1099/vir.0.2008/003731-0

24. Scherret JH, Poidinger M, Mackenzie JS, Broom AK, Deubel V, Lipkin WI, et al. The relationships between West Nile and Kunjin viruses. Emerg Infect Dis. 2001;7:697–705. http://dx.doi.org/10.3201/eid0704.017418

25. Brault AC, Huang CY, Langevin SA, Kinney RM, Bowen RA, Ramey WN, et al. A single positively selected West Nile viral mutation confers increased virogenesis in American crows. Nat Genet. 2007;39:1162–6. http://dx.doi.org/10.1038/ng2097

26. Tan CS, Hobson-Peters JM, Stoermer MJ, Fairlie DP, Khromykh AA, Hall RA. An interaction between the methyltransferase and RNA dependent RNA polymerase domains of the West Nile virus NS5 protein. J Gen Virol. 2013;94:1961–71. http://dx.doi.org/10.1099/vir.0.054395-0

27. Prow NA, Setoh YX, Biron RM, Sester DP, Kim KS, Hobson-Peters J, et al. The West Nile virus-like flavivirus Koutango is highly virulent in mice due to delayed viral clearance and the induction of a poor neutralizing antibody response. J Virol. 2014;88:9947–62. http://dx.doi.org/10.1128/JVI.01304-14

28. Wright PJ, Warr HM, Westaway EG. Synthesis of glycoproteins in cells infected by the flavivirus Kunjin. Virology. 1981;109:418–27. http://dx.doi.org/10.1016/0042-6822(81)90512-2

29. Hall-Mendelin S, Ritchie SA, Johansen CA, Zborowski P, Cortis G, Dandridge S, et al. Exploiting mosquito sugar feeding to detect mosquito-borne pathogens. Proc Natl Acad Sci U S A. 2010;107:11255–9. http://dx.doi.org/10.1073/pnas.1002040107

30. van den Hurk AF, Hall-Mendelin S, Townsend M, Kurucz N, Edwards J, Ehlers G, et al. Applications of a sugar-based surveillance system to track arboviruses in wild mosquito populations. Vector Borne Zoonotic Dis. 2014;14:66–73. http://dx.doi.org/10.1089/vbz.2013.1373

31. Badman R, Campbell J, Aldred J. Arbovirus infection in horses—Victoria. Commun Dis Intell. 1984;17:5–6.

32. Bingham J, Payne J, Harper J, Frazer L, Eastwood S, Wilson S, et al. Evaluation of a mouse model for the West Nile virus group for the purpose of determining viral pathotypes. J Gen Virol. 2014;95:1221–32. http://dx.doi.org/10.1099/vir.0.063537-0

33. van den Hurk AF, Nisbet DJ, Foley PN, Ritchie SA, Mackenzie JS, Beebe NW. Isolation of arboviruses from mosquitoes (Diptera: Culicidae) collected from the Gulf Plains region of northwest Queensland, Australia. J Med Entomol. 2002;39:786–92. http://dx.doi.org/10.1603/0022-2585-39.5.786

34. Prow NA. The changing epidemiology of Kunjin virus in Australia. Int J Environ Res Public Health. 2013;10:6255–72. http://dx.doi.org/10.3390/ijerph10126255

35. Coffey LL, Forrester N, Tsetsarkin K, Vasilakis N, Weaver SC. Factors shaping the adaptive landscape for arboviruses: implications for the emergence of disease. Future Microbiol. 2013;8:155–76. http://dx.doi.org/10.2217/fmb.12.139

36. Duggal NK, D'Anton M, Xiang J, Seiferth R, Day J, Nasci R, et al. Sequence analyses of 2012 West Nile virus isolates from Texas fail to associate viral genetic factors with outbreak magnitude. Am J Trop Med Hyg. 2013;89:205–10. http://dx.doi.org/10.4269/ajtmh.13-0140

37. van den Hurk AF, Hall-Mendelin S, Webb CE, Tan CS, Frentiu FD, Prow NA, et al. Role of enhanced vector transmission of a new West Nile virus strain in an outbreak of equine disease in Australia in 2011. Parasites & Vectors. 2014;7:586. http://dx.doi.org/10.1186/s13071-014-0586-3

Address for correspondence: Roy A. Hall or Alexander A. Khromykh, The University of Queensland, St. Lucia, 4072, Queensland, Australia; email: roy.hall@uq.edu.au or a.khromykh@uq.edu.au

Microgeographic Heterogeneity of Border Malaria During Elimination Phase, Yunnan Province, China, 2011–2013

Xin Xu,[1] Guofa Zhou,[1] Ying Wang, Yue Hu, Yonghua Ruan, Qi Fan,
Zhaoqing Yang, Guiyun Yan, Liwang Cui

To identify township-level high-risk foci of malaria transmission in Yunnan Province, China, along the international border, we retrospectively reviewed data collected in hospitals and clinics of 58 townships in 4 counties during 2011–2013. We analyzed spatiotemporal distribution, especially hot spots of confirmed malaria, using geographic information systems and Getis-Ord $G_i^*(d)$ cluster analysis. Malaria incidence, transmission seasonality, and *Plasmodium vivax:P. falciparum* ratio remained almost unchanged from 2011 to 2013, but heterogeneity in distribution increased. The number of townships with confirmed malaria decreased significantly during the 3 years; incidence became increasingly concentrated within a few townships. High-/low-incidence clusters of *P. falciparum* shifted in location and size every year, whereas the locations of high-incidence *P. vivax* townships remained unchanged. All high-incidence clusters were located along the China–Myanmar border. Because of increasing heterogeneity in malaria distribution, microgeographic analysis of malaria transmission hot spots provided useful information for designing targeted malaria intervention during the elimination phase.

Malaria, one of the most devastating infectious diseases, creates an enormous public health burden in the developing world (*1*). Since 2000, increased financial support has strengthened malaria control programs, leading to substantially reduced malaria incidence and death rates, even in the high-transmission areas of sub-Saharan Africa (*1*). The estimated worldwide malaria death rate declined by 45% during 2000–2012. Of the 97 countries with malaria transmission in 2013, twelve are in the preelimination

phase and 7, including China, are in the elimination phase. In early 2009, China's Ministry of Health presented its Revised National Malaria Strategy 2010–2015; this strategy was followed by the Malaria Elimination Action Plan for 2010–2020, in which the Ministry of Health laid out a strategy to eliminate malaria by 2020 (*2,3*).

Control efforts, guided by the 1-3-7 strategy (reporting a malaria case within 1 day; confirming, treating, and investigating the case within 3 days; and delivering an appropriate public health response to prevent further transmission within 7 days) have drastically reduced malaria incidence in central China (*4*). As a result, malaria transmission is restricted to the southwestern Yunnan Province along the international borders (*5–8*). Currently, *Plasmodium vivax* is the predominant species of malaria parasites in China, and autochthonous *P. falciparum* occurs only in Yunnan Province (*7,8*).

In 2012, Yunnan Province reported an annual malaria incidence of 7.4 cases/100,000 population (*8*). Yunnan Province borders 3 malaria-endemic countries: Myanmar, Laos, and Vietnam. Previous studies found that cross-border migration from Myanmar was the major source of importation/reintroduction of *P. falciparum* malaria in Yunnan Province (*9*). Therefore, the control strategy during the elimination phase must focus on eliminating local transmission and cross-border introduction.

Elimination strategies can differ profoundly from control strategies because they require prospective, accurate identification of transmission foci and rapid control responses (*10–13*). Earlier studies in China relied exclusively on retrospective data acquired from county-level hospital records (*5–8*). The retrospective nature of these studies raises questions about diagnostic accuracy, whereas the county-level epidemiologic data provide limited spatial resolution. A county in China typically comprises many townships, sometimes ≈100 villages and totaling ≈1 million persons, and it might span ≈100 km (*14–17*), which limit the usefulness of county-level risk assessment for

[1]These authors contributed equally to this article.

guiding targeted malaria control and local malaria elimination. Thus, for spatially heterogeneous malaria transmission, finer-scale mapping is essential for deploying elimination measures.

We aimed to use prospectively confirmed malaria data to identify high-risk foci of malaria transmission at the township level in Yunnan Province along the international border. Specifically, we wanted to locate the transmission hot spots and determine whether malaria transmission is heterogeneous at the township level. Our goal was to provide data to help guide targeted malaria control response during the malaria elimination phase.

Methods

Study Area

The study area comprised 58 townships in 4 counties (Tengchong, Yingjiang, Longchuan, and Ruili) along the China–Myanmar border in Yunnan Province (Figure 1). Each township has 1 government-run healthcare center consisting of an inpatient hospital and other administrative facilities and sometimes a few small village-level clinics. In accordance with government policy, malaria diagnosis and treatment are free, regardless of the patient's nationality or origin of residence. The study area spans 13,200 km²; the population was ≈1.3 million in 2010. Approximately 85% of residents live in rural areas, and most are farmers. The climate is subtropical; average maximum/minimum

temperatures ranges from 13/4°C in January to 34/24°C in July. Annual rainfall in the study area is ≈2,200 mm, with 1 rainy season during April–July but no clear dry season. The topography is characterized by mountains separated by small, long, narrow basins dominated by rice fields. Among the 4 counties, Ruili is located in the largest basin of the study area. In 2012, Tengchong, Yingjiang, and Ruili counties were among China's leading 5 counties in malaria incidence (8).

Data Collection

We applied a prospective surveillance method and included all patients with fever who sought care at 58 local health centers and 4 hospitals in the study area during January 2011–December 2013. Local doctors screened persons with fever at local hospitals/clinics for malaria symptoms after patients signed consent or assent (for minors <18 years of age) forms (i.e., screening for suspected cases). A suspected malaria case was defined as malaria-related symptoms (fever with axillary temperature ≥37.5°C, chills, severe malaise, headache, or vomiting) at examination or 1–2 days before examination. In brief, before sample collection, study procedures (i.e., sampling procedures, study benefits, and potential risks and discomforts) were explained to patients. Before samples were collected, demographic data such as sex, age, home address and name of participant, travel history during the preceding 14 days, malaria infections during the preceding 6 months and prescriptions obtained, and use of preventive measures were recorded. Identification numbers were used in the final analysis, and each patient's real identity and address was kept confidential. Blood samples were collected by finger-pricking. Labeled slides with thin and thick blood smears were prepared for microscopic *Plasmodium* species identification and parasite density counts. Thick and thin blood films were stained with 10% Giemsa and examined according to a previously described method (18). The hospitals where the patients were admitted confirmed all reported cases. The blood slides were reexamined by 3 experienced microscopists, who provided the final confirmation of malaria cases. For slides that were confirmed positive, the asexual parasite density and gametocyte density were scored against 200 leukocytes. Confirmed malaria was defined as malaria-related symptoms at examination or 1–2 days before examination and a *Plasmodium*-positive blood smear confirmed by microscopy. Persons in whom malaria was diagnosed were treated in accordance with national malaria treatment guidelines (http://www.who.int/malaria/publications/atoz/9789241549127/en/).

Figure 1. Locations of hospitals and healthcare centers (center of each circle) and total confirmed malaria cases in each township, Yunnan Province, China, 2011–2013.

Data Analysis

We calculated the malaria incidence rate as cases per 100,000 population per year or month based on 2010

population census data. Nonlocal residents (e.g., visitors and travelers) were excluded from incidence rate calculation. We examined year-to-year differences in the number of townships where confirmed malaria was absent using a χ^2 test. We tested township-level year-to-year differences in incidence using the Tukey-Kramer honest significant difference (HSD) of analysis of variance (ANOVA) post hoc test. *P. vivax* and *P. falciparum* case ratio for each year was also calculated.

We mapped spatial distribution of incidence rate at the township level using ArcGIS 10 (ESRI, Redlands, CA, USA). Spatial heterogeneity of confirmed malaria cases was measured with median incidence rate, range of incidence rate, Kurtosis, skewness, and coefficient of variation of incidence among townships. To determine whether the distance from the hospital or healthcare centers to the nearest border affected malaria incidence rate, we calculated distances from the hospital or healthcare centers to the nearest border using ArcGIS and divided them into 4 categories (0–9, 10–29, 30–49, and ≥50 km); average incidence rate of *P. falciparum* and *P. vivax* were calculated for each distance group; and differences in incidence rate among different distance groups were compared using the Tukey-Kramer HSD of ANOVA post hoc test. To identify spatial clusters that might characterize the distribution of malaria at the China–Myanmar border, we used the Getis-Ord local $G_i^*(d)$ test to determine the sizes and locations of high- and low-incidence clusters at the township level (*19,20*). Getis-Ord $G_i^*(d)$ statistics have been commonly used for disease transmission hot spot analysis (*14,21–24*). We examined hot spots separately for *P. falciparum* and *P. vivax* and annually so we could track temporal changes in transmission hot spot.

Ethical Statement
The institutional review boards of Kunming Medical University (Kunming, China); University of California, Irvine (Irvine, CA, USA); and Pennsylvania State University (University Park, PA, USA) approved the study. We obtained written informed consent or assent (for minors <18 years of age) from all persons or parents or guardians who were willing to participate in the study.

Results

Descriptive Statistics of Confirmed Malaria
Blood smear examination by microscopy confirmed 468 malaria cases from the 915 suspected cases screened from ≈23,000 febrile persons. The annual confirmed malaria incidence rate was 13.1 cases/100,000 population. We detected all 4 human *Plasmodium* species; *P. vivax* and *P. falciparum* accounted for 334 (71.4%) and 123 (26.3%), respectively. We found only 1 (0.2%) *P. malariae* and 4 (0.9%) *P. ovale* infections. Six patients carried mixed infections by *P. falciparum* and *P. vivax*.

Temporal Trend in Confirmed Malaria
Confirmed malaria incidence showed strong seasonality and peaked during April–August each year (Figure 2). In December 2011 and October 2013, confirmed malaria infections were not detected in the study area, whereas during the peak months, incidence increased sharply to ≈40 cases/month (3.3 cases/100,000 population/month) in each year of the study. *P. vivax* and *P. falciparum* parasites were detected nearly every month, but the other parasites and mixed infections were detected only during the high-transmission season (Figure 2). The *P. vivax* and *P. falciparum* case ratio remained almost unchanged: 2.5 for 2011, 2.6 for 2012, and 2.8 for 2013. The percentage of townships with no confirmed malaria increased from 43.1% in 2011 to 53.4% in 2012 and 67.2% in 2013 (Figure 3; Table), indicating a continuous reduction in malaria transmission in the area. This reduction also is reflected in the median incidence rates; the 0 median incidence rate
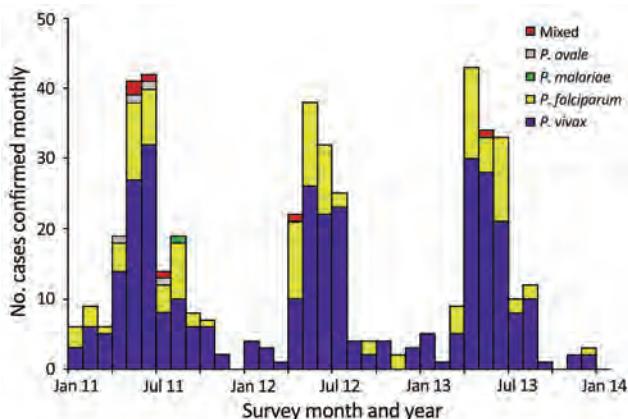
Figure 2. Monthly number of confirmed malaria cases of different *Plasmodium* species, Yunnan Province, China, 2011–2013.
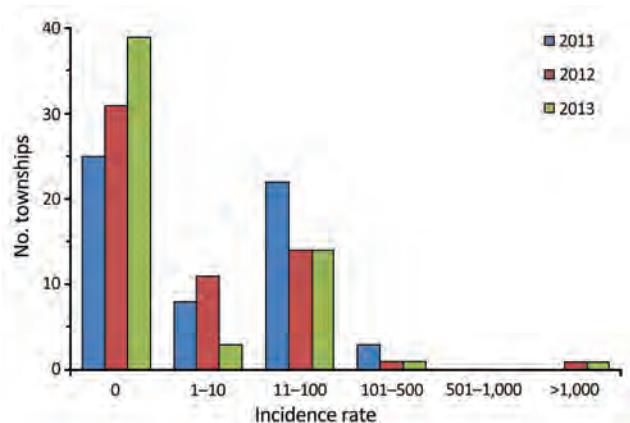
Figure 3. Malaria incidence (cases per 100,000 population), by year, Yunnan Province, China, 2011–2013.

Table. Measurement of heterogeneous distribution of confirmed township-level malaria incidence rate, Yunnan Province, China, January 2011–December 2013

Parameter	Year of surveillance		
	2011	2012	2013
No. townships with confirmed malaria*	33	27	19
No. malaria cases	170	144	149
Incidence rate†			
Mean (95% CI)	17.9 (8.2–27.6)	29.1 (0–68.3)	31.7 (0–71.3)
Median	5.4	0	0
Range	200	1133.3	1133.3
Kurtosis	14.3	55.2	52.6
Skewness	3.6	7.4	7.1
Coefficient of variation	205.6	513.9	475.3

*Significant differences (p<0.05) were determined by χ^2 test. The differences between 2011 and 2012 and between 2012 and 2013 were not significant; however, the difference between 2011 and 2013 was significant.
†Cases/100,000 population/year.

in 2012 and 2013 indicated that ≈50% of townships had no confirmed malaria. The increased mean incidence rates from 2011 to 2013 reflected the increased heterogeneity of the distribution.

Spatial Heterogeneity in Confirmed Malaria

Malaria was increasingly concentrated in fewer townships, and the heterogeneous level increased among townships over time (Table). The annual township-level incidence rate of malaria ranged from 0 to 200.0 cases/100,000 population in 2011 and from 0 to 1,133.3 cases/100,000 population in 2012 and 2013; however, the average incidence rate changed only from 17.9 to 31.7 cases/100,000 population annually from 2011 to 2013 (Table), and the increased mean incidence rate was caused primarily by a few extremely high-incidence townships. We detected malaria only from 33 townships during 2011, 27 during 2012, and 19 during 2013 (Figure 3). Coefficients of variation were well above 100% in all 3 years (Table). Spatial heterogeneity in incidence rate increased significantly over time (Table). These findings indicate a significantly heterogeneous distribution in township-level malaria incidence. Post hoc comparison indicated that differences in the annual average incidence rate at the township level were statistically insignificant among the 3 years (Tukey-Kramer HSD p>0.05), which indicated that the increasing mean annual incidences among townships from 2011 to 2013 most likely resulted from extreme variation in incidence rate among townships.

Confirmed Malaria versus Distance to the Border

The distance versus incidence rate analysis indicated that malaria incidence was 2- to 30-fold higher in areas within 10 km of the international border than it was in areas farther from the border, and the difference in incidence rate between the 2 categories increased during the 3 years. Within 10 km of the border, the annual *P. vivax* incidence was 21.48 during 2011, 57.89 during 2012, and 68.77 during 2013; for *P. falciparum*, incidence was 6.11 during 2011,

13.04 during 2012, and 22.62 during 2013 (Figure 4). This finding indicated that confirmed malaria incidence was increasingly aggregated along the border. However, because of the huge variances in each group, statistical tests did not show any significant differences in the incidence rate among different distance groups (data not shown).

Hot Spots of Confirmed Malaria

The distribution of malaria incidence rates (Figure 5) and the clusters of low and high incidence rates (Figure 6) showing hot spots of confirmed malaria varied throughout
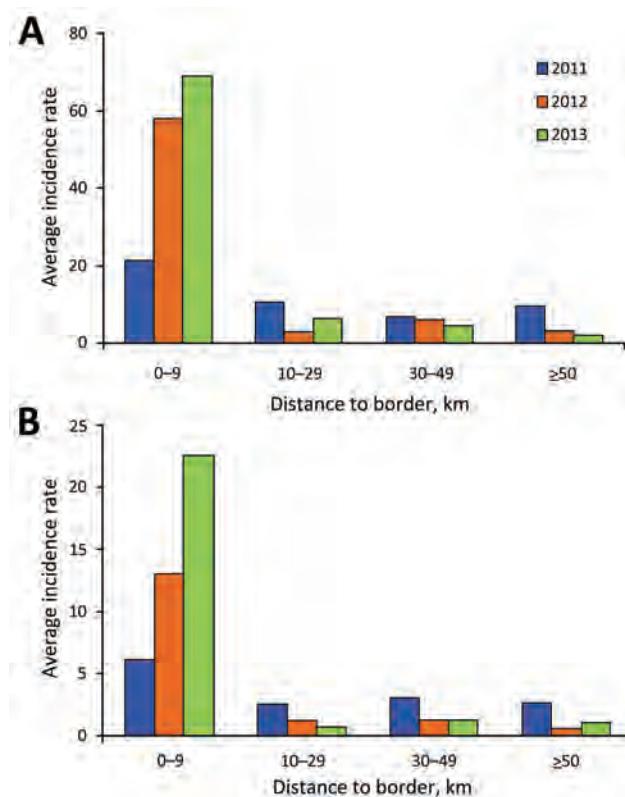
Figure 4. Malaria incidence (cases per 100,000 population) and distance to the nearest border, by year, Yunnan Province, China, 2011–2013. A) *Plasmodium vivax*. B) *P. falciparum*.
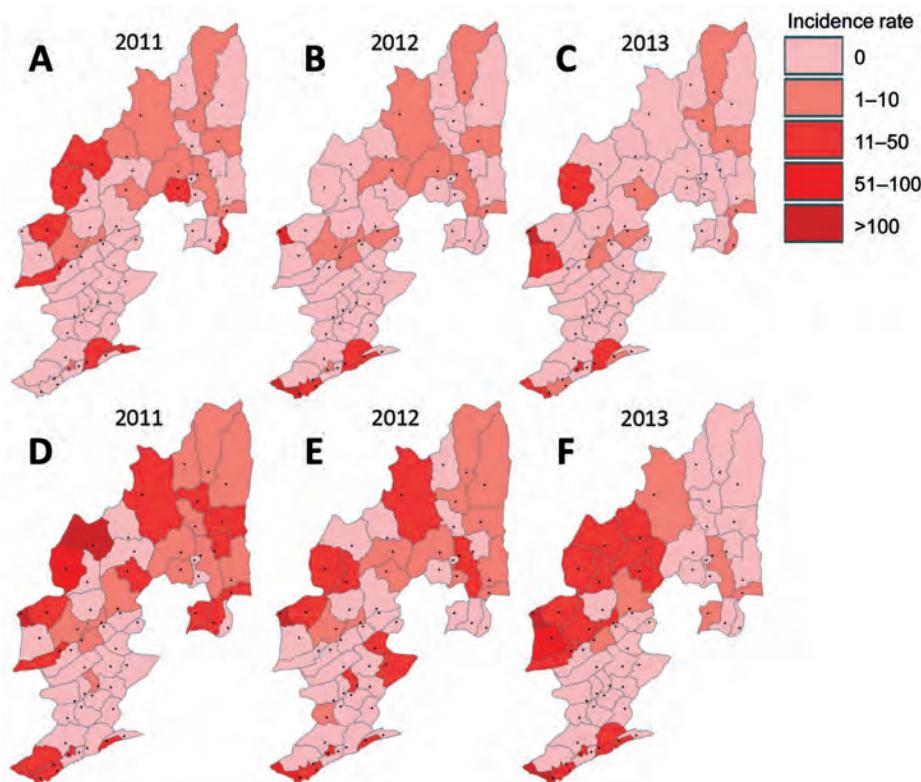
Figure 5. Distribution of township-level malaria incidence rate (cases per 100,000 population), Yunnan Province, China, 2011–2013. A–C) *Plasmodium falciparum*. D–F) *P. vivax*.

the years at the township level. Nevertheless, the transmission hot spots were generally located close to the international border.

The distribution maps of malaria incidence rates showed large spatial variation at the township level (Table; Figure 5). Townships with high incidences of *P. vivax* and *P. falciparum* were located mostly along the international border. However, many townships along the border had no confirmed malaria (Figure 5), illustrating the complex heterogeneous nature of malaria transmission in the border area. Compared with 2011, the geographic range of malaria incidence had shrunk in 2013. Clinical *P. falciparum* malaria cases were extremely scarce in 2013 (Figure 5, panel C), and *P. vivax* malaria cases were more aggregated in the central area along the border (Figure 5, panel F).

Results of the Getis-Ord $G_i^*(d)$ test indicated that all high-incidence clusters were located along the China–Myanmar border, namely Nabang, Xima, and Tongbiguan townships (Figure 6). The population of these 3 townships is ≈46,400, and the area is ≈1,530 km². However, for *P. falciparum* malaria, both the sizes and the exact locations of high- and low-incidence clusters shifted over time (Figure 6, panel A). On the other hand, high-incidence clusters of *P. vivax* remained in the same areas, although the size of clusters shrank from 2011 to 2012–2013. Coincidentally, high-incidence clusters comprised exactly the same

townships for both *P. falciparum* and *P. vivax* in 2013 (Figure 6, panels C, F).

Discussion

China successfully reduced illness and death from malaria during the 1980s–2000s and is now in the malaria elimination phase. Strategies to achieve and maintain malaria elimination should concentrate on identifying and eliminating transmission foci through passive and active methods of case detection (*12*). As malaria transmission declines, the number and sizes of the infection foci are shrinking. Thus, finer-scale transmission maps are required to identify small transmission hot spots. Because the township is the smallest administrative unit in China that has government-run healthcare centers, transmission mapping at the township level might be the best approach for elimination planning.

In Yunnan Province, *P. vivax*, which is difficult to eliminate, has become the predominant parasite species. Therefore, as overall malaria incidence rates fell in a region, we would expect the proportion of *P. vivax* cases to increase (*25*). Previous studies found that clinical *P. falciparum* malaria in Yunnan Province accounted for ≈15% of total cases during 1991 2006 and 22% during 2001 2005 (*26,27*). However, we did not find further decrease in the proportion of *P. falciparum* malaria during 2011–2013, which accounted for ≈27% of total clinical cases. Most
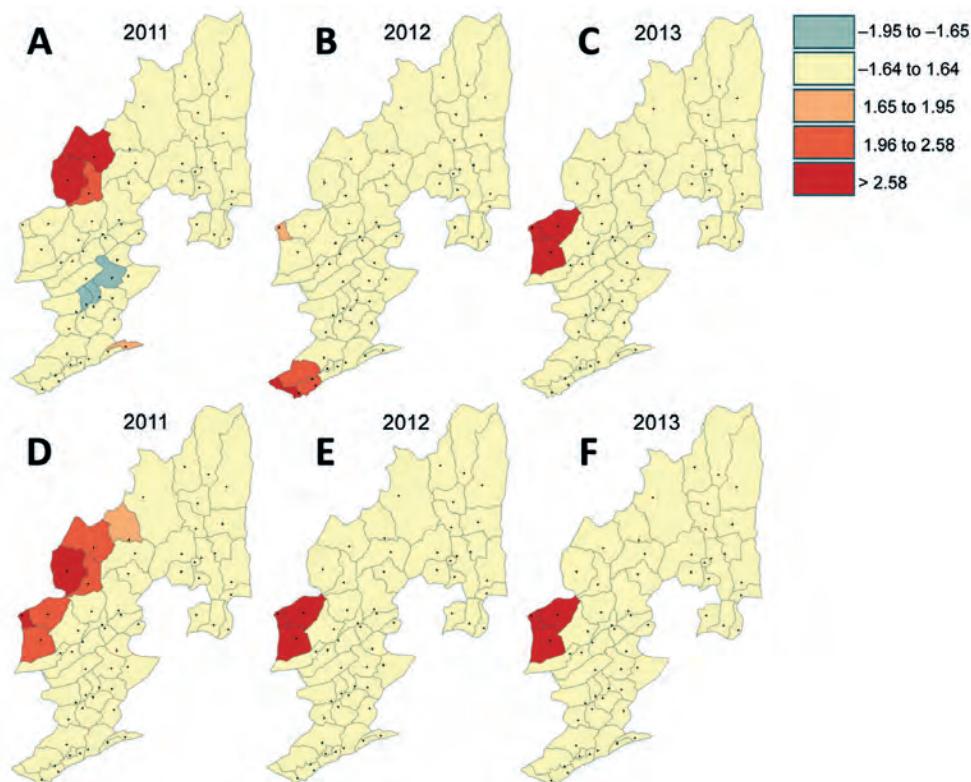
Figure 6. Clusters of low and high malaria incidence rates (cases per 100,000 population) detected at the township level and their shift over time, Yunnan Province, China, 2011–2013. A–C) *Plasmodium falciparum*. D–F) *P. vivax*.

P. falciparum cases occurred along the international border. Importation probably explains this unusual increase in the *P. falciparum* proportion. A previous study conducted in the same area found that clinical *P. falciparum* malaria was significantly associated with cross-border travel, especially travel to Myanmar (*9*).

Because malaria transmission rates are much higher in Myanmar than in China (*9,28*), persons living close to the border are at higher risk for infection. We found much a higher malaria incidence in the border area than in places farther from the border. Hot spot analysis found that high-incidence clusters of confirmed malaria were all located along the international border. Yet, the actual risk depends on the exact locations because malaria incidence rate in the border townships varied tremendously, from 0 to 1,133 cases/100,000 population annually in 2013. In addition, the hot spots of malaria changed over time and differed between *P. falciparum* and *P. vivax*. The shift of *P. falciparum* transmission hot spots might again be strongly linked to the pattern of cross-border population migration (*9,28,29*). The Getis-Ord local $G_i^*(d)$ test has been commonly used to determine clustering of transmission hot spots of different diseases (*14,21–24*); the test can be used in even finer-scale clustering analysis, such as village- or household-level hot spot analysis (*20,30,31*). The use of spatial clustering combined with geographic information systems clearly shows the locations and the sizes of the transmission hot spots. If this method is implemented in real-time monitoring, the development of hot spots can be detected early, thus enabling targeted interventions in a timely manner. Thus, this method can become a conventional parameter in a programmatic decision-making process by disease prevention and control authorities. We emphasize that, for active case tracking at the elimination stage, such a hot spot analysis at the village or household level might be worth investigating, even though it demands more resources (*31*). In addition, the spatial shift in malaria incidence hot spots from year to year is a challenge for the national malaria control program. For the national malaria control program to identify hot spots of malaria incidence and target malaria control in a timely manner, the spatial cluster analysis will need to be performed more frequently.

Regardless of the changing epidemiology, malaria cases continued to exhibit a seasonal transmission pattern, peaking in April–July, mostly reflecting the dynamics of monthly rainfall in this region (*9,32–34*). Seasonal migration patterns also might contribute to seasonal malaria transmission, as in other parts of the Greater Mekong Subregion such as western Thailand (*35–38*). Therefore, measures need to be developed to strengthen surveillance of cross-border migratory human populations to prevent malaria reintroduction. One limitation of our study is that we did not differentiate indigenous from definitive

imported cases because of the lack of travel history information for many persons with confirmed malaria. The clear seasonality of malaria cases and migratory populations should be considered in future malaria prediction analyses so that targeted monitoring and control efforts can be deployed more precisely.

The complex heterogeneous distribution of low but focalized and mobilized confirmed malaria transmission brings enormous challenges to malaria elimination plans. Strategies for malaria elimination in China should focus on these few transmission foci. For example, vector control measures should be enhanced in these areas; active case surveillance should be deployed to track the transmission; and more rigorous case management strategies should be implemented. In addition, Myanmar is considered the major source of parasite importation in the entire Greater Mekong Subregion (*39,40*), and human migration in the area plays an important role in malaria transmission in China (*35–38*; http://www.searo.who.int/entity/malaria/ documents/Mekong_pro/en/). Therefore, future elimination efforts should focus on the effects of cross-border activities on malaria parasite transmission, and strategies should include more intensive surveillance so that prevention and control activities can be directed at hot spot regions along the China–Myanmar border.

References
1. World Health Organization. World malaria report 2014 [cited 2015 Feb 15]. http://www.who.int/malaria/publications/world_malaria_ report_2014/en/
2. Ministry of Health of the People's Republic of China. From malaria control to eliminate: a revised national malaria strategy 2010–2015. Beijing: Ministry of Health of the People's Republic of China; 2009.
3. Ministry of Health of the People's Republic of China. Action plan of China malaria elimination (2010–2020) [cited 2015 Feb 15]. http://www.malariaeradication.org/elimination-programmes/ peoples-republic-china
4. Cao J, Sturrock HJ, Cotter C, Zhou S, Zhou H, Liu Y, et al. Communicating and monitoring surveillance and response activities for malaria elimination: China's "1-3-7" strategy. PLoS Med. 2014;11:e1001642. http://dx.doi.org/10.1371/journal. pmed.1001642
5. Clements AC, Barnett AG, Cheng ZW, Snow RW, Zhou HN. Space-time variation of malaria incidence in Yunnan Province, China. Malar J. 2009;8:180. http://dx.doi.org/10.1186/1475-2875-8-180
6. Lin H, Lu L, Tian L, Zhou S, Wu H, Bi Y, et al. Spatial and temporal distribution of *falciparum* malaria in China. Malar J. 2009;8:130. http://dx.doi.org/10.1186/1475-2875-8-130
7. Zhou SS, Wang Y, Li Y. Malaria situation in the People's Republic of China in 2010 [in Chinese]. Zhongguo Ji Sheng Chong Xue Yu Ji Sheng Chong Bing Za Zhi. 2011;29:401–3.
8. Xia ZG, Feng J, Zhou SS. Malaria situation in the People's Republic of China in 2012 [in Chinese]. Zhongguo Ji Sheng Chong Xue Yu Ji Sheng Chong Bing Za Zhi. 2013;31:413–8.
9. Zhou G, Sun L, Xia R, Duan Y, Xu J, Yang H, et al. Clinical malaria along the China–Myanmar border, Yunnan Province, China, January 2011–August 2012. Emerg Infect Dis. 2014;20:675–8. http://dx.doi.org/10.3201/eid2004.130647
10. Bejon P, Williams TN, Liljander A, Noor AM, Wambua J, Ogada E, et al. Stable and unstable malaria hotspots in longitudinal cohort studies in Kenya. PLoS Med. 2010;7:e1000304. http://dx.doi.org/10.1371/journal. pmed.1000304
11. Bousema T, Drakeley C, Gesase S, Hashim R, Magesa S, Mosha F, et al. Identification of hot spots of malaria transmission for targeted malaria control. J Infect Dis. 2010;201:1764–74. http://dx.doi.org/10.1086/652456
12. Moonen B, Cohen JM, Snow RW, Slutsker L, Drakeley C, Smith DL, et al. Operational strategies to achieve and maintain malaria elimination. Lancet. 2010;376:1592–603. http://dx.doi.org/10.1016/S0140-6736(10)61269-X
13. Bousema T, Griffin JT, Sauerwein RW, Smith DL, Churcher TS, Takken W, et al. Hitting hotspots: spatial targeting of malaria for control and elimination. PLoS Med. 2012;9:e1001165. http://dx.doi.org/10.1371/journal.pmed.1001165
14. Dhimal M, O'Hara RB, Karki R, Thakur GD, Kuch U, Ahrens B. Spatio-temporal distribution of malaria and its association with climatic factors and vector-control interventions in two high-risk districts of Nepal. Malar J. 2014;13:457. http://dx.doi.org/10.1186/1475-2875-13-457
15. Yin JH, Zhou SS, Xia ZG, Wang RB, Qian YJ, Yang WZ, et al. Historical patterns of malaria transmission in China. Adv Parasitol. 2014;86:1–19. http://dx.doi.org/10.1016/B978-0-12-800869-0.00001-9
16. Zhou XN, Xia ZG, Wang RB, Qian YJ, Zhou SS, Utzinger J, et al. Feasibility and roadmap analysis for malaria elimination in China. Adv Parasitol. 2014;86:21–46. http://dx.doi.org/10.1016/B978-0-12-800869-0.00002-0
17. Yin JH, Yan H, Huang F, Li M, Xiao HH, Zhou SS, et al. Establishing a China malaria diagnosis reference laboratory network for malaria elimination. Malar J. 2015;14:40. http://dx.doi.org/10.1186/s12936-015-0556-z
18. Tebit KE. Comparison of capillary and venous blood using blood film microscopy in the detection of malaria parasites: a hospital based study. Scientific J Microbiology. 2013;2:89–94.
19. Zhou G, Sirichaisinthop J, Sattabongkot J, Jones J, Bjørnstad ON, Yan G, et al. Spatio-temporal distribution of *Plasmodium falciparum* and *P. vivax* malaria in Thailand. Am J Trop Med Hyg. 2005;72:256–62.
20. Zhou G, Munga S, Minakawa N, Githeko AK, Yan G. Spatial relationship between adult malaria vector abundance and environmental factors in western Kenya highlands. Am J Trop Med Hyg. 2007;77:29–35.
21. Kelly-Hope LA, Hemingway J, McKenzie FE. Environmental factors associated with the malaria vectors *Anopheles gambiae* and *Anopheles funestus* in Kenya. Malar J. 2009;8:268. http://dx.doi.org/10.1186/1475-2875-8-268

22. Cartabia M, Campi R, Clavenna A, Bortolotti A, Fortino I, Merlino L, et al. Geographical epidemiology of antibacterials in the preschool age. Int J Health Geogr. 2012;11:52. http://dx.doi.org/10.1186/1476-072X-11-52

23. Haque U, Scott LM, Hashizume M, Fisher E, Haque R, Yamamoto T, et al. Modelling malaria treatment practices in Bangladesh using spatial statistics. Malar J. 2012;11:63. http://dx.doi.org/10.1186/1475-2875-11-63

24. Ruktanonchai CW, Pindolia DK, Striley CW, Odedina FT, Cottler LB. Utilizing spatial statistics to identify cancer hot spots: a surveillance strategy to inform community-engaged outreach efforts. Int J Health Geogr. 2014;13:39. http://dx.doi.org/10.1186/1476-072X-13-39

25. Vogel G. The forgotten malaria. Science. 2013;342:684–7. http://dx.doi.org/10.1126/science.342.6159.684

26. Li HX, Chen GW, Yang YC, Jiang H. Malaria situation in Yunnan Province during 2001–2005 [in Chinese]. Zhongguo Ji Sheng Chong Xue Yu Ji Sheng Chong Bing Za Zhi. 2008; 26:46–9.

27. Hui F-M, Xu B, Chen Z-W, Cheng X, Liang L, Huang H-B, et al. Spatio-temporal distribution of malaria in Yunnan Province, China. Am J Trop Med Hyg. 2009;81:503–9.

28. Li N, Parker DM, Yang Z, Fan Q, Zhou G, Ai G, et al. Risk factors associated with slide positivity among febrile patients in a conflict zone of north-eastern Myanmar along the China–Myanmar border. Malar J. 2013;12:361. http://dx.doi.org/10.1186/1475-2875-12-361

29. Kumar A, Chery L, Biswas C, Dubhashi N, Dutta P, Dua VK, et al. Malaria in South Asia: prevalence and control. Acta Trop. 2012;121:246–55. http://dx.doi.org/10.1016/j.actatropica.2012.01.004

30. Getis A, Morrison AC, Gray K, Scott TW. Characteristics of the spatial pattern of the dengue vector, *Aedes aegypti*, in Iquitos, Peru. Am J Trop Med Hyg. 2003;69:494–505.

31. Hu Y, Zhou G, Ruan Y, kLee MC, Xu X, Deng S, et al. Seasonal dynamics and microgeographical spatial heterogeneity of malaria along the China–Myanmar border. Acta Trop. 2016;157:12–9. http://dx.doi.org/10.1016/j.actatropica.2016.01.022

32. Bi Y, Hu W, Yang H, Zhou X-N, Yu W, Guo Y, et al. Spatial patterns of malaria reported deaths in Yunnan Province, China. Am J Trop Med Hyg. 2013;88:526–35. http://dx.doi.org/10.4269/ajtmh.2012.12-0217

33. Lu G, Zhou S, Horstick O, Wang X, Liu Y, Müller O. Malaria outbreaks in China (1990–2013): a systematic review. Malar J. 2014;13:269. http://dx.doi.org/10.1186/1475-2875-13-269

34. Zhao X, Chen F, Feng Z, Li X, Zhou X-H. Characterizing the effect of temperature fluctuation on the incidence of malaria: an epidemiological study in south-west China using the varying coefficient distributed lag non-linear model. Malar J. 2014;13:192. http://dx.doi.org/10.1186/1475-2875-13-192

35. Wiwanitkit V. High prevalence of malaria in Myanmar migrant workers in a rural district near the Thailand–Myanmar border. Scand J Infect Dis. 2002;34:236–7. http://dx.doi.org/10.1080/00365540110077272

36. Richards AK, Banek K, Mullany LC, Lee CI, Smith L, Oo EKS, et al. Cross-border malaria control for internally displaced persons: observational results from a pilot programme in eastern Burma/Myanmar. Trop Med Int Health. 2009;14:512–21. http://dx.doi.org/10.1111/j.1365-3156.2009.02258.x

37. Coker RJ, Hunter BM, Rudge JW, Liverani M, Hanvoravongchai P. Emerging infectious diseases in southeast Asia: regional challenges to control. Lancet. 2011;377:599–609. http://dx.doi.org/10.1016/S0140-6736(10)62004-1

38. Jitthai N. Migration and malaria. Southeast Asian J Trop Med Public Health. 2013;44(Suppl 1):166–200, discussion 306–7.

39. Cui L, Yan G, Sattabongkot J, Cao Y, Chen B, Chen X, et al. Malaria in the Greater Mekong Subregion: heterogeneity and complexity. Acta Trop. 2012;121:227–39. http://dx.doi.org/10.1016/j.actatropica.2011.02.016

40. Cui L, Yan G, Sattabongkot J, Chen B, Cao Y, Fan Q, et al. Challenges and prospects for malaria elimination in the Greater Mekong Subregion. Acta Trop. 2012;121:240–5. http://dx.doi.org/10.1016/j.actatropica.2011.04.006

Address for correspondence: Zhaoqing Yang, Department of Pathogen Biology and Immunology, Kunming Medical University, Kunming, China; email: zhaoqingy92@hotmail.com; Guiyun Yan, Program in Public Health, University of California, Irvine, Irvine, CA 92697, USA; email: guiyuny@uci.edu; Liwang Cui, Department of Entomology, Pennsylvania State University, University Park, PA 16802, USA; email: luc2@psu.edu

Phylogeographic Evidence for 2 Genetically Distinct Zoonotic *Plasmodium knowlesi* Parasites, Malaysia

Ruhani Yusof,[1] Md Atique Ahmed,[1] Jenarun Jelip, Hie Ung Ngian, Sahlawati Mustakim, Hani Mat Hussin, Mun Yik Fong, Rohela Mahmud, Frankie Anak Thomas Sitam, J. Rovie-Ryan Japning, Georges Snounou, Ananias A. Escalante, Yee Ling Lau

Infections of humans with the zoonotic simian malaria parasite *Plasmodium knowlesi* occur throughout Southeast Asia, although most cases have occurred in Malaysia, where *P. knowlesi* is now the dominant malaria species. This apparently skewed distribution prompted an investigation of the phylogeography of this parasite in 2 geographically separated regions of Malaysia, Peninsular Malaysia and Malaysian Borneo. We investigated samples collected from humans and macaques in these regions. Haplotype network analyses of sequences from 2 *P. knowlesi* genes, type A small subunit ribosomal 18S RNA and cytochrome c oxidase subunit I, showed 2 genetically distinct divergent clusters, 1 from each of the 2 regions of Malaysia. We propose that these parasites represent 2 distinct *P. knowlesi* types that independently became zoonotic. These types would have evolved after the sea-level rise at the end of the last ice age, which separated Malaysian Borneo from Peninsular Malaysia.

The number of malaria cases in Malaysia steadily decreased from a peak of 59,208 in 1995 to 3,850 confirmed cases in 2013; of these, 80% were reported in the 2 states of Malaysian Borneo and the remainder in 6 of the 11 states of Peninsular Malaysia (Figure 1) (*1*). In Malaysia, the simian malarial parasite species *Plasmodium knowlesi* is now the dominant species infecting humans and is >2 times more prevalent than *P. falciparum* or *P. vivax*.

Author affiliations: University of Malaya Faculty of Medicine, Kuala Lumpur, Malaysia (R. Yusof, M.A. Ahmed, M.Y. Fong, R. Mahmud, Y.L. Lau); Sabah State Health Department, Sabah, Malaysia (J. Jelip); Hospital Kapit, Sarawak, Malaysia (H.U. Ngian); Hospital Tengku Microbiology Laboratory, Ampuan Rahimah, Selangor, Malaysia (S. Mustakim); Kelantan State Health Department, Kelantan, Malaysia (H.M. Hussin); Department of Wildlife and National Parks Peninsular Malaysia, Kuala Lumpur, Malaysia (F.A.T. Sitam, J. Rovie-Ryan); Sorbonne Universités, INSERM, Paris, France (G. Snounou); Temple University, Philadelphia, PA, USA (G. Snounou, A.A. Escalante)

Humans were found to be susceptible to *P. knowlesi* when this species was experimentally transmitted to man in 1932, the year in which it was first described (*2,3*). In 1965, the first confirmed case of a naturally acquired infection in humans was recorded (*4*). The next naturally acquired confirmed cases were reported in 2004, when a stable focus of *P. knowlesi* was discovered in Sarawak, 1 of 2 states that make up Malaysian Borneo (*5*). Thereafter, transmission of *P. knowlesi* to humans occurred in the second state, Sabah (*6,7*), and in neighboring countries (*8,9*).

The natural hosts of *P. knowlesi* are principally the long-tailed (*Macaca fascicularis*) and pig-tailed (*M. nemestrina*) macaques (*10*), 2 species that are widely distributed in the Southeast Asia countries in which cases of *P. knowlesi* have been recorded. To date, human-to-human transmission has not been observed. Infections in humans can cause severe disease that can be fatal (*9,11*), underscoring the public health concern raised by this zoonotic simian parasite.

The 2 states of Malaysian Borneo appear to be the epicenter of zoonotic *P. knowlesi* infections: 1,391 cases in Malaysian Borneo and 423 cases in Peninsular Malaysia were recorded in 2012. A total of 1,407 PCR-confirmed cases were reported during 2004–2013 in Malaysia, which contrasts with the low number of cases (n = 136) reported from neighboring countries (*9*): Cambodia (n = 1), China (n = 36), Indonesia (n = 1), Myanmar (n = 14), the Philippines (n = 5), Singapore (n = 2), Thailand (n = 36), and Vietnam (n = 32). The reasons for this uneven distribution remain unclear. Geographic variation in mosquito species and human social factors could be an explanation; it is also possible that the parasite populations circulating on the island of Borneo are distinct from those found in continental Malaysia. The *P. knowlesi* strains that had been studied in earlier years displayed distinct biologic characteristics, which in some cases led malariologists to propose distinct *P. knowlesi* subspecies (*12*). Such differences
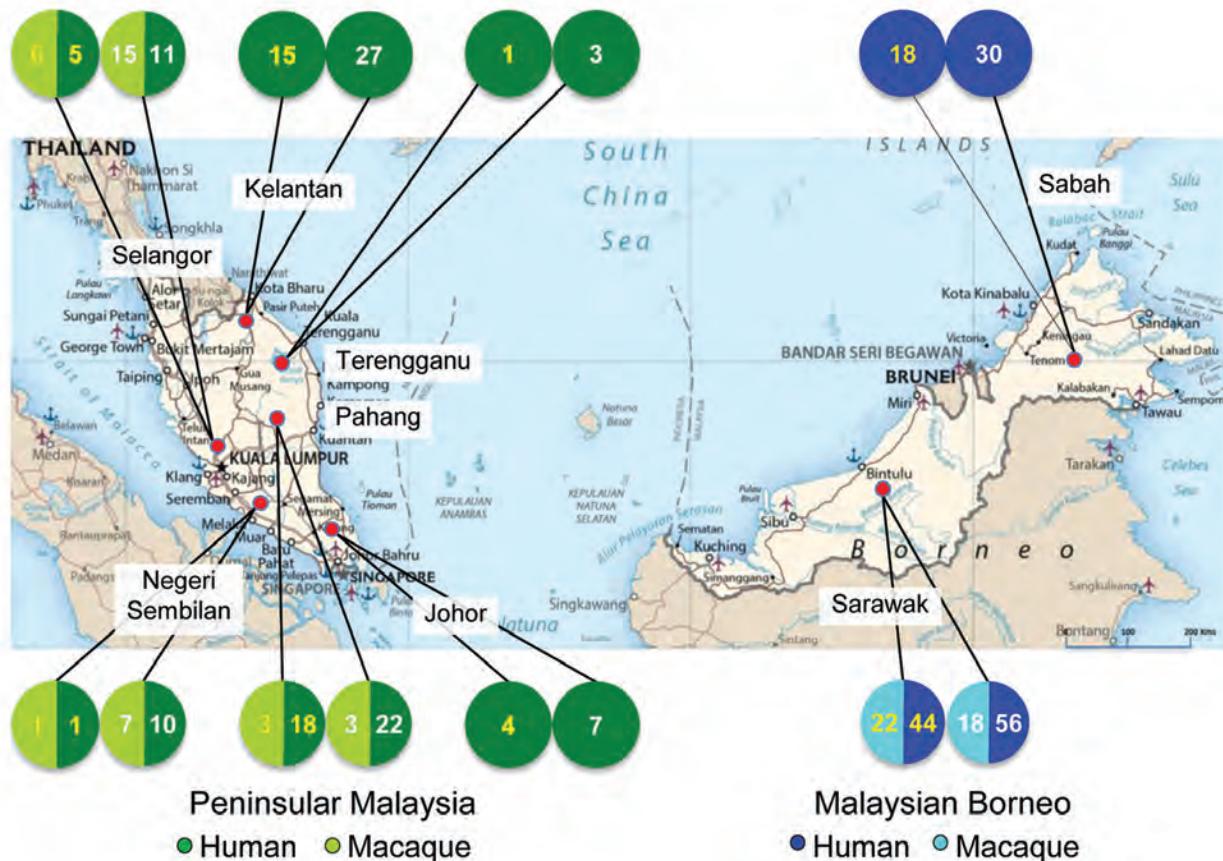
Figure 1. Geographic origin of the genetic sequences generated during study of Plasmodium knowlesi parasite populations, Malaysia. The numbers in each circle refer to the number of sequences (macaque or human) obtained for the genes P. knowlesi type A small subunit ribosomal 18S RNA (numbers in white) and P. knowlesi cytochrome oxidase subunit I (numbers in yellow).

could indicate that local ecologic factors are influential and that each *P. knowlesi* subspecies became a zoonosis independently in each geographic area.

To explore whether the *P. knowlesi* populations in Malaysia differed and independently became zoonoses, we focused on 2 genes that have been extensively used for phylogenetic studies (*13–16*): 1 nuclear, encoding the type A small subunit ribosomal 18S RNA (*PkA-type 18S rRNA*), and 1 mitochondrial, encoding the cytochrome oxidase subunit I protein (*PkCOX1*). Using samples collected from humans and macaques in both regions of the country, we generated the relevant sequences, compared them to those published previously (*17*), and conducted phylogenetic and population genetic analyses.

Materials and Methods

Sample Collection

The Medical Research Ethic Committee of the Ministry of Health Malaysia, Sabah State Director of Health, Kelantan State Director of Health, and directors of state and district hospitals approved this study. Ethical approval was granted by the Medical Research and Ethics Committee of the Malaysian Ministry of Health (Reference Number: KKM/NIHSEC/800/-2/2/2/P13–316), the Medical Ethics Committee of University Malaya Medical Centre, and the Department of Wildlife and National Parks.

We used previously collected human blood samples for this study (*7*): 78 microscopically confirmed *P. knowlesi*–positive blood samples from patients in 8 states in Malaysia, including Sabah and Sarawak in Malaysian Borneo (Figure 1). We also examined blood samples from 8 long-tailed macaques collected during routine surveys by the Department of Wildlife and National Parks in the Peninsular Malaysia states of Pahang, Selangor, and Negeri Sembilan. All samples were collected during September 2012–December 2013 (Tables 1, 2). In addition to these samples, we included previously published sequences deposited into GenBank during 2003–2015 in the analyses; these sequences were derived from samples collected from humans and macaques (online Technical Appendix Table, http://wwwnc.cdc.gov/EID/article/22/8/15-1885-Techapp1.pdf).

Table 1. Samples and sequences obtained for the *PkA-type 18S rRNA* gene used to distinguish 2 distinct *Plasmodium knowlesi* parasite populations in Malaysia*

| Population location | No. samples† | | No. sequences | | | | Total sequences obtained |
| | Human | Macaque | Human | | Macaque | | |
			This study‡	GenBank§	This study‡	GenBank§	
Peninsular Malaysia							
Kelantan	13	ND	27	ND	ND	ND	27
Johor	3	ND	7	ND	ND	ND	7
Selangor	7	5	11	ND	15	ND	26
Terengganu	2	ND	3	ND	ND	ND	3
Pahang	14	1	21	1	3	ND	25
Negeri Sembilan	4	2	10		6	1	17
Malaysian Borneo							
Sarawak	22	ND	48	8	ND	18	74
Sabah	13	ND	30	ND	ND		30
Total samples	86		78	8	8	6	86 human + 14 macaque
Total sequences	NA		157	9	24	19	166 human + 43 macaque

*NA, not applicable; ND, no data; *PkA-type 18S rRNA, P. knowlesi* type A small subunit ribosomal 18S RNA.
†Previously collected samples used for this study.
‡GenBank accession nos. KT852845–KT852938 and KJ917815–KJ917903.
§GenBank accession numbers listed in online Technical Appendix Table (http://wwwnc.cdc.gov/EID/article/22/8/15-1885-Techapp1.pdf).

Amplification and Sequencing of Gene Fragments

Genomic DNA was extracted from the human and macaque blood samples by using the DNeasy Blood Tissue Kit (QIA-GEN, Hilden, Germany), according to the manufacturers' protocol. An established nested PCR protocol was used to test the samples; all tested positive for *P. knowlesi* only (*5*).

The *PkA-type 18S rRNA* and *PkCOX1* genes were then amplified (MyCycler, Bio-Rad, Hercules, CA). In a primary amplification reaction, a *PkA-type 18S rRNA* fragment of 1.1. kb was obtained by using the oligonucleotide primer pair rPLU5+rPLU6 (*18*). The amplification reaction was completed in a mixture containing 1X Green Go Taq Flexi Buffer (Promega, Madison, WI, USA); 4.0 mol/Lmagnesium chloride solution; 0.2 mol/L dNTP Mix (Promega), 0.2 mM of each primer; 1 U GoTaq Flexi DNA Polymerase (Promega); and 4 mL of DNA template combined with nuclease–free water to obtain a final volume of 25 mL. The PCR amplification was initiated at 95°C for

10 min, then by 35 cycles of denaturation at 94°C for 30 s, annealing at 55°C for 30 s, extension at 72°C for 1 min, and a final extension at 72°C for 5 min. For the secondary amplification, 4 mL of the primary amplification product were used as a template by using forward primer Pkl1 (5′-ACATAACTGATGCCTCCGCGTA) and reverse primer Pkl2 (5′-CACACATCGTTCCTCTAAGAAGC) to obtain a 986 990-bp fragment. The reaction mixture and the cycling conditions were as above with minor modification for the 35 cycles: denaturation at 94°C for 1 min, annealing at 53°C for 1 min, extension at 72°C for 1 min, and final extension at 72°C for 10 min. The amplified PCR fragments were cloned into the pGEM-T Vector (Invitrogen, Carlsbad, CA, USA). Plasmids purified from ≥2 positive clones from each ligation mixture were selected for sequencing (First Base Laboratories Sdn Bhd, Malaysia). Any polymorphism that was not observed in ≥2 samples was only included in the analysis if its validity

Table 2. Samples and sequences obtained for the *PkCOX1* gene used to distinguish the 2 distinct *Plasmodium knowlesi* parasite populations in Malaysia*

| Location | No. samples† | | No. sequences | | | | Total sequences obtained |
| | Human | Macaque | Human | | Macaque | | |
			This study‡	GenBank§	This study‡	GenBank§	
Peninsular Malaysia							
Kelantan	13	ND	15	ND	ND	ND	15
Johor	3	ND	4	ND	ND	ND	4
Selangor	7	5	5	ND	5	1	11
Terengganu	2	ND	1	ND	0	ND	1
Pahang	14	1	18	ND	2	1	21
Negeri Sembilan	4	2	ND	1	1	ND	2
Malaysian Borneo							
Sarawak	22	ND	23	21	ND	22	66
Sabah	13	ND	18	ND	ND	ND	18
Total samples	NA	86	78	22	8	12	100 human + 20 macaque
Total sequences	NA	NA	84	22	8	24	106 human + 32 macaque

*NA, not applicable; ND, no data; *PkCOX1 P. knowlesi* cytochrome oxidase subunit I.
†Previously collected samples used for this study.
‡GenBank accession nos.KT900705–KT900797).
§GenBank accession numbers listed in online Technical Appendix Table (http://wwwnc.cdc.gov/EID/article/22/8/15-1885-Techapp1.pdf).

was confirmed by a repeated cycle of amplification, cloning, and sequencing.

For the *PkCOX1* gene, amplification was achieved by using forward (5′-GCCAGGATTATTTGGAGG) and reverse (5′-CAGGAATACGTCTAGGCA) primers to obtain a 1,116-bp fragment. These primers were designed based on a published gene sequence (GenBank accession no. AY598141). The amplification reaction was achieved as above. The PCR amplification was initiated at 95°C for 3 min, then denatured for 35 cycles at 94°C for 1 min, annealed at 52°C for 1 min, extended at 72°C for 1 minute, and put through final extension at 72°C for 10 min. The purified amplified fragments were then sent for sequencing.

Sequence Editing and Alignment

We analyzed the DNA sequences using BioEdit Sequence Alignment Editor Software (http://www.mbio.ncsu.edu/BioEdit/bioedit.html) on the reference *P. knowlesi* H-strain (GenBank accession no. AM910985) for the *PkA-type 18S rRNA* and the *P. knowlesi* mitochondrial sequence (GenBank accession no. NC 00723244) for the *PkCOX1* gene. Results were exported to MEGA 5.6 software (http://www.megasoftware.net) for further alignment and analysis. We performed similarity searches using BLAST (http://blast.ncbi.nlm.nih.gov/Blast.cgi). We obtained 28 additional *PkA-type 18S RNA* sequences derived from *P. knowlesi*–infected samples (9 from humans and 19 from macaques) and 46 additional *PkCOX1* sequences derived from *P. knowlesi*-infected samples (22 from humans and 24 from macaques) from GenBank and included these sequences in the analysis (online Technical Appendix Table).

Haplotype Network Analysis

We estimated polymorphism of the *PkA-type 18S rRNA* and *PkCOX1* genes by computing haplotype diversity (Hd), number of haplotypes (h), nucleotide diversity (p), number of polymorphic sites, and the average number of pairwise nucleotide differences using DnaSP version 5.10.01 software (BioSoft http://en.bio-soft.net/). We constructed haplotype networks for *PkA-type 18S rRNA* and *PkCOX1* genes based on their polymorphic sites by using the median-joining method in NETWORK version 4.6.1.2 software (Fluxus Technology Ltd, Suffolk, UK). We inferred the genealogical haplotype network using the sequences of *P. knowlesi* human and macaque isolates from Peninsular Malaysia and Malaysian Borneo. Where available, we included sequences from the *P. knowlesi* H and Nuri strains as references.

Population Genetic Structure Analysis

To define genetic structure of the *P. knowlesi* parasite population in Malaysia, we used STRUCTURE version 2.3.4 software (The Pritchard Lab, Stanford University, Stanford, CA, USA) that deploys the Bayesian model–based clustering approach. We estimated the most probable number of populations (K) using an admixture model. All sample data (for both genes) were run for values K = 1–8, each with a total of 15 iterations. We used 500,000 Markov Chain Monte Carlo generations for each run after a burn-in of 50,000 steps. The most likely number K in the data was estimated by calculating ΔK values and identifying the K value that maximizes the log probability of data, lnP(D) (*19*). The most probable K value was then calculated according to Evanno's method (*20*) by using the webpage interface STRUCTURE Harvester (*21*). We also used ARLEQUIN version 3.5.1.3 software (University of Berne, Berne, Switzerland) to compute pairwise differences (F_{ST}) between populations (i.e., humans and macaques from Peninsular Malaysia and Malaysian Borneo) (*22*) from haplotypes that showed 10,100 permutations. F_{ST} is a comparison of the sum of genetic variability within and between populations on the basis of the differences in allelic frequencies. We interpreted F_{ST} values as no (0), low (>0–0.05), moderate (0.05–0.15), and high (0.15–0.25) genetic differentiation.

Neutrality and Demographic Analysis

We examined departure from a strict neutral model, including demographic expansions, on the basis of pairwise mismatch distribution, the Tajima D test (*23*), Fu and Li D (*24*), Fu and Li F, and Fu Fs statistics (*25*) using DnaSP version 5.10.01 software (*26*). Significant negative values for these tests indicate either a purifying selection or population expansion, and positive values indicate balancing selection.

Results

The sequences analyzed in this study were derived from 130 *P. knowlesi*–infected blood samples obtained from 23 macaques and 107 humans. We analyzed a total of 209 *PkA-type 18S RNA* sequences (105 from Peninsular Malaysia and 104 from Malaysian Borneo) and 138 *PkCOX1* sequences (54 from Peninsular Malaysia and 84 from Malaysian Borneo).

Gene Diversity Indices

Analysis of the molecular polymorphism within the 209 partial *PkA-type 18S rRNA* sequences (945 bp) revealed moderately polymorphic sequences (p = 0.00324 ± 0.00019). Overall, 137 polymorphic sites yielded 93 haplotypes. Nucleotide and haplotype diversities were broadly similar for both Peninsular Malaysia and Malaysian Borneo samples (Table 3). Single-nucleotide polymorphisms were scattered throughout the gene; most the Peninsular Malaysia sequences displayed a distinct single nucleotide polymorphism (G→A at position 830) (online Technical Appendix Table).

Table 3. Genetic characteristics of the 2 genetically distinct zoonotic *Plasmodium knowlesi* parasite populations in Malaysia*

Gene and location	No. samples	No. haplotypes	No. polymorphic sites	Haplotype diversity ±SD	Nucleotide diversity ±SD	Average. no. nucleotide differences
PkA-type 18S rRNA						
Peninsular Malaysia	105	47	62	0.906 ±0.0.025	0. 0.00284 ±0.00024	2.66667
Malaysian Borneo	105	48	85	0.871 ±0.031	0.00276 ±0.0.00029	2.59341
Overall	210	93	137	0.941 ±0.0.011	0.00324 ±0.00019	3.03550
PkCOX1						
Peninsular Malaysia	53	20	20	0.827 ±0.039	0.00141 ±0.00018	1.52685
Malaysian Borneo	84	25	25	0.676 ±0.057	0.00115 ±0.00014	1.24498
Overall	137	44	39	0.848 ±0.025	0.00215 ±0.00013	2.33104
*PkA-type 18S rRNA, *P. knowlesi* type A small subunit ribosomal 18S RNA; *PkCOX1 P. knowlesi* cytochrome oxidase subunit I.						

Analysis of the molecular polymorphism within the 138 partial *P. knowlesi* mitochondrial *COX1* sequences (1,082 bp) revealed low instances of polymorphism (p = 0.00215 ± 0.00013). Overall, 61 polymorphic sites yielded 44 haplotypes. Although nucleotide diversities were similar for sequences from both regions, haplotype diversity was higher for the sequences from Peninsular Malaysia (h = 19, Hd = 0.827 ± 0.039) than for those from Malaysian Borneo (h = 25, Hd = 0.676 ± 0.057) (Table 3). Sequences from Malaysian Borneo were distinguished from those from Peninsular Malaysia by 2 distinct single nucleotide polymorphisms (G→A at position 166 and T→C at position 659) (online Technical Appendix figure).

Haplotype network

DNA sequence variation in our phylogeographic study is more clearly observed in a haplotype network. The network tree for the *PkA-type 18S RNA* haplotypes (Figure 2) showed 2 distinct *P. knowlesi* populations that, with 1 exception, clustered exclusively to 1 of the 2 regions of Malaysia: Peninsular Malaysia (n = 47) and Malaysian Borneo (n = 48). The exception was of 2 haplotypes derived from 1 macaque sample (haplotypes 88 and 89) from Peninsular Malaysia that clustered with the Malaysian Borneo haplotypes. In each cluster, only 2 haplotypes were shared by humans and macaques, but in each case 1 was dominant (in Malaysian Borneo, haplotype 1: n = 38, human = 27,
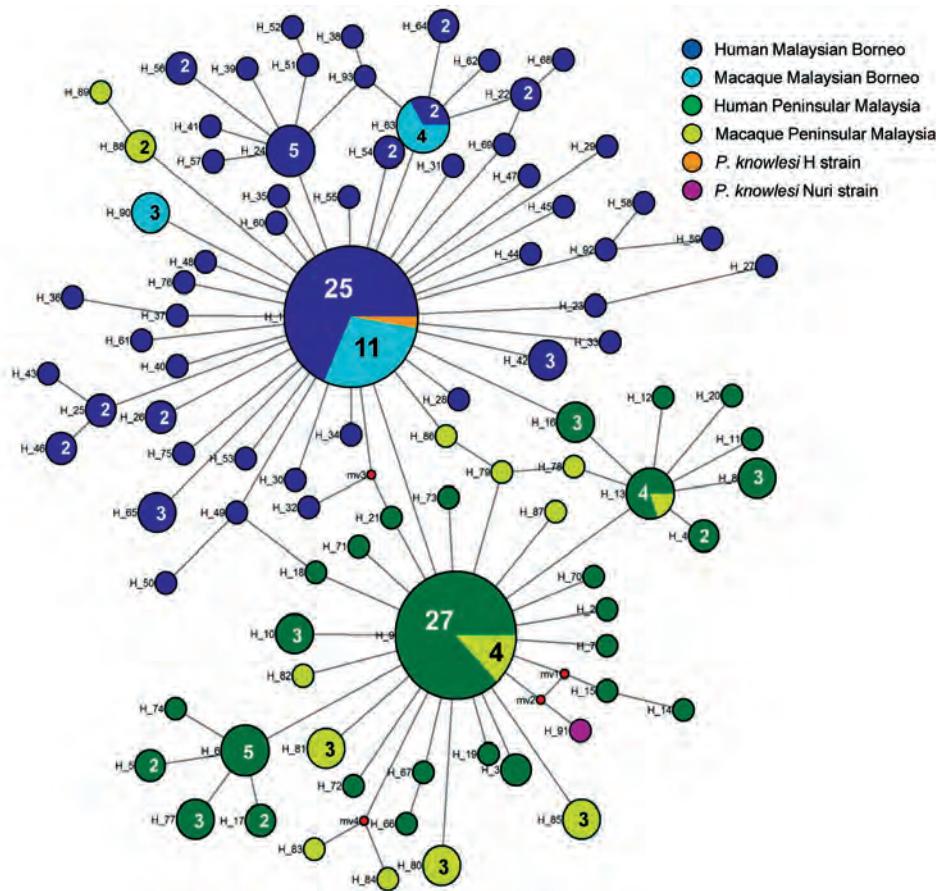
Figure 2. Median-joining networks of *Plasmodium knowlesi* type A small subunit ribosomal 18S RNA haplotypes from Malaysia. The genealogical haplotype network shows the relationships among the 93 haplotypes present in the 209 sequences obtained from human and macaque samples from Peninsular Malaysia and Malaysian Borneo. Each distinct haplotype has been designated a number (H_n). Circle sizes represent the frequencies of the corresponding haplotype (the number is indicated for those that were observed >1×). Small red nodes are hypothetical median vectors created by the program to connect sampled haplotypes into a parsimonious network. Distances between nodes are arbitrary.

macaque = 11; and in Peninsular Malaysia, haplotype 9: n = 31, human = 27, macaque = 4). The network tree for the *PkCOX1* genes showed a similar pattern to that of *PkA-type 18S rRNA*: it had 2 geographically distinct *P. knowlesi* populations (n = 19 for Peninsular Malaysia and n = 25 for Malaysian Borneo) (Figure 3), and dominant haplotypes in each cluster were shared between humans and macaques (Figure 3).

The excess of unique *PkA-type 18S rRNA* and *PkCOX1* haplotypes observed for the *P. knowlesi* populations in humans (Figures 2, 3) is indicative of an evolutionarily recent population expansion. A signature of population expansion was also evident from the unimodal shape of the pairwise mismatch distribution of the *PkA-type 18S rRNA* and *Pk-COX1* genes (Figure 4). Calculations by using Tajima D, Fu and Li D and F, and Fu Fs statistics also showed significant negative values (p = 0.05–0.001; Table 4). However, the low number of samples and consequent sequences from macaques precludes any meaningful comparison.

Population Structure

We used a Bayesian admixture model implemented in STRUCTURE to calculate the potential number of *P. knowlesi* parasite populations within Malaysia. Because the study samples were collected from 8 different states of Malaysia (Figure 1), we used K values from 1 to 8 for the analysis. For both genes, significant genetic structure was found between the parasite populations when K = 2 (Figure 5), indicating 2 distinct populations clustered to 1 of the 2 main regions of Malaysia (*PkA-type 18S rRNA*, K = 2, ΔK = 121.79; *PkCOX1*, K = 2, ΔK = 481.27). In *PkA-type 18S rRNA* and *PkCOX1* sequences, we also estimated pairwise F_{ST} values using ARLEQUIN software to determine to what extent population differentiation exists within *P. knowlesi* in Malaysia on the basis of host and geographic origin, i.e., between humans and macaques and between Peninsular Malaysia and Malaysian Borneo. This analysis revealed particularly high population differentiation F_{ST} values (>0.21 for *PkA-type 18S rRNA* and >0.60 for *Pk-COX1*) for samples originating from Peninsular Malaysia and Malaysian Borneo irrespective of the host (human or macaque) from which they were collected (Table 5). For the macaque and human population within the same geographic region, the F_{ST} values were low (<0.05) (Table 5), suggesting that parasitic transmission was confined to each of the regions. These results are concordant with the haplotype network analysis.

Discussion

The results of the various analyses conducted on the *P. knowlesi* parasites collected from Peninsular Malaysia and Malaysian Borneo strongly support the conclusion that the 2 geographically separated regions of this country harbor genetically distinct *P. knowlesi* populations. Haplotype diversity, a measure of species evenness (low values indicate skewing toward a few predominant haplotypes), was high
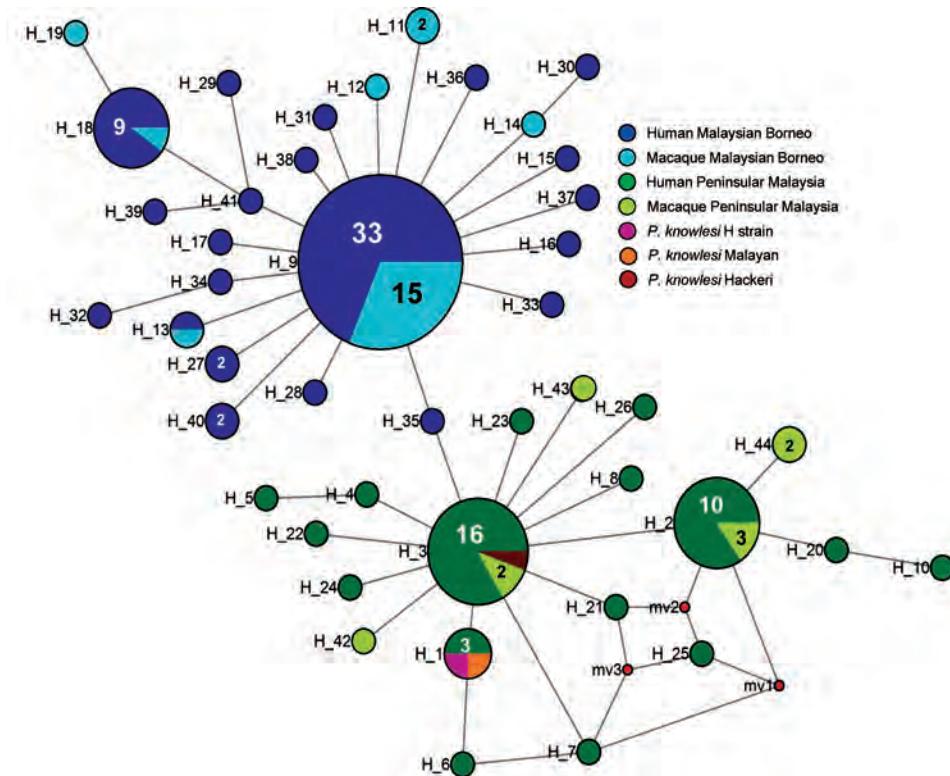
Figure 3. Median-joining networks of *Plasmodium knowlesi* cytochrome oxidase subunit I haplotypes from Malaysia. The genealogical haplotype network shows the relationships among the 44 haplotypes present in the 138 sequences obtained from human and macaque samples from Peninsular Malaysia and Malaysian Borneo. Each distinct haplotype has been designated a number (H_n). Circle sizes represents the frequencies of the corresponding haplotype (the number is indicated for those that were observed more than once). Small red nodes are hypothetical median vectors created by the program to connect sampled haplotypes into a parsimonious network. Distances between nodes are arbitrary.
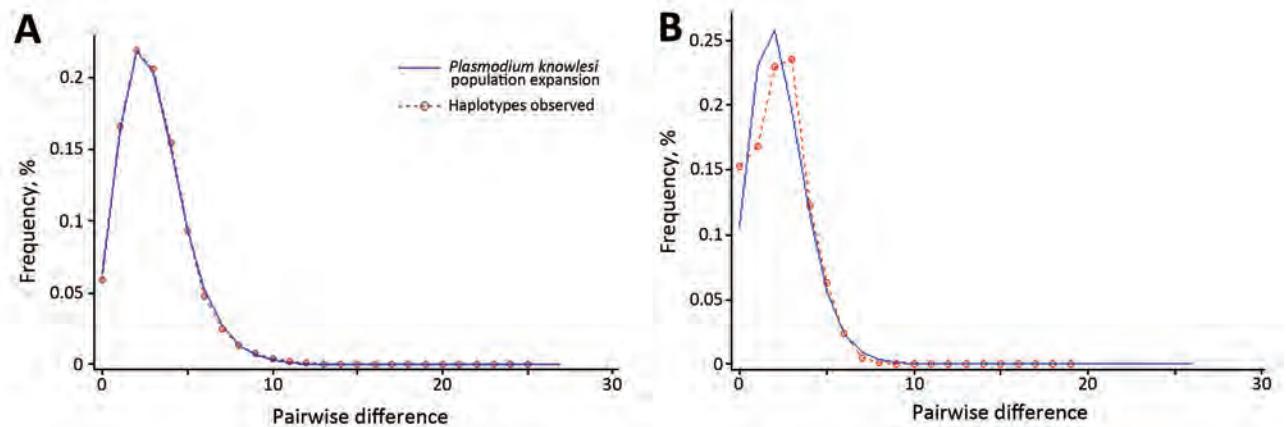
Figure 4. Pairwise mismatch distribution of *Plasmodium knowlesi* parasite populations, Malaysia. A) Type A small subunit ribosomal 18S RNA; B) cytochrome oxidase subunit I. Red dotted lines represent the observed frequencies of the pairwise differences among mitochondrial DNA sequences; blue lines represent the expected curve for a population that has undergone a demographic expansion.

for both the Peninsular Malaysia (0.906 ± 0. 0.025) and the Malaysian Borneo (0.871 ± 0.031) isolates, which may indicate a sustained transmission of *P. knowlesi* in both regions of Malaysia over long periods. Similar high haplotype diversity values have been reported for the *P. knowlesi csp* gene in isolates from Sarawak (*17*). Nucleotide diversity, however, was low for the genes analyzed in this study, irrespective of the samples' geographic or host origins, indicating that only minor differences occurred between the haplotypes observed (online Technical Appendix Table, Figure). A similar pattern has been observed for geographically separated *P. vivax* populations between which gene flow is limited (*14*).

The relatively large sample group size and the short genetic distances between the intraspecific sequences in this study are not suited for phylogenetic studies that aim to reconstruct genealogies. Therefore, we subjected the sequences to a median-joining haplotype network analysis, which showed that the network consisted mostly of unique haplotypes that clearly form 2 clusters: 1 comprised the samples obtained from Peninsular Malaysia, and the other the samples from Malaysian Borneo (Figures 2, 3). Within each cluster, the dominant haplotypes were shared

between humans and macaques; a similar observation was previously reported for a sample set collected in Sarawak (*17*). Additional population structure analyses showed very high genetic differentiation between 2 distinct *P. knowlesi* populations from the 2 geographic regions and very low genetic differentiation between the human and macaque parasites within each of these regions (Figure 5). These observations strongly support the conclusion that humans are susceptible to infection by any of the *P. knowlesi* types circulating in macaques.

The question arises as to how these 2 distinct populations arose. Analyses of the complete mitochondrial DNA revealed that *P. knowlesi* parasites were present in macaques around 65,000 years ago, before human settlement in Southeast Asia (*17*). Although DNA sequences isolated in our study are too short to perform a comparable analysis, it has been proposed that the macaque populations of Borneo became isolated from those of Peninsular Malaysia, Java, and Sumatra around 15,000 years ago, when the rise in the level of the South China Sea at the end of the last ice age submerged parts of Sundaland (*27*). Thus, *P. knowlesi* populations likely became isolated, along with their natural vertebrate and insect hosts, and consequently

Table 4. Results of statistical testing for neutrality of *Plasmodium knowlesi* parasite populations in Malaysia

Gene and location	Tajima D (*23*)	Fu and Li D (*24*)	Fu and Li F (*25*)	Fu Fs (*26*)
PkA-type 18S rRNA				
Peninsular Malaysia	−2.49764*	−3.71579 †	−3.85230 †	−56.133
Malaysian Borneo	−2.73586*	−6.47796 †	−5.87592 †	−59.698
Overall	−2.71801*	−7.08484†	−5.97285†	−151.882
PkCOX1				
Peninsular Malaysia	−2.06554‡	−3.20519‡	−3.33283†	−18.092
Malaysian Borneo	−2.28662†	−3.60846†	−3.71725†	−27.990
Overall	−2.02607‡	−4.40748†	−4.11218†	−48.131

PkA-type 18S rRNA, *P. knowlesi* type A small subunit ribosomal 18S RNA; *PkCOX1 P. knowlesi* cytochrome oxidase subunit I.
*p<0.001.
†p<0.02.
‡p<0.05.
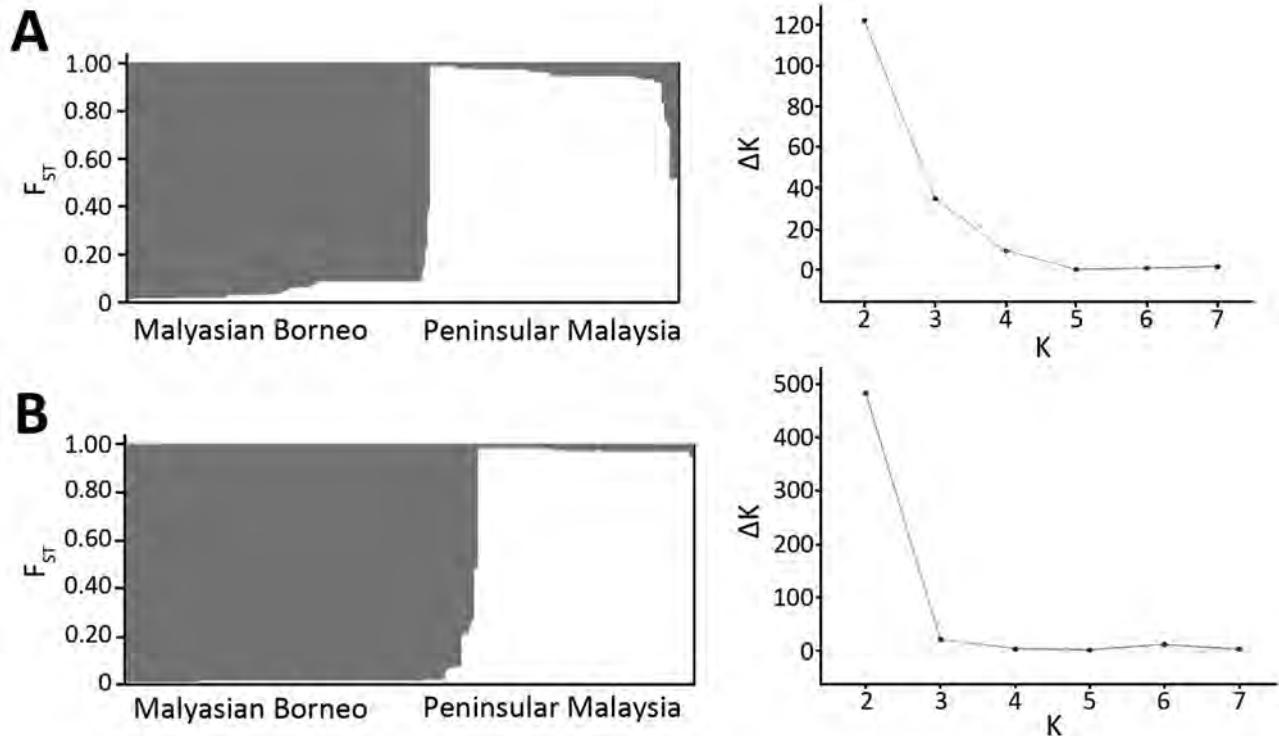
Figure 5. Most likely number of *Plasmodium knowlesi* parasite subpopulation haplotype clusters (K) in Malaysian Borneo (gray) and Peninsular Malaysia (white). A) Type A small subunit ribosomal 18S RNA (K = 2, ∆K = 121.79), including comparison of K and ∆K; B) cytochrome oxidase subunit I (K = 2, ∆K = 481.27), including comparison between K and ᴅK. Relationships were determined by using Bayesian model–based STRUCTURE version 2.3.4 software (The Pritchard Laboratory, Stanford University, Stanford, CA, SUA). ∆K = mean (|L″(K)|)/sd(L(K)). Vertical axes represent membership coefficient values.

evolved separately. This mechanism of geographic isolation and host demography is considered important in the differentiation and origin of *P. knowlesi* parasites and other closely related *Plasmodium* species, for which diversity is probably underestimated (*16,28*). We propose that the 2 distinct *P. knowlesi* populations currently circulating in Peninsular Malaysia and Malaysian of Borneo correspond to 2 independently evolving populations. The *PkCOX1* haplotypes available for the *P. knowlesi* isolates from Peninsular Malaysia (Malayan, GenBank accession no. AB444106.1; Hackeri, accession no. AB444107.1; H, accession no. AB444108) fall within the Peninsular Malaysia cluster; corresponding *PkA-type 18S rRNA* sequences are not available.

Table 5. F_{ST} results for pairwise population comparisons of 2 genetically distinct zoonotic *Plasmodium knowlesi* parasite populations and associated significance, Malaysia*†

Gene and location	Haplotype	F_{ST} values			
		HuPen	MaPen	HuBor	MaBor
PkA-type 18S rRNA					
Peninsular Malaysia	HuPen	NA	‡	‡	‡
	MaPen	0.0483	NA	‡	‡
Malaysian Borneo	HuBor	0.2710	0.2167	NA	NS
	MaBor	0.3134	0.3090	0.0008	NA
PkCOX1					
Peninsular Malaysia	HuPen	NA	§	‡	‡
	MaPen	0.0461	NA	‡	‡
Malaysian Borneo	HuBor	0.6008	0.6303	NA	NS
	MaBor	0.6219	0.6925	0.0007	NA

*HuBor, human haplotypes from Malaysian Borneo; HuPen, human haplotypes from Peninsular Malaysia; MaBor, Macaque haplotypes from Malaysian Borneo; MaPen, macaque haplotype from Peninsular Malaysia; NA, not applicable; NS, not significant; *PkA-type 18S rRNA*, *P. knowlesi* type A small subunit ribosomal 18S RNA; *PkCOX1 P. knowlesi* cytochrome oxidase subunit I.
†ARLEQUIN (University of Berne, Berne, Switzerland) software package version 3.5.1.3 was used to compute pairwise differences between populations (i.e., humans and macaques from Peninsular Malaysia and Malaysian Borneo).
‡p<0.001; p values computed with 10,100 permutations.
§p<0.05.

The 3 *P. knowlesi* subspecies proposed to date (*12*) were found in distinct locations (Taiwan, Java, and Peninsular Malaysia). These parasites were not studied further and confirmation of their subspecific status remains to be confirmed, but no material suitable for genetic analysis is available. We note that evidence of potential hybrid forms was obtained from a single sample from a macaque from Sabah and for the H strain. The low frequency of such forms suggests a recent admixture through increased human movement between the 2 geographic regions of Malaysia, biologic factors that limit their fitness, or both. The clear geographic genetic differentiation and the indiscriminate distribution between human and macaque hosts for the parasites within each cluster strongly indicate that *P. knowlesi* became zoonotic independently in the 2 regions. Given that *P. knowlesi* has long been zoonotic, the data also indicate that human-to-human transmission has not been established over time.

While our study was underway, *P. knowlesi* populations from Sarawak were shown to be dimorphic across their genome (*29,30*). Furthermore, analyses based on microsatellite diversity identified 2 distinct parasite groups across the whole of Malaysia that strongly cluster with the macaque host species but not in the human samples: 1 was dominant in *M. fascicularis* macaques and the other in *M. nemestrina* macaques (*31*). These distinct groups do not correspond to the 2 distinct clusters we propose because their pattern of distribution is incongruent with the marked geographic distribution we report. It is likely that they represent a more recent population structure driven by adaptation to the macaque as vector and host. Considering the differences in the mutation rates between mitochondrial and nuclear genes and microsatellites (*32,33*), the data from the microsatellite analyses would be expected to detect recent population structuring, and our data from the nuclear and mitochondrial genes would reveal a more ancient geographic isolation.

In conclusion, it is clear that the *P. knowlesi* malaria parasites are not a homogeneous group but form a complex of related types, possibly including emerging subspecies, of which evolution and distribution has been shaped by past and recent events. It is equally clear that further analyses encompassing a larger number of genetic loci or whole genomes from sample sets collected in Malaysia, as well as in neighboring countries, will be needed to obtain a more comprehensive picture of the phylogeographic distribution and population structure of *P. knowlesi*. The zoonotic potential of these parasites constitutes a threat to the efforts to eliminate malaria in Southeast Asia. Thus, more epidemiologic and biologic investigations are necessary to help devise strategies that will minimize if not eliminate this threat.

References

1. World Health Organization. World malaria report 2014. Geneva, Switzerland: World Health Organization; 2014 [cited 2/19/2015 Feb 19]. http://www.who.int/malaria/publications/world_malaria_report_2014/en
2. Knowles R, Das Gupta BM. A study of monkey-malaria, and its experimental transmission to man. (A preliminary report). Ind Med Gaz. 1932;67:301–20 [cited 2/19/2015 Feb 19]. http://www.cabdirect.org/abstracts/19322901628.html
3. Sinton JA, Mulligan HW. A critical review of the literature relating to the identification of the malarial parasites recorded from monkeys of the families *Cercopithecidæ* and *Colobidæ*. Rec Mal Surv Ind. 1932;3:357–80 [cited 2/19/2015 Feb 19]. http://www.cabdirect.org/abstracts/19342900941.html
4. Chin W, Contacos PG, Coatney GR, Kimball HR. A naturally acquired quotidian-type malaria in man transferable to monkeys. Science. 1965;149:865. http://dx.doi.org/10.1126/science.149.3686.865
5. Singh B, Sung LK, Matusop A, Radhakrishnan A, Shamsul SSG, Cox-Singh J, et al. A large focus of naturally acquired *Plasmodium knowlesi* infections in human beings. Lancet. 2004;363:1017–24. PubMed http://dx.doi.org/10.1016/S0140-6736(04)15836-4
6. Barber BE, William T, Dhararaj P, Anderios F, Grigg MJ, Yeo TW, et al. Epidemiology of Plasmodium knowlesi malaria in north-east Sabah, Malaysia: family clusters and wide age distribution. Malar J. 2012;11:401. http://dx.doi.org/10.1186/1475-2875-11-401
7. Yusof R, Lau YL, Mahmud R, Fong MY, Jelip J, Ngian HU, et al. High proportion of Knowlesi malaria in recent malaria cases in Malaysia. Malar J. 2014;13:168. http://dx.doi.org/10.1186/1475-2875-13-168
8. Cox-Singh J. Zoonotic malaria: *Plasmodium knowlesi*, an emerging pathogen. Curr Opin Infect Dis. 2012;25:530–6. http://dx.doi.org/10.1097/QCO.0b013e3283558780
9. Singh B, Daneshvar C. Human infections and detection of *Plasmodium knowlesi*. Clin Microbiol Rev. 2013;26:165–84. http://dx.doi.org/10.1128/CMR.00079-12
10. Coatney GR, Collins WE, Warren M, Contacos PG. The primate malarias. Washington (DC): US Department of Health, Education and Welfare; 1971.
11. Ahmed MA, Cox-Singh J. Plasmodium knowlesi—an emerging pathogen. ISBT Sci Ser. 2015;10(Suppl 1):134–40. http://dx.doi.org/10.1111/voxs.12115
12. Garnham PCC. Malaria parasites and other haemosporidia. Oxford: Blackwell Scientific Publications; 1966.
13. Pacheco MA, Battistuzzi FU, Junge RE, Cornejo OE, Williams CV, Landau I, et al. Timing the origin of human

malarias: the lemur puzzle. BMC Evol Biol. 2011;11:299. http://dx.doi.org/10.1186/1471-2148-11-299

14. Taylor JE, Pacheco MA, Bacon DJ, Beg MA, Machado RL, Fairhurst RM, et al. The evolutionary history of *Plasmodium vivax* as inferred from mitochondrial genomes: parasite genetic diversity in the Americas. Mol Biol Evol. 2013;30:2050–64. http://dx.doi.org/10.1093/molbev/mst104

15. Joy DA, Feng X, Mu J, Furuya T, Chotivanich K, Krettli AU, et al. Early origin and recent expansion of *Plasmodium falciparum.* Science. 2003;300:318–2. http://dx.doi.org/10.1126/science.1081449

16. Muehlenbein MP, Pacheco MA, Taylor JE, Prall SP, Ambu L, Nathan S, et al. Accelerated diversification of nonhuman primate malarias in Southeast Asia: adaptive radiation or geographic speciation? Mol Biol Evol. 2015;32:422–39. http://dx.doi.org/10.1093/molbev/msu310

17. Lee K-S, Divis PCS, Zakaria SK, Matusop A, Julin RA, Conway DJ, et al. *Plasmodium knowlesi*: reservoir hosts and tracking the emergence in humans and macaques. PLoS Pathog. 2011;7:e1002015. http://dx.doi.org/10.1371/journal.ppat.1002015

18. Singh B, Bobogare A, Cox-Singh J, Snounou G, Abdullah MS, Rahman HA. A genus- and species–specific nested polymerase chain reaction malaria detection assay for epidemiologic studies. Am J Trop Med Hyg. 1999;60:687–92.

19. Pritchard JK, Stephens M, Donnelly P. Inference of population structure using multilocus genotype data. Genetics. 2000;155:945–59.

20. Evanno G, Regnaut S, Goudet J. Detecting the number of clusters of individuals using the software STRUCTURE: a simulation study. Mol Ecol. 2005;14:2611–20. http://dx.doi.org/10.1111/j.1365-294X.2005.02553.x

21. Earl DA, von Holdt BM. STRUCTURE HARVESTER: a website and program for visualizing STRUCTURE output and implementing the Evanno method. Conserv Genet Resour. 2012;4:359–61 http://dx.doi.org/10.1007/s12686-011-9548-7.

22. Excoffier L, Lischer HE. Arlequin suite ver 3.5: a new series of programs to perform population genetics analyses under Linux and Windows. Mol Ecol Resour. 2010;10:564–7. http://dx.doi.org/10.1111/j.1755-0998.2010.02847.x

23. Tajima F. The effect of change in population size on DNA polymorphism. Genetics. 1989;123:597–601.

24. Fu YX. Statistical tests of neutrality of mutations against population growth, hitchhiking and background selection. Genetics. 1997;147:915–25.

25. Fu YX, Li WH. Statistical tests of neutrality of mutations. Genetics. 1993;133:693–709.

26. Librado P, Rozas J. DnaSP v5: a software for comprehensive analysis of DNA polymorphism data. Bioinformatics. 2009;25:1451–2. http://dx.doi.org/10.1093/bioinformatics/btp187

27. Hanebuth T, Stattegger K, Grootes PM. Rapid flooding of the sunda shelf: A late-glacial sea-level record. Science. 2000;288:1033–5. http://dx.doi.org/10.1126/science.288.5468.1033

28. Pacheco MA, Reid MJC, Schillaci MA, Lowenberger CA, Galdikas BMF, Jones-Engel L, et al. The origin of malarial parasites in orangutans. PLoS One. 2012;7:e34990. http://dx.doi.org/10.1371/journal.pone.0034990

29. Ahmed AM, Pinheiro MM, Divis PCS, Siner A, Zainudin R, Wong IT, et al. Disease progression in *Plasmodium knowlesi* malaria is linked to variation in invasion gene family members. PLoS Negl Trop Dis. 2014;8:e3086. http://dx.doi.org/10.1371/journal.pntd.0003086

30. Pinheiro MM, Ahmed MA, Millar SB, Sanderson T, Otto TD, Lu WC, et al. *Plasmodium knowlesi* genome sequences from clinical isolates reveal extensive genomic dimorphism. PLoS One. 2015;10:e0121303. http://dx.doi.org/10.1371/journal.pone.0121303

31. Divis PC, Singh B, Anderios F, Hisam S, Matusop A, Kocken CH, et al. Admixture in humans of two divergent *Plasmodium knowlesi* populations associated with different macaque host species. PLoS Pathog. 2015;11:e1004888. http://dx.doi.org/10.1371/journal.ppat.1004888

32. Haasl RJ, Payseur BA. Multi-locus inference of population structure: a comparison between single nucleotide polymorphisms and microsatellites. Heredity. 2011;106:158–71. http://dx.doi.org/10.1038/hdy.2010.21

33. Lehmann T, Blackston CR, Besansky NJ, Escalante AA, Collins FH, Hawley WA. The Rift Valley complex as a barrier to gene flow for *Anopheles gambiae* in Kenya: the mtDNA perspective. J Hered. 2000;91:165–8. http://dx.doi.org/10.1093/jhered/91.2.165

Address for correspondence: Yee Ling Lau, Tropical Infectious Disease Research & Education Centre (TIDREC), Department of Parasitology, Faculty of Medicine, University of Malaya, 50603 Kuala Lumpur, Malaysia; email: lauyeeling@um.edu.my

Hemolysis after Oral Artemisinin Combination Therapy for Uncomplicated *Plasmodium falciparum* Malaria

Florian Kurth, Tilman Lingscheid, Florian Steiner, Miriam S. Stegemann, Sabine Bélard, Nikolai Menner, Peter Pongratz, Johanna Kim, Horst von Bernuth, Beate Mayer, Georg Damm, Daniel Seehofer, Abdulgabar Salama, Norbert Suttorp, Thomas Zoller

Episodes of delayed hemolysis 2–6 weeks after treatment of severe malaria with intravenous artesunate have been described. We performed a prospective observational study of patients with uncomplicated malaria to investigate whether posttreatment hemolysis also occurs after oral artemisinin-based combination therapy. Eight of 20 patients with uncomplicated malaria who were given oral artemisinin-based combination therapy met the definition of posttreatment hemolysis (low haptoglobin level and increased lactate dehydrogenase level on day 14). Five patients had hemolysis persisting for 1 month. Patients with posttreatment hemolysis had a median decrease in hemoglobin level of 1.3 g/dL (interquartile range 0.3–2.0 g/dL) in the posttreatment period, and patients without posttreatment hemolysis had a median increase of 0.3 g/dL (IQR –0.1 to 0.7 g/dL; p = 0.002). These findings indicate a need for increased vigilance for hemolytic events in malaria patients, particularly those with predisposing factors for anemia.

Artemisinin-based drugs are the mainstay of current antimalarial treatment and play a key role in the World Health Organization (WHO) global strategy to reduce malaria illness and death caused by malaria. These drugs act rapidly against *Plasmodium* spp. and are usually well tolerated. Artemisinin-based combination therapies (ACTs) are the recommended first-line treatment for uncomplicated malaria in most countries (*1*).

Episodes of delayed hemolysis 2–6 weeks after treatment for severe malaria with intravenous artesunate have been observed in non–malaria-immune patients in Europe (*2*). This phenomenon, recently referred to as postartemisinin-delayed hemolysis (PADH) (*3,4*), has been confirmed in other nonimmune patients (*4,5*) and in children in Africa (*6*). Approximately 20%–30% of nonimmune patients given intravenous artesunate show signs of PADH that vary in intensity and duration (*5,7*). Hemolysis is usually self-limiting, but patients need to be actively followed up because transfusion of erythrocytes and rehospitalization might be necessary (*2,5*).

The pathophysiology of hemolysis after artemisinin therapy is not fully understood. Once-infected erythrocytes that have been cleared of parasites in the spleen have a shorter life span and play a role. Patients with higher concentrations of once-infected erythrocytes after artemisinin treatment are at higher risk for PADH (*4*). However, other features of posttreatment hemolysis, such as prolonged hemolytic reactions over several weeks (*2*), are not explained by this mechanism. Several reports suggest involvement of a drug-dependent autoimmune hemolysis mechanism (*8*), but systematic investigations have not been performed in most published cases (*2,9*). Given the key role of artemisinins in malaria treatment, WHO calls for prospective clinical studies and further research to improve the understanding of delayed hemolysis after artemisinin therapy (*10*).

Only 2 single cases and 2 patients in a recent analysis of surveillance data in the United States have been reported with signs of delayed hemolysis after oral ACT treatment (*11–13*). We hypothesize that delayed hemolysis occurs not only after intravenous treatment for severe malaria but also in a substantial number of patients given oral ACTs for uncomplicated malaria. Because delayed hemolysis has not been captured by safety studies on ACTs, we assume that delayed hemolysis after oral ACTs is less pronounced and occurs to a subclinical degree.

We conducted a study of patients with uncomplicated *Plasmodium falciparum* malaria to investigate the clinical, laboratory, and immunohematologic features of hemolysis and anemia during and after antimalarial treatment. This article presents data for patients investigated during the first 12 months of this ongoing study.

Methods

This prospective observational study was conducted at the University Hospital of Charité–Universitätsmedizin Berlin (Berlin, Germany). The study protocol was approved by the ethical committee of Charité–Universitätsmedizin Berlin and is registered at the WHO International Clinical Trials Registry Platform (DRKS00007104). All laboratory analyses and parasitologic examinations were performed in accredited laboratories at Charité-Universitätsmedizin, Berlin.

All patients who sought treatment at the hospital and were found to have microscopically confirmed uncomplicated *P. falciparum* malaria were included in the study after written informed consent was obtained. Patients were excluded if they had received antimalarial treatment (excluding prophylaxis) within 12 weeks before inclusion; had medical conditions that potentially cause hemolysis (e.g., glucose-6-phosphate dehydrogenase deficiency, hemoglobinopathy, mechanical heart valve, lymphoproliferative disease); or were taking medication that potentially causes hemolysis.

Patients were seen for study visits at admission before treatment (day 0). After the first treatment, they were seen again after the last treatment dose on day 3, on day 7 (range day 6–day 10), and on day 14 (range day 14–day 20). If symptoms or signs of hemolysis were detected, patients were seen on day 30 (range day 27–day 31) and thereafter if clinically indicated.

Study visits included obtaining a medical history and conducting a physical examination. Laboratory investigations were parasitologic (thick and thin blood smears), hematologic (differential blood count), and biochemical (haptoglobin, lactate dehydrogenase [LDH], C-reactive protein, potassium, and sodium levels and renal and liver function tests) examinations; screening for glucose-6-phosphate dehydrogenase deficiency; and immunohematologic examinations (direct and indirect antiglobulin test, including testing with enzyme-treated erythrocytes).

This analysis evaluated data for all patients given oral ACTs during the first 12 months of the study. The primary objective was to assess the proportion of patients with posttreatment hemolysis, which was defined as a low haptoglobin level (<0.3 g/L) and an LDH level above the age-dependent upper normal level 14 days after treatment. Secondary objectives were to compare in patients with posttreatment hemolysis and those without it possible risk factors (age, ethnicity, sex, initial parasitemia) and the course of anemia (hemoglobin [Hb] level, reticulocyte production index) during treatment, after treatment, and overall. Hemolysis with a loss of Hb ≥1.5 g/dL during days 3–14 was classified as uncompensated hemolysis; hemolysis without a decrease in Hb level or a decrease <1.5 g/dL during days 3–14 was classified as compensated hemolysis.

Differences between patients with and without signs of posttreatment hemolysis and between patients with compensated and uncompensated hemolysis were analyzed by using the Mann-Whitney U test for continuous data and the Fisher exact test for binary data at a 2-sided significance level of $\alpha = 0.05$. Data are presented as median and interquartile range (IQR). Statistical analysis was performed by using JMP version 7.0 (SAS Institute Inc., Cary, NC, USA).

The sample size of the ongoing study was calculated to detect an incidence of posttreatment hemolysis of 20% with a 95% CI, ± 7.5% precision, and 15% lost to follow-up. This calculation resulted in a sample size of 130 patients. This study evaluated 27 patients, which represented 21% of the intended total sample size. Because we could find no published prospective data for hemolysis after oral ACT treatment, we decided to communicate the findings of this interim analysis before completion of the study.

Results

During May 2014–April 2015, a total of 27 patients with uncomplicated *P. falciparum* malaria and a standard 3-day treatment course of oral ACT were included in the study. All malaria infections had been acquired in Africa, and none of the patients had taken antimalarial prophylaxis. Six patients did not complete all necessary follow-up visits, and 1 patient was excluded because of sickle cell disease. Twenty patients with ≥4 study visits until day 20 were available for this interim analysis; of these patients, 3 were children (Table). All patients showed rapid clinical improvement with clearance of peripheral asexual parasitemia no later than 72 hours after initiation of treatment. There were no treatment failures.

The criteria for posttreatment hemolysis (haptoglobin and LDH levels) on day 14 were met by 8 (40%) of 20 patients. An additional 2 patients showed signs of in vitro hemolysis on day 14 (increased LDH and potassium levels but haptoglobins level within reference ranges). The LDH values of these patients were excluded from further analysis and these patients were classified as patients without hemolysis. Patient characteristics showed no differences between those with and without hemolysis, with the exception of slightly higher Hb levels on day 0 and day 3 in patients with posttreatment hemolysis (Table).

After treatment (during days 3–14), patients with posttreatment hemolysis showed a decrease in Hb level (median change –1.3 g/dL, IQR –2.0 to –0.3), and patients without posttreatment hemolysis showed an increase in Hb level (median change 0.3 g/dL, IQR –0.1 to 0.7; p = 0.002) (Figure 1, panel C). During treatment (during days 0–3), patients with posttreatment hemolysis showed a tendency toward a smaller decrease in Hb level (median change –0.15 g/dL, IQR –0.6 to 0.6) than did patients without

Table. Baseline characteristics and follow-up laboratory data for patients with uncomplicated *Plasmodium falciparum* malaria who were given ACT*

Characteristic	All, n = 20	Without posttreatment hemolysis, n = 12	With posttreatment hemolysis, n = 8	p value	With compensated posttreatment hemolysis, n = 4	With uncompensated posttreatment hemolysis, n = 4	p value
Baseline							
Age, y	35 (26–40)	31 (17–40)	38 (30–43)	0.18	32 (22–42)	40 (27–46)	0.15
Children	3/20 (15.0)	3/12 (25.0)	0/8 (0)	0.24	0/4 (0)	0 (0)	
African ethnicity	13/20 (65.0)	9/12 (75.0)	4/8 (50.0)	0.35	4/4 (100.0)	0/4 (0)	0.001
Female sex	9/20 (45.0)	7/12 (58.3)	2/8 (25.0)	0.19	2/4 (50.0)	0/4 (0)	0.42
Treatment with ARM/LUM	5/20 (25.0)	4/12 (33.3)	1/8 (12.5)	0.60	0/4 (0)	1/4 (25.0)	1.0
Treatment with DHA/PPQ	15/20 (75.0)	8/12 (75.0)	7/8 (87.5)	0.60	4/4 (100.0)	3/4 (75.0)	1.0
Parasitemia†	0.4 (0.2–1.1)	0.3 (0.1–0.9)	0.9 (0.4–1.4)	0.12	1.15 (0.4–1.9)	0.8 (0.2–1.1)	0.40
Hb d0‡	12.5 (11.1–14.0)	11.3 (10.5–13.5)	13.1 (12.5–14.1)	0.11	12.7 (12.4–13.8)	13.7 (12.6–14.6)	0.30
Laboratory follow-up‡							
Hb d3	12.2 (10.6–13.6)	11.1 (9.7–12.7)	13.2 (12.2–14.3)	0.02	12.8 (11.9–13.4)	14.2 (12.5–14.6)	0.15
Hb d7	12.1 (11.1–13.0)	11.7 (10.5–12.5)	12.5 (11.9–12.6)	0.33	12.6 (11.8–13.1)	12.7 (11.5–12.9)	0.66
Hb d14	12.0 (10.9–12.6)	11.7 (10.5–12.6)	12.2 (11.9–12.6)	0.33	12.5 (12.2–12.8)	11.9 (10.5–12.5)	0.11
ΔHb d0–d3	−0.4 (−0.8 to 0.0)	−0.5 (−1.0 to −0.3)	−0.1 (−0.6 to 0.6)	0.07	−0.4 (−1.1 to 0.7)	0.1 (−0.2 to 0.6)	0.40
ΔHb d3–d7	0.0 (−0.8 to 0.5)	0.3 (0.3–0.8)	−0.8 (−1.5 to −0.1)	0.007	−0.3 (−0.6 to 0.2)	−1.5 (−1.7 to −1.0)	NA
ΔHb d7–d14	0.1 (−0.5 to 0.5)	0.3 (0.1–0.5)	−0.4 (−0.9 to 0.1)	0.04	0.0 (−0.4 to 0.4)	−0.8 (−1.2 to −0.3)	NA
ΔHb d3–d14	0.0 (−0.7 to 0.5)	0.3 (−0.1 to 0.7)	−1.3 (−2.0 to −0.3)	0.002	−0.3 (−0.6 to 0.3)	−1.9 (−2.6 to −1.9)	NA
ΔHb d0–d14	−0.7 (−1.1 to 0.1)	−0.4 (−0.8 to 0.4)	−1.3 (−2.1 to −0.3)	0.03	−0.4 (−1.3 to 0.2)	−1.9 (−2.8 to −1.3)	NA
LDH d7, U/L	250 (225–331)	244 (222–274)	327 (229–407)	0.16	329 (211–495)	327 (248–381)	0.77
LDH d14, U/L	256 (210–283)	210 (197–247)	280 (256–365)	0.006	273 (255–394)	298 (234–365)	1.0
RPI d3	0.5 (0.3–0.7)	0.4 (0.2–0.7)	0.7 (0.4–0.7)	0.22	0.7 (0.4–0.7)	0.6 (0.5–0.7)	1.0
RPI d7	1.4 (0.9–1.6)	1.4 (0.9–1.5)	1.3 (0.8–2.0)	0.66	1.7 (1.2–2.7)	1.0 (0.4–1.8)	0.24
RPI d14	1.4 (1.0–1.8)	1.1 (1.0–1.6)	1.9 (1.4–2.6)	0.015	2.5 (1.9–2.9)	1.5 (1.1–1.9)	0.04

*Values are median (interquartile range) or n/N (%). ACT, artemisinin-based combination therapy; ARM, artemether; d, day; Δ, period between indicated days; DHA, dihydroartemisinin; Hb, hemoglobin; LDH, lactate dehydrogenase; LUM, lumefantrine; NA, not applicable; PPQ, piperaquine; RPI, reticulocyte production index.
†Percentage of erythrocytes infected.
‡Hb levels are in grams/deciliter.

posttreatment hemolysis (median change −0.5 g/dL, IQR −1.0 to −0.3; p = 0.07) (Figure 1, panel B). Overall (during days 0–14), patients with posttreatment hemolysis showed a larger decrease in Hb level (median change −1.35 g/dL, IQR −2.1 to −0.3) than did patients without posttreatment hemolysis (median change −0.45 g/dL, IQR −0.8 to 0.4; p = 0.03) (Figure 1, panel A).

Analysis of the course of anemia in the 8 patients with posttreatment hemolysis showed that a decrease in Hb level during days 3–14 occurred in only 4 patients (uncompensated hemolysis). The other 4 patients with hemolysis maintained stable Hb levels during days 3–14 (compensated hemolysis) (Figure 2, Panel C). Consistent with this observation, we found that patients with compensated posttreatment hemolysis showed a higher reticulocyte production index on day 14 than did patients with uncompensated posttreatment hemolysis or without hemolysis on day 14.

No differences were observed in median LDH levels and initial parasitemia between patients with compensated or uncompensated posttreatment hemolysis (Table). All patients with compensated posttreatment hemolysis were of African ethnicity, and all patients with uncompensated posttreatment hemolysis were Caucasian.

Five patients with posttreatment hemolysis (4 patients with uncompensated hemolysis and 1 patient with compensated hemolysis) were followed-up until day 30. All of these patients had persistent low haptoglobin levels (<0.3 g/L) on day 30, and 2 patients still had LDH levels above the age-dependent upper reference level on day 30. Exemplary cases of a patient without hemolysis (Figure 3, panel A), a patient with compensated hemolysis (Figure 3, panel B), and a patient with uncompensated hemolysis (Figure 3, panel C) show the course of laboratory values over time. The patient with compensated hemolysis had a low haptoglobin level
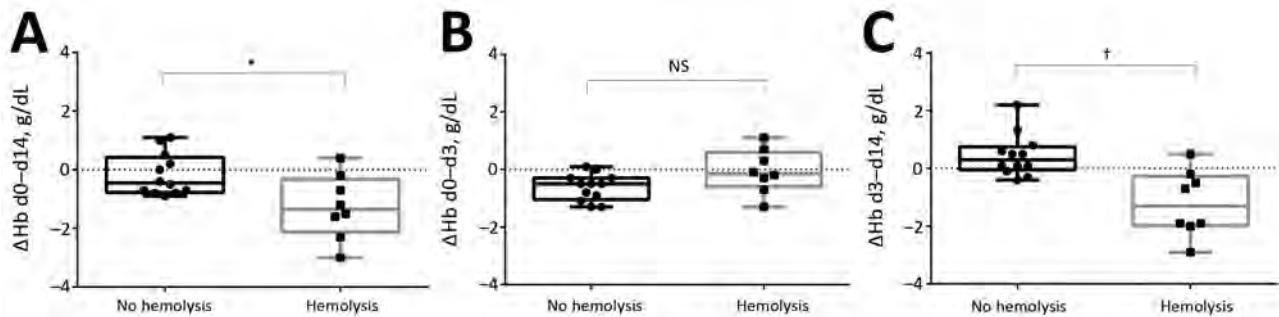
Figure 1. Changes in hemoglobin levels (DHb) for patients with and without posttreatment hemolysis after treatment with oral artemisinin-based combination therapy for uncomplicated *Plasmodium falciparum* malaria. A) Day (d) 0 to d 14 (overall); B) d 0 to d 3 (treatment period); C) d 3 to d 14 (posttreatment period). Horizontal lines indicate median values, boxes indicate interquartile ranges, whiskers indicate ranges, and solid squares and circles indicate individual patient data points. The Mann-Whitney U test was used for comparative analysis. *p<0.05; †p<0.01; NS, not significant.

(<0.3 g/L) and an increased reticulocyte count 8 weeks after treatment on day 56 (Figure 2, panel B).

Immunohematologic testing showed that serum samples from 5 (25%) of 20 patients were reactive only with enzyme-treated erythrocytes after therapy (3 patients with and 2 patients without posttreatment hemolysis). The direct antiglobulin test result was weakly positive for 3 patients; none of them had posttreatment hemolysis. None of the patients with hemolysis showed coating of erythrocytes with IgG, IgM, or C3d.

Discussion

Hemolytic anemia after treatment of severe malaria with intravenous artesunate has been described in malaria-endemic and non–malaria-endemic countries. However, evidence of hemolytic anemia after treatment of malaria with oral ACTs is limited to 2 case reports. Data from the current prospective study confirm our hypothesis that delayed posttreatment hemolysis also occurs after oral artemisinin treatment and provide insight into its frequency and clinical course. In 40% of the patients in our study with uncomplicated malaria and oral ACT treatment, laboratory

signs of hemolysis were detected 2 weeks after therapy. In 5 patients, hemolysis persisted 1 month after treatment. Patients with posttreatment hemolysis showed a larger decrease in Hb levels after treatment than did patients without hemolysis. The intensity of hemolysis was mild compared with that after intravenous artesunate. In many reported cases of PADH after intravenous artesunate, patients received blood transfusions (2,9). In other studies, patients with hemolysis after oral ACT treatment had decreases in Hb levels of 2.1 g/dL–3.6 g/dL in the posttreatment period (11–13).

The decrease in Hb levels during treatment in the current study was smaller in patients with posttreatment hemolysis than in patients without posttreatment hemolysis. Consistent with this finding, we found that the patient group with the largest decrease in Hb levels after treatment (i.e., patients with uncompensated hemolysis) showed a small increase in Hb levels during treatment (Figure 2). This observation could be explained by involvement of once-infected erythrocytes: during treatment, erythrocytes are spared by removal of parasites without destruction of the cell. The Hb level therefore remains stable. After treatment,
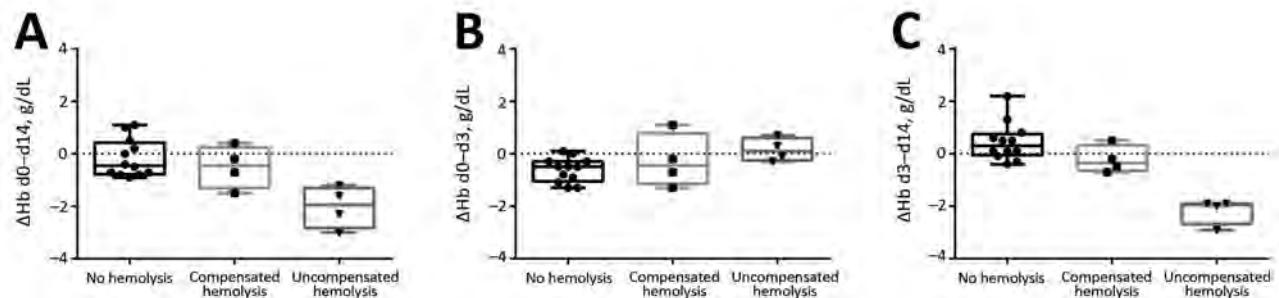
Figure 2. Changes in hemoglobin levels (DHb) for patients without posttreatment hemolysis, with compensated posttreatment hemolysis, and with uncompensated posttreatment hemolysis after treatment with oral artemisinin-based combination therapy for uncomplicated *Plasmodium falciparum* malaria. A) day (d) 0 to d 14 (overall); B) d 0 to d 3 (treatment period); C) d 3 to d 14 (posttreatment period). Horizontal lines indicate median values, boxes indicate interquartile ranges, whiskers indicate ranges, and solid squares, circles, and triangles indicate individual patient data points.
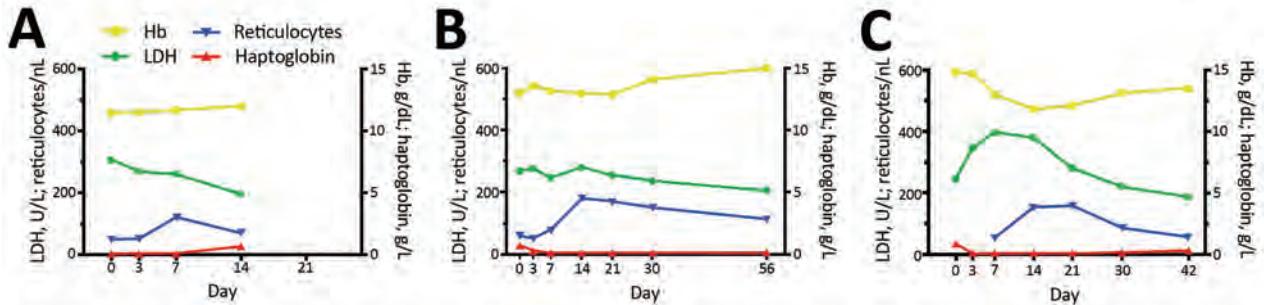
Figure 3. Laboratory values over time for exemplary patients with and without posttreatment hemolysis after treatment with oral artemisinin-based combination therapy for uncomplicated *Plasmodium falciparum* malaria. A) Patient without posttreatment hemolysis, B) patient with compensated posttreatment hemolysis, and C) patient with uncompensated posttreatment hemolysis. Hb, hemoglobin; LDH, lactate dehydrogenase.

the once-infected, pitted erythrocytes hemolyze because of their shorter life spans, which results in a postponed loss of Hb during the posttreatment period (*4*). Our data therefore give additional support to the relevance of this mechanism as a cause of late hemolysis.

Half of the patients with posttreatment hemolysis showed erythropoietic activity at day 14 that was sufficient for compensating the postponed loss of Hb. These patients were all of African origin, unlike those with uncompensated hemolysis, who were all Caucasian. The reason for this observation is unknown. Malaria-related dyserythropoiesis (*14*) might be less pronounced in African patients than in European patients. Impairment of erythropoiesis by artemisinins has been described in vitro (*15*), but no differences regarding ethnicity have been reported.

Different reported clinical courses of delayed hemolysis after artemisinin therapy suggest involvement of mechanisms other than pitting (*4,16*). In some patients, the decrease in Hb level far exceeds the loss of erythrocytes expected from destruction of once-infected erythrocytes (*16*). In a recent case report, drug-dependent autoimmune hemolysis was reported as a probable cause of PADH (*8*). Several other reports failed to demonstrate immune-mediated hemolysis or drug-induced antibodies in patients with severe malaria (*2,9,17*). In our patients, results from immunohematologic testing were inconclusive. No antibody or complement coating of erythrocytes was found that could trigger bystander hemolysis of uninfected erythrocytes.

Baseline Hb levels were comparatively high in our patients. The mild loss of Hb therefore did not result in clinical symptoms. However, in settings in which chronic anemia is common because of concomitant infections and nutritional deficiencies, posttreatment hemolysis after antimalarial treatment might be a clinically relevant factor. Recently, a large study in Nigeria reported a >5% decrease in hematocrit levels in 23% of African children with uncomplicated malaria 14–28 days after ACT treatment (*18*). Although no further assessments were performed in this study, the authors assumed an association with postartemisinin

hemolysis. Further prospective investigations of this phenomenon in malaria-endemic areas are needed and should include markers for detection of hemolysis.

The dataset used for this analysis has several limitations. The most relevant limitation is that this study has, so far, not included patients who are receiving oral antimalarial drugs other than ACTs. At this time, we cannot rule out that similar hemolytic reactions occur after non-ACT antimalarial treatment because no prospective studies are available with a comparable method to detect hemolysis. More data on posttreatment anemia, hemolysis, and erythropoiesis after non-ACT treatment are therefore needed for comparison. However, this analysis also included patients with no evidence of posttreatment hemolysis after malaria and ACT therapy; it is therefore unlikely that hemolysis generally occurs after antimalarial therapy. The main objective of this study was to prospectively collect evidence for posttreatment hemolysis after oral ACT treatment. Some uncertainty might arise from the limited number of patients regarding other conclusions, such as different reticulocyte responses in patients from Africa and Europe. These conclusions have to be confirmed with larger sample sizes.

In conclusion, our study provides evidence that a mild form of posttreatment hemolysis commonly occurs after oral ACT treatment for uncomplicated malaria. The role of this observation for clinical practice in malaria-endemic and non–malaria-endemic settings remains to be defined but should prompt increased vigilance for hemolytic events, particularly for patients with preexisting anemia or those for whom mild anemia constitutes a clinical problem. Larger studies are needed to investigate observations and hypotheses concerning underlying pathophysiology and to eventually identify potential risk factors.

Dr. Kurth is a physician and scientist in the Department of Infectious Diseases and Respiratory Medicine at Charité Medical University, Berlin, Germany, and in the Infectious Disease Control Group at the Centre de Recherches Medicales de Lambaréné, Lambaréné, Gabon. His primary research interests are pathophysiology of malaria and artemisinin treatment.

References

1. World Health Organization. Guidelines for the treatment of malaria. 3rd ed. [cited 2016 Apr 15]. http://www.who.int/malaria/publications/atoz/9789241549127/en/
2. Zoller T, Junghanss T, Kapaun A, Gjorup I, Richter J, Hugo-Persson M, et al. Intravenous artesunate for severe malaria in travelers, Europe. Emerg Infect Dis. 2011;17:771–7. http://dx.doi.org/10.3201/eid1705.101229
3. Arguin PM. Case definition: postartemisinin delayed hemolysis. Blood. 2014;124:157–8. http://dx.doi.org/10.1182/blood-2014-06-578922
4. Jauréguiberry S, Ndour PA, Roussel C, Ader F, Safeukui I, Nguyen M, et al. Postartesunate delayed hemolysis is a predictable event related to the lifesaving effect of artemisinins. Blood. 2014;124:167–75. http://dx.doi.org/10.1182/blood-2014-02-555953
5. Jauréguiberry S, Thellier M, Ndour PA, Ader F, Roussel C, Sonneville R, et al. Delayed-onset hemolytic anemia in patients with travel-associated severe malaria treated with artesunate, France, 2011–2013. Emerg Infect Dis. 2015;21:804–12. http://dx.doi.org/10.3201/eid2105.141171
6. Rolling T, Agbenyega T, Issifou S, Adegnika AA, Sylverken J, Spahlinger D, et al. Delayed hemolysis after treatment with parenteral artesunate in African children with severe malaria: a double-center prospective study. J Infect Dis. 2014;209:1921–8. http://dx.doi.org/10.1093/infdis/jit841
7. Rehman K, Lotsch F, Kremsner PG, Ramharter M. Haemolysis associated with the treatment of malaria with artemisinin derivatives: a systematic review of current evidence. International journal of infectious diseases. Int J Infect Dis. 2014;29:268–73. http://dx.doi.org/10.1016/j.ijid.2014.09.007
8. Raffray L, Receveur MC, Beguet M, Lauroua P, Pistone T, Malvy D. Severe delayed autoimmune haemolytic anaemia following artesunate administration in severe malaria: a case report. Malar J. 2014;13:398. http://dx.doi.org/10.1186/1475-2875-13-398
9. Kreeftmeijer-Vegter AR, van Genderen PJ, Visser LG, Bierman WF, Clerinx J, van Veldhuizen CK, et al. Treatment outcome of intravenous artesunate in patients with severe malaria in the Netherlands and Belgium. Malar J. 2012;11:102. http://dx.doi.org/10.1186/1475-2875-11-102
10. World Health Organization. WHO/GMP information note on delayed haemolytic anaemia following treatment with artesunate, 2013 [cited 2016 Mar 9]. http://www.who.int/malaria/publications/atoz/who_note_delayed_haemolytic_anaemia_oct13.pdf
11. Corpolongo A, De Nardo P, Ghirga P, Gentilotti E, Bellagamba R, Tommasi C, et al. Haemolytic anaemia in an HIV-infected patient with severe falciparum malaria after treatment with oral artemether-lumefantrine. Malar J. 2012;11:91. http://dx.doi.org/10.1186/1475-2875-11-91
12. De Nardo P, Oliva A, Giancola ML, Ghirga P, Mencarini P, Bibas M, et al. Haemolytic anaemia after oral artemether-lumefantrine treatment in a patient affected by severe imported falciparum malaria. Infection. 2013;41:863–5. http://dx.doi.org/10.1007/s15010-013-0451-x
13. Gray AM, Arguin PM, Hamed K. Surveillance for the safety and effectiveness of artemether-lumefantrine in patients with uncomplicated Plasmodium falciparum malaria in the USA: a descriptive analysis. Malar J. 2015;14:349.
14. Haldar K, Mohandas N. Malaria, erythrocytic infection, and anemia. Hematology Am Soc Hematol Educ Program. 2009;87–93. http://dx.doi.org/10.1182/asheducation-2009.1.87
15. Finaurini S, Basilico N, Corbett Y, D'Alessandro S, Parapini S, Olliaro P, et al. Dihydroartemisinin inhibits the human erythroid cell differentiation by altering the cell cycle. Toxicology. 2012;300:57–66. http://dx.doi.org/10.1016/j.tox.2012.05.024
16. Plewes K, Haider MS, Kingston HW, Yeo TW, Ghose A, Hossain MA, et al. Severe falciparum malaria treated with artesunate complicated by delayed onset haemolysis and acute kidney injury. Malar J. 2015;14:246. http://dx.doi.org/10.1186/s12936-015-0760-x
17. Rolling T, Wichmann D, Schmiedel S, Burchard GD, Kluge S, Cramer JP. Artesunate versus quinine in the treatment of severe imported malaria: comparative analysis of adverse events focussing on delayed haemolysis. Malar J. 2013;12:241. http://dx.doi.org/10.1186/1475-2875-12-241
18. Sowunmi A, Akano K, Ayede AI, Ntadom G, Fatunmbi B, Aderoyeje T, et al. Temporal changes in haematocrit following artemisinin-based combination treatments of uncomplicated falciparum malaria in children. BMC Infect Dis. 2015;15:454. http://dx.doi.org/10.1186/s12879-015-1219-y

Address for correspondence: Florian Kurth, Department of Infectious Diseases and Respiratory Medicine, Charité Campus Virchow Klinikum, Südring 2, Augustenburger Platz 1, 13353 Berlin, Germany; email: florian.kurth@charite.de

Enterovirus D68 Infection in Children with Acute Flaccid Myelitis, Colorado, USA, 2014

Negar Aliabadi, Kevin Messacar, Daniel M. Pastula, Christine C. Robinson, Eyal Leshem,
James J. Sejvar, W. Allan Nix, M. Steven Oberste, Daniel R. Feikin, Samuel R. Dominguez

During August 8, 2014–October 14, 2014, a total of 11 children with acute flaccid myelitis and distinctive neuroimaging changes were identified near Denver, Colorado, USA. A respiratory prodrome was experienced by 10, and nasopharyngeal specimens were positive for enterovirus D68 (EV-D68) for 4. To determine whether an association exists between EV-D68 infection and acute flaccid myelitis, we conducted a retrospective case–control study comparing these patients with 2 groups of outpatient control children (1 group tested for acute respiratory illness and 1 for *Bordetella pertussis* infection). Adjusted analyses indicated that, for children with acute flaccid myelitis, the odds of having EV-D68 infection were 10.3 times greater than for those tested for acute respiratory infection and 4.5 times greater than for those tested for *B. pertussis* infection. No statistical association was seen between acute flaccid myelitis and non–EV-D68 enterovirus or rhinovirus infection. These findings support an association between EV-D68 infection and acute flaccid myelitis.

Enterovirus D68 (EV-D68) shares features with rhinoviruses (*1*) and primarily causes respiratory disease. Clusters of respiratory disease caused by EV-D68 have been reported in Asia, Europe, and the United States (*2,3*). Although EV-D68 has been identified in the central nervous system of 2 patients with limb weakness (*4,5*), its role in causing neuroinvasive disease has not been clearly defined.

From August 8, 2014, through October 14, 2014, a cluster of cases of acute limb weakness, cranial nerve dysfunction, or both, in children with characteristic radiologic findings of myelitis were identified at Children's Hospital Colorado (CHCO), in Aurora, Colorado, USA. These cases represented a substantial increase over the number

of children admitted with this same constellation of signs and symptoms in the previous 4 years at CHCO (*6–8*). This cluster prompted the Centers for Disease Control and Prevention (CDC) to create a case definition for acute flaccid myelitis (AFM; a subset of acute flaccid paralysis, characterized by appearance of myelitis on radiologic scans) and publish a national call for cases through a health alert announcement (*9*), which led to identification of cases nationally (*10*) and an additional case in Colorado.

The Colorado AFM cluster occurred during an outbreak of EV-D68 respiratory disease (*3*). During this period, CHCO emergency department visits and admissions for respiratory complaints to the hospital increased over prior years (*11*); EV-D68 detection among hospitalized patients subsequently increased (*7*). Although no etiology for the neurologic disease was identified among the Colorado cluster of patients (despite extensive testing, including metagenomic sequencing of cerebrospinal fluid), EV-D68 was found in the nasopharynx of 45% of these patients (*7,12*). We further investigated a possible epidemiologic association between EV-D68 and AFM by conducting a case–control study comparing the presence of EV-D68 in upper respiratory specimens of case-patients and 2 groups of control children. This analysis was determined by human subjects review at CDC and CHCO to be nonresearch and was conducted as a public health investigation.

Methods

Study Design and Setting

We conducted a retrospective case–control study of children who had received medical care for any illness necessitating collection of nasopharyngeal specimens for respiratory pathogen testing in Colorado during August 3, 2014–October 18, 2014 (the epidemiologic weeks when confirmed AFM cases were identified). AFM case-patients were defined as children <21 years of age who had acute neurologic illness characterized by focal weakness of ≥1 limbs, magnetic resonance imaging (MRI) findings of spinal cord lesions largely restricted to gray matter, and no identified etiology, per CDC case definition (*6,7,9,10*).

We also identified 2 control groups of children for whom nasopharyngeal specimens had been obtained while they were CHCO outpatients during the study period. We selected outpatients as controls because most AFM case-patients had respiratory signs and symptoms and were evaluated as outpatients before neurologic symptoms developed. The first control group (respiratory pathogen panel [RPP]–tested controls) included children who were evaluated as outpatients and for whom nasopharyngeal specimens had been tested by multiplex RPP PCR (FilmArray; BioFire Diagnostics LLC, Salt Lake City, UT, USA), which detects adenovirus; coronaviruses HKU1, NL63, 229E, OC43; influenza viruses A(H1N1)pdm09, A(H3), and B; meta-pneumovirus, parainfluenza viruses 1–4; respiratory syncytial viruses A and B; enterovirus/rhinovirus; *Bordetella pertussis*; *Chlamydophila pneumoniae;* and *Mycoplasma pneumoniae*. The second control group (*B. pertussis* [BP]–tested controls) included children who were evaluated as outpatients and who had nasopharyngeal specimens obtained for PCR testing for *B. pertussis*. We excluded from the study infants <12 months of age and children >18 years of age because AFM patients in these age groups had not been identified in Colorado during this period. If multiple specimens from the same child were submitted for testing from different times during the study, only the first was included. Specimens submitted for RPP and BP testing from the same child and on the same date were considered for the RPP analysis only.

We also analyzed results of FilmArray testing for all patients admitted to the pediatric intensive care unit (PICU) at CHCO during July–November 2014. We chose this population because all patients admitted with respiratory symptoms routinely undergo FilmArray testing and results would provide a representative view of pathogens circulating in the community and resulting in severe respiratory illness at the time of the outbreak.

Laboratory Testing

Nasopharyngeal specimens from AFM patients were initially tested by using the FilmArray panel, which has a sensitivity of 83.7% and a specificity of 100% for detecting enteroviruses and rhinoviruses but is unable to distinguish between them (13). Specimens positive for enterovirus/rhinovirus were sent to CDC for enterovirus viral protein (VP) 1 seminested reverse transcription PCR (RT-PCR) (14), followed by molecular sequencing of the VP1 amplicons. In October 2014, a new, highly sensitive, EV-D68 real-time RT-PCR (rRT-PCR) assay was developed at CDC (15), and samples from all AFM patients were also tested by using this assay. FilmArray testing was first conducted for the RPP-tested controls; specimens that were positive for enterovirus/rhinovirus were subsequently sent to CDC, along with all BP-tested specimens. At CDC, the RPP- and

BP-tested control specimens were tested by using an rRT-PCR assay for pan-enteroviruses, which performs similarly to the VP1 seminested PCR assay (16). Specimens were also tested by rRT-PCR for EV-D68. All specimens positive by pan-enterovirus RT-rPCR that were not EV-D68 were also molecularly sequenced for virus identification. Samples from PICU patients were tested first with the FilmArray panel at CHCO; positive samples were sent to CDC, where they underwent the same series of testing as controls.

Main Exposure and Covariates

The main exposure of interest was EV-D68 infection, defined as positive EV-D68 results obtained by rRT-PCR of a nasopharyngeal specimen. The second exposure of interest was infection with another enterovirus/rhinovirus, defined as a positive result by pan-enterovirus rRT-PCR but a negative result by EV-D68 rRT-PCR; that is, infection with any enteroviruses/rhinoviruses other than EV-D68. This group, referred to as enteroviruses/rhinoviruses excluding EV-D68, was chosen to provide a comparison with the EV-D68–positive group. Covariates included continuous variables (age, sex, days between symptom onset and collection of nasopharyngeal specimen, epidemiologic week of naso-pharyngeal specimen collection) and categorical variables (fever [yes/no]; upper and/or lower respiratory symptoms including nasal congestion, rhinorrhea, sore throat, cough, wheeze, or respiratory distress [yes/no]; hospitalization for respiratory symptoms [yes/no]; and type of nasopharyngeal specimen obtained [swab/aspirate]). Although enterovirus detection in nasopharyngeal aspirates and nasopharyngeal swab samples is similar, more pathogens might be identified in nasopharyngeal swab samples (17). To ensure that no differences existed between groups with regard to this variable, we included it in our models.

Statistical Analyses

Descriptive analyses reported characteristics of the AFM case-patients and control children. Medians and interquartile ranges were provided for age and days between symptom onset and collection of nasopharyngeal specimen because these variables were not normally distributed. Proportions were reported for categorical variables. The nonparametric Wilcoxon-Mann-Whitney 2-sample test was used to detect significant differences between continuous variables and between proportions for categorical variables. Those variables that differed significantly between AFM case-patients and controls (p<0.1) were included in the adjusted multivariable models, with the exception of epidemiologic week of sample collection, which was included in the adjusted models regardless of statistical significance. Models assessing AFM case-patients versus RPP-tested controls were adjusted for age, time between respiratory symptom

onset and specimen collection, and epidemiologic week of specimen collection. Models assessing AFM case-patients versus BP-tested controls were adjusted for type of nasopharyngeal specimen, presence of fever, and epidemiologic week of sample collection. We report odds ratios, 95% CIs, and p values from logistic regression analyses in our models performed by using exact conditional analysis for small sample sizes. In the multivariable models, p<0.05 was considered statistically significant.

We tested 2 models for comparisons between AFM and each control group. Model 1 tested the association between EV-D68 and AFM; model 2 tested the association between enterovirus/rhinovirus excluding EV-D68 and AFM. To determine the sensitivity of our models among cases of neurologic weakness, which included acute cranial nerve deficits with or without limb weakness, we also conducted a sensitivity analysis among all patients in Colorado with acute neurologic weakness for whom nasopharyngeal specimens were available. Models and covariates used for this analysis were the same as those used in the main analysis. All analyses were performed with SAS statistical software package version 9.3 (SAS Institute, Inc., Cary, NC, USA).

Results

The peak of AFM diagnoses coincided with the peak of EV-D68 respiratory infection detections at CHCO (6,7). Viral analyses of the specimens from PICU patients indicated that the predominant virus causing severe respiratory illness during the outbreak was EV-D68, followed by enterovirus/rhinovirus species excluding EV-D68 (Figure 1). Of the 203 specimens from PICU patients that were positive by RPP and sent to CDC for further testing, 100 (49%) were positive for EV-D68 (Figure 2). Among the other enterovirus/rhinovirus species, no predominant virus was

in circulation. These species included human rhinoviruses, echoviruses, and coxsackieviruses A and B; some specimens could not be typed.

Overall, during the outbreak period in Colorado, we identified 13 patients who had acute neurologic disease with limb weakness, cranial nerve dysfunction, or both. Use of the CDC AFM case definition resulted in exclusion of 2 patients with acute neurologic disease who did not have limb weakness but who had cranial nerve deficits only. Of the remaining 11 patients, 10 were reported from CHCO and 1 was reported from another Denver metropolitan area hospital. From CHCO, we identified 105 RPP-tested controls and 232 BP-tested controls. All AFM patients had an antecedent acute illness; most (91%) reported respiratory illness (Table 1).

Comparing AFM case-patients with RPP-tested controls, we found that AFM case-patients were older (median age 8 years vs. 5 years, respectively; p = 0.05) and that specimens from AFM case-patients were collected later than specimens from RPP-tested controls (median 10 vs. 5 days after respiratory symptom onset, respectively; p<0.001). We found no statistically significant differences between these 2 groups with regard to sex, presence of upper or lower respiratory symptoms, presence of fever, hospitalizations for respiratory symptoms, type of specimen obtained, or epidemiologic week of specimen collection.

Comparing AFM case-patients with BP-tested controls, we found that AFM case-patients were more often febrile (91% vs. 32%, respectively; p<0.001) and had fewer nasopharyngeal specimens collected by swab than by aspiration (55% vs. 83%, respectively; p = 0.04). We found no statistically significant differences between these 2 groups with regard to sex, age, presence of respiratory symptoms, hospitalizations for respiratory symptoms, timing of specimen
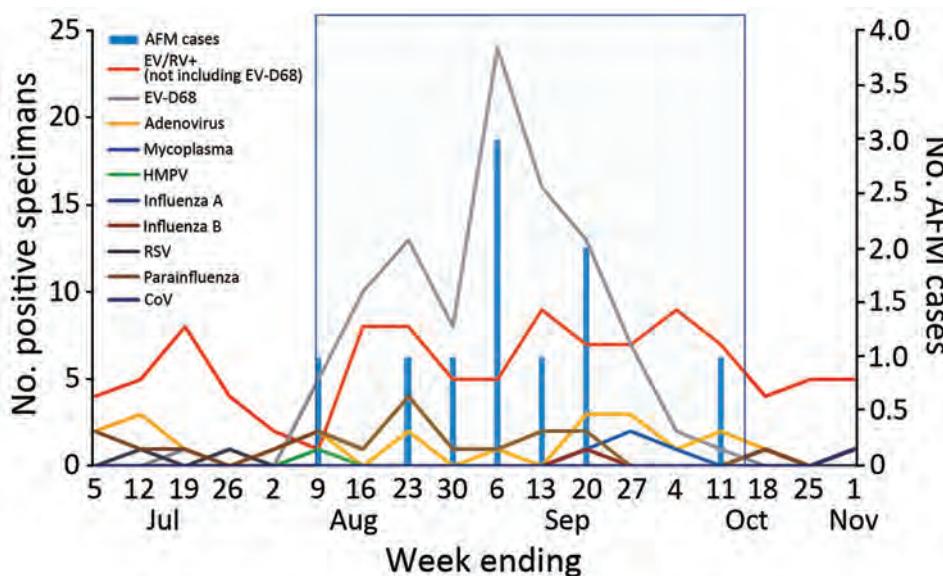
Figure 1. Pathogens isolated from patients with acute flaccid myelitis and from patients in a pediatric intensive care unit, Colorado, USA, July–November, 2014. Box indicates study period. AFM, acute flaccid myelitis; CoV, coronavirus; EV, enterovirus; HMPV, human metapneumovirus; RPP, respiratory pathogen panel; RSV, respiratory syncytial virus; RV, rhinovirus.
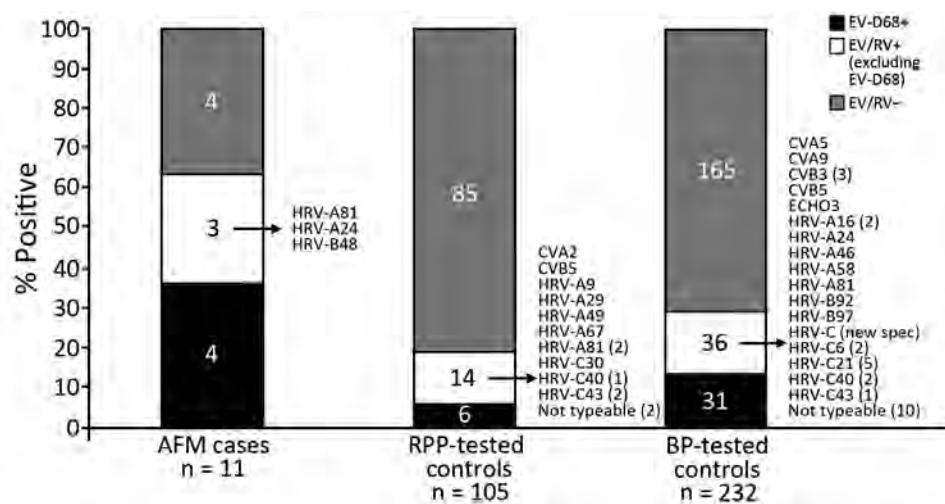
Figure 2. Results of enterovirus testing among case-patients and controls in study of acute flaccid myelitis, Colorado, USA, July–November, 2014. Arrows indicate specific strains identified in those specimens; numbers in parentheses indicate number of that type of strain. AFM, acute flaccid myelitis; BP, *Bordetella pertussis*; CV, coxsackievirus; echo, echovirus; EV, enterovirus; HRV, human rhinovirus; RPP, respiratory pathogen panel; RV, rhinovirus; RPP, respiratory pathogen panel.

collection, and epidemiologic week of specimen collection. Furthermore, epidemiologic week of specimen collection was not found to be a confounder (data not shown).

Of the 11 AFM case-patients, 4 were infected with EV-D68, 4 were negative for enterovirus/rhinovirus according to pan-enteroviral RT-PCR, and 3 were positive according to pan-enteroviral RT-PCR; further typing of specimens from these 3 patients indicated a variety of rhinoviruses (Figure 3). One case-patient who was initially negative according to VP1 testing had a positive result on EV-D68 rRT-PCR, which was confirmed on repeat analysis. This discordance resulted from low EV-D68 RNA copy numbers in the specimen, at the limit of detection for both assays. The EV-D68 rRT-PCR cycle threshold for this specimen was 43.9 with a clear sigmoid curve. Given that we used the EV-D68 rRT-PCR for case-patients and controls, this patient was classified as EV-D68 positive.

Among the AFM case-patients, characteristics did not differ among those positive and those negative for EV-D68 (data not shown). EV-D68 was detected more frequently in the nasopharyngeal specimens of AFM case-patients than in those of RPP-tested controls (36% vs. 6%, respectively; p = 0.02) and BP-tested controls (36% vs. 13%, respectively; p = 0.03) (Table 1). The non–EV-D68 enterovirus/rhinoviruses

Table 1. Characteristics of patients with acute flaccid myelitis and control patients, Colorado, August 3–October 18, 2014*

Characteristic	Case-patients, n = 11	Control patients			
		RPP-tested†	p value	BP-tested‡	p value
Sex, no. (%)					
M	8 (73)	62 (59)	0.52	124 (53)	0.24
F	3 (27)	43 (41)	NA	108 (47)	NA
Age, y, median (IQR, range)	8 (9, 1–18)	5 (8, 1–18)	0.05	7 (8, 1–18)	0.14
Respiratory symptoms, no. (%)	10 (91)	82 (79)§	0.69	221 (97)¶	0.25
Fever, no. (%)	10 (91)	79 (76)§	0.45	73 (32)#	<0.001
Hospitalized for respiratory symptoms, no. (%)	0	11 (11)**	0.60	12 (5)¶	1.00
Enterovirus testing, no. (%)					
EV/RV negative	4 (36)	85 (81)	NA	165 (71)	NA
EV/RV positive, excluding EV-D68	3 (27)	14 (13)	0.08††	36 (16)	0.12††
EV-D68 positive	4 (36)	6 (6)	0.02‡‡	31 (13)	0.03‡‡
Type of specimen, no. (%)					
Nasopharyngeal swab	6 (55)	57 (54)	1.00	192 (83)	0.04
Nasopharyngeal aspirate/wash	5 (45)	48 (46)	NA	40 (17)	NA
Time to specimen collection, d, median (IQR, range)§§	10 (7, 7–36)	5 (5, 0–31)¶¶	<0.001	14 (14, 1–120)##	0.91
Epidemiologic wk of specimen collection, median (range)	37 (33–42)	38 (32–42)	0.58	38 (32–42)	0.89

*BP, *Bordetella pertussis*; EV, enterovirus; IQR, interquartile range; NA, not applicable; RPP, respiratory pathogen panel; RV, rhinovirus.
†Unless otherwise stated, denominator is 105 for RPP-tested controls.
‡Unless otherwise stated, denominator is 232 for BP-tested controls. Denominators vary slightly because some observations were missing for covariates.
§n = 104.
¶n = 227.
#n = 226.
**n = 103.
††p value comparing EV/RV-positives excluding EV-D68 with EV/RV negatives.
‡‡p value comparing EV-D68 with EV/RV-negatives.
§§No. days between symptom onset and collection of nasopharyngeal specimen.
¶¶n = 102.
##n = 222.

Figure 3. Sequencing results for 203 specimens from patients in a pediatric intensive care unit, Colorado, USA, 2014. All respiratory pathogen panel–positive samples were sent to the Centers for Disease Control and Prevention for further testing. Of these, 148 were positive by EV RT-PCR and 55 were negative by pan-EV RT-PCR. The 148 specimens positive by pan-EV RT-PCR were tested by EV-D68 real-time RT-PCR, and of these, 100 were positive (EV-D68). The remaining non–EV-D68 specimens were sent for molecular sequencing and were identified as 26 various HRVs, 4 echoviruses, and 3 CVs; 16 specimens were not typeable. One specimen was co-infected with HRV and CV. CV, coxsackievirus; EV, enterovirus: HRV, human rhinoviruses; RT-PCR, reverse transcription PCR.
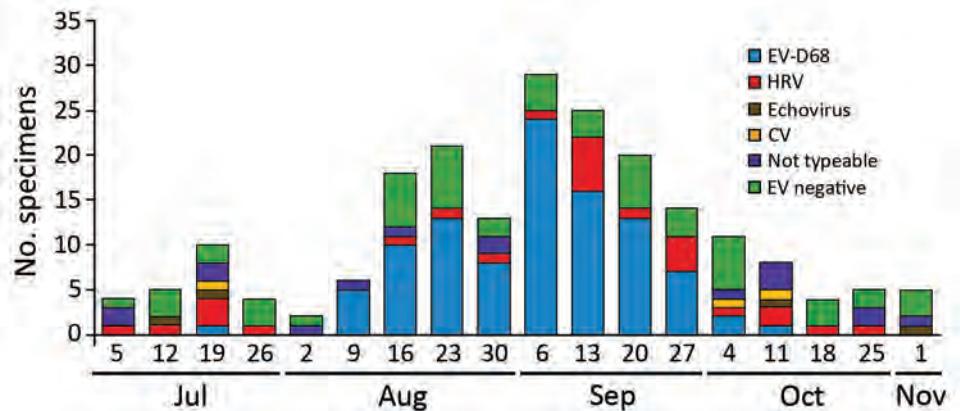
among the control groups included a mixture of coxsackieviruses, echoviruses, and rhinoviruses; some samples could not be typed. The odds of EV-D68 infection for AFM case-patients compared with RPP-tested controls were 10.3 (95% CI 1.8–64.8) when adjusted for age, days between respiratory symptoms and nasopharyngeal specimen collection, and the epidemiologic week of specimen collection (Table 2). The odds of EV-D68 infection for AFM case-patients compared with BP-tested controls were 4.5 (95% CI 1.0–21.2) when adjusted for the presence of fever, type of specimen collected, and epidemiologic week of specimen collection (Table 3). In this latter model, the odds of fever for AFM case-patients were nearly 19 times that for BP-tested controls. We found no association between enterovirus/rhinovirus excluding EV-D68 and AFM in comparison with either control group. Although epidemiologic week of specimen collection did not differ between groups (Table 1), this variable was further tested as a possible confounder in all models and did not meet criteria (data not shown).

Sensitivity Analysis

We conducted a sensitivity analysis and included children who met the original Colorado case definition. This definition included 2 patients with cranial nerve dysfunction who did not meet the CDC AFM case definition criteria because they lacked acute limb weakness, compatible spinal MRI findings, or both (7). A nasopharyngeal specimen was collected from only 1 of these 2 patients and was positive for EV-D68, yielding 12 cases in this subanalysis. These results did not differ appreciably from those of the main analysis (Table 4).

Discussion

Our study demonstrated an epidemiologic association between EV-D68 infection and AFM among children during

the 2014 Colorado outbreak. The odds of EV-D68 infection were 10 times higher for children with AFM than for RPP-tested controls and 4.5 times higher than for BP-tested controls. The odds of fever were also higher for AFM case-patients than for BP-tested controls; this finding was not surprising, given the clinical picture associated with pertussis. The elevated odds of EV-D68 infection for AFM case-patients compared with RPP-tested controls suggest that the prevalence of EV-D68 infection among these AFM case-patients was not likely to reflect background circulation of the virus during the outbreak. Moreover, during the outbreak, this association seems to be unique to EV-D68 because infection with other enteroviruses, rhinoviruses, or other common respiratory pathogens identified through FilmArray was not significantly associated with AFM.

Age was a confounder in this analysis. RPP-tested controls were younger, reflecting the median 5 years of age reported during the 2014 EV-D68 respiratory outbreak (18). The older age of the AFM case-patients was similar to the median 7.6 years reported in the US description of AFM cases (10). However, data from Europe and Wales describe similar disease in younger children. In a report of 3 cases of neurologic dysfunction and laboratory evidence of EV-D68 infection in Europe, these patients were 4, 5, and 6 years of age (19,20). In addition, in Wales, the ages of a cluster of 4 children with acute flaccid paralysis (3 who had respiratory symptoms preceding the acute flaccid paralysis and 2 who were positive for EV-D68) was predominantly <2 years (21). These slightly discrepant data may be indicative of the small sample size of AFM cases and highlight the need for continued surveillance to better define the epidemiology of AFM cases.

The prevalence of EV-D68 in the nasopharyngeal specimens of the controls in our study (6%–13%) was

Table 2. EV-D68 and EV/RV association with acute flaccid myelitis compared with RPP-tested controls, Colorado, USA, 2014*

Model	RPP-tested controls	
	Unadjusted models, OR (95% CI)	Adjusted models, OR (95% CI)
EV-D68	9.1 (1.9–42.0)†	10.3 (1.8–64.8)‡
Patient age	NA	1.0 (0.9–1.2)
Time to specimen collection	NA	1.1 (1.0–1.2)
Epidemiologic wk of specimen collection	NA	0.9 (0.7–1.3)
EV/RV excluding EV-D68	4.5 (0.8–23.9)§	6.9 (0.8–66.0)¶
Patient age	NA	1.1 (0.9–1.3)
Time to specimen collection	NA	1.1 (1.0–1.2)
Epidemiologic wk of specimen collection	NA	0.9 (0.6–1.2)

*Denominators vary slightly within models because some observations were missing for covariates. EV, enterovirus; NA, not applicable; OR, odds ratio; RPP, respiratory pathogen panel; RV, rhinovirus.
†n = 105.
‡n = 102.
§n = 99.
¶n = 96.

lower than expected, given the common presence of EV-D68 in PICU patients. Although the rate of EV-D68 in communities during the 2014 US outbreak is unknown, data from other EV-D68 respiratory illness outbreaks in Asia and Europe suggest a similar low prevalence rate of EV-D68 positivity in nasopharyngeal specimens: 2.3%–10.9% among hospitalized children with respiratory symptoms (2,22–25) and 2.0% among outpatients with respiratory symptoms (25). The prevalence of EV-D68 among the controls was much lower than that seen among PICU patients, suggesting either a disproportionately high acuity of EV-D68 respiratory disease testing or selective testing by clinicians in the outpatient setting compared with the intensive care setting. As the outbreak was

Table 3. EV-D68 association with acute flaccid myelitis compared with BP-tested controls, Colorado, USA, 2014*

Model	BP-tested controls	
	Unadjusted models, OR (95% CI)	Adjusted models, OR (95% CI)
EV-D68	3.7 (0.9–13.5)†	4.5 (1.0–21.2)‡
Fever	NA	18.9 (3.0–424.1)
Type of specimen	NA	0.2 (0.05–0.9)
Epidemiologic wk of specimen collection	NA	1.0 (0.8–1.3)
EV/RV excluding EV-D68	3.4 (0.6–17.2)§	2.5 (0.4–13.9)¶
Fever	NA	11.6 (1.6–276.5)
Type of specimen	NA	0.2 (0.04–1.2)
Epidemiologic wk of specimen collection	NA	1.1 (0.8–1.4)

*Denominators vary slightly within models because some observations were missing for covariates. BP, *Bordetella pertussis*; EV, enterovirus; NA, not applicable; OR, odds ratio; RV, rhinovirus.
†n = 232.
‡n = 226.
§n = 201.
¶n = 195.

progressing, the official CHCO respiratory illness algorithm discouraged clinicians from testing all children with respiratory symptoms seen in emergency or outpatient settings for EV-D68 because the clinical management would not change for those who were treated as outpatients. As such, children with routine respiratory symptoms seen in the emergency room, urgent care, or other outpatient clinics were not being sampled for EV-D68, and children who were infected would have been missed. We tried to account for the potential decline in outpatient testing in 2 ways. First, although we did not find week of specimen collection to be a statistical confounder, we nonetheless included it in the multivariable model. Second, we chose an additional control group of children tested for *B. pertussis*. The clinical syndrome of pertussis in these children probably differed from the respiratory symptoms among children with acute respiratory illness, and the BP-tested children were probably sampled more systematically to rule out *B. pertussis* infection. These specimens were thus less likely to have a testing bias than were those from the RPP-tested control group. In the BP-tested controls, we saw a positive association between AFM case-patients and the presence of EV-D68.

A similar clinical presentation of some other picornaviruses lends biological plausibility to the association of EV-D68 and AFM. Enteroviruses such as enterovirus A71 (EV-A71) and poliovirus cause neurologic syndromes including acute flaccid paralysis, aseptic meningitis, and rhomboencephalitis. The MRI findings for the cluster of children in our study are similar to those induced by EV-A71 and poliovirus, both of which show tropism for the anterior horn cells of the spinal cord, although they infrequently infect the central nervous system (26,27). Similar to EV-D68, EV-A71 was initially linked to nonneurologic syndromes, specifically herpangina and hand, foot, and mouth disease, before outbreak data conclusively revealed an association between EV-A71 and neurologic syndromes. Other studies of the 2014 cluster of AFM cases have detected EV-D68 in the upper respiratory tract and, in 1 patient, in blood (10,12). However, EV-D68 is expected to be found at these sites in persons with EV-D68 respiratory illness, and detection of EV-D68 in these specimens does not prove causation of AFM. Identification of EV-D68 in cerebrospinal fluid, which provides the most definitive evidence of causation, was not reported from the 2014 cluster. Nonetheless, our study compares EV-D68 detection in AFM case-patients with detection in contemporaneous control patients with mild respiratory illness, lending additional epidemiologic support to the ecologic association between EV-D68 and AFM.

Our analysis was subject to several limitations. First, although an ideal control group would have included

Table 4. EV-D68 association with acute neurologic disease compared with that of RPP-tested and BP–tested controls, adjusted models*

Exposure	RPP-tested controls†		BP-tested controls‡	
	OR (95% CI)	p value	OR (95% CI)	p value
EV-D68	12.9 (2.5–76.4)†	0.002	5.7 (1.3–25.5)‡	0.02
EV/RV excluding EV-D68	6.9 (0.8–66.0)§	0.08	2.5 (0.4–13.9)¶	0.30

*Of 13 cases of neurologic disease identified in Colorado during the outbreak period, only 12 provided nasopharyngeal specimens for analysis. RPP models were adjusted for age, time to specimen collection, epidemiologic week of sample collection. *B. pertussis* models were adjusted for presence of fever, type of specimen collected, and epidemiologic week of specimen collection. BP, *Bordetella pertussis*; EV, enterovirus; OR, odds ratio; RPP, respiratory pathogen panel; RV, rhinovirus.
†n = 102.
‡n = 226.
§n = 96.
¶n = 195.

population-based sampling of all age-appropriate children in the Denver metropolitan area who did not have AFM during the outbreak, such a group was logistically not possible. Therefore, we used retrospective outpatient controls for whom RT-PCR diagnostic testing was performed at the discretion of providers at CHCO and specimens were retained and available for further testing. As such, our controls probably do not reflect all children in the community, and the sample might have been biased, representative only of children with mild respiratory symptoms not requiring hospitalization. The higher prevalence of EV-D68 among PICU patients suggests that prevalence in the community is higher than in the sample of children with mild respiratory symptoms for whom upper respiratory specimens were collected. However, given that most of the AFM case-patients were children with a mild respiratory prodrome, our control groups were more representative of the degree of respiratory illness seen in the case-patients than in PICU patients. Second, respiratory specimens were obtained after a much shorter interval from patients in the RPP-control group than from patients in the AFM case-patient and BP-control groups. This delay might have led to a lower prevalence of EV-D68 (or other pathogens) in these latter 2 groups than would have been found if testing had been performed sooner (*28*). Third, nasopharyngeal specimens are not sterile; presence of viruses in these samples might be coincidental and not causative of AFM. The association of the presence of EV-D68 in the nasopharynx and AFM might also have been biased by an unmeasured or unrecognized confounder. Fourth, RPP-negative specimens at CHCO were not sent to CDC for enterovirus/rhinovirus and EV-D68 rRT-PCR testing. Although sensitivity of the FilmArray assay is 83.7%, this test may have missed EV-D68–positive cases. Fifth, we also noted positive measures of association between non–EV-D68 enterovirus/rhinovirus exposure and AFM among both control groups, although neither association was statistically significant. However, this analysis did not have an adequate sample size to enable further exploration of this association. Last, although our models included a variable

for the timing of specimen collection, because of the limited sample size of AFM case-patients we were unable to completely control for this variable through analyses that more closely matched with time of specimen collection (not shown).

In conclusion, we found an epidemiologic association between AFM and EV-D68 infection among children with respiratory illness during 2014 in Colorado. This finding goes beyond previously reported temporal associations between AFM clusters with increases in hospital admissions for respiratory symptoms and detection of EV-D68 in AFM case-patients. These epidemiologic data, combined with the biological plausibility of this association, suggest a possible causal link; however, a gap remains between the epidemiologic data and the data from extensive testing of laboratory specimens. CDC recommends continued surveillance, and a revised case definition without age restrictions has been implemented (*29*). For further investigation of this association, improved surveillance for AFM with timely and comprehensive specimen collection and testing for EV-D68 are needed.

Dr. Aliabadi is an Epidemic Intelligence Service officer in the National Center for Immunization and Respiratory Diseases at CDC and a board-certified physician specialized in internal medicine. In addition to acute flaccid myelitis, her research interests include surveillance for rotavirus before and after rotavirus vaccine introduction in resource-poor settings and epidemiologic and infection control support for the Ebola response in West Africa.

References

1. Oberste MS, Maher K, Schnurr D, Flemister MR, Lovchik JC, Peters H, et al. Enterovirus 68 is associated with respiratory illness and shares biological features with both the enteroviruses and the rhinoviruses. J Gen Virol. 2004;85:2577–84. http://dx.doi.org/10.1099/vir.0.79925-0

2. Imamura T, Fuji N, Suzuki A, Tamaki R, Saito M, Aniceto R, et al. Enterovirus 68 among children with severe acute respiratory infection, the Philippines. Emerg Infect Dis. 2011;17:1430–5.

3. Midgley CM, Jackson MA, Selvarangan R, Turabelidze G, Obringer E, Johnson D, et al. Severe respiratory illness associated with enterovirus D68—Missouri and Illinois, 2014. MMWR Morb Mortal Wkly Rep. 2014;63:798–9.

4. Kreuter JD, Barnes A, McCarthy JE, Schwartzman JD, Oberste MS, Rhodes CH, et al. A fatal central nervous system enterovirus 68 infection. Arch Pathol Lab Med. 2011;135:793–6.

5. Khetsuriani N, Lamonte-Fowlkes A, Oberst S, Pallansch MA; Centers for Disease Control and Prevention. Enterovirus surveillance—United States, 1970–2005. MMWR Surveill Summ. 2006;55:1–20.

6. Pastula DM, Aliabadi N, Haynes AK, Messacar K, Schreiner T, Maloney J, et al. Acute neurologic illness of unknown etiology in children—Colorado, August–September 2014. MMWR Morb Mortal Wkly Rep. 2014;63:901–2.

7. Messacar K, Schreiner TL, Maloney JA, Wallace A, Ludke J, Oberste MS, et al. A cluster of acute flaccid paralysis and cranial nerve dysfunction temporally associated with an outbreak of enterovirus D68 in children in Colorado, USA. Lancet. 2015;385:1662–71. http://dx.doi.org/10.1016/S0140-6736(14)62457-0

8. Maloney JA, Mirsky DM, Messacar K, Dominguez SR, Schreiner T, Stence NV. MRI findings in children with acute flaccid paralysis and cranial nerve dysfunction occurring during the 2014 enterovirus D68 outbreak. AJNR Am J Neuroradiol. 2015;36:245–50. http://dx.doi.org/10.3174/ajnr.A4188

9. Centers for Disease Control and Prevention. Acute neurological illness with focal limb weakness of unknown etiology in children. Health Alert Network. 2014 [cited 2016 Feb 1]. http://emergency.cdc.gov/HAN/han00370.asp

10. Division of Viral Diseases, National Centers for Immunization and Respiratory Diseases, Centers for Disease Control and Prevention; Division of Vector-Borne Diseases, Division of High-Consequence Pathogens and Pathology, National Center for Emerging and Zoonotic Infectious Diseases, Centers for Disease Control and Prevention; Children's Hospital Colorado, Council of State and Territorial Epidemiologists. Notes from the field: acute flaccid myelitis among persons aged ≤21 years—United States, August 1–November 13, 2014. MMWR Morb Mortal Wkly Rep. 2015;63:1243–4.

11. Messacar K, Hawkins SM, Baker J, Pearce K, Tong S, Dominguez SR, et al. Resource burden during the 2014 enterovirus D68 respiratory disease outbreak at Children's Hospital Colorado: an unexpected strain. JAMA Pediatr. 2016;170:294–7.

12. Greninger AL, Naccache SN, Messacar K, Clayton A, Yu G, Somasekar S, et al. A novel outbreak enterovirus D68 strain associated with acute flaccid myelitis cases in the USA (2012–14): a retrospective cohort study. Lancet Infect Dis. 2015;15:671–82. http://dx.doi.org/10.1016/S1473-3099(15)70093-9

13. Popowitch EB, O'Neill SS, Miller MB. Comparison of the Biofire FilmArray RP, Genmark eSensor RVP, Luminex xTAG RVPv1, and Luminex xTAG RVP fast multiplex assays for detection of respiratory viruses. J Clin Microbiol. 2013;51:1528–33. http://dx.doi.org/10.1128/JCM.03368-12

14. Nix WA, Oberste MS, Pallansch MA. Sensitive, seminested PCR amplification of VP1 sequences for direct identification of all enterovirus serotypes from original clinical specimens. J Clin Microbiol. 2006;44:2698–704. http://dx.doi.org/10.1128/JCM.00542-06

15. Centers for Disease Control and Prevention. Enterovirus D68 2014 real-time RT-PCR assay [cited 2015 Jul 1]. http://www.fda.gov/downloads/MedicalDevices/Safety/Emergency-Situations/UCM446784.pdf

16. Oberste MS, Penaranda S, Rogers SL, Henderson E, Nix WA. Comparative evaluation of TaqMan real-time PCR and semi-nested VP1 PCR for detection of enteroviruses in clinical specimens. J. Clin Virol. 2010;49:73–4. http://dx.doi.org/10.1016/j.jcv.2010.06.022 PMID: 20667767

17. Heikkinen T, Marttila J, Salmi AA, Ruuskanen O. Nasal swab versus nasopharyngeal aspirate for isolation of respiratory viruses. J Clin Microbiol. 2002;40:4337–9. http://dx.doi.org/10.1128/JCM.40.11.4337-4339.2002

18. Midgley CM, Watson JT, Nix WA, Curns AT, Rogers SL, Brown BA, et al. Severe respiratory illness associated with a nationwide outbreak of enterovirus D68 in the USA (2014): a descriptive epidemiological investigation. Lancet Respir Med. 2015;3:879–87. http://dx.doi.org/10.1016/S2213-2600(15)00335-5

19. Lang M, Mirand A, Savy N, Henquell C, Maridet S, Perignon R, et al. Acute flaccid paralysis following enterovirus D68 associated pneumonia, France, 2014. Euro Surveill. 2014;19;pii:20952.

20. Pfeiffer HC, Bragstad K, Skram MK, Dahl H, Knudsen PK, Chawla MS, et al. Two cases of acute severe flaccid myelitis associated with enterovirus D68 infection in children, Norway, autumn 2014. Euro Surveill. 2015;20; pii:21062.

21. Williams CJ, Thomas RH, Pickersgill TP, Lyons M, Lowe G, Stiff RE, et al. Cluster of atypical adult Guillain-Barré syndrome temporally associated with neurological illness due to EV-D68 in children, South Wales, United Kingdom, October 2015 to January 2016. Euro Surveill. 2016;21. http://dx.doi.org/10.2807/1560-7917

22. Centers for Disease Control and Prevention. Clusters of acute respiratory illness associated with human enterovirus 68—Asia, Europe, and United States, 2008–2010. MMWR Morb Mortal Wkly Rep. 2011;60:1301–4.

23. Esposito S, Ruggiero L, Madini B, Niesters H, Principi N. Enterovirus D68–associated community-acquired pneumonia in children living in Milan, Italy. J Clin Virol. 2015;68:94–6. http://dx.doi.org/10.1016/j.jcv.2015.05.017

24. Poelman R, Scholvinck EH, Borger R, Niesters HG, van Leer-Buter C. The emergence of enterovirus D68 in a Dutch University Medical Center and the necessity for routinely screening for respiratory viruses. J Clin Virol. 2015;62:1–5. http://dx.doi..org/10.1016/j.jcv.2014.11.011

25. Bragstad K, Jakobsen K, Rojahn AE, Skram MK, Vainio K, Holberg-Petersen M, et al. High frequency of enterovirus D68 in children hospitalised with respiratory illness in Norway, autumn 2014. Influenza Other Respir Viruses. 2015;9:59–63. http://dx.doi.org/10.1111/irv.12300

26. Kornreich L, Dagan O, Grunebaum M. MRI in acute poliomyelitis. Neuroradiology. 1996;38:371–2. http://dx.doi.org/10.1007/BF00596591

27. Chen CY, Chang YC, Huang CC, Lui CC, Lee KW, Huang SC. Acute flaccid paralysis in infants and young children with enterovirus 71 infection: MR imaging findings and clinical correlates. AJNR Am J Neuroradiol. 2001;22:200–5.

28. World Health Organization. Polio laboratory manual. 4th ed. 2004 [cited 2016 Feb 1]. http://whqlibdoc.who.int/hq/2004/WHO_IVB_04.10.pdf

29. Council of State and Territorial Epidemiologists. Standardized case definition for acute flaccid myelitis [cited 2016 Feb 1]. http://c.ymcdn.com/sites/www.cste.org/resource/resmgr/2015PS/2015PSFinal/15-ID-01.pdf

Address for correspondence: Negar Aliabadi, Centers for Disease Control and Prevention, 1600 Clifton Rd NE, Mailstop A34, Atlanta, GA 30329-4027, USA; email: ydh6@cdc.gov

Middle East Respiratory Syndrome Coronavirus Transmission in Extended Family, Saudi Arabia, 2014

M. Allison Arwady, Basem Alraddadi, Colin Basler, Esam I. Azhar, Eltayb Abuelzein,
Abdulfattah I. Sindy, Bakr M. Bin Sadiq, Abdulhakeem O. Althaqafi, Omaima Shabouni,
Ayman Banjar, Lia M. Haynes, Susan I. Gerber, Daniel R. Feikin, Tariq A. Madani

Risk factors for human-to-human transmission of Middle East respiratory syndrome coronavirus (MERS-CoV) are largely unknown. After MERS-CoV infections occurred in an extended family in Saudi Arabia in 2014, relatives were tested by using real-time reverse transcription PCR (rRT-PCR) and serologic methods. Among 79 relatives, 19 (24%) were MERS-CoV positive; 11 were hospitalized, and 2 died. Eleven (58%) tested positive by rRT-PCR; 8 (42%) tested negative by rRT-PCR but positive by serology. Compared with MERS-CoV–negative adult relatives, MERS-CoV–positive adult relatives were older and more likely to be male and to have chronic medical conditions. Risk factors for household transmission included sleeping in an index patient's room and touching respiratory secretions from an index patient. Casual contact and simple proximity were not associated with transmission. Serology was more sensitive than standard rRT-PCR for identifying infected relatives, highlighting the value of including serology in future investigations.

Middle East respiratory syndrome coronavirus (MERS-CoV) was first reported in September 2012 in a patient in Saudi Arabia (*1,2*). MERS-CoV is known to cause a severe acute febrile respiratory illness in humans after an incubation period of 2–14 days (*3*). As of May 1, 2016, a total of 1,728 laboratory-confirmed cases, including 624 deaths, had been reported globally (*4*); all patients have been linked to the Arabian Peninsula (*5,6*). Studies suggest dromedary camels as a possible natural host (*7*), although most patients report no exposure to camels (*8*).

Sustained human-to-human transmission in community settings has not been observed (*6*), but transmission has been documented in healthcare settings (*9,10*) and in households (*11–14*). Specific risk factors for secondary transmission remain unknown.

In Saudi Arabia, real-time reverse transcription PCR (rRT-PCR) of nasopharyngeal or oropharyngeal swabs is used for routine MERS-CoV diagnosis and contact tracing. rRT-PCR identifies and amplifies viral RNA, indicating active infection. More recently developed serologic assays identify antibodies to MERS-CoV, indicating previous infection. MERS-CoV antibodies are rare in the general population; a nationwide serosurvey in Saudi Arabia in 2013 found antibodies in 15 (0.15%) of 10,009 persons (*15*).

MERS-CoV cases in Saudi Arabia increased substantially during March–April 2014 (*16*) in association with transmission in healthcare settings (*9,10*). In May 2014, as the number of urban cases decreased (*10,17*), a new cluster was identified 400 km south of Jeddah, in an area that had not previously reported cases. All identified patients were members of 1 extended family from the town of Al-Qouz, near Al-Qunfudah. The first MERS-CoV diagnosis was reported on May 20, 2014, in a hospitalized patient after 14 days of worsening respiratory symptoms and impending respiratory failure; by May 29, this man's wife, brother, and nephew and the nephew's paternal uncle had been hospitalized with confirmed MERS-CoV. These 5 relatives lived in 4 different households within Al-Qouz.

On June 4–5, 2014, representatives from the Saudi Arabia Ministry of Health (Jeddah), US Centers for Disease Control and Prevention (CDC; Atlanta, GA, USA), and King Abdulaziz University (Jeddah) joined the Al-Qunfudah Regional Health Department to investigate the family cluster. The objectives were to characterize the cluster by identifying additional cases through both rRT-PCR for viral RNA and serologic testing for MERS-CoV antibodies; to determine transmission risk factors for MERS-CoV within the affected households; and to assess possible

MERS-CoV infections in the larger community, sampling both local healthcare settings and local animal workers.

Methods

Cluster Investigation

To find cases, we interviewed clinicians, reviewed regional records, and searched a national laboratory database. We interviewed all persons who had received a MERS-CoV diagnosis in the region and reviewed hospitalized patients' medical charts; proxy interviews were conducted for patients who were in the intensive care unit or who had died. We then conducted a retrospective cohort study to assess infection risk factors among household members. We aimed to interview and test all members of the 4 households of the 5 known MERS-CoV–infected patients, as well as relatives who regularly visited these households and were present on the day of the on-site investigation.

On June 5, trained nurses collected 1 oropharyngeal and 1 nasopharyngeal swab for rRT-PCR and 1 blood sample for serologic testing from all available household members and visiting relatives. Hospitalized persons, persons who previously had tested positive by rRT-PCR, and children <14 years of age did not undergo serologic testing. Local public health officials had previously collected oropharyngeal swabs for rRT-PCR in the households during May 20–29; we reviewed these records. On June 5, trained physicians administered a standardized questionnaire to household members and visiting relatives to identify symptoms and healthcare exposures and infection risk factors, including animal contact, recent travel, underlying medical conditions, tobacco use, and details of exposure to each household's index patient. An index patient was defined as the person with rRT-PCR confirmation of MERS-CoV who had the earliest date of symptom onset in the household.

Healthcare Worker and Community Transmission

To understand whether this outbreak was affecting the broader community, we collected data at the town's hospital, at the outpatient clinic nearest the family's homes, at 2 local slaughterhouse facilities, and at the town's weekly livestock animal market. All hospital staff members who had treated the first identified MERS-CoV patient from his admission on May 9 until his MERS-CoV diagnosis on May 20 underwent hospital-based rRT-PCR of oropharyngeal swabs May 21–23; serologic testing was not performed. At the outpatient clinic, all staff and a convenience sample of patients who visited the clinic on June 4 with respiratory symptoms or fever were interviewed with a standardized questionnaire and tested for MERS-CoV by using nasopharyngeal and oropharyngeal swabs for rRT-PCR and blood for serologic testing. All animal workers at 2 local slaughterhouse facilities and a convenience sample

of persons with daily animal contact who were present at the town's weekly livestock animal market on June 4 were interviewed and tested by using the same methods.

Laboratory Testing

Specimens from hospitalized patients and hospital staff members underwent rRT-PCR at the Ministry of Health's Jeddah regional laboratory, according to Ministry of Health protocol (18). Nasopharyngeal and oropharyngeal flocked swabs collected in the households, at the community clinic, and in animal workers were placed in viral transport media and transferred at 4°C to King Abdulaziz University, where rRT-PCR amplification of consensus viral RNA targets (upstream of E and open reading frame 1a) was undertaken (19). Serum samples were sent to CDC and screened for MERS-CoV antibodies by the recombinant MERS-CoV nucleocapsid protein ELISA, and confirmatory testing was conducted with immunofluorescence assay and microneutralization (20).

Data Analysis and Ethics Review

We analyzed questionnaire data using Epi Info 7.0 (CDC, Atlanta, GA, USA). Proportions were compared by using the χ^2 or Fischer exact test and medians by using Wilcoxon rank-sum. Risk ratios (RRs) were calculated. We compared questionnaire data for all MERS-CoV–positive (by rRT-PCR or serology) relatives ≥14 years of age with questionnaire data for all MERS-CoV–negative relatives ≥14 years of age. We excluded children from analysis because they had not had antibody testing of serum. A household secondary transmission analysis comprised relatives ≥14 years of age residing only in the 4 affected households. Results for MERS-CoV–positive household members who had illness onset (or tested MERS-CoV–positive) at least 2 days after the household's index patient's illness onset were compared with results for MERS-CoV–negative household members.

Because this investigation was part of a public health response, it was not considered by CDC and the Saudi Arabia Ministry of Health to be research that was subject to review by an institutional review board. Participants gave verbal consent.

Results

Nineteen extended family members had evidence of MERS-CoV by rRT-PCR or presence of MERS-CoV antibodies (Figure 1). Seventy-nine relatives were interviewed and tested for MERS-CoV by both rRT-PCR and (unless already positive by rRT-PCR or <14 years of age) serology. These persons comprised 50 (96%) of the 52 relatives living in the 4 original households (including 13 children <14 years of age); 26 relatives visiting those households (including 6 children <14 years of age); and 3 ill adults
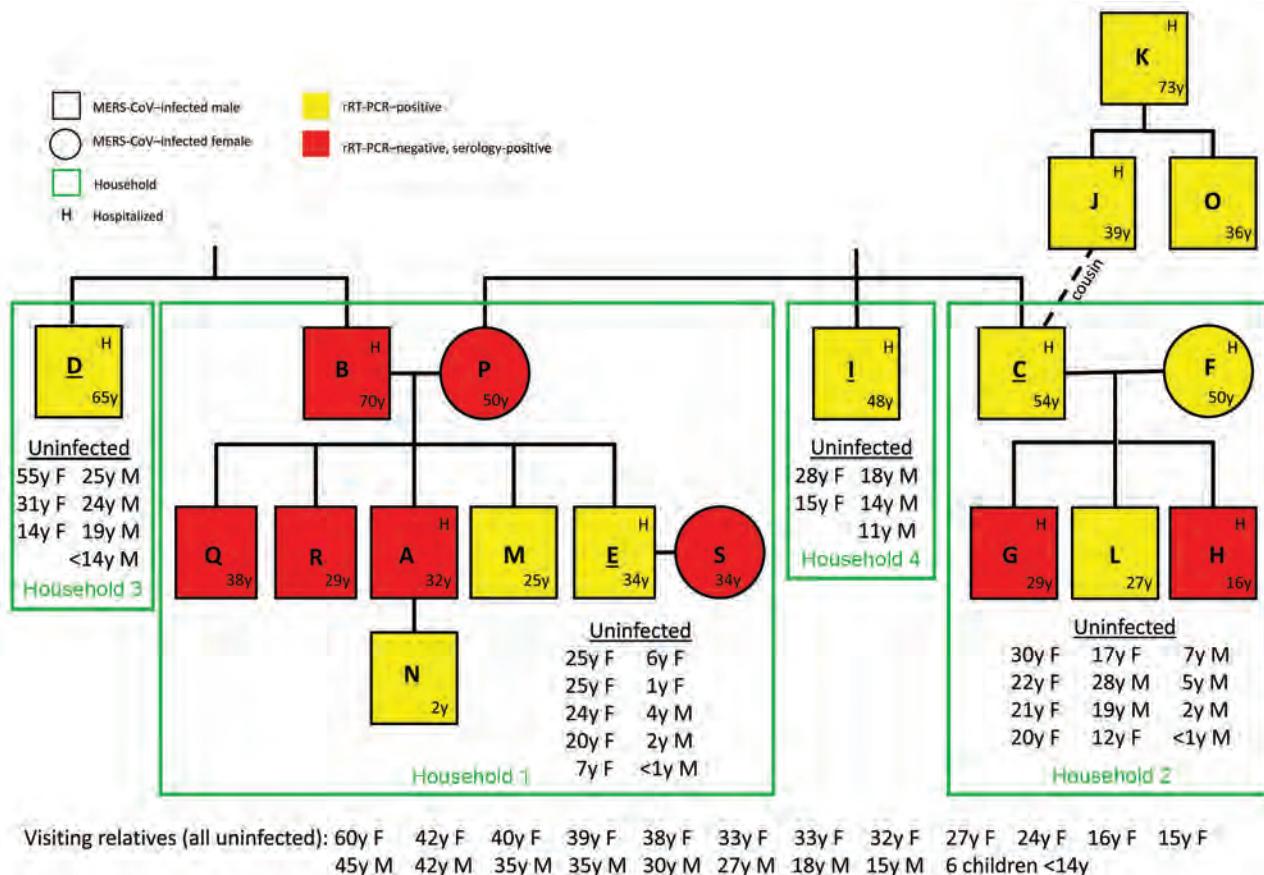
Figure 1. Family relationships and household distribution of persons infected with MERS-CoV, Al-Qouz, Saudi Arabia, 2014. Black lines denote standard family tree relationships. Patients are lettered in order of symptom onset or, if asymptomatic, by test date. Green boxes indicate households; all persons living in households 1–4 were tested, except for 2 adults living in household 4 (not shown). Index patient (person with earliest symptom onset diagnosed by rRT-PCR) in each household is underlined. Uninfected indicates person in household with negative rRT-PCR results and (if ≥14 years of age) negative serologic testing for MERS-CoV. Visiting relatives indicates extended family members who regularly visited the 4 households and were present in the households on the day of the field investigation. MERS-CoV, Middle East respiratory syndrome coronavirus; rRT-PCR, real-time reverse transcription PCR.

identified in a separate branch of the family tree (J, K, and O; Figure 1) after the household investigation. All 26 visiting relatives were MERS-CoV–negative by both rRT-PCR and (for adults) serology.

Standard Diagnosis and Disease Presentation

MERS-CoV was diagnosed in 11 (58%) of the 19 patients by rRT-PCR, the standard method in Saudi Arabia (Table 1, http://wwwnc.cdc.gov/EID/article/22/8/15-2015-T1.htm). For 7 of these, including the 5 original patients, illness was diagnosed during May 20–June 9 while they were hospitalized (Figure 2). For the other 4 patients (L, M, N, and O), MERS-CoV infection was diagnosed during May 22–June 11 through routine contact tracing and rRT-PCR by regional health officers. One of these contacts denied symptoms, 2 reported mild symptoms (i.e., cough, subjective fever) but had not sought medical care, and 1 (N, the only

child given a MERS-CoV diagnosis) had visited an emergency department with fever. In the 4 households, all non-hospitalized family members were rRT-PCR–negative when tested on June 5, indicating little risk for ongoing household transmission.

Serologic Diagnosis and Disease Presentation

For 8 (42%) of the 19 positive family members, MERS-CoV infection was diagnosed only retrospectively by using serology. All 8 previously had tested negative by rRT-PCR during April 21–May 29 while hospitalized or during routine contact tracing, and all again tested negative on June 5. Two of these rRT-PCR–negative patients (A and B) had extended hospitalizations; 2 patients (G and H) had brief hospitalizations; 2 patients (R and S) had sought medical care but not required hospitalization; and 2 (P and Q) denied symptoms. Some of these patients had
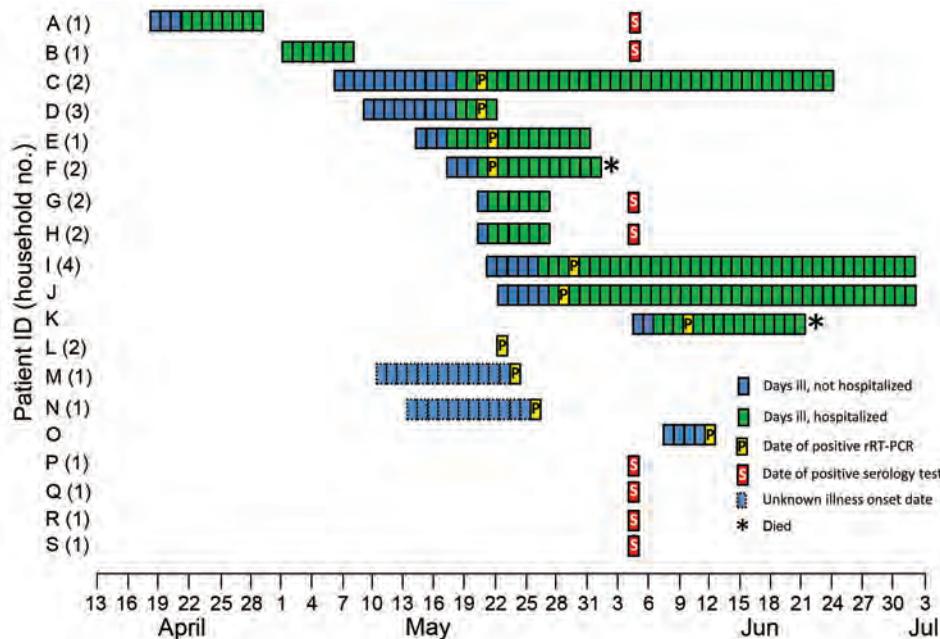
Figure 2. Timeline of illness onset and testing for MERS-CoV–positive family members, Al-Qouz, Saudi Arabia, 2014. Patients M and N had mild symptoms during 2 weeks before their rRT-PCR–positive results but did not identify a specific onset date; their illness dates are estimated. Patients R and S reported symptoms during the month preceding their positive serology tests but also without a specific onset date; their illness dates are not displayed. Patients L, P, and Q denied symptoms at any time. HH, household; MERS-CoV, Middle East respiratory syndrome coronavirus; Pt, patient; rRT-PCR, real-time reverse transcription PCR; S, positive serology date for rRT-PCR–negative persons.

multiple negative tests; during an April 2014 hospitalization in Jeddah, patient A, the first patient in this family to become ill, had 3 negative rRT-PCR results of nasopharyngeal swabs.

Among the 19 relatives in whom MERS-CoV infection was diagnosed, 11 (58%) were hospitalized; 3 (16%) were treated in an emergency department for symptoms but not hospitalized; 2 (11%) reported mild symptoms but had not sought medical care; and 3 (16%) were asymptomatic. Five (26%) were intubated, 2 of whom (11%) died while hospitalized. Fever was the most commonly reported symptom (74%), followed by cough (63%), shortness of breath (44%), and diarrhea (44%). The 11 hospitalized patients were ill at home for a median of 3 days before hospital admission (range 0–9 days) (Figure 2).

Infection Risk Factors among Adults
Fifteen (83%) of 18 MERS-CoV–positive adults were male, compared with 15 (37%) of 41 MERS-CoV–negative adults (p = 0.0009; Table 2). MERS-CoV–positive adults were more likely to have smoked sheesha, the traditional water pipe for flavored tobacco, than were MERS-CoV–negative adults (2/18 [11%] vs. 0/41; p = 0.003) and were more likely to have traveled to Jeddah (10 [56%] vs. 9 [22%]; p = 0.011) and visited a hospital there (7 [39%] vs. 5 [12%]; p = 0.019) during the month before becoming ill. MERS-CoV–positive adults were older (median age 37 years vs. 25 years; p = 0.0011) and more likely to report chronic medical problems (8 [44%] vs. 5 [12%]; p = 0.006), including diabetes mellitus and heart disease. All MERS-CoV–positive relatives denied animal contact during the 14 days before testing.

Household Transmission
In household 1, eight of the 12 adults (a husband and wife, 5 of their adult sons, and 1 son's wife) and 1 of the 7 children received a MERS-CoV diagnosis (household attack rate 44%; household adult attack rate 64%) (Figure 1). In household 2, five of the 12 adults (a husband and wife and 3 of their adult sons) received a MERS-CoV diagnosis (household attack rate 29%; household adult attack rate 42%). In households 3 and 4, only the index patients (both adult men) tested positive; no secondary patients were identified. All family members in whom MERS-CoV symptoms developed or who had positive rRT-PCR results reported contact with at least 1 ill relative in the preceding 14 days (Figure 3).

When we compared results for the 9 secondary adult patients (adults who tested MERS-CoV–positive with illness onset after the presumed index patient) in these 4 households with the results for 21 adults in the households who tested negative, we identified several major risk factors for MERS-CoV transmission in univariate analysis (Table 3). These risk factors included sleeping in the same room as an index patient (RR 4.1, 95% CI 1.5–11.2), touching his respiratory secretions (RR 4.0, 95% CI 1.6–9.8), and removing his biological waste (RR 3.2, 95% CI 1.2–8.4). Notable variables not associated with being a secondary patient included hugging or social kissing; sharing plates, cups, meals, sheesha, or a toilet; and cleaning or feeding the index patient.

Community Transmission
Except for members of this extended family, the regional hospital admitted no other MERS-CoV patients. Of 131

Table 2. Demographic, risk factor and symptom characteristics of adults with MERS-CoV–positive and MERS-CoV–negative test results in an extended family, Al-Qouz, Saudi Arabia, 2014*

Characteristic†	Test results, no. (%)		Risk ratio (95% CI)
	Positive, n = 18	Negative, n = 41	
Male sex	15 (83)	15 (37)	**4.8 (1.6–15.0)**
Reported chronic medical problem	8 (44)	5 (12)	**2.8 (1.4–5.7)**
Diabetes mellitus	5 (28)	1 (2)	**3.4 (1.9–6.1)**
Hypertension	4 (22)	3 (7)	**2.1 (1.0–4.6)**
Asthma	1 (6)	1 (2)	1.7 (0.4–7.1)
Heart disease	4 (22)	0	**3.1 (1.6–5.8)**
Smoked cigarettes	2 (11)	1 (2)	2.3 (0.9–5.7)
Smoked sheesha	2 (11)	0	**3.6 (2.4–5.4)**
Reported activities			
Visited animal market during preceding 14 d	0	2 (5)	0 (undefined)
Touched live animal during preceding 14 d	0	1 (2)	0 (undefined)
Touched camel during preceding 14 d	0	0	0 (undefined)
Traveled to Jeddah during preceding month	10 (56)	9 (22)	**2.6 (1.2–5.6)**
Visited Jeddah hospital during preceding month	7 (39)	5 (12)	**2.5 (1.2–5.0)**
Illness at any time during preceding month			
Sought medical care	13 (72)	4 (10)	**6.4 (2.7–15.2)**
Admitted to hospital	11 (61)	0 (0)	**6.9 (3.5–13.6)**
Fever	13 (72)	3 (7)	**7.0 (3.0–16.5)**
Cough	12 (67)	5 (23)	**4.9 (2.2–11.0)**
Shortness of breath	8 (44)	1 (2)	**4.4 (2.4–8.1)**
Diarrhea	8 (47)‡	3 (8)§	**3.7 (1.9–7.4)**
Vomiting	2 (12)‡	1 (3)§	**2.4 (1.0–6.0)**
Chills	5 (29)‡	1 (3)§	**3.5 (1.9–6.5)**
Body aches	9 (53)‡	1 (3)§	**5.3 (2.7–10.3)**

*Bold indicates statistical significance. Analysis includes all relatives 14 y of age tested for MERS-CoV (n = 59), regardless of household or visitor status. Positive indicates positive rRT-PCR or serologic antibody testing for MERS-CoV; negative indicates negative rRT-PCR and serologic antibody testing. Children (one 2-year-old rRT-PCR–positive child and 19 rRT-PCR–negative children) were excluded because they did not have serologic antibody testing. Listed chronic medical problems were self-reported; no one reported chronic lung or kidney disease, and other self-reported problems (hyperthyroidism, allergies, and solitary kidney) were excluded. MERS-CoV, Middle East respiratory syndrome coronavirus; rRT-PCR, real-time reverse transcription PCR.
†Ages were as follows: MERS-CoV positive: median 37 y (range 16–73 y); MERS-CoV-negative: median 25 y (range 14–60y).
‡Of the 17 persons for whom this information was reported.
§Of the 40 persons for whom this information was reported.

hospital workers who cared for patient C, 1 (0.8%), a nurse who remained asymptomatic, tested positive by rRT-PCR on May 23. All 44 persons tested at the outpatient clinic (21 patients with respiratory complaints and 23 staff) were MERS-CoV–negative by both rRT-PCR and serology. All 11 slaughterhouse workers and 10 livestock market participants tested negative by rRT-PCR. One (5%) asymptomatic slaughterhouse worker demonstrated antibodies to MERS-CoV by serology. He had no known contact with any family members in the cluster.

Discussion

This investigation defined the epidemiology of a large family cluster of MERS-CoV infection in Saudi Arabia, identified multiple possible household transmission risk factors, and highlighted the useful role of serology in describing the extent of family clusters and spectrum of illness. For approximately half (42%) of the 19 MERS-CoV–infected family members, rRT-PCR results were negative while they were ill or after recognized exposure, and infection was diagnosed only retrospectively by serology; this included patients tested during extended hospitalizations and demonstrates real-world limitations in rRT-PCR or timing of specimen collection, transport, and testing. This finding

highlights the need for clinicians to consider MERS-CoV diagnoses in appropriate clinical settings, even in patients with negative rRT-PCR results. Clinicians should consider obtaining lower respiratory tract specimens to improve the sensitivity of rRT-PCR, particularly if nasopharyngeal and oropharyngeal test results are negative and clinical suspicion is high, and they should consider follow-up serologic testing. Most importantly, clinicians should apply appropriate infection control practices for patients with clinically suspected illness, regardless of initial rRT-PCR results.

Only 3 of the 19 MERS-CoV–infected family members were women, all wives of patients. Infection predominance in males has characterized MERS-CoV since its identification (64% of patients globally have been male [5]) and might reflect biologic or behavior differences, such as men and women socializing separately (21,22). Underlying illness has previously been linked to more severe MERS-CoV symptoms and signs (23), but whether underlying illness also makes persons more susceptible to initial MERS-CoV infection is less clear. This study, in which 96% of household members were tested, found an increased infection risk among persons with underlying chronic illnesses.

Our data indicate close contact (e.g., sleeping in the same room as an index patient) and direct patient care
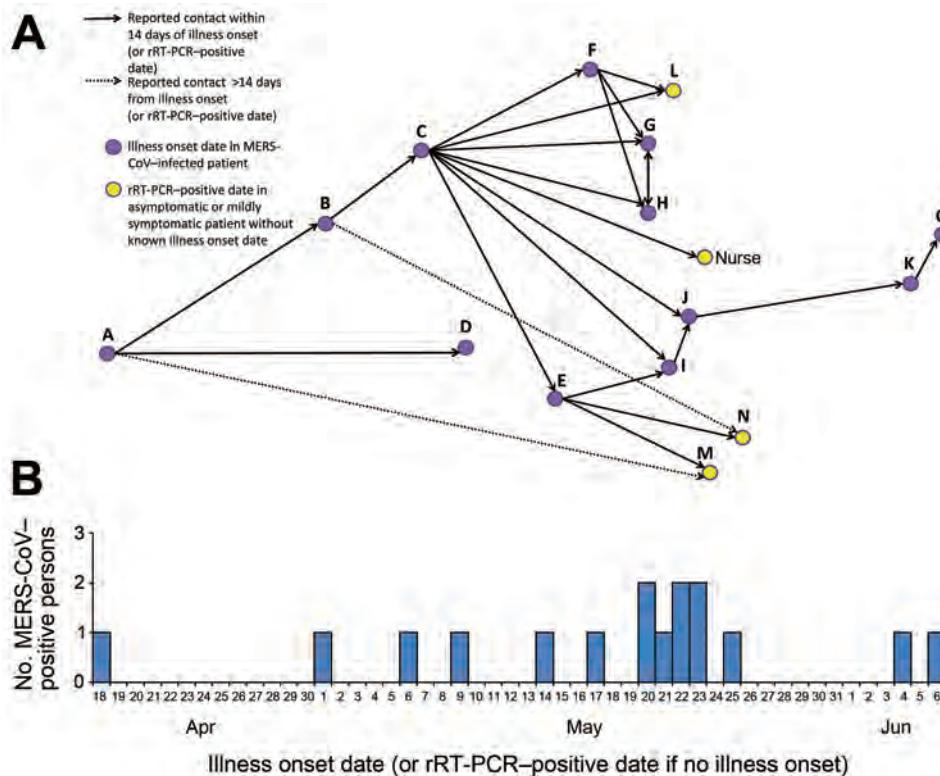
Figure 3. Reported contact among family members who received a MERS-CoV diagnosis and illness onset timeline, Al-Qouz, Saudi Arabia, 2014. Patients L, M, and N, as well as the infected nurse, reported no or mild symptoms and could not identify onset dates; for these 4 persons, the rRT-PCR–positive date is listed. All persons were questioned about ill family members with whom they had close contact during illness. Solid arrows indicate contact between persons within 14 days (MERS–CoV incubation period is ≤14 days) and indicate a likely infection source. Dashed arrows indicate contact after the 14-day incubation period; they are included for patients M and N because these patients could not identify their precise illness onset dates. MERS-CoV, Middle East respiratory syndrome coronavirus; rRT-PCR, reverse transcription PCR.

activities (e.g., touching a patient's respiratory secretions and removing his body waste), rather than casual contact or simple proximity, increases risk for transmission. Although smoking sheesha was a statistically significant risk factor for infection, the 2 infected family members who smoked sheesha denied smoking together, making it an unlikely mechanism of transmission. Guidance on preventing household transmission of MERS-CoV should emphasize minimizing close contact with patients. Outside of this extended family (and 1 asymptomatic exposed nurse and 1 asymptomatic camel slaughterhouse worker), we did not find evidence for wider community transmission of MERS-CoV.

Two (11%) of the infected family members died. As of May 1, 2016, Saudi Arabia had reported 588 deaths among 1,380 confirmed MERS-CoV patients, for an overall 43% case-fatality rate (*17*). The substantially lower fatality rate in this family most likely reflects aggressive contact tracing and use of serology to identify mildly symptomatic and asymptomatic patients. Patients in this family also were younger (median age 37 years) than MERS-CoV patients globally (median 48 years [*5*]). The case-fatality rate in this cluster might reflect the broader population across the spectrum of illness.

Previously described MERS-CoV family clusters and household contact investigations have reported household attack rates ranging from ≤1% to 19% (*11–14*). Household attack rates in this investigation were markedly higher; 64% and 42% of the adults in 2 households were infected. This difference could be due to methodologic differences in our investigation; serology identified mildly symptomatic and asymptomatic patients, which would increase the attack rate over investigations that relied only on rRT-PCR. The attack rate, however, could have actually been higher in this cluster for several reasons. First, MERS-CoV diagnoses were missed or delayed among the first cases in the family. The first 2 patients to become ill (patients A and B) were hospitalized but had negative rRT-PCR results during illness; their subsequent positive serologic results confirmed that the earlier illness had in fact been undiagnosed MERS-CoV. The third patient (patient C) was ill for 14 days before receiving a diagnosis, a time during which many other family members reported contact with him. Because this community had not previously experienced MERS-CoV infections, family members and local hospital staff might have had limited suspicion for MERS-CoV infection and not limited close contact. In contrast, when MERS-CoV infection was diagnosed in index patients in households 3 and 4, the family (and local hospital staff) was highly attuned to the possibility of MERS-CoV infection and took precautions to prevent its spread.

Second, patient C might have been part of a superspreading event because up to 8 other infected persons might have been infected through contact with him (Figure

Table 3. Exposures to MERS-CoV index patients by household adult members with and without secondary MERS-CoV infection living in 4 households, Al-Qouz, Saudi Arabia, 2014*

Exposure/activity	Infected by secondary transmission, no. (%), n = 9	Uninfected, no. (%), n = 21	Risk ratio (95% CI)
Daily household activities			
Treated index patient during time he was ill at home before hospitalization	8 (89)	13 (62)	3.4 (0.5–23.5)
Shared meal	6 (67)	11 (52)	1.5 (0.5–5.0)
Ate from same plate with hands	6 (67)	8 (38)	2.3 (0.7–7.5)
Hugged	7 (78)	8 (38)	3.5 (0.9–14.2)
Kissed	7 (78)	9 (43)	3.1 (0.8–12.4)
Shook hands	6 (67)	11 (52)	1.5 (0.5–5.0)
Shared drinking cup	4 (44)	9 (43)	1.0 (0.3–3.1)
Shared sheesha	0	0	Undefined
Shared utensils	1 (11)	7 (33)	0.3 (0.1–2.3)
Slept in same room	5 (56)	2 (10)	**4.1 (1.5–11.2)**
Shared toilet	4 (44)	6 (29)	1.6 (0.5–4.7)
Caregiving activities			
Helped care for index patient at home	6 (67)	8 (38)	2.3 (0.7–7.5)
Changed or washed clothes, sheets	5 (56)	4 (19)	**2.9 (1.0–8.4)**
Cleaned index patient	4 (44)	5 (15)	2.6 (0.9–7.3)
Cleaned in room	4 (44)	4 (19)	2.2 (0.8–6.2)
Administered medicine	5 (56)	6 (29)	2.2 (0.7–6.4)
Fed index patient	5 (56)	7 (33)	1.9 (0.6–5.6)
Touched index patient's respiratory secretions	4 (44)	1 (5)	**4.0 (1.6–9.8)**
Removed index patient's waste	4 (44)	2 (10)	**3.2 (1.2–8.4)**
Proximity to index patient			
Within 1 m during time he was sick at home	8 (89)	12 (57)	4.0 (0.6–27.8)
Within 1 m every day	7 (78)	9 (43)	3.1 (0.8–12.4)
Within 1 m on day preceding hospitalization	7 (78)	11 (52)	2.3 (0.6–9.3)
Visited index patient in the hospital	6 (67)	10 (48)	1.8 (0.5–5.7)

*Bold indicates statistical significance. This household transmission analysis included relatives ≥14 y of age living in the 4 households of the index patients, defined as the first patient in the household who received a MERS-CoV diagnosis by rRT-PCR. Secondary transmission is defined as onset of illness or testing positive for MERS-CoV after the household's index patient had received a diagnosis. Two MERS-CoV–infected household members were excluded from analysis because they had illness onsets before the presumed household index patient's illness and were subsequently reported to have MERS-CoV antibodies. MERS-CoV, Middle East respiratory syndrome coronavirus; rRT-PCR, real-time reverse transcription PCR.

3). The concept of a super-spreading event was described during the outbreak of severe acute respiratory syndrome coronavirus in 2003 (*24,25*) and more recently was observed in the MERS-CoV outbreak in healthcare facilities in South Korea, where each of 3 patients was associated with infection in >20 other persons (*26,27*). Finally, although all infected persons denied animal contact and the range of symptom onset dates indicated ongoing person-to-person spread, an environmental point-source of infection might have been missed.

Our study had several limitations. First, in household 1, two persons had, in fact, been ill with MERS-CoV before the presumed household index patient received a diagnosis. These persons had negative rRT-PCR results while ill, and infection was diagnosed retrospectively when later serologic test results were positive. The study questionnaire focused primarily on household exposures to the presumed index patient, but persons in this household might have had a range of exposures to all 3 persons, making isolation of the specific exposure that resulted in secondary infection more difficult. Second, the small sample size did not enable multivariable risk factor analysis and confounding and collinearity could not be evaluated. Third, serologic testing was not conducted for children <14 years

of age, and they were excluded from risk factor analysis; the observed lower incidence of infection among children could be investigated by including children in future serologic investigations. Fourth, sequential serologic testing was not performed, so it is possible that persons identified as MERS-CoV-negative might not yet have seroconverted, although none had developed respiratory illnesses before or after testing. Finally, specimens were not available for genome sequencing, which might have helped to clarify transmission chains within the family.

More studies are needed to define the virologic and epidemiologic factors involved in household transmission of MERS-CoV to inform future public health response. Including serologic methods in these investigations will help better identify the spectrum of MERS-CoV clinical presentations. As testing methods evolve, maintaining strict infection control practices for ill patients with strong epidemiologic risk factors for MERS-CoV remains crucial to containing further spread.

Dr. Arwady, who completed this work while in CDC's Epidemic Intelligence Service, is now the chief medical officer

RESEARCH

at the Chicago Department of Public Health (Chicago, Illinois). Her research interests include improving communicable disease outbreak responses and promoting health equity in the United States and globally.

References

1. Zaki AM. Novel coronavirus—Saudi Arabia: human isolate. ProMED. 2012 Sep 20 [cited 2016 May 1]. http://www.promedmail.org, archive no. 20120920.1302733.
2. Zaki AM, van Boheemen S, Bestebroer TM, Osterhaus AD, Fouchier RA. Isolation of a novel coronavirus from a man with pneumonia in Saudi Arabia. N Engl J Med. 2012;367:1814–20. http://dx.doi.org/10.1056/NEJMoa1211721
3. Assiri A, McGeer A, Perl TM, Price CS, Al Rabeeah AA, Cummings DA, et al. Hospital outbreak of Middle East respiratory syndrome coronavirus. N Engl J Med. 2013;369:407–16. http://dx.doi.org/10.1056/NEJMoa1306742
4. World Health Organization. Middle East respiratory syndrome coronavirus (MERS-CoV) [cited 2016 May 1]. http://www.who.int/emergencies/mers-cov/en/
5. World Health Organization. Middle East respiratory syndrome coronavirus (MERS-CoV): summary of current situation, literature update and risk assessment—7 July 2015 [cited 2016 Feb 28]. http://apps.who.int/iris/bitstream/10665/179184/2/WHO_MERS_RA_15.1_eng.pdf
6. European Centre for Disease Control and Prevention. Rapid risk assessment: severe respiratory disease associated with Middle East respiratory syndrome-coronavirus, 21 October 2015. Figure 2 [cited 2016 Feb 28]. http://ecdc.europa.eu/en/publications/Publications/MERS-rapid-risk-assessment-update-october-2015.pdf
7. Azhar EI, El-Kafrawy SA, Farraj SA, Hassan AM, Al-Saeed MS, Hashem AM, et al. Evidence for camel-to-human transmission of MERS coronavirus. N Engl J Med. 2014;370:2499–505. http://dx.doi.org/10.1056/NEJMoa1401505
8. Kayali G, Peiris M. A more detailed picture of the epidemiology of Middle East respiratory syndrome coronavirus. Lancet Infect Dis. 2015;15:495–7. http://dx.doi.org/10.1016/S1473-3099(15)70128-3
9. Drosten C, Muth D, Corman VM, Hussain R, Al Masri M, HajOmar W, et al. An observational, laboratory-based study of outbreaks of Middle East respiratory syndrome coronavirus in Jeddah and Riyadh, Kingdom of Saudi Arabia, 2014. Clin Infect Dis. 2015;60:369–77. http://dx.doi.org/10.1093/cid/ciu812
10. Oboho IK, Tomczyk SM, Al-Asmari AM, Banjar AA, Al-Mugti H, Aloraini MS, et al. 2014 MERS-CoV outbreak in Jeddah—a link to health care facilities. N Engl J Med. 2015;372:846–54. http://dx.doi.org/10.1056/NEJMoa1408636
11. Memish ZA, Zumla AI, Al-Hakeem RF, Al-Rabeeah AA, Stephens GM. Family cluster of Middle East respiratory syndrome coronavirus infections. N Engl J Med. 2013;368:2487–94. http://dx.doi.org/10.1056/NEJMoa1303729
12. Drosten C, Meyer B, Müller MA, Corman VM, Al-Masri M, Hossain R, et al. Transmission of MERS-coronavirus in household contacts. N Engl J Med. 2014;371:828–35. http://dx.doi.org/10.1056/NEJMoa1405858
13. Abroug F, Slim A, Ouanes-Besbes L, Hadj Kacem MA, Dachraoui F, Ouanes I, et al. Family cluster of Middle East respiratory syndrome coronavirus infections, Tunisia, 2013. Emerg Infect Dis. 2014;20:1527–30. http://dx.doi.org/10.3201/eid2009.140378
14. Omrani AS, Matin MA, Haddad Q, Al-Nakhli D, Memish ZA, Albarrak AM. A family cluster of Middle East respiratory syndrome coronavirus infections related to a likely unrecognized asymptomatic or mild case. Int J Infect Dis. 2013;17:e668–72. http://dx.doi.org/10.1016/j.ijid.2013.07.001
15. Müller MA, Meyer B, Corman VM, Al-Masri M, Turkestani A, Ritz D, et al. Presence of Middle East respiratory syndrome coronavirus antibodies in Saudi Arabia: a nationwide, cross-sectional, serological study. Lancet Infect Dis. 2015;15:599–64. http://dx.doi.org/10.1016/S1473-3099(15)70090-3
16. Gulland A. WHO voices concern over rising numbers of MERS-CoV cases. BMJ. 2014;348:g2968. http://dx.doi.org/10.1136/bmj.g2968
17. Kingdom of Saudi Arabia Ministry of Health. MERS-CoV statistics [cited 2016 May 1]. http://www.moh.gov.sa/en/CCC/PressReleases/Pages/default.aspx
18. Kingdom of Saudi Arabia Ministry of Health. Case definition and surveillance guidance for MERS-CoV testing in Saudi Arabia. 13 May 2014 [cited 2015 Apr 15]. http://www.moh.gov.sa/en/Documents/MoHCaseDefinitionMERSCoVVersion-May132014.pdf
19. Corman VM, Müller MA, Costabel U, Timm J, Binger T, Meyer B, et al. Assays for laboratory confirmation of novel human coronavirus (hCoV-EMC) infections. Euro Surveill. 2012; 17:pii20334.
20. Kapoor M, Pringle K, Kumar A, Dearth S, Liu L, Lovchik J, et al. Clinical and laboratory findings of the first imported case of Middle East respiratory syndrome coronavirus to the United States. Clin Infect Dis. 2014;59:1511–8. http://dx.doi.org/10.1093/cid/ciu635
21. World Health Organization. Middle East respiratory syndrome coronavirus (MERS–CoV) summary and literature update—as of 9 May 2014 [cited 2015 Apr 15]. http://www.who.int/csr/disease/coronavirus_infections/MERS_CoV_Update_09_May_2014.pdf?ua=1
22. Memish ZA, Al-Tawfiq JA, Makhdoom HQ, Al-Rabeeah AA, Assiri A, Alhakeem RF, et al. Screening for Middle East respiratory syndrome coronavirus infection in hospital patients and their healthcare worker and family contacts: a prospective descriptive study. Clin Microbiol Infect. 2014;20:469–74. http://dx.doi.org/10.1111/1469-0691.12562
23. Assiri A, Al-Tawfiq JA, Al-Rabeeah AA, Al-Rabiah FA, Al-Hajjar S, Al-Barrak A, et al. Epidemiological, demographic, and clinical characteristics of 47 cases of Middle East respiratory syndrome coronavirus disease from Saudi Arabia: a descriptive study. Lancet Infect Dis. 2013;13:752–61. http://dx.doi.org/10.1016/S1473-3099(13)70204-4
24. Chow KY, Lee CE, Ling ML, Heng DM, Yap SG. Outbreak of severe acute respiratory syndrome in a tertiary hospital in Singapore, linked to an index patient with atypical presentation: epidemiological study. BMJ. 2004;328:195. http://dx.doi.org/10.1136/bmj.37939.465729.44
25. Wang SX, Li YM, Sun BC, Zhang SW, Zhao WH, Wei MT, et al. The SARS outbreak in a general hospital in Tianjin, China—the case of super-spreader. Epidemiol Infect. 2006;134:786–91. http://dx.doi.org/10.1017/S095026880500556X
26. Cowling BJ, Park M, Fang VJ, Wu P, Leung GM, Wu JT. Preliminary epidemiological assessment of MERS-CoV outbreak in South Korea, May to June 2015. Euro Surveill. 2015;20:7–13. http://dx.doi.org/10.2807/1560-7917.ES2015.20.25.21163
27. Korea Centers for Disease Control and Prevention. Middle East respiratory syndrome coronavirus outbreak in the Republic of Korea, 2015. Osong Public Health Res Perspect. 2015;6:269–78. http://dx.doi.org/10.1016/j.phrp.2015.08.006

Address for correspondence: Tariq A. Madani, Department of Medicine, Faculty of Medicine, King Abdulaziz University, PO Box 80215, Jeddah 21589, Saudi Arabia; email: tmadani@kau.edu.sa

Exposure-Specific and Age-Specific Attack Rates for Ebola Virus Disease in Ebola-Affected Households, Sierra Leone

Hilary Bower, Sembia Johnson, Mohamed S. Bangura, Alie Joshua Kamara, Osman Kamara, Saidu H. Mansaray, Daniel Sesay, Cecilia Turay, Francesco Checchi, Judith R. Glynn

Using histories of household members of Ebola virus disease (EVD) survivors in Sierra Leone, we calculated risk of EVD by age and exposure level, adjusting for confounding and clustering, and estimated relative risks. Of 937 household members in 94 households, 448 (48%) had had EVD. Highly correlated with exposure, EVD risk ranged from 83% for touching a corpse to 8% for minimal contact and varied by age group: 43% for children <2 years of age; 30% for those 5–14 years of age; and >60% for adults ≥30 years of age. Compared with risk for persons 20–29 years of age, exposure-adjusted relative risks were lower for those 5–9 (0.70), 10–14 (0.64), and 15–19 (0.71) years of age but not for children <2 (0.92) or 2–4 (0.97) years of age. Lower risk for 5–19-year-olds, after adjustment for exposure, suggests decreased susceptibility in this group.

In Ebola epidemics in West Africa and elsewhere, children appear to have been relatively spared (1–5). Published notification data for the West Africa outbreak that began in 2013 show a linear increase in incidence of Ebola virus disease (EVD) with age in persons up to ≈35 years of age, followed by a plateau in incidence for older age groups (6). Among children, the World Health Organization has reported a slightly increasing incidence with increasing age in Liberia and Sierra Leone but no clear pattern in Guinea (4). In contrast, published case-fatality rates for EVD are lowest for persons 10–15 years of age and highest for young children and older adults (4,7).

These age patterns could result from bias in recognizing, diagnosing, or reporting cases; differences in exposure; or differences in susceptibility to disease. Official data from the West Africa outbreak are known to be inaccurate (8,9).

In previous, smaller outbreaks, case ascertainment could have been more complete because of the smaller scale, but EVD cases might have been missed, especially mild cases; deaths may also have been missed because the elderly and very young are more likely to sicken and die from other causes. Children with fever are less likely than adults to visit health facilities for care, and children may be underreported as contacts (10).

Exposure patterns are likely to differ by age and sex. Women may be more at risk from caring for the sick and men from carrying sick persons to the hospital. Children may be deliberately kept away from sick persons and funeral rites, and lower incidence among children has been attributed to these factors (1,11). However, preventing exposure of young children in Ebola-affected households is difficult. Children need to be held, fed, and cared for and often share beds with adults or other children; they may also be exposed through breastfeeding (12).

The high case-fatality rate observed in children <5 years of age and especially in those <1 year of age (4) suggests that young children are particularly susceptible to Ebola; consequently, low incidence in young children may reflect low exposure or low ascertainment. In a study of 27 Ebola-affected households after the Kikwit outbreak in 1995, children <18 years of age had lower risks of disease than adults, after adjustment for reported exposures (13).

Assessing whether risk by age depends on exposure or susceptibility requires a comparison of exposures in persons with and without EVD. A recent systematic review of risk factors for transmission of Ebola virus found few studies reporting data on risks (14) and no previous study large enough to stratify in detail by age (3,13,15–19). We interviewed a large cohort of EVD survivors and their household members to determine exposure levels of all members, living and dead, and to calculate attack rates and relative risks by age, sex, and type of exposure. The Sierra Leone Ethics and Scientific Review Committee and the Ethics Committee of the London School of Hygiene and Tropical Medicine approved the study.

Methods

All survivors who were discharged from Kerry Town Ebola Treatment Centre (ETC), Sierra Leone, during November 2014–March 2015 and who lived in the Western Area were eligible for the study. During July–August 2015, members of the study team, which had assisted in survivor reintegration into the community, contacted survivors or their parents or guardians and asked them to bring all household members who were present at the time Ebola was affecting their household to an interview to be conducted at 1 of various locations. To make contact, the field team went to addresses of survivors when addresses were available and complete enough to locate or used telephone numbers when available. Team members were university graduates, nurses, and paramedics and included Ebola survivors; they received extensive training in interview techniques and were supervised by the first 2 authors (H.B. and S.J.), 1 or both of whom attended all interviews.

After obtaining individual written informed consent from each participant or parents or guardians of participants <18 years of age, the interviewers compiled a list of all members in each household and included information on age, sex, and household members who had had EVD and those who had died of EVD. Households were defined as persons eating from the same pot at the time EVD was in the household, regardless of how much time had been spent in the household, and included persons who joined the household to assist someone who was ill.

We asked household members to describe in their own words what had occurred in the household. For each person reported as having had EVD, we asked what symptoms occurred at home and which persons had helped that person during his or her EVD illness, shared a bed or had contact with the person, or had contact with the body if the person died. Adults spoke for young children and corroborated information from older children. Using probing questions and predefined exposure levels, we assigned a maximum exposure for persons who had been present in the household. The levels, which we developed on the basis of the literature and discussion with ETC staff, included touching the corpse of someone who died from EVD; direct contact with body fluids of a wet patient (i.e., with diarrhea, vomiting, or bleeding); direct contact with a wet patient; direct contact with a dry patient (i.e., without diarrhea, vomiting, or bleeding); indirect contact with a wet patient (e.g., washing clothes); indirect contact with a dry patient; minimal contact (e.g., shared meals); or no known contact (Table 1). We also asked about exposures outside the home and classified these exposures by using the same scale. For those reported as not having had EVD, we asked about any symptoms at the same time that others in the household had EVD. Study team members, all of whom are multilingual, conducted interviews in the participants' language and recorded key outcomes in English.

Definitions

Laboratory-confirmed EVD survivors who were reported from Kerry Town ETC, survivors from other ETCs, and all persons reported by the family as having died of EVD were counted as EVD case-patients. Deaths for which the family was unsure of the cause and symptomatic persons who were not tested or did not receive a diagnosis of EVD were classified as probable EVD case-patients if they fit the Sierra Leone case definition for probable cases (20).

For each household, the first person who became ill was identified as the likely primary case-patient. Some households reported 2 people who became ill at the same time, and they are counted as co-primary case-patients. No household described >1 period when Ebola occurred in the household. To avoid overburdening participants, we did not collect time sequences or dates and defined all nonprimary case-patients in a household as subsequent case-patients.

Analysis

Our initial descriptive analysis of outcomes by age and sex included all household members. We subsequently analyzed primary case-patients separately because their exposure occurred outside the household, and we compared their characteristics with those of all other household members.

Table 1. Classification of level of exposure to EVD patients in study of EVD risk for household members, Sierra Leone, 2014–2015*

Level	Definition
1	Contact with the body of EVD patient after death/prepared the body for burial
2	Direct contact with body fluids (e.g., blood, diarrhea, vomit, urine, or a baby breastfed by an EVD-positive woman)
3	Direct close contact with wet case; i.e., with diarrhea/vomiting/bleeding (e.g., person helped dress, embraced, carried, helped care for, or shared bed of an EVD patient with wet symptoms; or mother breastfed an EVD-positive child)
4	Direct close contact with dry case (i.e., without wet symptoms at the time) (e.g., person helped dress, embraced, carried, helped care for, or shared bed with an EVD patient without wet symptoms)
5	Indirect close contact with wet case (e.g., washed clothes or bed linen of an EVD patient with wet symptoms, or slept in the same room but not the same bed)
6	Indirect close contact with dry case (e.g., person washed clothes or bed linen of EVD patient without wet symptoms; formal/informal health workers without known contact with an EVD patient; ETC workers in PPE; Ebola Intervention workers (outside household only); person attended funeral without contact with the body (outside household only)
7	Minimal contact (e.g., person shared meals or utensils or sat In the same room; children placed in observation centers [outside household only])
8	No actual contact (e.g., person kept distance once EVD patient was symptomatic)

*ETC, Ebola Treatment Centre; EVD, Ebola virus disease; PPE, personal protective equipment.

In the analysis of risks for disease by age, sex, and exposure level, we excluded primary case-patients and household members who were alive but not present for the interview and unable to consent to individual data collection. We explored the following variables for their effects on disease risk and as confounders of the associations of other variables and disease risk: having a spouse who contracted EVD first; occupation; being household head versus household member; and household-level variables (i.e., household size; crowding [number of persons/number of rooms]; and access to water, soap, and latrine). Our analysis used logistic regression and adjusted for household clustering by using random effects. Because risks were large, we used marginal standardization to estimate risk ratios (RRs) and the delta method to estimate 95% CIs (*21,22*). All analyses used Stata 14 (http://www.stata.com). We also performed a sensitivity analysis that excluded case-patients and deaths classified as probable EVD cases.

Results

Study Population

Of 151 EVD survivors discharged from Kerry Town ETC, we included 123 survivors from 94 households in the study. The other 28 survivors had a similar age distribution to those included (39% of survivors not included vs. 36% of those included were <15 years of age) and a slightly higher proportion of males (54% of those not included vs. 38% of included survivors). We collected detailed

information for 937 persons, including exposure histories for 909 (Figure 1).

Overall, 448 persons were reported as having had EVD or probable EVD, of whom 238 (53%) died; 227 deaths were reported as caused by EVD, and the 11 other deaths fit the EVD case definition. Among survivors, 123 were EVD patients at the Kerry Town ETC, and 45 were at other ETCs. An additional 42 household members had probable EVD; the remaining 485 household members had no evidence of EVD.

Risk for EVD was lowest for children 5–14 years of age but higher for children <2 years of age and for adults (Table 2). Risk increased with age for adults up to ≈35 years of age and then plateaued for older adults (Figure 2, panel A). Because most probable case-patients were children, the lower risk for children was more extreme when probable case-patients were excluded (Table 2). EVD risk was similar for male and female study participants, even when results were stratified by age (Figure 2, panel B).

Primary Case-Patients

Primary case-patients were identified for 91 households and co-primary case-patients in 3 households. Compared with all other household members, primary case-patients were older, usually ≥30 years of age; slightly more likely to be male; and more likely to be household heads, healthcare or EVD front-line workers, or religious or community leaders (Table 3). Children or students were least likely to be primary case-patients. In 5 households,
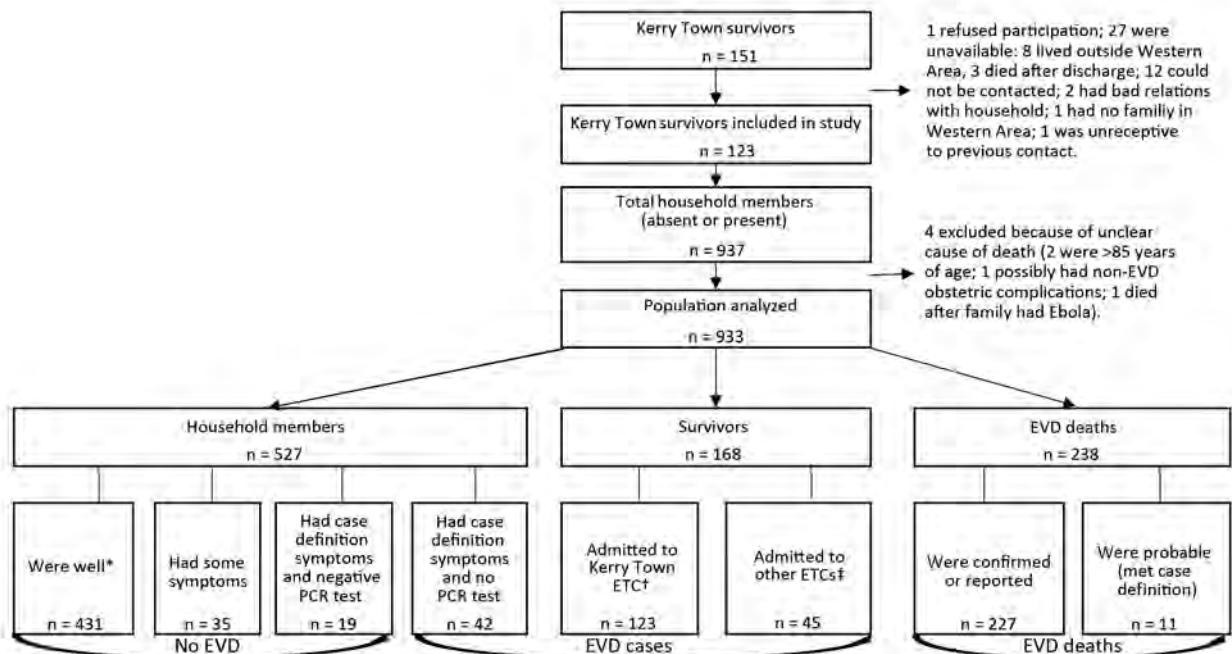
Figure 1. Flow diagram showing the population composition for study of Ebola-affected households related to survivors from the Kerry Town Ebola Treatment Centre (ETC), Sierra Leone, 2014–2015. EVD, Ebola virus disease. *Includes 23 not present for interview. †Includes 1 who died after discharge. ‡Includes 5 not present for interview.

Table 2. Distribution of outcomes by age and sex among Kerry Town Ebola Treatment Centre survivors and their household members, Sierra Leone, 2014–2015*

		No. (%)							
Characteristic	Total	Persons with no symptoms	Persons with some symptoms†	SympCD and neg test‡	SympCD and no test§	EVD survivors	Probable EVD deaths¶	EVD deaths	Overall % EVD#
Total	933	431 (46.2)	35 (3.8)	19 (2.0)	42 (4.5)	168 (18.0)	11 (1.2)	227 (24.3)	48
Sex									
M	399	184 (46.1)	19 (4.8)	11 (2.8)	20 (5.0)	62 (15.5)	5 (1.3)	98 (24.6)	46
F	534	247 (46.3)	16 (3.0)	8 (1.5)	22 (4.1)	106 (19.9)	6 (1.1)	129 (24.2)	49
Age, y**									
<2	54	27 (50.0)	2 (3.7)	0	1 (1.9)	4 (7.4)	1 (1.9)	19 (35.2)	46
2–4	86	49 (57.0)	2 (2.3)	2 (2.3)	8 (9.3)	9 (10.5)	1 (1.2)	15 (17.4)	38
5–9	131	82 (62.6)	4 (3.1)	4 (3.1)	11 (8.4)	15 (11.5)	0	15 (11.5)	31
10–14	121	78 (64.5)	3 (2.5)	3 (2.5)	8 (6.6)	18 (14.9)	0	11 (9.1)	31
15–19	107	57 (53.3)	4 (3.7)	2 (1.9)	1 (0.9)	28 (26.2)	0	15 (14.0)	41
20–29	178	76 (42.7)	8 (4.5)	4 (2.2)	10 (5.6)	49 (27.5)	1 (0.6)	30 (16.9)	51
30–39	114	31 (27.2)	3 (2.6)	3 (2.6)	3 (2.6)	26 (22.8)	3 (2.6)	45 (39.5)	68
40–49	62	12 (19.4)	4 (6.5)	1 (1.6)	0	12 (19.4)	4 (6.5)	29 (46.8)	73
>50	76	18 (23.7)	5 (6.6)	0	0	7 (9.2)	0	46 (60.5)	70

*Excluded are 4 persons who died with uncertain cause (3 females, 1 male). EVD, Ebola virus disease.
†Persons had some EVD symptoms but did not fulfill case definition.
‡Persons met EVD case definition on interview but reported a negative PCR test for Ebola.
§Persons met EVD case definition on interview but were never tested.
¶Description of symptoms leading to death were compatible with Ebola, but EVD was not diagnosed at the time.
#Overall % EVD includes EVD cases and deaths, SympCD and no test, and Probable EVD deaths as case-patients.
**Age missing for 4 persons (2 reported EVD deaths, 1 probable EVD death, 1 with no symptoms).

primary case-patients joined the household when they were already ill.

Likely sources of infection were identified for 68 (70%) of 97 primary case-patients. When >1 source of infection was possible, we selected the highest exposure level (Table 1). Thirty primary case-patients visited a household with an EVD patient; 16 of those 30 went to help the ill patient. Eight prepared bodies for burial or touched the corpse; 6 attended funerals; 4 carried a person with EVD symptoms; 8 attended healthcare facilities; and 12 worked as healthcare or front-line workers, 5 of whom were known to have treated an EVD patient.

Subsequent Case-Patients

The overall risk for acquiring EVD was 43% and was similar for male and female participants (Table 4); the risk by

age was J-shaped, as for the full study population. Among household members, 60% reported direct contact with a wet patient or their fluids or with a person who died of EVD (Table 4). Only 10 (1.2%) household members had a substantially higher level of exposure outside the household than inside.

Attack rates increased steeply and linearly with the predefined exposure levels. Exposure levels were high at all ages and for males and females (Figure 3), but exposure to EVD corpses increased with age, and direct exposure to fluids was higher for children <2 years of age, largely because of breastfeeding, and for older adults. After adjustment for age and sex, attack rates varied by occupation and were higher in larger and more crowded households. We found no clear associations with household-level measures of sanitation nor with having a spouse who developed EVD first (Table 4).
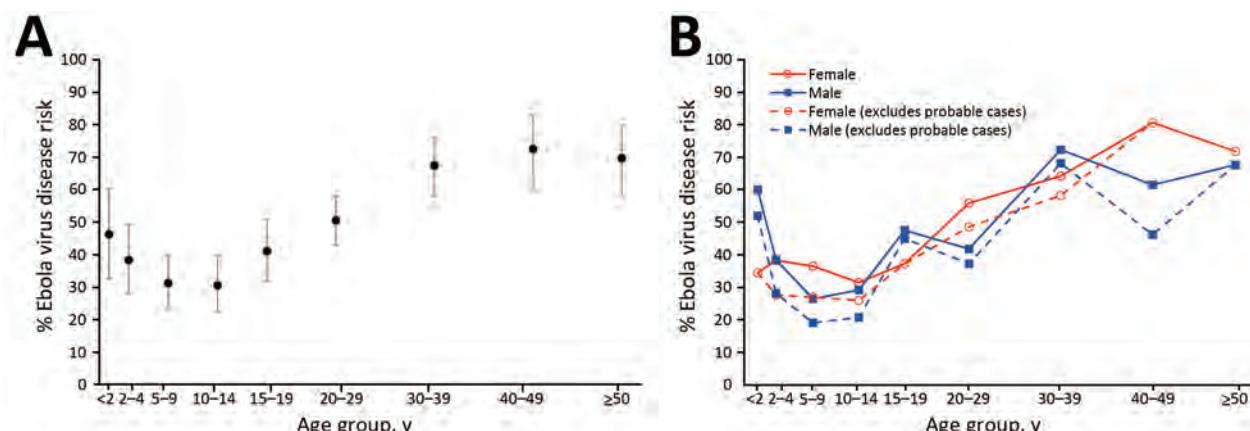
Figure 2. Risk for Ebola virus disease in Ebola-affected households of Kerry Town Ebola Treatment Centre survivors, by age and sex, Sierra Leone, 2014–2015. A) Risk by age group; bars indicate 95% CIs. B) Risk by sex and age group with and without probable cases.

Table 3. Risk factors associated with being the first EVD case in a household, compared with all other household members in households of Ebola Treatment Centre survivors, Kerry Town, Sierra Leone, 2014–2015*

Risk factor	Total population	No. primary cases	Risk,%	Adjusted RR* (95% CI)	p value†
Sex					
M	400	47	11.8	1.3 (0.93–1.9)	
F	537	50	9.3	1	0.1
Age, y‡					
<2	54	3	5.6	0.57 (0.17–1.9)	
2–4	86	2	2.3	0.24 (0.06–1.0)	
5–9	131	2	1.5	0.15 (0.04–0.65)	
10–14	121	3	2.5	0.26 (0.08–0.86)	
15–19	107	7	6.5	0.69 (0.30–1.6)	
20–29	179	17	9.5	1	
30–39	114	26	22.8	2.4 (1.4–4.2)	
40–49	63	15	23.8	2.5 (1.3–4.7)	
≥50	78	20	25.6	2.6 (1.5–4.7)	<0.001
Occupation§					
Heathcare worker, formal and informal	21	10	47.6	3.9 (2.0–7.5)	
Ebola front-line worker	11	3	27.3	2.5 (0.86–7.1)	
Driver	23	6	26.1	1.7 (0.67–4.1)	
Religious leader/chief/teacher	12	5	41.7	2.7 (1.1–6.9)	
Farmer/fisherman/unskilled	54	12	22.2	1.7 (0.83–3.3)	
Office/business	47	8	17.0	1.3 (0.62–2.8)	
Child/student	511	15	2.9	0.41 (0.12–1.4)	
Trader/tailor/service	205	25	12.2	1	0.01
Position in household					
Household head	87	32	36.8	2.3 (1.5–3.8)	
Household member	850	65	7.6	1	<0.001

*EVD, Ebola virus disease; RR, risk ratio. Adjusted for age, sex, and household clustering.
†p values calculated from likelihood ratio test in logistic regression model.
‡Age missing for 4 persons.
§No occupation recorded for 29 persons, including 28 with no individual-level data.

A multivariable analysis (Table 4) showed that developing EVD as a subsequent case-patient was strongly associated with age (p = 0.004), level of exposure (p<0.001), not being a household head (p = 0.03), and household size (p = 0.01). Sex was kept in the model a priori but was not associated with EVD risk. Occupation was not associated with EVD risk after adjustment for exposure level (p = 0.2). In the full model, the association with age was still J-shaped. The lowest risk was for persons 5–19 years of age, and risks were higher for older than younger adults. Additional adjustment for other available variables had little effect on associations. In the sensitivity analysis that excluded probable EVD cases, associations with exposure levels were stronger, and the J-shaped association with age was more marked (Table 5).

Discussion

In Ebola-affected households in our study, the age pattern for EVD incidence in children differed from that reported for the overall epidemic by the World Health Organization (4) and was closer to the age pattern of reported case-fatality rates; children <5 years of age had higher risks than older children (4,7). Among adults, the pattern was similar to previous findings (6), with
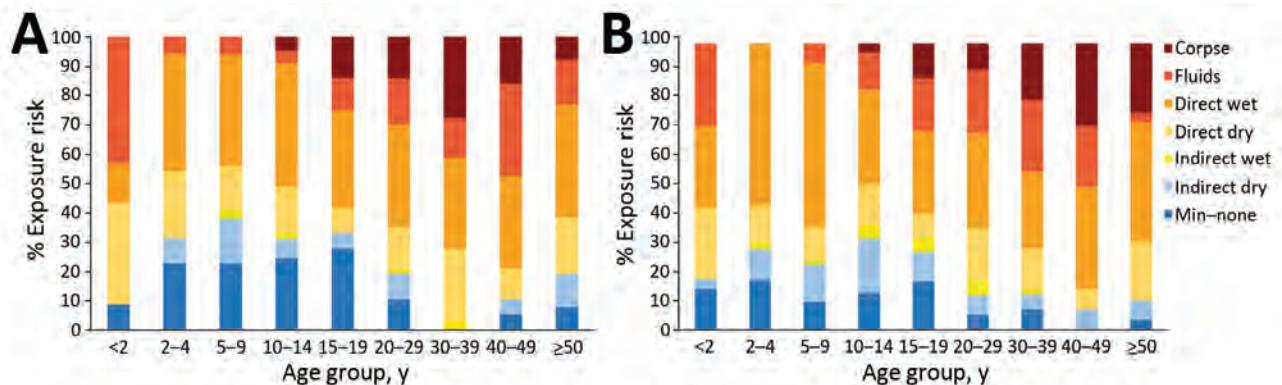
Figure 3. Levels of exposure to Ebola virus disease among households of Kerry Town survivors, excluding primary case-patients, by age and sex, Sierra Leone, 2014–2015. A) Male participants; B) female participants. Levels of exposure correspond to those shown in Table 1. Min–none, minimum or no exposure.

Table 4. Risk factors associated with development of EVD in subsequent case-patients in Ebola-affected households, Kerry Town, Sierra Leone, 2014–2015*

Risk factor	No. patients/no. total (%),† N = 809	Adjusted RR‡ (95% CI)	Adjusted RR§ (95% CI)	Multivariable RR¶ (95%CI)	p value#
Sex					
M	136/337 (40.4)	1.1 (0.87–1.4)	1.06 (0.85–1.3)	1.03 (0.87–1.2)	
F	211/472 (44.7)	1	1	1	0.7
Age, y					
<2	22/51 (43.1)	0.79 (0.49–1.3)	0.80 (0.49–1.3)	0.92 (0.64–1.3)	
2–4	31/81 (38.3)	0.70 (0.45–1.1)	0.70 (0.46–1.1)	0.97 (0.72–1.3)	
5–9	38/127 (29.9)	0.44 (0.28–0.68)	0.44 (0.28–0.69)	0.70 (0.50–0.97)	
10–14	34/114 (29.8)	0.41 (0.25–0.67)	0.41 (0.25–0.67)	0.64 (0.45–0.93)	
15–19	35/95 (36.8)	0.53 (0.33–0.84)	0.53 (0.33–0.84)	0.71 (0.49–1.02)	
20–29	72/155 (46.5)	1	1	1	
30–39	51/85 (60.0)	1.2 (0.82–1.6)	1.2 (0.82–1.6)	1.1 (0.83–1.4)	
40–49	30/46 (65.2)	1.2 (0.82–1.8)	1.2 (0.83–1.8)	1.1 (0.80–1.6)	
≥50	33/53 (62.3)	1.3 (0.87–1.8)	1.3 (0.88–1.8)	1.3 (0.97–1.8)	0.004
Maximum exposure					
Handled corpse	60/72 (83.3)	18.1 (7.4–44.1)	13.5 (5.4–33.5)	11.1 (4.5–27.4)	
Handled fluids	73/120 (60.8)	13.1 (5.4–31.9)	9.7 (3.9–24.1)	8.5 (3.5–20.6)	
Direct wet contact	146/297 (49.2)	10.4 (4.3–25.1)	8.3 (3.4–20.1)	7.1 (3.0–17.1)	
Direct dry contact	47/125 (37.6)	7.1 (2.9–17.7)	5.6 (2.3–13.9)	5.3 (2.2–12.9)	
Indirect wet contact	5/19 (26.3)	5.7 (1.6–20.1)	4.9 (1.4–16.8)	4.7 (1.5–14.6)	
Indirect dry contact	8/74 (10.8)	1.4 (0.43–4.6)	1.3 (0.40–4.2)	1.3 (0.41– 4.0)	
Minimal/no contact**	8/102 (7.8)	1	1	1	<0.001
Position in household					
Household head	24/52 (46.2)	1.2 (0.79–1.79)	0.62 (0.35–1.1)	0.62 (0.39–1.0)	
Household member	323/757 (42.7)	1	1	1	0.03
Household size					
≥16	120/209 (57.4)	5.2 (1.6–16.9)	5.0 (1.5–16.8)	2.9 (1.1–7.8)	
11–15	98/290 (33.8)	2.4 (0.70–7.9)	2.4 (0.70–8.3)	1.7 (0.63–4.6)	
6–10	121/270 (44.8)	3.7 (1.2–12.0)	3.9 (1.2–12.8)	2.7 (1.04–7.0)	
1–5	8/40 (20.0)	1	1	1	0.01
Occupation					
HCW (formal and informal)	8/11 (72.7)	1.6 (1.1–2.5)	1.8 (0.91–3.6)		
Ebola front-line worker	1/8 (12.5)	0.16 (0.02–1.5)	0.14 (0.02–1.3)		
Driver	11/17 (64.7)	1.2 (0.67–2.0)	1.1 (0.55–2.3)		
Religious leader/chief/teacher	5/7 (71.4)	1.6 (0.95–2.8)	1.8 (0.70–4.4)		
Farmer/fisherman/unskilled	18/41 (43.9)	0.81 (0.49–1.4)	0.85 (0.48–1.5)		
Office/business	26/39 (66.7)	1.3 (0.89–1.8)	1.4 (0.87–2.2)		
Child/student	173/484 (35.7)	0.52 (0.40–0.69)	1.0 (0.63–1.6)		
Trader/tailor/service	96/177 (54.2)	1	1		
Water available					
Sometimes	45/131 (34.4)	0.58 (0.2–1.3)	0.59 (0.28–1.3)		
Most days	118/265 (44.5)	1.0 (0.59–1.59)	0.96 (0.60–1.5)		
Every day	182/408 (44.6)	1	1		
Soap available					
Sometimes	64/194 (33.0)	0.78 (0.42–1.4)	0.84 (0.47–1.5)		
Most days	113/200 (56.5)	1.5 (0.90–5.5)	1.4 (0.84–2.3)		
Every day	168/410 (41.0)	1	1		
Latrine					
Household's own	107/286 (37.4)	0.7 (0.43–1.2)	0.72 (0.43–1.2)		
Shared/none	238/518 (45.9)	1	1		
Crowding					
High	126/238 (52.9)	2.1 (0.89–4.7)	2.4 (1.0–5.4)		
Medium	189/483 (39.1)	1.4 (0.63–3.2)	1.6 (0.71–3.6)		
Low	30/83 (36.1)	1	1		
Spouse with Ebola first					
Yes	45/77 (58.4)	1.6 (1.2–2.1)	1.0 (0.68–1.5)		
No	302/732 (41.3)	1	1		

*Subsequent case-patients were any household members who contracted Ebola virus disease after the first (primary) case-patient. Data were excluded for 4 deaths from uncertain cause, 27 persons with no individual-level data, and 97 primary cases. Data were missing for 2 persons with no recorded age, 6 persons with no recorded occupation, and 5 persons (in 1 household) with no recorded information about water, soap, latrine, and crowding. EVD, Ebola virus disease; HCW, healthcare worker; RR, risk ratio.
†Number of subsequent case-patients/total number of household members in study, excluding primary case-patients.
‡Adjusted for household clustering.
§Adjusted for age, sex, and household clustering.
¶Adjusted for clustering and all other factors included in the model.
#p values for multivariable model calculated from likelihood ratio test in logistic regression model.
**Only 7 persons reported no contact, so these 2 categories are combined.

a plateau occurring >35 years of age. This pattern was similar whether probable case-patients were included or not. Children were less likely than adults to be primary case-patients, and among child primary case-patients, no particular trend by age was observed (Table 3). The higher risk for EVD among children <5 years of age than among older children may suggest that very young children have been disproportionately missed in notification data.

Our study included only survivor households because it was conducted by building on survivor-support links; consequently, it missed households with only fatal cases and those in which no one sought care. Compared with all Ebola-affected households, households in our study were likely to be larger; to include more EVD patients, which increases the chance that ≥1 household member survived; and to include more children ≥5 years of age, who have a lower case-fatality rate than younger children. These characteristics would tend to increase attack rates and may explain the high attack rate overall and the association of attack rate with household size. These characteristics might also increase the proportion of cases among

children, although children ≥5 years of age had a relatively low incidence of EVD.

After excluding primary case-patients, we examined the extent to which age patterns could be explained by exposure levels. After we adjusted age-specific incidence data by exposure, children 5–19 years of age still had a lower risk for EVD, although the lower risk was less marked, and the increased risk with age for adults no longer plateaued but continued upward. If we measured exposure accurately, these findings suggest that some of the variation in risk by age within households results from differences in susceptibility. In the interviews, we avoided lengthy questionnaires with each person to try to reduce questionnaire fatigue, respondents' forgetting or denying types of exposure, and possibly overburdening already traumatized households. Instead, we encouraged families to tell their stories, ensuring that we learned which household members had contact with each EVD patient and what type of contact. Consequently, the conversation flowed naturally, with different household members contributing and providing details, helping to minimize recall bias. This approach also enabled us to acquire details for

Table 5. Sensitivity analysis excluding probable cases showing risk factors associated with development of EVD as a subsequent case-patient in Ebola-affected households, Kerry Town, Sierra Leone, 2014–2015*

Risk factor	Total, excluding probable cases, N = 764		
	No. patients/no. total (%)†	Adjusted RR‡ (95% CI)	p value§
Sex			
M	114/315 (36.2)	1.0 (0.83–1.2)	
F	188/449 (41.9)	1	1.0
Age, y			
<2	21/50 (42.0)	0.99 (0.66–1.5)	
2–4	22/72 (30.6)	0.98 (0.68–1.4)	
5–9	27/116 (23.3)	0.69 (0.47–1.0)	
10–14	26/106 (24.5)	0.60 (0.39–0.93)	
15–19	34/94 (36.2)	0.77 (0.52–1.1)	
20–29	63/146 (43.2)	1	
30–39	47/81 (58.0)	1.2 (0.86–1.6)	
40–49	28/44 (63.6)	1.2 (0.82–1.8)	
≥50	33/53 (62.3)	1.5 (1.1–2.0)	0.002
Maximum exposure			
Handled corpse	60/72 (83.3)	40.6 (8.5–194.5)	
Handled fluids	65/112 (58.0)	30.5 (6.4–144.8)	
Direct wet contact	125/276 (45.3)	24.1 (5.2–113.2)	
Direct dry contact	41/119 (34.5)	16.7 (3.6–78.1)	
Indirect wet contact	5/19 (26.3)	17.2 (3.1–94.7)	
Indirect dry contact	4/70 (5.7)	2.3 (0.37–14.3)	
Minimal/no contact	2/96 (2.1)	1	<0.001
Position in household			
Household head	22/50 (44.0)	0.58 (0.35–0.98)	
Household member	280/714 (39.2)	1	0.02
Household size			
≥16	108/197 (54.8)	2.6 (0.98–6.7)	
11–15	90/282 (31.9)	1.5 (0.57–3.9)	
6–10	96/245 (39.2)	2.3 (0.89–5.7)	
1–5	8/40 (20.0)	1	0.04

*Subsequent case-patients were any household members who contracted EVD after the first (primary) case-patient. EVD, Ebola virus disease; RR, risk ratio.
†Excluded data: 4 deaths from uncertain cause; 27 persons with no individual-level data, 97 primary case-patients; 45 case-patients were classified as having EVD on the basis of their histories but had no diagnosis of EVD at the time. Missing data: 2 persons with age unknown.
‡Adjusted for clustering and all variables in the model.
§p values calculated from likelihood ratio test in logistic regression model.

children and for persons who had died, although use of proxy respondents may have limited accuracy of exposure measurement. We conducted the interviews 4–9 months after the illness, but participants provided considerable detail in their responses. Inaccuracies in recall would lead to a failure to adjust completely for exposure level, whereas any tendency to recall greater exposures for household members with EVD would increase the association with exposure and result in the association between age and EVD being overadjusted for exposure level.

We predefined exposure levels so that we could record only the highest level and not probe for details for possible lower levels. This approach differed from that of other studies (*13,14,16*), which recorded several exposures and adjusted during analysis. Our hierarchy of exposure appears to be accurate; we found strong correlations between EVD risk and each increase in exposure level.

As others have reported (*13,14,16*), the highest risk for EVD exposure was from contact with dead bodies. Risk was also high from direct contact with fluids and with wet patients and was lower but still considerable (5-fold [17-fold in the sensitivity analysis], compared with minimal risk) from direct contact with dry patients and indirect contact with wet patients (Tables 4,5). We found no discernible increase in risk from indirect contact with dry patients compared with exposures classified as minimal risk (Table 1). Overall, after exclusion of primary and co-primary case-patients, we found a high household attack rate, higher than found in previous studies (*23*), perhaps reflecting the urban setting and the bias toward households with multiple cases.

Children had lower exposure than adults, but exposure levels in these households were high overall; >50% of each age group had at least direct exposure to a wet patient. In the sensitivity analysis, correlation between exposure levels and outcome was stronger, suggesting misclassification of some case-patients included as probable EVD cases; this analysis also showed a markedly lower EVD risk in children >5 years of age.

A lower susceptibility to EVD among children is possible. Lower attack rates or case-fatality rates in children have been found for other viral diseases, including varicella (*24*), smallpox (*25*), and West Nile virus disease (*26*). For EVD, different cytokine and chemokine responses related to survival have been noted for adults and children (*27*).

We found little difference in risk by sex, even when stratified by age. Household-level measures of sanitation had surprisingly little effect on the outcome (*28*). Having a spouse who contracted EVD first was not a risk factor after we adjusted for age; consequently, sexual transmission did not appear to be an important factor in the acute phase.

We established likely sources of infection for 70% of primary case-patients. Although some were linked to high-risk activities, more were related to visits to friends and relatives, including some visits to nurse sick relatives. Other households were infected by taking in sick relatives. These activities show remarkable altruism at a stage of the epidemic when Ebola was well known. More support to families to protect themselves in the home when they helped those not known to have EVD might have prevented these transmissions.

Much of what we know about risks for Ebola virus transmission comes from anecdotal reports or case series (*29*). Few studies have measured risk associated with particular exposures directly (*13,15,16,18,23*), and none have been large enough to examine risk by age in detail. This study collected information on >800 contacts, enabling estimates of exposure-specific and age-specific attack rates. After we adjusted for exposure, age patterns for Ebola attack rates were similar to those for case-fatality rates. Inherent differences in susceptibility, which warrant further investigation, likely underlie both distributions.

Ms. Bower is a research fellow in the Department of Infectious Disease Epidemiology, London School of Hygiene and Tropical Medicine. Her research interests include emerging infectious diseases and humanitarian emergencies.

References

1. Dowell SF. Ebola hemorrhagic fever: why were children spared? Pediatr Infect Dis J. 1996;15:189–91. http://dx.doi.org/10.1097/00006454-199603000-00002
2. Rosello A, Mossoko M, Flasche S, Van Hoek AJ, Mbala P, Camacho A, et al. Ebola virus disease in the Democratic Republic of the Congo, 1976–2014. eLife. 2015;4: e09015. http://dx.doi.org/10.7554/eLife.09015
3. Ebola hemorrhagic fever in Zaire, 1976. Bull World Health Organ. 1978;56:271–93.
4. World Health Organization Ebola Response Team; Agua-Agum J, Ariyarajah A, Blake IM, Cori A, Donnelly CA, Dorigatti I, et al. Ebola virus disease among children in West Africa. N Engl J Med. 2015;372:1274–7. http://dx.doi.org/10.1056/NEJMc1415318
5. World Health Organization Ebola Response Team; Agua-Agum J, Ariyarajah A, Aylward B, Blake IM, Brennan R, Cori A, et al. West African Ebola epidemic after one year—slowing but not yet under control. N Engl J Med. 2015;372:584–7. http://dx.doi.org/10.1056/NEJMc1414992
6. Glynn JR. Age-specific incidence of Ebola virus disease. Lancet. 2015;386:432. http://dx.doi.org/10.1016/S0140-6736(15)61446-5
7. World Health Organization Ebola Response Team. Ebola virus disease among male and female persons in West Africa. N Engl J Med. 2016;374:96–8. http://dx.doi.org/10.1056/NEJMc1510305
8. World Health Organization Ebola Response Team. Ebola virus disease in West Africa—the first 9 months of the epidemic and forward projections. N Engl J Med. 2014;371:1481–95. http://dx.doi.org/10.1056/NEJMoa1411100
9. Gignoux E, Idowu R, Bawo L, Hurum L, Sprecher A, Bastard M, et al. Use of capture-recapture to estimate underreporting of Ebola virus disease, Montserrado County, Liberia. Emerg Infect Dis. 2015;21:2265–7. http://dx.doi.org/10.3201/eid2112.150756

10. Helleringer S, Noymer A, Clark SJ, McCormick T. Did Ebola relatively spare children? Lancet. 2015;386:1442–3. http://dx.doi.org/10.1016/S0140-6736(15)00415-8

11. Kourtis AP, Appelgren K, Chevalier MS, McElroy A. Ebola virus disease: focus on children. Pediatr Infect Dis J. 2015;34:893–7. http://dx.doi.org/10.1097/INF.0000000000000707

12. Moreau M, Spencer C, Gozalbes JG, Colebunders R, Lefevre A, Gryseels S, et al. Lactating mothers infected with Ebola virus: EBOV RT-PCR of blood only may be insufficient. Euro Surveill. 2015;20:21017. http://dx.doi.org/10.2807/1560-7917.ES2015.20.3.21017

13. Dowell SF, Mukunu R, Ksiazek TG, Khan AS, Rollin PE, Peters CJ. Transmission of Ebola hemorrhagic fever: a study of risk factors in family members, Kikwit, Democratic Republic of the Congo, 1995. Commission de Lutte contre les Epidémies à Kikwit. J Infect Dis. 1999;179(Suppl 1):S87–91. http://dx.doi.org/10.1086/514284

14. Brainard J, Hooper L, Pond K, Edmunds K, Hunter PR. Risk factors for transmission of Ebola or Marburg virus disease: a systematic review and meta-analysis. Int J Epidemiol. 2016;45:102–16. http://dx.doi.org/10.1093/ije/dyv307

15. Baron RC, McCormick JB, Zubeir OA. Ebola virus disease in southern Sudan: hospital dissemination and intrafamilial spread. Bull World Health Organ. 1983;61:997–1003.

16. Francesconi P, Yoti Z, Declich S, Onek PA, Fabiani M, Olango J, et al. Ebola hemorrhagic fever transmission and risk factors of contacts, Uganda. Emerg Infect Dis. 2003;9:1430–7. http://dx.doi.org/10.3201/eid0911.030339

17. Wamala JF, Lukwago L, Malimbo M, Nguku P, Yoti Z, Musenero M, et al. Ebola hemorrhagic fever associated with novel virus strain, Uganda, 2007–2008. Emerg Infect Dis. 2010;16:1087–92. http://dx.doi.org/10.3201/eid1607.091525

18. World Health Organization. Ebola hemorrhagic fever in Sudan, 1976. Report of a WHO International Study Team. Bull World Health Organ. 1978;56:247–70.

19. Roels TH, Bloom AS, Buffington J, Muhungu GL, Mac Kenzie WR, Khan AS, et al. Ebola hemorrhagic fever, Kikwit, Democratic Republic of the Congo, 1995: risk factors for patients without a reported exposure. J Infect Dis. 1999;179(Suppl 1):S92–7. http://dx.doi.org/10.1086/514286

20. World Health Organization; Sierra Leone Ministry of Health. Clinical management of patients in the Ebola Treatment Centres and other care centres in Sierra Leone: a pocket guide. Interim emergency guidelines—Sierra Leone adaptation of the WHO generic clinical management of patients with viral haemorrhagic fever: a pocket guide for front-line health workers. Interim emergency guidance for West Africa—for country adaptation. March 2014 [cited 2016 Apr 28]. http://nerc.sl/sites/default/files/docs/Sierra%20Leone%20Ebola%20Treatment%20Centre%20pocket%20guide%2015%20Dec%20%202014%281%29.pdf

21. Localio AR, Margolis DJ, Berlin JA. Relative risks and confidence intervals were easily computed indirectly from multivariable logistic regression. J Clin Epidemiol. 2007;60:874–82. http://dx.doi.org/10.1016/j.jclinepi.2006.12.001

22. Santos CA, Fiaccone RL, Oliveira NF, Cunha S, Barreto ML, do Carmo MB, et al. Estimating adjusted prevalence ratio in clustered cross-sectional epidemiological data. BMC Med Res Methodol. 2008;8:80. http://dx.doi.org/10.1186/1471-2288-8-80

23. Dean NE, Halloran ME, Yang Y, Longini IM. Transmissibility and pathogenicity of Ebola virus: a systematic review and meta-analysis of household secondary attack rate and asymptomatic infection. Clin Infect Dis. 2016;ciw114. http://dx.doi.org/10.1093/cid/ciw114

24. Seward J, Galil K, Wharton M. Epidemiology of varicella. In: Arvin AM, Gershon AA, editors. Varicella-zoster virus: virology and clinical management. Cambridge: Cambridge University Press; 2000.

25. Fenner F, Henderson DA, Arita I, Jezek Z, Ladnyi ID. Smallpox and its eradication. Geneva: World Health Organization; 1988.

26. Lindsey NP, Staples JE, Lehman JA, Fischer M; Centers for Disease Control and Prevention. Surveillance for human West Nile virus disease—United States, 1999–2008. MMWR Surveill Summ. 2010;59:1–17.

27. McElroy AK, Erickson BR, Flietstra TD, Rollin PE, Nichol ST, Towner JS, et al. Biomarker correlates of survival in pediatric patients with Ebola virus disease. Emerg Infect Dis. 2014;20:1683–90. http://dx.doi.org/10.3201/eid2010.140430

28. Fallah MP, Skrip LA, Gertler S, Yamin D, Galvani AP. Quantifying poverty as a driver of Ebola transmission. PLoS Negl Trop Dis. 2015;9:e0004260. http://dx.doi.org/10.1371/journal.pntd.0004260

29. Dietz PM, Jambai A, Paweska JT, Yoti Z, Ksaizek TG. Epidemiology and risk factors for Ebola virus disease in Sierra Leone—23 May 2014 to 31 January 2015. Clin Infect Dis. 2015;61:1648–54.

Address for correspondence: Judith R. Glynn, Department of Infectious Disease Epidemiology, London School of Hygiene & Tropical Medicine, Keppel St, London WC1E 7HT, UK; email: judith.glynn@lshtm.ac.uk

Outbreak of *Achromobacter xylosoxidans* and *Ochrobactrum anthropi* Infections after Prostate Biopsies, France, 2014

Skerdi Haviari, Pierre Cassier, Cédric Dananché, Monique Hulin, Olivier Dauwalder,
Olivier Rouvière, Xavier Bertrand, Michel Perraud, Thomas Bénet, Philippe Vanhems

We report an outbreak of healthcare-associated prostatitis involving rare environmental pathogens in immunocompetent patients undergoing transrectal prostate biopsies at Hôpital Édouard Herriot (Lyon, France) during August 13–October 10, 2014. Despite a fluoroquinolone-based prophylaxis, 5 patients were infected with *Achromobacter xylosoxidans* and 3 with *Ochrobactrum anthropi*, which has not been reported as pathogenic in nonimmunocompromised persons. All patients recovered fully. Analysis of the outbreak included case investigation, case–control study, biopsy procedure review, microbiologic testing of environmental and clinical samples, and retrospective review of hospital records for 4 years before the outbreak. The cases resulted from asepsis errors during preparation of materials for the biopsies. A low-level outbreak involving environmental bacteria was likely present for years, masked by antimicrobial drug prophylaxis and a low number of cases. Healthcare personnel should promptly report unusual pathogens in immunocompetent patients to infection control units, and guidelines should explicitly mention asepsis during materials preparation.

The diagnosis of prostate cancer relies heavily on transrectal ultrasound-guided prostate biopsy (TUPB), which 0.1%–0.3% of the total population undergoes each year in developed countries. An estimated 1 million biopsies are performed annually in the United States (*1*) and ≈63,000 in France (*2*). This invasive practice, essential to diagnose prostate cancer properly and to guide future treatment, takes several prostate samples by means of a biopsy

Author affiliations: Hospices Civils de Lyon, Lyon, France
(S. Haviari, P. Cassier, C. Dananché, M. Hulin, O. Dauwalder,
O. Rouvière, M. Perraud, T. Bénet, P. Vanhems); Université
Claude Bernard, Lyon (S. Haviari, P. Cassier, C. Dananché,
O. Dauwalder, O. Rouvière, M. Perraud, T. Bénet, P. Vanhems);
Centre International de Recherche en Infectiologie, Lyon
(P. Cassier, O. Dauwalder, T. Bénet, P. Vanhems); Centre
Hospitalier Régional Universitaire de Besançon, Besançon,
France (X. Bertrand); Laboratoire des Pathogènes Émergents–
Fondation Mérieux, Lyon (T. Bénet, P. Vanhems)

needle, which passes through the intestinal barrier. This process makes proper asepsis challenging, and the attack rate of iatrogenic urinary tract infections (UTIs) after biopsy is ≈3%, although rates vary for different countries and clinics (*3*). Endogenous gram-negative bacteria, mostly *Escherichia coli*, are the main causative agents of complications after prostate biopsies (*4*). Antimicrobial drug prophylaxis is recommended for patients undergoing these procedures, mostly to reduce risk of infection. However, the choice of antimicrobial drug is always a compromise because a single drug cannot target all microorganisms (*5–7*). Fluoroquinolones targeting digestive gram-negative bacteria are the most common choice (*3,8,9*), as described in relevant guidelines (*10,11*).

Reports of a few outbreaks resulting from nonsterile handling of materials or inadequate procedures (*12–14*) have involved unexpected pathogens, such as naturally occurring environmental bacteria that are antimicrobial-drug resistant. These pathogens' resistance to antimicrobial prophylaxis could theoretically facilitate outbreaks caused by asepsis errors. We investigated an outbreak of healthcare-associated UTIs occurring after prostate biopsies to stop its spread and determine its causes and risk factors.

Materials and Methods

Outbreak Description and Setting

In October 2014, the urology team of Hôpital Édouard Herriot, a teaching hospital with ≈850 beds, located in Lyon, France, alerted the radiology department that in the previous 3 weeks, 6 patients had dysuria and UTIs involving unusual pathogens <10 days after each had a prostate biopsy. The radiology department, which performed the biopsies, asked the hospital infection control unit to investigate, and the investigation began immediately.

Of the 6 initial case-patients, 4 had *Achromobacter xylosoxidans* UTIs and 2 had *Ochrobactrum anthropi* UTIs, all occurring after a TUPB. The radiology department performs ≈450 biopsies per year, all in the same ultrasound room. According to hospital records, ≈1% of patients call

back to report symptoms of infections and need to submit urine or blood cultures within 15 days after biopsy.

Biopsy Protocol

All biopsies were preceded by a single dose of antimicrobial drug prophylaxis (400 mg ofloxacin), as recommended by national guidelines at the time of the procedures (*11*). As a preliminary step, nonsterile sponges were soaked in a 0.9% solution of sodium chloride (NaCl) and placed in small plastic cases on a table beside the patient. During the first part of the procedure, the main operator undertook transrectal ultrasonography with a probe covered by an inner layer of gel, a protective plastic sheath, and an outer layer of gel. During the second part of the procedure, a needle guide was mounted on top of the plastic sheath, and the operator worked the automatic biopsy gun with his or her main hand, while holding the ultrasound probe with the other hand. After a sample was taken, the needle was scraped against one of the sponges to remove the biopsy core (Figure 1, panels A, B); the needle was then reused until all relevant samples were obtained. At the end of the procedure, the integrity of the probe sheath was checked, and all equipment was discarded or sanitized. Patients were advised to call their radiologist or urologist if they had fever, pain, difficulty urinating, or prolonged bleeding.

Case–Control Study and Retrospective Surveillance

Administrative, clinical, and microbiologic records of all patients who underwent a TUPB at the hospital during September 1–October 31, 2014, were reviewed to find putative additional cases. The urology team was also asked to report any additional cases found as a result of systematic postbiopsy follow-up consultation. Confirmed cases were defined as patients having fever, pain, or dysuria and a positive urine or blood culture requested <15 days after biopsy that showed presence of *A. xylosoxidans* or *O. anthropi* infection. Controls were all patients who underwent a TUPB in the same ultrasound

room during the same 2-month period but who were not asked to submit a blood or urine culture. Possible cases were retrospectively defined as patients for whom a clinician had requested ≥1 urine or blood culture <15 days after biopsy, regardless of the result, because of a clinical suspicion of prostatis (i.e., presence of fever, pain, or dysuria). Possible cases were not included in our statistical calculations.

Temporal distribution of cases involved an index case that occurred in August 2014, a month before the other cases occurred in September and October 2014 at a rate of ≈2 per week. All possible control-patients (n = 44) whose biopsies occurred between the first and last case of the September–October cluster were included. In addition, 6 temporally matched control-patients were included for the August case-patient; these patients were biopsied on the same day or <1 week before the case-patient.

Records were reviewed to assess organizational risk factors (e.g., operator identity or order in which patients had biopsies during the day) and individual features (e.g., patient age or histologic evidence of localized inflammation). Retrospective surveillance was also conducted by accessing an electronic database that contained dates and patient names for all prostate biopsies in the radiology unit and that contained dates, patient names, and results (i.e., species and antibiograms) for all blood and urine cultures in the hospital network laboratory during January 2011–November 2014. Records for November 2014–March 2015 were similarly analyzed to confirm the clinician-reported absence of new cases after implementation of corrective measures.

Microbiologic Methods and Molecular Typing

All biopsy materials were investigated microbiologically. Tap water was gathered in sterile containers (Dominique Dutscher, Brumath, France). Sterile cotton swabs (Biolys, Taluyers, France) were used for transducer probe and sink drain samples. Worktop and handwashing sink samples were plated on Count Tact Agar plates (bioMérieux, Marcy
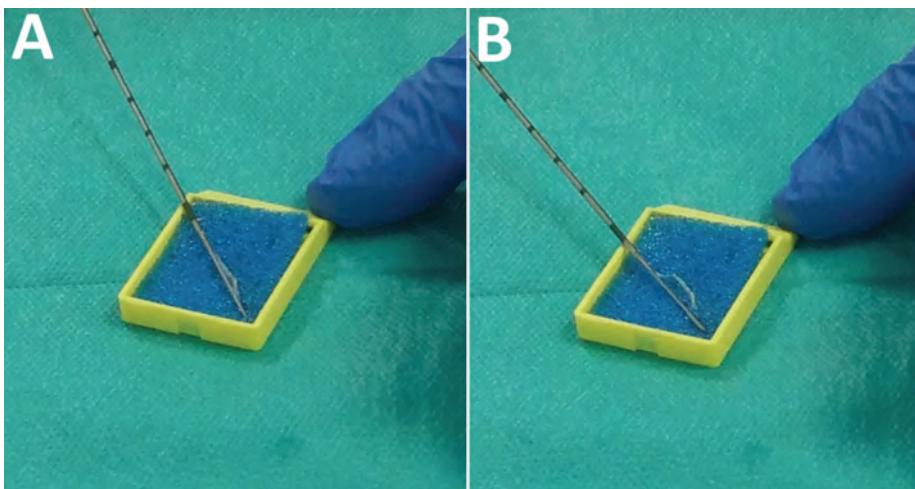
Figure 1. Application of biopsy needle on sponge used during transrectal ultrasound-guided prostate biopsy. A) Needle before scraping a biopsy core on sponge; B) needle after scraping to detach a biopsy core on sponge.

l'Etoile, France). For *A. xylosoxidans* and *O. anthropi*, trypticase soy broth (TSB) was used as preenrichment broth, supplemented with cetrimide (2 g/L) for *A. xylosoxidans* and amoxicillin (10 mg/L) for *O. anthropi*. Brain–heart infusion (BHI) enrichment broth, supplemented with aztreonam (32 mg/L) and vancomycin (32 mg/L), was also used for both bacteria, as described (*15*).

For each species, 200 mL of tap water and 0.9% sterile NaCl were filtered through sterile 0.45-μm membrane filters (Millipore, Darmstadt, Germany). The membrane was placed either on plate count agar enriched with cetrimide (2 g/L) or on trypticase soy agar (TSA) enriched with amoxicillin (10 mg/L). Sponges, reused soaking container, probe, gel, plastic cases, and drain swab samples were first enriched with 10 mL of TSB supplemented with either cetrimide or amoxicillin for 48 h at 30°C or with BHI supplemented with aztreonam for 72 h at 37°C. One drop of each enrichment culture (i.e., TSB and centrimide, TSB and amoxicillin, and BHI and aztreonam) was respectively plated on TSA supplemented with cetrimide; on TSA supplemented with amoxicillin and incubated for 48 h at 30°C; and on MacConkey agar and incubated for 48 h at 37°C. Count Tact Agar plates were incubated for 7 days at 30°C.

Isolates were identified phenotypically by API 20NE and API 20E strips (bioMérieux) for non-*Enterobacteriacae* and *Enterobacteriacae*, respectively. Identification was confirmed by matrix-assisted laser desorption/ionization time-of-flight mass spectrometry with the VITEK MS system (bioMérieux).

The macrorestriction profile of the total DNA of the clinical and environmental isolates was charted by pulsed-field gel electrophoresis (PFGE) (CHEF-DR III,

Bio-Rad, Hercules, California), as described (*16*). *Xba*I and *Spe*I served as restriction enzymes for *A. xylosoxidans* and *O. anthropi*, respectively. We ensured that the gels were comparable by including *Staphylococcus aureus* strain NCTC 8325 (including *Sma*I as the restriction enzyme) for reference. We compared PFGE patterns by visual inspection.

Statistical Analysis

Descriptive statistics, including median and interquartile ranges, were computed for quantitative variables. Categorical data were compared by using the Fisher exact test and quantitative data by using the Mann-Whitney U test. Statistical analysis was conducted with R statistical software (*17*). All tests were 2-tailed, and p values ≤0.05 were considered statistically significant. Logistic regression was performed with general linear models with bias reduction as implemented in R, brglm (*18,19*). Multiple logistic regression that used an entry threshold of p = 0.15 and a backward elimination cutoff of p = 0.05 searched for factors that correlated independently with infection. Interactions between variables in the resulting model were also tested.

Results

Clinical Course

We identified 8 confirmed case-patients: 1 was biopsied on August 13, 2014; the other 7 were biopsied during September 12–October 10 and were evenly distributed during that period. An additional 2 possible case-patients with no microbiologic evidence of infection were biopsied on

Table 1. Clinical and microbiologic history of the 8 confirmed cases in the cluster of *Achromobacter xylosoxidans* and *Ochrobactrum anthropi* infections occurring after prostate biopsies, France, 2014*

Characteristic	Patient ID							
	1	2	3	4	5	6	7	8
Date of biopsy	Aug 13	Sep 12	Sep 15	Sep 30	Sep 30	Oct 3	Oct 8	Oct 10
Patient age at onset, y	66	60	59	62	65	54	68	69
Days between biopsy and urinalysis	13	2	3	10	3	6	8	7
Highest fever level, °C	39	39	38.5	38.6	39.1	NR	39	38.3
Localized symptoms	No	Yes	No	Yes	No	NR	Yes	No
Hospitalization	Yes	Yes	Yes	Yes	Yes	No	No	No
Urine culture result	Negative	*A. xyl*	*A. xyl*	*A. xyl*	*A. xyl*	*O. ant*	*A. xyl*	*O. ant*
Blood culture result	*O. ant*	*A. xyl*	*A. xyl*	NA	*A. xyl*	NA	NA	NA
Curative antimicrobial treatment†	Yes	Yes	Yes	Yes	Yes	NR	Yes	No
Apyrexia without effective antimicrobial drug	Yes	No	Yes	No	Yes	NR	Yes	Yes
Immunosuppressive drugs	No	No	No	No	No	No	No	No

*A. xyl, *Achromobacter xylosoxidans*; NA, cultures not requested; NR, not recorded; *O. ant, *Ochrobactrum anthropi*.
†All patients received a single dose of 400 mg ofloxacin. Most received curative treatments: Patient 1, 2 g ceftriaxone/d intravenously for 3 d; then 200 mg ofloxacin/d orally for 10 d. Patient 2, ceftazidime, modalities unknown (treated outside the university hospital network). Patient 3, 2 g ceftriaxone 1× intravenously; then 200 mg ofloxacin 2×/d orally for 15 d. Patient 4, 2 g ceftriaxone/d intravenously for 3 d; then 1,200 mg amikacin 1× intravenously; then 800/160 mg co-trimoxazole 2×/d orally for 15 d. Patient 5, 2 g ceftriaxone/d intravenously for 3 d; then 4 g piperacillin 3×/d intravenously and 800/160 mg co-trimoxazole 3×/d orally for 4 d; then co-trimoxazole for 15 d. Patient 7, 1 g ceftriaxone/d intravenously for 2 d and 200 mg ofloxacin 2×/d orally for 21 d. Antibiogram of *A. xylosoxidans* for patients 2, 3, 4, 5, and 7 showed sensitivity to amoxicillin, ticarcillin, piperacillin (with or without β-lactamase inhibitors), ceftazidime, colistin, co-trimoxazole, and carbapenems and resistance to cefalotine, cefoxitine, cefotaxime, cefepime, aminoglycosides, quinolones, tigecyclin, fosfomycin, and rifampin. Antibiogram of *O. anthropi* for patient 1 showed sensitivity to carbapenems, aminoglycosides, ciprofloxacin, tigecyclin, rifampin, and co-trimoxazole and resistance to amoxicillin, ticarcillin, piperacillin (with or without β-lactamase inhibitors), cefalotine, cefoxitine, cefotaxime, ceftazidime, cefepime, aztreonam, norfloxacin, and fosfomycin. Antibiogram of *O. anthropi* for patient 8 was the same as for patient 1 except for sensitivity to norfloxacin. In hindsight, co-trimoxazole should probably have been used as first-line therapy.

October 6 and 7 (Table 1). On the basis of confirmed cases, the attack rate during August 13–October 10 was 9.4% (8/85 patients). At the height of the outbreak (i.e., September 12–October 10), the rate was 13.2% (7/53). These rates compare with a baseline long-term rate of 1.4% (27/1,927 patients) for endogenous postbiopsy infections, which are defined as cultures collected <15 days postbiopsy and growing no environmental bacterial strains (determined from hospital records for January 2011–August 2014).

Of the 10 confirmed and possible case-patients, 6 were hospitalized. None were in intensive care, and all recovered fully. Five patients were infected with an *A. xylosoxidans* strain resistant to ceftriaxone and ofloxacin; 3 of these patients reached apyrexia within 48 hours of treatment initiation with ceftriaxone (2 g/24 h), ofloxacin (400 mg/24 h), or both, as first-line regimens, despite the in vitro resistance to these agents. Three patients had *O. anthropi* infection; 1 received no curative antimicrobial drug treatment. The first outbreak patient (biopsied on August 13) had *O. anthropi* bacteremia and was a kidney-transplant recipient. The 2 possible case-patients with no identifiable culture also recovered quickly.

Onsite Investigation

Facility inspection and a review of practices identified mistakes in the sterile handling of sponges, which were sometimes accidentally touched by an aide with contaminated hands (aide 1 in Table 2). The container in which the sponges were soaked was reused from day to day, reportedly for up to several weeks. The container was commonly left overnight with sponges inside and never completely dried during the course of use. Other practices causing risk included application of nonsterile gel on the outer layer of the ultrasound probe and lack of a proper log of probe disinfection procedures.

The plastic container was identified as a likely source of environmental contamination of the biopsy needle, with bacteria being spread by the sponges. The container was immediately taken for microbiologic examination and replaced by sterile single-use cups. Biopsies continued to be performed while the investigation continued.

Samples were also collected from the sterile saline flask periodically used to refill the container and from the plastic cases; sponges (dry and soaked); ultrasound gel; transducer probe; tap water; and biopsy room environment (i.e., worktop, sink, and drain). A total of 52 samples were collected from 20 soaked sponges, 6 dry sponges, 2 plastic cases, 1 NaCl 0.9% flask, 1 ultrasound gel bottle, 4 water samples, and 18 surfaces.

Microbiologic Studies and Molecular Typing

All samples tested negative except for sponges retrieved from the saline-filled plastic container; those samples tested positive for 5 bacterial species: *A. xylosoxidans*, *O. anthropi*, *Stenotrophomonas maltophilia*, *Roseomonas mucosa*, and *Enterobacter cloacae*. Neither the dry sponges nor the sterile NaCl 0.9% flask used to soak them was contaminated. Of the 5 bacterial isolates, only *A. xylosoxidans* was resistant to fluoroquinolones. PFGE confirmed that all 5 patients infected by *A. xylosoxidans* were contaminated by the same strain (Figure 2). However, the clinical and environmental *O. anthropi* isolates had different PFGE profiles.

Table 2. Characteristics and risk factors of patients and controls in the study of an outbreak of *Achromobacter xylosoxidans* and *Ochrobactrum anthropi* infections occurring after prostate biopsies, France, 2014*

Variables	Cases, n = 8	Controls, n = 50	p value	Crude OR (95% CI)	Adjusted OR (95% CI)
Quantitative variables, median (IQR)†					
Age, y	63.5 (59.6–67.2)	67.1 (60.4–73.7)	0.12	0.55 (0.180–1.43)‡	–
Prostate-specific antigen, μg/L	6.94 (6.22–8.5)	6.0 (4.61–8.0)	0.3	1.36 (0.429–3.39)‡	–
Prostate size, mL§	40.0 (30.5–54.0)	37.2 (26.2–58.8)	0.39	1.28 (0.680–2.37)‡	–
No. cores sampled	14.5 (12.8–15.2)	15.0 (13.2–15.8)	0.92	0.97 (0.694–1.20)‡	–
Categorical variables, no. (%)¶					
Organizational factors					
Previous unaffected patient that day#	0	31 (62)	0.001	0.04 (0.000–0.319)	–
First patient of the day	7 (87.5)	14 (28)	0.002	12.6 2.44–353)	14.5 (2.49–558)
Operator A	5 (62.5)	9 (18)	0.02	6.86 1.56–43.0)	8.49 (1.55–104)
Aide 1 alone	7 (87.5)	27 (54)	0.12	4.27 (0.844–116)	–
Physiologic factors					
Previously had biopsy	4 (50)	41 (82)	0.07	0.23 (0.044–1.08)	–
Inflammatory histology	2 (25)	5 (10)	0.24	3.18 (0.373–17.9)	–
Previous localized treatment**	0	10 (20)	0.33	0.23 (0.000–2.09)	–
Neoplasic histology	5 (62.5)	41 (82)	0.34	0.36 (0.075–2.04)	–

*HIFU, high-intensity focused ultrasound; OR, odds ratio; –, not included in the final multiple regression model.
†p values determined by using the Mann-Whitney U test.
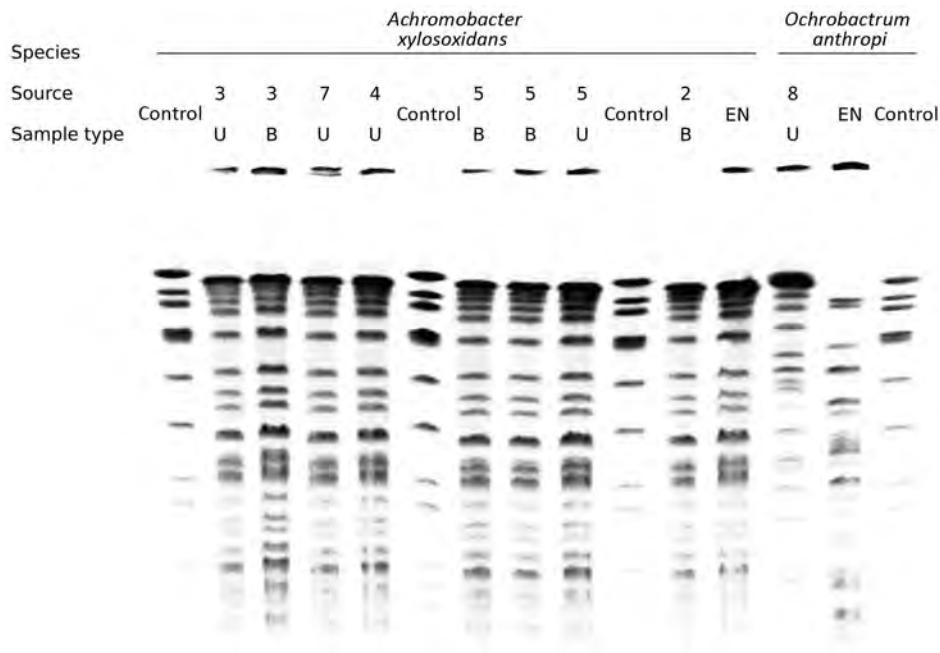‡For every additional 10 y in age, 5 μg/L (prostate-specific antigen), 20 mL (prostate size), and additional core (number of cores).
§n = 6 for cases, n = 44 for controls.
¶p values determined by using Fisher exact test.
#This variable was not included in the multiple model because it was closely correlated wtih the variable "first patient of the day."
**Resection or HIFU.

Figure 2. Pulsed-field gel electrophoresis of clinical and environmental strains of *Achromobacter xylosoxidans* and *Ochrobactrum anthropi* infections in patients after undergoing prostate biopsies at Hôpital Édouard Herriot, Lyon, France. Patient numbers match those in Table 1. EN, environmental; B, blood; U, urine; control, reference sample for calibration (described in Methods).

Infection Control Measures and Outbreak Termination

On the day of the alert, investigators conducting facility inspection identified the plastic container as a potential hazard and removed it from use. Beginning the following morning, the sponges were soaked in sterile cups, and a new cup was used for each patient. In early 2015, all sponges were systematically sterilized before being placed for soaking in sterile single-use cups. Radiology staff were retrained in clean and sterile handling of materials. No microbiologically confirmed infections occurred during October 10, 2014–March 30, 2015.

Case–Control Study

Case–control investigation determined that among potential risk factors considered (Table 2), first procedure of the day and identity of the main operator were associated with increased infection risk (adjusted odds ratio 14.5 [95% CI 2.49–558] and 8.49 [95% CI 1.55–104], respectively). No other significant differences between case-patients and control-patients were apparent; an interaction term variable was also considered and was not statistically significant. A sensitivity analysis, whether it included possible cases or excluded August cases and controls, retained the same variables in the final model (data not shown).

Retrospective Surveillance

After being informed by radiology staff of prolonged sporadic reuse of the plastic containers, we reviewed databases for January 2011–August 2014 for TUPBs and blood or urine cultures, looking for past cases involving 1 of the 5 species isolated from the container or other rare, environmental, waterborne pathogens. For 32 (1.7%) of 1,927

patients undergoing the procedure, a blood or urine sample was taken <15 days after the biopsy. Overall, cultures for 23 of the 32 patients were negative; among the other 9 patients, 2 had positive urine cultures with >2 bacteria (suggesting contamination by digestive flora), 1 had *Klebsiella pneumoniae*, 1 had *E. coli*, 1 had *O. anthropi* (patient 1 from Table 1), and 4 had *S. maltophilia* (1 of the 5 species found in the container) (Table 3).

During 2011 and 2012, four *S. maltophilia* cases clustered in 2 pairs, for which TUPBs occurred 19 days and 45 days apart. The first pair of patients had identical antibiograms, indicating that they were likely infected by the same strain. Minor differences were found in the antibiograms of the second pair. All strains were resistant to fluoroquinolones and third-generation cephalosporins. No complications occurred. All 4 patients were the first to undergo a biopsy on the day of their procedure.

Discussion

Our investigation showed that an outbreak of infections with uncommon pathogens after TUPBs in a radiology clinic resulted from inadequate preparation of supplies for the procedure. An aide seems to have accidentally contaminated a container, and its prolonged reuse for soaking small sponges enabled proliferation of uncommon waterborne pathogens and contamination of the sponges. For each patient, the biopsy needle was repeatedly in contact with contaminated sponges (Figure 1, panels A, B) and was reused to obtain additional biopsy cores, inoculating some patients with pathogens and causing infections. Because an ultrasound gel contaminated with *A. xylosoxidans* had been previously linked to an outbreak (*12*), we tested

Table 3. Clinical and microbiologic history of retrospective surveillance patients in the study of an outbreak of *Achromobacter xylosoxidans* and *Ochrobactrum anthropi* infections occurring after prostate biopsies, France*

Characteristic	Patient ID					
	A	B	C	D	E	F
Date of biopsy	2011 Nov 23	2011 Dec 16	2012 May 7	2012 May 31	2012 July 9	2012 Nov 30
Patient age at onset, y	57	79	75	65	76	68
Days between biopsy and urinalysis	5	1	8	3	9	2
Highest fever, °C	40	39	None	39	38.4	None
Localized symptoms	Yes	Yes	Yes	No	Yes	Yes
Hospitalization	No	Yes	No	No	No	No
Urine culture result	*S. malt*	*S. malt*	*E. coli*	*S. malt*	*S. malt*	Mixed flora
Blood culture result	NA	Negative	NA	Negative	NA	*K. pne*
Antimicrobial resistance profile†	1	1	NR	2	3	NR
Curative antimicrobial drug treatment	Yes	Yes	Yes	Yes	Yes	Yes
Apyrexia without proper antimicrobial regimen	Yes	Yes	No	Yes	Yes	Yes
Immunosuppressants	No	No	No	No	No	No

E. coli, Escherichia coli; K. pne, Klebsiella pneumoniae; NA, cultures not requested; NR, not recorded; *S. malt, Stenotrophomonas maltophilia*.
†The antimicrobial-drug resistance profile is shown for *S. maltophilia* only. Profiles 1 and 2 had only 1 difference across 17 different antimicrobial drugs (ceftazidime-I vs. -S). Of 14 antimicrobial drugs tested for all 4 *S. maltophilia* patients, profile 3 had 2 differences from profile 2 and 3 differences from profile 1.

both unopened and opened bottles of gel from the radiology clinic; all results were negative. Other outbreaks involving *A. xylosoxidans* have been reported (*12,20–23*) and sometimes attributed to this environmental organism's ability to colonize reusable plastic containers (*20,21*). Its resistance to common disinfectants, especially quaternary ammonium compounds (*20,21,24*), makes single-use equipment all the more critical.

We found other reports suggesting particular prostate susceptibility to this type of organism. One report involved this species after prostate biopsies (*12*); others involved the same organ and other lung pathogens classically associated with cystic fibrosis, such as *Pseudomonas aeruginosa* and *Burkholderia cepacia* (*13,14*). We found 3 *O. anthropi*–related outbreaks reported in the literature; all involved specific patient populations that received immunosuppressants systemically (*25,26*) or locally (*27*). In contrast, 2 of the 3 patients infected with *O. anthropi* described in our study were immunocompetent.

In the outbreak we report, 5 cases were caused by *A. xylosoxidans*, a waterborne opportunistic pathogen that rarely causes clinically relevant infections. The same strain was responsible for all 5 of these infections and was fluoroquinolone resistant, enabling the strain to escape prophylaxis and facilitating the outbreak (Figure 3).

The other species, *O. anthropi*, was the source of infection for 3 case-patients. This pathogen caused symptomatic infections despite its susceptibility to antimicrobial drug prophylaxis (ofloxacin). Our study's retrospective nature resulted in our inability to ascertain definitely whether prophylaxis had been taken properly or whether this strain was capable of surviving despite its in vitro susceptibility. Because the contamination of the plastic container was extensive and because a PFGE mismatch occurred (Figure 2), other hypotheses for the proliferation of the strain include the possibilities that a large inoculum of the pathogen occurred or that several strains of this species were involved in these infections.

No pathogen could be identified in 2 possible cases occurring during the outbreak period. These patients might correspond to either false positives or to real cases despite having negative cultures because of prophylaxis (i.e., 4 of 5 strains isolated from the container were sensitive to fluoroquinolones); these cases' occurrence during the time of the other cases argues for the latter hypothesis. We excluded these 2 cases from the case–control analysis because their status could not be ascertained.

We also found 4 cases of infection with *S. maltophilia*, another pathogen associated with stagnant water, from 2011–2012. At that time, radiology staff members were reusing plastic containers over a period of several days or weeks. We cannot attribute these past infections to similar contamination with certainty. However, postbiopsy infections with *S. maltophilia* are nearly nonexistent in the literature (*4,28*), and an isolate of this species was retrieved from environmental contamination during the 2014 outbreak. The clinical isolates from 2011–2012 were resistant to antimicrobial drug prophylaxis (ofloxacin) in vitro, whereas the environmental isolate from 2014 was not; this change in susceptibility could explain why *S. maltophilia* infections occurred in 2011–2012 but not in 2014. The same type of mishandling of materials, although with less severe contamination, was likely responsible for the *S. maltophilia* cases occurring in 2011–2012. These cases were overlooked, probably because no sizeable cluster occurred, unlike in 2014.

During prostate biopsy, all items that enter sterile tissue are critical and should be sterile, along with items that will not be in contact with patients but will be in contact with critical items, as discussed in national recommendations (*11*) and elsewhere (*29*). Generally, all reusable items should be cleaned or sterilized (*30*). Although the

Figure 3. Patients with positive urine or blood cultures taken <15 days after prostate biopsy at Hôpital Édouard Herriot, Lyon, France, 2011–2015. Only nondigestive species matching those found in a contaminated pot in 2014 are shown. All represented patients are from hospital data files. For consistency, 1 patient with *Ochrobactrum anthropi* infection treated in primary care in October 2014 is not shown.

nonsterile nature of the rectum and antimicrobial drug prophylaxis might result in healthcare workers' being less vigilant in following recommendations, outbreaks caused by prophylaxis-resistant environmental bacteria indicate the need for rigorous implementation of sterile practices in all settings. We found no specific mention of the need for such materials to be sterile in various recommendations (*30–33*), with the exception of an annex in French national guidelines (*11*). This omission in recommendations might contribute to oversights such as those reported in this article, especially given the frequency of the procedure. After the outbreak, practices were modified and now comply fully with French guidelines.

Other preventive measures have been discussed in the literature. Some are specifically aimed at endogenous bacteria, such as the use of a transperineal route (*34*) or pre-biopsy rectal cultures to guide antimicrobial-drug prophylaxis (*9*); others are more general, such as providone/iodine enemas (*9*) and formalin disinfection of biopsy needles (*35*). Such preventive measures have had good preliminary results and could possibly have prevented this outbreak.

This outbreak highlights the usefulness of analyzing the order of procedures to detect environmental contamination. In our investigation, the first patient of the day had a higher infection risk than subsequent patients. The bacterial inoculum was likely highest for the first procedure of the day and then decreased for remaining patients because the highly contaminated sponges, which often soaked overnight, had been used and new ones were soaked only briefly in the plastic container.

Some limitations reduce the strength of our study. The urgent need to terminate the outbreak made the data observational, the sample size low, and the study mostly retrospective and subject to recording and reporting bias. Also, the possibility exists of limited sensitivity of a diagnosis that is based on voluntary consultation, especially given that the UTIs were generally mild and, for some patients, symptoms might have been present and worrying but were overlooked by physicians inside or outside the university hospital, contributing to a misclassification bias. However, this possible bias might be limited because little time had passed between clinical onset of cases and the investigation and because all

patients had to consult with urologists to obtain their biopsy results. Previous cases involving other bacteria might have escaped our analysis because of antimicrobial drug prophylaxis, which likely biased the microbiologic results for some patients, and because no cluster of cases existed to draw increased scrutiny from clinical teams.

In summary, an outbreak of healthcare-associated infections after TUPBs was caused by improper handling of biopsy materials and involved 2 unusual pathogens, *O. anthropi* and *A. xylosoxidans*. The latter was resistant to standard fluoroquinolone-based antimicrobial drug prophylaxis. Infections by uncommon microorganisms should quickly be reported to infection control units, especially when they cluster in time. Invasive outpatient procedures, such as TUPBs, could be the source of other outbreaks involving multidrug-resistant environmental bacteria. Such procedures require rigorous sterile handling of all relevant materials during operating room surgery.

References

1. Loeb S, Carter HB, Berndt SI, Ricker W, Schaeffer EM. Complications after prostate biopsy: data from SEER-Medicare. J Urol. 2011;186:1830–4. http://dx.doi.org/10.1016/j.juro.2011.06.057
2. Polton D, Ricordeau P. Le SNIIRAM et les bases de donnees de l Assurance Maladie en 2011. 2011 Mar 30 [cited 2015 Mar 30]. http://www.sante.gouv.fr/IMG/pdf/Le_SNIIRAM_et_les_bases_de_donnees_de_l_Assurance_Maladie_en_2011.pdf
3. Loeb S, Vellekoop A, Ahmed HU, Catto J, Emberton M, Nam R, et al. Systematic review of complications of prostate biopsy. Eur Urol. 2013;64:876–92. http://dx.doi.org/10.1016/j.eururo.2013.05.049
4. Loeb S, van den Heuvel S, Zhu X, Bangma CH, Schröder FH, Roobol MJ. Infectious complications and hospital admissions after prostate biopsy in a European randomized trial. Eur Urol. 2012;61:1110–4. http://dx.doi.org/10.1016/j.eururo.2011.12.058

5. Liss MA, Johnson JR, Porter SB, Johnston B, Clabots C, Gillis K, et al. Clinical and microbiological determinants of infection after transrectal prostate biopsy. Clin Infect Dis. 2015;60:979–87.

6. Steensels D, Slabbaert K, De Wever L, Vermeersch P, Van Poppel H, Verhaegen J. Fluoroquinolone-resistant *E. coli i*n intestinal flora of patients undergoing transrectal ultrasound-guided prostate biopsy—should we reassess our practices for antibiotic prophylaxis? Clin Microbiol Infect. 2012;18:575–81. http://dx.doi.org/10.1111/j.1469-0691.2011.03638.x

7. Dumford D III, Suwantarat N, Bhasker V, Kundrapu S, Zabarsky TF, Drawz P, et al. Outbreak of fluoroquinolone-resistant *Escherichia coli* infections after transrectal ultrasound-guided biopsy of the prostate. Infect Control Hosp Epidemiol. 2013;34:269–73.

8. Wagenlehner FME, van Oostrum E, Tenke P, Tandogdu Z, Çek M, Grabe M, et al.; GPIU investigators. Infective complications after prostate biopsy: outcome of the Global Prevalence Study of Infections in Urology (GPIU) 2010 and 2011, a prospective multinational multicentre prostate biopsy study. Eur Urol. 2013;63:521–7. http://dx.doi.org/10.1016/j.eururo.2012.06.003

9. Taylor AK, Murphy AB. Preprostate biopsy rectal culture and postbiopsy sepsis. Urol Clin North Am. 2015;42:449–58. http://dx.doi.org/10.1016/j.ucl.2015.06.005

10. American Urological Association. Antimicrobial prophylaxis: best practice policy statement on urologic surgery antimicrobial prophylaxis. 2008 [cited 2016 Mar 11]. https://www.auanet.org/education/guidelines/antimicrobial-prophylaxis.cfm

11. Ouzzane A, Coloby P, Mignard J-P, Allegre J-P, Soulie M, Rebillard X, et al. Recommendations for best practice for prostate biopsy [in French]. Prog En Urol J Assoc Fr Urol Société Fr Urol. 2011;21:18–28.

12. Olshtain-Pops K, Block C, Temper V, Hidalgo-Grass C, Gross I, Moses AE, et al. An outbreak of *Achromobacter xylosoxidans* associated with ultrasound gel used during transrectal ultrasound guided prostate biopsy. J Urol. 2011;185:144–7. http://dx.doi.org/10.1016/j.juro.2010.08.093

13. Hutchinson J, Runge W, Mulvey M, Norris G, Yetman M, Valkova N, et al. *Burkholderia cepacia* infections associated with intrinsically contaminated ultrasound gel: the role of microbial degradation of parabens. Infect Control Hosp Epidemiol. 2004; 25:291–6. http://dx.doi.org/10.1086/502394

14. Gillespie JL, Arnold KE, Noble-Wang J, Jensen B, Arduino M, Hageman J, et al. Outbreak of *Pseudomonas aeruginosa* infections after transrectal ultrasound-guided prostate biopsy. Urology. 2007;69:912–4. http://dx.doi.org/10.1016/j.urology.2007.01.047

15. Amoureux L, Bador J, Fardeheb S, Mabille C, Couchot C, Massip C, et al. Detection of *Achromobacter xylosoxidans* in hospital, domestic, and outdoor environmental samples and comparison with human clinical isolates. Appl Environ Microbiol. 2013;79:7142–9. http://dx.doi.org/10.1128/AEM.02293-13

16. Cholley P, Gbaguidi-Haore H, Bertrand X, Thouverez M, Plésiat P, Hocquet D, et al. Molecular epidemiology of multidrug-resistant *Pseudomonas aeruginosa* in a French university hospital. J Hosp Infect. 2010;76:316–9. http://dx.doi.org/10.1016/j.jhin.2010.06.007

17. R Core Team. R: A language and environment for statistical computing. Vienna: R Foundation for Statistical Computing; 2015 [cited 2016 Mar 11]. http://www.R-project.org

18. Kosmidis I, Firth D. A generic algorithm for reducing bias in parametric estimation. Electron J Stat. 2010;4:1097–112. http://dx.doi.org/10.1214/10-EJS579.

19. Kosmidis I. brglm: bias reduction in binomial-response generalized linear models. 2013 [cited 2015 Apr 20]. http://www.ucl.ac.uk/~ucakiko/software.html

20. Molina-Cabrillana J, Santana-Reyes C, González-García A, Bordes-Benítez A, Horcajada I. Outbreak of *Achromobacter xylosoxidans* pseudobacteremia in a neonatal care unit related to contaminated chlorhexidine solution. Eur J Clin Microbiol Infect Dis. 2007;26:435–7. http://dx.doi.org/10.1007/s10096-007-0311-7

21. Tena D, Carranza R, Barberá JR, Valdezate S, Garrancho JM, Arranz M, et al. Outbreak of long-term intravascular catheter-related bacteremia due to *Achromobacter xylosoxidans* subspecies xylosoxidans in a hemodialysis unit. Eur J Clin Microbiol Infect Dis. 2005;24:727–32. http://dx.doi.org/10.1007/s10096-005-0028-4

22. McGuckin MB, Thorpe RJ, Koch KM, Alavi A, Staum M, Abrutyn E. An outbreak of *Achromobacter xylosoxidans* related to diagnostic tracer procedures. Am J Epidemiol. 1982;115:785–93.

23. Reina J, Antich M, Siquier B, Alomar P. Nosocomial outbreak of *Achromobacter xylosoxidans* associated with a diagnostic contrast solution. J Clin Pathol. 1988;41:920–1. http://dx.doi.org/10.1136/jcp.41.8.920-c

24. Siebor E, Llanes C, Lafon I, Ogier-Desserrey A, Duez JM, Pechinot A, et al. Presumed pseudobacteremia outbreak resulting from contamination of proportional disinfectant dispenser. Eur J Clin Microbiol Infect Dis. 2007;26:195–8. http://dx.doi.org/10.1007/s10096-007-0260-1

25. Ezzedine H, Mourad M, Van Ossel C, Logghe C, Squifflet JP, Renault F, et al. An outbreak of *Ochrobactrum anthropi* bacteraemia in five organ transplant patients. J Hosp Infect. 1994;27:35–42. http://dx.doi.org/10.1016/0195-6701(94)90066-3

26. Christenson JC, Pavia AT, Seskin K, Brockmeyer D, Korgenski EK, Jenkins E, et al. Meningitis due to *Ochrobactrum anthropi:* an emerging nosocomial pathogen. A report of 3 cases. Pediatr Neurosurg. 1997;27:218–21. http://dx.doi.org/10.1159/000121256

27. Mattos FB, Saraiva FP, Angotti-Neto H, Passos AF. Outbreak of *Ochrobactrum anthropi* endophthalmitis following cataract surgery. J Hosp Infect. 2013;83:337–40. http://dx.doi.org/10.1016/j.jhin.2012.11.027

28. Tal R, Livne PM, Lask DM, Baniel J. Empirical management of urinary tract infections complicating transrectal ultrasound guided prostate biopsy. J Urol. 2003;169:1762–5. http://dx.doi.org/10.1097/01.ju.0000061280.23447.29

29. Galosi AB, Muzzonigro G, Lacetera V, Mazzucchelli R. Specimen orientation by marking the peripheral end: (potential) clinical advantages in prostate biopsy. Prostate Cancer. 2011;2011:270403.

30. Turner B, Aslet P, Drudge-Coates L, Forristal H, Gruschy L, Hieronymi S, et al. Evidence-based guidelines for best practice in health care. Transrectal ultrasound guided biopsy of the prostate. 2011 [cited 2015 Mar 12]. http://www.medicalcity-iq.net/medlib/EAUN_TRUS_Guidelines_EN_2011_LR.pdf

31. El-Hakim A, Moussa S. CUA guidelines on prostate biopsy methodology. Can Urol Assoc J. 2010;4:89–94. http://dx.doi.org/10.5489/cuaj.10021

32. American Urological Association. AUA/SUNA white paper on the incidence, prevention and treatment of complications related to prostate needle biopsy. 2012 [cited 2015 Jul 16]. https://www.auanet.org/common/pdf/practices-resources/quality/patient_safety/Prostate-Needle-Biopsy-White-Paper.pdf

33. British Association of Urological Surgeons; British Association of Urological Nurses. Transrectal ultrasound and prostatic biopsy: guidelines and recommendations for training. 2015 Apr [cited 2015 Jul 16]. http://www.baus.org.uk/_userfiles/pages/files/Publications/Transrectal%20Ultrasound%20%20Prostatic%20Biopsy%20FINAL.pdf

34. Shen P-F, Zhu Y-C, Wei W-R, Li Y-Z, Yang J, Li Y-T, et al. The results of transperineal versus transrectal prostate biopsy: a systematic review and meta-analysis. Asian J Androl. 2012;14:310–5. http://dx.doi.org/10.1038/aja.2011.130

35. Issa MM, Al-Qassab UA, Hall J, Ritenour CWM, Petros JA, Sullivan JW. Formalin disinfection of biopsy needle minimizes the risk of sepsis following prostate biopsy. J Urol. 2013;190:1769–75. http://dx.doi.org/10.1016/j.juro.2013.04.134

Address for correspondence: Skerdi Haviari, Unité d'Hygiène et d'Épidémiologie, Hôpital Edouard Herriot, 5 place d'Arsonval, 69437 Lyon CEDEX 03, France; email: skerdihaviari@gmail.com

Cutaneous Melioidosis Cluster Caused by Contaminated Wound Irrigation Fluid

Adam J. Merritt, Mariani Peck, Dionne Gayle, Avram Levy, Yi-Horng Ler, Edward Raby, Tristan M. Gibbs, Timothy J.J. Inglis

Author affiliations: PathWest Laboratory Medicine, Nedlands, Western Australia, Australia (A.J. Merritt, M. Peck, D. Gayle, A. Levy, Y.-H. Ler, T.M. Gibbs, T.J.J. Inglis); University of Western Australia, Crawley, Western Australia, Australia (A.J. Merritt, T.J.J. Inglis); Royal Perth Hospital, Perth, Western Australia, Australia (E. Raby)

Melioidosis usually occurs after environmental exposure to *Burkholderia pseudomallei* in the tropics. A cluster of 5 cutaneous melioidosis cases occurred in suburban southwest Australia after an earlier case in January 2012. We collected environmental samples at the first patient's home in January 2012 and from a nearby health center in December 2013 after 2 new cases occurred in the same postal district. We isolated genotypically identical *B. pseudomallei* from the first patient and 5 other patients in the district. Environmental

sampling implicated an opened bottle of saline wound irrigation fluid containing >10^6 *B. pseudomallei*/mL. The bottle included instructions to discard within 24 hours of opening. No further cases of *B. pseudomallei* infection occurred after removing the contaminated bottle. This cutaneous melioidosis cluster demonstrates that *B. pseudomallei* can survive and disseminate in widely used medical fluids beyond its known geographic distribution, highlighting a need to use these products according to manufacturers' instructions.

Melioidosis, caused by infection with the bacterium *Burkholderia pseudomallei*, is a disease with manifestations ranging from rapidly fatal septicemia, pneumonia, or meningoencephalitis to localized abscess formation, cellulitis, and asymptomatic seroconversion. This disease occurs most commonly in Southeast Asia and northern Australia after exposure to contaminated soil or surface water (*1*). The US National Notifiable Diseases Surveillance Systems case definition describes cutaneous melioidosis as "an acute or chronic localized infection which may or may not include symptoms of fever and muscle aches. Such infection often results in ulcer, nodule, or skin abscess" (*2*).

Sporadic cases outside melioidosis-endemic regions usually occur in persons who have a history of travel in the tropics, which can be as long as several decades previously because of the ability of *B. pseudomallei* to persist undetected after the initial inoculation event (*3*). In these cases, *B. pseudomallei* infection might not be considered in the differential diagnosis. Detection of sporadic cases of melioidosis by clinical pathology laboratories requires microbiology laboratories to have robust bacterial identification procedures. Even with advanced equipment, a lack of awareness of the characteristic features of *B. pseudomallei* can result in misidentification of cultured organisms (*4*). Only a few point-source outbreaks of melioidosis have been reported (*5*). Two of these occurred in Western Australia; 1 was attributed to movement of livestock from the tropical north to the temperate southwest (*6*), and the other was caused by contamination of a potable water supply (*7*). Neither cluster was healthcare-associated. Only a few cases of healthcare-associated melioidosis have been reported. Some of the earliest accounts of melioidosis identified opiate injection as a potential source of infection (*8*). In animal healthcare, injected medication was thought responsible for a series of animal infections in northern Australia (*9*). The first report of hospital-acquired melioidosis originated in Hawaii, USA, and described pulmonary infection after bronchoscopy with a scope contaminated with *B. pseudomallei* (*10*). This report indicated that the contaminated bronchoscope had previously been used on a returned traveler with melioidosis. A second report described 2 patients with *B. pseudomallei* urinary tract infection on different wards of a hospital on whose grounds *B. pseudomallei* was

isolated (*11*). Nosocomial contamination associated with faulty hospital hygiene and ineffective disinfectant solution was reported from a hospital in Thailand treating patients with melioidosis (*12*). More recently, cases of neonatal melioidosis from a hospital in Thailand were thought to be healthcare-associated, although the full details of transmission could not be determined (*13*).

Melioidosis became a notifiable infection in Western Australia in January 2000 (*14*). Physicians, pathology service providers, and the state public health laboratory are required to report a diagnosis of melioidosis to the State Disease Control Directorate. Melioidosis notification is largely laboratory-generated in Western Australia because confirmation of infection according to the Australian Laboratory Case Definition relies on culture of *B. pseudomallei* from clinical specimens. Pathology service providers therefore routinely refer presumptive *B. pseudomallei* isolates to the state public health laboratory for confirmation, genotyping, and archiving in a reference culture collection (Western Australian *Burkholderia* Collection). Here we report the laboratory investigation of a cluster of cutaneous melioidosis in the temperate southwest of Australia, the identification of its source, and means of control.

Methods

In January 2012, a patient residing in temperate Western Australia who had a superficial soft tissue infection had a preliminary isolation of *B. pseudomallei*. We interviewed the patient to determine a detailed local, national, and international travel history; potential means of *B. pseudomallei* exposure; and melioidosis-associated concurrent conditions.

The patient's home property was visited by staff from PathWest Laboratory Medicine (Nedlands, Western Australia) for inspection and environmental sampling of garden beds (1 sample), potable water (2 samples), storm water drainage (1 sample), and a nearby nature reserve (1 sample). Soil samples were processed by suspending 10 g of soil in 20 mL of sterile water and incubated overnight with agitation. Samples were kept stationary for 2 h to allow the soil to settle, and 50 μL supernatant was spread across Ashdown's agar and *B. pseudomallei* selective agar (*15*,*16*). Solid media was incubated for 48 hours at 37°C followed by 5 days at room temperature. One milliliter of supernatant was also inoculated into 10 mL of Ashdown's broth (*17*) and incubated at 37°C overnight before being spread onto selective solid media as described. Plates were checked every 24 h and suspect colonies picked to nonselective blood agar with a 10-μg gentamicin disk placed on the second sector.

In December 2013, after 2 additional cases of culture-confirmed cutaneous melioidosis had been detected in the same postal district associated with a local healthcare facility, we conducted environmental sampling in and around

the facility. Additional environmental samples were collected from public accessed land and building excavations in the neighborhood to identify other potential sources of *B. pseudomallei* external to the health facility. These samples were processed as described previously. Samples included all wound care products in current use, whether sealed or already open. We also sampled fixed surfaces patients were likely to come into contact with during wound care and soil at locations surrounding the health facility that could provide either a primary source or reservoir for later distribution. Laboratory-based surveillance for melioidosis cases from the region was performed for 12 months after the conclusion of the field investigation. This process included referral of all suspected *B. pseudomallei* by all pathology service providers in Western Australia, multilocus sequence typing (MLST) of all confirmed *B. pseudomallei*, and matrix-assisted laser desorption/ionization time-of-flight (MALDI-TOF) mass spectrometry identification of all wound swab bacterial isolates processed at the state public health laboratory (*4*).

Solid samples were inoculated onto 5% horse blood agar, Ashdown's selective agar, and *Burkholderia* selective agar and then incubated for 48 h at 37°C. Bulk liquids were sampled in a class II biological safety cabinet not previously used for *B. pseudomallei* work, and 1.0 mL dispensed into thioglycollate broth in accordance with standard microbial contamination assessment methods. A ≈100-mL aliquot of each bulk liquid was filtered through a 0.22-µm membrane filter and used to inoculate the same series of selective and nonselective agars. Positive fluid samples were used for detailed bacterial count studies by using a serial 10-fold dilution to 1:10^7, a spiral plating device, and triplicates of each dilution.

One environmental sample yielded *B. pseudomallei*: a 1,000-mL bottle of wound irrigation fluid. Turbidity of the residual wound irrigation fluid in the bottle was not visible because the container walls were semi-opaque. To determine the extent of bacterial colonization and identify any specific higher-density bacterial localization within it, the bottle was dissected from its screw top down to its bottom, sampling at 2.5-cm intervals. Plastic surfaces contaminated with *B. pseudomallei* were cut into ≈0.5-cm square portions and processed for scanning electron microscopy. Samples were fixed overnight (2.5% glutaraldehyde [vol/vol] in 0.05 mol/L cacodylate buffer pH 7.4), then washed in the same buffer before postfixation for 30 min (1% aqueous osmium tetroxide) and sequential dehydration in ethanol series for 5 min each. Reagents were supplied by the PathWest Electron Microscopy Unit (Nedlands, Western Australia). Critical point drying was achieved by using liquid carbon dioxide; the plastic squares were then attached to aluminum stubs by using double-sided carbon tape with edges painted with carbon solution and coated with 15 nm of carbon. Samples were viewed through a Zeiss SUPRA 55 Variable Pressure SEM

operating at 3–5 kV with either in-lens or SE2 detectors, depending on magnification required.

Preliminary identification of *B. pseudomallei* was made by using a MALDI-TOF mass spectrometer with a 70% formic acid partial extraction protocol and a locally generated *Burkholderia* mass spectrum database (*4*). Definitive confirmation of *B. pseudomallei* was made by using a panel of real-time PCR assays targeting independent genes (*18,19*). The mutually exclusive *B. thailandensis*–like flagellar (BTFC)/*Yersinia*-like fimbrial (YLF) genetic markers were used for preliminary molecular characterization, which used primers and probes developed in-house based on the previously published sequences (*20*). MLST was performed by using the current PCR and sequencing primers as previously described (http://bpseudomallei.mlst.net/misc/info2.asp) (*21*). Sequencing was performed on an ABI 3130xl sequencer by using forward and reverse primers with ABI BigDye version 3.1 sequencing chemistry (Applied Biosystems, Foster City, CA, USA). MEGA5 was used to construct a neighbor-joining tree of MLST sequence from all outbreak-associated isolates, including the wound irrigation fluid isolate, to show their genetic relationship to reference *B. pseudomallei* isolates in the Western Australian *Burkholderia* Collection (*22,23*). *B. thailandensis* E264 was used as an outgroup and root for the neighbor-joining tree. Bootstrap values >50 (>1,000 replicates) were included next to the tree's branches (*24*), and evolutionary distances were computed by using a maximum composite likelihood method with units of the number of base substitutions per site (*25*). The rate variation among sites was modeled with a gamma distribution (shape parameter = 4).

Results

Case Summary

The state public health laboratory started its investigation in 2012 after confirming a diagnosis of cutaneous melioidosis in a patient who had not left the temperate southwest region of Western Australia during the previous 18 years (patient A). No further cases of cutaneous melioidosis occurred throughout 2012. In September 2013, an isolate of suspected *B. pseudomallei* was referred from another resident of the same postal district (patient C) who had a purulent wound infection at the site of a minor procedure 1 month before. We commenced more intensive public health investigations after a further case of culture-confirmed cutaneous melioidosis (discharge at site of leg injury [patient D]) and prioritized referral of all suspected *B. pseudomallei* isolates from pathology service providers in Western Australia. Four further cases occurred after this time (patients E through H). An additional 2012 case was detected (patient B) after retrospective review. *B. pseudomallei* isolates were available from a total of 8 cases (Table). We excluded 2

Table. Summary characteristics of a cutaneous melioidosis cluster caused by contamination of wound irrigation fluid, Western Australia, 2012–2013*

Isolate source	Source	Date of collection	Pathology request notes	MALDI-TOF MS score	YLF/BTFC	MLST ST
Patient A	Wound	2012 Jan 20	Cellulitis (left shin and toe), unresponsive to first-line antibiotics	2.6	BTFC	1112
Patient B	Pulmonary	2012 Mar 30	Cough and shortness of breath, fine needle aspirate of lung lesion, fever and chills afterwards	2.476	YLF	84
Patient C	Wound	2013 Sep 25	Purulent, dehiscing wound at site of lesion removed 1 month previously	2.61	BTFC	1112
Patient D	Wound	2013 Nov 12	Leg injury, slough	2.376	BTFC	1112
Patient E	Wound	2013 Nov 29	Cellulitis (left shin), worsening despite first-line antibiotics	2.146	BTFC	1112
Patient F	Wound	2013 Dec 05	Nonhealing wound (right forearm)	2.394	BTFC	1112
Patient G	Wound	2013 Dec 13	Wound sustained in QLD, swabbed to check for cutaneous melioidosis	2.7	BTFC	1112
Patient H	Pulmonary† and cutaneous	2013 Dec 20	Subgaleal abscess pus	2.211	YLF	176
Saline	Wound irrigation fluid	2013 Dec 20	NA	2.3	BTFC	1112

*Patients ordered by date of specimen collection. Isolates from patients B and H have sequence types previously documented in Southeast Asia. BTFC, *B. thailandensis*–like flagellar gene cluster; MALDI-TOF MS, matrix-assisted laser desorption/ionization time-of-flight mass spectrometry; MLST, multilocus sequence typing; NA, not applicable; QLD, Queensland; ST, sequence type; YLF, *Yersinia*-like fimbrial gene cluster.
†Molecular detection only; no isolate recovered.

cases (patients B and H) from further investigation of the cluster after genotyping yielded sequence types (STs) already documented in clinical and environmental isolates from Southeast Asia (ST-84 and ST-176) and both were shown to be YLF types (Table). These 2 patients had different clinical features and a history of travel to a known melioidosis region.

The patient from January 2012 and all subsequent patients with cutaneous infections associated with the common genotype had minor wounds dressed at a health facility in the same postal district. One patient (patient G) had a traumatic wound swabbed to check whether cutaneous melioidosis was present and thus might represent a case of contamination or colonization. Apart from patients B and H, all other patients were reported to have local skin inflammation or cellulitis with or without discharge; infection in 3 patients had not responded to presumptive antimicrobial therapy.

Isolate Characterization

Our state public health laboratory confirmed the identity of all isolates by MALDI-TOF mass spectrometry and a real-time PCR assay panel. Specimens from the January 2012 patient and all subsequent patients with cutaneous melioidosis yielded cultures of *B. pseudomallei* belonging to the BTFC clade of *B. pseudomallei* (Table). Bacterial isolates belonged to a single MLST genotype, previously unreported in the global *B. pseudomallei* database (Figure 1). For this genotype, the *gltB* locus had 1 single nucleotide polymorphism variant (G276A) of *gltB* allele 16, given allele number 85, and a new ST, ST-1112. The closest related strains in the *B. pseudomallei* MLST database are all double-locus variants of ST-1112 and are

all identified as Australian human or veterinary clinical isolates. Comparison with clinical and environmental isolates from Western Australia identified a previous clinical *B. pseudomallei* isolate (C30) that varied at a single locus, from the town of Derby in the north of the state in 2007 (Figure 1).

Environmental Sampling

Environmental sampling followed a spiral plan, beginning in the health facility and working outwards into the grounds and wider neighborhood, based on potential for public exposure. This process generated a total of 62 samples, including surface swabs, wound dressing materials, fluids, ointments, creams, garden soil, and building site soil. The bottle of wound irrigation fluid that yielded *B. pseudomallei* had been in intermittent use since September 2013 (Figure 2, panels A and B). PCR assays and MLST performed on the wound irrigation fluid isolate confirmed the presence of *B. pseudomallei* BTFC/ST-1112, matching the clinical isolates from the patients with cutaneous melioidosis. Another previously opened bottle of wound irrigation fluid and unopened bottles from the same supplier batch all were culture-negative for *B. pseudomallei*. However, other fluid samples, including in-use disinfectants, grew small quantities of *Pseudomonas aeruginosa*, which was also present in the *B. pseudomallei*–contaminated wound irrigation fluid bottle. The contaminated wound irrigation fluid contained 1.83×10^6 CFU/mL *B. pseudomallei* and 1.89×10^3 CFU/mL *P. aeruginosa* (Figure 2, panels C and D). The bottle was supplied during March 18–27, 2013, first opened in September 2013, and removed from use when sampling was performed in December 2013.
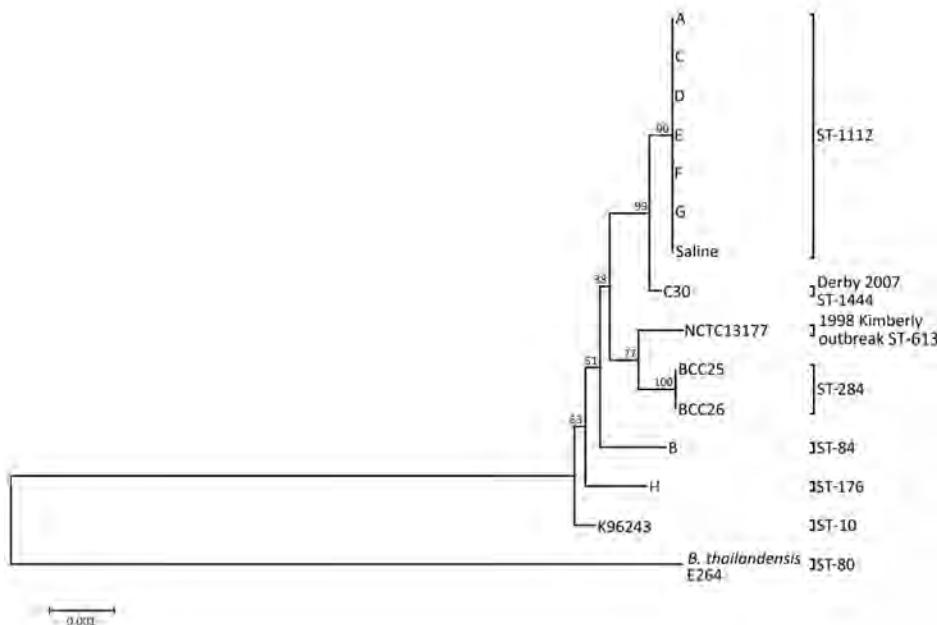
Figure 1. Neighbor-joining tree of aligned multilocus sequence typing sequences of *Burkholderia pseudomallei* clinical isolates from a 2012–2013 cutaneous melioidosis cluster in the temperate southern region of Western Australia (patients A and C–G) and indistinguishable environmental isolate (saline) with sequence type (ST) 1112 and their genetic relatedness to other isolates from the Western Australian *Burkholderia* Collection (C30, NCTC13177, BCC25, and BCC26). Isolates from patients B and H are shown as less closely related to the ST-1112 cluster. *B. thailandensis* E264 is used as an outgroup and root for the tree. Tree inference was performed in MEGA5 (*22*). Bootstrap values >50 (>1,000 replicates) are shown. Scale bar indicates base substitutions per site (*20–24*).

Electron Microscopy

Scanning electron microscopy of the contaminated wound irrigation fluid bottle confirmed extensive bacterial colonization of the inner surfaces. The density of bacterial colonization varied depending on the location analyzed within the bottle. Few bacteria were at the neck of the bottle, many were on the sides of the bottle, and the highest concentration was at the base of the bottle. Bacteria were tethered by short adhesions (Figure 3, panel A) and were occasionally associated with fibrillary material that had a globular structure at high magnification (Figure 3, panel B inset). Decayed bacteria were common (Figure 3, panel C, arrows), and although duplex cells were observed, healthy dividing cells were uncommon. Numerous clusters and microcolonies were observed, particularly at the base of the bottle, which also showed a greater proportion of decayed cells and more extensive extracellular adhesions than the other samples (Figure 3, panel D). The plastic washer inside the bottle lid was covered in a mature biofilm.

Discussion

Recent events in the continental United States highlight the ability of *B. pseudomallei* to breach ecologic or biologic boundaries (*26–30*). A review of U.S. state and territory cases identified 3 persons with culture-positive melioidosis in the absence of relevant travel to melioidosis-endemic regions and concluded with a recommendation that physicians and healthcare workers should be more aware of the disease (*31*). A lack of familiarity with this bacterial species in an unusual clinical setting, such as occurred in the cluster we describe here, can cause difficulty in identifying

the primary source. The previous Western Australia cluster occurred in a very different setting, a remote community in the tropical north of the state (*7*). Only 1 other melioidosis cluster has been reported in temperate Western Australia; that cluster was attributed to livestock transported from a melioidosis-endemic region (*6*). The melioidosis cluster we describe here was notable for its occurrence in urban Western Australia, which is not considered to be endemic for melioidosis, and for its association with a contaminated wound care product.

We recovered *B. pseudomallei* isolates with the same multilocus ST from 6 melioidosis patients in 1 postal district and excluded another 2 cases of melioidosis from our investigation on the basis of clinical features, travel history, biogeographic bacterial clade, and MLST genotype. Isolation of *B. pseudomallei* of the same ST from contaminated wound irrigation fluid explains the 5 cases in 2013 because the bottle of wound irrigation fluid was used without replacement throughout this period. Although the manufacturer's instructions advise that the bottle should be discarded within 24 hours of opening and label the fluid as single-use, it is common practice to use such large volumes of fluid as a stock during wound care procedures, providing decanting is conducted as a no-touch procedure. This melioidosis cluster highlights the public health risks of such a practice. Because the contaminated wound irrigation fluid bottle had not yet been received when the 2012 patient had wound care at the same health facility, the wound irrigation fluid probably was not contaminated before opening. We note that the connection between the January 2012 case and the September–December 2013 cases remains unexplained.
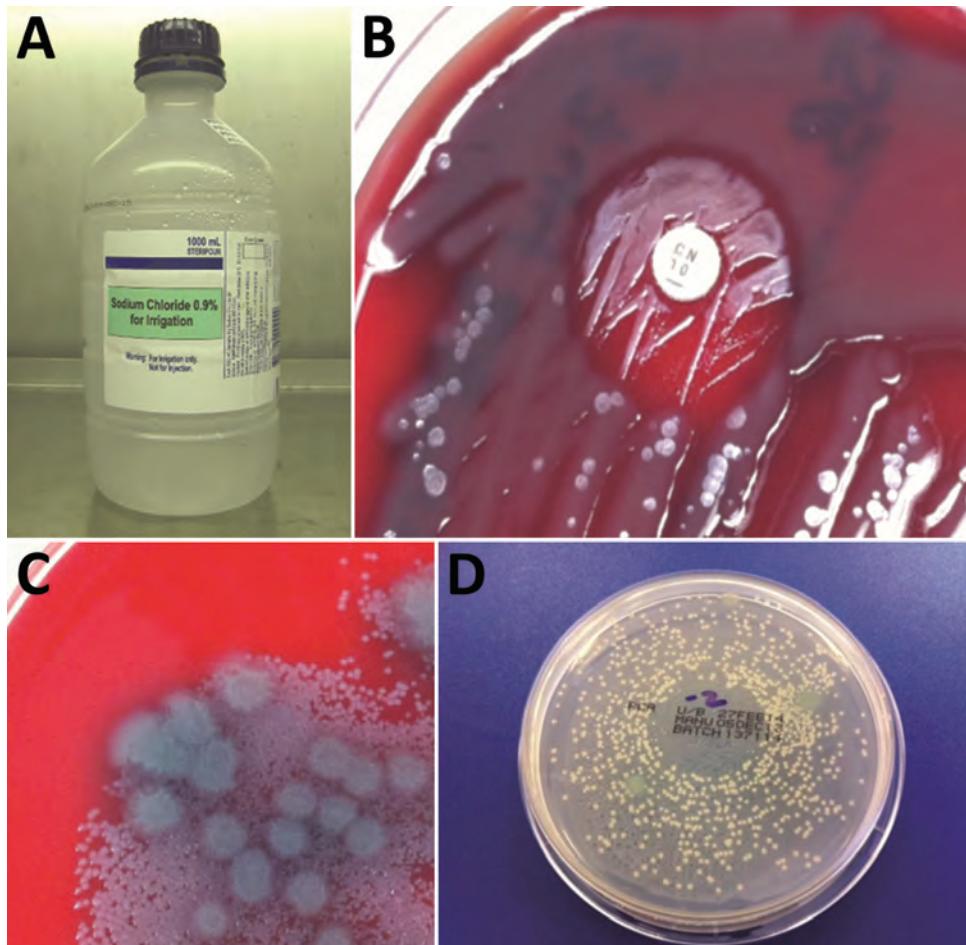
Figure 2. Bacterial culture results for 1,000-mL bottle of wound irrigation fluid in laboratory investigation of a 2012–2013 cutaneous melioidosis cluster in the temperate southern region of Western Australia. A) Wound irrigation fluid in original bottle. B) Direct primary culture of wound irrigation fluid on blood agar plate, showing growth inhibition of *Pseudomonas aeruginosa* and revealing *Burkholderia pseudomallei* around gentamicin disk. C) Filtrate of wound irrigation fluid from same bottle showing higher count of *B. pseudomallei* colonies than *P. aeruginosa.* D) Dilution of wound irrigation fluid (1:100), dispensed by spiral plating device, showing *B. pseudomallei* colonies and relatively sparse *P. aeruginosa* colonies.

Given that other patients received wound care during this period without evidence of cutaneous melioidosis, the existence of an earlier contaminated bottle with subsequent transfer to the contaminated bottle is improbable. Possible explanations for this interval include an undetected past case of chronic, unresolved cutaneous melioidosis with multiple introductions of *B. pseudomallei* into medical products or an external environmental reservoir common to the 2012 patient and the first or first few 2013 patients. The previous report of nosocomial melioidosis in Australia identified environmental *B. pseudomallei* that was biochemically similar to the clinical isolates, but that report lacked the strength of molecular epidemiology evidence (*10*). All previous reports of nosocomial melioidosis come from locations in the tropics (*8–12*).

The melioidosis cluster we report represents an unusual healthcare-associated outbreak in a temperate suburban setting. *B. pseudomallei* was not isolated from any other solution or environmental sample from the facility. It is not clear whether the count of *B. pseudomallei* found in the contaminated irrigation fluid was the result of an initial seeding event with subsequent bacterial growth or by

gross contamination without further growth. Previous in vitro studies indicate that *B. pseudomallei* will tolerate a wide range of nutrient-free aqueous environments (*32*), and survival of 10^7 CFU/mL *B. pseudomallei* in sterile distilled water over 16 years has been reported (*33*). Electron microscopy showed complex colonization patterns and extensive bacterial adhesion, consistent with long-term bacterial colonization. The initial seeding event probably included sufficient nutrients to support bacterial proliferation. The senescent bacteria we observed could reflect a larger original bacterial population introduced to the bottle. Although not healthcare-associated, 2 cases of cutaneous melioidosis attributed to a contaminated hand wash solution noted in another report further highlight the potential for contamination and subsequent transmission of *B. pseudomallei* in an occupational setting (*34*).

We investigated cause and effect in this laboratory outbreak investigation by using a set of stringent rules for emerging infectious disease causality (*35*), establishing the laboratory evidence to link a series of cutaneous infections in a geographically restricted cluster, identifying a probable source, and introducing early environmental controls. We
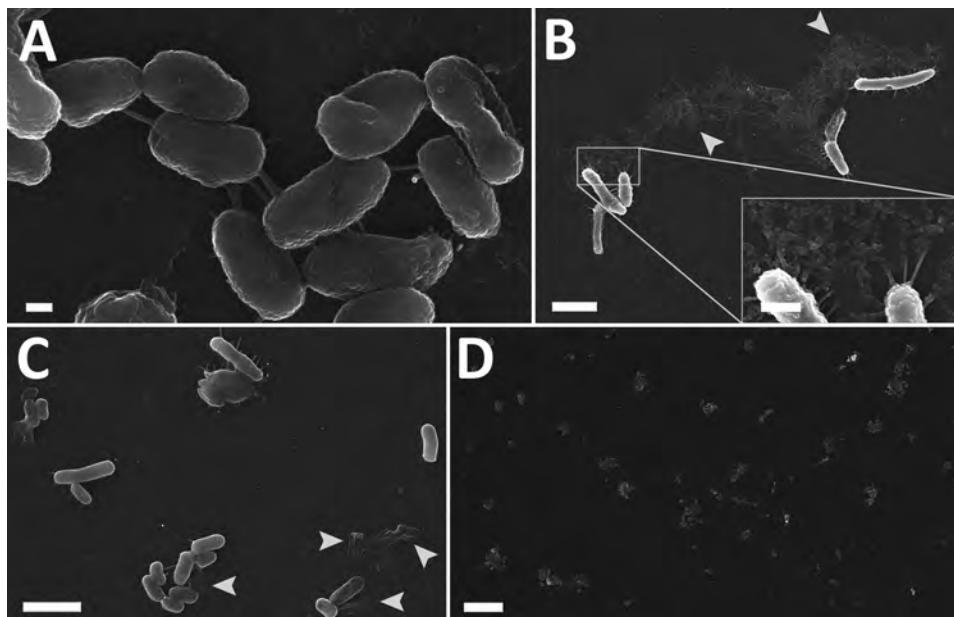
Figure 3. Scanning electron micrographs of internal plastic surface of contaminated irrigation fluid bottle implicated in a 2012–2013 cutaneous melioidosis cluster in the temperate southern region of Western Australia. A–C) Bacilli tethered to each other and to the surface by short peritrichous or polar adhesions (A, C) and occasionally by fibrillary material (B), which appeared to have a globular structure at higher magnification. Decayed cells were common (arrows). D) Clusters of cells were regularly dispersed over the surface. Scale bars indicate 2 μm (A); 200 nm (B and C); 500 nm (B, inset); and 10 μm (D).

used a combination of molecular epidemiology, microscopy, and culture-based bacteriologic methods to identify and study a point source for healthcare-associated infection in this investigation of a cluster of cutaneous melioidosis cases in temperate southwest Australia. We obtained circumstantial evidence that bacterial contamination combined with incorrect use of wound irrigation fluid to form a chain of events necessary for subsequent infection. The contaminated wound irrigation fluid is a plausible vehicle for infection, but uncertainty exists about its essential role in the case of patient A. Although we halted the series of infections by removing the source of *B. pseudomallei* infection from use, we have not yet been able to identify the initial environmental reservoir. Therefore, the long duration of the previous temperate Western Australia cluster leads us to expect additional sporadic cases in the area over an extended period and represents a continuing public health risk (*4*). However, we have not identified any other cases of cutaneous melioidosis in the same area or ST-1112 infections elsewhere during the subsequent 12 months of laboratory-based surveillance.

Although the inoculum of *B. pseudomallei* causing human cutaneous infection was measured, the circumstances of wound contamination in this cluster did not allow us to determine the probability of subsequent dissemination from an already infected wound. Additional questions raised are 1) whether pouring contaminated wound irrigation fluid limited infection to an already damaged epidermis without generating sufficient aerosol for pulmonary infection, and 2) whether others in this suburban community were exposed to *B. pseudomallei* ST-1112 without clinical consequences. Specific aspects of virulence phenotype, genetics, and circumstance that resulted in the notable absence of pneumonia or septicemic infection are the focus of further study.

Mr. Merritt is a senior clinical microbiology laboratory scientist in the Molecular Diagnostics Laboratory of the Western Australian State Pathology Service and a part-time graduate research student at the University of Western Australia. His primary research interests include molecular methods for melioidosis diagnosis and bioreconnaissance, the phylogeography of *Burkholderia* species, and the laboratory response to emerging infectious diseases.

References

1. Cheng AC, Currie BJ, Dance DA, Funnell SG, Limmathurotsakul D, Simpson AJ, et al. Clinical definitions of melioidosis. Am J Trop Med Hyg. 2013;88:411–3. http://dx.doi.org/10.4269/ajtmh.12-0555
2. Centers for Disease Control and Prevention. National Notifiable Diseases Surveillance System. Melioidosis (*Burkholderia pseudomallei*) 2012 case definition [cited 2015 Jul 7]. http://wwwn.cdc.gov/nndss/conditions/melioidosis/case-definition/2012
3. Frangoulidis D, Schwab D, Scholz H, Tomaso H, Hogardt M, Meyer H, et al. 'Imported' melioidosis in Germany: relapse after

10 years. Trans R Soc Trop Med Hyg. 2008;102(Suppl 1):S40–1. http://dx.doi.org/10.1016/S0035-9203(08)70011-7

4. Inglis TJ, Healy PE, Fremlin LJ, Golledge CL. Use of matrix-assisted laser desorption/ionization time-of-flight mass spectrometry analysis for rapid confirmation of *Burkholderia pseudomallei* in septicemic melioidosis. Am J Trop Med Hyg. 2012;86:1039–42. http://dx.doi.org/10.4269/ajtmh.2012.11-0454

5. Currie BJ, Haslem A, Pearson T, Hornstra H, Leadem B, Mayo M, et al. Identification of melioidosis outbreak by multilocus variable number tandem repeat analysis. Emerg Infect Dis. 2009;15:169–74. http://dx.doi.org/10.3201/eid1502.081036

6. Currie B, Smith-Vaughan H, Golledge C, Buller N, Sriprakash KS, Kemp DJ. *Pseudomonas pseudomallei* isolates collected over 25 years from a non-tropical endemic focus show clonality on the basis of ribotyping. Epidemiol Infect. 1994;113:307–12. http://dx.doi.org/10.1017/S0950268800051736

7. Inglis TJ, Garrow SC, Henderson M, Clair A, Sampson J, O'Reilly L, et al. *Burkholderia pseudomallei* traced to water treatment plant in Australia. Emerg Infect Dis. 2000;6:56–9.

8. Whitmore A. An account of a Glanders-like disease occurring in Rangoon. J Hyg (Lond). 1913;13:1–34.

9. Choy JL, Mayo M, Janmaat A, Currie BJ. Animal melioidosis in Australia. Acta Trop. 2000;74:153–8. http://dx.doi.org/10.1016/S0001-706X(99)00065-0

10. Markovitz A. Inoculation by bronchoscopy. West J Med. 1979;131:550.

11. Ashdown LR. Nosocomial infection due to *Pseudomonas pseudomallei*: two cases and an epidemiologic study. Rev Infect Dis. 1979;1:891–4. http://dx.doi.org/10.1093/clinids/1.5.891

12. Sookpranee M, Lumbiganon P, Puapermpoonsiri S, Tattawasatra A, Nopwinyoovongs J. Contamination of Savlon solution with *Pseudomonas pseudomallei* at Srinagarind Hospital. In: Punyagupta S, Sirisanthana T, Stapatayavong B, editors. Melioidosis. Bangkok: Bangkok Medical Publisher; 1989. p. 211–3.

13. Thatrimontrichai A, Maneenil G. Neonatal melioidosis: systematic review of the literature. Pediatr Infect Dis J. 2012;31:1195–7. http://dx.doi.org/10.1097/INF.0b013e318265ac62

14. Inglis TJ, O'Reilly L, Merritt AJ, Levy A, Heath CH. The aftermath of the Western Australian melioidosis outbreak. Am J Trop Med Hyg. 2011;84:851–7. http://dx.doi.org/10.4269/ajtmh.2011.10-0480

15. Ashdown LR. An improved screening technique for isolation of *Pseudomonas pseudomallei* from clinical specimens. Pathology. 1979;11:293–7. http://dx.doi.org/10.3109/00313027909061954

16. Howard K, Inglis TJ. Novel selective medium for isolation of *Burkholderia pseudomallei*. J Clin Microbiol. 2003;41:3312–6. http://dx.doi.org/10.1128/JCM.41.7.3312-3316.2003

17. Wuthiekanun V, Dance DA, Wattanagoon Y, Supputtamongkol Y, Chaowagul W, White NJ. The use of selective media for the isolation of *Pseudomonas pseudomallei* in clinical practice. J Med Microbiol. 1990;33:121–6. http://dx.doi.org/10.1099/00222615-33-2-121

18. Merritt A, Inglis TJ, Chidlow G, Harnett G. PCR-based identification of *Burkholderia pseudomallei*. Rev Inst Med Trop Sao Paulo. 2006; 48:239–44. http://dx.doi.org/10.1590/S0036-46652006000500001

19. Novak RT, Glass MB, Gee JE, Gal D, Mayo MJ, Currie BJ, et al. Development and evaluation of a real-time PCR assay targeting the type III secretion system of *Burkholderia pseudomallei*. J Clin Microbiol. 2006;44:85–90. http://dx.doi.org/10.1128/JCM.44.1.85-90.2006

20. Tuanyok A, Auerbach RK, Brettin TS, Bruce DC, Munk AC, Detter JC, et al. A horizontal gene transfer event defines two distinct groups within *Burkholderia pseudomallei* that have

dissimilar geographic distributions. J Bacteriol. 2007;189:9044–9. http://dx.doi.org/10.1128/JB.01264-07

21. Godoy D, Randle G, Simpson AJ, Aanensen DM, Pitt TL, Kinoshita R, et al. Multilocus sequence typing and evolutionary relationships among the causative agents of melioidosis and glanders, *Burkholderia pseudomallei* and *Burkholderia mallei*. J Clin Microbiol. 2003;41:2068–79. http://dx.doi.org/10.1128/JCM.41.5.2068-2079.2003

22. Tamura K, Peterson D, Peterson N, Stecher G, Nei M, Kumar S. MEGA5: molecular evolutionary genetics analysis using maximum likelihood, evolutionary distance, and maximum parsimony methods. Mol Biol Evol. 2011;28:2731–9. http://dx.doi.org/10.1093/molbev/msr121

23. Saitou N, Nei M. The neighbor-joining method: a new method for reconstructing phylogenetic trees. Mol Biol Evol. 1987;4:406–25.

24. Felsenstein J. Confidence limits on phylogenies: an approach using the bootstrap. Evolution. 1985;39:783–91. http://dx.doi.org/10.2307/2408678

25. Tamura K, Nei M, Kumar S. Prospects for inferring very large phylogenies by using the neighbor-joining method. Proc Natl Acad Sci U S A. 2004;101:11030-5.

26. Herriman R. Melioidosis—USA: (LA) primate, human. ProMED. 2015 Feb 10 [cited 2015 Jul 7]. http://www.promedmail.org, archive no. 20150210.3157436.

27. Berger S. Melioidosis—USA (02): background. ProMED. 2015 Feb 11 [cited 2015 Jul 7]. http://www.promedmail.org, archive no. 20150211.3159588.

28. Owen MP. Melioidosis—USA (04): update. ProMED. 2015 Mar 3 [cited 2015 Jul 7]. http://www.promedmail.org, archive no. 20150302.3202447.

29. Roberts FA. Melioidosis—USA (05): 2 new seropositive monkeys. ProMED. 2015 Mar 7 [cited 2015 Jul 7]. http://www.promedmail.org, archive no. 20150307.3215130.

30. Centers for Disease Control and Prevention. Conclusion of select agent inquiry into *Burkholderia pseudomallei* release at Tulane National Primate Research Center [cited 2015 July 7]. http://www.cdc.gov/media/releases/2015/s0313-burkholderia-pseudomallei.html

31. Benoit TJ, Blaney DD, Gee JE, Elrod MG, Hoffmaster AR, Doker TJ, et al. Melioidosis cases and selected reports of occupational exposures to *Burkholderia pseudomallei*—United States, 2008–2013. MMWR Surveill Summ. 2015;64(5):1–9.

32. Robertson J, Levy A, Sagripanti JL, Inglis TJ. The survival of *Burkholderia pseudomallei* in liquid media. Am J Trop Med Hyg. 2010;82:88–94. http://dx.doi.org/10.4269/ajtmh.2010.09-0226

33. Pumpuang A, Chantratita N, Wikraiphat C, Saiprom N, Day NP, Peacock SJ, et al. Survival of *Burkholderia pseudomallei* in distilled water for 16 years. Trans R Soc Trop Med Hyg. 2011;105:598–600. http://dx.doi.org/10.1016/j.trstmh.2011.06.004

34. Gal D, Mayo M, Smith-Vaughan H, Dasari P, McKinnon M, Jacups SP, et al. Contamination of hand wash detergent linked to occupationally acquired melioidosis. Am J Trop Med Hyg. 2004;71:360–2.

35. Inglis TJ. *Principia aetiologica*: taking causality beyond Koch's postulates. J Med Microbiol. 2007;56:1419–22. http://dx.doi.org/10.1099/jmm.0.47179-0

Address for correspondence: Timothy J.J. Inglis, Department of Microbiology PathWest Laboratory Medicine, Western Australia, PP Building, QEII Medical Centre, Hospital Ave, Nedlands, WA 6009, Australia; email: tim.inglis@health.wa.gov.au

Possible Role of Fish and Frogs as Paratenic Hosts of *Dracunculus medinensis*, Chad

Mark L. Eberhard, Michael J. Yabsley, Hubert Zirimwabagabo, Henry Bishop, Christopher A. Cleveland, John C. Maerz, Robert Bringolf, Ernesto Ruiz-Tiben

Copepods infected with *Dracunculus medinensis* larvae collected from infected dogs in Chad were fed to 2 species of fish and tadpoles. Although they readily ingested copepods, neither species of fish, Nile tilapia (*Oreochromis niloticus*) nor fathead minnow (*Pimephalis promelas*), were found to harbor *Dracunculus* larvae when examined 2–3 weeks later. Tadpoles ingested copepods much more slowly; however, upon examination at the same time interval, tadpoles of green frogs (*Lithobates* [*Rana*] *clamitans*) were found to harbor small numbers of *Dracunculus* larvae. Two ferrets (*Mustela putorius furo*) were fed fish or tadpoles that had been exposed to infected copepods. Only the ferret fed tadpoles harbored developing *Dracunculus* larvae at necropsy 70–80 days postexposure. These observations confirm that *D. medinensis*, like other species in the genus *Dracunculus*, can readily survive and remain infective in potential paratenic hosts, especially tadpoles.

The global campaign to eradicate dracunculiasis (or Guinea worm disease [GWD]), which began at the Centers for Disease Control and Prevention (CDC) in 1980 and has been led by the Carter Center since 1986, has assisted 17 of 21 affected countries to interrupt transmission. In 1986, an estimated 3.5 million cases occurred annually in 20 countries (the separation of Sudan and South Sudan created a 21st country in 2011). Today, only 4 countries (Chad, Ethiopia, Mali, and South Sudan) still have endemic transmission of GWD. In 2014, only 126 cases were reported from these 4 countries, and only 22 cases were reported during January–November 2015 (*1*). Since the beginning of the campaign, all interventions against GWD have focused on preventing contamination of stagnant sources of drinking water by patients with patent GWD

Author affiliations: Centers for Disease Control and Prevention, Atlanta, Georgia, USA (M.L. Eberhard, H. Bishop); University of Georgia College of Veterinary Medicine, Athens, Georgia, USA (M.J. Yabsley, C.A. Cleveland); University of Georgia Warnell School of Forestry and Natural Resources, Athens (M.J. Yabsley, C.A. Cleveland, J.C. Maerz, R. Bringolf); Carter Center, Atlanta (H. Zirimwabagabo, E. Ruiz-Tiben)

and preventing ingestion of infected copepods. However, in 2013, several unusual epidemiologic findings were noted in Chad, including absence of disease outbreaks associated with sources of drinking water common to many residents year-to-year in affected villages and a relatively common infection of domestic dogs with Guinea worms genetically indistinguishable from those from human cases. This finding led to the hypothesis that an aquatic paratenic host (an intermediate host that serves as transport host for parasite larvae) was involved in the transmission of *Dracunculus medinensis* in Chad (*2*). Since 2013, the sporadic pattern of human cases in Chad has continued, the number of infections in dogs has continued to increase, and the presence of a paratenic host in the transmission cycle seems more likely.

The purpose of our study was to expose, under laboratory conditions, 2 species of fish and 2 species of tadpoles to *D. medinensis*–infected copepods, in an effort to determine whether these species would support viable larvae (and thus serve as a paratenic host). These potential paratenic hosts were then fed to an experimental definitive host (a domestic ferret) to determine if any third-stage larvae (L3) present would undergo further development in ferrets.

Materials and Methods

During July 20–22, 2015, batches of first-stage larvae (L1) were recovered from 5 Guinea worms removed from infected dogs resident in villages within the dracunculiasis-endemic zone along the Chari River between the cities of Guelendeng and Bousso in the Mayo-Kebbi Est region of Chad. Copepods were collected locally in the Guelendeng area (dracunculiasis-endemic zone) and exposed to the L1 per standard methods (*3*). L1 were mixed with copepods in a ratio of ≈3–5:1 to ensure a high rate of infection but not high enough to cause copepod mortality. Infected copepods were maintained for 5–7 days in 1.5-L water bottles and then transported to laboratories at CDC (Atlanta, GA, USA), where they were maintained in culture per standard practices (*3*). Beginning at day 12 after exposure, copepods were dissected to determine level of infection and stage of development of larvae. Many larvae observed at day 12

were early (and infective) L3. To allow full maturation of the infective larvae, no copepods were used in experimental studies before day 14.

For experimental trials, 2 species of fish (29 Nile tilapia [*Oreochromis niloticus*] and 36 fathead minnows [*Pimephalis promelas*]) and 2 species of tadpoles (20 Fowler's toads [*Bufo fowleri*] and 10 green frogs [*Lithobates* (*Rana*) *clamitans*]) were used. Both fish species were captive-raised and the tadpoles were wild-caught (green frogs raised from egg masses in captivity) in Georgia. Because the toads and some of the ranid tadpoles were very young at the time of exposure, species identity was confirmed by amplification and sequencing of a ≈500-bp region of the 16S rRNA gene with primers Amph-sp-F (5′-CTGTTTACCAAAAACATCG-3′) and Ecto-univ-R (5′-ATCCAACATCGAGGTCGT-3′). Sequences were a 100% match to GenBank accession numbers AY680224 (toads) and DQ283185 (ranids) confirming their identity. Finally, 2 age classes of green frog tadpoles were used.

Beginning at day 14 after exposure to *D. medinensis* L1, batches of infected copepods were fed to groups of fish or tadpoles. Fish and tadpoles, separated by species, were exposed to copepods in shallow water in a 500-mL beaker with a bubbling air source. Both fish species immediately began to ingest copepods, all of which had been ingested by 24 hours. In contrast, tadpoles ingested copepods more slowly, and some copepods remained uneaten after 3 days of exposure.

Beginning 1 week after exposure, groups of 4–5 fish and tadpoles were examined for *Dracunculus* larvae. Fish and tadpoles were euthanized by overdose of pH-neutral buffered tricaine methane sulfonate (MS-222), followed by decapitation, and then examined grossly under a dissecting scope to see if any larvae could be visualized in fin or tail fin or under skin. Then, the entire body, including head and viscera, was dissected to fully separate all tissues, and macerated tissues were examined under a dissecting microscope. If no larvae were observed, the tissues were allowed to sit in phosphate-buffered saline for 1–2 hours and reexamined under a dissecting or compound microscope. A total of 19 tilapia, 19 fathead minnows, 11 *Bufo* tadpoles, and 9 *Lithobates* tadpoles were examined by dissection. For a subset of 6 fish (3 of each type), tissues were grossly macerated, examined microscopically, and then digested in a 0.5% pepsin solution for 1 hour before examination for larvae.

Two colony-reared ferrets (*Mustela putorius furo*) were fed either tadpoles or fish mixed in canned cat food to determine infectivity of L3 from aquatic hosts. All dissected fish and the additional 5 tilapia and 11 fathead minnows that were not dissected were fed to 1 ferret. The other ferret was fed all dissected tadpoles and an additional 9

Bufo and 3 *Lithobates* tadpoles that had not been dissected. Ferrets were euthanized and examined at 70–83 days after exposure to fish or tadpoles. Animals were examined per previously proven methods for detecting developing *Dracunculus* (*3*). All animal procedures were reviewed and approved by the University of Georgia Institutional Animal Care and Use Committee (no. A2014 11–010).

Results

No *Dracunculus* larvae were detected in dissected fish or *Bufo* tadpoles, but 4 of 7 *Lithobates* tadpoles were infected with 1–3 *Dracunculus* L3. Infections were noted in both age classes. The exact locations of the larvae were not determined, but they were recovered from the body musculature or head. No larvae were observed in the body cavity or viscera. The larvae recovered from tadpoles were slightly larger and more active than L3 recovered from copepods.

No worms were detected in the ferret that had been fed fish, but in the ferret that had ingested tadpoles, 3 young developing worms were recovered. All 3 worms were females and measured 1.4, 2.0, and 2.7 cm in length by 295–350 μm in maximum diameter. Two of the worms were recovered from the right hind leg, and the third worm was recovered from the lower left abdominal wall. The largest worm was coiled under the muscle fascia, whereas the other 2 worms were present in adipose tissue.

Discussion

These results, although limited in scope, clearly confirm that *D. medinensis*, like *D. insignis*, can use an aquatic paratenic host; specifically, at least 2 species of amphibians (*4–6*). Although tadpoles consumed far fewer copepods, most tadpoles exposed to infected copepods subsequently had infections, which is consistent with previous data that showed a high percentage of adult frogs (*L. pipiens* and *L. clamitans*) acquired infections when a very high dose of infected copepods (n = 200–500) were given by mouth (*4*).

D. insignis larvae recovered from tadpoles previously were stated to be slightly larger and more active than infective larvae recovered from copepods, which is what we noted in our study with *D. medinensis* (*4,6*), in which the larvae grew ≈20% after 15–18 days. Previously these *D. insignis* larvae recovered from tadpoles or frogs were infective to a single raccoon or ferrets, respectively, proving that these larger larvae are infectious (*4,5*). Similarly, the larger *D. medinensis* larvae we recovered from tadpoles were infectious for a domestic ferret.

The absence of larvae in the 2 species of fish we included in this study does not rule out a role of fish as paratenic hosts. Previously, a low percentage of fish exposed to L3 recovered from copepods subsequently had infections

(*4*). Although sample sizes were low, 2 of 4 white suckers (*Catostomus commersonii*) and 1 of 2 rainbow trout (*Oncorhynchus mykiss*) had 1–2 larvae recovered after exposure to 100–180 L3. Thus, we may not have exposed our fish to enough larvae to become infected (*4*). However, fish species variability in susceptibility is probable, given that common shiners (*Luxilus cornutus*) failed to become infected even though 3 were exposed to ≥200 larvae (*4*). Future studies should investigate the fate of *Dracunculus*-infected copepods after ingestion by fish hosts, dose required to establish infections in fish, and additional trials with other species of fish (e.g., *Gambusia* [mosquito fish]) that are known to predate copepods. Tilapia, 1 type of fish used in this study, is common in Chad and widely used as a food source. However, many other types of fish are present in Chad, and continued study of tilapia and other native fish should also be undertaken before ruling out fish as potential paratenic hosts.

Collectively, our data and the findings of previous reports indicate that *Dracunculus* larvae in general, and *D. medinensis* larvae specifically, are well-adapted to using a paratenic host and that tadpoles of *Lithobates* (*Rana*) and *Xenopus* species are appropriate hosts (*4,5*). *Lithobates* spp. are members of the family Ranidae, which has a near global distribution that includes more than 180 known species in sub-Saharan Africa (*7*). This study also confirms that domestic ferrets, like domestic cats, domestic dogs, and monkeys, can serve as experimental definitive hosts for *D. medinensis*. The recovered worms were of consistent size and development as previously reported for worms of similar age recovered from dogs or monkeys (*8,9*). Finally, these results also suggest that a more extensive examination of tadpoles and frogs in Chad is warranted. Although a small number (n = 28) of ranid frogs from Chad were previously examined for *Dracunculus* larvae and all were negative (*2*), sample sizes were low. Because natural infections of tadpoles or frogs have not been documented for either *D. medinensis* or *D. insignis,* the prevalence of natural infections is unknown; therefore, larger numbers of wild-caught frogs should be examined in future efforts. In addition to identifying which aquatic animals are acting as paratenic hosts for *D. medinensis* in Chad, it would be important to also identify which wild animals are predators of these transport hosts and whether those predators develop patent infections, thus helping maintain transmission of the parasite.

References

1. Hopkins DR, Ruiz-Tiben E, Eberhard ML, Roy SL. Progress toward global eradication of dracunculiasis, January 2014–June 2015. MMWR Morb Mortal Wkly Rep. 2015;64:1161–5. http://dx.doi.org/10.15585/mmwr.mm6441a1
2. Eberhard ML, Ruiz-Tiben E, Hopkins DR, Farrell C, Toe F, Weiss A, et al. The peculiar epidemiology of dracunculiasis in Chad. Am J Trop Med Hyg. 2014;90:61–70. http://dx.doi.org/10.4269/ajtmh.13-0554
3. Eberhard ML, Ruiz-Tiben E, Wallace SV. *Dracunculus insignis*: experimental infection in the ferret, *Mustela putorius furo*. J Helminthol. 1988;62:265–70. http://dx.doi.org/10.1017/S0022149X00011640
4. Crichton VFJ, Beverley-Burton M. Observations on the seasonal prevalence, pathology and transmission of *Dracunculus insignis* (Nematoda: Dracunculoidea) in the raccoon (*Procyon lotor* (L.) in Ontario. J Wildl Dis. 1977;13:273–80. http://dx.doi.org/10.7589/0090-3558-13.3.273
5. Eberhard ML, Brandt FH. The role of tadpoles and frogs as paratenic hosts in the life cycle of *Dracunculus insignis* (Nematoda: Dracunculoidea). J Parasitol. 1995;81:792–3. http://dx.doi.org/10.2307/3283979
6. Anderson RC. Nematode parasites of vertebrates: their development and transmission. Wallingford (UK): CAB International; 1992. p. 320–35.
7. Poynton JC. Distribution of amphibians in sub-Saharan Africa, Madagascar, and Seychelles. In: patterns and distribution of amphibians: a global perspective. Duellman WE, editor. Baltimore (MD): Johns Hopkins University Press; 1999. p. 483–540.
8. Onabamiro SD. The early stages of the development of *Dracunculus medinensis* (Linnaeus) in the mammalian host. Ann Trop Med Parasitol. 1956;50:157–66. http://dx.doi.org/10.1080/00034983.1956.11685755
9. Muller R. *Dracunculus* and dracunculiasis. Adv Parasitol. 1971;9:73–151. http://dx.doi.org/10.1016/S0065-308X(08)60160-8

Address for correspondence: Mark L. Eberhard, Centers for Disease Control and Prevention, 1600 Clifton Rd NE, Mailstop D-64, Atlanta, GA 30329-4018, USA; email: mle1@cdc.gov

Assessment of Community Event–Based Surveillance for Ebola Virus Disease, Sierra Leone, 2015

Ruwan Ratnayake,[1] Samuel J. Crowe,[1] Joseph Jasperse, Grayson Privette, Erin Stone, Laura Miller, Darren Hertz, Clementine Fu, Matthew J. Maenner, Amara Jambai, Oliver Morgan

In 2015, community event–based surveillance (CEBS) was implemented in Sierra Leone to assist with the detection of Ebola virus disease (EVD) cases. We assessed the sensitivity of CEBS for finding EVD cases during a 7-month period, and in a 6-week subanalysis, we assessed the timeliness of reporting cases with no known epidemiologic links at time of detection. Of the 12,126 CEBS reports, 287 (2%) met the suspected case definition, and 16 were confirmed positive. CEBS detected 30% (16/53) of the EVD cases identified during the study period. During the subanalysis, CEBS staff identified 4 of 6 cases with no epidemiologic links. These CEBS-detected cases were identified more rapidly than those detected by the national surveillance system; however, too few cases were detected to determine system timeliness. Although CEBS detected EVD cases, it largely generated false alerts. Future versions of community-based surveillance could improve case detection through increased staff training and community engagement.

Community event–based surveillance (CEBS) systems have been used for case finding during outbreaks and to increase sensitivity for detection of diseases targeted for eradication (*1–5*), but this type of surveillance has not been implemented rapidly on a national scale during a large health emergency. In October 2014, near the peak of the Ebola virus disease (EVD) epidemic in West Africa, the International Rescue Committee, Sierra Leone's Bo District Health Management Team, and the US Centers for Disease Control and Prevention developed CEBS in Sierra Leone to serve as a village-level active surveillance system for reporting possible EVD cases (*6*). At that time, many infected persons were not detected until after they had died by the national surveillance system, which consisted of contact tracing, healthcare facility surveillance, and a telephone hotline for reporting events; thus, opportunities for virus transmission were prolonged (*6*). CEBS was designed to supplement the national surveillance system by training community members to identify, within their own communities, unsafe burials and persons with signs and symptoms compatible with EVD infection. Through its community presence, CEBS was positioned to detect EVD cases that were not epidemiologically linked to other confirmed cases at the time of detection; identification of such cases could provide early warning of new chains of transmission.

A brief pilot study in Bo District during November and December 2014 demonstrated that community leadership accepted CEBS and that CEBS could identify possible EVD cases. Thus, the Ebola Response Consortium, led by the International Rescue Committee and consisting of 15 humanitarian organizations committed to stopping the Ebola virus epidemic, worked with the Sierra Leone Ministry of Health and Sanitation to implement CEBS in 9 of Sierra Leone's 14 districts (Figure 1). CEBS began operations on February 27, 2015, when the surveillance system recorded its first alert.

During February 27–September 30, 2015, we evaluated the ability of CEBS to detect possible EVD cases and unsafe burials in the 9 districts. We also conducted a subanalysis of the system during its first 6 weeks of operation in Kambia District to assess the sensitivity, positive predictive value (PPV), and timeliness of case detection for persons with no epidemiologic links at the time of detection. Among the districts in which CEBS was operational, Kambia District was the only one that experienced ongoing active virus transmission during the subanalysis period.

Methods

Data Collection, Data Flow, and Reporting
The CEBS system included community health monitors, community surveillance supervisors, and community health officers, each of whom received job-specific training in the month before beginning operations. Formal

Author affiliations: International Rescue Committee, New York, New York, USA (R. Ratnayake); Centers for Disease Control and Prevention, Atlanta, Georgia, USA (S.J. Crowe, M.J. Maenner, O. Morgan); International Rescue Committee, Freetown, Sierra Leone (J. Jasperse, G. Privette, E. Stone, L. Miller, D. Hertz); Action contre la Faim, Kambia, Sierra Leone (C. Fu); Sierra Leone Ministry of Health and Sanitation, Freetown (A. Jambai)

[1]These first authors contributed equally to this article.

Figure 1. Nine districts (dark gray shading) where community event–based surveillance for Ebola virus disease was operational, Sierra Leone, February 27–September 30, 2015.

evaluations of staff knowledge were not conducted due to the rapid nature of the system deployment, but some districts provided informal refresher training when possible. Community health monitors were volunteers or existing community health workers who were trained to detect 6 trigger events suggestive of Ebola virus transmission: 1) ≥2 sick or dead members in a household, 2) a sick or dead person after an unsafe burial or corpse washing, 3) a sick or dead health worker or traditional healer, 4) a sick or dead traveler, 5) a sick or dead contact of an EVD patient, or 6) an unsafe burial or corpse washing. A seventh category, "other," was included so that community health monitors could report and describe other unusual events that did not fall under any of the 6 defined trigger events. Community health monitors reported events to their community surveillance supervisors via mobile telephone calls; the supervisors then conducted preliminary investigations. The community health officers, who were trained professionals within the national public health system, often assisted surveillance supervisors with preliminary investigations, but some delegated that responsibility to the supervisors and only assisted when needed. The surveillance supervisors or community health officers then reported events that remained suspect to their local District Ebola Response Center for follow-up.

Community health monitors were responsible for their own village and sometimes, to help ensure adequate coverage, a few small villages within walking distance of where they lived. Surveillance supervisors were assigned a larger area but were provided with motorcycles to facilitate investigations. All CEBS staff were given a mobile telephone

with monthly phone credit or a subscription in a prepaid, closed user-group network. Community health monitors were expected to immediately contact their surveillance supervisors to report alerts and to contact them weekly to confirm the absence of reportable events.

When a surveillance supervisor received an alert from a community health monitor, the supervisor recorded the alert information on a standardized form, a weekly alert log. The following data were captured: date; time; trigger event involved; type of alert (sickness, death, unsafe burial, or other); and age, sex, and location of the person(s) concerned. The surveillance supervisor also recorded what, if any, actions were taken to respond to the alert; whether the alert was raised to the District Ebola Response Center; and whether local social mobilization teams were notified to provide health education activities.

Surveillance supervisors submitted alert logs to the CEBS district lead at the end of each week. On a weekly basis, the district lead entered the data into a standardized spreadsheet, checked for duplicate reporting, and submitted the document to the CEBS coordination unit in Freetown, Sierra Leone. The district lead also cross-checked each CEBS alert against those in the District Ebola Response Center alert records and confirmed the final alert status as 1) the identified illness or death did not meet the suspected case definition, 2) the alert involved a suspected or probable case-patient who tested negative, or 3) the alert identified a confirmed case. In Sierra Leone, a suspected case-patient was defined as 1) a person with a fever (temperature >38°C) who was a known contact of a suspected, probable, or confirmed EVD clinical case-patient; 2) a person with ≥3 EVD-compatible symptoms (e.g., headache, vomiting, and diarrhea) and who had had contact with a clinical case-patient; 3) a person with fever and ≥3 EVD-compatible symptoms; 4) a person with inexplicable bleeding or miscarriage; or 5) a deceased person with an unexplained death. A probable EVD case-patient was defined as a person who was determined likely to have EVD based on clinical or epidemiologic factors. A confirmed case-patient was defined as a person who tested positive for Ebola virus RNA by quantitative reverse transcription PCR or a similar diagnostic test (7).

By September 30, 2015, CEBS had been implemented by 7,416 community health monitors and 137 surveillance supervisors across 9 districts in Sierra Leone (Figure 1). Implementation was undertaken by the International Rescue Committee (in Bo, Kenema, Kono, and Tonkolili Districts); Save the Children International (in Kailahun and Pujehun Districts); CARE International (in Bombali District); Action contre la Faim (in Kambia and Moyamba Districts); and ABC Development (in Kambia District). The Ebola Response Consortium provided technical assistance for system implementation and operations.

As a new surveillance system, CEBS had no trained staff, field equipment (e.g., telephones and motorbikes), or reporting infrastructure. The startup costs were estimated at US$1.3 million. Once the system was operational, the monthly costs were ≈US$129,000, which covered training, telephones, motorbikes, fuel, and incentives.

Methods of Evaluation

We described the alerts by type (illness, death, unsafe burial, and other) and by trigger event used. We calculated alert rates and death rates per 100,000 persons per day by district, using 2004 district population estimates (8). The sensitivity of CEBS for case detection was assessed using the Ministry of Health and Sanitation's surveillance data (9). Sensitivity was evaluated by dividing the number of CEBS-detected confirmed cases by the total number of confirmed cases detected by the overall surveillance system. PPV of confirmed case detection was determined by dividing the confirmed cases detected by CEBS by the suspected, probable, and confirmed cases detected by CEBS.

During April 13–May 30, 2015 (i.e., from the date CEBS first became operational in Kambia to the end date of our team's field investigations), we evaluated cases in persons in Kambia District who had no identified epidemiologic links at the time of detection. We used the Ministry of Health and Sanitation's Epi Info database to identify all confirmed cases in Kambia during the evaluation period (10). The database served as the line list of suspected, probable, and confirmed cases in Sierra Leone and integrated information from the epidemiologic investigation, including date of symptom onset and potential risk factors. By interviewing frontline public health and CEBS staff, we were able to determine whether and how CEBS was involved in case detection. We considered case-patients to have no identified epidemiologic links at the time of detection if they were not on the contact list used by the district contact tracers and, therefore, were not being actively monitored. The timeliness of detection of these cases was determined by calculating the interval in days between the date of symptom onset and the date of detection.

This assessment was a part of a nonresearch public health response activity and thus did not undergo institutional review board review. In addition, we used only information that had already been collected for public health surveillance purposes, so informed consent was not obtained.

Results

During February 27–September 30, 2015, a total of 12,126 alerts were reported through CEBS in 9 Sierra Leone districts (Figure 2). Tonkolili was the first district to report on a consistent basis, beginning on February 27, followed by
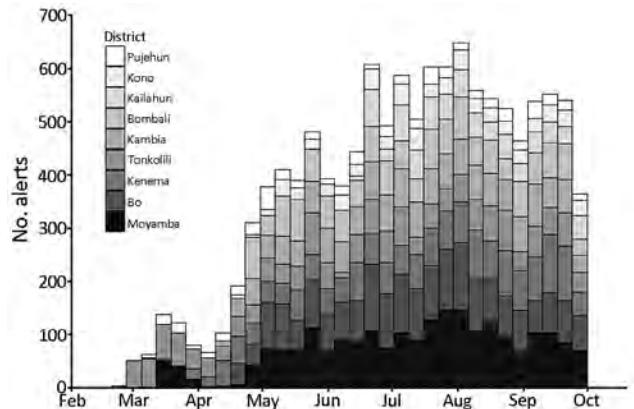
Figure 2. Weekly alerts from community event–based surveillance for Ebola virus disease, by district, Sierra Leone, February 27–September 30, 2015.

Moyamba (March 6), Pujehun (March 14), Kenema (March 31), Kambia (April 13), Bo (April 18), Kono (April 23), Bombali (April 27), and Kailahun (June 14). From June 14 onward, the districts were collectively reporting an average of 79 alerts per day.

Of the 12,126 alerts reported, 86% (10,421) were for deaths, 14% (1,646) for illnesses, and <1% for unsafe burials (7) or other (52) (Table 1). The alert rate per 100,000 persons per day differed by district and alert type. Of note, Moyamba and Kambia generated the highest rates of death alerts (3.81 and 2.19, respectively), and Kailahun and Bombali reported the highest rates of sick alerts (0.67 and 0.32, respectively) (Table 2). The CEBS death reporting rates were substantially lower than the

Table 1. CEBS for Ebola virus disease, Sierra Leone, 2015*

Surveillance variable	No. (%)
Alerts, n = 12,126	
Death	10,421 (86)
Sickness	1,646 (14)
Unsafe burial	7 (<1)
Other†	52 (<1)
Trigger events	
≥2 persons sick or dead in household	205 (2)
Sickness or death after unsafe burial	59 (<1)
Sickness or death in HCW	70 (<1)
Sickness or death in traveler	191 (2)
Sickness or death in contact of case-patient	36 (<1)
Unsafe burial or washing of corpse	7 (<1)
Other‡	11,558 (95)
Cases	
Suspected, probable, or confirmed	287 (2)
Tested and ruled negative	271
Confirmed	16
Did not meet case definition	10,173 (84)
Not escalated as an alert	774 (6)
Lost to follow-up§	892 (7)

*This analysis was conducted during February 27–September 30, 2015. CEBS, community event–based surveillance; HCW, healthcare worker.
†Alerts for unusual events that did not fall under any of the first 6 events listed in the trigger events section of the table.
‡A total of 10,042 (86.9%) of these events were deaths in the community.
§No follow-up or missing information on follow-up.

Table 2. CEBS Ebola virus disease alert rates, by type and district, Sierra Leone, February 27–September 30, 2015*

District	Population estimate†	Days of CEBS operation	Death alerts		Sick alerts	
			Total no. alerts	Rate‡	Total no. alerts	Rate‡
Moyamba	278,119	208	2,203	3.81	74	0.13
Bombali	494,139	156	1,137	1.47	250	0.32
Kambia	341,690	170	1,273	2.19	148	0.25
Bo	654,142	165	1,775	1.64	238	0.22
Tonkolili	434,937	215	1,343	1.44	192	0.21
Kenema	653,013	183	1,327	1.11	308	0.26
Kono	325,003	160	573	1.10	48	0.09
Pujehun	335,574	200	432	0.64	108	0.16
Kailahun	465,048	108	358	0.71	339	0.67

*CEBS (community event–based surveillance) was conducted in 9 of the country's 14 districts.
†Estimates from the 2004 Population and Housing Census: Analytical Report on Population Projection for Sierra Leone (8).
‡No. alerts/100,000 persons/d.

expected crude death rate of 4.66 deaths/100,000 persons/ day used by the World Health Organization (11).

In terms of the 6 defined trigger events, the most commonly cited was ≥2 sick or dead household members (n = 205, 2%). Sickness or death of a traveler was the second most cited (n = 191, 2%). In total, the 6 defined trigger events accounted for <5% of the alerts (Table 1). The seventh trigger event category (i.e., other) accounted for the most alerts (n = 11,558, 95%); a total of 10,042 (87%) of the alerts categorized as other were for deaths in the community (Table 1). Surveillance supervisors and community health officers escalated 93% of the alerts to the District Ebola Response Centers for follow-up.

A total of 287 (2%) of all persons who triggered alerts met the suspected, probable, or confirmed case definitions. Of these 287 persons, 215 (75%) were detected after death, and 271 (94%) tested negative for EVD. During the study period, 16 confirmed EVD cases were reported by CEBS in Kambia (n = 13) and Tonkolili (n = 3); half of the infected persons were detected while alive. During this same period, the Ministry of Health and Sanitation documented 53 confirmed cases in the CEBS districts. Overall, the sensitivity for confirmed case detection by CEBS was 30% (16/53 confirmed cases), and the PPV was 6% (16/287 suspected, probable, or confirmed cases). Sensitivity was 27% (13/49 confirmed cases) in Kambia and 75% (3/4 confirmed cases) in Tonkolili; PPV was 7% (13/175 suspected, probable, or confirmed cases) in Kambia and 9% (3/33 suspected, probable, or confirmed cases) in Tonkolili.

During the 6-week subanalysis in Kambia, the Ministry of Health and Sanitation database identified 13 confirmed EVD cases in the district. CEBS staff reported 8 of these patients, of whom 7 were alive at the time of the alert. Upon further investigation, we found that 3 of the cases were reported by community health monitors who also served as contact tracers through the contact tracing reporting system. Therefore, CEBS was not the main reporting source for these 3 cases, and the cases were

not recorded in the CEBS database or counted as cases detected by CEBS. For the remaining 5 cases, 3 were classified as other trigger events, 1 was in a sick contact of a confirmed case-patient, and 1 was a sick member of a household.

Six of the 13 confirmed case-patients in Kambia had no epidemiologic links when they were detected; CEBS staff identified 4 of these case-patients. The time from symptom onset to detection ranged from 1 to 3 days for the 4 cases identified by CEBS and was 5 and 7 days, respectively, for the 2 cases detected by other components of the national surveillance system (Table 3). For the latter 2 cases, 1 of the ill persons lived in a village that was not covered by a community health monitor at the time of detection, and the case was identified after the person had died; the other person resided in a CEBS-covered village, but the case was not detected until the ill person was admitted to a local hospital.

During the subanalysis in Kambia, surveillance staff from other districts indicated that the CEBS network had detected additional outbreaks that were not caused by Ebola. Community health monitors identified 2 measles clusters in Kono and 1 measles cluster in Bombali, leading to the initiation of investigations and implementation of control measures, including isolation of ill persons and vaccination of susceptible children. Community health monitors in Bombali and Kono also reported suspected chickenpox clusters.

Table 3. Timeliness of identification of confirmed Ebola virus disease cases with no known epidemiologic links to other confirmed cases at detection, Kambia District, Sierra Leone, 2015*

Detected by CEBS	Patient age, y/sex	Symptom onset date	Detection date	Days from onset to detection
Yes	52/M	Apr 17	Apr 20	3
No	45/M	Apr 17	Apr 22	5
Yes	23/F	Apr 23	Apr 25	2
Yes	25/F	Apr 24	Apr 27	3
No	56/F	Apr 23	Apr 30	7
Yes	29/M	May 28	May 29	1

*The data are for April 13–May 30, 2015. CEBS, community event–based surveillance.

Discussion

Our evaluation indicates that, during its period of operation, CEBS effectively generated alerts for and detected nearly one third of all EVD cases found in its districts. Although this would rightly be considered a low sensitivity for an independent surveillance system, CEBS was designed to supplement a larger, established system. The low PPV of CEBS also was expected because of the tendency of event-based systems to provide higher sensitivity while generating a large number of false alerts (*12*) and because there were few true EVD cases. Ruling out EVD in times of low transmission requires investigation of all alerts and isolation and testing of all suspected case-patients (*13*), most of whom will be determined to be uninfected.

Our data from the subanalysis in Kambia are too few to draw a meaningful conclusion, but they suggest that CEBS may be capable of quickly finding cases with no identified epidemiologic links. If this is true, the system could be used to detect the early stages of new infectious disease outbreaks or to rapidly identify the spread of disease to new geographic areas during ongoing outbreaks or epidemics. Nevertheless, even within this small sample of cases, CEBS failed to detect 2 cases with no known epidemiologic links, which highlights the need for adequate coverage of villages by community health monitors, development of stronger links between communities and health monitors, and vigilance by the monitors.

One unexpected finding was that CEBS detected a large number of deaths in the community. Although not intended to serve as a reporting system for community deaths, CEBS did contribute to death reporting, which was a major initiative of the national government and social mobilization programs. By detecting dead bodies that were then tested and found to be negative for Ebola infection, CEBS helped to confirm the lack of virus transmission, thereby providing some evidence that the epidemic had, in fact, ended in a given district. However, death reports are a late indicator of infection and, thus, do not enable isolation of patients early in the disease course, a control measure that could result in reduced transmission (*14–16*). The death reporting rates also were considerably lower in most CEBS districts than would be expected based on estimated death rates (*11*); consequently, CEBS reporting rates were not a substitute for death surveillance or registration.

Another unexpected finding was the detection of 3 measles outbreaks. Given extensive undervaccination and undertreatment of other communicable diseases during the epidemic, it was expected that a large number of disease outbreaks would go undetected (*17,18*), but we did not anticipate that CEBS would detect a few of them. CEBS staff might have detected these clusters because some of the trigger events, such as ≥2 sick or dead persons

in a household, were not specific to EVD. The staff also might have identified the clusters because they were looking for signs of illness in their communities, irrespective of the cause or signs or symptoms. This finding provides some indication that community-based surveillance could be used to provide early warning of a variety of diseases of public health concern.

Our evaluation also revealed several critical weaknesses in CEBS, some of which may be due to the rapid implementation of the system. First, community health monitors primarily relied on the trigger category other to classify community deaths and alerts, rather than the defined trigger events that they were taught to seek out. This lack of use of defined trigger events could imply that some of the triggers were not sensitive enough to capture Ebola virus transmission. It is also possible that the staff miscategorized the alerts and that many alerts did, in fact, fit a trigger event category. However, most alerts categorized as other were not reported with sufficient information to assess whether they fit a defined trigger event category. Before future systems are widely implemented, the validity of triggers should be more rigorously tested, and refresher training of staff should be regularly provided to reinforce trigger event recall. Rapid implementation at scale is difficult to achieve while also providing comprehensive training and developing strong links between the community and the surveillance team. Ideally, community-based surveillance should be developed and implemented when a large outbreak is not underway. Such a system would then be in place and available for adaptation if a public health crisis arises.

Another weakness of CEBS is that community health monitors reported relatively few illnesses, which is concerning for a system that aimed to detect illness quickly to reduce opportunities for virus transmission. The low proportion of illness alerts may indicate that the intended meaning of illness was unclear or, more likely, that community health monitors were concerned about negative consequences from the community for reporting an event, particularly if the affected person was not infected with Ebola virus.

A final weakness of note is that CEBS detected few unsafe burials. This lack of reporting could reflect the general challenge faced by EVD surveillance in exposing a cultural tradition that communities intentionally guard closely. However, by February 2015, when awareness of the Ebola virus transmission risks of traditional burials were more fully understood, community members may have bypassed their community health monitors to relay information about unsafe burials directly to the preexisting burial management alert system (*19*).

Our evaluation has several limitations. First, we conducted the evaluation during a period of low Ebola virus

transmission; therefore, we cannot draw conclusions about how CEBS would perform in a high-transmission environment. Second, the subanalysis in Kambia lasted only 6 weeks and involved only a few cases. Consequently, the results regarding the ability of CEBS to find cases with no identified epidemiologic links at the time of detection cannot be considered conclusive. Additional implementation and evaluation of CEBS in future EVD outbreaks would provide data to assess the relative merits of this approach. Third, we could not analyze the sensitivity of CEBS to detect other disease outbreaks because no reference standard exists to inform the denominator, and no reporting mechanism exists within CEBS to inform the numerator. Fourth, CEBS was implemented primarily in rural settings, so we do not know how the system would perform in a densely populated urban setting, such as a capital city. Last, an anthropologic understanding of the lack of illness and burial reporting would inform a more comprehensive interpretation of these results.

The Sierra Leone Ministry of Health and Sanitation plans to use community-based surveillance as part of its Integrated Disease Surveillance and Response system, which is tasked with detecting and responding to several priority diseases, conditions, and events (20). Community-based surveillance could extend disease surveillance beyond district health clinics to the village level and provide an early warning function. This would contribute to meeting the core capacity requirements of the International Health Regulations to detect and report disease at the community level to facilitate the immediate implementation of control measures before an outbreak expands further (21,22). Nonetheless, our evaluation reveals several challenges that should be addressed. Detailed assessments should be undertaken to determine how community health monitors recognize and categorize symptomatic illness and the barriers to their ability and willingness to report illness. The assessment results should then be applied to refine trigger definitions and processes. Given that valid disease measures are the basis of an effective surveillance system, these issues are the most pressing ones that need to be studied and addressed to strengthen future iterations of community-based surveillance. In addition, trigger definitions should remain simple to ensure that community health monitors can understand and correctly apply them, which may mean that a few salient, event-based triggers would be more effective than several case-based, specific triggers. Alternatively, more extensive, regularly repeated training of community health monitors might be needed to ensure adequate recall and reporting of more complicated triggers. Furthermore, to sustain efficacy and performance, community-based surveillance must be fully integrated into the overall surveillance system and adequately supported to ensure response capacity.

References

1. Dagina R, Murhekar M, Rosewell A, Pavlin B. Event-based surveillance in Papua New Guinea: strengthening an International Health Regulations (2005) core capacity. Western Pac Surveill Response J. 2013;4:19–25. http://dx.doi.org/10.5365/wpsar.2013.4.2.001
2. Toyama Y, Ota M, Beyene BB. Event-based surveillance in north-western Ethiopia: experience and lessons learnt in the field. Western Pac Surveill Response J. 2015;6:22–7. http://dx.doi.org/10.5365/wpsar.2015.6.2.002
3. Santa-Olalla P, Gayer M, Magloire R, Barrais R, Valenciano M, Aramburu C, et al. Implementation of an alert and response system in Haiti during the early stage of the response to the cholera epidemic. Am J Trop Med Hyg. 2013;89:688–97. http://dx.doi.org/10.4269/ajtmh.13-0267
4. Curry D, Bisrat F, Coates E, Altman P. Reaching beyond the health post: community-based surveillance for polio eradication. Dev Pract. 2013;23:69–78 http://dx.doi.org/10.1080/09614524.2013.753410.
5. International Federation of Red Cross and Red Crescent Societies. Epidemic control for volunteers: a training manual [cited 2016 Jan 19]. http://www.ifrc.org/Global/Publications/Health/epidemic-control-en.pdf
6. Crowe S, Hertz D, Maenner M, Ratnayake R, Baker P, Lash RR, et al.; Centers for Disease Control and Prevention (CDC). A plan for community event–based surveillance to reduce Ebola transmission—Sierra Leone, 2014–2015. MMWR Morb Mortal Wkly Rep. 2015;64:70–3.
7. Sierra Leone Ministry of Health and Sanitation. Clinical management of patients in the Ebola treatment centres and other care centres in Sierra Leone [cited 2016 Mar 14]. https://extranet.who.int/ebolafmt/content/clinical-management-patients-ebola-treatment-centres-and-other-care-centres-sierra-leone
8. Koroma D, Turay AB, Moigua MB. Republic of Sierra Leone 2004 population and housing census: analytical report on population projection for Sierra Leone [cited 2016 Jan 19]. http://statistics.sl/2004_pop._&_hou._census_analytical_reports/2004_population_and_housing_census_report_on_projection_for_sierra_leone.pdf
9. World Health Organization. Ebola data and statistics [cited 2016 Jan 19]. http://apps.who.int/gho/data/view.ebola-sitrep.ebola-country-SLE-new-conf-prob-districs-20151007-data?lang=en
10. Centers for Disease Control and Prevention. The Epi Info viral hemorrhagic fever application [cited 2016 Jan 19]. https://epiinfovhf.codeplex.com/
11. World Health Organization. Ebola situation report—18 November 2015 [cited 2016 Jan 19]. http://apps.who.int/ebola/current-situation/ebola-situation-report-18-november-2015
12. World Health Organization. A guide to establishing event-based surveillance [cited 2016 Jan 19]. http://www.wpro.who.int/emerging_diseases/documents/docs/eventbasedsurv.pdf

13. World Health Organization. Emergency guidance: surveillance strategy during phase 3 of the Ebola response [cited 2016 Jan 19]. http://apps.who.int/iris/bitstream/10665/192997/1/WHO_EVD_ Guidance_Sur_15.1_eng.pdf

14. Faye O, Boëlle PY, Heleze E, Faye O, Loucoubar C, Magassouba N, et al. Chains of transmission and control of Ebola virus disease in Conakry, Guinea, in 2014: an observational study. Lancet Infect Dis. 2015;15:320–6. http://dx.doi.org/10.1016/ S1473-3099(14)71075-8

15. Lindblade KA, Kateh F, Nagbe TK, Neatherlin JC, Pillai SK, Attfield KR, et al. Decreased Ebola transmission after rapid response to outbreaks in remote areas, Liberia, 2014. Emerg Infect Dis. 2015;21:1800–7. http://dx.doi.org/10.3201/ eid2110.150912

16. Frieden TR, Damon I, Bell BP, Kenyon T, Nichol S. Ebola 2014—new challenges, new global response and responsibility. N Engl J Med. 2014;371:1177–80. http://dx.doi.org/10.1056/NEJMp1409903

17. Takahashi S, Metcalf CJ, Ferrari MJ, Moss WJ, Truelove SA, Tatem AJ, et al. Reduced vaccination and the risk of measles and other childhood infections post-Ebola. Science. 2015;347:1240–2. http://dx.doi.org/10.1126/science.aaa3438

18. Truelove SA, Moss WJ, Lessler J. Mitigating measles outbreaks in West Africa post-Ebola. Expert Rev Anti Infect Ther. 2015;13:1299–301. http://dx.doi.org/10.1586/14787210.201 5.1085305

19. Nielsen CF, Kidd S, Sillah AR, Davis E, Mermin J, Kilmarx PH; Centers for Disease Control and Prevention. Improving burial practices and cemetery management during an Ebola virus disease epidemic—Sierra Leone, 2014. MMWR Morb Mortal Wkly Rep. 2015;64:20–7.20. World Health Organization. Integrated disease surveillance [cited 2016 Jan 19]. http://www.who.int/csr/ labepidemiology/projects/diseasesurv/en/

21. World Health Organization. International Health Regulations (2005) [cited 2016 Jan 19]. http://www.who.int/ ihr/9789241596664/en/

22. Moon S, Sridhar D, Pate MA, Jha AK, Clinton C, Delaunay S, et al. Will Ebola change the game? Ten essential reforms before the next pandemic. The report of the Harvard–LSHTM Independent Panel on the Global Response to Ebola. Lancet. 2015;386:2204–21. http://dx.doi.org/10.1016/S0140-6736(15)00946-0

Address for correspondence: Ruwan Ratnayake, International Rescue Committee, 122 E 42nd St, New York, NY 10168, USA; email: ruwan.ratnayake@rescue.org; Sam Crowe, Centers for Disease Control and Prevention, 1600 Clifton Rd NE, Mailstop A38, Atlanta, GA 30329-4027, USA; email: yeo2@cdc.gov

etymologia

Dracunculus medinensis [drə-kung'ku-ləs med-in-en'sis]

Also known as Guinea worm for its formerly high prevalence along the Gulf of Guinea, *Dracunculus medinensis* ("little dragon from Medina") is a parasitic nematode that infects humans and domestic animals through contaminated water. *D. medinensis* was described in Egypt as early as the 15th century BCE and may have been the "fiery serpent" of the Israelites described in the Bible.

Guinea worm disease was once a substantial cause of illness in tropical and subtropical Africa and Asia, but cases declined as water sanitation improved in the 19th century. In 1986, the World Health Organization resolved to eradicate the parasite, and in 2015, due in large part to the work of the Carter Center, led by former Centers for Disease Control and Prevention Deputy Director Donald R. Hopkins, there were only 22 cases in 4 countries (Chad, Ethiopia, Mali, and South Sudan).

This 2004 photograph depicted the entrance to a Nigerian Guinea worm containment center. The sign at the entrance displayed a drawing of a Guinea worm sufferer. Photo by E. Staub, CDC/Carter Center.

Sources

1. Biswas G, Sankara DP, Agua-Agum J, Maiga A. Dracunculiasis (Guinea worm disease): eradication without a drug or vaccine. Philos Trans R Soc Lond B Biol Sci. 2013;368:20120146.

2. Guinea worm disease nears eradication. Lancet Infect Dis. 2016;16:131.

3. World Health Organization. Dracunculiasis: historical background. 5 Aug 2014 [cited 2016 Jun 20]. Available at http://www.who.int/dracunculiasis/ background/en/.

Address for correspondence: Ronnie Henry, Centers for Disease Control and Prevention, 1600 Clifton Rd NE, Mailstop E03, Atlanta, GA 30329-4027, USA; email: boq3@cdc.gov

Time Lags between Exanthematous Illness Attributed to Zika Virus, Guillain-Barré Syndrome, and Microcephaly, Salvador, Brazil

Igor A.D. Paploski,[1] Ana Paula P.B. Prates,[1] Cristiane W. Cardoso, Mariana Kikuti,
Monaise M. O. Silva, Lance A. Waller, Mitermayer G. Reis, Uriel Kitron,[1] Guilherme S. Ribeiro[1]

Zika virus infection emerged as a public health emergency after increasing evidence for its association with neurologic disorders and congenital malformations. In Salvador, Brazil, outbreaks of acute exanthematous illness (AEI) attributed to Zika virus, Guillain-Barré syndrome (GBS), and microcephaly occurred in 2015. We investigated temporal correlations and time lags between these outbreaks to identify a common link between them by using epidemic curves and time series cross-correlations. Number of GBS cases peaked after a lag of 5–9 weeks from the AEI peak. Number of suspected cases of microcephaly peaked after a lag of 30–33 weeks from the AEI peak, which corresponded to time of potential infections of pregnant mothers during the first trimester. These findings support the association of GBS and microcephaly with Zika virus infection and provide evidence for a temporal relationship between timing of arboviral infection of pregnant women during the first trimester and birth outcome.

In late 2014, cases of acute exanthematous illness (AEI), involving widespread rash of unclear etiology, were reported in several municipalities in northeastern Brazil. By April 2015, Zika virus was identified in patients from the states of Bahia (*1*) and Rio Grande do Norte, Brazil (*2*). In Salvador, the capital of Bahia, during February–June 2015, ≈15,000 cases of indeterminate AEI were reported (*3*). Reverse transcription PCR performed on 58 serum samples from AEI outbreak case-patients identified Zika virus in 3 (5.2%) of them. (*3*). Although chikungunya and dengue viruses were also detected at similar frequencies, the low frequency of fever (35.1%) and arthralgia (26.5%) among AEI

Author affiliations: Centro de Pesquisas Gonçalo Moniz, Salvador, Brazil (I.A.D. Paploski, M. Kikuti, M.M.O. Silva, M.G. Reis, U. Kitron, G.S. Ribeiro); Universidade Federal da Bahia, Salvador (I.A.D. Paploski, M. Kikuti, M.G. Reis, G.S. Ribeiro); Secretaria Municipal de Saúde de Salvador, Salvador (A.P.P.B. Prates, C.W. Cardoso); Emory University, Atlanta, Georgia, USA (L.A. Waller, U. Kitron)

patients suggested that Zika virus was the likeliest etiology for the outbreak (*3*).

The virus has continued to spread, and by the end of 2015, laboratory-confirmed autochthonous Zika virus cases have been identified in all 5 regions of Brazil; the Brazilian Ministry of Health estimated that 500,000-1.5 million persons were infected (*4*). Zika virus has since spread to other regions of the Americas and resulted in large epidemics (*5*).

Studies conducted during a Yap Island (Federated States of Micronesia) outbreak found that ≈20% of Zika virus infections showed clinical symptoms (*6*). For most patients in whom symptoms develop, the disease is self-limited and clinical manifestations (exanthema [rash], arthralgia, fever, and conjunctivitis) are mild (*6*). However, during the outbreak in French Polynesia, a 20-fold increase in the incidence of GBS was observed (*7*), and concerns about an association between Zika virus infection and GBS were first raised. A case–control study subsequently identified strong associations of GBS with positive Zika virus seroneutralization and Zika virus IgM or IgG (*8*). Since 2015, an increase in GBS rates has also been observed in Brazil, Colombia, El Salvador, Suriname, and Venezuela (*9*).

The increase in newborns with microcephaly in northeastern Brazil in late 2015 called global attention to Zika virus as a major public health threat to pregnant women and their newborns (*10*). Even without a conclusive association between a prenatal Zika virus infection and neurologic disorders in the offspring, the Brazilian Ministry of Health and World Health Organization declared a public health emergency (*11*). Since then, clinical evidence increasingly supports an association of prenatal Zika virus infection with birth of babies with microcephaly, and other neurologic and ophthalmologic complications, as well as miscarriages and stillbirths (*12–17*).

Salvador, the largest city in northeastern Brazil (2015 population of 2.9 million persons) has been one of the main epicenters for epidemics of Zika virus infection, GBS, and

microcephaly. Using raw and smoothed temporal data collected during these outbreaks, we investigated the temporal associations and determined the time lags between epidemiologic curves of the suspected Zika virus infection outbreak, reported cases of GBS, and reported suspected cases of microcephaly.

Methods

Data Collection and Case Definitions

In April 2015, the Centers for Information and Epidemiologic Surveillance of Salvador (CIES) established 10 public emergency health centers as sentinel units for systematic surveillance of patients with AEI of unknown cause in Salvador. A case-patient was defined as a resident of Salvador who had a rash, with or without fever, and whose clinical and epidemiologic characteristics did not satisfy the criteria for dengue, chikungunya, measles, or rubella (18). The public health units searched retrospectively for suspected cases by review of medical charts of patients treated starting on February 15, 2015; continued with prospective case detection; and submitted weekly reports of identified cases to CIES. On May 25, 2015, because of the sharp decrease in the number of outbreak cases, CIES reduced the number of sentinel health units to the 3 that reported the most cases, although several of the other units continued to report AEI cases voluntarily. For our analyses, we used the reported number of cases for February 15–December 31, 2015.

After neurologic syndrome cases in adults potentially associated with a previous Zika virus infection were first reported in Salvador in late May, CIES initiated surveillance for hospitalizations caused by neurologic manifestations that might be linked to Zika. Cases were identified retrospectively during April–May and followed by prospective case detection. CIES regularly contacted all city hospital epidemiologic services and investigated all suspected case-patients who resided in Salvador. Surveillance personnel, supported by infectious disease physicians and neurologists, ruled out cases for which clinical and laboratory manifestations indicated other diagnoses, and only included cases of GBS and its variants (e.g., Miller-Fisher syndrome). For our analyses, we used the number of hospitalized patients with GBS or GBS variants identified in Salvador during 2015.

After the increase in number of cases of microcephaly in newborns first noticed in Pernambuco State in September 2015, and the request from the Brazilian Ministry of Health that all suspected cases of microcephaly in newborns be reported, CIES established a reporting system in October 2015. Since then, CIES has requested and received reports of all newborns with suspected neurologic impairments and has been investigating all potential cases of microcephaly.

Suspected cases of microcephaly in newborns were reported on the basis of a reduced occiptofrontal perimeter at birth. The initial criteria for reporting was newborns delivered after ≥37 gestational weeks with an occiptofrontal perimeter ≤33 cm, or newborns delivered before 37 gestational weeks with a perimeter less than the third percentile of the Fenton curve (19). In December, 2015, the Brazilian Ministry of Health changed the first criterion to an occiptofrontal perimeter <32 cm (20).

For our analyses, we only included suspected microcephaly case-patients that fulfilled these latest criteria. The first such case-patient was born on July 11, 2015, and a search of the national information system on live births from Salvador for the AEI outbreak period produced no additional cases of congenital malformation fulfilling these criteria. We included all of suspected cases of microcephaly up to March 10, 2016 (the 10th epidemiologic week of 2016); and data for the last case-patient was updated on March 17, 2016.

We opted to analyze all reported suspected cases of microcephaly, instead of only those investigated and confirmed, because only 27.7% of the reported cases had been investigated. Limiting analysis to only confirmed cases could potentially introduce bias because cases that were reported earlier during the outbreak were more likely to have had the investigation concluded. In contrast, including all reported cases might introduce some false-positive diagnoses. Because both inclusion criteria are not free of a potential bias, we analyzed all reported suspected cases of microcephaly.

CIES served as the repository of all AEI, GBS, and suspected microcephaly data from all contributing sources. CIES evaluated and integrated data, including merging of different reporting spreadsheets, and removed duplicate information (on the basis of name, age, date of reporting, and sanitary districts of residence) and nonsense data (e.g., all missing information). Numbers of cases of AEI, GBS, and suspected microcephaly per epidemiologic week were then tabulated.

Data Analysis

We analyzed case-patients with AEI, GBS, and suspected microcephaly by date of medical care, date of hospitalization, and date of birth, respectively. We used the documented date of medical care or hospitalization, rather than the presumed day when symptoms began, to avoid recall error and reduce missing information.

We constructed epidemiologic curves by week and with 3-week and 5-week moving averages by using Stata software (21). We smoothed data by using 3-week and 5-week moving averages to reduce week-to-week variation, wherein the count of events for a given week was averaged with values of the previous and following weeks (3 weeks)

or with the 2 previous and 2 following weeks (5 weeks). Because the weekly increase in cases during the outbreak was much larger than the observed weekly variation, there was little difference between crude and smoothed data.

We assessed temporal correlations between our time series by using standard estimation of lagged time-series cross-correlations (22) to identify lag times showing the highest correlations between weekly numbers of AEI and ensuing weekly numbers of 1) GBS cases and 2) suspected cases of microcephaly. Although one could evaluate statistical significance by comparing cross-correlations to those expected under a null hypothesis of no association (22), our primary focus was to estimate lags with the strongest correlation (i.e., at what lags do the strongest correlations occur?), not a strict evaluation of whether any correlations occurred. Because both time series showed single large increases, our goal was to identify time lags between these series. Specifically, we examined lag times of 0–40 weeks and compared the AEI time series to those for GBS and suspected microcephaly to cover the full pregnancy period. Because of observed timing of initial epidemic curves, we present only results for positive time lags (i.e., AEI preceding GBS or suspected microcephaly). We also assessed cross-correlations for raw and 3-week and 5-week smoothed data.

Results

During the study, CIES recorded 17,503 reported cases of AEI (5.99 cases/1,000 persons during 2015), 51 hospitalizations of persons with of GBS (1.74 cases/100,000 persons during 2015), and 367 newborns with suspected microcephaly (15.6 cases/1,000 newborns during July 2015–February 2016, which peaked at 31.4 cases/1,000 newborns in December) (Table, http://wwwnc.cdc.gov/EID/article/22/8/16-0496-T1.htm). Raw and smoothed data (3-week and 5-week moving averages) had a clear initiation, peak, and reduction of cases, and followed a classic epidemic time series of incidence for AEI, GBS, and suspected microcephaly (Figure 1).

Number of AEI cases with available data for date of medical care (16,986 [97.1%]) (Figure 1, panel A) peaked during week 18 (May 3–9, 2015), as reported (3). The peak during week 18 was confirmed by 3-week and 5-week moving averages. During weeks 16–20 (April 19–May 23, 2015), >1,000 AEI cases/week were reported.

Number of GBS cases with a known date of hospitalization (49 [96.1%]) (Figure 1, panel B) peaked during weeks 23–27 (June 7–July 11, 2015). Using the 5-week moving average, we found that ≥4 cases were reported during weeks 23–27. The 5-week and 3-week moving averages provided a clearer picture of the GBS epidemic curve, which was susceptible to higher variability, given the relatively low number of cases per week.

Suspected cases of microcephaly that satisfied our criteria and included a date of birth (357 [97.3%]) (Figure 1, panel C) peaked during weeks 47–49 (November 22–December 12, 2015), during which there were >20 cases/week. Moving averages helped smooth the epidemiologic curve, which is susceptible to uneven time lags between a potential prenatal infection and outcome (i.e., a mother could have been infected at any time during the first trimester or even later). The 18-week period of increase in the number of suspected cases of microcephaly (weeks 31–48)
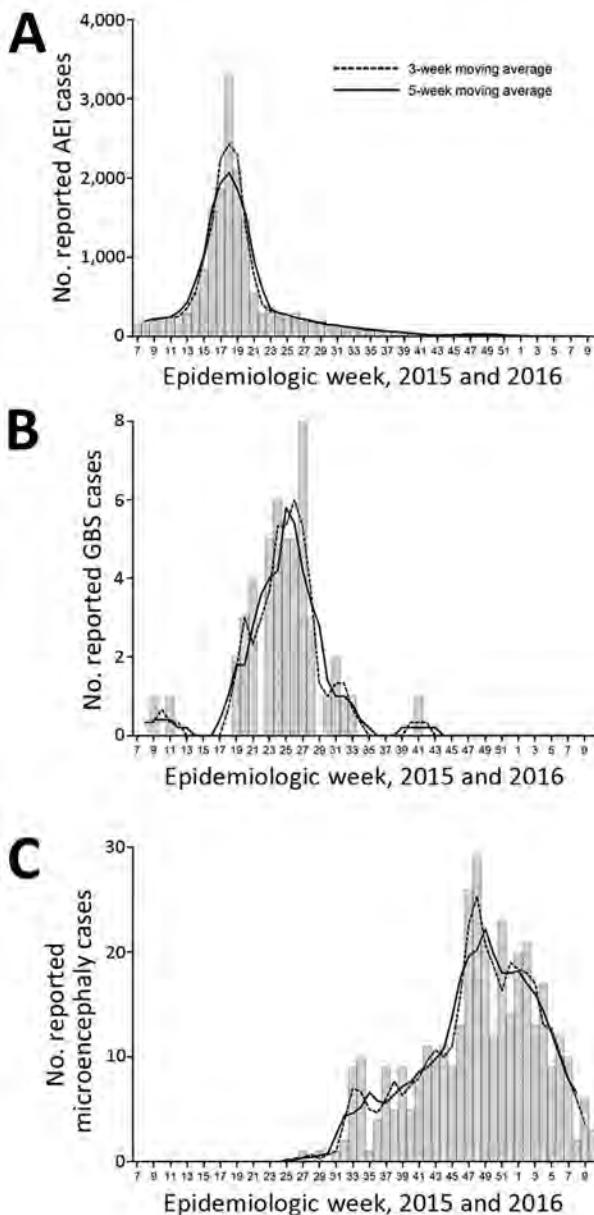
Figure 1. Epidemiologic curves of weekly cases and moving averages of 3 weeks and 5 weeks for A) acute exanthematous illness (AEI), B) Guillain-Barré syndrome, and C) suspected microcephaly, Salvador, Brazil, 2015–2016. The specific starting date during week 7 was February 15, 2105.

corresponds to a 12-week increase in number of AEI cases (weeks 7–18), and is probably longer because pregnant women throughout the first trimester might have been infected at the onset of the AEI outbreak. For 328 (91.9%) of 357 suspected cases of microcephaly for which data on gestational age at birth were available, the median gestational week was 39 weeks (range 34–41 weeks), which coincided with the first trimester of pregnancy when the AEI outbreak peaked.

Cross-correlation analyses (Figure 2) confirmed the patterns shown in Figure 1 (i.e., a strong positive correlation between temporally lagged time series driven by observed time lags between peaks in case numbers). Findings were consistent for results based on the raw time series and either the 3-week or 5-week moving averages, and peak correlations differed by $\leq$1 week. Number of GBS cases peaked after a lag of 5–9 weeks from the peak in AEI cases (Figure 2, panel A), thus providing strong support for a direct association of the GBS outbreak with the AEI outbreak 1–2 months earlier.

The number of suspected cases of microcephaly peaked after a lag of 30–33 weeks from the peak in AEI cases (Figure 2, panel B), which corresponded to potential infections of mothers during the first trimester of gestation (7–8 months before giving birth). Negative correlations observed at early lag periods were a function of the fact that most AEI cases occurred early in the study period when there were no suspected cases of microcephaly.

Discussion

Our analyses showed clear and strong cross-correlations for GBS and suspected cases of microcephaly with the original AEI outbreak in Salvador during 2015. These correlations were particularly noteworthy, given delays in case reporting, challenges with diagnosis, and ongoing

investigations. Correlations were particularly clear-cut for GBS when a lag of 5–9 weeks from AEI was considered. These results complement a recent case–control study (8), which reported an association of GBS with Zika virus in French Polynesia.

Of even more public health interest might be the strong association between outbreaks of AEI and children born with suspected microcephaly (30–33 weeks apart), which demonstrated a strong temporal association between potential exanthematous disease in the first trimester of pregnancy and birth outcome. These results also complement results of studies that linked febrile rash illness suggestive of Zika virus infection during the first trimester of pregnancy and an increased incidence of microcephaly in newborns (23,24). The ongoing decrease in number of suspected cases of microcephaly in 2016, which has occurred despite continuing and increasing public health and media attention to this serious pregnancy outcome, is particularly noteworthy and matches the reduction in number of cases of microcephaly predicted for Salvador in early 2016 (25,26).

Recent statements by researchers in Brazil and elsewhere and reports in the media have raised doubts about the actual baseline number of cases of microcephaly in Brazil and questioned the number of cases associated with exposure to Zika virus, given limited baseline data and greatly increased recognition and attention to this phenomenon (27). Our results support the link between births of children suspected of having microcephaly and exposure of a pregnant woman to an AEI putatively caused by Zika virus during the first trimester of pregnancy. This link was based on the time-lagged correlation between these 2 factors and the decrease in incidence of congenital manifestations since mid-December 2015.

Although such temporal associations do not prove causation, their strength and pattern makes a major contribution
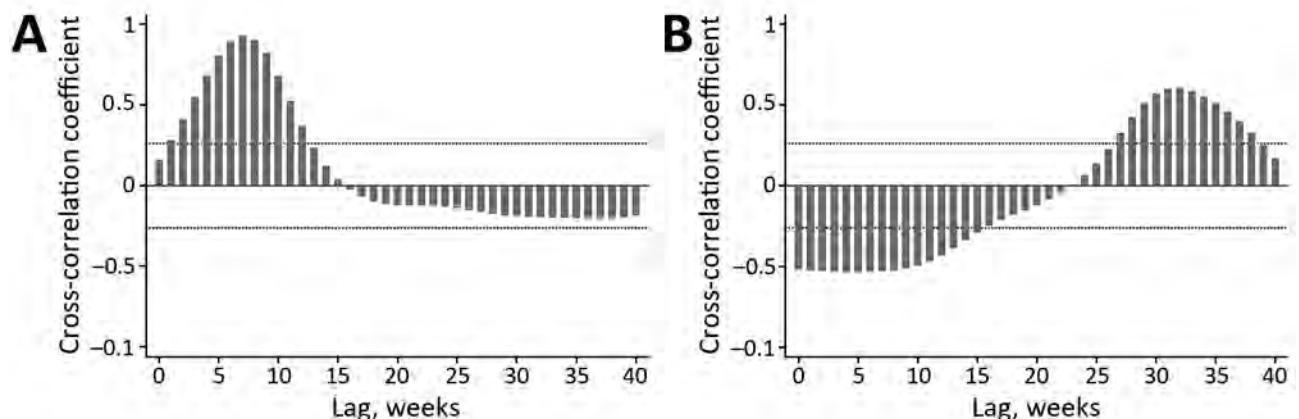
Figure 2. Cross-correlation of acute exanthematous illness with A) Guillain-Barré syndrome and B) suspected microcephaly, Salvador, Brazil, 2015–2016, for a 5-week moving average. Dotted horizontal lines indicate 95% tolerance intervals for a null model of no association. Negative correlations observed at early lag periods are a function of large numbers of acute exanthematous illness cases that occurred early in the study period when there were no suspected cases of microcephaly.

to the growing body of data supporting the association of GBS and congenital malformations with previous exposure to Zika virus (or, at least, an AEI). Furthermore, estimated time lags provide insight into the high-risk exposure period that might lead to these complications and, consequently, help public health and vector control authorities target control and protection efforts more effectively. Additional individual and population level investigations, both clinical and epidemiologic (case–control and cohort studies) are needed, as are increased resources for surveillance, vector control, and diagnostic capabilities to make definitive connections. With emerging infectious diseases increasing worldwide (28), investing in public health surveillance on the city, state, national, and global levels is one of the most cost effective way to help address these ongoing and increasing challenges (29).

As an epidemiologic investigation relying on population-level analyses, this study had several limitations. Our data were collected by CIES from different sources, diagnoses were not always definitive, and case definition criteria and case ascertainment were prone to changes, as is common during initial outbreak investigations of novel events. This limitation is particularly true for the AEI outbreak, for which cases were not subjected to an extensive laboratory investigation. In a previous study, we showed that Zika virus, chikungunya virus (CHIKV), and dengue virus were circulating and associated with AEI cases during the outbreak (3). On the basis of clinical manifestations for reported AEI case-patients and epidemiologic evidence for the spread of Zika virus in Brazil and to the rest of the Americas, and given the challenges in identifying Zika virus in serum samples, this virus was probably the main arbovirus involved in the AEI outbreak in Salvador during our study. Furthermore, although dengue (30,31) and chikungunya (32,33) have been associated with GBS, dengue epidemics have occurred for decades without any associated outbreaks of microcephaly or other severe congenital malformations, and CHIKV infections that occur in pregnant women before the peripartum period do not appear to pose congenital risks (34,35).

In French Polynesia, during the chikungunya outbreak in 2014–2015, an increase in GBS cases was observed (33). Thus, Zika virus and CHIKV might have played a role in emergence of GBS cases in Salvador. Unfortunately, our study design (because of limited available diagnostic data) precluded determining the frequency of each circulating arbovirus during the AEI outbreak. These data are needed to determine whether different arboviral infections peaked at the same time or whether the AEI peak represented the junction of distinct epidemic curves for sequential arbovirus outbreaks.

The presence of 2 infectious triggers, whose temporal distribution might not have coincided at the AEI peak,

might partly explain why we observed GBS cases peaking 5–9 weeks after the peak of AEI cases, while in French Polynesia, the lag between peaks of GBS and cases of Zika virus infection was only 3 weeks (8). Use of date of medical care for AEI and date of hospitalization for GBS, rather than the presumed day when symptoms began, also might have contributed to the difference in observed time lags. For case-patients for whom data were available, the median interval between AEI symptoms onset and medical care was 1 day, and the median interval between onset of GBS symptoms and hospitalization was 5 days. In addition, patients with AEI might have been less likely to seek medical care for their symptoms, once the community perceived Zika virus infection as benign, making the AEI epidemic curve shorter. Therefore, actual time lags might be shorter than what we observed.

Another limitation was the change in case ascertainment for AEI from retrospective to prospective, and then from using 10 health units to using the 3 units that reported most cases (although several of the other units continued to report AEI cases voluntarily). Retrospective data collection is the common method for detecting a baseline level and initiating an outbreak investigation, and reduction of the number of health units was made after the large decrease in AEI cases. Thus, the effect of these changes on the shape of the epidemic curve is small.

As another limitation, the epidemiologic curve for suspected cases of microcephaly potentially overestimated the actual number of cases. Ongoing investigation of the 5,909 reported suspected cases of microcephaly and other central nervous system impairments in newborns, stillbirths, and abortions in Brazil was completed for 1,687 cases by mid-February 2016. Of these cases, 641 (38.0%) were confirmed (36). In Salvador, CIES investigated 99 reported cases of Zika virus congenital syndrome, of which 43 (43.4%) were confirmed.

On the basis of the reported number of suspected cases of microcephaly and the number of births in Salvador during the study, 3.1% of newborns were reported as having suspected cases of microcephaly during the peak month of December 2015. However, if we consider that in December only 20 (58%) of the 34 investigated cases were confirmed, a more realistic estimation for the suspected microcephaly risk in that period is 1.8 cases/100 newborns. We believe that the temporal distribution of reported cases parallels that of actual cases. Also, by analyzing all reported cases, we reduced a major source of observation bias (i.e., investigations of cases reported earlier were more likely to have been completed). The consistent shape and mode of the epidemiologic curves, with or without smoothing, support the robustness of our data and findings.

Our case ascertainments of suspected cases of microcephaly were also potentially influenced by spontaneous

and nonspontaneous abortions. Although spontaneous abortions could have occurred because of virus effects during embryogenesis, nonspontaneous abortions might have increased after intense media coverage of the microcephaly outbreak. Abortion is prohibited in Brazil (except for a few situations, such as rape, anencephaly, or risk for death of the mother), but it is commonly performed illegally, and 16.4% of women reported having had ≥1 abortion (37). Unfortunately, no official data are available to help understand the likely effect of abortions on the outbreak of congenital Zika virus syndrome. In addition, the database for suspected microcephaly is restricted to live births, and data on stillbirths and abortions are not available.

Finally, we focused on cross-correlation between the time series because we did not have individual links between GBS cases and earlier AEI in the same person or between suspected microcephaly and prior AEI of the mother. Retrospective studies indicate a recall of AEI by women who have given birth to microcephalic babies, but there are few direct demonstrations of virus transfer (17). Use of aggregate data enabled us to test for a temporal association between AEI, GBS, and suspected microcephaly, taking advantage of the establishment in Salvador of a surveillance system for detecting and recording AEI cases early during the outbreak. Consequently, Salvador recorded 17,503 of the 72,062 suspected cases of Zika virus infection in Brazil by February 25, 2016 (38).

After the AEI outbreak in Salvador, attention was given to the increased number of cases of microcephaly. However, it is becoming clear that newborns also manifest other congenital malformations (12,16), and that microcephaly might be the most extreme outcome of arboviral infection of the mother. The recently proposed term congenital Zika syndrome (39) might better capture the spectrum of possible clinical manifestation of newborns exposed to Zika virus during gestation. The Brazilian Ministry of Health is now conducting surveillance of microcephaly or changes in the central nervous system (36). As neonatal outcomes are likely to be observed in other countries, attention must be given to the full range of potential congenital malformations.

Acknowledgments

Dr. Paploski is a veterinarian and public health doctoral candidate at the Federal University of Bahia, Salvador, Brazil. His primary research interests are epidemiology of arboviruses and infectious diseases that disproportionally affect neglected populations.

References

1. Campos GS, Bandeira AC, Sardi SI. Zika virus outbreak, Bahia, Brazil. Emerg Infect Dis. 2015;21:1885–6. http://dx.doi.org/10.3201/eid2110.150847
2. Zanluca C, de Melo VC, Mosimann AL, dos Santos GI, dos Santos CN, Luz K. First report of autochthonous transmission of Zika virus in Brazil. Mem Inst Oswaldo Cruz. 2015;110:569–72. http://dx.doi.org/10.1590/0074-02760150192
3. Cardoso CW, Paploski IA, Kikuti M, Rodrigues MA, Silva MM, Campos GS, et al. Outbreak of exanthematous illness associated with Zika, chikungunya, and dengue viruses, Salvador, Brazil. Emerg Infect Dis. 2015;21:2274–6. http://dx.doi.org/10.3201/eid2112.151167
4. Ribeiro GS, Kitron U. Zika virus pandemic: a human and public health crisis [in Portuguese]. Revista da Sociedade Brasileira de Medicina Tropical. 2016;49:1–3. http://dx.doi.org/10.1590/0037-8682-0036-2016
5. Weaver SC, Costa F, Garcia-Blanco MA, Ko AI, Ribeiro GS, Saade G, et al. Zika virus: history, emergence, biology, and prospects for control. Antiviral Res. 2016;130:69–80. http://dx.doi.org/10.1016/j.antiviral.2016.03.010
6. Duffy MR, Chen T-H, Hancock WT, Powers AM, Kool JL, Lanciotti RS, et al. Zika virus outbreak on Yap Island, Federated States of Micronesia. N Engl J Med. 2009;360:2536–43. http://dx.doi.org/10.1056/NEJMoa0805715
7. Oehler E, Watrin L, Larre P, Leparc-Goffart I, Lastere S, Valour F, et al. Zika virus infection complicated by Guillain-Barre syndrome–case report, French Polynesia, December 2013. Euro Surveill. 2014;19:20720. http://dx.doi.org/10.2807/1560-7917.ES2014.19.9.20720
8. Cao-Lormeau V-M, Blake A, Mons S, Lastère S, Roche C, Vanhomwegen J, et al. Guillain-Barré syndrome outbreak associated with Zika virus infection in French Polynesia: a case–control study. Lancet. 2016;387:1531–9. http://dx.doi.org/10.1016/S0140-6736(16)00562-6
9. World Health Organization. Zika situation report, February 26, 2016 [cited 2016 Mar 2]. http://who.int/emergencies/zika-virus/situation-report/26-february-2016/en/
10. Zika virus—Brazil (16): (Pernambuco) Microcephaly cause undetermined. ProMED-mail [cited 2016 Apr 27]. http://www.promedmail.org archive no. 20151118.3799192.
11. World Health Organization. WHO Director-General summarizes the outcome of the emergency committee regarding clusters of microcephaly and Guillain-Barré syndrome, 2016 [cited 2016 Mar 2]. http://www.who.int/mediacentre/news/statements/2016/emergency-committee-zika-microcephaly/en/
12. Sarno M, Sacramento GA, Khouri R, do Rosáario MS, Costa F, Archanio G, et al. Zika virus infection and stillbirths: a case of hydrops fetalis, hydranencephaly and fetal demise. PLoS Negl Trop Dis. 2016;10:e0004517. http://dx.doi.org/10.1371/journal.pntd.0004517
13. Schuler-Faccini L, Ribeiro EM, Feitosa IM, Horovitz DD, Cavalcanti DP, Pessoa A, et al. Possible association between Zika

virus infection and microcephaly—Brazil, 2015. MMWR Morb Mortal Wkly Rep. 2016;65:59–62. http://dx.doi.org/10.15585/mmwr.mm6503e2

14. Mlakar J, Korva M, Tul N, Popović M, Poljšak-Priiateli M, Mraz J, et al. Zika virus associated with microcephaly. N Engl J Med. 2016;374:951–8. http://dx.doi.org/10.1056/NEJMoa1600651

15. Calvet G, Aguiar RS, Melo AS, Sampaio SA, de Filippis I, Fabri A, et al. Detection and sequencing of Zika virus from amniotic fluid of fetuses with microcephaly in Brazil: a case study. Lancet Infect Dis. 2016;Feb 17:pii: S1473-3099(16)00095-5.

16. de Paula Freitas B, de Oliveira Dias JR, Prazeres J, Sacramento GA, Ko AI, Maia M, et al. Ocular findings in infants with microcephaly associated with presumed Zika virus congenital infection in Salvador, Brazil. JAMA Ophthalmol. 2016 Feb 9. http://dx.doi.org/10.1001/jamaophthalmol.2016.0267

17. Brasil P, Pereira JP Jr, Raja Gabaglia C, Damasceno L, Wakimoto M, Ribeiro Nogueira RM, et al. Zika virus infection in pregnant women in Rio de Janeiro—preliminary report. [Epub ahead of print]. N Engl J Med. 2016. http://dx.doi.org/10.1056/NEJMoa1602412

18. Government of the State of Bahia. Alert for indeterminate and exanthema disease transmission risk of epidemics of dengue and chikungunya fever in the State of Bahia, June 4, 2015. Technical note [in Portuguese] [cited 2016 Mar 2]. http://www.suvisa.ba.gov.br/sites/default/files/doenca_transmissao_vetorial/arquivo/2015/05/14/NOTA T%C3%89CNICA 02–2015 Doen%C3%A7a Exantem%C3%A1tica Indeterminada.pdf

19. Ministry of Health of Brazil. Information note N01/2015. COES microcephaly, 2015 [in Portuguese] [cited 2016 May 2]. http://portalsaude.saude.gov.br/images/pdf/2015/novembro/18/microcefalia-nota-informativa-17nov2015-c.pdf

20. Ministry of Health of Brazil. Surveillance and response protocol for occurrence of microcephaly, 2016 [in Portuguese] [cited 2016 May 2]. http://portalsaude.saude.gov.br/images/pdf/2016/janeiro/22/microcefalia-protocolo-de-vigilancia-e-resposta-v1-3-22jan2016.pdf

21. Stata statistical software: release 14. College Station (TX): StataCorp LP; 2015 [cited 2016 Apr 27]. http://www.stata.com/

22. Diggle P. Time series: a biostatistical introduction. New York: Oxford University Press; 1990.

23. Kleber de Oliveira W, Cortez-Escalante J, De Oliveira WT, do Carmo GM, Henriques CM, Coelho GE, et al. Increase in reported prevalence of microcephaly in infants born to women living in areas with confirmed Zika virus transmission during the first trimester of pregnancy—Brazil, 2015. MMWR Morb Mortal Wkly Rep. 2016;65:242–7. http://dx.doi.org/10.15585/mmwr.mm6509e2

24. Cauchemez S, Besnard M, Bompard P, Dub T, Guillemette-Artur P, Evrolle-Guignot D, et al. Association between Zika virus and microcephaly in French Polynesia, 2013–15: a retrospective study. Lancet. 2016;Mar 15:pii: S0104-6736(16)00651-6.

25. Reefhuis J, Gilboa SM, Johansson MA, Valencia D, Simeone RM, Hills SL, et al. Projecting month of birth for at-risk infants after Zika virus disease outbreaks. Emerg Infect Dis. 2016;22:828–32.

26. Nah K, Mizumoto K, Miyamatsu Y, Yasuda Y, Kinoshita R, Nishiura H. Estimating risks of importation and local transmission of Zika virus infection. PeerJ. 2016;4:e1904. http://dx.doi.org/10.7717/peerj.1904

27. Butler D. Zika virus: Brazil's surge in small-headed babies questioned by report. Nature. 2016;530:13–4. http://dx.doi.org/10.1038/nature.2016.19259

28. Cutler SJ, Fooks AR, van der Poel WH. Public health threat of new, reemerging, and neglected zoonoses in the industrialized world. Emerg Infect Dis. 2010;16:1–7. http://dx.doi.org/10.3201/eid1601.081467

29. Vazquez-Prokopec GM, Chaves LF, Ritchie SA, Davis J, Kitron U. Unforeseen costs of cutting mosquito surveillance budgets. PLoS Negl Trop Dis. 2010;4:e858. http://dx.doi.org/10.1371/journal.pntd.0000858

30. Esack A, Teelucksingh S, Singh N. The Guillain-Barré syndrome following dengue fever. West Indian Med J. 1999;48:36–7.

31. Santos NQ, Azoubel AC, Lopes AA, Costa G, Bacellar A. Guillain-Barré syndrome in the course of dengue: case report. Arq Neuropsiquiatr. 2004;62:144–6. http://dx.doi.org/10.1590/S0004-282X2004000100025

32. Lebrun G, Chadda K, Reboux A-H, Martinet O, Gaüzère B-A. Guillain-Barré syndrome after chikungunya infection. Emerg Infect Dis. 2009;15:495–6. http://dx.doi.org/10.3201/eid1503.071482

33. Oehler E, Fournier E, Leparc-Goffart I, Larre P, Cubizolle S, Sookhareea C, et al. Increase in cases of Guillain-Barré syndrome during a chikungunya outbreak, French Polynesia, 2014 to 2015. Euro Surveill. 2015;20:30079. http://dx.doi.org/10.2807/1560-7917.ES.2015.20.48.30079

34. Gérardin P, Sampériz S, Ramful D, Boumahni B, Bintner M, Alessandri JL, et al. Neurocognitive outcome of children exposed to perinatal mother-to-child chikungunya virus infection: the CHIMERE cohort study on Reunion Island. PLoS Negl Trop Dis. 2014;8:e2996. http://dx.doi.org/10.1371/journal.pntd.0002996

35. Fritel X, Rollot O, Gérardin P, Gauzere BA, Bideault J, Lagarde L, et al. Chikungunya virus infection during pregnancy, Réunion, France, 2006. Emerg Infect Dis. 2010;16:418–25. http://dx.doi.org/10.3201/eid1604.091403

36. Ministry of Health of Brazil. Epidemiological report N15. Epidemiological week (IF) 8/2016 (21 to 2/27/2016) monitoring cases of microcephaly in Brazil, 2016 [in Portuguese] [cited 2016 Mar 3]. http://portalsaude.saude.gov.br/images/pdf/2016/marco/01/coes-microcefalia-informe-epid15-se08-2016-01mar2016.pdf

37. Cecatti JG, Guerra GVQL, Sousa MH, Menezes GM. Abortion in Brazil: a demographic approach [in Portuguese]. Rev Bras Ginecol Obstet. 2010;32:105–11. http://dx.doi.org/10.1590/S0100-72032010000300002

38. Pan American Health Organization/World Health Organization. Cumulative Zika suspected and confirmed cases reported by countries and territories in the Americas, 2015–2016, Updated as of February 25, 2016, with data received by February 24, 2016 [cited 2016 Mar 2]. http://ais.paho.org/phip/viz/ed_zika_cases.asp

39. Costa F, Sarno M, Khouri R, de Paulo Freitas B, Siqueira I, Ribeiro GS, et al. Emergence of congenital Zika syndrome: viewpoint from the front lines. Ann Intern Med. 2016 Feb 24; http://dx.doi.org/10.7326/M16-0332

Address for correspondence: Guilherme S. Ribeiro, Centro de Pesquisas Gonçalo Moniz, Fundação Oswaldo Cruz, Rua Waldemar Falcão, 121, Candeal, 40296-710 Salvador, BA, Brazil; email: guilherme.ribeiro@bahia.fiocruz.br

Human Babesiosis, Bolivia, 2013

Simona Gabrielli, Valentina Totino,
Fabio Macchioni, Freddy Zuñiga, Patricia Rojas,
Yuni Lara, Mimmo Roselli,
Alessandro Bartoloni, Gabriella Cancrini

To investigate human babesiosis in the Bolivian Chaco, in 2013 we tested blood samples from 271 healthy persons living in 2 rural communities in this region. Microscopy and PCR indicated that 3.3% of persons were positive for *Babesia microti* parasites (US lineage); seroprevalence was 45.7%. Appropriate screening should mitigate the risk for transfusion-associated babesiosis.

Babesiosis is an emerging tickborne disease worldwide resulting from ≈100 *Babesia* parasite species that can infect a broad range of hosts in which it induces malaria-like disorders. Like trypanosomes and *Plasmodium* spp., *Babesia* spp. can be transmitted through vertical routes and blood transfusions (*1*). Babesiosis has the greatest effect on the cattle industry and on companion animals; however, occasional human babesiosis has attracted increased attention. In immunocompetent persons, the infection is rarely detected because it can be asymptomatic or cause mild, self-resolving symptoms. However, babesiosis can be life-threatening in certain populations, such as neonates/infants, elderly persons, asplenic patients, and otherwise immunocompromised persons (*2*).

The predominant species that causes of human babesiosis in the United States and is a rare cause of disease in Europe and Asia is *Babesia microti* (*3*), a complex that includes at least 4 named types and an unknown number of other strains (*4*). The second-most important zoonotic species, *B. divergens*, causes several clinical cases in Europe (*5*). Other species, such as *B. duncani*, *B. venatorum*, and some *B. divergens*–like parasites, can cause further human infections worldwide (*6*). Many ixodid tick species can transmit *Babesia* parasites to their natural hosts; *Ixodes scapularis* and *I. ricinus* are the most important human-biting vector ticks in the United States and Europe, respectively (*7*).

Three cases of uncharacterized babesiosis have been reported from South America, 2 from Brazil and 1 from

Author affiliations: Università "Sapienza" di Roma, Rome, Italy
(S. Gabrielli, V. Totino, G. Cancrini); Università degli Studi di Pisa,
Pisa, Italy (F. Macchioni); Distrito de Salud Cordillera, Santa Cruz,
Bolivia (F. Zuñiga, P. Rojas); Hospital S. Antonio de Los Sauces,
Monteagudo, Bolivia (Y. Lara); Università di Firenze, Florence,
Italy (M. Roselli, A. Bartoloni)

Colombia (*8,9*). In Bolivia, only cattle have been investigated, highlighting the prevalence of the species *B. bovis* and *B. bigemina*, unstable and endemic in the east of the country (*10*); no data are available on *B. microti*. Our objective was to investigate human babesiosis in the Bolivian Chaco, a rural region in southeastern Bolivia.

The Study

In 2013, a total of 271 healthy volunteers, residents of 2 rural communities in southeastern Bolivia, Bartolo (Hernando Siles Province, Department of Chuquisaca) and Ivamirapinta (Cordillera Province, Department of Santa Cruz), completed a questionnaire interview asking for anamnestic data (sex, age, fever attacks, history of tick bite or transfusion) and provided blood samples for testing. The participants represented ≈50% and ≈25% of the population of the 2 communities, respectively. The Bolivian Ministry of Health and the Regional Health Departments approved the study design, including its ethical aspects; the Guaraní political organization (Asamblea del Pueblo Guaraní) supported the field work and conducted the interviews.

Blood drawn was immediately used to prepare thick and thin smears and to impregnate filter papers (100 mL); serum was obtained from each remaining sample. Smears were Giemsa stained and examined by microscopy at 400× and 1,000×. DNA was extracted from all the dried blood spots by using Dried Blood Spot DNA Isolation Kit (Norgen Biotek Corp., Thorold, ON, Canada) and amplified by PCR with generic apicomplexan 18S rRNA-specific primers (*11*). Amplicons (≈1,700 bp) were purified (Sure Clean kit; Bioline, Rome, Italy) and then sequenced. Sequences were aligned and compared with those available in GenBank. To investigate the *B. microti* strain, we further examined all positive samples by lineage-specific PCR based on the subunit 7 (η) of the chaperonin-containing t-complex polypeptide 1 (CCTη) gene, following the published protocol (*4*). PCR-positive samples and further randomly chosen serum samples (n = 47 for each community) were checked by an indirect fluorescent antibody test (IFAT) (IgG IFA kit; Fuller Laboratories, Fullerton, CA, USA) for reactivity to *B. microti*, following the manufacturer's instructions and fixing the cutoff value at dilution 1:64. Positive and negative control sera supplied by the kit were included on each IFAT slide. IFAT sensitivity and specificity in detecting *B. microti* antibodies, reported by the kit data sheet, are 88%–96% and 90%–100%, respectively (*12*). To ensure the specificity of the results, we further tested all reactive serum samples and 10 negative serum samples with the Falciparum-Spot

Table. *Babesia microti* results from microscopy, PCR, and serology in persons living in 2 rural communities, southeastern Bolivia, 2013*

	No. positive/no. examined (%)			
	Bartolo		Ivamirapinta	
Age group, y	Microscopy and PCR	IFAT	Microscopy and PCR	IFAT
1–10	2/29 (6.9)	3/9 (33.3)	1/21(4.7)	5/6 (83.3)
11–20	1/16 (6.2)	1/3 (33.3)	0/42 (0)	3/10 (30)
21–30	1/23 (4.3)	7/7 (100)	1/15 (6.6)	1/3 (33.3)
31–40	0/19 (0)	3/4 (75)	1/21 (4.7)	2/3 (66.6)
41–50	0/11 (0)	0/2 (0)	0/13 (0)	3/4 (75)
51–60	1/11 (9.0)	2/8 (25)	0/13 (0)	2/6 (33)
61–70	0/10 (0)	5/10 (50.0)	1/15 (6.6)	4/11 (36.4)
>70	0/4 (0)	1/4 (25)	0/8 (0)	1/4 (25)
Total	5/123 (4.1)	22/47 (46.8)	4/148 (2.7)	21/47 (44.7)
*IFAT, indirect fluorescent antibody test.				

IF kit (bioMérieux, Marcy l'Etoile, France) to detect plasmodial antibodies.

We conducted statistical analyses using the χ^2 test. We considered p<0.05 as significant.

Of the 271 serum samples, 9 (3.3%; 95% CI 0.97%–5.03%) thin and thick smears, from 5 (4.1%) and 4 (2.7%) participants living in Bartolo and Ivamirapinta, respectively, were positive for *B. microti* (Table; Figure). Infection rates did not differ significantly by community (p = 0.55), sex, or age, despite early infection in Bartolo.

Testing of blood from the 9 positive participants by molecular amplification and sequencing confirmed morphologic diagnosis (99% nt identity with the *B. microti* 18S rRNA gene; GenBank accession no. AY693840.1); moreover, results classified all the remaining blood spots as negative. PCR on the CCTη gene and sequencing showed that all positive samples belonged to the US lineage Gray strain (100% nt identity with GenBank accession no. AB362586.1). Sequences obtained were deposited in GenBank under accession nos. KT318131, KT318132, and KT844553–KT844568.

IFAT showed reactivity to *B. microti* antigens in all positive survey participants and in 34 of 85 additional persons, providing an overall seroprevalence of 45.7% (95% CI 35.7%–55.7%). We observed no differences between the 2 communities (p = 0.836) by age group or between early (0–30-year-olds) or late (>30-year-olds) developed seroreactivity (Bartolo: p = 0.209; Ivamirapinta: p = 0.760). We found no cross-reactivity to plasmodial antigens.

Conclusions

Although our study has some limitations, including the cross-sectional design, the limited number of human samples, and the nonrandom sampling, we detected *B. microti* antigens in ≈3% of persons living in the rural communities of the Bolivian Chaco. Moreover, we detected an overall seroprevalence rate of ≈45%, higher than that reported in Colombia (30.6%) (*13*), and with exposure starting from an early age. None of the positive study participants had signs or symptoms of babesiosis at the time of sample collection. Considering that many intra-erythrocytic cycles are needed before the immune system responds to the parasite and starts antibody production (*14*), the contemporary detection in some cases of blood parasite and serum-specific antibodies suggests a late infection stage.

The presence of *B. microti* antigens in persons without a history of tick infestation or transfusions indicates that contact between ticks and humans is not rare (mainly in young persons), as confirmed by a serosurvey that evidenced human exposure to other tickborne pathogens, such as *Borrelia* spp. (*15*). Furthermore, this finding suggests that, even though the primary reservoir, the white-footed
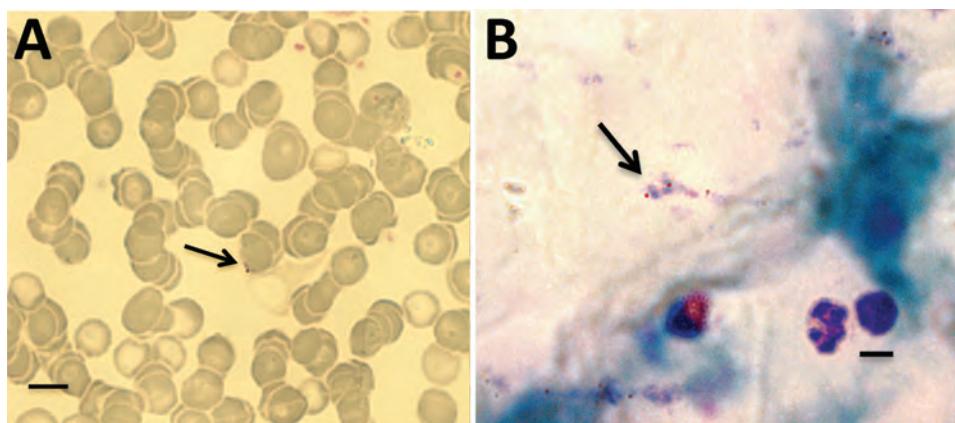
Figure. *Babesia microti* parasites (arrows) detected in Giemsa-stained thin (A) and thick (B) blood smears from persons living in 2 rural communities, southeastern Bolivia, 2013. Scale bars indicate 10 μm.

mouse (*Peromyscus leucopus*), has been reported only in North and Central America, natural animal hosts of this protozoon are widespread in the studied area. Inhabitants of both communities live in close contact with domestic animals, such as dogs, chickens, and pigs, and with deer and other wild animals, which might contribute to the maintenance and spread of the ticks. Because this zoonotic babesiosis is due to the Gray strain, previously documented in humans in the United States, Germany, Russia, China, South Korea, and Japan, where it is harbored by various small mammals, further studies are needed to explore its vectors and reservoirs in the rural areas here investigated.

Human babesiosis is probably an underestimated health problem in the Bolivian Chaco. Residents should therefore be alerted to the threat posed by ticks, and physicians should be aware of infection with *B. microti* parasites as a potential life-threatening disease. The presence of *B. microti* antigens in the blood of asymptomatic persons is of concern in terms of the possible risk for transfusion-associated babesiosis and should prompt the need to evaluate implementation of appropriate screening measures.

References

1. Leiby DA. Transfusion-transmitted *Babesia* spp.: bull's-eye on *Babesia microti*. Clin Microbiol Rev. 2011;24:14–28. http://dx.doi.org/10.1128/CMR.00022-10
2. Gray J, Zintl A, Hildebrandt A, Hunfeld KP, Weiss L. Zoonotic babesiosis: overview of the disease and novel aspects of pathogen identity. Ticks Tick Borne Dis. 2010;1:3–10. http://dx.doi.org/10.1016/j.ttbdis.2009.11.003
3. Vannier E, Krause PJ. Update on babesiosis. Interdiscip Perspect Infect Dis. 2009;2009:984568. Epub 2009 Aug 27. http://dx.doi.org/10.1155/2009/984568
4. Nakajima R, Tsuji M, Oda K, Zamoto-Niikura A, Wei Q, Kawabuchi-Kurata T, et al. *Babesia microti*–group parasites compared phylogenetically by complete sequencing of the CCTeta gene in 36 isolates. J Vet Med Sci. 2009;71:55–68. http://dx.doi.org/10.1292/jvms.71.55
5. Centeno-Lima S, do Rosário V, Parreira R, Maia AJ, Freudenthal AM, Nijhof AM, et al. A fatal case of human babesiosis in Portugal: molecular and phylogenetic analysis. Trop Med Int Health. 2003;8:760–4. http://dx.doi.org/10.1046/j.1365-3156.2003.01074.x
6. Gray JS. Identity of the causal agents of human babesiosis in Europe. Int J Med Microbiol. 2006;296(Suppl 40):131–6. http://dx.doi.org/10.1016/j.ijmm.2006.01.029
7. Yabsley MJ, Shock BC. Natural history of zoonotic *Babesia*: role of wildlife reservoirs. Int J Parasitol Parasites Wildl. 2012;2:18–31. http://dx.doi.org/10.1016/j.ijppaw.2012.11.003
8. Ríos L, Alvarez G, Blair S. Serological and parasitological study and report of the first case of human babesiosis in Colombia. Rev Soc Bras Med Trop. 2003;36:493–8. http://dx.doi.org/10.1590/S0037-86822003000400010
9. Rech A, Bittar CM, de Castro CGJ Jr, Azevedo KR, dos Santos RP, Machado ARL, et al. Asymptomatic babesiosis in a child with hepatoblastoma. J Pediatr Hematol Oncol. 2004;26:213. http://dx.doi.org/10.1097/00043426-200403000-00015
10. Carrique JJ, Morales GJ, Edelsten M. Endemic instability for babesiosis and anaplasmosis in cattle in the Bolivian Chaco. Vet J. 2000;160:162–4. http://dx.doi.org/10.1016/S1090-0233(00)90489-1
11. Herwaldt BL, Cacciò S, Gherlinzoni F, Aspöck H, Slemenda SB, Piccaluga P, et al. Molecular characterization of a non-*Babesia divergens* organism causing zoonotic babesiosis in Europe. Emerg Infect Dis. 2003;9:942–8. http://dx.doi.org/10.3201/eid0908.020748
12. Krause PJ, Telford SR III, Ryan R III, Conrad PA, Wilson M, Thomford JW, et al. Diagnosis of babesiosis: evaluation of a serologic test for the detection of *Babesia microti* antibody. J Infect Dis. 1994;169:923–6. http://dx.doi.org/10.1093/infdis/169.4.923
13. Buelvas F, Alvis N, Buelvas I, Miranda J, Mattar S. A high prevalence of antibodies against *Bartonella* and *Babesia microti* has been found in villages and urban populations in Cordoba, Colombia [in Spanish]. Rev Salud Publica (Bogota). 2008;10:168–77. http://dx.doi.org/10.1590/S0124-00642008000100016
14. Chappell LH, Cox FEG. Modern parasitology, 2nd ed., Oxford (UK): Blackwell Scientific Publications; 1993.
15. Ciceroni L, Bartoloni A, Guglielmetti P, Paradisi F, Barahona HG, Roselli M, et al. Prevalence of antibodies to *Borrelia burgdorferi*, *Borrelia parkeri* and *Borrelia turicatae* in human settlements of the Cordillera Province, Bolivia. J Trop Med Hyg. 1994;97:13–7.

Address for correspondence: Alessandro Bartoloni, Università degli Studi di Firenze, Clinica Malattie Infettive, Dipartimento di Medicina Sperimentale e Clinica, Largo Brambilla 3, Florence 50134, Italy; email: alessandro.bartoloni@unifi.it

Use of Unamplified RNA/cDNA–Hybrid Nanopore Sequencing for Rapid Detection and Characterization of RNA Viruses

Andy Kilianski, Pierce A. Roth, Alvin T. Liem,
Jessica M. Hill, Kristen L. Willis,
Rebecca D. Rossmaier, Andrew V. Marinich,
Michele N. Maughan, Mark A. Karavis,
Jens H. Kuhn, Anna N. Honko,
C. Nicole Rosenzweig

Nanopore sequencing, a novel genomics technology, has potential applications for routine biosurveillance, clinical diagnosis, and outbreak investigation of virus infections. Using rapid sequencing of unamplified RNA/cDNA hybrids, we identified Venezuelan equine encephalitis virus and Ebola virus in 3 hours from sample receipt to data acquisition, demonstrating a fieldable technique for RNA virus characterization.

Portable and reliable molecular epidemiology techniques and field approaches for assessing virus genomes are desired to inform clinical diagnostics and public health operations. Need for such methods has been highlighted by the recent Middle East respiratory syndrome and Ebola virus disease (EVD) epidemics, during which it became necessary to characterize novel viruses and to evaluate genetic drift, transmission chains, and zoonotic introductions.

To determine if nanopore sequencing can be used as an accelerated viral genome sequencing tool, we utilized a rapid cDNA/RNA–hybrid library preparation procedure to sequence cell cultures of Venezuelan equine encephalitis virus vaccine (VEEV) strain TC-83 or Ebola virus (EBOV) isolate Makona-C05 stock IRF0137. To evaluate nanopore sequencing for rapid, field-deployable pathogen characterization, we collected raw read data and statistics for VEEV and EBOV sequence runs on the MinION sequencing device (Oxford Nanopore Technologies, Oxford, UK). To determine the level of identification and accuracy of genome characterization over sequencing runtime, these

Author affiliations: US Army Edgewood Chemical Biological Center, Aberdeen Proving Ground, Maryland, USA (A. Kilianski, P.A. Roth, A.T. Liem, J.M. Hill, K.L. Willis, R.D. Rossmaier, A.V. Marinich, M.N. Maughan, M.A. Karavis, C.N. Rosenzweig); Defense Threat Reduction Agency, Fort Belvoir, Virginia, USA (K.L. Willis); National Institutes of Health, Fort Detrick, Frederick, Maryland, USA (J.H. Kuhn, A.N. Honko)

reads were then mapped to VEEV and EBOV genomes and to reference databases (RefSeq [http://www.ncbi.nlm.nih.gov/RefSeq/]). From the results of these analyses, we determined that the current and future versions of nanopore sequencing technology can be used to rapidly identify and characterize pathogens.

The Study

This approach for pathogen identification and characterization differs from the previously used methods on the MinION platform. Biased techniques, such as amplicon sequencing, have proven to be effective in complex sample backgrounds in which titers of the target pathogen might be low, but such approaches limit characterization to known pathogens and require additional viral genome amplification (*1–4*). Unbiased techniques that require viral genome amplification (*5*) or that have been optimized for bacterial genomes (*6,7*) require longer sample and library preparation times, but can detect low pathogen titers or create highly accurate genomic data. We sequenced unamplified poly(A)-tailed viral RNA using rapid cDNA library preparation coupled with real-time data analysis to determine its potential application for pathogen genomic characterization.

VEEV has a single-stranded, linear, poly(A)-tailed RNA genome. Thus, poly-dT primers can be used for cDNA production without further genomic RNA manipulation. The workflow to isolate the RNA and prepare it for sequencing (online Technical Appendix, http://wwwnc.cdc.gov/article/22/8/16-0270-Techapp1.pdf) took ≈3 hours from the initiation of sample processing to data acquisition on MinION (Figure, panel A). The sequencing of VEEV genomic RNA/cDNA hybrids attained in hours by using MinION revealed reads that mapped to the VEEV TC-83 genome within minutes by using the LAST (Computational Biology Research Consortium, Tokyo, Japan) multiple sequence alignment program (online Technical Appendix; Figure, panel B [*2,4,6*]). The coverage increased from 15–60 min from the 3′ end of the VEEV genome with reads aligning directionally from the 3′ to 5′ end of the VEEV genome (Figure, panel B). These alignment characteristics are indicative of the poly-dT priming strategy for poly(A)-tailed RNA.

To determine if the reads generated from VEEV TC-83 would align to the correct viral genome within a set

Figure. Use of unamplified RNA/cDNA--hybrid nanopore sequencing for genomic characterization of Venezuelan equine encephalitis virus (VEEV) TC-83. A) Sample preparation workflow for nanopore sequencing. First, viral RNA from BHK21 cell cultures of VEEV TC-83 was isolated, then single strand complimentary DNA (cDNA) was synthesized. The resulting RNA/cDNA hybrids were then prepared for nanopore sequencing and sequenced with data analysis occurring in real time. B) Genome organization and sequencing coverage over time of VEEV TC-83. VEEV is an alphavirus; its genome consists of a single strand of positive-sense RNA that can be translated into a polyprotein. Translation is critically dependent on the genomic 3′ poly(A)-tail. This tail can be used for reverse transcription priming by using poly-(dT) primers that anneal to it. Read data were aligned to VEEV TC-83 (accession number L01443) by using the multiple sequence alignment program LAST (Computational Biology Research Consortium, Tokyo, Japan [online Technical Appendix, wwwnc.cdc.gov/ article/22/8/16-0270-Techapp1.pdf). The coverage map shows the depth of genome coverage over 15, 30, 45, and 60 minutes of sequencing runtime, with the greatest depth observed at the 3′ end of the VEEV genome. Nsp, nonstructural protein; C, capsid; E, envelope.

of reference sequences, we used the viral genome reference sequences (http://www.ncbi.nlm.nih.gov/genomes/GenomesGroup.cgi?taxid=10239&opt=Virus), plus the VEEV TC-83 genome database (GenBank accession no. L01443). We then used LAST to align nanopore reads against this set of references (online Technical Appendix). These alignments were used to generate a top hit table and the associated read alignment statistics against each hit. VEEV TC-83 was the top hit based on LAST alignment versus virus RefSeq genome sequences; wild-type VEEV placed second (Table). VEEV TC-83 was also identified as the top hit when the 15- and 60–min sequencing datasets were compared with alphavirus genome sequences (online Technical Appendix) (Table), demonstrating accuracy and depth achieved in a short time. We also analyzed the VEEV TC-83 dataset using the cloud-based metagenomic detection platforms Pathosphere (*8*) and One Codex (www.onecodex.com), and found that the sample contained VEEV (online Technical Appendix).

Molecular epidemiology, including use of viral genomics, played a major role during the 2013–2016 EVD response, informing contact tracing, diagnostic operability, and public health measures (*9–11*). To determine if EBOV is amenable to the same rapid sequencing methodology that

was used for VEEV, unamplified negative-stranded RNA isolated from EBOV in Trizol (Thermofisher Scientific, http://www.thermofisher.com/us/en/home/brands/product-brand/trizol.html) was poly(A)-tailed, a single complementary strand of cDNA synthesized, and RNA/cDNA hybrids sequenced. The EBOV samples sequenced on MinION rapidly provided usable, accurate data, despite less raw data than the VEEV TC-83 dataset (137kbp for EBOV versus 2.4Mbp for VEEV at 60 min). Using 15-and 60-min time points and an identical alignment strategy to VEEV TC-83 above, we detected EBOV as the top hit within the sequencing dataset when compared to all virus RefSeq sequences (Table).

Despite success against the RefSeq database, the lack of depth within the dataset did not enable differentiation between the EBOV isolate sequenced here and the >1,500 EBOV draft genomes sequenced during the 2013–2016 outbreak (*10*,*12*,*13*), which indicates a limitation in this sequencing approach for negative-stranded RNA viruses. The poly(A)-tailing method was chosen because the reverse transcription primer adapters designed by Oxford Nanopore were developed to interact directly with the motor protein necessary for guiding DNA through the nanopores. This method greatly reduced preparation time and eliminated need for adaptor ligation reagents. This approach can

Table. Alignment statistics for detection of VEEV TC-83 and EBOV/Mak-C05 using unamplified RNA/cDNA-hybrid nanopore sequencing*

Virus samples and time points, min	Top hits (GenBank accession no.)	LAST score	Total bases mapped, %	Coverage, %	Average base depth	Per read accuracy, %
VEEV TC-83 (GenBank accession no. L01443)						
Viral genomes (RefSeq databases†)						
15	VEEV TC-83 (L01443)	138,321	5.54	76.14	50.94x	59–80
	VEEV WT (NC_001449.1)	789	0.05	18.59	1.76x	60–78
60	VEEV TC-83 (L01443)	419,153	17.17	78.54	153.16x	57–80
	VEEV WT (NC_001449.1)	1,182	0.08	32.12	1.82x	58–78
Alphavirus genomes						
15	VEEV TC-83 (L01443)	31,320	1.13	48.92	16.21x	67–69
	VEEV E541/73 (AF093102.1)	6,463	0.27	95.07	5.26x	62–73
	VEEV 71–180 (AF069903.1)	5,865	0.22	30.18	5.08x	65–73
60	VEEV TC-83 (L01443)	96,348	3.55	48.92	50.84x	62–74
	VEEV E541/73 (AF093102.1)	21,411	0.89	99.91	16.36x	61–73
	VEEV 71–180 (AF069903.1)	16,429	0.64	51.04	8.78x	65–73
EBOV/Mak-C05 (GenBank accession no. KX000400)						
Viral genomes (RefSeq databases)						
15	EBOV/Mak-137 (KX000400)	529	0.11	9.29	1.00x	68
	Bovine herpesvirus (NC_024303.1)	73	0.02	0.18	1.00x	67
60	EBOV/Mak-137 (KX000400)	2,371	0.53	22.23	2.09x	66–71
	Bovine herpesvirus (NC_024303.1)	239	0.04	0.27	1.58x	67–74

*VEEV, Venezuelan equine encephalitis virus; EBOV, Ebola virus; LAST (Computational Biology Research Consortium, Tokyo, Japan), multiple sequence alignment program.
†RefSeq, NCBI Reference Sequence Database (http://www.ncbi.nlm.nih.gov/RefSeq/).

be revisited for sequencing negative-strand RNA viruses (*2,5*). Despite this limitation, the RefSeq alignments and nearest neighbor calls were possible with limited data, demonstrating the potential power of long-read rapid sequencing on nanopore platforms.

Conclusions

The current Middle East respiratory syndrome, EVD, and Zika virus disease outbreaks illustrate the necessity for rapid characterization of pathogens for environmental detection, clinical evaluation, and epidemiologic investigation. To determine whether nanopore sequencing can fill this role in a fieldable platform, we tested an RNA/cDNA–hybrid sequencing approach on VEEV TC-83 (a positive-stranded RNA virus) and EBOV (a negative-stranded RNA virus) prepared from cell-culture supernatants. This method definitively identified VEEV TC-83 and differentiated it from wild-type VEEV in ≈3 hours, including only 15 min of data acquisition on MinION. VEEV TC-83 was also differentiated from other alphavirus genomes, facilitating strain-level identification of TC-83. EBOV was also identified rapidly by this approach, differentiating the virus in the sample analyzed here from available virus reference genomes. However, variant/isolate level characterization was not possible due to limited data generated from the RNA/cDNA–hybrid approach.

The method applied here is greatly accelerated compared to traditional next-generation sequencing library preparation, and was used with reagents and equipment suitable for austere conditions (e.g., little need for cold chain, steps not requiring PCR). This study confirmed the possibility of accurate RNA virus genome characterization from RNA/cDNA hybrids by using limited sample manipulation, albeit from relatively pure samples. If samples derived directly from clinical matrices (e.g., blood, saliva) were used, this method would probably not support the necessary depth to characterize virus genomes unless the pathogen titer within these samples was high. As the depth of sequence data obtained from nanopore sequencing approaches continues to improve (*14*) and other pore types (such as RNA-specific sequencing pores) are integrated into commercial products, these unamplified techniques can transition from the laboratory to the field for more complex analysis.

Utilization of nanopore sequencing in Western Africa (*2,3*) has demonstrated potential for its use, and newly developed methods like this RNA/cDNA–hybrid approach can be integrated into fieldable protocols. For the emerging Zika virus, insufficiently high virus titers in clinical samples usually necessitates virus culture before genomic sequencing (*15*). Genomic Zika virus isolate characterization efforts would greatly benefit from the approaches outlined here, especially regarding materials needed for genomic library preparation and the time reduction for strain-level identification (*15*). By preparing and sequencing RNA/cDNA hybrids, the sample-to-answer time for RNA sequencing is greatly reduced, providing pathogen identification and characterization rapidly to inform future decision making.

Dr. Kilianski is a National Research Council fellow in the BioSciences Division at Edgewood Chemical Biological Center. His research focuses on biosurveillance, emerging viral pathogens, and the identification and characterization of novel agents that threaten today's warfighter.

References

1. Kilianski A, Haas JL, Corriveau EJ, Liem AT, Willis KL, Kadavy DR, et al. Bacterial and viral identification and differentiation by amplicon sequencing on the MinION nanopore sequencer. Gigascience. 2015;4:12. http://dx.doi.org/10.1186/s13742-015-0051-z

2. Hoenen T, Groseth A, Rosenke K, Fischer RJ, Hoenen A, Judson SD, et al. Nanopore sequencing as a rapidly deployable Ebola outbreak tool. Emerg Infect Dis. 2016;22:331–4; Epub ahead of print.

3. Quick J, Loman NJ, Duraffour S, Simpson JT, Severi E, Cowley L, et al. Real-time, portable genome sequencing for Ebola surveillance. Nature. 2016;530:228–32. http://dx.doi.org/10.1038/nature16996

4. Wang J, Moore NE, Deng Y-M, Eccles DA, Hall RJ. MinION nanopore sequencing of an influenza genome. Front Microbiol. 2015;6:766. http://dx.doi.org/10.3389/fmicb.2015.00766

5. Greninger AL, Naccache SN, Federman S, Yu G, Mbala P, Bres V, et al. Rapid metagenomic identification of viral pathogens in clinical samples by real-time nanopore sequencing analysis. Genome Med. 2015;7:99. http://dx.doi.org/10.1186/s13073-015-0220-9

6. Quick J, Ashton P, Calus S, Chatt C, Gossain S, Hawker J, et al. Rapid draft sequencing and real-time nanopore sequencing in a hospital outbreak of *Salmonella.* Genome Biol. 2015;16:114. http://dx.doi.org/10.1186/s13059-015-0677-2

7. Ashton PM, Nair S, Dallman T, Rubino S, Rabsch W, Mwaigwisya S, et al. MinION nanopore sequencing identifies the position and structure of a bacterial antibiotic resistance island. Nat Biotechnol. 2014;33:296–300; Epub ahead of print. http://dx.doi.org/10.1038/nbt.3103

8. Kilianski A, Carcel P, Yao S, Roth P, Schulte J, Donarum GB, et al. Pathosphere.org: pathogen detection and characterization through a web-based, open source informatics platform. BMC Bioinformatics. 2015;16:416. http://dx.doi.org/10.1186/s12859-015-0840-5

9. Mate SE, Kugelman JR, Nyenswah TG, Ladner JT, Wiley MR, Cordier-Lassalle T, et al. Molecular evidence of sexual transmission of Ebola virus. N Engl J Med. 2015;373:2448–54. http://dx.doi.org/26465384

10. Park DJ, Dudas G, Wohl S, Goba A, Whitmer SLM, Andersen KG, et al. Ebola virus epidemiology, transmission, and evolution during seven months in Sierra Leone. Cell. 2015;161:1516–26. http://dx.doi.org/10.1016/j.cell.2015.06.007

11. Kugelman JR, Sanchez-Lockhart M, Andersen KG, Gire S, Park DJ, Sealfon R, et al. Evaluation of the potential impact of Ebola virus genomic drift on the efficacy of sequence-based candidate therapeutics. MBiol. 2015;6. http://dx.doi.org/10.1128/mBio.02227-14

12. Gire SK, Goba A, Andersen KG, Sealfon RSG, Park DJ, Kanneh L, et al. Genomic surveillance elucidates Ebola virus origin and transmission during the 2014 outbreak. Science. 2014;345:1369–72. http://dx.doi.org/10.1126/science.1259657

13. Carroll MW, Matthews DA, Hiscox JA, Elmore MJ, Pollakis G, Rambaut A, et al. Temporal and spatial analysis of the 2014–2015 Ebola virus outbreak in West Africa. Nature. 2015;524:97–101. http://dx.doi.org/10.1038/nature14594

14. Ip CLC, Loose M, Tyson JR, de Cesare M, Brown BL, Jain M, et al. MinION analysis and reference consortium: phase 1 data release and analysis. F1000Research. 2015;4:1075. http://dx.doi.org/10.12688/f1000research.7201.1 PMID: 26834992

15. Faria NR. Azevedo R do S da S, Kraemer MUG, Souza R, Cunha MS, Hill SC, et al. Zika virus in the Americas: early epidemiological and genetic findings. Science. 2016;352:345–9. http://dx.doi.org/10.1126/science.aaf5036

Address for correspondence: C. Nicole Rosenzweig, BioDefense Branch, BioSciences Division, Edgewood Chemical Biological Center, Aberdeen Proving Ground, MD 21010, USA; email: carolyn.n.rosenzweig.civ@mail.mil

SPOTLIGHT

Zika virus is spread to people through mosquito bites. Outbreaks of Zika have occurred in areas of Africa, Southeast Asia, the Pacific Islands, and the Americas. Because the *Aedes* species mosquitoes that spread Zika virus are found throughout the world, it is likely that outbreaks will spread to new countries. In December 2015, Puerto Rico reported its first confirmed Zika virus case. In May 2015, the Pan American Health Organization issued an alert regarding the first confirmed Zika virus infection in Brazil.

Learn more at **http://wwwnc.cdc.gov/eid/page/zika-spotlight**

Importation of Hybrid Human-Associated *Trypanosoma cruzi* Strains of Southern South American Origin, Colombia

Louisa A. Messenger, Juan David Ramirez, Martin S. Llewellyn, Felipe Guhl, Michael A. Miles

We report the characterization of *Trypanosoma cruzi* of southern South American origin among humans, domestic vectors, and peridomestic hosts in Colombia using high-resolution nuclear and mitochondrial genotyping. Expanding our understanding of the geographic range of lineage TcVI, which is associated with severe Chagas disease, will help clarify risk of human infection for improved disease control.

Chagas disease is the most common parasitic infection in Latin America, annually affecting ≈5–6 million persons and putting another 70 million at risk (*1*). The etiologic agent, *Trypanosoma cruzi*, displays remarkable genetic diversity, which is widely thought to contribute to the considerable biologic, epidemiologic, and clinical variation observed in regions where the disease is endemic (*2*). Seven discrete typing units (DTUs) are currently recognized (TcI–TcVI and TcBat) (*2*); TcV and TcVI are natural interlineage hybrids of TcII and TcIII (*3*). It is unknown whether these hybrids arose from multiple independent recombination events (*3*) or a single incidence of hybridization followed by clonal divergence (*4*). Molecular dating indicates these lineages evolved recently (<1 million years ago) (*3,4*), suggesting that genetic exchange may still be driving the emergence of novel recombinants (*3,4*).

Historically, most *T. cruzi* DTUs have had broadly distinct, but often overlapping, geographic and ecologic distributions (*2*). TcV and TcVI are largely confined to domestic transmission cycles and are sympatric with severe chronic and congenital human disease in southern South America (*2*). Increased sampling indicates that the geographic ranges of TcV and TcVI are more extensive than previously suggested. Putative domestic hybrid strains were identified recently as far north as Colombia (*5*); it is unclear whether these are bona fide TcV and TcVI isolates (suggesting long-range introduction) or progeny of a novel, independent, and local recombination event(s). Elucidation of the molecular epidemiology of TcV and TcVI has been

complicated by limited sample collections and difficulties distinguishing these genotypes from their parental DTUs (*6*) and each other (*7*). We undertook high-resolution nuclear and mitochondrial genotyping of hybrid clones from Colombia to resolve their putative status as novel recombinants and provide further insights into the evolutionary origin(s) of TcV and TcVI.

The Study

For analysis, we assembled a panel of 57 *T. cruzi* biologic clones from a range of representative hosts/vectors across South America: 24 uncharacterized clones from Colombia and 33 reference clones (Figure 1; online Technical Appendix 1 Table 1, http://wwwnc.cdc.gov/EID/article/22/8/15-0786-Techapp1.pdf). From 2002–2010, we isolated the uncharacterized clones from humans; triatomine vectors (*Panstrongylus geniculatus, Rhodnius prolixus*, and *Triatoma venosa* insects); and sylvatic mammalian hosts (*Dasypus* spp. armadillos) in 3 *T. cruzi*–endemic departments in northern Colombia.

We genotyped all isolates using nuclear housekeeping genes *GPX*, *GTP*, *Met-II*, *TcAPX,* and *TcMPX* (*6,8*) (online Technical Appendix 1 Table 2); 25 microsatellite loci (online Technical Appendix 1 Table 3) (*9*); and 10 mitochondrial gene fragments (*10*). Diploid multilocus sequence typing (MLST) data were analyzed by locus and concatenated according to their relative chromosomal positions in MLSTest (*11*); heterozygous variable sites were handled as average states. Gene haplotypes were inferred using PHASE version 2.1 (*12*). PCR products were cloned and sequenced to confirm ambiguous gene phases. We constructed maximum-likelihood and Bayesian phylogenies for nuclear haplotypic and concatenated mitochondrial data (*13*).

For microsatellite loci, we defined sample clustering using a neighbor-joining tree based on pairwise distances between multilocus genotypes (Figure 2) (*13*). We calculated DTU-level heterozygosity (Bonferroni-corrected) and evaluated genetic diversity using sample size–corrected allelic richness and private allele frequency per locus (Table). To examine TcV/TcVI allele inheritance, we classified genotypes at each locus as hybrid (TcII/TcIII) or nonhybrid (TcII/TcII or TcIII/TcIII) based on the presence or absence of specific parental alleles (online Technical Appendix 2, http://wwwnc.cdc.gov/EID/article/22/8/15-0786-Techapp2.xlsx).

Author affiliations: London School of Hygiene and Tropical Medicine, London, UK (L.A. Messenger, M.S. Llewellyn, M.A. Miles); Universidad del Rosario, Bogotá, Colombia (J.D. Ramirez); Universidad de Los Andes, Bogotá (F. Guhl)

All putative hybrids from Colombia were highly heterozygous and minimally diverse. They possessed TcII and TcIII alleles at an approximate 1:1 ratio and, compared with parental DTUs, they displayed fewer private alleles or single-nucleotide polymorphisms; these strains fulfilled all the expectations of progeny from a recent Mendelian hybridization event(s) (Table). Based on nuclear MLST and microsatellite data, all hybrids from Colombia were classified as TcVI, not novel recombinants.

Examination of TcII and TcIII alleles across 5 nuclear loci showed that hybrid haplotypes from Colombia were shared among other TcVI strains from the Southern Cone region of South America and showed negligible affinities to parental alleles from Colombia (online Technical Appendix 1 Figures 1, 2). Microsatellite profiles also supported this allopatric inheritance: only a minority of private parental alleles from Colombia were common to local TcVI hybrids. At mitochondrial loci, TcVI clones from Colombia were noticeably divergent from local TcIII maxicircle haplotypes and those observed in reference TcVI strains (Figure 2). Of note, 1 hybrid from Colombia (AACf2 cl11), which was unequivocally classified as TcVI by both types of nuclear loci, possessed a TcV-type mitochondria. All isolates in this study were biologic clones, ruling out mixed infections as a potential confounder.

Overall, our data support the hypothesis that 2 separate recombination events led to the formation of TcV and TcVI. These interlineage hybrids have distinct nuclear and mitochondrial MLST genotypes and related but independent microsatellite profiles, and most alleles that distinguish between hybrid DTUs (70.4% [38/54 alleles]) were also present in their corresponding parental strains. Interlineage differences (fixed at 84% [21/25 of loci]) between TcV and TcVI are not consistent with allelic sequence divergence (Meselson effect); for such divergence, a much higher frequency of private alleles, compared with parental genotypes, would be expected at rapidly evolving microsatellite loci.

TcVI clones from Colombia had more private microsatellite alleles per locus (0.86) than their southern counterparts (0.43), despite their unequivocal origin in the Southern Cone. This phenomenon could be attributable to de novo mutations or a founder effect with respect to the northerly introduction of TcVI. Support for the latter cause is evidenced by an overall reduction in genetic diversity among hybrids from Colombia compared with TcVI strains from the Southern Cone (allelic richness 1.87 vs. 2.46, respectively). However, we cannot discount some sampling bias because reference Southern Cone strains represented a much wider geographic range.

A novel observation among TcVI strains from Colombia was the presence of an anomalous TcV maxicircle.

Figure 1. Geographic distribution of TcII, TcIII, TcV, and TcVI *Trypanosoma cruzi* clones, South America, 2002–2010. A total of 57 *T. cruzi* biologic clones were assembled for analysis. Of these, 24 were isolated from humans; triatomine vectors (*Panstrongylus geniculatus, Rhodnius prolixus*, and *Triatoma venosa* insects); and sylvatic mammalian hosts (*Dasypus* spp. armadillos) in Antioquia, Boyaca, and Casanare Departments in northern Colombia. The remaining 33 were reference clones derived from a range of representative hosts and vectors across South America (online Technical Appendix 1 Table 1, http://wwwnc.cdc.gov/EID/article/22/8/15-0786-Techapp1.pdf). Dots indicate geographic strain origin of biologic clones; colors denote isolate discrete typing units.

This pattern of inheritance could reflect 1) recent mitochondrial introgression from TcV into TcVI, leaving undetectable signatures of nuclear hybridization by our markers or, possibly, none at all (*10,14*), or 2) potential backcrossing of TcVI into TcIII. Genetic exchange has not been described among hybrid DTUs, but it might be expected to be more permissive between closely related strains (*14*). We also isolated hybrid AACf2 cl11 from a dog. *T. cruzi* hybridization has been proposed to arise within mammalian cells (*14*), and mixed infections in such hosts are common. Alternatively, TcV and TcVI may have evolved from the beneficiaries of different alleles during a single hybridization event between heterozygous parents with mixed TcIII-type mitochondrial complements; although, to date, reported levels of mitochondrial heteroplasmy in *T. cruzi* are low (*10*).

DISPATCHES
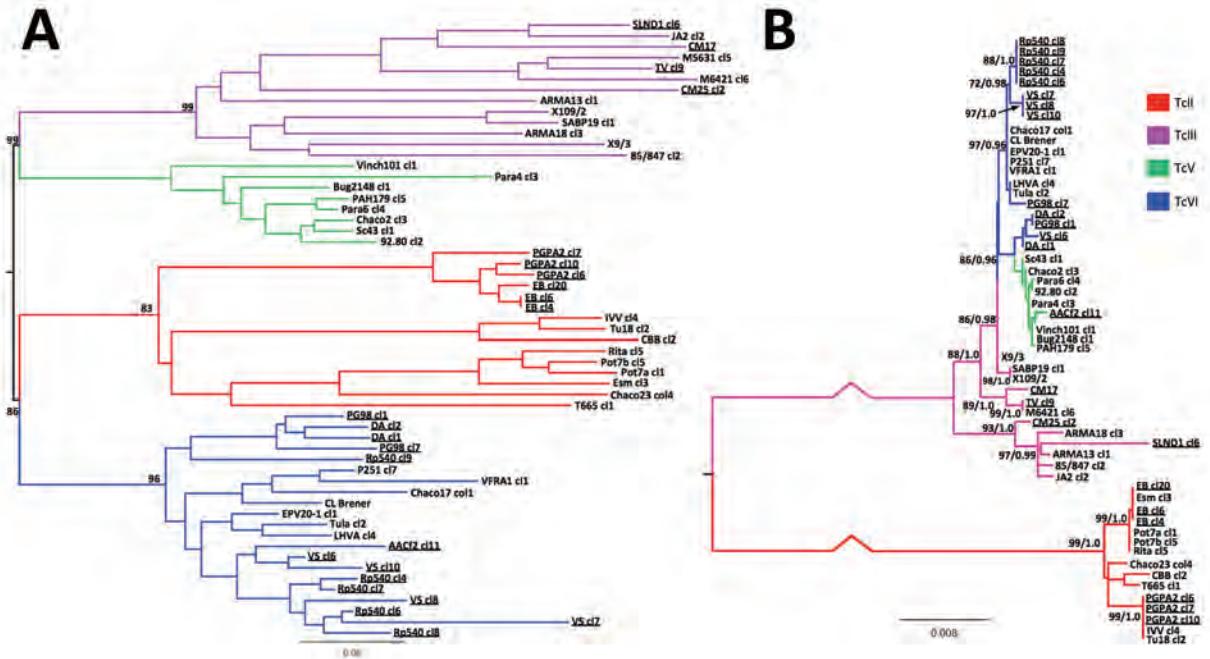
Figure 2. Phylogenetic trees showing relationships between *Trypanosoma cruzi* hybrids from Colombia and reference *T. cruzi* strains from across South America. A) Unrooted neighbor-joining tree based on pairwise distances between microsatellite loci. B) Maximum-likelihood tree from concatenated maxicircle sequences. Pairwise distance–based bootstrap values were calculated as the mean across 1,000 random diploid resamplings of the dataset; those >70% are shown for relevant nodes. A maximum-likelihood topology was constructed from concatenated maxicircle sequences for all clones. The most appropriate nucleotide substitution model was the general time reversible plus gamma distribution (9 substitution rate categories) based on the Akaike information criterion. Statistical support for major clades is given as equivalent bootstraps and posterior probabilities from consensus maximum-likelihood (1,000 pseudo-replicates) and Bayesian trees (based on the Hasegawa-Kishino-Yano plus gamma distribution model), respectively. Note that strain AACf2 cl11 is phylogenetically incongruent between nuclear and mitochondrial topologies. Branch colors indicate isolate discrete typing unit. Labels for clones from Colombia are underlined. Scale bars indicate genetic distance (A) and nucleotide substitutions per site (B).

Conclusions

Our understanding of the geographic and ecologic distribution of *T. cruzi* DTUs is changing because of parallel improvements in sampling strategies and genotyping techniques. Human Chagas disease in Colombia is currently associated with DTUs TcI, TcII (to a lesser extent), and oral outbreaks of TcIV (*5*). In this study, we isolated *T. cruzi* hybrids from 3 domestic triatomine vectors, a peridomestic dog, and congenital infections among local patients. Given that no reservoir hosts of TcV and TcVI have been described (*15*), the hybrids from Colombia are more likely the result of long-range anthropogenic introduction than local sylvatic invasion, especially considering the successful establishment of these DTUs among domestic infections in the Southern Cone. Further intensive sampling efforts in northern South America are warranted to elucidate the transmission cycle ecology of TcVI and to accurately assess the epidemiologic risk of

Table. Population genetic parameters for *Trypanosoma cruzi* discrete typing units, South America, 2002–2010*

Discrete typing unit	No. multilocus genotypes/no. isolates	Proportion shared alleles ± SD	No. polymorphic loci	Mean no. private alleles per locus ± SE	Mean A_r ± SE†	Mean expected/observed heterozygosity†	% Loci with deficit/excess heterozygosity‡
TcII	14/15 (5/6)	0.44 ± 0.23 (0.062 ± 0.053)	24 (15)	1.76 ± 0.20 (0.68 ± 0.14)	3.94 ± 0.29 (1.65 ± 0.12)	0.58/0.65 (0.91/0.58)	29.2/20.8 (40.0/0)
TcIII	13/13 (4/4)	0.48 ± 0.15 (0.30 ± 0.16)	22 (21)	2.35 ± 0.48 (1.76 ± 0.27)	4.26 ± 0.43 (2.35 ± 0.18)	0.45/0.70 (0.46/0.69)	4.5/27.3 (9.5/38.1)
TcV	8/8	0.15 ± 0.092	22	0.16 ± 0.07	2.38 ± 0.20	0.85/0.58	54.6/4.5
TcVI	21/21 (14/14)	0.24 ± 0.87 (0.22 ± 0.103)	21 (20)	0.43 ± 0.12 (0.86 ± 0.20)	2.46 ± 0.21 (1.87 ± 0.11)	0.60/0.49 (0.71/0.54)	41.7/16.7 (40.0/15.0)

*Values represent findings for reference clones derived from a range of representative hosts and vectors across South America and, in parentheses, clones isolated from humans, triatomine vectors, and sylvatic mammalian hosts in northern Colombia. Values were calculated from microsatellite data for 25 analyzed loci. Ar, allelic richness.
†Across all loci.
‡After sequential Bonferroni correction.

human Chagas disease associated with this low-diversity hybrid lineage.

Dr. Messenger is postdoctoral researcher at the London School of Hygiene and Tropical Medicine. Her research interests include population genetics, molecular epidemiology, clinical parasitology, and disease control.

References

1. World Health Organization. Chagas disease in Latin America: an epidemiological update based on 2010 estimates [cited 2015 Jun 2]. http://www.who.int/wer/2015/wer9006/en/
2. Messenger LA, Miles MA, Bern C. Between a bug and a hard place: *Trypanosoma cruzi* genetic diversity and the clinical outcomes of Chagas disease. Expert Rev Anti Infect Ther. 2015;13:995–1029. http://dx.doi.org/10.1586/14787210.2015.1056158
3. Lewis MD, Llewellyn MS, Yeo M, Acosta N, Gaunt MW, Miles MA. Recent, independent and anthropogenic origins of *Trypanosoma cruzi* hybrids. PLoS Negl Trop Dis. 2011;5:e1363. http://dx.doi.org/10.1371/journal.pntd.0001363
4. Flores-López CA, Machado CA. Analyses of 32 loci clarify phylogenetic relationships among *Trypanosoma cruzi* lineages and support a single hybridization prior to human contact. PLoS Negl Trop Dis. 2011;5:e1272. http://dx.doi.org/10.1371/journal.pntd.0001272
5. Guhl F, Ramírez JD. Retrospective molecular integrated epidemiology of Chagas disease in Colombia. Infect Genet Evol. 2013;20:148–54. http://dx.doi.org/10.1016/j.meegid.2013.08.028
6. Yeo M, Mauricio IL, Messenger LA, Lewis MD, Llewellyn MS, Acosta N, et al. Multilocus sequence typing (MLST) for lineage assignment and high resolution diversity studies in *Trypanosoma cruzi*. PLoS Negl Trop Dis. 2011;5:e1049. http://dx.doi.org/10.1371/journal.pntd.0001049
7. Venegas J, Rojas T, Díaz F, Miranda S, Jercic MI, González C, et al. Geographical structuring of *Trypanosoma cruzi* populations from Chilean *Triatoma infestans* triatomines and their genetic relationship with other Latino American counterparts. Ann Trop Med Parasitol. 2011;105:625–46. http://dx.doi.org/10.1179/2047773211Y.0000000002
8. Lauthier JJ, Tomasini N, Barnabé C, Rumi MM, D'Amato AM, Ragone PG, et al. Candidate targets for multilocus sequence typing of *Trypanosoma cruzi*: validation using parasite stocks from the Chaco region and a set of reference strains. Infect Genet Evol. 2012;12:350–8. http://dx.doi.org/10.1016/j.meegid.2011.12.008
9. Llewellyn MS, Miles MA, Carrasco HJ, Lewis MD, Yeo M, Vargas J, et al. Genome-scale multilocus microsatellite typing of *Trypanosoma cruzi* discrete typing unit I reveals phylogeograhic structure and specific genotypes linked to human infection. PLoS Pathog. 2009;5:e1000410. http://dx.doi.org/10.1371/journal.ppat.1000410
10. Messenger LA, Llewellyn MS, Bhattacharyya T, Franzén O, Lewis MD, Ramírez JD, et al. Multiple mitochondrial introgression events and heteroplasmy in *Trypanosoma cruzi* revealed by maxicircle MLST and next generation sequencing. PLoS Negl Trop Dis. 2012;6:e1584.
11. Tomasini N, Lauthier JJ, Llewellyn MS, Diosque P. MLSTest: novel software for multi-locus sequence data analysis in eukaryotic organisms. Infect Genet Evol. 2013;20:188–96. http://dx.doi.org/10.1016/j.meegid.2013.08.029
12. Stephens M, Smith N, Donnelly P. A new statistical method for haplotype reconstruction from population data. Am J Hum Genet. 2001;68:978–89. http://dx.doi.org/10.1086/319501
13. Messenger LA, Garcia L, Vanhove M, Huaranca C, Bustamante M, Torrico M, et al. Ecological host fitting of TcI in Bolivia: mosaic population structure, hybridization and a role for humans in Andean parasite dispersal. Mol Ecol. 2015;24:2406–22. http://dx.doi.org/10.1111/mec.13186
14. Messenger LA, Miles MA. Evidence and importance of genetic exchange among field populations of *Trypanosoma cruzi*. Acta Trop. 2015;151:150–5. http://dx.doi.org/10.1016/j.actatropica.2015.05.007
15. dos Santos Lima V, Xavier SC, Maldonado IF, Roque AL, Vicente AC, Jansen AM. Expanding the knowledge of the geographic distribution of *Trypanosoma cruzi* TcII and TcV/TcVI genotypes in the Brazilian Amazon. PLoS ONE. 2014;9:e116137. http://dx.doi.org/10.1371/journal.pone.0116137

Address for correspondence: Louisa A. Messenger, Department of Pathogen Molecular Biology, Faculty of Infectious and Tropical Diseases, London School of Hygiene and Tropical Medicine, London WC1E 7HT, UK; email: louisa.messenger@lshtm.ac.uk
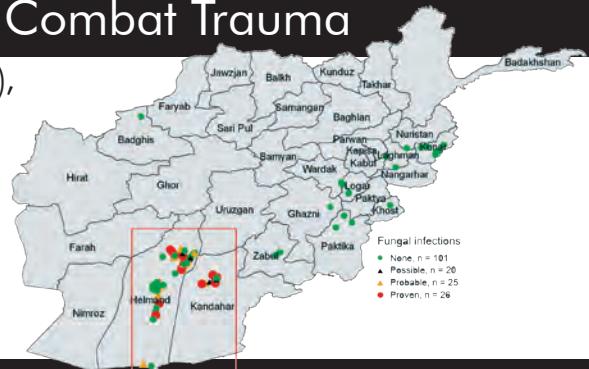
Lyssavirus in Indian Flying Foxes, Sri Lanka

Panduka S. Gunawardena,[1] Denise A. Marston,[1] Richard J. Ellis, Emma L. Wise, Anjana C. Karawita, Andrew C. Breed, Lorraine M. McElhinney, Nicholas Johnson, Ashley C. Banyard, Anthony R. Fooks

A novel lyssavirus was isolated from brains of Indian flying foxes (*Pteropus medius*) in Sri Lanka. Phylogenetic analysis of complete virus genome sequences, and geographic location and host species, provides strong evidence that this virus is a putative new lyssavirus species, designated as Gannoruwa bat lyssavirus.

There are 14 recognized species in the genus *Lyssavirus*: rabies virus (RABV), Lagos bat virus, Mokola virus (MOKV), Duvenhage virus, European bat lyssavirus types 1 and 2, Australian bat lyssavirus (ABLV), Aravan virus (ARAV), Khujand virus, Irkut virus, Shimoni bat virus, Bokeloh bat lyssavirus, West Caucasian bat virus, and Ikoma lyssavirus (IKOV) (*1*). RABV has a global distribution and is the dominant lyssavirus circulating in nonvolant (incapable of flight) mammals across Asia, including Sri Lanka. Bats are known reservoir hosts of all lyssaviruses except MOKV and IKOV. Discovery of new lyssaviruses in bats has stimulated research and surveillance efforts to identify additional members of this genus in bat populations (*2*).

Although lyssaviruses circulate in bats in Asia (*2*), RABV in bats in Asia remains unconfirmed. Irkut virus was the first bat lyssavirus identified in China (*3*). ARAV, Khujand virus, and West Caucasian bat virus have been isolated exclusively from insectivorous bats in Eurasia. Pathogen discovery in insectivorous and hematophagous bats is progressing. However, surveillance for lyssaviruses in fruit bats remains limited, particularly across Asia. Frugivorous bats in the Americas, which are distant genetically from bats of the family *Pteropodidae*, are independent reservoirs of RABV (*4*).

Although several regions contain fruit bats of the genus *Pteropus*, only pteropid bats in Australia have been identified as reservoirs for a lyssavirus species, ABLV, which has been isolated from all 4 *Pteropus* species in Australia. Moreover, ABLV has also been detected in at least 1 insectivorous bat (*Saccolaimus flaviventris*) (*5*). Although lyssavirus-specific antibodies have been detected in bats from several countries in Asia (*2*), the only lyssaviruses reportedly isolated from fruit bats in Asia have not been characterized (*6,7*).

In Sri Lanka, lyssavirus surveillance has focused on canine RABV as the primary public health concern. The Indian flying fox (*P. medius*, formerly known as *P. giganteus*), is a large frugivorous and nectarivorous bat that lives in forest, urban, and rural areas and is one of the most persecuted (e.g., cutting down of roosting trees and hunting) bats in southern Asia (*8*). These bats can fly long distances (≤150 km) to forage and have a wide distribution (India, China, Bangladesh, Bhutan, Myanmar, the Maldives, Nepal, Pakistan, and Sri Lanka). We report identification of a lyssavirus in Indian flying foxes in Sri Lanka.

The Study

Ethical clearance was obtained from the ethics committee of the Faculty of Veterinary Medicine and Animal Science at the University of Peradeniya (Peradeniya, Sri Lanka) and the Animal and Plant Health Agency (Addlestone, UK). Specimens were collected under permit no. WL/3/2/62/14 from the Sri Lanka Department of Wildlife Conservation.

During January 1, 2014–October 31, 2015, a total of 62 grounded bats were collected in an area inhabited by a long-established roost of ≈20,000 Indian flying foxes in Gannoruwa, Peradeniya, Sri Lanka (7°16′N, 80°36′E), which is located 600 m above sea level. Most bats were found dead. One bat (AK-42), which had clinical signs of illness, died shortly after capture (Table).

The first bat collected (AK-15) was a fresh carcass of a mature male that weighed 1.5 kg. A detailed necropsy showed that the animal had been healthy and had well-developed pectoral muscles. Except for a few multifocal hemorrhages in the lungs and mild, diffuse hyperemia and edema in the brain, gross pathologic findings were unremarkable. However, Negri bodies of various sizes were identified in the brain (Figure 1, panel A). Numerous aggregations of lyssavirus nucleocapsid antigen were observed in brain smears subjected to a direct fluorescence antibody test (dFAT) (Figure 1, panel B). Histopathologic examination of brain and spinal cord showed mild nonsuppurative lesions, leptomeningitis, and encephalomyelitis. Three additional dFAT-positive samples were identified from the 62

Author affiliations: University of Peradeniya, Peradeniya, Sri Lanka (P.S. Gunawardena, A.C. Karawita); Animal and Plant Health Agency, Addlestone, UK (D.A. Marston, R.J. Ellis, E.L. Wise, A.C. Breed, L.M. McElhinney, N. Johnson, A.C. Banyard, A.R. Fooks); University of Liverpool, Liverpool, UK (L. M. McElhinney, A.R. Fooks)

[1]These authors contributed equally to this article.

Table. Characteristics of 4 Indian flying foxes infected with Gannoruwa bat lyssavirus, Sri Lanka*

Original ID no.	APHA ID no.	Collection date	Location	Weight, g/age/sex	Clinical signs/condition	GenBank accession no.
AK-15	RV3266	2014 Sept 17	Peradeniya	1,500/mature/M	Dead at collection	KU244266
AK-40	RV3267	2015 May 8	Peradeniya	350/immature/F	Dead at collection	KU244267
AK-42	RV3268	2015 May 25	Peradeniya	500/immature/M	Cachectic, paresis, unable to fly, nystagmus, intermittent seizures (≈10 s), spontaneous vocalization, aggressiveness, biting, died shortly after capture	KU244268
AK-74	RV3269	2015 Sep 11	Gannoruwa	212.5/immature/F	Dead at collection	KU244269
*APHA, Animal and Plant Health Agency; ID, identification.						

bats tested (Table). Subsequent virus isolation and molecular analysis were conducted for these 4 brain samples.

Virus was isolated by using N2A cells (*9*). After 5 days of incubation, 3 of 4 samples were positive for virus. Two of the isolates, RV3267 and RV3269, were subsequently cultured in BHK cells. RNA was extracted by using TRIzol reagent (Invitrogen, Paisley, UK). A pan-lyssavirus reverse transcription PCR yielded a specific 606-bp amplicon for the virus nucleoprotein gene (*10*). Results for a differential real-time reverse transcription PCR with a TaqMan probe specific for RABV showed no amplification for the 4 RNA samples. A specific 145-bp amplicon was visualized after electrophoresis on a 2% agarose gel. Thus, pan-lyssavirus primers used in the real-time assay detected this virus, but the RABV-specific probe did not bind to the amplicon, which suggested presence of a non-RABV lyssavirus.

Complete genome sequences (GenBank accession nos. KU244266–9) were obtained from brain RNA samples by using next-generation sequencing according to previous methods (*11,12*). Phylogenetic analysis of complete genome sequences, including representatives of all lyssavirus species, showed that sequences of the new non-RABV lyssavirus clustered with each other and had a common ancestor with ABLV and RABV in phylogroup 1 (Figure 2). This novel virus was designated as Gannoruwa bat lyssavirus (GBLV).

Representative canine and golden palm civet RABV sequences from Sri Lanka were included in the dataset, but those sequences clustered with other RABVs, distinct from the GBLV sequence (nucleotide identity 78%). Nucleotide identity across the complete genome ranged from 61% (IKOV) to 76.5% (ABLV), which showed that GBLV is a member of the genus *Lyssavirus* but is distinct from viruses circulating in nonvolant mammals in Sri Lanka.

Conclusions

We report isolation of a novel non-RABV lyssavirus (GBLV) that is most closely related to RABV and ABLV. GBLV is pathogenic; it caused fatal disease in 4 Indian flying foxes, and clinical signs for these flying foxes were similar to those observed in other bat lyssavirus infections (Table). Diagnostic tests identified Negri bodies by staining with hematoxylin and eosin and lyssavirus antigens by dFAT in brain and spinal cord tissue (Figure 1). Molecular techniques identified lyssavirus nucleic acid, and full-genome analysis indicated that GBLV was divergent from known RABVs circulating in Sri Lanka (Figure 2).

Although rabies is prevalent in Sri Lanka, and a number of wildlife species have been confirmed as being rabid, most of the RABVs involved have not been genetically typed. Furthermore, over a 12-year period, only 1 bat tested for RABV was shown to be uninfected (*13*).

We report a novel non-RABV lyssavirus identified in Sri Lanka, which indicates that Indian flying foxes are a reservoir for lyssaviruses on the Indian subcontinent and nearby regions. Indian flying foxes are widespread in urban and rural areas and occasionally come in contact with humans and domestic dogs, which provides opportunities for virus spillover. Indian flying foxes are also reservoirs for
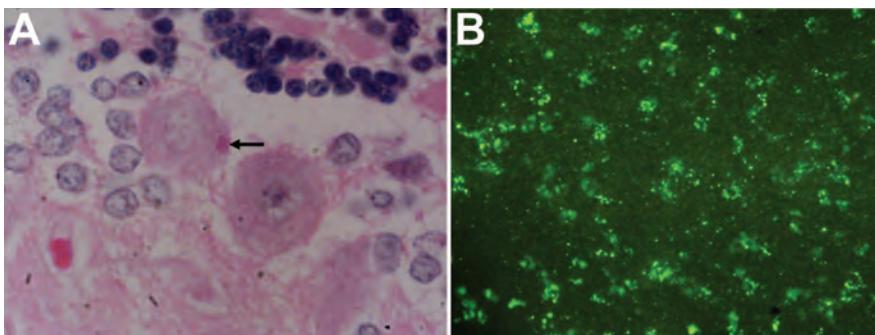
Figure 1. Negri bodies and lyssavirus antigens in brain tissue from an Indian flying fox, Sri Lanka. A) Degenerate Purkinje's cell with an eosinophilic, intracytoplasmic inclusion body and a Negri body (arrow). Hematoxylin and eosin stain, original magnification ×1,000. B) Fluorescence indicative of lyssavirus nucleoprotein in a brain smear subjected to a direct fluorescence antibody test with fluorescein isothiocyanate–conjugated monoclonal antibody. Original magnification ×100. A color version of this figure is available online (http://wwwnc.cdc.gov/EID/article/22/8/15-1986-F1.htm).
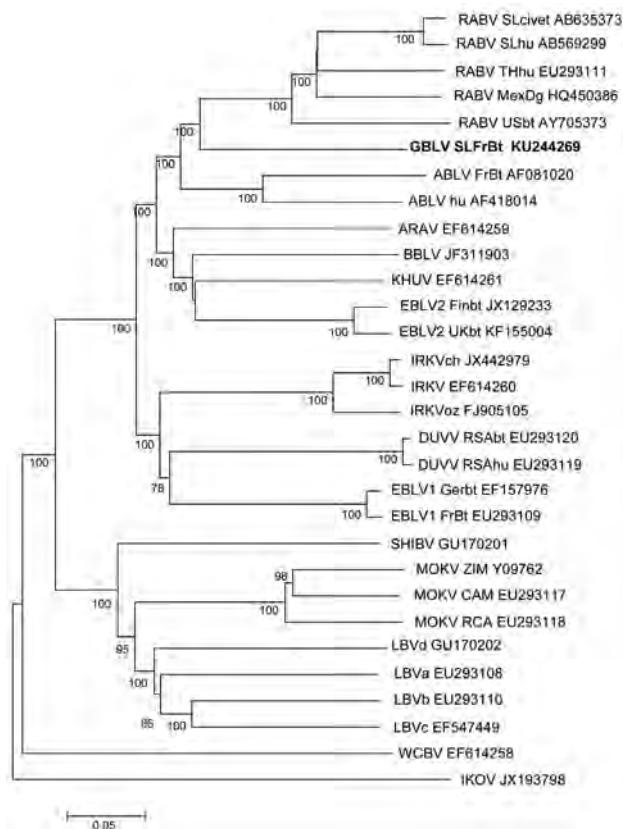
Figure 2. Phylogenetic relationships between representatives from all classified lyssaviruses and novel Gannoruwa bat lyssavirus (GBLV) on the basis of complete genome sequences. All 4 GBLV sequences form a monophyletic clade and are >99.9% identical across the genome; therefore, only 1 sequence (in bold) is shown. Relationships are shown as an unrooted phylogram, which was constructed by using the maximum-likelihood method and a general time reversible plus gamma distribution plus proportion of invariable sites model, and are identified by using the model test implemented in MEGA6 (http://www.megasoftware. net). Bootstrap values ≥70 (1,000 replicates) are indicated next to branches; sequences are listed with GenBank accession numbers. RABV, rabies virus; ABLV, Australian bat lyssavirus; ARAV, Aravan virus; BBLV, Bokeloh bat lyssavirus; KHUV, Khujand virus; EBLV, European bat lyssavirus; IRKV, Irkut virus; DUVV, Duvenhage virus; SHIBV, Shimoni bat virus; MOKV, Mokola virus; LBV, Lagos bat virus; WCBV, West Caucasian bat virus; IKOV, Ikoma lyssavirus. Scale bar indicates nucleotide substitutions per site.

Nipah virus in Bangladesh and India, where transmission to humans has resulted in outbreaks and human deaths. Other bat species, including insectivorous bats, might also be reservoir hosts for lyssaviruses in the study region. Thus, further surveillance is required to understand the role that bats play in the epidemiology of lyssaviruses in Asia.

Continued and extended surveillance of bats and other mammalian species is necessary to determine the distribution and prevalence of GBLV. Detailed phylogenetic analysis and monoclonal typing and antigenic mapping will help clarify the evolutionary relationship between GBLV and other lyssaviruses, in particular RABV and ABLV. In vitro and in vivo cross-neutralization and protection studies will elucidate properties of GBLV and provide information on protection from this virus by available prophylaxis.

Dr. Gunawardena is a senior lecturer and head of the Division of Veterinary Pathology, Faculty of Veterinary Medicine and Animal Science, University of Peradeniya, Peradeniya, Sri Lanka. His main research interests include disease etiology, pathogenesis, and control of neurologic diseases in animals.

References

1. Dietzgen R, Calisher, CH, Kurath, G, Kuzmin, IV, Rodriguez, LL, Stone, DM, et al. Rhabdoviridae. In: King A, Adams, MJ, Carstens, EB, Lefkowitz, EJ, editors. Virus taxonomy: classification and nomenclature of viruses. Ninth Report of the International Committee on Taxonomy of Viruses. San Diego: Elsevier; 2011. p. 654–81.
2. Banyard AC, Hayman D, Johnson N, McElhinney L, Fooks AR. Bats and lyssaviruses. Adv Virus Res. 2011;79:239–89. http://dx.doi.org/10.1016/B978-0-12-387040-7.00012-3
3. Wang L, Tang Q, Liang G. Rabies and rabies virus in wildlife in mainland China, 1990–2013. Int J Infect Dis. 2014;25:122–9. http://dx.doi.org/10.1016/j.ijid.2014.04.016
4. Escobar LE, Peterson AT, Favi M, Yung V, Medina-Vogel G. Bat-borne rabies in Latin America. Rev Inst Med Trop Sao Paulo. 2015; 57:63–72. http://dx.doi.org/10.1590/S0036-46652015000100009
5. Gould AR, Kattenbelt JA, Gumley SG, Lunt RA. Characterisation of an Australian bat lyssavirus variant isolated from an insectivorous bat. Virus Res. 2002;89:1–28. http://dx.doi.org/10.1016/S0168-1702(02)00056-4
6. Pal SR, Arora B, Chhuttani PN, Broor S, Choudhury S, Joshi RM, et al. Rabies virus infection of a flying fox bat, *Pteropus policephalus* in Chandigarh, northern India. Trop Geogr Med. 1980;32:265–7.
7. Smith PC, Lawhaswasdi K, Vick WE, Stanton JS. Isolation of rabies virus from fruit bats in Thailand. Nature. 1967;216:384. http://dx.doi.org/10.1038/216384a0
8. Molur S, Srinivasulu C, Bates P, Francis C. *Pteropus giganteus*. The IUCN red list of threatened species, 2008 [cited 2016 Jan 12]. http://dx.doi.org/10.2305/IUCN.UK.2008.RLTS.T18725A8511108.en

9. Webster WA, Casey GA. Virus isolation in neuroblastoma cell culture. In: Meslin F-X, Kaplan MM, Koprowski H, editors. Laboratory techniques in rabies. 4th ed. Geneva: World Health Organization; 1996. p. 96–104.
10. Heaton PR, Johnstone P, McElhinney LM, Cowley R, O'Sullivan E, Whitby JE. Heminested PCR assay for detection of six genotypes of rabies and rabies-related viruses. J Clin Microbiol. 1997;35:2762–6.
11. Marston DA, McElhinney LM, Ellis RJ, Horton DL, Wise EL, Leech SL, et al. Next generation sequencing of viral RNA genomes. BMC Genomics. 2013;14:444. http://dx.doi.org/10.1186/1471-2164-14-444
12. Atkinson B, Marston DA, Ellis RJ, Fooks AR, Hewson R. Complete genomic sequence of Issyk-Kul virus. Genome Announc. 2015;3:e00662–15. http://dx.doi.org/10.1128/genomeA.00662-15
13. Karunanayake D, Matsumoto T, Wimalaratne O, Nanayakkara S, Perera D, Nishizono A, et al. Twelve years of rabies surveillance in Sri Lanka, 1999–2010. PLoS Negl Trop Dis. 2014;8:e3205. http://dx.doi.org/10.1371/journal.pntd.0003205

Address for correspondence: Anthony R. Fooks, Wildlife Zoonoses and Vector-Borne Diseases Research Group, Animal and Plant Health Agency, Weybridge, New Haw, Addlestone, Surrey KT15 3NB, UK; email: tony.fooks@apha.gsi.gov.uk

May 2016: **Vectorborne Diseases**

Including:

- An Operational Framework for Insecticide Resistance Management Planning
- *Plasmodium falciparum* K76T *pfcrt* Gene Mutations and Parasite Population Structure, Haiti, 2006–2009
- Outbreak of Middle East Respiratory Syndrome at Tertiary Care Hospital, Jeddah, Saudi Arabia, 2014
- Differences in Genotype, Clinical Features, and Inflammatory Potential of *Borrelia burgdorferi* sensu stricto Strains from Europe and and the United States
- Expansion of Shiga Toxin–Producing *Escherichia coli* by Use of Bovine Antibiotic Growth Promoters
- Projecting Month of Birth for At-Risk Infants after Zika Virus Disease Outbreaks
- Genetic Characterization of Archived Bunyaviruses and Their Potential for Emergence in Australia
- *Plasmodium falciparum* In Vitro Resistance to Monodesethylamodiaquine, Dakar, Senegal, 2014
- Astrovirus MLB2, a New Gastroenteric Virus Associated with Meningitis and Disseminated Infection
- Spectrum of Viral Pathogens in Blood of Malaria-Free Ill Travelers Returning to Canada
- Expanded Geographic Distribution and Clinical Characteristics of *Ehrlichia ewingii* Infections, United States
- *Rickettsia parkeri* Rickettsiosis, Arizona, USA
- Acute Human Inkoo and Chatanga Virus Infections, Finland

http://wwwnc.cdc.gov/eid/articles/issue/22/05/table-of-contents
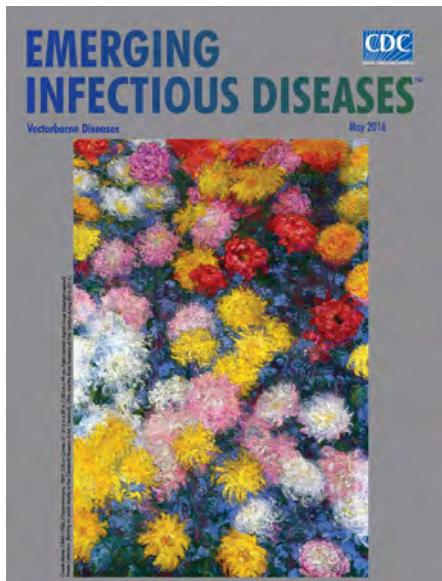
Survival and Growth of *Orientia tsutsugamushi* in Conventional Hemocultures

**Sabine Dittrich, Elizabeth Card,
Weerawat Phuklia, Williams E. Rudgard,
Joy Silousok, Phonelavanh Phoumin,
Latsaniphone Bouthasavong, Sarah Azarian,
Viengmon Davong, David A.B. Dance,
Manivanh Vongsouvath,
Rattanaphone Phetsouvanh, Paul N. Newton**

Orientia tsutsugamushi, which requires specialized facilities for culture, is a substantial cause of disease in Asia. We demonstrate that *O. tsutsugamushi* numbers increased for up to 5 days in conventional hemocultures. Performing such a culture step before molecular testing could increase the sensitivity of *O. tsutsugamushi* molecular diagnosis.

*O*rientia tsutsugamushi, the causative agent of scrub typhus, has long been a pathogen of major public health concern in the Asia-Pacific region (*1,2*). Reports from India, China, and Southeast Asia suggest that a substantial proportion of fevers and central nervous system infections are caused by this bacterium (*3,4*). The World Health Organization has called scrub typhus "probably one of the most underdiagnosed and underreported febrile illnesses requiring hospitalization in the region" (*5*). Furthermore, *Orientia*-infected patients are emerging outside the so-called tsutsugamushi triangle, from the Middle East, Africa, and South America (*6–8*). *Orientia* spp. DNA was recently detected in rodents from Asia, Europe, and Africa (*9*).

To improve patient management and clarify the epidemiology and pathogenicity of *O. tsutsugamushi*, physicians and researchers need sensitive and specific diagnostic tools (*10*). The current diagnostic reference standard is a 4-fold antibody rise between acute- and convalescent-phase serum samples; however, because results are determined retrospectively, they cannot influence patient management. *O. tsutsugamushi* is an intracellular pathogen, and traditionally its growth has been assumed to require specialized cell

Author affiliations: Mahosot Hospital, Vientiane, Laos (S. Dittrich, E. Card, W. Phuklia, W.E. Rudgard, J. Silousok, P. Phoumin, L. Bouthasavong, S. Azarian, V. Davong, D.A.B. Dance, M. Vongsouvath, R. Phetsouvanh, P.N. Newton); Centre for Tropical Medicine and Global Health–University of Oxford, Oxford, United Kingdom (S. Dittrich, D.A.B. Dance, R. Phetsouvanh, P.N. Newton); London School of Hygiene and Tropical Medicine, London, United Kingdom (W.E. Rudgard, S. Azarian, P.N. Newton)

culture at Biosafety Level 3, which is only available at a limited number of specialized centers. Therefore, molecular detection of *O. tsutsugamushi* in patients' EDTA-blood buffy coat has become the tool of choice for routine diagnosis and epidemiologic studies (*11,12*). In other pathogens with low bacterial loads, propagation of the organism before molecular amplification has increased target density and improved sensitivity of diagnostic tools such as quantitative PCR (qPCR) or isolation in cell cultures (*13*). In line with these findings, we hypothesized that *O. tsutsugamushi* can survive and potentially grow in conventional hemoculture media within the co-inoculated human host cells and that this capacity for growth could be used to improve diagnostic and analytical sensitivities.

The Study

We conducted this study at the Microbiology Laboratory, Mahosot Hospital, Vientiane, Laos, the only microbiology laboratory in Vientiane with a routine, accessible hemoculture service for sepsis diagnosis (*4,14*). Study patients provided written informed consent; ethical approval was granted by the Oxford Tropical Research Ethics Committee, University of Oxford (Oxford, UK), and the National Ethics Committee for Health Research, Laos.

One pair of hemocultures was incubated aerobically at 35°C–37°C for 7 days. As part of a weekly routine molecular diagnostic service, admission EDTA anti-coagulated buffy coats (≈200 μL) from febrile patients were collected to test for *O. tsutsugamushi* and *Rickettsia* spp. by qPCR (*11*). Serial dilutions of plasmids (pGEM-T Vector Systems; Promega, Southhampton, UK) and nontemplate controls were included in all runs as external controls; they always showed the appropriate result. During the 2014 rainy season (May–October), we collected consecutive hemoculture fluids after 24 h of incubation (0.5 mL/bottle; total 1 mL/patient; n = 760) (*15*). Each aliquot contained ≈0.1 mL blood or 0.01 mL buffy coat per mL media. If the EDTA buffy coat qPCR result (cycle quantitation value <40) was positive within the 7-day hemoculture incubation period (n = 11), the respective bottles were sampled at subsequent times so PCR positivity could be estimated (Table).

Hemoculture fluids were centrifuged (10 min at 15,900 × g) to pellet intracellular and extracellular bacteria, and DNA was extracted by using a method that removes inhibitors with benzyl alcohol (guanidine hydrochloride lysis/column extraction) (*16*). The same qPCR protocols were used for buffy coat (1 μL/reaction) and hemoculture fluids

Table. Results of testing HCF from 21 patients whose samples had tested positive for *Orientia tsutsugamushi* by qPCR on EDTA buffy coat after ≥1 days of incubation, Laos, 2014*

Patient code	Day of incubation of HCF†				
	1	2	3	5	7
29931	+ (Cq ≈34)				
30009	−				
30029	−				
30100	− (Cq ≈42)		−	+ (Cq ≈35)	+ (Cq ≈38)
30104	+ (Cq ≈38)				
30316	+ (Cq ≈37)		−		+ (Cq ≈38)
30329		+ (Cq≈39)		+ (Cq ≈35)	+ (Cq ≈37)
30379	+ (Cq ≈34)				
30416	+ (Cq ≈35)		+ (Cq≈40)	+ (Cq ≈40)	
30442	−				−
30446	+ (Cq ≈37)				−
30581	−		+ (Cq≈32)	+ (Cq ≈30)	+ (Cq ≈34)
30600	−				+ (Cq ≈32)
30862	+ (Cq ≈33)				
30874	+ (Cq ≈30)				
30920					
31120	+ (Cq ≈31)				
31199	+ (Cq ≈30)				
31209	+ (Cq ≈31)				+ (Cq ≈21)
31230	+ (Cq ≈31)			+ (Cq ≈31)	+ (Cq ≈32)
31231	+ (Cq ≈32)			+ (Cq ≈30)	+ (Cq ≈37)

*For each patient, 2 hemocultures bottles were used (Pharmaceutical Factory No. 2, Vientiane, Laos): 1.7 g tryptic hydrolysate casein, 0.3 g soy peptone, 0.5 g sodium chloride, 0.25 g potassium phosphate, 0.25 g dextrose, 0.025 g sodium polyanetholsulfonate/100 mL) were inoculated with blood in a 1:10 dilution. Cq, cycle quantitation; HCF, hemoculture fluids; qPCR, quantitative PCR; −, sample available/negative; +, sample available/positive; blank cell, no sample available.
†Cq values are noted in parentheses to illustrate the increase in template.

(7 μL/reaction), with bovine serum albumin (40 μg/reaction) added in the latter (*11,13*). We estimated bacterial loads using plasmid standard curves and calculated bacterial multiplication factor by dividing bacterial numbers, at follow-up days, by the number in the first sample.

Of the 760 buffy coat samples, 21 were positive for *O. tsutsugamushi* by qPCR; therefore, to estimate survival and growth, we collected aliquots of hemoculture fluids during days 1–7 (n = 11). During that period, 100/760 (13%) hemocultures were positive for other organisms; however, none of the known *O. tsutsugamushi*–infected patients were co-infected with an alternative pathogen. In addition, hemoculture fluids from the first 277 patients with buffy coats negative for *O. tsutsugamushi* by qPCR, underwent *O. tsutsugamushi* qPCR testing to explore whether using hemoculture fluids as an additional diagnostic sample could improve molecular detection of *O. tsutsugamushi*.

For nearly all (20/21) of the *O. tsutsugamushi*–positive patients, ≥1 hemoculture samples were available. Of these, ≥1 hemoculture sample from 17/20 (85%) patients tested positive (Table). Despite the initial 1:10 dilution of blood in hemoculture fluid, 66% (14/21) of patients with buffy coat–positive qPCR results also had a positive result in the first hemoculture fluid sample (Table). Due to logistical constraints, only 11/21 patients could be tested at multiple time points; samples from 7/11 (63%) showed a marked increase in *O. tsutsugamushi* density between day 1 and day 7 (Figure). The increase ranged from 2-fold to 210-fold (median

3.25-fold), and data suggest that *Orientia* bacterial density peaked in the first 5 days and subsequently declined (Figure).

During the same period, 10/760 patients were diagnosed with *Rickettsia* spp. infection by blood culture qPCR. In contrast to the positive results for *O. tsutsugamushi*, all samples were negative by *Rickettsia* spp. hemoculture fluid qPCR, regardless of sampling day.

Of samples from the 277 patients tested for *O. tsutsugamushi* in hemoculture fluid incubated for 24 h, those from an additional 3 patients, negative by qPCR at admission, were positive (cycle quantitation value <40). In this pilot study, combining buffy coat and hemoculture fluid testing, the number of *O. tsutsugamushi*–positive patients increased by 3 (27%). Results are consistent with our hypothesis that qPCR on incubated hemoculture fluid alone or in combination with admission buffy coat testing could improve the sensitivity of molecular diagnosis of *O. tsutsugamushi* infection.

Conclusions

Our findings suggest that *O. tsutsugamushi* remains viable and growing in hemoculture, presumably in human leukocytes. This observation opens up new possibilities for detecting *O. tsutsugamushi* and other intracellular organisms, albeit seemingly not *Rickettsia* spp. With the discovery of *Orientia* spp. outside the tsutsugamushi triangle, improved tools are needed to aid the timely identification of infections in disease-endemic communities and among returning travelers to facilitate appropriate

Figure. Growth curve of *Orientia tsutsugamushi* in hemoculture bottles from individual patients, Ventiane, Laos, 2014. The increase in bacterial numbers is represented as bacterial multiplication factor and plotted on a log$_2$ axis. Patient codes in key match those listed in the Table.

and assess multiplication rates of host cells and pathogens in these fluids. Such studies can provide evidence for the optimal system and number of incubation days that would maximize the effects for the *O. tsutsugamushi* diagnostic. These findings could also affect the detection of other underdiagnosed intracellular pathogens that scientists assume cannot be detected in hemoculture fluids.

Dr. Dittrich is a molecular microbiologist with a specific interest in infectious disease diagnostics. This work was carried out while she was working for the University of Oxford based in Laos, where her main focus was to understand the causative agents of disease and improve diagnostic tools for their detection. She currently works as a senior scientific officer in the Acute Febrile Illness Program at the Foundation of Innovative New Diagnostics (FIND) in Geneva, Switzerland.

References

1. Kelly DJ, Fuerst PA, Ching WM, Richards AL. Scrub typhus: the geographic distribution of phenotypic and genotypic variants of *Orientia tsutsugamushi*. Clin Infect Dis. 2009;48(Suppl 3): S203–30. http://dx.doi.org/10.1086/596576
2. Sayen JJ, Pond HS, Forrester JS, Wood FC. Scrub typhus in Assam and Burma; a clinical study of 616 cases. Medicine (Baltimore). 1946;25:155–214. http://dx.doi.org/10.1097/00005792-194605000-00003
3. Varghese GM, Janardhanan J, Mahajan SK, Tariang D, Trowbridge P, Prakash JA, et al. Molecular epidemiology and genetic diversity of *Orientia tsutsugamushi* from patients with scrub typhus in 3 regions of India. Emerg Infect Dis. 2015;21:64–9. http://dx.doi.org/10.3201/eid2101.140580
4. Dittrich S, Rattanavong S, Lee SJ, Panyanivong P, Craig SB, Tulsiani SM, et al. Orientia, rickettsia, and leptospira pathogens as causes of CNS infections in Laos: a prospective study. Lancet Glob Health. 2015;3:e104–12. http://dx.doi.org/10.1016/S2214-109X(14)70289-X
5. Paris DH, Shelite TR, Day NP, Walker DH. Unresolved problems related to scrub typhus: a seriously neglected life-threatening disease. Am J Trop Med Hyg. 2013;89:301–7. http://dx.doi.org/10.4269/ajtmh.13-0064
6. Balcells ME, Rabagliati R, Garcia P, Poggi H, Oddo D, Concha M, et al. Endemic scrub typhus-like illness, Chile. Emerg Infect Dis. 2011;17:1659–63. http://dx.doi.org/10.3201/eid1709.100960
7. Izzard L, Fuller A, Blacksell SD, Paris DH, Richards AL, Aukkanit N, et al. Isolation of a novel *Orientia* species (*O. chuto* sp. nov.) from a patient infected in Dubai. J Clin Microbiol. 2010;48:4404–9. http://dx.doi.org/10.1128/JCM.01526-10
8. Ghorbani RP, Ghorbani AJ, Jain MK, Walker DH. A case of scrub typhus probably acquired in Africa. Clin Infect Dis. 1997;25:1473–4. http://dx.doi.org/10.1086/516990

treatment (*4*). In areas without sophisticated laboratory facilities, the combination of hemoculture amplification and direct diagnostic (e.g., antigen capture) has been proposed for simplified *Salmonella enterica* serovar Typhi diagnosis and resistance molecular screening (*13*). Similarly, innovative approaches to identify *O. tsutsugamushi* infections after ≥1 days could be developed. Because *O. tsutsugamushi* is categorized as a Hazard Group 3 pathogen, sampling and processing of hemocultures from patients with suspected scrub typhus should be conducted with appropriate biosafety precautions.

Furthermore, the possibility of using hemoculture as a simple transport tool for samples from remote areas should be investigated. Clinical isolates from remote areas can also show *O. tsutsugamushi* diversity, which can guide the development of diagnostic tests and vaccines (*3*).

The underlying mechanisms and the reason *O. tsutsugamushi*, but not *Rickettsia* spp., grows in hemoculture fluid are unclear. We compared the diagnostic possibilities of preincubating blood samples in hemoculture fluid before qPCR with using qPCR on buffy coat samples to investigate its advantage as a diagnostic tool. Further investigations are needed to confirm our findings, explore whether *O. tsutsugamushi* really multiplies in hemoculture fluids,

9. Cosson JF, Galan M, Bard E, Razzauti M, Bernard M, Morand S, et al. Detection of Orientia *sp.* DNA in rodents from Asia, West Africa and Europe. Parasit Vectors. 2015;8:172. http://dx.doi.org/10.1186/s13071-015-0784-7
10. La Scola B, Raoult D. Laboratory diagnosis of rickettsioses: current approaches to diagnosis of old and new rickettsial diseases. J Clin Microbiol. 1997;35:2715–27.
11. Mayxay M, Castonguay-Vanier J, Chansamouth V, Dubot-Pérès A, Paris DH, Phetsouvanh R, et al. Causes of non-malarial fever in Laos: a prospective study. Lancet Glob Health. 2013;1:e46–54. http://dx.doi.org/10.1016/S2214-109X(13)70008-1
12. Paris DH, Blacksell SD, Nawtaisong P, Jenjaroen K, Teeraratkul A, Chierakul W, et al. Diagnostic accuracy of a loop-mediated isothermal PCR assay for detection of *Orientia tsutsugamushi* during acute scrub typhus infection. PLoS Negl Trop Dis. 2011;5:e1307. http://dx.doi.org/10.1371/journal.pntd.0001307
13. Nic Fhogartaigh C, Dance DA, Davong V, Tann P, Phetsouvanh R, Turner P, et al. A novel technique for detecting antibiotic-resistant typhoid from rapid diagnostic tests. J Clin Microbiol. 2015; 53:1758–60. http://dx.doi.org/10.1128/JCM.00531-15
14. Phetsouvanh R, Phongmany S, Soukaloun D, Rasachak B, Soukhaseum V, Soukhaseum S, et al. Causes of community-acquired bacteremia and patterns of antimicrobial resistance in Vientiane, Laos. Am J Trop Med Hyg. 2006;75:978–85.
15. Dittrich S, Rudgard WE, Woods KL, Silisouk J, Phuklia W, Davong V, et al. The utility of blood culture fluid for the molecular diagnosis of *Leptospira*: a prospective evaluation. Am J Trop Med Hyg. 2016;94:736–40. http://dx.doi.org/10.4269/ajtmh.15-0674
16. Villumsen S, Pedersen R, Krogfelt KA, Jensen JS. Expanding the diagnostic use of PCR in leptospirosis: improved method for DNA extraction from blood cultures. PLoS ONE. 2010;5:e12095. http://dx.doi.org/10.1371/journal.pone.0012095

Address for correspondence: Sabine Dittrich, Foundation for Innovative New Diagnostics (FIND), Geneva, Switzerland; email: sabine-dittrich@gmx.de

July 2016: **Zoonoses**
Including:

- Turtle-Associated Salmonellosis, United States, 2006–2014 S.
- Pregnancy, Labor, and Delivery after Ebola Virus Disease and Implications for Infection Control in Obstetric Services, United States, 2015
- Response to Middle East Respiratory Syndrome Coronavirus, Abu Dhabi, United Arab Emirates, 2013–2014
- Current Guidelines, Common Clinical Pitfalls, and Future Directions for Laboratory Diagnosis of Lyme Disease, United
- Two Linked Enteroinvasive *Escherichia coli* Outbreaks, Nottingham, United Kingdom, June 2014
- Comparing Disease Characteristics of Sporadic and Outbreak-Associated Foodborne Illnesses, United States, 2004–2011
- African Swine Fever Epidemic, Poland, 2014–2015
- Restaurant Cooking Trends and Increased Risk for *Campylobacter* Infection
- Heatwave-Associated Vibriosis, Sweden and Finland,
- A Literature Review of Zika Virus
- High Incidence of Chikungunya Virus and Frequency of Viremic Blood Donations during Epidemic, Puerto Rico, USA,
- *Tropheryma whipplei* as a Cause of Epidemic Fever, Senegal, 2010–2012
- Outbreak of *Vibrio parahaemolyticus* Sequence Type 120, Peru, 2009
- Clinical Manifestations of Senecavirus A Infection in Neonatal Pigs, Brazil, 2015
- Infection with Possible Novel Parapoxvirus in Horse, Finland, 2013
- Vesicular Disease in 9-Week-Old Pigs Experimentally Infected with Senecavirus
- Hepatitis E Virus in Dromedaries, North and East Africa, United Arab Emirates and Pakistan, 1983–2015

http://wwwnc.cdc.gov/eid/articles/issue/22/07/table-of-contents

Multilocus Sequence Typing Tool
for *Cyclospora cayetanensis*

Yaqiong Guo, Dawn M. Roellig, Na Li,
Kevin Tang, Michael Frace, Ynes Ortega,
Michael J. Arrowood, Yaoyu Feng,
Yvonne Qvarnstrom, Lin Wang, Delynn M. Moss,
Longxian Zhang, Lihua Xiao

Because the lack of typing tools for *Cyclospora cayetanensis* has hampered outbreak investigations, we sequenced its genome and developed a genotyping tool. We observed 2 to 10 geographically segregated sequence types at each of 5 selected loci. This new tool could be useful for case linkage and infection/contamination source tracking.

*C*yclospora cayetanensis* is an emerging parasitic pathogen responsible for numerous foodborne outbreaks of cyclosporiasis in North America, primarily associated with imported fresh produce from cyclosporiasis-endemic areas (*1*). The lack of genotyping tools has hampered case linkage and infection/contamination source tracking (*2*). In this study, we developed a multilocus sequence typing (MLST) tool to help with identification of this protozoan.

The Study

To identify potential genotyping markers, we sequenced the genome of 1 *C. cayetanensis* isolate (CHN_HEN01) from Henan, China (*3*), and searched for microsatellite and minisatellite sequences among the first 40 of 4,811 assembled contigs by using Tandem Repeat Finder software (http://tandem.bu.edu/trf/trf.html). We designed primers for nested PCR analysis of the targets based on flanking nucleotide sequences.

The total volume of PCR mixture was 50 mL, which contained 1 mL of DNA (for primary PCR) or 2 mL of the primary PCR product, 250 nmol/L primers, 3 mmol/L magnesium chloride, 200 µmol/L deoxynucleotide triphosphates, 1× GeneAmp PCR buffer (Applied Biosystems, Foster City, CA, USA), and 1.5 U of Taq polymerase (Promega, Madison, WI, USA). The amplification consisted of

Author affiliations: Centers for Disease Control and Prevention, Atlanta, Georgia, USA (Y. Guo, D.M. Roellig, K. Tang, M. Frace, M.J. Arrowood, Y. Qvarnstrom, D.M. Moss, L. Xiao); East China University of Science and Technology, Shanghai, China (Y. Guo, N. Li, Y. Feng, L. Wang); University of Georgia, Griffin, Georgia, USA (Y. Ortega); Henan Agricultural University, Zhengzhou, China (L. Zhang)

an initial denaturation at 94°C for 5 min; 35 cycles at 94°C for 45 s; a specified annealing temperature (Table; online Technical Appendix Table 1, http://wwwnc.cdc.gov/EID/article/22/8/15-1696-Techapp1.pdf) for 45 s and 72°C for 1 min; and a final extension at 72°C for 7 min. The secondary PCR products were sequenced in both directions on an ABI 3130 Genetic Analyzer (Applied Biosystems).

The sequences obtained from each locus were aligned by using ClustalX version 2.1 (http://www.clustal.org). A neighbor-joining analysis was used to assess the genetic relatedness of various *C. cayetanensis* sequences for each locus and concatenated sequences of 5 loci. Unique sequences generated from the 5 MLST loci were deposited in GenBank (accession nos. KP723491–KP723518).

Altogether, 15 loci were chosen for evaluations (Table; online Technical Appendix Table 1). These loci included 13 microsatellite and 2 minisatellite loci. Six specimens from China and Peru were used in the initial evaluation of the PCR primers designed. Five microsatellite loci (CYC3, CYC13, CYC15, CYC21, and CYC22) exhibiting high PCR amplification efficiency and nucleotide sequence polymorphism in the initial evaluation were chosen for further evaluations of the nature of nucleotide sequence polymorphism by using a total of 64 *C. cayetanensis* specimens from China (n = 26), Nepal (n = 3), Indonesia (n = 1), Guatemala (n = 2), Peru (n = 8), Spain (n = 1), and the United States (n = 23) (online Technical Appendix Table 2). Of these, 63 specimens were amplified by PCR at the CYC3 locus, 61 at the CYC13 locus, 63 at the CYC15 locus, 62 at the CYC21 locus, and 64 at the CYC21 locus (Table). However, 1–11 specimens did not produce readable sequences at each locus.

Nucleotide sequence alignment led to the identification of 4 sequence types at locus CYC3, 10 at locus CYC13, 2 at locus CYC15, 8 at locus CYC21, and 4 at locus CYC22 (online Technical Appendix Table 2). As expected, all 5 loci showed differences in the number of microsatellite repeats. In addition, single nucleotide polymorphisms were present at all loci (online Technical Appendix Figures 1–5). Sequences from CYC3, CYC13, CYC21, and CYC22 formed 2–3 major groups in neighbor-joining trees (Figure 1). Clear geographic clustering of sequences was observed at most loci, with specimens from China largely clustering together and US outbreak specimens often clustering with specimens from Peru (Figure 1). Of the 9 specimens from a 2013 Texas outbreak, 1 had a different sequence from the remaining specimens at CYC3, 2 had different sequences

Table. Primer sequences of microsatellite loci used in multilocus sequence analysis of *Cyclospora cayetanensis*

Locus	Contig no.	Targeted repeat*	Primer sequence, 5′ → 3′†	Annealing temp, °C	Expected size, bp	Amplification efficiency, no. positive/no. analyzed
CYC3	00003	$TGTA_{63}$ and $TATA_{23}$	F1: GAAGATGAAGCGTTGGTACG; R1: TACCGCTGCTGGAGTGCAT; F2: TTGTGCATGGCACCCAATGC; R2: CCAGACAGTAGTTCGTGTCTT	55	598	4/4
CYC13	00008	GAT_{15}	F1: TTGGAGCAGGACGAGTTTCG; R1: ATGGAAGCGGCTATGAAATTGG; F2: CCTCGGAGTCCTCTGAGTG; R2: AGCCGTCGCAGTGTGTAGCA	58	595	4/4
CYC15	00009	TGC_{11}	F1: AGTAGCTACGTGCCAAGACGA; R1: TCGTTCTATCTGACCATAGTAGTG; F2: CGCTGTGCAAGAGGCGATCTA; R2: AAGCACTGCAGGGTCCGTAAC	58	609	4/4
CYC21	00036	AT_{31}	F1: TAGTGGCGACTGCGACATG; R1: GCACCTTGCTGATGAGGCA; F2: CTA AGGCTGTCTTGAGCGG; R2: CGCCCACATGCTTCGTATAC	55	471	4/4
CYC22	00037	AC_{20}	F1: CACTATGCCGTGTGACACGT; R1: GTAGATTTGCAAGAACTCATGCTA; F2: ATAGTATTCAGGCGCAAACTAAG; R2: GAGGCTTTCCAAAGGTCTAGTT	55	512	4/4

*Tandem repeat identified in the sequence from whole genome sequencing.
†Six *C. cayetanensis* specimens were used in initial evaluation of PCR primers: specimens 22231, 22234, 22238, and 28709 were used to evaluate PCR primers from loci CYC3, whereas specimens 22231, 22234, 24550, and 24552 were used for PCR primers from the remaining loci.

from the remaining specimens at CYC13 and CYC21, and at CYC22, PCR products from 7 specimens produced unreadable sequences (online Technical Appendix Table 2).

A total of 34 specimens had complete sequence data at 5 loci, forming 25 MLST types (online Technical Appendix Table 2). Most of the MLST types had only 1 specimen, except for 4 MLST types (MS3, MS15, MS16, and MS17), which had 3 or 4 specimens (online Technical Appendix Table 2). A neighbor-joining analysis of the concatenated sequences of 2,317 bp showed clear geographic clustering of MLST types (Figure 2). Most specimens from China clustered together in 1 major group, whereas specimens from outbreaks in the United States formed 2 other groups with specimens from Peru. The specimen from Spain appeared to be distinct.
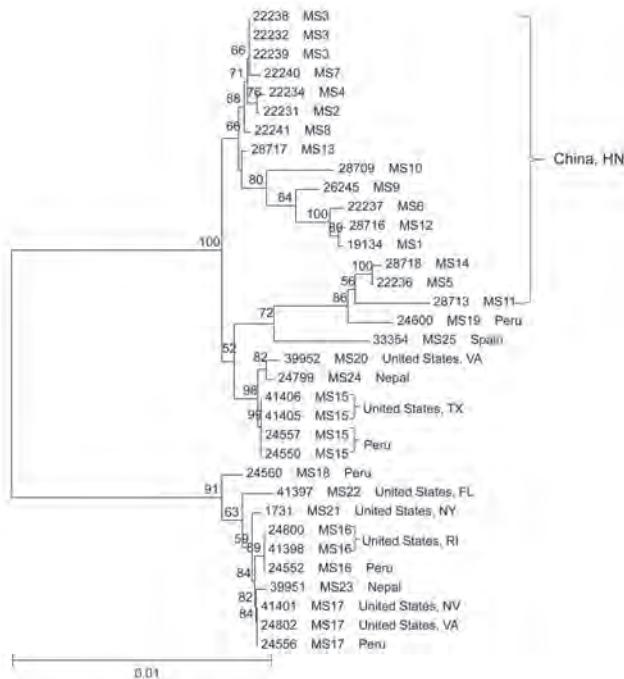
Conclusions

In this study, we sequenced the genome of *C. cayetanensis* protozoa and developed a genotyping tool. Noticeable geographic clustering was observed at some of the loci, with specimens from China forming 1–2 groups at each of these loci. In contrast, the US outbreak specimens mostly grouped together with Peru specimens, probably because of the imported nature of pathogens from Central and South America. The geographic clustering pattern of specimens from the same country at 1 locus does not conform to patterns at other loci, probably because of the occurrence of genetic recombination among parasites in a particular area. Therefore, the use of a single genetic marker is probably not useful in geographic tracking of infection sources of this species.

Data generated from this study have demonstrated the high resolution of the MLST tool. Although genotyping

resulted in complete data at all 5 loci for only 34 of the 64 specimens, 25 MLST types were detected. The failure in obtaining informative sequences from some amplicons was mainly attributable to the presence of PCR products with different repeat lengths, leading to overlapped signals following the tandem repeat region. This highlights some potential challenges in investigations of cyclosporiasis outbreaks using genotyping tools. Only 2 of the 9 specimens from the 2013 outbreak of cyclosporiasis in Texas produced complete MLST data because of inability to obtain readable sequences from CYC22. Sequence analysis at other loci suggested that at least 3 types of *C. cayetanensis* protozoa were present in specimens from the outbreak. The occurrence of mixed *C. cayetanensis* populations probably led to unreadable sequences for most specimens from the outbreak at CYC22.

The occurrence of mixed *C. cayetanensis* populations in large outbreaks is expected because divergent MLST types are apparently present in a small community or geographic area. For example, the Peru specimens in this study were from a small shantytown, Pampas de San Juan de Miraflores, in Lima (*4*), but the specimens had at least 5 MLST types among them. Similarly, 14 MLST types were detected among the 26 Chinese specimens collected from 2 neighboring cities (Kaifeng and Zhengzhou) in Henan Province (*5*). Fresh produce is frequently contaminated by *C. cayetanensis* protozoa through irrigation water (*6*) and thus has a higher probability of containing multiple *C. cayetanensis* genotypes. It might be possible to use only 2 or 3 loci that are highly polymorphic and easier to sequence in *C. cayetanensis* genotyping, such as CYC13 and CYC21.

Figure 1. Phylogenetic relationships among sequence types of *Cyclospora cayetanensis* at 5 microsatellite loci: A) CYC3, B) CYC13, C) CYC15, D) CYC21, and E) CYC22. Tree was constructed on the basis of neighbor-joining analyses of the nucleotide sequences, using genetic distances calculated by the Kimura 2-parameter model. Numbers on branches are bootstrap values from 1,000 replicate analyses. Only values >50% are displayed on the left of each node. Scale bars indicate substitution rates per nucleotide. HN, Henan.

Figure 2. Phylogenetic relationships among concatenated multilocus sequence types of *Cyclospora cayetanensis* as assessed by a neighbor-joining analysis of the nucleotide sequences, using genetic distances calculated by the Kimura 2-parameter model. Numbers on branches are bootstrap values from 1,000 replicate analyses. Only values >50% are displayed on the left of each node. Scale bar indicates substitution rates per nucleotide. HN, Henan.

In summary, whole-genome sequence data from *C. cayetanensis* protozoa enabled the development of a MLST tool for characterizing isolates in outbreak investigations. The high resolution of the typing tool and the apparent presence of geographic clusters might facilitate the identification of outbreaks and infection sources. Nevertheless, extensive characterization of specimens from diverse areas and wide application of the developed tool in outbreak investigations are needed to better understand *C. cayetanensis* transmission.

Ms. Guo is a lecturer at East China University of Science and Technology. Her research interests include molecular epidemiology and genomics of foodborne, waterborne, and zoonotic parasites.

References

1. Hall RL, Jones JL, Herwaldt BL. Surveillance for laboratory-confirmed sporadic cases of cyclosporiasis—United States, 1997–2008. MMWR Surveill Summ. 2011;60:1–11.
2. desVignes-Kendrick M, Reynolds K, Lee T, Gaul L, Klein K, Irvin K, et al. Outbreaks of cyclosporiasis—United States, June–August 2013. MMWR Morb Mortal Wkly Rep. 2013;62:862.
3. Tang K, Guo Y, Zhang L, Rowe LA, Roellig DM, Frace MA, et al. Genetic similarities between *Cyclospora cayetanensis* and cecum-infecting avian *Eimeria* spp. in apicoplast and mitochondrial genomes. Parasit Vectors. 2015;8:358. http://dx.doi.org/10.1186/s13071-015-0966-3
4. Cama VA, Bern C, Roberts J, Cabrera L, Sterling CR, Ortega Y, et al. *Cryptosporidium* species and subtypes and clinical manifestations in children, Peru. Emerg Infect Dis. 2008;14:1567–74. http://dx.doi.org/10.3201/eid1410.071273
5. Zhou Y, Lv B, Wang Q, Wang R, Jian F, Zhang L, et al. Prevalence and molecular characterization of *Cyclospora cayetanensis*, Henan, China. Emerg Infect Dis. 2011;17:1887–90. http://dx.doi.org/10.3201/eid1710.101296
6. Mota P, Rauch CA, Edberg SC. Microsporidia and *Cyclospora*: epidemiology and assessment of risk from the environment. Crit Rev Microbiol. 2000;26:69–90. http://dx.doi.org/10.1080/10408410091154192

Address for correspondence: Yaoyu Feng, State Key Laboratory of Bioreactor Engineering, School of Resources and Environmental Engineering, East China University of Science and Technology, 130 Meilong Rd, Shanghai 200237, China; email: yyfeng@ecust.edu.cn

Letters

Letters commenting on recent articles as well as letters reporting cases, outbreaks, or original research are welcome. Letters commenting on articles should contain no more than 300 words and five references; they are more likely to be published if submitted within four weeks of the original article's publication. Letters reporting cases, outbreaks, or original research should contain no more than 800 words and ten references. They may have one Figure or Table and should not be divided into sections. All letters should contain material not previously published and include a word count.

Chagas Disease Screening in Maternal Donors of Publicly Banked Umbilical Cord Blood, United States

**James M. Edwards, Jennifer B. Gilner,
Jose Hernandez, Joanne Kurtzberg,
R. Phillips Heine**

To assess patterns of Chagas disease, we reviewed results of screening umbilical cord blood from a US public cord blood bank during 2007–2014. Nineteen maternal donors tested positive for *Trypanosoma cruzi* parasites (0.04%). Because perinatal transmission of Chagas disease is associated with substantial illness, targeted prenatal programs should screen for this disease.

Chagas disease, a parasitic disease caused by *Trypanosoma cruzi*, is increasingly seen in non–disease-endemic areas, secondary to population movements (*1*). Vertical transmission of this parasite to a developing fetus occurs at a rate of ≈4.7% and can cause substantial perinatal illness and death (*2*). Adverse pregnancy-related outcomes include increased rates of preterm delivery, restricted fetal growth, low birthweight, premature rupture of membranes, and polyhydramnios (*3*). Mortality rates among congenitally infected infants approach 5%, mostly secondary to myocarditis and meningoencephalitis. Long-term maternal and child conditions include dilated cardiomyopathy and gastrointestinal disorders, with mortality rates as high as 13% (*4*). Fortunately, infants within the first year of life tolerate treatment well, and the infection is usually cured (*3*).

Because screening for and treating this infection has potential benefits, the World Health Assembly adopted a resolution recommending screening for Chagas disease among pregnant women in non–disease-endemic areas who were born in disease-endemic areas, who lived extensively in disease-endemic areas, or who were born to mothers who lived in disease-endemic areas (*5*). The US Food and Drug Administration instituted guidelines for screening in 2007 (*6*). This screening also applied to mothers donating their newborn infants' cord blood to public cord blood banks. Therefore, we reviewed identified cases of Chagas disease in maternal donors to a public umbilical cord blood bank to estimate disease prevalence and population characteristics in a non–disease-endemic area of the United States.

Author affiliation: Duke University Medical Center, Durham, North Carolina, USA

The Study

We performed a retrospective cohort study of the seroprevalence of *Trypanosoma cruzi* parasites in all cord blood samples donated to the Carolinas Cord Blood Bank (CCBB) during July 1, 2007–December 31, 2014. The CCBB is a public cord blood bank (licensed by the US Food and Drug Administration) that collects donations from multiple sites across the state of North Carolina as well as from Boston, Massachusetts, and Atlanta, Georgia. A kit donation program also enables donations to be made from any US state. Initial donor screening selects patients with singleton, nonanomalous pregnancies without known preexisting infection. After CCBB received general written informed consent for cord blood donation at the time of delivery, we assessed blood samples from mothers whose cord blood donations met specifications of initial donor screening, volume, and cell count. Donor demographic information, including maternal age, race, ethnic background, state of collection, and date of collection, was recorded.

Maternal blood samples from cord blood donors were routinely screened for infectious agents at the American Red Cross National Donor Testing Laboratory (Charlotte, NC, USA). These agents were hepatitis B, hepatitis C, HIV-1 and -2, human T-lymphotrophic viruses I and II, *Treponema pallidum* (for syphilis, by rapid plasma regain test), cytomegalovirus, West Nile virus, *T. cruzi*, and any bacterial contamination. *T. cruzi* screening was performed by indirect hemagglutination assay. If results were positive, a confirmatory radioimmunoprecipitation assay (RIPA) was performed. Positive confirmatory testing triggered referral of mother and neonate for further evaluation and treatment. Because CCBB records are not linked to patient records, we were unable to obtain follow-up information regarding additional maternal and neonatal evaluation and treatment. After the study received exempt status from the Duke University Institutional Review Board (Pro00064159), we performed a retrospective cohort study and collected demographic data from mothers whose umbilical cord blood donations were positive for *T. cruzi*. Descriptive statistics were then performed and results were analyzed. All statistical analyses were performed with R version 3.2.2 (https://www.r-project.org/).

We screened samples from 58,817 maternal donors who donated cord blood during the 8.5-year period covered by the study. Twenty-five samples were positive by indirect hemaglutination assay (0.043%), and 19 were positive by

confirmatory RIPA testing (0.032%). For 3 donors, confirmatory RIPA results were indeterminate, and results for 3 other donors were negative. One donor with a positive confirmatory test result had a positive rapid plasma regain result, and another was co-infected with hepatitis C virus. The remaining 17 donors from the cohort had no identified co-infections.

Of the donors with positive samples, 20 were from North Carolina, 1 was from Florida, 1 was from Massachusetts, and 3 were of unknown origin. When the total screened population was assessed, a substantial amount of missing data precluded the possibility of further analysis. We also attempted to assess maternal age but were unable to do so because of missing data.

The incidence of confirmed Chagas disease among mothers who donated their neonate's cord blood varied over time, from an incidence of 0.3 cases/1,000 donors in 2007 to 1.6 cases/1,000 donors in 2014 (Figure). The ethnic distribution of donors with confirmed positive results was significantly different from that of the full population of screened donors (p = 0.002) (Table). The primary difference was that the number of Hispanic patients increased as the numbers of African American case-patients and Asian–Pacific Islander case-patients decreased.

Conclusion

Chagas disease is an emerging infection in non–disease-endemic regions, such as the United States, secondary to emigration from disease-endemic areas, including Central and South America. In the pregnant population studied, we found a prevalence of Chagas disease of 0.32 cases/1,000 persons screened over an 8.5-year period. In comparison, the risk of invasive group B *Streptococcus* (GBS) disease in the current era of universal maternal screening and treatment is similar, 0.3 case/1,000 live births. Although only 5% of maternal Chagas cases are estimated to be associated with perinatal transmission, the long-term illnesses and deaths associated with unrecognized Chagas disease are notable. This situation is similar to that of invasive GBS, which has a 3% case-fatality rate and a 5%–10% rate of sepsis meningitis, which will cause long-term neurologic effects in half of affected patients (*7*).
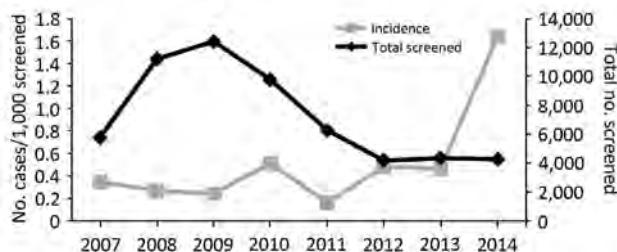
Figure. Chagas disease incidence in donated cord blood, United States, 2007–2014.

Table. Distribution by ethnicity of maternal cord blood donors with confirmed Chagas disease, United States, 2007–2014

Ethnicity	No. (%) patients with Chagas disease, n = 19	No. (%) screened donors
Caucasian	8 (32)	30,332 (52)
Hispanic	7 (28)	9,112 (16)
African American	2 (8)	10,277 (18)
Asian–Pacific Islander	0	1,833 (3)
Other	0	5,387 (10)
Unknown	2 (8)	854 (1)

The incidence of Chagas disease varied over time. During the last year of the study period, an ≈3-fold increase in incidence occurred, although this finding is based on small numbers. Screening test methods remained constant throughout this period. We are unsure of the cause of this increase in incidence. Although it may have been secondary to continued immigration from Chagas disease endemic areas, the small numbers of cases makes identification of factors difficult.

In addition, the difference in ethnicity between the cohort with Chagas disease and the overall screened donors was significant, with an increase in self-identified Hispanic patients. These changes are consistent with the worldwide prevalence of the disease (*8*)

A strength of this study is its large sample size, particularly because the incidence of this disease is low. The study does, however, have several limitations. First, Chagas disease screening was limited to maternal donors of cord blood units donated to a public cord blood bank. Therefore, ascertainment bias is a possibility, despite use of a bilingual staff and consent and donor materials available in Spanish. However, this phenomenon would likely cause disease prevalence in the overall population to be underestimated. In addition, this sample primarily consists of donations across the state of North Carolina, with smaller proportions coming from Atlanta, Georgia; and Boston, Massachusetts. Therefore, these results may not be generalizable to all non–disease-endemic areas.

Our future work will focus on expanding the number of patients assessed by including other cord blood screening programs across the United States. We aim to determine patient demographics that will enable creation of targeted antenatal screening programs to reduce perinatal illness and death associated with congenital Chagas disease.

Dr. Edwards is a third-year maternal-fetal medicine fellow at Duke University Medical Center. His research interests focus on infectious complications of pregnancy, in particular, the neonatal effects of maternal infection.

References

1. Pérez-López FR, Chedraui P. Chagas disease in pregnacy: a non-endemic problem in a globalized world. Arch Gynecol Obstet. 2010;282:595–9. http://dx.doi.org/10.1007/s00404-010-1553-7

2. Howard EJ, Xiong X, Carlier Y, Sosa-Estani S, Buekens P. Frequency of the congenital transmission of *Trypanosoma cruzi*: a systematic review and meta-analysis. BJOG. 2014;121:22–33. http://dx.doi.org/10.1111/1471-0528.12396

3. Cevallos AM, Hernandez R. Chagas' disease: pregnancy and congenital transmission. Biomed Res Int. 2014:401864.

4. Sicuri E, Munoz J, Pinazo MJ, Posada E, Sanchez J, Alonso PL, et al. Economic evaluation of Chagas disease screening of pregnant Latin American women and of their infants in a non endemic area. Acta Trop. 2011;118:110–7. http://dx.doi.org/10.1016/j.actatropica.2011.02.012

5. Carlier Y, Torrico F, Sosa-Estani S, Russomando G, Luquetti A, Freilij H, et al. Congenital Chagas disease: recommendations for diagnosis, treatment and control of newborns, siblings and pregnant women. PLoS Negl Trop Dis. 2011;5:e1250. http://dx.doi.org/10.1371/journal.pntd.0001250

6. US Department of Health and Human Services. Guidance for industry: use of serological tests to reduce the risk of transmission of *Trypanosoma cruzi* infection in whole blood and blood components intended for transfusion. Rockville (MD): US Department of Health and Human Services; 2010 [cited 2016 Jun 6] http://www.fda.gov/BiologicsBloodVaccines/GuidanceCompliance-RegulatoryInformation/Guidances/Blood/ucm235855.htm

7. Ahmadzia HK, Heine RP. Diagnosis and management of group B streptococcus in pregnancy. Obstet Gynecol Clin North Am. 2014;41:629–47. http://dx.doi.org/10.1016/j.ogc.2014.08.009

8. Bern C. Chagas' disease. N Engl J Med. 2015;373:456–66. http://dx.doi.org/10.1056/NEJMra1410150

Address for correspondence: James M. Edwards, Duke University Medical Center 3967, Durham, NC 27710, USA; email: james.edwards@duke.edu
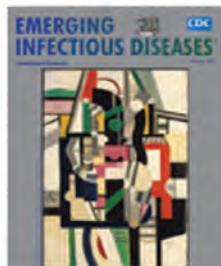
Borrelia miyamotoi Infection in Patients from Upper Midwestern United States, 2014–2015

**Dean A. Jobe, Steven D. Lovrich,
Darby G. Oldenburg, Todd J. Kowalski,
Steven M. Callister**

We confirmed *Borrelia miyamotoi* infection in 7 patients who had contracted an illness while near La Crosse, Wisconsin, USA, an area where *Ixodes scapularis* ticks are endemic. *B. miyamatoi* infection should now be considered among differential diagnoses for patients from the midwestern United States who have signs and symptoms suggestive of tickborne illness.

The upper midwestern United States, which includes the region surrounding La Crosse, Wisconsin, is a well-described focus of *Ixodes scapularis* ticks. As a result, annual incidence of Lyme disease has been high (*1*) and prevalence of human granulocytic anaplasmosis (*2*) and babesiosis has been increasing (*3*). At the Gundersen Health System in La Crosse, we therefore use multiple laboratory procedures to screen patients with suspected *I. scapularis* tick–associated illness; the procedures include a whole-cell *Borrelia burgdorferi* ELISA and Western blot for confirming Lyme disease and PCRs for detecting infection with *Anaplasma phagocytophilum* or *Babesia microti*. However, other human illnesses caused by pathogenic microorganisms transmitted from *I. scapularis* ticks continue to emerge. Primary among them is *Borrelia miyamotoi* (*4*), a spirochete bacterium that colonizes blood and typically causes relapsing fevers accompanied by chills, headache, fatigue, myalgia, arthralgia (*5–8*), and (rarely) meningoencephalitis (*9*).

The first case of human infection with *B. miyamotoi* was documented in 2011 in a patient from Russia (*5*); additional cases have since been detected in Russia, Europe, Asia, and the United States (*7–11*). Although cases seem to have occurred only in patients who contracted the organism from infected *I. scapularis* ticks in the northeastern United States (*8,10,11*), persons in the upper midwestern United States (upper Midwest) are also commonly bitten by these ticks. In addition, Hamer et al. (*12*) detected *B. miyamotoi* DNA in *I. scapularis* ticks that had been captured from several sites in the upper Midwest during the 2006 and 2007 tick-questing seasons. We therefore conducted a retrospective investigation to determine whether patients at our healthcare facility

with clinically suspected illness caused by tick bite could be infected with *B. miyamotoi*. To do so we also conducted *B. miyamotoi* DNA testing on blood samples submitted for *A. phagocytophilum* or *B. microti* DNA testing.

The Study

A total of 2,150 DNA samples were obtained from blood of patients evaluated during 2014–2015 for illness and tested for either *A. phagocytophilum* or *B. microti* because of clinical complaints or abnormalities suggestive of tickborne illness. Because our current laboratory procedures for confirming either infection require extraction of DNA from a blood sample before PCR testing, we also evaluated the extracted DNA for *B. miyamotoi*. Ethics approval for detecting and sequencing unique bacterial DNA from routine clinical samples and linkage to patient data without individual informed consent was obtained from the Gundersen Institutional Review Board with the stipulation that patient identifiers be appropriately redacted and information be used only as surveillance data for public health purposes.

We initially screened the DNA samples with a modification of a previously described *B. miyamatoi* screening PCR (*13*), which amplified a 70-bp DNA fragment of the 16S ribosomal RNA gene specific for *B. miyamatoi*. In brief, we combined 5 μL of extracted DNA with 20 μL of a master mix that contained 12.5 μL of buffer (AmpliTaq Gold DNA Polymerase with GeneAmp 10X PCR Gold Buffer; Life Technologies, Austin, TX, USA); 2.5 mmol/L magnesium chloride, deoxynucleoside triphosphates; 7 μL of a primer/probe mix comprising forward primer 5′-GCTGTAAACGATGCACACTTGGT-3′, reverse primer 5′-GGCGGCACACTTAACACGTTAG-3′, and probe 5′-HEX-CGGTACTAACCTTTCGATTA-3′; and 0.5 μL (1.5 U) AmpliTaq Gold DNA Polymerase under the following conditions: 1 cycle at 95°C for 10 min, 45 cycles at 95°C for 15 s, 63°C for 1 min, and a final cycle at 25°C for 5 s. For a positive control, we used strain HS1 (ATCC 35209) of *Borrelia hermsii* because *B. miyamotoi* DNA or viable spirochetes are not easily obtained.

We amplified *B. miyamotoi* DNA from 7 patients (1 male, 6 female) whose previous anaplasmosis and babesiosis test results were negative. Mean patient age was 51 years (range 3–70 years), and 3 patients confirmed that they had been bitten by a tick suspected to be *I. scapularis* within the 10 days before becoming ill. The patients also resided in or near La Crosse; although none reported recent travel outside the region, we cannot rule out the possibility

that the infections were acquired elsewhere. Further supporting local acquisition, however, we also recently detected *B. miyamotoi* DNA by the PCR used in this study in a small number (≈2%) of *I. scapularis* ticks collected locally (data not shown).

The clinical signs and symptoms strongly supported PCR positivity for *B. miyamotoi* (*5*–*8*). The most common clinical sign was fever; 1 patient reported additional episodes of fever during the 2 months before seeking treatment (Table). In addition, skin lesions were not detected, although 1 patient may have been co-infected with *B. burgdorferi*; an IgM Western blot test performed in the clinical laboratory also yielded reactivity sufficient to provide sero-diagnostic confirmation of early Lyme disease (*14*). Moreover, elevated levels of serum alanine aminotransferase (n = 2) or aspartate aminotransferase (n = 1) were detected in the only 2 patients for whom *B. miyamotoi* DNA was identified and who were tested for these liver enzyme abnormalities. In addition, the infected patients received doxycycline therapy for at least 7 days (mean 10 days; range 7–14 days), which uniformly resulted in complete resolution of clinical signs and symptoms.

For final confirmation of infection with *B. miyamotoi*, we then reamplified a 142-bp fragment (bp 636–777) of the glycerophosphodiester phosphodiesterase (*glpQ*) gene from the remaining DNA sample from each patient positive for *B. miyamotoi* by PCR. The *glpQ* gene was targeted because the GlpQ protein is absent in the *Borrelia* species that cause Lyme disease (*15*), which are detected relatively frequently in patients from the region (*1*). In brief, 5 µL of DNA was combined with 20 µL of a master mix that contained 12.5 µL of buffer, 0.5 µmol/L of forward (5′-GATAATATTCCTGTTATAATGC-3′) and reverse (5′-CACTGAGATTTAGTGATTTAAGTTC-3′) primers, and 0.5 µL (1.5 U) of AmpliTaq Gold DNA polymerase. The DNA was then amplified under the following conditions: 1 cycle at 95°C for 3 min followed by 50 cycles at 95°C for 45 s, 56°C for 30 s, and 72°C for 60 s, followed by a final extension at 72°C for 7 min. Amplified material was purified (QIAquick PCR Purification Kit; QIAGEN, Hilden, Germany) and forwarded to Laragen Inc. (Culver City, CA, USA) for sequencing. In each instance, the sequence of the amplified fragment was 100% homologous with that of *B. miyamotoi* LB-2001 (GenBank accession no. CP006647.2).

Conclusions

Researchers have documented human illness caused by *B. miyamotoi* transmitted from *I. scapularis* ticks (*5*,*7*–*9*,*11*), but infections in patients from the United States have to date been described only for residents of the northeastern part of the country (*10*). In this study, however, we confirmed characteristic illness caused by infection with *B. miyamotoi* in 7 patients who resided in the *I. scapularis* tick–endemic focus surrounding La Crosse, Wisconsin. Given these findings, clinicians in the upper Midwest must now also consider the possibility of *B. miyamotoi* infection in patients with suspected tickborne illness, especially because even more cases will probably be detected as appropriate methods, such *B. miyamotoi*-specific anti-GlpQ antibody testing (*8*,*15*) or *B. miyamotoi* DNA detection, become more widely available. Studies to provide additional insight into human infection with *B. miyamotoi* remain necessary because the prevalence of the illness will probably increase even more as *I. scapularis* ticks continue to disperse.

References

1. Kowalski TJ, Tata S, Berth W, Mathiason MA, Agger WA. Antibiotic treatment duration and long-term outcomes of patients with early Lyme disease from a Lyme disease–hyperendemic area. Clin Infect Dis. 2010;50:512–20. http://dx.doi.org/10.1086/649920
2. Lovrich SD, Jobe DA, Kowalski TJ, Policepatil SM, Callister SM. Expansion of the midwestern focus for human granulocytic anaplasmosis into the region surrounding La Crosse, Wisconsin. J Clin Microbiol. 2011;49:3855–9. http://dx.doi.org/10.1128/JCM.05025-11
3. Kowalski TJ, Jobe DA, Dolan EC, Kessler A, Lovrich SD, Callister SM. The emergence of clinically relevant babesiosis in southwestern Wisconsin. WMJ. 2015;114:152–7.
4. Fukunaga M, Takahashi Y, Tsuruta Y, Matsushita O, Ralph D, McClelland M, et al. Genetic and phenotypic analysis of *Borrelia miyamotoi* sp. nov. isolated from the ixodid tick *Ixodes persulcatus*, the vector for Lyme disease in Japan. Int J Syst Bacteriol. 1995;45:804–10. http://dx.doi.org/10.1099/00207713-45-4-804
5. Platonov AE, Karan LS, Kolyasnikova NM, Makhneva NA, Toporkova MG, Maleev VV, et al. Humans infected with relapsing fever spirochete *Borrelia miyamotoi*, Russia. Emerg Infect Dis. 2011;17:1816–23. http://dx.doi.org/10.3201/eid1710.101474
6. Krause PJ, Fish D, Narasimhan S, Barbour AG. *Borrelia miyamotoi* infection in nature and humans. Clin Microbiol Infect. 2015;21:631–9. http://dx.doi.org/10.1016/j.cmi.2015.02.006

Table. Clinical manifestations in 7 *Borrelia miyamotoi*–infected patients from the midwestern United States, 2014–2015

Manifestation	No. (%) patients
Fever	6 (86)*
Chills	3 (43)
Myalgia	3 (43)
Fatigue	3 (43)
Arthralgia	2 (29)
Headache	1 (14)
Nausea	1 (14)
Stiff neck	1 (14)
Vomiting	1 (14)
Skin lesion	0

*Fever was recurrent for 1 patient.

7. Sato K, Takano A, Konnai S, Nakao M, Ito T, Koyama K, et al. Human infections with *Borrelia miyamotoi*, Japan. Emerg Infect Dis. 2014;20:1391–3. http://dx.doi.org/10.3201/eid2008.131761n

8. Molloy PJ, Telford III Sr, Howdri HR, Lepore TJ, Gugliotta JL, Weeks KE, et al. *Borrelia miyamotoi* disease in the northeastern United States. Ann Intern Med. 2015;163:91–8. http://dx.doi.org/10.7326/M15-0333

9. Gugliotta JL, Goethert HK, Berardi VP, Telford III Sr. Meningoencephalitis from *Borrelia miyamotoi* in an immunocompromised patient. N Engl J Med. 2013;368:240–5. http://dx.doi.org/10.1056/NEJMoa1209039

10. Krause PJ, Narasimhan S, Wormser GP, Rollend L, Fikrig E, Lepore T, et al. Human *Borrelia miyamotoi* infection in the United States. N Engl J Med. 2013;368:291–3. http://dx.doi.org/10.1056/NEJMc1215469

11. Chowdri HR, Gugliotta JL, Berardi VP, Goethert HK, Molloy PJ, Sterling SL, et al. *Borrelia miyamotoi* infection presenting as human granulocytic anaplasmosis: a case report. Ann Intern Med. 2013;159:21–7. http://dx.doi.org/10.7326/0003-4819-159-1-201307020-00005

12. Hamer SA, Hickling GJ, Walker ED, Tsao JI. Increased diversity of zoonotic pathogens and *Borrelia burgdorferi* strains in established versus incipient *Ixodes scapularis* populations across the midwestern United States. Infect Genet Evol. 2014;27:531–42. http://dx.doi.org/10.1016/j.meegid.2014.06.003

13. Barbour AG, Bunikis J, Travinsky B, Hoen AG, Duik-Wasser MA, Fish D, et al. Niche partitioning of *Borrelia burgdorferi* and *Borrelia miyamotoi* in the same vector and mammalian reservoir species. Am J Trop Med Hyg. 2009;81:1120–31. http://dx.doi.org/10.4269/ajtmh.2009.09-0208

14. Centers for Disease Control and Prevention. Recommendations for test performance and interpretation from the Second National Conference on Serologic Diagnosis of Lyme Disease. MMWR Morb Mortal Wkly Rep. 1995;44:590–1.

15. Schwan TG, Schrumpf ME, Hinnebusch BJ, Anderson DE, Konkel ME. GlpQ: an antigen for serological discrimination between relapsing fever and Lyme borreliosis. J Clin Microbiol. 1996;34:2483–92.

Address for correspondence: Steven M. Callister, Microbiology Research and Molecular Diagnostics Laboratories, Health Science Center, Rm 5032, 1300 Badger St, La Crosse, WI 54601, USA; email: smcallis@gundersenhealth.org

Whole-Genome Sequencing Detection of Ongoing *Listeria* Contamination at a Restaurant, Rhode Island, USA, 2014

Jonathan S. Barkley, Michael Gosciminski, Adam Miller[1]

In November 2014, the Rhode Island Department of Health investigated a cluster of 3 listeriosis cases. Using whole-genome sequencing to support epidemiologic, laboratory, and environmental investigations, the department identified 1 restaurant as the likely source of the outbreak and also linked the establishment to a listeriosis case that occurred in 2013.

Infection with *Listeria monocytogenes*, a foodborne bacterial pathogen, causes listeriosis, which can lead to severe illness, typically among persons with compromised immune systems and pregnant women and their fetuses. The pathogen can survive at high salt concentrations and grow at refrigeration temperatures (*1*). These properties enable the bacteria to persist in food processing and food service establishments for extended periods. Listeriosis has a long incubation period (3–70 days), making exposure recall difficult. Retail delicatessens are a potential source of *L. monocytogenes* because they hold ready-to-eat foods at refrigeration temperatures; however, a risk assessment by the United States Department of Agriculture's Food Safety and Inspection Service suggests that thorough sanitization of food contact surfaces, proper maintenance of equipment and facilities, safe product handling practices, and good employee practices to avoid cross-contamination can help prevent listeriosis cases associated with retail food establishments (*2*).

Since 1998, PulseNet (http://www.cdc.gov/pulsenet/index.html) has used pulsed-field gel electrophoresis (PFGE) to look at genetic differences in *L. monocytogenes* subtypes and to identify outbreaks. However, distantly related strains can appear indistinguishable by PFGE; thus, greater differentiation may be needed to distinguish between outbreak and sporadic cases of listeriosis. Whole-genome sequencing (WGS) offers an opportunity to further discriminate between strains and identify outbreaks. WGS has historically been used retrospectively to provide additional insight into outbreak investigations (*3*). However, since September 2013, WGS has been performed on all clinical *L. monocytogenes* isolates identified in the United States by the Centers for Disease Control and Prevention (Atlanta, GA) and several state public health laboratories (*4*). *L. monocytogenes* is a good candidate for WGS because it causes a relatively rare condition that can result in serious illness, it has a small genome that is relatively easy to analyze, and epidemiologic surveillance and food regulatory program components for the bacterium are strong (*5*).

Data obtained from WGS has been analyzed using whole-genome multilocus sequence typing (wgMLST), a technique that examines allelic differences from thousands of loci, and ≈96% of *L. monocytogenes* coding sequences have been identified as loci in the wgMLST scheme (S. Stroika, Centers for Disease Control and Prevention, pers. comm., 2016 Jan 29). To discriminate between strains and identify outbreaks, alleles within the coding sequence (i.e., loci) are compared with ≈178 reference genomes. A unique combination of alleles at each locus specifies the sequence type, which enables comparison of isolates (*6*); the smaller the number of allelic differences between isolates, the more related they are.

The Rhode Island Department of Health (RIDOH) attempts interviews and, when applicable, conducts environmental investigations for all reports of listeriosis. Each year during 2011–2013, RIDOH received ≈3 reports of listeriosis, most of which were sporadic cases. However, in November 2014, a cluster of cases was detected from laboratory reports and examined using WGS in conjunction with epidemiologic, laboratory, and environmental investigations. Isolates were confirmed to be *L. monocytogenes* and submitted for PFGE analysis. The Centers for Disease Control and Prevention performed WGS on clinical isolates; the Food and Drug Administration performed WGS on food isolates.

The Investigation

During October 27–November 5, 2014, RIDOH's Center for Acute Infectious Disease Epidemiology was notified of 3 *L. monocytogenes*–infected persons residing in the same city. The 3 case-patients were all non-Hispanic white persons >60 years of age; 2 had an immunocompromising condition. Interviews conducted by the Center for Acute Infectious Disease Epidemiology identified a single

[1]All authors contributed equally to this article.

common restaurant visited by the 3 patients. RIDOH's Center for Food Protection performed inspections and collected food and environmental samples at the establishment.

PFGE analysis showed that clinical *L. monocytogenes* isolates from the 3 case-patients shared an identical, common PFGE pattern (Figure). To determine the relationship between the isolates, RIDOH collaborated with federal partners to conduct WGS. Results of wgMLST showed that the isolates were closely related (0–5 allelic differences) (Figure) and a close genetic match (median allelic differences 4) to a clinical isolate from a 2013 patient, who was reinterviewed and reported eating at the same restaurant. A sliced prosciutto sample from the restaurant tested positive for *L. monocytogenes*, and PFGE patterns for this isolate matched those for isolates from the 2013 and 2014 case-patients. Results of wgMLST showed that the isolate from the prosciutto differed by 0–5 alleles (median 3) from the 2014 clinical samples and by 0–11 alleles (median 4) from the 2013 clinical sample (Figure). Sequences for the isolates were uploaded to GenBank (*7*) (clinical isolates: accession nos. SAMN02400177, SAMN03253348–49, SAMN03253359; isolate from prosciutto: accession no. SAMN03218571).

A total of 10 food and environmental food samples were initially collected from the restaurant. Swab samples were obtained from the food slicer, preparation tables, and walk-in cooler. Environmental investigation of the restaurant identified issues related to control of *L. monocytogenes*: the temperature of the refrigerated unit that held sliced meat and other food items was elevated (52°F [11°C]), and cleanliness issues were observed with the preparation tables and slicer. An additional 19 environmental samples were later collected from the establishment; however, the refrigerated unit and preparation tables had been replaced, so additional swab samples could not be collected from those surfaces. The sample of sliced prosciutto was the only *L. monocytogenes*–positive sample identified at the restaurant; however, just 1 of the 2014 case-patients reported eating prosciutto (in an antipasto salad) at the restaurant. Other foods reported included green salad and coleslaw.

RIDOH tested a sample of prosciutto from an unopened package from the establishment and collaborated with the Food Safety and Inspection Service to see if the processing plant had recently tested positive for *L. monocytogenes*. The sample tested negative, and no positive tests had been reported at the plant in at least 1 year.

Conclusions

Epidemiologic, environmental, and laboratory investigation results implicated a restaurant with sanitation issues and improper sliced meat storage as the likely source of a multiyear listeriosis outbreak. A long incubation period makes WGS an effective technology to use during listeriosis outbreak investigations and to identify outbreak-associated cases originally believed to be sporadic cases. This technology can help overcome difficulties associated with investigating listeriosis cases and can be useful for the investigation of other pathogens. In this investigation, WGS (wgMLST) helped link the 2013 listeriosis case, which was originally believed to be a sporadic case, to the 2014 outbreak. Furthermore, given that the 4 isolates had a common PFGE pattern, this technology increased confidence that the restaurant, which was the only common restaurant among the 4 patients, was the source of the outbreak. The allelic differences observed are consistent with slow, spontaneous mutation occurring over a long period due to persistent contamination.

There is no set number of allelic differences used to determine whether clusters of cases are part of actual outbreaks (*8*). Thus, WGS is not sufficient by itself to identify outbreaks and must be performed in conjunction with epidemiologic, laboratory, and environmental investigations (*8,9*). In the investigation we describe, WGS was used in this supporting role. The close relationship that WGS showed between the clinical isolates and the isolate from meat provides additional evidence that the restaurant was the likely source of contamination for the cases in 2013 and 2014.

Our findings support the need to control *L. monocytogenes* at retail food establishments. Storing meat at ≤41°F
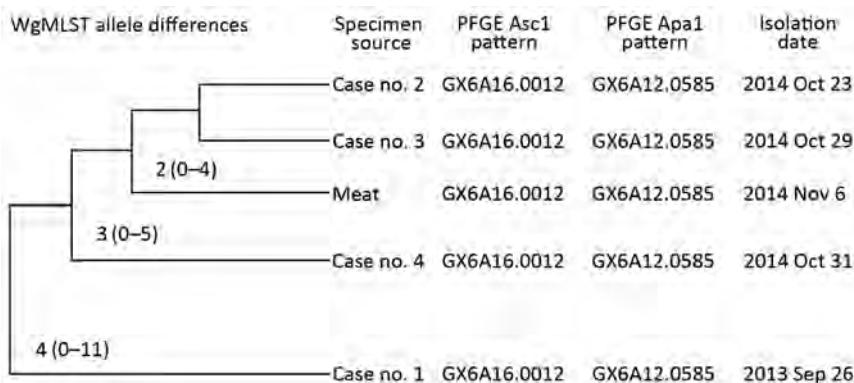
Figure. Median (minimum–maximum) allele differences and pulsed-field gel electrophoresis (PFGE) patterns for *Listeria monocytogenes* isolates from clinical and food samples associated with a 2014 cluster of listeriosis cases and a 2013 listeriosis case, Rhode Island, USA. Allele differences were determined by whole-genome multilocus sequence typing (wgMLST). Adapted from data provided by the Enteric Diseases Laboratory Branch, National Center for Emerging and Zoonotic Infectious Diseases, Centers for Disease Control and Prevention (Atlanta, GA, USA).

WgMLST allele differences	Specimen source	PFGE Asc1 pattern	PFGE Apa1 pattern	Isolation date
	Case no. 2	GX6A16.0012	GX6A12.0585	2014 Oct 23
2 (0–4)	Case no. 3	GX6A16.0012	GX6A12.0585	2014 Oct 29
3 (0–5)	Meat	GX6A16.0012	GX6A12.0585	2014 Nov 6
	Case no. 4	GX6A16.0012	GX6A12.0585	2014 Oct 31
4 (0–11)	Case no. 1	GX6A16.0012	GX6A12.0585	2013 Sep 26

(5°C) can prevent ≈9% of listeriosis cases (2). In addition, retail delicatessens and food establishments can prevent *L. monocytogenes*–associated illnesses among customers by controlling cross-contamination, cleaning and sanitizing food contact surfaces, and eliminating environmental niches.

Acknowledgments

We thank the Rhode Island State Laboratory for performing confirmatory *L. monocytogenes* testing on clinical and food samples and for coordinating PFGE and WGS testing; the Massachusetts William A. Hinton State Laboratory for performing PFGE testing of the clinical and food samples; and the Centers for Disease Control and Prevention and Food and Drug Administration for performing WGS of clinical and food samples, respectively.

Mr. Barkley is a public health epidemiologist at the Center for Food Protection, Rhode Island Department of Health. His research interests include understanding risk factors of foodborne illness associated with retail food establishments.

References

1. Ferreira V, Wiedmann M, Teixeira P, Stasiewicz MJ. *Listeria monocytogenes* persistence in food-associated environments: epidemiology, strain characteristics, and implications for public health. J Food Prot. 2014;77:150–70. http://dx.doi.org/10.4315/0362-028X.JFP-13-150
2. United States Department of Agriculture, Food Safety and Inspection Service. Best practices guidance for controlling *Listeria monocytogenes* in retail delicatessens. June 2015 [cited 2016 Feb 1]. http://www.fsis.usda.gov/wps/wcm/connect/29d51258-0651-469b-99b8-e986baee8a54/Controlling-LM-Delicatessens.pdf?MOD=AJPERES
3. Le VT, Diep BA. Selected insights from application of whole-genome sequencing for outbreak investigations. Curr Opin Crit Care. 2013;19:432–9. http://dx.doi.org/10.1097/MCC.0b013e3283636b8c
4. Centers for Disease Control and Prevention. Advanced molecular detection (AMD). AMD projects: learning from Listeria [cited 2015 Oct 23]. http://www.cdc.gov/amd/project-summaries/listeria.html
5. Jackson B, Jackson K, Tarr C, Evans P, Klimke W, Kubota K, et al. Improving detection and investigation of listeriosis outbreaks using real-time whole-genome sequencing. Presented at: IDWeek 2014; Philadelphia, PA, USA; 2014 Oct 8–12.
6. Larsen MV, Cosentino S, Rasmussen S, Friis C, Hasman H, Marvig RL, et al. Multilocus sequence typing of total-genome-sequenced bacteria. J Clin Microbiol. 2012;50:1355–61. http://dx.doi.org/10.1128/JCM.06094-11
7. Benson DA, Clark K, Karsch-Mizrachi I, Lipman DJ, Ostell J, Sayers EW. GenBank. Nucleic Acids Res. 2015;43:D30–5. http://dx.doi.org/10.1093/nar/gku1216
8. Jackson B. Everything in sequence: listeriosis outbreak investigations in the era of WGS. Presented at: Integrated Foodborne Outbreak Response and Management (InFORM) 2015 Conference; Phoenix, AZ, USA; 2015 Nov 17–20.
9. Leekitcharoenphon P, Nielsen EM, Kaas RS, Lund O, Aarestrup FM. Evaluation of whole genome sequencing for outbreak detection of *Salmonella enterica*. PLoS ONE. 2014;9:e87991. http://dx.doi.org/10.1371/journal.pone.0087991

Address for correspondence: Jonathan S. Barkley, Rhode Island Department of Health, Center for Food Protection, 3 Capitol Hill, Rm 203, Providence, RI 02908-5097, USA; email: jonathan.barkley@health.ri.gov

April 2015: **Emerging Viruses**
Including:

- Reappearance of Chikungunya, Formerly Called Dengue, in the Americas
- Hantavirus Pulmonary Syndrome, Southern Chile, 1995–2012
- Animal-Associated Exposure to Rabies Virus among Travelers, 1997–2012
- Evolution of Ebola Virus Disease from Exotic Infection to Global Health Priority, Liberia, Mid-2014
- Population Structure and Antimicrobial Resistance of Invasive Serotype IV Group B Streptococcus, Toronto, Ontario, Canada
- Norovirus Genotype Profiles Associated with Foodborne Transmission, 1999–2012
- Sequence Variability and Geographic Distribution of Lassa Virus, Sierra Leone
- Deaths Associated with Respiratory Syncytial and Influenza Viruses among Persons ≥5 Years of Age in HIV-Prevalent Area, South Africa, 1998–2009
- Highly Pathogenic Avian Influenza A(H5N1) Virus Infection among Workers at Live Bird Markets, Bangladesh, 2009–2010
- Increased Risk for Group B Streptococcus Sepsis in Young Infants Exposed to HIV, Soweto, South Africa, 2004–2008
- La Crosse Virus in *Aedes japonicus japonicus* Mosquitoes in the Appalachian Region, United States
- Pathogenicity of 2 Porcine Deltacoronavirus Strains in Gnotobiotic Pigs
- Multidrug-Resistant *Salmonella enterica* Serotype Typhi, Gulf of Guinea Region, Africa

http://wwwnc.cdc.gov/eid/articles/issue/21/4/table-of-contents

Onchocerca lupi Nematodes in Dogs Exported from the United States into Canada

Guilherme G. Verocai,[1] Gary Conboy,
Manigandan Lejeune, Fany Marron, Paul Hanna,
Erin MacDonald, Brian Skorobohach,
Brian Wilcock, Susan J. Kutz, John S. Gilleard

The *Onchocerca lupi* nematode is an emerging helminth capable of infecting pets and humans. We detected this parasite in 2 dogs that were imported into Canada from the southwestern United States, a region to which this nematode is endemic. We discuss risk for establishment of *O. lupi* in Canada.

*O*nchocerca lupi is species of vectorborne nematode found in dogs, and rarely cats, which was recently recognized as an emerging zoonotic parasite in the United States and Old World countries in Europe and the Middle East (*1–3*). Infection in most cases in dogs and cats involves the eyes (*4–6*). Incidence of canine cases appears to be increasing; cases have been reported in Germany, Greece, Hungary, Portugal, Romania, Switzerland, and the United States (*2,5,6*). Only 3 cases of ocular onchocerciasis have been reported in cats: 2 in the United States and 1 in Portugal (*4,7*).

Human cases of infection with *O. lupi* nematodes have been reported Old World countries, including Albania, Crimea, Iran, Tunisia, and Turkey (*3,8–11*). All case-patients had ocular disease caused by subconjunctival nodules containing nematodes. In the United States, these nematodes are emerging zoonotic parasites, and cases are clustered in the southwest, a region to which canine onchocerciasis is endemic. In contrast with Old World zoonotic infections, all human cases in the United States are non-ocular. *O. lupi* nematodes have been found in masses compressing the cervical spinal canal of young children in Arizona and New Mexico (*1,11,12*). Additional human cases have been found in the same region (*13*).

Author affiliations: University of South Florida, Tampa, Florida, USA (G.G. Verocai); University of Calgary, Calgary, Alberta, Canada (G.G. Verocai, B. Skoroboach, S.J. Kutz, J.S. Gilleard); Atlantic Veterinary College, Charlottetown, Prince Edward Island, Canada (G. Conboy, F. Marron, P. Hanna); Canadian Wildlife Health Cooperative, Calgary (M. Lejeune, S.J. Kutz); Summerside Animal Hospital, Summerside, Prince Edward Island, Canada (E. MacDonald); Calgary Animal Referral and Emergency Centre, Calgary (B. Skoroboach); Histovet, Guelph, Ontario, Canada (B. Wilcock)

Little is known about the biology or epidemiology of this emerging zoonotic parasite. As with most *Onchocerca* species, black flies (Simuliidae) serve as biological vectors for *O. lupi*. To date, the only black fly species from which nematode DNA has been isolated is *Simulium tribulatum*, which is endemic to southern California (*5*). We report cases of canine ocular onchocerciasis in Canada.

The Study

In 2012 and 2014, respectively, 2 privately owned dogs with ocular disease were referred to veterinary practices in Canada. Both animals originated from the southwestern United States.

The first dog (dog A) was from Summerside, Prince Edward Island, in eastern Canada. This dog was a 3-year-old toy fox terrier purchased from a breeder in New Mexico and was taken to Canada months before its death from an unrelated cause (inflammatory bowel disease).

The second dog (dog B) was from Calgary, Alberta in western Canada. This dog was a 7-year-old female pit bull mixed breed that was obtained in Utah 2 years before it developed periodic swelling in the right eye that occurred over ≈1.5 years. This dog underwent surgery for removal of subconjunctival nodules. Two months after surgery, the dog had a friable nodule on the previously healthy left eye. This nodule was also surgically removed.

Adult nematodes were detected in histologic sections of both eyes and microfilaria were detected in skin from an ear of dog A. Nematodes were recovered from surgically removed nodules of dog B. Morphologic examination of nematodes from both dogs showed a cuticular pattern consistent with that of *O. lupi* nematodes, with 2 inner transverse striae per each interval between outer cuticular ridges (Figure 1). Histopathologic analysis of specimens from dog A showed nodular, lymphocytic, granulomatous, eosinophilic conjunctivitis, which is consistent with *O. lupi* nematode infection.

Genomic DNA was extracted from nematode fragments from dog B, and a 420-bp fragment of the mitochondrial NADH dehydrogenase subunit 5 gene was amplified by using PCR and sequenced by using described methods (*14*). Resulting sequences were phylogenetically compared with those of other *O. lupi* nematode isolates from the United States and Europe and other *Onchocerca* species by using MEGA6 (http://www.megasoftware.net/)
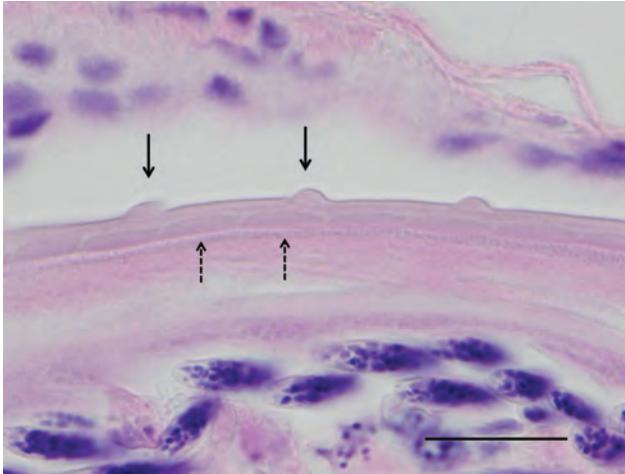
Figure 1. Histologic section of the eye of a dog infected with *Onchocerca lupi* nematodes, Summerside, Prince Edward Island, Canada. The typical *O. lupi* nematode cuticular pattern is shown, with 2 inner transverse striae (dashed arrows) within the interval between 2 outer cuticular ridges (solid arrows). Hematoxylin and eosin stain, original magnification ×100. Scale bar indicates 20 μm.

(Figure 2). Phylogenetic comparison confirmed species identity. All isolates from North America showed 100% similarity and differed by 1–6 bp from isolates from Portugal, Greece, and Hungary.

Conclusions

We confirmed through molecular and morphological approaches that *O. lupi* nematodes were the causative agent of canine ocular onchocerciasis in 2 dogs in Canada. Both dogs were imported from southwestern United States, which indicates the potential for international dog

transportation in contributing to introduction and establishment of zoonotic parasites in nonendemic areas.

The black fly *S. tribulatum*, a putative nematode vector in California (*5*), is widely distributed across the United States and Canada, including areas of southern Alberta, where Calgary is located (*15*). This fly is one of many species in the *S. vittatum* species complex and is also found in Prince Edward Island, Canada (*15*). The wide occurrence of the confirmed vector and related potential vectors in these areas of Canada and many areas of the United States reinforce the need for diagnosis and treatment of onchocerciasis before importation of dogs from disease-endemic areas.

The biology of *O. lupi* nematodes is poorly understood. However, theses nematodes appear to have a long life span. Consequently, microfilariae might be available for long periods (a few years) in skin of infected dogs. Available microfilariae might be ingested by competent black fly vectors, which will feed on the ubiquitous vertebrate hosts for *O. lupi* nematodes (e.g., dogs, cats, and humans) and thus pose a risk for establishment of the parasite in areas where it has been introduced. Clinical ocular cases are believed to occur in only a small portion of overall canine infections (*6*). Nonclinical cases, together with rare nonocular clinical cases, in dogs and potential wildlife reservoirs (e.g., wolves, coyotes) might make a larger contribution to the epidemiology of canine onchocerciasis.

Reappearance of an *O. lupi* nodule in the previously healthy eye of dog B ≈3 months after surgical removal of the first nodules remains enigmatic. Presumably, the second nodule was also caused by exposure in the United States. It seems unlikely that during the 2 years spent in Canada, dog B served as a source of infection for the local black flies,
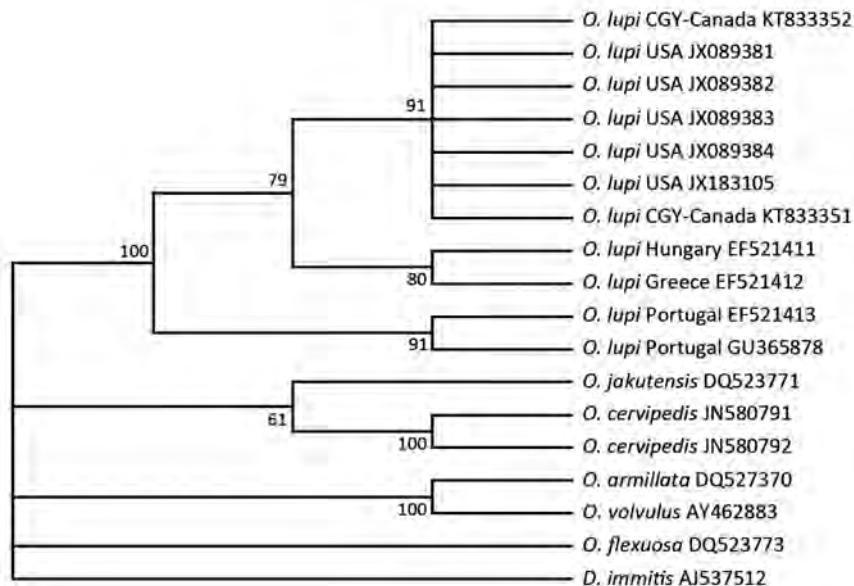
Figure 2. Phylogenetic relationship among the *Onchocerca lupi* nematode isolates from a dog in Calgary, Alberta, Canada (GeneBank accession nos. KT833351 and KT833352), and other filarial nematodes in the family *Onchocercidae* on the basis of the mitochondrial NADH dehydrogenase subunit 5 gene. The parsimonious tree depicts reciprocal monophyly of gene sequence derived from *O. lupi* nematodes from North America and Europe. Bootstrap consensus was inferred from 1,000 replicates. Values along branches are bootstrap values. Branches corresponding to <50% bootstrap replicates are collapsed. GenBank accession numbers are shown for all isolates. Analysis was performed by using MEGA 6 (http://www.megasoftware.net/). Canine heartworm (*Dirofilaria immitis*) was used as an outgroup.

which would have led to a second exposure of the same dog in Canada. We are not aware of any reports of local cases. Both dogs probably had long-term patent infections while in Canada. As adult dogs of active breeds, with a history of outdoor activities and travel, these 2 dogs might have been exposed to black flies during months of optimal environmental conditions for these vectors. Dog A traveled frequently to other parts of Canada and the United States as a show dog, including multiple trips in the spring/summer months.

A recent study hypothesized that *O. lupi* nematodes were recently introduced to the United States, possibly by dogs from Europe (*6*). Similarly, moving infected animals to areas of the United States and Canada to which *O. lupi* nematodes are not endemic might facilitate range expansion. Because purchase or adoption of pets from the United States is a common practice in Canada, additional clinical and nonclinical cases of canine onchocerciasis might be present in Canada, which would increase the risk for establishment of this zoonotic parasite.

Currently, diagnosis in dogs before onset of ocular disease would require recovery of microfilariae from a skin biopsy specimen. The unfamiliarity of diagnostic laboratories in North America with such testing and its unknown sensitivity make it unlikely that current infrastructure could effectively screen the number of dogs crossing the border to prevent introduction. The only current requirement for dog and cat importation into Canada by the Canadian Food Inspection Agency is having an up-to-date rabies immunization (http://www.inspection.gc.ca/animals/terrestrial-animals/imports/policies/live-animals/pets/eng/1326600389775/1326600500 578). Because suitable intermediate and definitive hosts of *O. lupi* nematodes are already present in Canada, there is an ongoing risk for the nematode to become established, which might be dependent on climatic and ecologic factors.

Dr. Verocai is an assistant research scientist and director of the Parasitology Diagnostic Laboratory in the Department of Infectious Diseases at the University of Georgia College of Veterinary Medicine, Athens, Georgia. His research interests include biodiversity, ecology, and genetics of parasites of veterinary and public health importance.

References

1. Eberhard ML, Ostovar GA, Chundu K, Hobohm D, Feiz-Erfan I, Mathison BA, et al. Zoonotic *Onchocerca lupi* infection in a 22-month-old child in Arizona: first report in the United States and a review of the literature. Am J Trop Med Hyg. 2013;88:601–5. http://dx.doi.org/10.4269/ajtmh.12-0733
2. Grácio AJ, Richter J, Komnenou AT, Grácio MA. Onchocerciasis caused by *Onchocerca lupi*: an emerging zoonotic infection. Systematic review. Parasitol Res. 2015;114:2401–13. http://dx.doi.org/10.1007/s00436-015-4535-7
3. Otranto D, Dantas-Torres F, Cebeci Z, Yeniad B, Buyukbabani N, Boral OB, et al. Human ocular filariasis: further evidence on the zoonotic role of *Onchocerca lupi*. Parasit Vectors. 2012;5:84. http://dx.doi.org/10.1186/1756-3305-5-84
4. Labelle AL, Daniels JB, Dix M, Labelle P. *Onchocerca lupi* causing ocular disease in two cats. Vet Ophthalmol. 2011;14:105–10. http://dx.doi.org/10.1111/j.1463-5224.2011.00911.x
5. Hassan HK, Bolcen S, Kubofcik J, Nutman TB, Eberhard ML, Middleton K, et al. Isolation of *Onchocerca lupi* in dogs and black flies, California, United States. Emerg Infect Dis. 2015;21:789–96. http://dx.doi.org/10.3201/eid2105.142011
6. Otranto D, Giannelli A, Latrofa MS, Dantas-Torres F, Trumble NS, Chavkin M, et al. Canine infections with *Onchocerca lupi* nematodes, United States, 2011–2014. Emerg Infect Dis. 2015;21:868–71. http://dx.doi.org/10.3201/eid2105.141812
7. Maia C, Annoscia G, Latrofa MS, Pereira A, Giannelli A, Pedroso L, et al. *Onchocerca lupi* nematode in cat, Portugal. Emerg Infect Dis. 2015;21:2252–4. http://dx.doi.org/10.3201/eid2112.150061
8. Ilhan HD, Yaman A, Morishima Y, Sugiyama H, Muto M, Yamasaki H, et al. *Onchocerca lupi* infection in Turkey: a unique case of a rare human parasite. Acta Parasitol. 2013;58:384–8. http://dx.doi.org/10.2478/s11686-013-0152-8
9. Otranto D, Sakru N, Testini G, Gurlu VP, Yakar K, Lia RP, et al. Case report: first evidence of human zoonotic infection by *Onchocerca lupi* (Spirurida, Onchocercidae). Am J Trop Med Hyg. 2011;84:55–8. http://dx.doi.org/10.4269/ajtmh.2011.10-0465
10. Mowlavi G, Farzbod F, Kheirkhah A, Mobedi I, Bowman DD, Naddaf SR. Human ocular onchocerciasis caused by *Onchocerca lupi* (Spirurida, Onchocercidae) in Iran. J Helminthol. 2014;88:250–5. http://dx.doi.org/10.1017/S0022149X13000060
11. Chen T, Moon K, deMello DE, Feiz-Erfan I, Theodore N, Bhardwaj RD. Case report of an epidural cervical *Onchocerca lupi* infection in a 13-year-old boy. J Neurosurg Pediatr. 2015;16:217–21. http://dx.doi.org/10.3171/2014.12.PEDS14462
12. Dudley RW, Smith C, Dishop M, Mirsky D, Handler MH, Rao S. A cervical spine mass caused by *Onchocerca lupi*. Lancet. 2015;386:1372. http://dx.doi.org/10.1016/S0140-6736(14)62255-8
13. Cantey PT, Weeks J, Edwards M, Rao S, Ostovar GA, Dehority W, et al. The emergence of zoonotic *Onchocerca lupi* infection in the United States: a case-series. Clin Infect Dis. 2016;62:778–83. http://dx.doi.org/10.1093/cid/civ983
14. McFrederick QS, Haselkorn TS, Verocai GG, Jaenike J. Cryptic *Onchocerca* species infecting North American cervids, with implications for the evolutionary history of host association in *Onchocerca*. Parasitology. 2013;140:1201–10. http://dx.doi.org/10.1017/S0031182012001758
15. Adler PH, Currie DC, Wood M. The black flies (Simuliidae) of North America. New York: Comstock Books; 2004.

Address for correspondence: Guilherme G. Verocai, Department of Infectious Diseases, College of Veterinary Medicine, University of Georgia, Athens, GA 30602, USA; email: gverocai@gmail.com

Baylisascaris procyonis–Associated Meningoencephalitis in a Previously Healthy Adult, California, USA

Charles Langelier, Michael J. Reid, Cathra Halabi,
Natalie Wietek, Alejandro LaRiviere,
Maulik Shah, Michael R. Wilson,
Peter Chin-Hong, Vanja Douglas,
Kevin R. Kazacos, Jennifer M. Babik

After severe neurocognitive decline developed in an otherwise healthy 63-year-old man, brain magnetic resonance imaging showed eosinophilic meningoencephalitis and enhancing lesions. The patient tested positive for antibodies to *Baylisascaris* spp. roundworms, was treated with albendazole and dexamethasone, and showed improvement after 3 months. Baylisascariasis should be considered for all patients with eosinophilic meningitis.

Over the past 30 years, the raccoon-associated roundworm *Baylisascaris procyonis* has emerged as an uncommon but noteworthy human pathogen associated with devastating eosinophilic meningoencephalitis in 25 patients (*1–4*). We report a case of neural larva migrans in an otherwise generally healthy man in California, USA.

Case Report

On May 18, 2015, a 63-year-old man was hospitalized in Humboldt County, California, after 2 weeks of fatigue, memory impairment, and progressive confusion accompanied by right-sided occipital headache and right-sided allodynia involving his arm and head. He was confused and disoriented to date but could recognize family; engage in brief, logical conversations; and walk independently. His medical history included essential thrombocytosis, hypothyroidism, and a remote episode of shingles. Vital signs were normal; physical examination showed no focal abnormalities. His complete blood count showed a leukocyte count of 11.5×10^9 cells/L (reference range 3.4–10 $\times 10^9$ cells/L), eosinophil count of 0.75×10^9 cells/L (reference range $<0.4 \times 10^9$ cells/L), and neutrophil count of 6.1×10^9/L (reference range 1.8–6.8 $\times 10^9$ cells/L).

Author affiliations: University of California, San Francisco, California, USA (C. Langelier, M.J. Reid, C. Halabi, N. Wietek, A. LaRiviere, M. Shah, M.R. Wilson, P. Chin-Hong, V. Douglas, J.M. Babik); Purdue University College of Veterinary Medicine, West Lafayette, Indiana, USA (K.R. Kazacos)

Chemistry and liver panel results were normal. A brain magnetic resonance imaging (MRI) demonstrated no intracranial pathology. Cerebrospinal fluid (CSF) showed a leukocyte count of 183×10^9 cells/L (60% lymphocytes, 27% monocytes, 9% eosinophils, 4% neutrophils); protein level of 155 mg/dL; and glucose level of 45 mg/dL (Figure 1). He was started on empiric vancomycin, ceftriaxone, and acyclovir.

Over the next 3 days, the patient sustained precipitous cognitive and functional declines; incontinence, right-sided facial droop, dysarthria, diffuse hyperreflexia, and ataxia developed. Initial infectious disease diagnostics returned negative results (Table 1), so antimicrobial drugs were discontinued. CSF analysis on day 11 showed persistent pleocytosis and marked elevation of eosinophils to 34% (Figure 1). CSF cytologic and flow cytometric testing showed no malignant cells but did show reactive lymphocytes and many eosinophils, consistent with chronic inflammation.

A brain MRI on day 13 showed new nodular enhancement at the gray–white junction (Figure 2, panels A–D) and patchy T2 signal abnormalities in the cerebellar, pontine, and supratentorial white matter. Due to progressive severe functional and cognitive decline, an unclear diagnosis, and concerning MRI abnormalities, the patient was transferred on day 15 to the University of California San Francisco Medical Center for evaluation. Upon transfer, he was lethargic and had moderate global aphasia and echolalia, a left forehead–sparing facial droop, spasticity in the arms, diffuse hyperreflexia, and mute plantar responses.

Additional history from his family revealed that the patient had worked as a contractor for >40 years in northern California. Several weeks before symptom onset, he had completed a project under his house, where raccoons and a skunk had been observed, and he had spent significant time working in a rural area with suspected raccoon activity. His occupation necessitated routine contact with soil, dust, and yard debris, and his wife said he regularly ate lunch at job sites without washing his hands. The patient was an avid hunter and had consumed bear meat 3 months before symptom onset.

Based on the patient's exposure history, we considered infection with *Baylisascaris*, *Toxocara*, *Trichinella*, *Coccidioides*, or other microbial pathogens (Table 1).
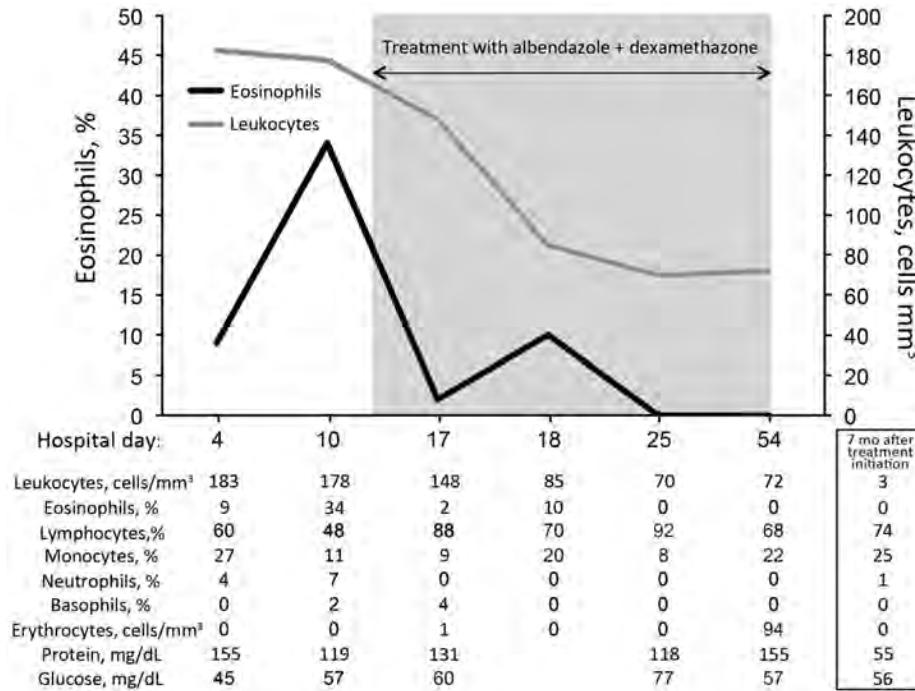
Figure 1. Cell counts and laboratory values in cerebrospinal fluid from a previously healthy adult with *Baylisascaris* meningoencephalitis, California, USA. Hospital day 4 was June 1, 2015; hospital day 54 was July 25, 2015. Samples for 7-month values were obtained on January 1, 2016.

Hospital day:	4	10	17	18	25	54	7 mo after treatment initiation
Leukocytes, cells/mm³	183	178	148	85	70	72	3
Eosinophils, %	9	34	2	10	0	0	0
Lymphocytes,%	60	48	88	70	92	68	74
Monocytes, %	27	11	9	20	8	22	25
Neutrophils, %	4	7	0	0	0	0	1
Basophils, %	0	2	4	0	0	0	0
Erythrocytes, cells/mm³	0	0	1	0	0	94	0
Protein, mg/dL	155	119	131	60	118	155	55
Glucose, mg/dL	45	57	60		77	57	56

Because of the patient's rapid neurologic decline, we initiated albendazole (20 mg/kg/d, given in doses every 12 h) and dexamethasone (4 mg every 6 h) on day 17 for empiric treatment of baylisascariasis or other helminth infection;

we also initiated empiric fluconazole and doxycycline. His neurologic symptoms stabilized 1 week later.

On day 17, serum and CSF samples were sent to the Centers for Disease Control and Prevention (Atlanta,

Table 1. Microbiologic diagnostics obtained during testing of a previously healthy patient with *Baylisascaris* meningoencephalitis, California, USA*

Diagnostic study	Site	Result
Bacterial cultures ×4	Blood and CSF	Negative
Coxiella antibody	Blood	Negative
Bartonella henselae and *B. quintana* antibodies	Blood	Negative
Mycoplasma antibody	Blood	IgM negative, IgG 1:5
Rickettsial antibody panel	Blood	Negative
Venereal Disease Research Laboratory test	CSF	Negative
Lyme disease antibody	CSF	Negative
Cytomegalovirus PCR	CSF	Negative
Epstein–Barr virus PCR	CSF	Negative
Enterovirus PCR	CSF	Negative
Herpes simplex virus PCR	CSF	Negative
Lymphocytic choriomeningitis virus IgM, IgG	CSF	IgM 1:2, IgG negative†
Varicella zoster virus PCR, IgM, IgG	CSF	Negative
West Nile virus IgM, IgG	CSF	Negative
Baylisascaris antibody	Blood and CSF	Positive
Strongyloides antibody	Blood	Negative
Trichinella antibody	Blood	Negative
Toxocara antibody	Blood	Negative
Toxoplasma antibody	Blood	Negative
Ova and parasite stain	CSF	Negative
Fungal stains and cultures ×4	Blood and CSF	Negative
Coccidiodes antibody by complement fixation	Blood and CSF	Negative
Coccidiodes antibody by immunodiffusion	Blood	Negative
Cryptococcal antigen	Blood and CSF	Negative
AFB stains and cultures ×4	CSF	Negative
Broad-range PCR (bacteria, fungi, AFB)	CSF	Negative
Cytology	CSF	Chronic inflammation

*AFB, acid-fast bacilli; CSF, cerebrospinal fluid.
†A low-titer IgM for lymphocytic choriomeningitis virus was considered to be a false-positive result.
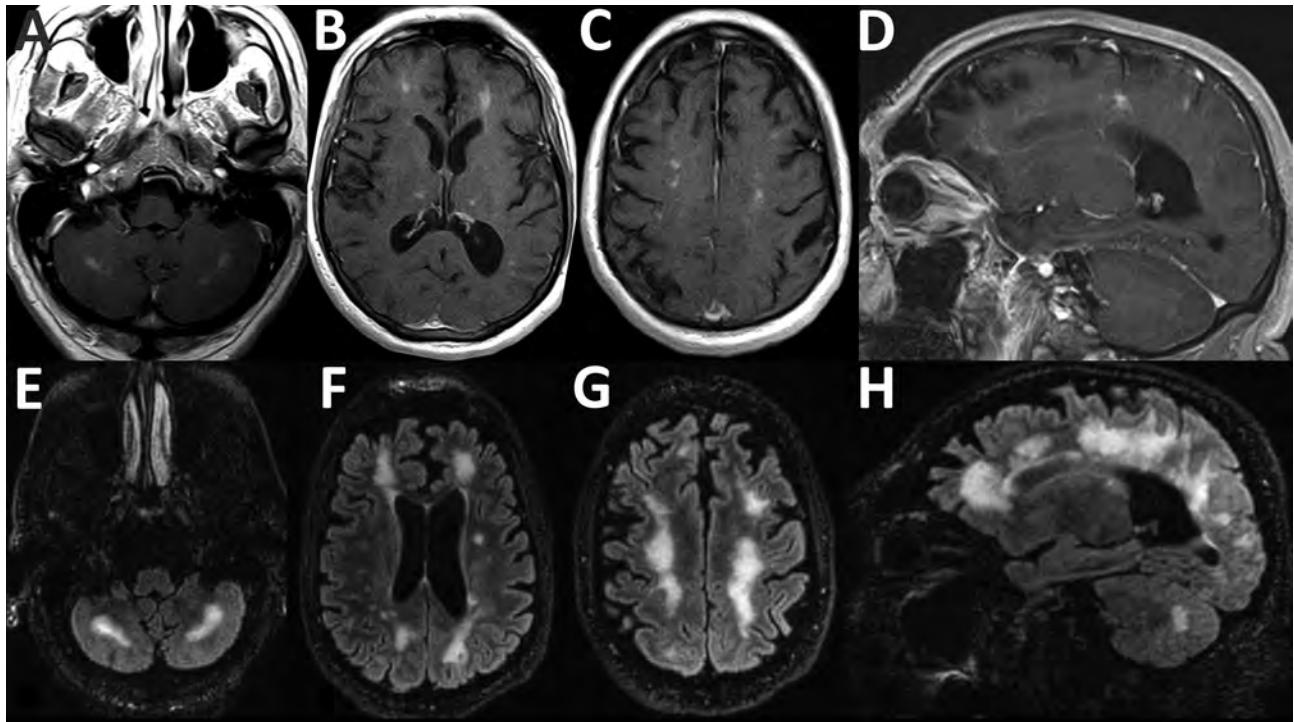
Figure 2. Magnetic resonance imaging scans showing brain abnormalities in a previously healthy adult with *Baylisascaris* meningoencephalitis, California, USA. A–D) Postgadolinium contrast T1 images obtained 4 weeks after symptom onset. A–C) Axial images, moving inferiorly to superiorly, demonstrating nodular bilateral enhancement within the cerebellar hemispheres, thalami, and subcortical white matter. D) Sagittal image further demonstrates multifocal areas of enhancement in cerebral hemispheres. Additional, mild T2 abnormalities (not shown) were present at the same time. E–H) T2/FLAIR (fluid attenuation inversion recovery) images obtained 6 weeks after symptom onset. E–G) Axial images, moving inferiorly to superiorly, demonstrating patchy and confluent hyperintense lesions throughout the supratentorial white matter and cerebellum. H) Sagittal image further demonstrates the high degree of white matter abnormality, which was not present on the earlier imaging. Postcontrast enhancement on T1 imaging (not shown) had nearly resolved at this time.

GA, USA) for *Baylisascaris procyonis* immunoassay testing. This test uses a recombinant BpRAG1 antigen and has a sensitivity of 88% and specificity of 98% (*5*). Thirteen days later, the results showed *B. procyonis* antibodies in the serum and CSF samples; results for all other studies were negative (Table 1). Repeat brain MRI on day 29 showed progression of white matter hyperintensity, near complete resolution of enhancement, and

mild atrophy (Figure 2, panels E–H). The patient began to show slow, but tangible, improvement in neurologic function after 4 weeks on albendazole and dexamethasone. This combination was continued for 6 weeks, after which albendazole was stopped and a 12-week dexamethasone taper was initiated. By 3 months, the patient had recovered orientation to person and place and limited motor coordination. After 7 months, he could walk with

Table 2. Cases of cerebrospinal fluid infection with *Baylisascaris* spp. roundworms in adults and adolescents, United States and Canada, 1986–2015

Year	Patient age, y	Location	Risk factor(s)	Treatment	Outcome	Reference
1986	21	Oregon, USA	Developmental delay and geophagia	Not recorded	Persistent residual deficits	(*7*)
2000	17	California, USA	Developmental delay and geophagia	Albendazole and antiinflammatory drugs	Died	(*8*)
2007	17	Oregon, USA	Altered mentation from drug abuse	None	Aphasia and memory deficits	(*9*)
2009	54	Missouri, USA	Intellectual disability; eating food scraps from public garbage cans	None	Died	(*10*)
2012	73	British Columbia, Canada	Dementia	None	Identified at time of autopsy	(*11*)
2015	63	California, USA	Home or occupational exposure	Albendazole (20 mg/kg/d) + dexamethasone (1 mg/kg/d)	Partial recovery after 6 weeks	This report

assistance, engage in simple conversations, and perform basic activities of daily living. At that time, CSF showed normalized cell counts (Figure 1).

Most *B. procyonis* roundworm infections occur in young children because their frequency of oral exploration predisposes children to ingestion of infective eggs (*1–6*). However, *B. procyonis* infections have been reported in 3 adults and 2 teenagers (*7–11*). Of note, those 5 patients had preexisting neuropsychiatric conditions that predisposed them to ingestion of infective eggs via geophagic pica (Table 2) (*7–11*). In the case we report, the patient had no predisposing condition, but he probably had occupational exposure, potentiated by insufficient hand hygiene, to raccoon feces.

Most symptomatic cases of neural larva migrans caused by infection with *Baylisascaris* roundworms have resulted in irreversible neurologic damage, and 5 deaths have been reported (*1–3*). Partial to complete recovery occurred in 4 cases, presumably due to a low level of infection at the time of diagnosis, early aggressive treatment, or both (*9,12–14*).

Because the differential diagnosis for eosinophilic meningitis is relatively restricted, we principally considered infectious etiologies consistent with the patient's demographics and exposure history. His risk factors associated with an infectious etiology included living and working near a region where *Coccidioides immitis* is endemic and exposure to raccoon-associated *Baylisascaris* roundworms. For this patient, MRI findings similar to those for other *B. procyonis*–infected patients included subcortical nodular enhancement and linear hyperintensities in the cerebellar white matter on T1- and T2-weighted images (Figure 2) (*14*).

The optimal treatment for baylisascariasis in adults is not known; the current recommendation for albendazole (25–50 mg/kg/d) comes from successful empiric regimens used in children (http://www.cdc.gov/parasites/baylisascaris/health_professionals/index.html#tx). Albendazole is the cornerstone of therapy for *B. procyonis* neural larva migrans and is combined with a corticosteroid to enhance central nervous system (CNS) penetration and mitigate inflammation-associated tissue necrosis (*3,4,15*). Due to low CNS penetration, ivermectin is ineffective for treating *B. procyonis* neural larva migrans (*1,3*). Despite treatment, outcomes are often poor because extensive CNS inflammatory damage and tissue necrosis usually occurs before diagnosis (*3,4,6*); thus, early recognition of baylisascariasis and prompt initiation of treatment are essential. Because of concern for adverse side effects, including agranulocytosis and hepatotoxicity, we used a 6-week regimen of albendazole plus dexamethasone. We observed reversal of disease progression and a modest neurocognitive recovery after 3 months.

Conclusions

This case demonstrates that severe neurologic disease from infection with *B. procyonis* roundworms can develop in otherwise healthy adults with incidental exposures. The patient in this report had no history of overt immune compromise and few concurrent conditions and was generally well until the inadvertent ingestion of occult *B. procyonis* eggs. This case highlights the importance of considering baylisascariasis in all patients with eosinophilic meningitis, and it underscores the importance of obtaining a detailed exposure history, understanding the causes of eosinophilic meningitis, and initiating early aggressive therapy when infection is suspected.

References

1. Kazacos KR. *Baylisascaris* and related species. In: Samuel WM, Pybus MJ, Kocan AA, editors. Parasitic diseases of wild mammals, 2nd ed. Ames (IA): State University Press; 2001. p. 301–41.
2. Murray WJ, Kazacos KR. Raccoon roundworm encephalitis. Clin Infect Dis. 2004;39:1484–92. http://dx.doi.org/10.1086/425364
3. Gavin PJ, Kazacos KR, Shulman ST. Baylisascariasis. Clin Microbiol Rev. 2005;18:703–18. http://dx.doi.org/10.1128/CMR.18.4.703-718.2005
4. Kazacos KR, Jelicks LA, Tanowitz HB. *Baylisascaris* larva migrans. Handb Clin Neurol. 2013;114:251–62. http://dx.doi.org/10.1016/B978-0-444-53490-3.00020-0
5. Rascoe LN, Santamaria C, Handali S, Dangoudoubiyam S, Kazacos KR, Wilkins PP, et al. Interlaboratory optimization and evaluation of a serological assay for diagnosis of human baylisascariasis. Clin Vaccine Immunol. 2013;20:1758–63. http://dx.doi.org/10.1128/CVI.00387-13
6. Kazacos KR. Protecting children from helminthic zoonoses. Contemp Pediatr. 2000;17(Suppl):1–24.
7. Cunningham CK, Kazacos KR, McMillan JA, Lucas JA, McAuley JB, Wozniak EJ, et al. Diagnosis and management of *Baylisascaris procyonis* infection in an infant with nonfatal meningoencephalitis. Clin Infect Dis. 1994;18:868–72. http://dx.doi.org/10.1093/clinids/18.6.868
8. Kazacos KR, Gavin PJ, Shulman ST, Tan TQ, Gerber SI, Kennedy WA, et al. Raccoon roundworm encephalitis—Chicago, Illinois, and Los Angeles, California. MMWR Morb Mortal Wkly Rep. 2002;50:1153–5.
9. Chun CS, Kazacos KR, Glaser C, Bardo D, Dangoudoubiyam S, Nash R. Global neurologic deficits with baylisascaris encephalitis in a previously healthy teenager. Pediatr Infect Dis J. 2009;28:925–7. http://dx.doi.org/10.1097/INF.0b013e3181a648f1
10. Ciarlini P, Gutierrez Y, Gambetti P, Cohen M. Necrotizing eosinophilic meningoencephalitis. Presented at the 87th Annual Meeting of the American Association of Neuropathologists; 2011 Jun 23–26; Seattle, WA, USA.

11. Hung T, Neafie RC, Mackenzie IRA. *Baylisascaris procyonis* infection in elderly person, British Columbia, Canada. Emerg Infect Dis. 2012;18:341–2. http://dx.doi.org/10.3201/eid1802.111046

12. Pai PJ, Blackburn BG, Kazacos KR, Warrier RP, Bégué RE. Full recovery from *Baylisascaris procyonis* eosinophilic meningitis. Emerg Infect Dis. 2007;13:928–30. http://dx.doi.org/10.3201/eid1306.061541

13. Hajek J, Yau Y, Kertes P, Soman T, Laughlin S, Kanani R, et al. A child with raccoon roundworm meningoencephalitis: a pathogen emerging in your own backyard? Can J Infect Dis Med Microbiol. 2009;20:e177–80. http://dx.doi.org/10.1155/2009/304625

14. Peters JM, Madhavan VL, Kazacos KR, Husson RN, Dangoudoubiyam S, Soul JS. Good outcome with early empiric treatment of neural larva migrans due to *Baylisascaris procyonis.* Pediatrics. 2012;129:e806–11. http://dx.doi.org/10.1542/peds.2011-2078

15. Centers for Disease Control and Prevention. Parasites—*Baylisascaris* infection. Resources for health professionals [cited 2016 Feb 1]. http://www.cdc.gov/parasites/baylisascaris/health_professionals/index.html#tx

Address for correspondence: Charles Langelier, University of California San Francisco, Division of Infectious Diseases, 513 Parnassus Ave, Rm S-380, San Francisco, CA 94143, USA; email: chaz.langelier@ucsf.edu

January 2016: Sexually Transmitted Infections

Including:

- Asymptomatic Lymphogranuloma Venereum in Men who Have Sex with Men, United Kingdom

- Waterborne *Elizabethkingia meningoseptica* in Adult Critical Care

- Human Papillomavirus Vaccination at a Time of Changing Sexual Behavior

- Multiorgan WU Polyomavirus Infection in Bone Marrow Transplant Recipient

- Multifacility Outbreak of Middle East Respiratory Syndrome in Taif, Saudi Arabia

- Falling *Plasmodium knowlesi* Malaria Death Rate among Adults despite Rising Incidence, Sabah, Malaysia, 2010–2014
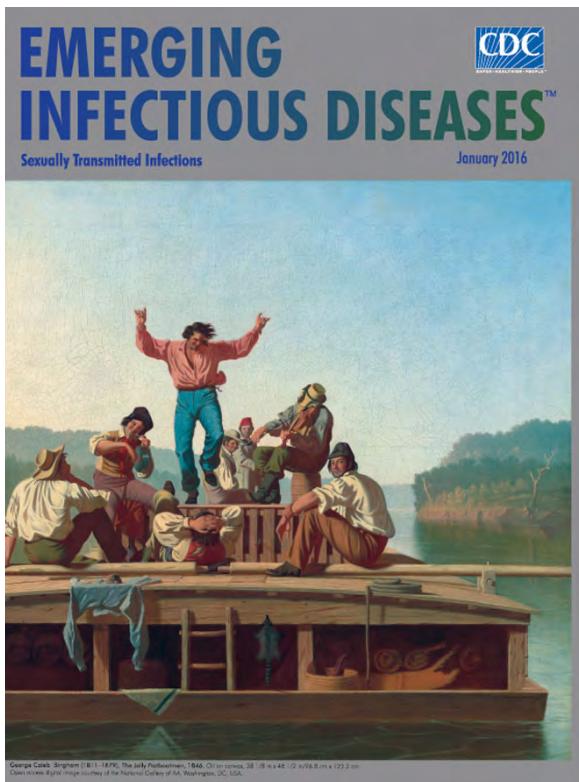
- Epidemiology of *Haemophilus ducreyi* Infections

- Risk Factors for Primary Middle East Respiratory Syndrome Coronavirus Illness in Humans, Saudi Arabia, 2014

- Human Papillomavirus Prevalence and Herd Immunity after Introduction of Vaccination Program, Scotland, 2009–2013

- Porcine Epidemic Diarrhea Virus and Discovery of a Recombinant Swine Enteric Coronavirus, Italy

- Increase in Sexually Transmitted Infections among Men Who Have Sex with Men, England, 2014

- Seroepidemiology of Human Enterovirus 71 Infection among Children, Cambodia

- Outbreak of Panton-Valentine Leukocidin–Associated Methicillin-Susceptible *Staphylococcus aureus* Infection in a Rugby Team, France, 2010–2011

http://wwwnc.cdc.gov/eid/articles/issue/22/01/table-of-contents

Human Tick-Borne Encephalitis and Characterization of Virus from Biting Tick

Anna J. Henningsson, Richard Lindqvist, Peter Norberg, Pontus Lindblom, Anette Roth, Pia Forsberg, Tomas Bergström, Anna K. Överby, Per-Eric Lindgren

We report a case of human tick-borne encephalitis (TBE) in which the TBE virus was isolated from the biting tick. Viral growth and sequence were characterized and compared with those of a reference strain. Virus isolation from ticks from patients with TBE may offer a new approach for studies of epidemiology and pathogenicity.

Tick-borne encephalitis (TBE), a notable public health problem in many parts of Europe and Asia (*1*), is a severe infection affecting the central nervous system that may cause death or long-term illness (*2*). Most available sequences of the European TBE virus (TBEV) are derived from ticks, because the virus is rarely isolated from patients, and clinical samples generally are PCR negative at onset of neurologic symptoms (*3–5*). This situation hampers TBEV molecular studies. Furthermore, data are limited on viral transmission from ticks to humans. We describe a human case of TBE in Sweden and isolation and characterization of the TBEV isolated from the biting tick.

Case Report

On August 18, 2011, a 67-year-old man in Habo, Jönköping County, Sweden, noticed a tick bite on his foot (Figure 1). When he visited his primary healthcare center the same day, he was included a study of tickborne diseases (*6,7*); ethical approval was given by the Regional Ethics Committee, Linköping, Sweden, M132-06. He donated the tick and a blood sample and filled out a questionnaire. On August 20, 2011, the patient experienced fever, neck pain, and myalgia. On August 23, he again visited his primary health center with a temperature of 38°C. Lyme borreliosis was suspected, and doxycycline (200 mg/d for 10 d) was prescribed. After 3 days, the fever disappeared.

Author affiliations: Region Jönköping County, Jönköping, Sweden (A.J. Henningsson, P.-E. Lindgren); Umeå University, Umeå, Sweden (R. Lindqvist, A.K. Överby); University of Gothenburg, Gothenburg, Sweden (P. Norberg, A. Roth, T. Bergström); Linköping University, Linköping, Sweden (P. Lindblom, P. Forsberg, P.-E. Lindgren); Linköping University Hospital, Linköping (P. Forsberg)

On September 4, the fever returned and the patient felt dizzy and experienced leg weakness. The following day, he returned to his primary health center with a temperature of 39°C, difficulty walking, and a severe headache. He was referred to the hospital, where a lumbar puncture was performed; cerebrospinal fluid (CSF) analysis revealed pleocytosis.

The patient was hospitalized for 10 days. He had difficulty walking, a headache, and pronounced fatigue but remained mentally lucid. Results of neurologic examination were normal in all other respects. Test results revealed high levels of serum TBEV IgM and IgG. He had not been vaccinated for TBE or yellow fever. CSF analyses for bacterial culture, *Borrelia burgdorferi* antibodies, varicella zoster virus DNA, and herpes simplex virus DNA were negative. The patient was discharged from the hospital on September 14 because his condition had improved. At a follow-up visit on October 28, he felt completely recovered, and a neuropsychiatric test showed no cognitive sequelae.

For study purposes, we obtained serum/plasma samples from the patient at inclusion in the tickborne disease study on August 18 and serum/plasma and CSF samples at hospital admission on September 5. We also obtained serum/plasma samples 2.5 months later. All samples were stored at -80°C. We analyzed TBEV antibodies in serum and CSF (IMMUNOZYM FSME [TBE] IgG and IgM; PROGEN Biotechnik GmbH, Heidelberg, Germany). In the serum samples from August 18, we could not detect any TBEV antibodies. The serum obtained on September 5 had high levels of TBEV IgG (368 Vienna units (VIEU)/mL) and IgM (571 VIEU/mL). No TBEV antibodies were detected in CSF. In the serum collected on October 28, the IgG titer had increased (>650 VIEU/mL), but IgM was not detectable.

TBEV quantitative PCR (qPCR) was performed as described (*7*) on all serum/plasma and CSF samples from the patient. TBEV RNA was not detectable in patient samples; however, no sample was obtained during the patient's first fever episode, the assumed viremic phase.

We bisected the tick (*Ixodes ricinus* nymph) obtained from the patient using a sterile scalpel and extracted RNA from one half of it. TBEV was quantified by using qPCR (*7*), and high levels of TBEV RNA (>10^7 copies) were detected. This result prompted us to isolate the new TBEV strain, tick/SWE/Habo/2011/1, directly from the tick, characterize its growth properties in cell culture, and sequence its genome.
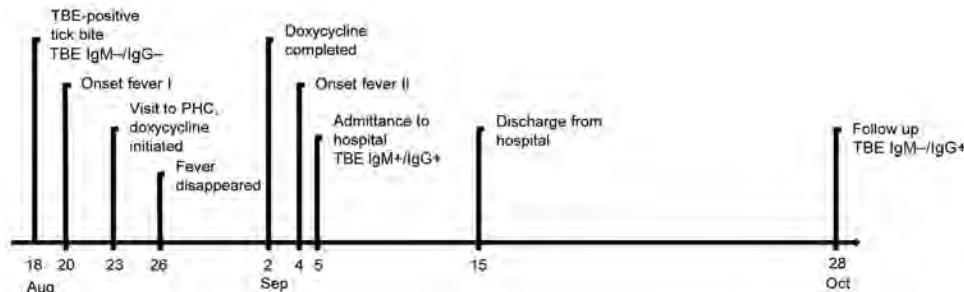
Figure 1. Time course of tick-borne encephalitis (TBE) in a 67-year-old man in Sweden, 2011. A classic biphasic onset of symptoms is shown. PHC, primary healthcare center.

The other half of the tick was homogenized in inoculation media (Dulbecco modified Eagle medium, 10X penicillin/streptomycin, 2% fetal calf serum, and 20 mM HEPES buffer) by FastPrep-24 (MP Biomedicals, Santa Ana, CA, USA) using lysing matrix A. After the mixture was centrifuged, we used the supernatant to inoculate Vero B4 African green monkey kidney cells. At 1 hour postinfection, cells were washed 3 times with inoculation media before infection media were added (Dulbecco modified Eagle medium, 1X penicillin/streptomycin, 2% fetal calf serum, and 20 mM HEPES buffer). The TBEV was harvested when cells showed cytopathic effects. Virus titers were determined by using a focus-forming assay (8).

A549 cells were infected with tick/SWE/Habo/2011/1 or Hypr 71 (9) at multiplicity of infection 0.1. Total RNA was extracted at different time points, and virus titers were determined with a focus-forming assay. Viral RNA was detected as previously described (10,11) (Figure 2). Tick/SWE/Habo/2011/1 replication was similar to that of the cell culture-adapted, highly pathogenic reference strain Hypr, originally isolated in Czechoslovakia from human blood (9). Progeny particle levels, however, were very different, indicating tick/SWE/Habo/2011/1 was less virulent.

We performed nucleotide sequencing of tick/SWE/Habo/2011/1 using 2 assays. First, deep sequencing was performed on the virus isolate. RNA was extracted from viral stock and real-time reverse transcription PCR was performed (12). The libraries were prepared by using modified TruSeq RNA Library Preparation Kit version 2 (Illumina, Inc., San Diego, CA, USA) and sequenced using MiSeq Desktop Sequencer (Illumina). De novo assembly was performed with Velvet algorithms (13), and a sequence of 10,899 nt was obtained. In the second assay, the strain was sequenced directly from PCR amplicons of RNA extracted from the tick (14) and yielded a sequence of 3,382 nt (nt 38–3,419). Sequences were submitted to GenBank under accession no. KU923573.

When we compared the 2 sequences from these assays, we found homologous sequences even though 2 approaches and techniques had been used and the possibility that isolation in cell culture might constitute a selection. Results demonstrated a difference of 9 nt, all insertion/deletion mutations, between the deep-sequenced virus isolate from cell culture and the PCR-derived sequence obtained directly from the tick. Because any of these differences would lead to frame shifts in the genome, and such changes could not be detected in reference sequences of European TBEV strains, the insertion/deletion mutations most likely were artifacts. When we removed all gaps in the sequence alignment, the sequences were identical over the 3,382 nt. In addition to a comparison of 2 sequence methods, this result suggests that virus isolation did not introduce a selection bias in regard to the compared nucleotide sequences.

Figure 2. Time course of tick-borne encephalitis virus (TBEV) multiplication from sample from a 67-year-old man in Sweden, 2011. A549 cells were infected with the virus isolated from the tick in this study, tick/SWE/Habo/2011/1, and reference strain Hypr at multiplicity of infection 0.1. Total cellular RNA and cell culture supernatants were collected at different time points postinfection. A) Intracellular levels of viral RNA quantified by real-time reverse

transcription PCR analysis. B) Virus titers in cell culture supernatants as determined by focus-forming assay (FFU). Mean values from 3 independent experiments are shown; error bars indicate SD. p values determined by Student *t* test.
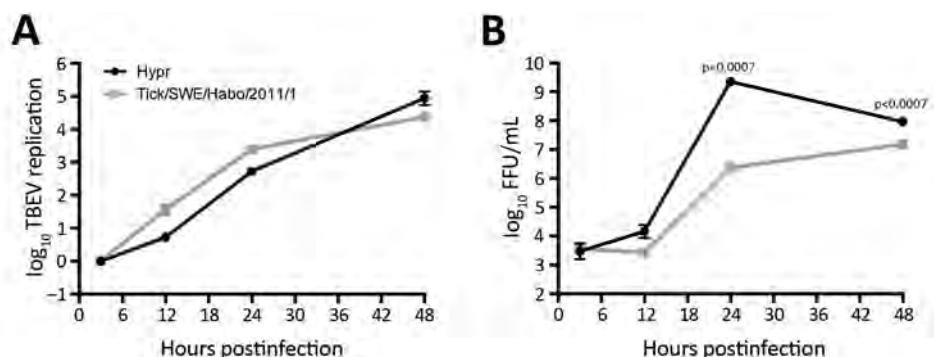
Conclusions

Data on molecular epidemiology and TBEV transmission from ticks to humans are limited. This study shows that tick bites can cause TBE, confirming earlier epidemiologic associations. The median time between the tick bite and onset of the initial symptoms has previously been reported to be 8 days (range 4–28 days) (15). This case shows a shorter incubation period of 2 days, possibly because of a high viral load in the tick or because the TBEV strain was highly virulent. However, when growth characteristics were compared with those of the highly pathogenic Hypr strain, Hypr produced 1.000-fold more virus at 24 hours postinfection. The patient recovered without sequelae, which also indicates moderate virulence of the identified strain, tick/SWE/Habo/2011/1. TBE diagnosis was serologically confirmed, but unfortunately, TBEV could not be isolated from the patient samples, which has also been the case in previous studies (4,5).

Our findings demonstrate a strong link between a TBEV-infected tick and a patient with TBE, with an incubation time of only 2 days. PCR amplification, virus isolation, and genetic sequencing of TBEV from ticks detached from persons in whom TBE later develops may be a novel tool for studies of epidemiology and pathogenicity of this virus, which is difficult to isolate from patient samples.

Acknowledgments

Dr. Henningsson is a specialist in infectious diseases and clinical microbiology. She has pursued research in the field of tickborne diseases in close collaboration with Linköping University for more than 10 years.

References

1. World Health Organization. Vaccines against tick-borne encephalitis: WHO position paper. Wkly Epidemiol Rec. 2011; 86:241–56.
2. Haglund M, Günther G. Tick-borne encephalitis—pathogenesis, clinical course and long-term follow-up. Vaccine. 2003;21(Suppl. 1):S11–8. http://dx.doi.org/10.1016/S0264-410X(02)00811-3
3. Puchhammer-Stöckl E, Kunz C, Mandl CW, Heinz FX. Identification of tick-borne encephalitis virus ribonucleic acid in tick suspensions and in clinical specimens by a reverse-transcription-nested polymerase chain reaction assay. Clin Diagn Virol. 1995;4:321–6. http://dx.doi.org/10.1016/0928-0197(95)00022-4
4. Haglund M, Vene S, Forsgren M, Günther G, Johansson B, Niedrig M, et al. Characterisation of human tick-borne encephalitis virus from Sweden. J Med Virol. 2003;71:610–21. http://dx.doi.org/10.1002/jmv.10497
5. Saksida A, Duh D, Lotric-Furlan S, Strle F, Petrovec M, Avsic-Zupanc T. The importance of tick-borne encephalitis virus RNA detection for early differential diagnosis of tick-borne encephalitis. J Clin Virol. 2005;33:331–5. http://dx.doi.org/10.1016/j.jcv.2004.07.014
6. Wilhelmsson P, Fryland L, Börjesson S, Nordgren J, Bergström S, Ernerudh J, et al. Prevalence and diversity of *Borrelia* species in ticks that have bitten humans in Sweden. J Clin Microbiol. 2010;48:4169–76. http://dx.doi.org/10.1128/JCM.01061-10
7. Lindblom P, Wilhelmsson P, Fryland L, Sjöwall J, Haglund M, Matussek A, et al. Tick-borne encephalitis virus in ticks detached from humans and follow-up of serological and clinical response. Ticks Tick-borne Dis. 2014;5:21–8. http://dx.doi.org/10.1016/j.ttbdis.2013.07.009
8. Overby AK, Popov VL, Niedrig M, Weber F. Tick-borne encephalitis virus delays interferon induction and hides its double-stranded RNA in intracellular membrane vesicles. J Virol. 2010;84:8470–83. http://dx.doi.org/10.1128/JVI.00176-10
9. Klockmann U, Krivanec K, Stephenson J, Hilfenhaus J. Protection against European isolates of tick-borne encephalitis virus after vaccination with a new tick-borne encephalitis vaccine. Vaccine. 1991;9:210–2. http://dx.doi.org/10.1016/0264-410X(91)90157-2
10. Upadhyay AS, Vonderstein K, Pichlmair A, Stehling O, Bennett KL, Dobler G, et al. Viperin is an iron-sulfur protein that inhibits genome synthesis of tick-borne encephalitis virus via radical SAM domain activity. Cell Microbiol. 2014;16:834–48. http://dx.doi.org/10.1111/cmi.12241
11. Schwaiger M, Cassinotti P. Development of a quantitative real-time RT-PCR assay with internal control for the laboratory detection of tick borne encephalitis virus (TBEV) RNA. J Clin Virol. 2003;27:136–45. http://dx.doi.org/10.1016/S1386-6532(02)00168-3
12. Frey S, Essbauer S, Zöller G, Klempa B, Dobler G, Pfeffer M. Full genome sequences and preliminary molecular characterization of three tick-borne encephalitis virus strains isolated from ticks and a bank vole in Slovak Republic. Virus Genes. 2014;48:184–8. http://dx.doi.org/10.1007/s11262-013-0985-0
13. Zerbino DR, Birney E. Velvet: algorithms for de novo short read assembly using de Bruijn graphs. Genome Res. 2008;18:821–9. http://dx.doi.org/10.1101/gr.074492.107
14. Norberg P, Roth A, Bergström T. Genetic recombination of tick-borne flaviviruses among wild-type strains. Virology. 2013;440:105–16. http://dx.doi.org/10.1016/j.virol.2013.02.017
15. Kaiser R. The clinical and epidemiological profile of tick-borne encephalitis in southern Germany 1994–98. A prospective study of 656 patients. Brain. 1999;122:2067–78. http://dx.doi.org/10.1093/brain/122.11.2067

Address for correspondence: Anna J. Henningsson, Clinical Microbiology, Division of Medical Diagnostics, Region Jönköping County S-551 85, Jönköping, Sweden; email: anna.jonsson.henningsson@rjl.se

Major Persistent 5′ Terminally Deleted Coxsackievirus B3 Populations in Human Endomyocardial Tissues

Alexis Bouin, Yohan Nguyen, Michel Wehbe, Fanny Renois, Paul Fornes, Firouze Bani-Sadr, Damien Metz, Laurent Andreoletti

We performed deep sequencing analysis of the enterovirus 5′ noncoding region in cardiac biopsies from a patient with dilated cardiomyopathy. Results displayed a mix of deleted and full-length coxsackievirus B3, characterized by a low viral RNA load (8.10^2 copies/μg of nucleic acids) and a low viral RNA positive-sense to RNA negative-sense ratio of 4.8.

Enteroviruses (EVs) are common human pathogens that are small, naked, single-stranded, positive-sense RNA viruses of ≈7,400 nt. Their genome is flanked on the 5′ end by a noncoding region (NCR), which is crucial for the initiation of the replication and translation of the virus genome (*1*). These viruses, especially group B coxsackieviruses (CV-B), are considered to be a common cause of acute myocarditis in children and young adults. This disease is a precursor to 10%–20% of chronic myocarditis cases and dilated cardiomyopathy (DCM), which is a leading cause of heart transplantation worldwide (*2*). The molecular mechanisms related to the switch from the acute to the persistent CV-B infection in human cardiac tissue are still unknown, but they could be related to terminal deletions on the 5′ NCR cloverleaf structure, resulting in low replication levels. One published report described the presence of EV-B strains containing genomic 5′ terminally deleted populations in heart tissues from a patient who had died of fulminant myocarditis (*3*). Several published studies reporting the presence of persistent EV infection in various human tissues, including heart tissue, did not investigate the presence of terminally deleted EV populations (*4–7*). We report a next-generation sequencing (NGS) strategy enabling a retrospective analysis of EV 5′ NCR of virus populations detected in heart tissue biopsies from a patient with idiopathic DCM (IDCM).

Authors affiliations: University of Reims Champagne-Ardenne, Reims, France (A. Bouin, Y. Nguyen, M. Wehbe, F. Renois, P. Fornes, F. Bani-Sadr, L. Andreoletti); Centre Hospitalier Universitaire de Reims, France (Y. Nguyen, F. Renois, P. Fornes, F. Bani-Sadr, D. Metz, L. Andreoletti); Centre Azm pour la Recherche en Biotechnologie et ses Applications, Tripoli, Lebanon (M. Wehbe)

The Study

In September 2011, a 47-year-old immune-competent woman was referred to University Hospital Center of Reims, Reims, France, because of stage 2 dyspnea (per New York Heart Association functional classifications, http://professional.heart.org/professional/General/UCM_423811_Classification-of-Functional-Capacity-and-Objective-Assessment.jsp) that began 1 month before. Transthoracic echocardiogram revealed a decreased left ventricle ejection fraction (LVEF) (45%) and a dilated left ventricle with a telediastolic diameter of 36 mm/m². Coronary artery disease was ruled out by coronarography; no other etiologic causes of DCM were indicated by heart magnetic resonance imaging (*2*). Endomyocardial biopsies (n = 5) were performed at the time of hospitalization to assess the potential causes of IDCM (*8*). Classical and immunohistologic analyses indicated only a slight cardiomyocyte hypertrophy without myocarditis per the Dallas criteria (*8*). The clinical outcome was good, with a slight LVEF increase (54%) 4 years later after symptomatic treatment by b-blocker, therefore excluding the hypothesis of familial DCM.

Total nucleic acids were retrospectively extracted from flash-frozen cardiac tissues by using NucliSens easyMAG instrument protocols (bioMérieux, Marcy l'Etoile, France) according to the manufacturer's instructions. Real-time quantitative reverse transcription PCR was performed for quantitative detection of total and strand-specific EV-genus genomic RNA according to previously published protocols (*7*). Generic EV-genus real-time quantitative reverse transcription PCR protocols showed the presence of EV total RNA detection with a low viral load of 8.10^2/μg of total extracted nucleic acids and a low viral RNA positive-sense (RNA+) to RNA negative-sense (RNA–) ratio value of 4.8 (*7*).

Classical reverse transcription PCR sequencing of the viral protein 2 puff region enabled us to perform a genotypic identification of an original CV-B3 strain (GenBank accession no. KU608309); nucleotide and amino acid sequence homologies were 79% and 92%, respectively, with the CV-B3 Nancy strain (GenBank accession no. JX312064.1) (*3*,*9*). The genomic differences between the sample virus and the prototype strains ruled out the possibility of laboratory contamination events (*10*).

To identify the 5′ NCR terminal deletion, we performed a rapid amplification of cDNA ends (RACE) PCR followed by an in-house NGS strategy. RNA-backboned oligonucleotides (trP1 and trP1c) were linked on 5′ extremity of EV RNA+

Table. Primer sequences used to detect and identify 5′ terminal deletions in enterovirus populations detected in cardiac tissue of a patient with idiopathic dilated cardiomyopathy, Reims, France, September 2011

Primers	Oligonucleotide sequences
trP1 RNA*	5′H-CCTCTCTATGGGCAGTCGGTGAT-3′
trP1c RNA*	5′P-ATCACCGACTGCCCATAGAGAGG-3′H
trP1	5′-CCT CTC TAT GGG CAG TCG GTG AT-3′
AvcRev	5′-AACAGGCGCACAAAGCTACCG-3′
A+AvcRevBC2–1	5′-CGACTCAGTAAGGAGAACGATAACAGGCGCACAAAGCTACCG-3′
A+AvcRevBC2–2	5′-CCATCTCATCCCTGCGTGTCTCCGACTCAGTAAGGAGAACGATAAC-3′

*RNA backbone oligonucleotides.

and 3′ extremity of RNA–, respectively (Table). A retrotranscription step was then performed by using trP1 or AvcRev for a specific hybridization on viral RNA– or RNA+, respectively (Table). For the RACE PCR strategy, the amplification step was performed by using AvcRev and trP1 primers. For the NGS strategy, the amplicons were generated by using 2 successive PCRs (forward primers: A+AvcRevBC2–1 and A+AvcRevBC2–2 for the first and second PCRs, respectively; reverse primer: trP1) (Table; online Technical Appendix, http://wwwnc.cdc.gov/EID/article/22/8/16-0186-Techapp1.pdf). The libraries obtained were sequenced by using an Ion PGM sequencer (Life Technologies, Saint Aubin, France) according to the manufacturer's instructions. Only reads containing both A and trP1 sequences were selected and aligned against the 5′ NCR regions of human EV genomes by using CLC Genomics Workbench software version 8.5.1 (CLC Bio, Aarhus, Denmark).

Our results estimated a major proportion (84.8%) of reads presenting with a terminal 48-nt deletion associated with minor proportions of reads deleted of 15 nt (14.3%) and nondeleted (0.9%) (Figure). Because read lengths could induce variation in the amplification efficiency, our NGS strategy corresponded to a semi-quantitative detection of the EV populations. We concluded that the persistent viral population in the cardiac samples consisted of a major proportion of deleted populations, with deletions ranging in size from 15 to 48 nt (Figure).

Conclusions

Our study demonstrated the existence of major 5′ terminally deleted CV-B3 populations in endomyocardial tissues taken from a patient with IDCM at the time of her clinical diagnosis. We observed low viral RNA load values associated with a low viral RNA+ to RNA– ratio (<5), indicating that these viral forms were compatible with persistent endomyocardial EV-B populations (7).

One previous study reported a detection of 5′ terminally deleted CV-B2 populations ranging in size from 22 to 36 nt in cardiac tissues taken from an immune competent patient in Japan who died of fulminant myocarditis (3). We demonstrated the existence of major persistent cardiac EV-B viral populations characterized by 15 and 48 nt deletions in the 5′ NCR at the time of chronic DCM (Figure). These deletions induce a loss of a part of the 5′ untranslated region
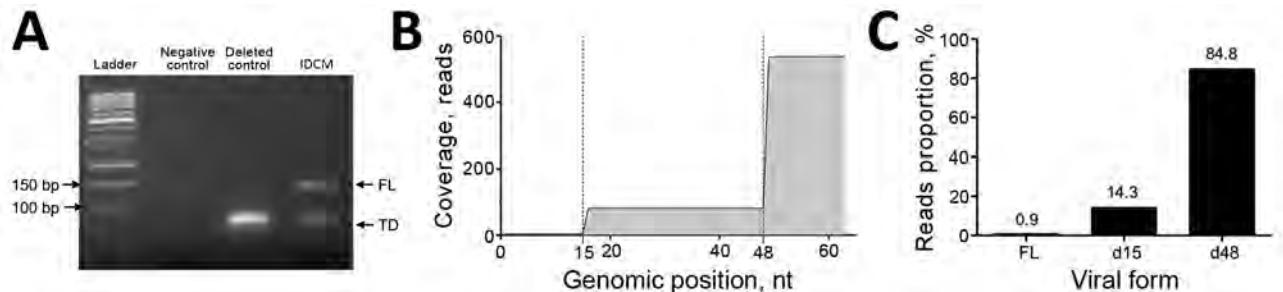
Figure. Identification of the major and minor 5′ terminally deleted or full-length enterovirus populations detected in the cardiac tissues of a patient with IDCM, Reims, France, September 2011. A) Gel electrophoresis analysis (4% agarose) of amplicons generated by using the rapid amplification of cDNA ends PCR strategy. Deleted control lane, synthetic RNA presenting with a 50-nt terminal deletion (3); IDCM lane, rapid amplification of cDNA ends PCR analysis of extracted RNA from heart tissues of the IDCM patient. B) Coverage data obtained by next-generation sequencing analysis of the cardiac tissue taken from IDCM patient. Reads obtained were filtered by bar code first to obtain 8,512,538 reads. A second discriminant step selected only reads containing both A and trP1 sequences, eliminating all artifacts resulting from early stops of the polymerase during amplification or sequencing. Following these steps, 7,354,283 reads were selected and aligned against the aligned human enterovirus group B genomes by using CLC Genomics software (CLC Bio, Aarhus, Denmark). Of these reads, only 538 were successfully aligned against enterovirus group B sequences and, more specifically, against coxsackieviruses B3 strain Nancy (Gen Bank accession no. JX312064.1). We observed that the persistent viral population in the cardiac samples consisted of a major proportion of deleted populations, with deletions ranging from 15 to 48 nt. C) Reads proportion obtained for each viral form from the IDCM patient. Coverage data were used to identify the full-length and deleted viral forms and indicate each populations' proportions. IDCM, idiopathic dilated cardiomyopathy; FL, full-length; TD, terminally deleted.

cloverleaf structure, but the viral RNA polymerase (3CD) binding site remains intact (*11*). Such terminally deleted populations have been previously described in persistent murine cardiac infection characterized by low RNA+ to RNA– ratio associated with a low production level of infectious particles in cell cultures. Furthermore, murine and in vitro models have demonstrated that EV-2A proteinase is sufficient to induce DCM (*12,13*). As a result, low replicative terminally deleted viral forms could be generated and selected in heart tissues during the early acute viral replication phase (myocarditis) and could establish an ongoing persistent human cardiac infection leading to chronic myocarditis and the DCM clinical phase. Moreover, the NGS strategy showed that these 5′ terminally deleted populations were associated with a minor full-length virus population, which could potentially affect persistence by acting as a helper virus through genomic transcomplementation (*14*) or genomic recombination mechanisms (*15*). Persistent low replicative EV-B deleted and undeleted collaborative populations might contribute to the pathogenesis of unexplained DCM cases.

The clinical data associated with our molecular results argued for a CV-B3–induced DCM stage that developed several years after an undiagnosed clinical CV-B3–related myocarditis event. Taken together with the unique published CV-B2–induced myocarditis case, our findings support the hypothesis that the emergence and the selection of terminally deleted EV-B forms could occur during the early acute viral replication phase and might explain the pathophysiological progression from acute viral myocarditis to the DCM phase, in which cardiac persistent terminally deleted virus populations would be advantaged (*3*). Further NGS investigations on a large number of cardiac tissues of myocarditis and DCM adult patients might enable a better understanding of the molecular mechanisms implicated in cardiac EV persistence.

Acknowledgments

Dr. Bouin is currently a postdoctoral fellow in the Department of Microbiology and Molecular Genetics at the University of California, Irvine, CA, USA. His primary research interests include persistent coxsackievirus replication and enterovirus terminal deletion mechanisms.

References

1. Racaniello VR. Picornaviridae: the viruses and their replication. In: Knipe DM, Howley PM, editors. Fields virology, vol. 1. 5th ed. Philadelphia: Lippincott Williams & Wilkins; 2007. p. 795–838.
2. Dennert R, Crijns HJ, Heymans S. Acute viral myocarditis. Eur Heart J. 2008;29:2073–82. http://dx.doi.org/10.1093/eurheartj/ehn296
3. Chapman NM, Kim K-S, Drescher KM, Oka K, Tracy S. 5′ terminal deletions in the genome of a coxsackievirus B2 strain occurred naturally in human heart. Virology. 2008;375:480–91. http://dx.doi.org/10.1016/j.virol.2008.02.030
4. Arbustini E, Grasso M, Porcu E, Bellini O, Diegoli M, Fasani R, et al. Enteroviral RNA and virus-like particles in the skeletal muscle of patients with idiopathic dilated cardiomyopathy. Am J Cardiol. 1997;80:1188–93. http://dx.doi.org/10.1016/S0002-9149(97)00638-3
5. Kim JKS, Zhu Z, Casale G, Koutakis P, McComb RD, Swanson S, et al. Human enterovirus in the gastrocnemius of patients with peripheral arterial disease. J Am Heart Assoc. 2013;2:e000082. http://dx.doi.org/10.1161/jaha.113.000082
6. Richardson SJ, Willcox A, Bone AJ, Foulis AK, Morgan NG. The prevalence of enteroviral capsid protein VP1 immunostaining in pancreatic islets in human type 1 diabetes. Diabetologia. 2009;52:1143–51. http://dx.doi.org/10.1007/s00125-009-1276-0
7. Lévêque N, Renois F, Talmud D, Nguyen Y, Lesaffre F, Boulagnon C, et al. Quantitative genomic and antigenomic enterovirus RNA detection in explanted heart tissue samples from patients with end-stage idiopathic dilated cardiomyopathy. J Clin Microbiol. 2012;50:3378–80. http://dx.doi.org/10.1128/jcm.01612-12
8. Cooper LT, Baughman KL, Feldman AM, Frustaci A, Jessup M, Kuhl U, et al. The role of endomyocardial biopsy in the management of cardiovascular disease: a scientific statement from the American Heart Association, the American College of Cardiology, and the European Society of Cardiology. J Am Coll Cardiol. 2007;50:1914–31. http://dx.doi.org/10.1016/j.jacc.2007.09.008
9. Nasri D, Bouslama L, Omar S, Saoudin H, Bourlet T, Aouni M, et al. Typing of human enterovirus by partial sequencing of VP2. J Clin Microbiol. 2007;45:2370–9. http://dx.doi.org/10.1128/jcm.00093-07
10. Oberste MS, Maher K, Kilpatrick DR, Pallansch MA. Molecular evolution of the human enteroviruses: correlation of serotype with VP1 sequence and application to picornavirus classification. J Virol. 1999;73:1941–8.
11. Sharma N, Ogram SA, Morasco BJ, Spear A, Chapman NM, Flanegan JB. Functional role of the 5′ terminal cloverleaf in Coxsackievirus RNA replication. Virology. 2009;393:238–49. http://dx.doi.org/10.1016/j.virol.2009.07.039
12. Wessely R, Klingel K, Santana LF, Dalton N, Hongo M, Jonathan Lederer W, et al. Transgenic expression of replication-restricted enteroviral genomes in heart muscle induces defective excitation-contraction coupling and dilated cardiomyopathy. J Clin Invest. 1998;102:1444–53. http://dx.doi.org/10.1172/jci1972
13. Xiong D, Yajima T, Lim B-K, Stenbit A, Dublin A, Dalton ND, et al. Inducible cardiac-restricted expression of enteroviral protease 2A is sufficient to induce dilated cardiomyopathy. Circulation. 2007;115:94–102. http://dx.doi.org/10.1161/circulationaha.106.631093
14. Collis PS, O'Donnell BJ, Barton DJ, Rogers JA, Flanegan JB. Replication of poliovirus RNA and subgenomic RNA transcripts in transfected cells. J Virol. 1992;66:6480–8.
15. Holmblat B, Jégouic S, Muslin C, Blondel B, Joffret M-L, Delpeyroux F. Nonhomologous recombination between defective poliovirus and coxsackievirus genomes suggests a new model of genetic plasticity for picornaviruses. MBio. 2014;5:e01119–14. http://dx.doi.org/10.1128/mbio.01119-14

Address for correspondence: Laurent Andreoletti, Laboratoire de Virologie Médicale et Moléculaire, CHU de Reims et EA-4684, SFR CAP-SANTE, URCA, Av Général Koenig, 51100 Reims CEDEX, France; email: landreoletti@chu-reims.fr

Seroconversions for *Coxiella* and Rickettsial Pathogens among US Marines Deployed to Afghanistan, 2001–2010

Christina M. Farris, Nhien Pho, Todd E. Myers, Allen L. Richards

We assessed serum samples from 1,000 US Marines deployed to Afghanistan during 2001–2010 to find evidence of 4 rickettsial pathogens. Analysis of predeployment and postdeployment samples showed that 3.4% and 0.5% of the Marines seroconverted for the causative agents of Q fever and spotted fever group rickettsiosis, respectively.

Rickettsial and rickettsial-like diseases have played a considerable role in military activities throughout much of recorded history (*1*). These diseases, which have worldwide distribution and cause a high number of deaths and illnesses, include the select agents (http://www.selectagents.gov/SelectAgentsandToxinsList.html) *Rickettsia prowazekii* and *Coxiella burnetii*, the causative agents of epidemic typhus and Q fever, respectively. Furthermore, outbreaks caused by rickettsial disease pathogens, such as scrub typhus (*Orientia tsutsugamushi*) in Laos, Vietnam, and Cambodia and African tick-bite fever (*Rickettsia africae*) in Botswana, have affected military forces in recent history (*2*,*3*). *O. tsutsugamushi* was the leading cause of fever of unknown origin in US soldiers during the Vietnam conflict and caused >16,000 cases of scrub typhus among Allied forces during World War II (*1*).

The epidemiology of rickettsial pathogens is not well understood in Central Asia, where >100,000 US and allied troops have been engaged in military operations since 2001. Retrospective studies from military personnel deployed during Operation Desert Shield/Desert Storm in 1991 revealed exposures of 9.8% and 5.7% for spotted fever group rickettsiae (SFGR) and typhus group rickettsiae (TGR), respectively; however, no seroconversions were observed (*4*). Since 2001 in Iraq, >150 cases of Q fever have been confirmed in US troops and civilians (*5*–*8*). An outbreak of Q fever and brucellosis in local residents in the Bamyan province of Afghanistan during 2011 (*9*) and the historic presence of SFGR and vectors known to carry

SFGR (*10*) highlight the inherent risk of contracting rickettsial-like diseases in Afghanistan. We estimated the risk for rickettsial infections in military personnel deployed to Afghanistan by measuring the rate of seroconversion for SFGR, TGR, scrub typhus group *Orientiae* (STGO), and *C. burnetii* among US Marines stationed in Afghanistan during 2001–2010.

The Study

Serum samples from US Marines 18–45 years of age who served ≥180 days in Afghanistan during 2001–2010 were obtained from the US Department of Defense Serum Repository (DoDSR). Documentation of prior exposure to Q fever or rickettsioses and sample volume <0.5 mL were exclusion criteria. We selected the most recent 1,000 postdeployment specimens that fit the inclusion criteria for our study.

Military service members have blood drawn every 2 years for HIV testing and during postdeployment screenings, and a portion of each sample is stored at the DoDSR. All predeployment samples were collected <1 year before the start of Afghanistan service, and postdeployment samples were collected within ≈1 year after the end of Afghanistan service. Paired predeployment and postdeployment samples were irreversibly stripped of personal identifiers by DoDSR and labeled with an internal DoDSR code. Only DoDSR has access to the key linking the code to personal identifiers. The Naval Medical Research Center Institutional Review Board approved the study.

We screened specimens for antibodies against TGR, SFGR, and STGO by ELISA, as described (*11*), and determined titers for positive specimens. Seroconversion (i.e., titer <100 in the predeployment sample and titer ≥400 in the paired postdeployment sample) or a 4-fold rise in titer between the predeployment and paired postdeployment sample was used to determine acute infection.

We tested specimens for antibodies against *C. burnetii* by using the Q fever Immunodot assay (GenBio, San Diego, CA, USA), according to the manufacturer's instructions. Specimens were considered positive for acute infection if antibodies against phase I and phase II antigen were present. Seroconversion was defined by the presence of antibodies against phase I antigen in the postdeployment sample but not in the predeployment sample.

Author affiliations: US Naval Medical Research Unit 2, Phnom Penh, Cambodia (C.M. Farris); Naval Medical Research Center, Silver Spring, Maryland, USA (C.M. Farris, T.E. Myers, A.L. Richards); Uniformed Services University of Health Science, Bethesda, Maryland, USA (N. Pho)

Table. Prevalence of antibodies against 4 rickettsial pathogens in samples from US Marines deployed to Afghanistan during 2001–2010

Pathogen	Total no. samples tested	No. (%)		
		Predeployment samples with detectable antibody	Postdeployment samples showing seroconversion	Total samples with detectable antibody
Coxiella burnetii	879	87 (9.9)	30 (3.4)	117 (13.3)
Spotted fever group *Rickettsia*	1,000	18 (1.8)	5 (0.5)	23 (2.3)
Typhus group *Rickettsia*	1,000	0	0	0
Orientia tsutsugamushi	3,654	1 (0.1)	0	1 (0.1)

Of the 1,000 postdeployment serum samples screened for SFGR, TGR, and STGO, only 879 were screened for Q fever because the volume of 121 samples was depleted from earlier testing. The screening assays showed that 87, 18, and 1 samples were positive for antibodies against *C. burnetii*, SFGR, and STGO, respectively, before deployment. No antibodies against TGR were detectable in any samples. Seroconversions to *C. burnetii* and SFGR occurred in 3.4% and 0.5% of the paired serum samples, respectively (Table). *C. burnetii* infection was most prevalent among the agents tested both before deployment (n = 87) and during deployment (n = 30). Of 879 specimens, 117 (13.3%) were positive.

Most of the 30 *C. burnetii* seroconversions occurred in Marines who began deployment in 2008 (n = 12) and 2009 (n = 8) (Figure, panel A). However, most (634/879 [72.1%]) of the sample population were deployed during this period (Figure, panel B), so higher rates for these years likely do not indicate higher risk. With the exception of 1 fixed-wing pilot, all *C. burnetii* and SFGR seroconversions occurred in general infantrymen, who represented 93.1% of *C. burnetii*–positive samples and 92.6% of total samples.

Range of deployment time was 180–450 days, and average length of deployment was 271 (SD 104.49) days. Average length of deployment for those who seroconverted for *C. burnetii* or SFGR was 286.2 (SD 112.01) and 342.4

(SD 131.65) days, respectively. Analysis by *t*-test showed no correlation between length of deployment and seroconversion for either *C. burnetii* (p = 0.98) or SFGR (p = 1.0).

Predeployment serum samples were collected 3–364 (mean 183, SD 111.07) days before deployment, and postdeployment samples were collected <443 (mean 61.3, SD 111.02) days after return. Samples showing seroconversions for *C. burnetii* and SFGR were collected an average of 179.3 (SD 93.94) and 151.6 (SD 126.76) days, respectively, predeployment and 76.9 (SD 87.64) and 129.8 (SD 127.85) days, respectively, postdeployment.

Conclusions

Acute febrile illness can be difficult to diagnose because many infections have similar symptoms and signs and are difficult to differentiate without appropriate diagnostic tools. The rate of *C. burnetii* seroconversions (3.4%) in Marines in our study is similar to that reported in United Kingdom military personnel deployed to Afghanistan during 2008–2011 (*7*); the study from the United Kingdom also confirms the presence of rickettsiae in the region. The rate of *C. burnetii* seropositivity in the United States is ≈3% but ranges dramatically; nearby Nova Scotia, Canada, has rates >14% (*8*,*12*). With proper treatment of infections, the case-fatality rate for Q fever and rickettsial infections is <2%. However, rates can be >30%; among hospitalized
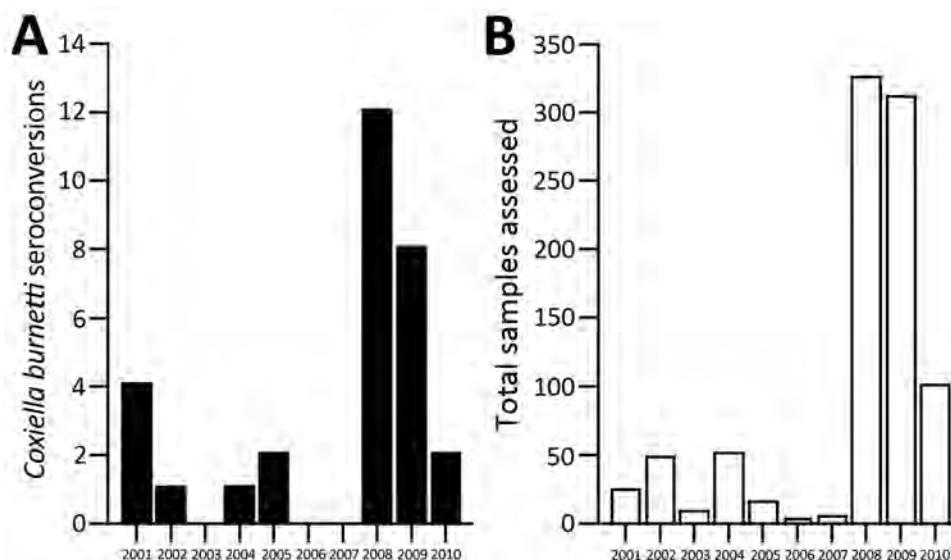
Figure. Serum samples assessed for evidence of seroconversion for *Coxiella burnetii* among US Marines deployed to Afghanistan, by year deployment began, 2001–2010. A) Number of *Coxiella burnetii* seroconversions (n = 30). B) Total number of samples assessed for antibodies against *Coxiella burnetii* (n = 879).

Mediterranean spotted fever patients in Portugal in 1997, the case-fatality rate was 32.5% (*13*).

In our study, gaps between dates of blood draws and start and end dates of deployment provided an opportunity for exposure to agents of Q fever and SFGR outside the deployment period. The nature of retrospective, blinded studies prevents follow-up with participants to ascertain additional information, including whether symptoms developed or treatment was sought. This limitation is especially true for studies of military populations, for whom routine blood draws are typically used, rather than samples being specifically collected for research studies. However, results from these studies provide valuable information, and in our study, this limitation does not discount the documented prevalence of Q fever in Iraq and Afghanistan (*4–10,14*) or the inherent risk to deployed US military personnel. Our results highlight the risk of contracting Q fever and the need for Q fever diagnostics in military engagements in Central Asia.

Dr. Farris is a Lieutenant in the United States Navy and is currently stationed at the Naval Medical Research Unit 2 detachment in Phnom Penh, Cambodia. Her research interests include intracellular bacteria and vectorborne diseases.

References

1. Kelly DJ, Richards AL, Temenak J, Strickman D, Dasch GA. The past and present threat of rickettsial diseases to military medicine and international public health. Clin Infect Dis. 2002; 34(Suppl 4):S145–69. http://dx.doi.org/10.1086/339908
2. Corwin A, Soderquist R, Suwanabun N, Sattabongkot J, Martin L, Kelly D, et al. Scrub typhus and military operations in Indochina. Clin Infect Dis. 1999;29:940–1. http://dx.doi.org/10.1086/520468
3. Smoak BL, McClain JB, Brundage JF, Broadhurst L, Kelly DJ, Dasch GA, et al. An outbreak of spotted fever rickettsiosis in U.S. Army troops deployed to Botswana. Emerg Infect Dis. 1996;2:217–21. http://dx.doi.org/10.3201/eid0203.960309
4. Richards AL, Malone JD, Sheris S, Weddle JR, Rossi CA, Ksiazek TG, et al. Arbovirus and rickettsial infections among combat troops during Operation Desert Shield/Desert Storm. J Infect Dis. 1993;168:1080–1. http://dx.doi.org/10.1093/infdis/168.4.1080
5. Faix DJ, Harrison DJ, Riddle MS, Vaughn AF, Yingst SL, Earhart K, et al. Outbreak of Q fever among US military in western Iraq, June–July 2005. Clin Infect Dis. 2008;46:e65–8. http://dx.doi.org/10.1086/528866
6. Newman EN, Johnstone P, Bridge H, Wright D, Jameson L, Bosworth A, et al. Seroconversion for infectious pathogens among UK military personnel deployed to Afghanistan, 2008–2011. Emerg Infect Dis. 2014;20:2015–22. http://dx.doi.org/10.3201/eid2012.131830
7. White B, Brooks T, Seaton RA. Q fever in military and paramilitary personnel in conflict zones: case report and review. Travel Med Infect Dis. 2013;11:134–7. http://dx.doi.org/10.1016/j.tmaid.2012.11.001
8. Gutiérrez RL, Hartzell JD. Fever, dyspnea, and hepatitis in an Iraq veteran. Cleve Clin J Med. 2012;79:623–30. http://dx.doi.org/10.3949/ccjm.79a.11136
9. Saeed KMI, Ansari J, Asghar RJ, Ahadi J. Concurrent brucellosis and Q fever infection: a case control study in Bamyan Province, Afghanistan in 2011. Int J Infect Dis. 2012;16(Suppl 1):e37 http://dx.doi.org/10.1016/j.ijid.2012.05.094.
10. Wallace MR, Hale BR, Utz GC, Olson PE, Earhart KC, Thornton SA, et al. Endemic infectious diseases of Afghanistan. Clin Infect Dis. 2002;34(Suppl 5):S171–207. http://dx.doi.org/10.1086/340704
11. Jiang J, Myers TE, Rozmajzl PJ, Graf PC, Chretien JP, Gaydos JC, et al. Seroconversions to rickettsiae in US military personnel in South Korea. Emerg Infect Dis. 2015;21:1073–4. http://dx.doi.org/10.3201/eid2106.141487
12. Marrie TJ, Pollak PT. Seroepidemiology of Q fever in Nova Scotia: evidence for age dependent cohorts and geographical distribution. Eur J Epidemiol. 1995;11:47–54. http://dx.doi.org/10.1007/BF01719945
13. de Sousa R, Nóbrega SD, Bacellar F, Torgal J. Mediterranean spotted fever in Portugal: risk factors for fatal outcome in 105 hospitalized patients. Ann N Y Acad Sci. 2003;990:285–94. http://dx.doi.org/10.1111/j.1749-6632.2003.tb07378.x
14. Anderson AD, Baker TR, Littrell AC, Mott RL, Niebuhr DW, Smoak BL. Seroepidemiologic survey for *Coxiella burnetii* among hospitalized US troops deployed to Iraq. Zoonoses Public Health. 2011;58:276–83. http://dx.doi.org/10.1111/j.1863-2378.2010.01347.x

Address for correspondence: Christina M. Farris, Naval Medical Research Unit 2 Detachment Phnom Penh, Unit 8166 Box P, APO, AP 96546, USA; email: christina.farris.mil@namru2.org.kh

Asymptomatic *Plasmodium* Infections in Children in Low Malaria Transmission Setting, Southwestern Uganda[1]

Michelle E. Roh,[2] Caesar Oyet,[2] Patrick Orikiriza, Martina Wade, Gertrude N. Kiwanuka, Juliet Mwanga-Amumpaire, Sunil Parikh,[3] Yap Boum II[3]

A survey of asymptomatic children in Uganda showed *Plasmodium malariae* and *P. falciparum* parasites in 45% and 55% of microscopy-positive samples, respectively. Although 36% of microscopy-positive samples were negative by rapid diagnostic test, 75% showed *P. malariae* or *P. ovale* parasites by PCR, indicating that routine diagnostic testing misses many non–*P. falciparum* malarial infections.

Since 2000, substantial progress has been made in reducing malaria worldwide. In Uganda, malaria transmission is heterogeneous, yet 97% of all cases are attributed to *P. falciparum* (*1*). Accordingly, detection and treatment algorithms have targeted *P. falciparum* over less virulent species. Inadequate attention to non–*P. falciparum* infections has several implications for malaria transmission. For example, gametocytemia can occur earlier (e.g., *P. vivax* and perhaps *P. ovale*) and remain undetected for longer periods because of milder clinical symptoms (e.g., *P. malariae* and *P. ovale*) than for *P. falciparum* infections, enabling persistent transmission of non–*P. falciparum* infections (*2*).

In the southwestern region of Uganda, *Plasmodium* transmission is low and unstable. In 2004 and 2010, we conducted surveys that showed progress in decreasing *P. falciparum* infections in this region, although comparatively little is known about the prevalence of other species in this region (*3*). To determine the comparative species prevalence by multispecies rapid diagnostic test (RDT) and blood-smear microscopy, we conducted a cross-sectional survey of 631 children <5 years of age during the low transmission season of 2014 in 3 districts in southwestern Uganda (Mbarara, Bushenyi, and Isingiro) (Figure). These

Author affiliations: University of California, San Francisco, California, USA (M.E. Roh); Yale School of Public Health, New Haven, Connecticut, USA (M.E. Roh, M. Wade, S. Parikh); Mbarara University of Science and Technology, Mbarara, Uganda (C. Oyet, G.N. Kiwanuka, Y. Boum II); Médecins Sans Frontières Epicentre Mbarara Research Centre, Mbarara (P. Orikiriza, J. Mwanga-Amumpaire, Y. Boum II)

Figure. Districts where surveys of asymptomatic children were conducted to determine *Plasmodium* infections, southwestern Uganda.

3 districts represent a range of transmission intensities from low to high, respectively (*4*).

The Study

Stratified, 2-stage cluster sampling was used to select study participants. We administered questionnaires to gather information about standard knowledge, attitudes, and practices related to malaria and collected blood for testing with microscopy, RDT, and PCR (online Technical Appendix, http://wwwnc.cdc.gov/EID/article/22/8/16-0619-Techapp1.pdf). RDT was a combined *P. falciparum*–specific, histidine-rich protein-2 (HRP-2)/pan-*Plasmodium* lactate dehydrogenase (pLDH) RDT (SD Bioline Malaria Ag P.f/Pan [*P. falciparum* or other *Plasmodium* species]; Standard Diagnostics, Gyeonggi-do, South Korea). Nested PCR was performed on all RDT- or microscopy-positive

[1]Preliminary results from this study were presented at the 64th Annual Meeting of the American Society of Tropical Medicine and Hygiene, October 25–29, 2015, Philadelphia, Pennsylvania, USA.

[2]These first authors contributed equally to this article.

[3]These senior authors contributed equally to this article.

Table 1. Characteristics of asymptomatic children surveyed for *Plasmodium* infections, by district, southwestern Uganda*

Characteristic	District†				p value‡
	Mbarara, n = 242	Bushenyi, n = 157	Isingiro, n = 232	Total, N = 631†	
Mean age, y ± SD	2.4 ± 1.2	2.3 ± 1.2	2.4 ± 1.3	2.4 ± 1.3	0.850
Sex					0.958
M	122 (50.4)	80 (51.0)	120 (51.7)	322 (51.0)	
F	120 (49.6)	77 (49.0)	112 (48.3)	309 (49.0)	
Rural	177 (73.1)	133 (84.7)	202 (87.1)	512 (81.1)	0.472
Wealth quartile					<0.001
1st	42 (17.4)	45 (28.7)	97 (41.8)	184 (29.2)	
2nd	27 (11.2)	58 (36.9)	55 (23.7)	140 (22.2)	
3rd	83 (34.3)	32 (20.4)	56 (24.1)	171 (27.1)	
4th	90 (37.2)	22 (14.0)	24 (10.3)	136 (21.6)	
Roofing material					<0.001
Corrugated metal	237 (97.9)	152 (96.8)	206 (88.8)	595 (94.3)	
Thatch or leaf	3 (1.2)	5 (3.2)	17 (7.3)	25 (4.0)	
Other	2 (0.8)	0	9 (3.9)	11 (1.7)	
Household crowding§					0.239
1–2	68 (28.1)	52 (33.1)	61 (26.3)	181 (28.7)	
3	123 (50.8)	71 (45.2)	134 (57.8)	328 (52.0)	
≥4	51 (21.1)	34 (21.7)	37 (16.0)	122 (19.3)	
Consistent bed net use	228 (94.2)	151 (96.2)	198 (85.7)	577 (91.6)	0.003
Indoor residual spraying	4 (1.7)	1 (0.6)	0	5 (0.8)	0.122
Malaria prevalence					
By RDT	4 (1.7)	8 (5.1)	30 (13.0)	42 (6.7)	<0.001
Pf+	1	3	7	11	
Pan+	2	0	1	3	
Pf/Pan+	1	5	22	28	
By microscopy	4 (1.7)	5 (3.2)	13 (5.6)	22 (3.5)	0.067
P. falciparum	2	3	4	9	
P. malariae	0	1	6	7	
P. ovale	1	1	1	3	
Mixed *Pf/Pm*	1	0	2	3	

*Values are no. (%) children surveyed except as indicated. Pan+, positive for non–*P. falciparum* infection only; Pf+, positive for *P. falciparum* monoinfection only; Pf/Pan+, positive for *P. falciparum* monoinfection or *P. falciparum* mixed infection; RDT, rapid diagnostic test; mixed *Pf/Pm*, positive for *P. falciparum* monoinfection or *P. malariae* mixed infection.
†Totals in columns may not add up to total because of missing data.
‡Determined by Fisher exact test or χ^2 test, as appropriate.
§Defined as number of persons who sleep in the same room.

samples. Predictors of malaria were selected a priori (online Technical Appendix).

We surveyed 631 children with a mean age of 2.4 years (Table 1). Bed net coverage was high (91.6%) and met targets for 2014 (*5*). Only 5 households (0.8% of children surveyed) reported use of indoor residual spraying. Of the 3 districts, Isingiro had the highest proportion of children living in the lowest wealth quartile (41.8%) and in households with thatched or leaf roofing (7.3%); this district also had the lowest consistent bed net use (85.7%) (Table 1).

Overall prevalence of parasitemia by microscopy was 3.5% (95% CI 1.9%–5.1%). Speciation by microscopy revealed a higher proportion of non–*P. falciparum* infections than *P. falciparum* monoinfections. Of 22 microscopy-positive samples, 9 (40.9%) were *P. falciparum* monoinfections, 7 (31.8%) were *P. malariae* monoinfections, 3 (13.6%) were *P. ovale* monoinfections, and 3 (13.6%) were *P. falciparum*/*P. malariae* mixed infections. Most *P. malariae* monoinfections occurred in Isingiro district. Sixteen (72.7%) of 22 blood-smear readings correlated directly with PCR results (online Technical Appendix Table 2).

Malaria parasite prevalence was 2-fold higher by RDT than by microscopy (6.7% vs. 3.5%; Table 1). RDT correctly identified 9 of 12 *P. falciparum* monoinfections and mixed infections. A comparison of the diagnostic performance of RDT and microscopy (uncorrected by PCR) indicates that agreement of results from these methods was high (>94%); however, agreement was poor in detecting non–*P. falciparum* infections (k = 0.15) compared with detecting overall infection (k = 0.41) and *P. falciparum* infection (k = 0.33) (Table 2). PCR detected parasite DNA in 53.7% (22/41) of RDT-positive samples; of these, 55% (12/22) correlated with the correct RDT band pattern interpretation (online Technical Appendix Table 2).

Approximately one third (8/22) of children with microscopy-positive cultures had negative RDT results (online Technical Appendix Table 3). Of these 8 discordant cases, 5 harbored PCR-confirmed *P. malariae* or *P. ovale* monoinfections; all had parasite densities <1,060/ μL (online Technical Appendix Table 2). Conversely, two thirds (28/42) of RDT-positive samples were negative by microscopy. Of the 28 children with RDT-positive and microscopy-negative samples, 8 (28.6%) had a malaria

Table 2. Diagnostic performance of RDT and microscopy for *Plasmodium* infections in children in 3 districts, southwestern Uganda*

Diagnostic accuracy of RDT†	*Plasmodium* infection	*P. falciparum* infection	Non–*P. falciparum* infection‡
Sensitivity (95% CI)	63.6 (40.7–82.8)	75.0 (42.8–94.5)	10.0 (0.3–44.5)
Specificity (95% CI)	95.4 (93.4–96.9)	95.1 (93.1–96.7)	99.8 (99.1–100.0)
PPV (95% CI)	33.3 (19.6–49.5)	23.1 (11.1–39.3)	50.0 (1.3–98.7)
NPV (95% CI)	98.6 (97.3–99.4)	99.5 (98.5–99.9)	98.6 (97.3–99.3)
Agreement, %	94.3	94.8	98.3
κ	0.41	0.33	0.15

*NPV, negative predictive value; PPV, positive predictive value; RDT, rapid diagnostic test.
†SD Bioline Malaria Ag Pf/Pan (*P. falciparum* or other *Plasmodium* species; Standard Diagnostics, Gyeonggi-do, South Korea).
‡Children with mixed infections were excluded from analysis.

infection within the previous month; 4 of those had detectable parasite DNA.

Conclusions

Our findings indicate that strides in the control of *P. falciparum* malaria have continued in Uganda. Compared with data from 2010, *P. falciparum* prevalence by microscopy had a 4- and 5-fold decrease in urban and rural villages, respectively (*3*). Our estimates are consistent with prevalence estimates from 2009 (12%) and 2014–2015 (4%) (*1,6*).

In our study, 46% of asymptomatically infected children harbored non–*P. falciparum* species, particularly *P. malariae*, in contrast to the 1.2% non–*P. falciparum* species prevalence in 2009 (*6*). In addition, 1 *P. vivax* monoinfection was detected by PCR in Isingiro, confirming the continued presence of all 4 major species in Uganda (online Technical Appendix Table 2) (*1*). Furthermore, although most *P. malariae* cases were from Isingiro, recent studies in other regions of Uganda (i.e., northern and eastern) have also reported a rise in non–*P. falciparum* infections, particularly *P. malariae* (*7–9*).

One possible reason for the nearly equivalent prevalence of asymptomatic *P. falciparum* and non–*P. falciparum* infections is the influence of seasonal fluctuations in species prevalence; for example, *P. malariae* prevalence has been higher during the dry season in West Africa (*10*). Another possibility is that the use of *P. falciparum*–based RDTs, which are advantageous because of low infrastructure costs and high prevalence of this species in Uganda, has enabled non–*P. falciparum* prevalence to go undetected. Alternatively, our results may represent a true shift in species prevalence. What is apparent is that pLDH/HRP-2–based RDTs may not be the most sensitive diagnostic method to determine true prevalence in the future. In our study, RDT was negative in all 3 microscopy-identified *P. ovale* and in 3 of 7 *P. malariae* monoinfections, a finding that may be in part attributable to these species' low parasite densities (range 39–1,057/μL).

Identifying *P. malariae* and *P. ovale* infections is critical because *P. malariae* has been associated with chronic infections that can persist for years, including a chronic nephrotic syndrome that, once established, is unresponsive to treatment (*10*). Because these species have milder symptoms and lower parasite prevalence than *P. falciparum*, infections can remain undetected for extended periods, enabling persons to serve as reservoirs for ongoing transmission (*2*). These species may transmit gametocytes more efficiently at low parasite densities; a recent study found increased *P. falciparum* gametocyte production in the setting of mixed *P. malariae* infections (*11*). In our study, 30% of non–*P. falciparum* monoinfections harbored gametocytes. Finally, on the therapeutic side, studies have shown failure of parasite clearance after artemisinin-based combination therapy in non–*P. falciparum* infections, including *P. malariae* (*2,9,12*). *P. ovale* and *P. vivax* also form hypnozoites in the liver, and safe treatment with a 14-day course of primaquine is necessary to clear parasitemia. Six children in our study harbored *P. ovale* or *P. vivax* infections.

From a malaria control perspective, the performance of the pLDH/HRP-2–based RDT was suboptimal in our data, indicating a need for accurate diagnostic methods aimed at detecting *Plasmodium* infections in this region. A diagnostic method that has been effective in resource-constrained settings is loop-mediated isothermal amplification (LAMP), which affords higher sensitivity in detecting low-level parasitemia, especially *P. malariae* infections that tend to exhibit lower parasite densities than *P. falciparum* and *P. vivax* (*13*). In a 2013 rural Uganda study, the sensitivity of LAMP was ≈1.8-fold greater than microscopy, comparable to PCR (*14*). Wide-scale application of a field-friendly technique such as LAMP might be possible in southwestern Uganda, where asymptomatic persons might have low-density malaria infections that persist during the low malaria transmission season, enabling these persons to serve as reservoirs for ongoing transmission and disease (*15*). Effective methods for detecting and treating these infections are essential for controlling and eliminating malaria.

Ms. Roh completed this research while obtaining a master's degree in public health at the Yale School of Public Health in 2015. She is currently a predoctoral student in the Department of Epidemiology and Biostatistics at the University of California, San Francisco. Her primary research focuses on malaria transmission dynamics and evaluation of targeted interventions for malaria elimination.

References

1. Uganda Bureau of Statistics (UBOS) and ICF International. Uganda malaria indicator survey 2014–15: key indicators. 2015 Apr [cited 2016 Mar 24]. http://pdf.usaid.gov/pdf_docs/PBAAC390.pdf
2. White NJ. The role of anti-malarial drugs in eliminating malaria. Malar J. 2008;7(Suppl 1):S1–S8. http://dx.doi.org/10.1186/1475-2875-7-S1-S8
3. De Beaudrap P, Nabasumba C, Grandesso F, Turyakira E, Schramm B, Boum Y II, et al. Heterogeneous decrease in malaria prevalence in children over a six-year period in south-western Uganda. Malar J. 2011;10:132. http://dx.doi.org/10.1186/1475-2875-10-132
4. Uganda Ministry of Health. National Malaria Control Program. Uganda malaria quarterly bulletin. Issue 10. 2015 Apr–June [cited 2016 Apr 11]. http://www.health.go.ug/sites/default/files/Ugand%20Malaria%20Bulletin%20Issue%2010.pdf
5. President's Malaria Initiative. President's Malaria Initiative Uganda Malaria Operational Plan FY 2014. 2014 [cited 2016 Apr 05]. http://www.pmi.gov/docs/default-source/default-document-library/malaria-operational-plans/fy14/uganda_mop_fy14.pdf?sfvrsn=14
6. Uganda Bureau of Statistics (UBOS) and ICF Macro. Uganda malaria indicator survey 2009. 2010 Aug [cited 2016 Mar 24]. http://dhsprogram.com/pubs/pdf/MIS6/MIS6.pdf.
7. Proietti C, Pettinato DD, Kanoi BN, Ntege E, Crisanti A, Riley EM, et al. Continuing intense malaria transmission in northern Uganda. Am J Trop Med Hyg. 2011;84:830–7. http://dx.doi.org/10.4269/ajtmh.2011.10-0498
8. Pullan RL, Bukirwa H, Staedke SG, Snow RW, Brooker S. *Plasmodium* infection and its risk factors in eastern Uganda. Malar J. 2010;9:2. http://dx.doi.org/10.1186/1475-2875-9-2
9. Betson M, Sousa-Figueiredo JC, Atuhaire A, Arinaitwe M, Adriko M, Mwesigwa G, et al. Detection of persistent *Plasmodium* spp. infections in Ugandan children after artemether-lumefantrine treatment. Parasitology. 2014;141:1880–90. http://dx.doi.org/10.1017/S003118201400033X
10. Mueller I, Zimmerman PA, Reeder JC. *Plasmodium malariae* and *Plasmodium ovale*—the "bashful" malaria parasites. Trends Parasitol. 2007;23:278–83. http://dx.doi.org/10.1016/j.pt.2007.04.009
11. Bousema JT, Drakeley CJ, Mens PF, Arens T, Houben R, Omar SA, et al. Increased *Plasmodium falciparum* gametocyte production in mixed infections with *P. malariae*. Am J Trop Med Hyg. 2008;78:442–8.
12. Dinko B, Oguike MC, Larbi JA, Bousema T, Sutherland CJ. Persistent detection of *Plasmodium falciparum*, *P. malariae*, *P. ovale curtisi* and *P. ovale wallikeri* after ACT treatment of asymptomatic Ghanaian school-children. Int J Parasitol Drugs Drug Resist. 2013;3:45–50. http://dx.doi.org/10.1016/j.ijpddr.2013.01.001
13. Lau YL, Lai MY, Fong MY, Jelip J, Mahmud R. Loop-mediated isothermal amplification assay for identification of five human *Plasmodium* species in Malaysia. Am J Trop Med Hyg. 2016;94:336–9. http://dx.doi.org/10.4269/ajtmh.15-0569
14. Hopkins H, González IJ, Polley SD, Angutoko P, Ategeka J, Asiimwe C, et al. Highly sensitive detection of malaria parasitemia in a malaria-endemic setting: performance of a new loop-mediated isothermal amplification kit in a remote clinic in Uganda. J Infect Dis. 2013;208:645–52. http://dx.doi.org/10.1093/infdis/jit184
15. Bousema JT, Gouagna LC, Drakeley CJ, Meutstege AM, Okech BA, Akim IN, et al. *Plasmodium falciparum* gametocyte carriage in asymptomatic children in western Kenya. Malar J. 2004;3:18. http://dx.doi.org/10.1186/1475-2875-3-18

Address for correspondence: Sunil Parikh, Yale School of Public Health, 60 College Street, Room 724, New Haven, CT, 06520, USA; email: sunil.parikh@yale.edu
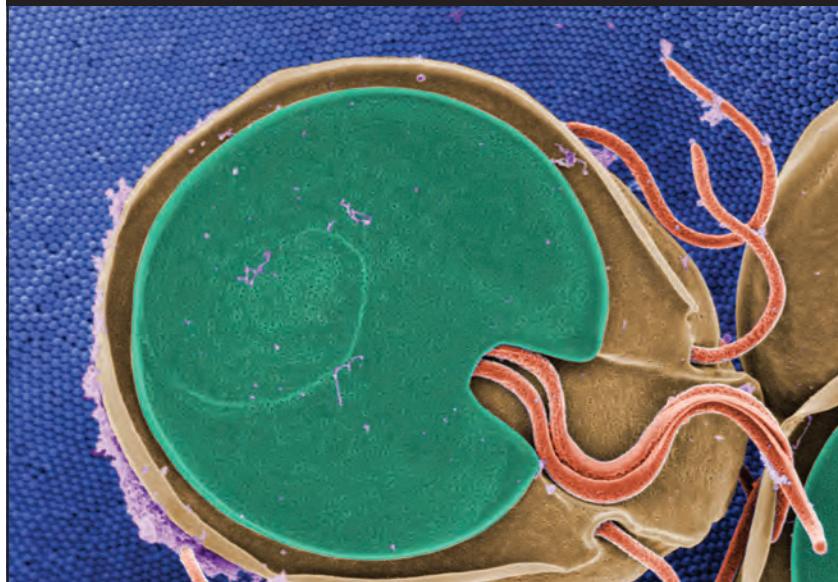
CDC PROVIDES INFORMATION ABOUT MRSA SKIN INFECTIONS.

Visit **www.cdc.gov/MRSA** or call **1-800-CDC-INFO** to order provider materials including:

> Clinician guidelines
> Evaluation & treatment recommendations
> Patient education materials
> Posters
> Fact sheets
> Flyers

Who Is This Person?

He studied the ecology of *Trypanosoma cruz*i, triatomine insects, and the insect hosts throughout the southwestern United States. His career capstone was publication of bibliographies "concerned with the world literature to the Triatominae and Triatominae-borne pathogens and clinical Chagas disease."

Is he:

A) Sherwin Wood

B) Robert Usinger

C) Raymond Ryckman

D) Charles Kofoid

E) Norman Woody

Decide first. Then turn the page. ➔

Raymond Edward Ryckman

Rachel Curtis-Robles and Charles B. Beard

This is a photograph of Raymond Edward Ryckman, PhD, a medical entomologist. His studies of triatomine bugs, *Trypanosoma cruzi*, and Chagas disease formed a rich library of information about vectors and hosts of *T. cruzi*, including the behavioral ecology of the vectors and the role of pack rats for sustaining *T. cruzi* in natural habitats.

Ryckman was born June 19, 1917, on a farm in southern Wisconsin, USA; fascinated at an early age by insects, he built an observation beehive and was eager to show the colony to visitors. He was drafted during World War II and served 4 years at the Presidio Army Base hospital in San Francisco, California, USA. After receiving a bachelor of science degree in zoology at the University of California, Berkeley, in 1950, Ryckman was recruited to teach at Loma Linda University in Loma Linda, California.

Soon after arriving at Loma Linda, he was approached by the Army Surgeon General's office and asked to research the dynamics of plague transmission, with regard to the Army's interest in troop health and safety in Southeast Asia. Ryckman used the natural plague system in southern California to study squirrel and flea population dynamics and potential insecticides. The innovative methods he used included electric-fence enclosures, ferrets trained to place devices within squirrel burrows, and crucible tongs used to gently handle unmanageable squirrels (*1–3*). His research played a major role in the understanding of the dynamics of plague transmission and control.

After the Army Surgeon General's plague grant ended, Ryckman returned to the University of California, Berkeley, where he completed his master's thesis on Cimicidae (bed bugs) and forged ahead with PhD studies under Dr. Robert Usinger. His research explored the systematics, hybridization, and reproduction of the triatomine *Triatoma protracta*—vector of *T. cruzi*, the agent of Chagas disease (*4*). He completed his PhD research while fulfilling teaching requirements at Loma Linda University. He educated hundreds of medical and graduate students at the School of Medicine at Loma Linda University until his retirement in 1987.

In addition to being a triatomine researcher, he was a naturalist eager to investigate organisms that captured his

Author affiliations: Texas A&M University, College Station, Texas, USA (R. Curtis-Robles); Centers for Disease Control and Prevention, Fort Collins, Colorado, USA (C.B. Beard)

interest, generally incidental to studies of triatomines. During his career he published articles about cactiphilic flies (*5*) and lizard mites (*6*). After his retirement, he continued to write, co-authoring a book about Edmund C. Jaeger, a naturalist who studied the desert ecology of the southwestern United States (*7*).

Ryckman traveled throughout Central and South America, generally returning with field-collected triatomines to start new colonies. His family frequently traveled with him, and he published several articles with his sons (*8–10*). Ryckman credits his wife with careful and patient review of his manuscripts before submission. He authored or co-authored ≈115 publications, most of which were 1- or 2-author publications.

Later in Ryckman's career, his focus turned to the publication of bibliographies. Before Internet and electronic searching were available, bibliographies were valuable sources of information for researchers, and their collation was a time-intensive, although perhaps underappreciated, achievement. In Ryckman's words, "A bibliographic monograph is the summation of our historical, cultural, and scientific heritage in a given field of endeavor" (*11*). His career capstone was the publication of bibliographies "concerned with the world literature to the Triatominae and Triatominae-borne pathogens and clinical Chagas' disease" (*12*). Careful curation was achieved with the help of assistants, requests via reprint request cards, use of a shopping cart to transport journals between the university library and copy shop, and use of a punch

card system to organize articles. Compiled over 16 years and containing >23,000 publications, these bibliographies are a unique contribution to the field of Chagas disease research (*11–13*). The hard copy (print) collection resides at the Centers for Disease Control and Prevention in Atlanta, Georgia, USA.

In addition to a legacy of bibliographies and publications, Ryckman's collection of >25,000 insects is available for study at the Bohart Museum of Entomology, University of California, Davis. This collection includes the triatomine specimens that resulted from Ryckman's many colonies of triatomines and other insects.

In honor of his contributions to the study of Chagas disease vectors, Ryckman was honored with an eponym in 1972: *Triatoma ryckmani*, a rare species from Central America (*14*). As an authority on triatomine ecology and Chagas disease, a patient teacher and mentor, an international scholar, and a family man, Raymond E. Ryckman is an admirably well-rounded scientist.

Ms. Curtis-Robles is a PhD candidate at Texas A&M University, College Station, studying Chagas disease eco-epidemiology in the southern United States. During the fall of 2014, Dr. Ryckman graciously returned her unsolicited phone call, and she has subsequently enjoyed many conversations and visits with this delightfully engaging, enthusiastic, spry-witted, and ever-a-teacher 99-year-old triatomine expert.

Dr. Beard currently serves as chief of the Bacterial Diseases Branch in the Division of Vector-Borne Diseases and associate director for climate change at the National Center for Emerging and Zoonotic Infectious Diseases at the Centers for Disease Control and Prevention in Fort Collins. He previously worked on Chagas disease for >15 years, inspired and mentored by Dr. Ryckman.

References

1. Ryckman RE. Plague vector studies. I. The rate of transfer of fleas among *Citellus*, *Rattus* and *Sylvilagus* under field conditions in southern California. J Med Entomol. 1971;8:535–40. http://dx.doi.org/10.1093/jmedent/8.5.535
2. Ryckman RE. Plague vector studies. II. The role of climatic factors in determining seasonal fluctuations of flea species associated with the California ground squirrel. J Med Entomol. 1971;8:541–9. http://dx.doi.org/10.1093/jmedent/8.5.541
3. Ryckman RE. Plague vector studies. III. The rate deparasitized ground squirrels are reinfested with fleas under field conditions. J Med Entomol. 1971;8:668–70. http://dx.doi.org/10.1093/jmedent/8.6.668
4. Ryckman RE. Biosystematics and hosts of the *Triatoma protracta* complex in North America: (Hemiptera, Reduviidae, Rodentia, Cricetidae). University of California Publications in Entomology. 1962;27:93–239.
5. Ryckman RE, Olsen LE. Studies on *Odontoloxozus longicornis* (Diptera: Neriidae). Part II. Distribution and ecology. Ann Entomol Soc Am. 1963;56:470–2. http://dx.doi.org/10.1093/aesa/56.4.470.
6. Newell IM, Ryckman RE. *Hirstiella pyriformis* sp. n. (Acari, Pterygosomidae), a new parasite of lizards from Baja California. J Parasitol. 1964;50:163–71. http://dx.doi.org/10.2307/3276056
7. Ryckman RE, Zackrison JL. Son of the living desert–Edmund C. Jaeger, 1887–1983: ecologist, educator, environmentalist, biologist, and philanthropist. Loma Linda (CA): Loma Linda University; 1998. p. 1–466.
8. Ryckman RE, Ryckman JV. Epizootiology of *Trypanosoma cruzi* in southwestern North America. XII. Does Gause's rule apply to the ectoparasitic Triatominae? (Hemiptera: Reduviidae) (Kinetoplastidae: Trypanosomidae) (Rodentia: Cricetidae). J Med Entomol. 1967;4:379–86. http://dx.doi.org/10.1093/jmedent/4.3.379
9. Ryckman RE, Ryckman AE. Reduviid bugs. In: Smith C, editor. Insect colonization and mass production. New York: Academic Press; 1966. p. 183–200.
10. Ryckman RE, Ryckman AE. Baja California Triatominae (Hemiptera: Reduviidae) and their hosts (Rodentia: Cricetidae). Ann Entomol Soc Am. 1961;54:142–3. http://dx.doi.org/10.1093/aesa/54.1.142
11. Ryckman RE, Blankenship CM. The Triatominae and Triatominae-borne trypanosomes of North and Central America and the West Indies, a bibliography with index. Bull Soc Vector Ecol. 1984;9:112–430.
12. Ryckman RE, Zackrison JL. A bibliography to Chagas' disease, the Triatominae and triatomine-borne trypanosomes of South America (Hemiptera: Reduviidae: Triatominae). Bull Soc Vector Ecol. 1987;12:1–464.
13. Ryckman RE, Archbold EF. The Triatominae and Triatominae-borne trypanosomes of Asia, Africa, Australia, and the East Indies. Bull Soc Vector Ecol. 1981;6:143–66.
14. Zeledón R, Ponce C. Description of a new Triatominae species of Honduras, Central America (Hemiptera: Reduviidae) [in Spanish]. Rev Biol Trop. 1972;20:275–9.

Address for correspondence: Rachel Curtis-Robles, 4458 TAMUS, Veterinary Integrative Biosciences Department, Texas A&M University, College Station, TX 77843, USA; email: rcurtis@cvm.tamu.edu

Baylisascaris procyonis Parasites in Raccoons, Costa Rica, 2014

Mario Baldi, Gilbert Alvarado, Steve Smith, Mario Santoro, Natalie Bolaños, Carlos Jiménez, Sabine E. Hutter, Chris Walzer

Author affiliations: University of Veterinary Medicine, Vienna, Austria (M. Baldi, S. Smith, S.E. Hutter, C. Walzer); Universidad Nacional, Heredia, Costa Rica (M. Baldi, N. Bolaños, C. Jiménez); Universidad de Costa Rica, San Pedro, Costa Rica (G. Alvarado); Istituto Zooprofilattico Sperimentale del Mezzogiorno, Naples, Italy (M. Santoro)

To the Editor: *Baylisascaris procyonis* (Ascaridoidea: Ascarididae) parasites are facultatively heteroxenous nematodes that are widely distributed in the United States and Canada, where prevalence rates reach 70%–90%. They colonize the small intestine of their final host, the northern raccoon (*Procyon lotor*), whose feces can contain up to 25 $\times 10^3$ eggs/g. Under ideal environmental conditions (100% humidity and 24°C), eggs become infective in soil (*1,2*). When ingested by other mammalian hosts, third-stage larvae can produce pathologic changes called larva migrans, which can lead to chronic neurologic disorders and even death (*1,3*). *B. procyonis* parasite infection of humans occurs by the fecal–oral route (ingestion of eggs in contaminated food) (*1*). Small children are particularly vulnerable through accidental geophagia. Public health concerns arise where raccoon and human populations overlap.

As elsewhere, raccoons in Costa Rica have expanded their range into human-dominated areas, becoming common in the Greater Metropolitan Area, an ≈2,000-km² portion of the Central Valley, home to 2.6 million persons. During the past decade, the government wildlife agency (Ministerio de Ambiente y Energía [MINAE]) reported a steep increase in raccoon-related complaints (*4*).

We examined raccoons for which a nuisance complaint was received by MINAE at 8 locations inside the Greater Metropolitan Area and report the southernmost range extension of *B. procyonis* parasites (previously not detected at latitudes below 31° N; Costa Rica [8°–11° N] is substantially farther south [*2*]). *B. procyonis* parasites in kinkajous (*Potos flavus*) have been reported, but that parasite was subsequently determined to be *B. potosis* (*5,6*).

For 10 months in 2014, raccoons were trapped in wooded areas and residential gardens by using baited traps (Havahart, Lititz, PA, USA) over 315 trap-nights. Fecal samples were collected from the animals and from communal latrines near the trapping sites, and the Sheather flotation technique was used to detect eggs in the feces (*1*). During raccoon necropsies, any adult roundworms (including *B. procyonis*) found in the gastrointestinal tract were fixed in 70% and 100% ethanol for morphologic and molecular identification, respectively.

Parasites were examined by light microscopy. Those identified as *B. procyonis* were counted and sexed. Voucher specimens of *B. procyonis* were deposited in the Natural History Museum, London, UK (accession no. NHMUK 2015.2.23 1–2). Nematodes were assigned to the genus *Baylisascaris* on the basis of genus-specific features. Species-specific features of *B. procyonis* (shape of lip denticles, male pericloacal rough areas, and male tail shape [*7*]) were used to distinguish *B. procyonis* from *B. columnaris* (*6,7*). Eggs were identified according to size and shell thickness. The shell has a characteristic soft granular surface (*3*). Mean size of the oval eggs was 57.0 μm (range 59.34–55.48) by 70.3 μm (range 51.5–72.1) (*1–3*).

We used DNA extracted from *B. procyonis* parasites to amplify the mitochondrial cytochrome c oxidase 2 gene, ribosomal ITS1–5.8S-ITS2, and ribosomal 28S genes by using the primers and protocol described by Franssen et al. (*8*). We found 100% identity between the sequences from *B. procyonis* parasites from Costa Rica and those from North America (GenBank accession nos. AF179908 [cytochrome c oxidase 2 region], JQ403615 [ITS1–5.8S-ITS2 region], and KC434770 [28S region]).

We found *B. procyonis* parasites in 10 of 20 captured raccoons (Table), from which 137 adult worms (78 females, 59 males) were recovered. Infection intensity was 1–60 parasites/raccoon (mean 12.5). Average specimen length was 11.6 cm (range 8.1–20 cm). *B. procyonis* infection was found in raccoons at all 8 locations.

Our sampling locations included 2 playgrounds and 1 school yard. A previous study found high prevalence of *Toxocara* spp. nematode eggs in dog feces from the same geographic region (*9*). Because egg identification can be difficult and that study was based exclusively on morphologic description without molecular confirmation or electron microscopy, it is possible that some *B. procyonis* eggs were misidentified as *Toxocara* spp. Both *Toxocara* spp. and *B. procyonis* parasites can cause larva migrans, the

Table. Age and sex of raccoons sampled for roundworm testing, Costa Rica, 2014

Raccoons	No. (%) raccoons	
	Sampled	Positive for *Baylisascaris procyonis* parasites
Age		
Juvenile	4 (20)	3 (30)
Adult	16 (80)	7 (70)
Sex		
M	6 (30)	2 (20)
F	14 (70)	8 (80)
Total	20	10

latter being more aggressive. In the Greater Metropolitan Area and Costa Rica in general, free-ranging dogs are common, including at playgrounds and school yards, sites also vulnerable to nocturnal visits by raccoons. Dogs can have patent *B. procyonis* parasite infections and can play a role in transmission of the parasite from raccoons to humans.

In Costa Rica, cases of larva migrans have been reported. The Unidad de Investigación y Análisis, Registros y Estadísticas de Salud at the National Children's Hospital, San José, Costa Rica, reported 135 cases of larva migrans ocularis and 21 cases of visceral larva migrans caused by nonspecifically identified ascarids during 2005–2014 (unpub. data). However, these diagnoses were based on IgG serologic testing results (Martinez J., National Children's Hospital; pers. comm., 2015), which do not identify ascarid species. Western blot testing would improve accuracy (*10*).

The eco-epidemiology of *B. procyonis* parasites in tropical settings is relevant to public health because it might play a yet-unrecognized role in larva migrans pathology, which can be severe. Increased contact between raccoons and humans also warrants further investigation to improve understanding and minimize zoonotic risk.

References

1. Kazacos KR. *Baylisascaris procyonis* and related species. In: Samuel WM, Pybus MJ, Kocan AA, editors. Parasitic diseases of wild mammals. 2nd ed. Ames (IA): Iowa State University Press; 2001. p.301–41.
2. Hernandez SM, Galbreath B, Riddle DF, Moore AP, Palamar MB, Levy MG, et al. *Baylisascaris procyonis* in raccoons (Procyon lotor) from North Carolina and current status of the parasite in the USA. Parasitol Res. 2013;112:693–8. http://dx.doi.org/10.1007/s00436-012-3186-1
3. Roussere GP, Murray WJ, Raudenbush CB, Kutilek MJ, Levee DJ, Kazacos KR. Raccoon roundworm eggs near homes and risk for larva migrans disease, California communities. Emerg Infect Dis. 2003;9:1516–22. http://dx.doi.org/10.3201/eid0912.030039
4. Soto M. Raccoons causing problems inside the Greater Metropolitan Area [in Spanish] [cited 2015 Jul 11]. http://wfnode01.nacion.com/2010-09-05/AldeaGlobal/Notas Secundarias/AldeaGlobal2507351.aspx
5. Tokiwa T, Nakamura S, Taira K, Une Y. *Baylisascaris potosis* n. sp., a new ascarid nematode isolated from captive kinkajou, *Potos flavus*, from the Cooperative Republic of Guyana. Parasitol Int. 2014;63:591–6. http://dx.doi.org/10.1016/j.parint.2014.03.003
6. Overstreet RM. *Baylisascaris procyonis* (Stefanski and Zarnowski, 1951) from the kinkajou, *Potos flavus*, in Colombia. J Parasitol. 1970;37:192–5.
7. Anderson RC, Chabaud AG, Willmott S. Keys to the nematode parasites of vertebrates: archival volume. Wallingford (UK): CAB International; 2009. p. 463.
8. Franssen F, Xie K, Sprong H, van der Giessen J. Molecular analysis of *Baylisascaris columnaris* revealed mitochondrial and nuclear polymorphisms. Parasit Vectors. 2013;6:124. http://dx.doi.org/10.1186/1756-3305-6-124
9. Paquet-Durand I, Hernández J, Dolz G, Zuñiga JJ, Schnieder T, Epe C. Prevalence of *Toxocara* spp., *Toxascaris leonina* and ancylostomidae in public parks and beaches in different climate zones of Costa Rica. Acta Trop. 2007;104:30–7. http://dx.doi.org/10.1016/j.actatropica.2007.06.011
10. Dangoudoubiyam S, Kazacos KR. Differentiation of larva migrans caused by *Baylisascaris procyonis* and *Toxocara* species by Western blotting. Clin Vaccine Immunol. 2009;16:1563–8. http://dx.doi.org/10.1128/CVI.00251-09

Address for correspondence: Mario Baldi, Institute of Wildlife Ecology, University of Veterinary Medicine; Savoyenstrasse 1, A-1160, Vienna, Austria; email: baldim@medvetuni.ac.at or mario.baldi.salas@una.cr

Artemisinin-Resistant *Plasmodium falciparum* K13 Mutant Alleles, Thailand–Myanmar Border

Mikael Boullé,[1] Benoit Witkowski,[1] Valentine Duru, Kanlaya Sriprawat, Shalini K. Nair, Marina McDew-White, Tim J.C. Anderson, Aung Pyae Phyo, Didier Menard, François Nosten

Author affiliations: Mahidol University Faculty of Tropical Medicine, Mae Sot, Thailand (M. BoulléSriprawat K, A.P. Phyo, F. Nosten); Institut Pasteur in Cambodia, Phnom Penh, Cambodia (B. Witkowski, V. Duru, D. Menard); Texas Biomedical Research Institute, San Antonio, Texas, USA (S.K. Nair, M. McDew-White; T.J.C. Anderson; F. Nosten); University of Oxford Nuffield Department of Medicine, Oxford, UK (F. Nosten)

To the Editor: Artemisinin resistance (ART-R) in *Plasmodium falciparum* phenotypes may have evolved independently in various areas of the Greater Mekong Subregion (*1,2*), prompting the World Health Organization to change its regional policy from containment to elimination (*3*). Risks associated with ART-R include compromised use of artemisinin combined therapy, partner drug resistance selection, total ART-R resistance, and geographic extension

---

[1]These authors contributed equally to this article.

to other malaria-endemic regions (2,3). Characterization of ART-R in each setting and rapid update of listed phenotypes classified as in vitro resistant to this antimalarial drug are needed.

Detected in western Cambodia in 2008, ART-R has been observed in neighboring countries, notably at the Thailand–Myanmar border (4,5). Resistance is partial and manifests by an increased parasite clearance half-life (PCHL) of >5 hours in patients receiving artemisinin monotherapy or artemisinin combined therapy (6). In vitro, ART-R phenotype has been characterized by the ring-stage survival assay (RSA$^{0–3h}$, cutoff 1%) (7) and mutations in the propeller domain of a *kelch* gene on chromosome 13 (K13) (8,9). However, tremendous K13 variability in different genetic backgrounds requires confirmation of specific alleles as ART-R markers (2,3); even statistically significant clinical associations are rarely unequivocal (5–9).

On the Thailand–Myanmar border where ART-R has been documented (4), we investigated K13 mutations in clinical and in vitro phenotypes. Patients with nonsevere *P. falciparum* hyperparasitemia infections treated during 2011–2013 at the Shoklo Malaria Research Unit (Mae Sot, Thailand) were treated with artesunate, then combined artesunate/mefloquine (5). We retrospectively selected 33 case-patients on the basis of PCHL outcome to analyze a broad parasite clearance distribution with available cryo-preserved isolates. Full written consent from all patients was obtained. PCHL was calculated on the basis of initial and repeated parasitemia measurement every 6 hours until undetectable asexual parasitemia (6) was achieved. Venous blood samples were cryopreserved before drug administration (day 0).

Short-term, culture–adapted parasites (3% hemato-crit; RPMI-1640 supplemented with 10% human serum, 0.05 mg/mL hypoxanthine, 2 mg/mL sodium bicarbonate, 2 mg/mL glucose, 0.04 mg/mL gentamicin, 0.3 mg/mL L-glutamine in a 37°C candle-jar atmosphere) were split for blinded RSA$^{0–3h}$ and K13 genotyping. We performed RSA$^{0–3h}$ in duplicate by selecting early rings (0–3 h) in a combination of percoll gradient and sorbitol lysis, followed by a 6-h exposure to 700 nmol/L dihydroartemisinin (7). RSA survival rate was measured microscopically 66 hours after drug removal and calculated as the quotient of para-sitemia upon DHA exposure over control parasitemia with dimethyl sulfoxide. Only 25 isolates that were successfully culture-adapted provided RSA survival rates.

After the phenotypical assays, the genotypes were obtained and K13 regions were amplified by using 3 primer sets: fragment 1 (1725380–1725680 bp, pos 211–302), F-tgaaaatatggtaggtgatt and R-atcgtttcctatgttcttct; frag-ment 2 (1725980–1726520 bp, pos 419–570), F-atc-taggggtattcaaagg, R-ccaaaagatttaagtgaaag; and fragment 3 (1726400–1726940 bp, pos 545–707), F-ctgccattcatttgtatct,

R-ggatatgatggctcttcta) before sequencing (8). The 33 mono-clonal isolates yielded clear K13 gene sequences. All except 4 isolates from patients who had PCHL >5 h had a single K13 mutant allele (19/23), and all isolates except 1 (G538V) from case-patients who had PCHL <5 h carried the K13 3D7 wild-type allele (9/10). PCHL was significantly different be-tween K13 wild-type (n = 13, median 4.3 h) and mutant (n = 20, median = 7.2 h) alleles (p<0.01 by Mann-Whitney U test). Among the 25 isolates successfully tested, RSA sur-vival rates differed significantly between K13 wild-type (n = 10, median 0.5%) and mutant (n = 15, median 3.5%) al-leles (p<0.001 by Mann-Whitney U test). When PCHL was present <5 h, RSA survival rates (n = 7, median 0.5%) were significantly lower than when PCHL was >5 hours (n = 18, median 3.1%) (p = 0.001 by Mann-Whitney U test).

In detail (Figure), C580Y and N458Y mutants were consistently associated with PHCL >5h and RSA values >1%. The C580Y allele has been repeatedly confirmed as a molecular marker of ART-R (5,7–9). Previous reports have inconsistently associated the N458Y mutation with ART-R; 7 case-patients with PCHL >5 h were reported by Ashley et al. (5), and 1 artemisinin sensitive case was reported at the China–Myanmar border (10). Nevertheless, this mutation has not been confirmed in vitro (3). We confirmed the mu-tation in vitro, and in vivo, according to the World Health Organization definition (3), this K13 allele as a molecular marker of ART-R.

Conflicting data observed between PCHL and RSA values for 4 mutant alleles (E252Q, P441L, G538V, and
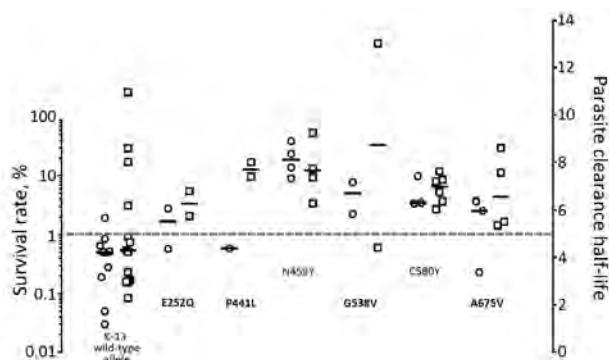
Figure. Distribution of parasite clearance half-lives (n = 33, squares) and Ring-stage survival assay survival rates (n = 25, circles) of *Plasmodium falciparum* isolates from patients on the Thailand–Myanmar border, determined on the basis of each K13 genotype. Mean survival rate of duplicate measures are showed for each isolate. Dashed line represents the cutoff value for parasite clearance half-life (artemisinin resistance >5 h) and RSA survival (artemisinin resistance >1%). K13 alleles N458Y and C580Y were consistently associated with parasite clearance half-life and survival rates above threshold. Bold text indicates K13 alleles with variable parasite clearance half-life and RSA associations. Horizontal bars represent median values for each K13 genotype. Survival rate for laboratory reference 3D7 strain was 0.2%.

A675V) require further targeted approaches to relate them to previous reports. In a study in which only PCHL were reported (*5*), the proportion of slowly clearing infections were 69%, 0%, 30%, and 61% for the P441L, E252Q, G538V, and A675V alleles, respectively. Discrepancies can result from confounding pharmacologic (drug level, partner drug), immunologic, and parasitologic (genetic background, parasitic stage at treatment initiation) factors.

RSA results and K13 genotypes were associated with delayed parasite clearance, emphasizing the pertinence of each method to define ART-R. In this area, N458Y is a marker of ART-R. To solve conflicts about specific mutations, more detailed characterization in vitro and in vivo is needed.

References
1. Takala-Harrison S, Jacob CG, Arze C, Cummings MP, Silva JC, Dondorp AM, et al. Independent emergence of artemisinin resistance mutations among *Plasmodium falciparum* in Southeast Asia. J Infect Dis. 2015;211:670–9. http://dx.doi.org/10.1093/infdis/jiu491
2. Fairhurst RM. Understanding artemisinin-resistant malaria: what a difference a year makes. Curr Opin Infect Dis. 2015;28:417–25. http://dx.doi.org/10.1097/QCO.0000000000000199
3. World Health Organization. Status report on artemisinin and ACT resistance—September 2015 [cited 2015 Dec 12]. http://www.who.int/malaria/publications/atoz/status-rep-artemisinin-resistance-sept2015.pdf
4. Phyo AP, Nkhoma S, Stepniewska K, Ashley EA, Nair S, McGready R, et al. Emergence of artemisinin-resistant malaria on the western border of Thailand: a longitudinal study. Lancet. 2012; 379:1960–6. http://dx.doi.org/10.1016/S0140-6736(12)60484-X
5. Ashley EA, Dhorda M, Fairhurst RM, Amaratunga C, Lim P, Suon S, et al. Spread of artemisinin resistance in *Plasmodium falciparum* malaria. N Engl J Med. 2014;371:411–23. http://dx.doi.org/10.1056/NEJMoa1314981
6. White LJ, Flegg JA, Phyo AP, Wiladpai-ngern JH, Bethell D, Plowe C, et al. Defining the *in vivo* phenotype of artemisinin-resistant falciparum malaria: a modelling approach. PLoS Med. 2015;12. http://dx.doi.org/10.1371/journal.pmed.1001823
7. Witkowski B, Amaratunga C, Khim N, Sreng S, Chim P, Kim S, et al. Novel phenotypic assays for the detection of artemisinin-resistant *Plasmodium falciparum* malaria in Cambodia: in-vitro and ex-vivo drug-response studies. Lancet Infect Dis. 2013;13:1043–9. http://dx.doi.org/10.1016/S1473-3099(13)70252-4
8. Ariey F, Witkowski B, Amaratunga C, Beghain J, Langlois AC, Khim N, et al. A molecular marker of artemisinin-resistant *Plasmodium falciparum* malaria. Nature. 2013;505:50–5. http://dx.doi.org/10.1038/nature12876
9. Straimer J, Gnadig NF, Witkowski B, Amaratunga C, Duru V, Ramadani AP, et al. Drug resistance. K13-propeller mutations confer artemisinin resistance in *Plasmodium falciparum* clinical isolates. Science. 2015;347:428–31. http://dx.doi.org/10.1126/science.1260867
10. Wang Z, Wang Y, Cabrera M, Zhang Y, Gupta B, Wu Y, et al. Artemisinin resistance at the China-Myanmar border and association with mutations in the K13 propeller gene. Antimicrob Agents Chemother. 2015;6952–9. http://dx.doi.org/10.1128/AAC.01255-15

Address for correspondence: Didier Ménard, Malaria Molecular Epidemiology Unit, Institut Pasteur in Cambodia, 5 Boulevard Monivong, PO Box 983, Phnom Penh, Cambodia; email: dmenard@pasteur-kh.org

Meningococcal Group W Disease in Infants and Potential Prevention by Vaccination

Sydel R. Parikh, Helen Campbell, Kazim Beebeejaun, Sonia Ribeiro, Steve J. Gray, Ray Borrow, Mary E. Ramsay, Shamez N. Ladhani

Author affiliations: Public Health England, London, UK (S.R. Parikh, H. Campbell, K. Beebeejaun, S. Ribeiro, S.J. Gray, R. Borrow, M.E. Ramsay, S.N. Ladhani); St. George's University of London, London (S.N. Ladhani)

To the Editor: We recently reported that postvaccination serum samples from infants immunized with a novel, protein-based multicomponent meningococcal serogroup B (MenB) vaccine (Bexsero; GlaxoSmithKline Vaccines, Verona, Italy) have bactericidal activity against the hypervirulent meningococcal group W (MenW) strain belonging to the sequence type (ST) 11 clonal complex (*1*). Historically, MenW has been a rare cause of invasive meningococcal disease (IMD), accounting for <5% of confirmed cases in England and Wales (*2*). Since 2009, MenW cases caused by

this hypervirulent strain have rapidly increased in England (*2*). During the 2014–15 epidemiologic year (July 1–June 30), this capsular group accounted for 176 (24%) of 724 IMD cases in England (*3*). In response to this outbreak, in August 2015, the United Kingdom introduced an emergency adolescent conjugate vaccination program against meningococcal capsular groups ACW and Y. Over 2 years, the program aims to provide vaccine to all youth 13–18 years of age and to new university entrants <25 years of age. This program is expected to protect adolescents (25 of 176 [14%] MenW cases during 2014–15 were in those 15–19 years of age), and, by targeting youth with the highest carriage rates, to protect others through indirect (herd) protection, which has been consistently observed in vaccine programs, including that for meningococcal group C (*4,5*). Indirect protection associated with the adolescent immunization program will likely take several years to manifest (*6*).

Infants <1 year of age have the highest incidence of IMD and the highest number of IMD cases and deaths (*5*). During the 2014–15, 127 (18%) of the 724 IMD cases in England occurred in this group: 101 (80%) meningococcal group B (MenB) cases, 21 (16%) MenW cases, 1 (1%) group C case, and 4 (3%) group Y cases (*7*). In September 2015, MenB vaccine was introduced into the UK infant

immunization program under a 2-, 4-, and 12-month schedule. We analyzed the epidemiology and long-term trends for MenW disease in infants in England to assess the potential effects of the infant MenB immunization program for preventing MenW cases in this highly vulnerable age group.

During the epidemiologic period 1998–99 through 2014–15, a total of 176 MenW cases were confirmed in infants. The number of cases peaked during 2000–01 (n = 28) because of a national outbreak associated with the Hajj pilgrimage and then declined rapidly after mandatory vaccination for pilgrims was instigated (Figure, panel A). During that outbreak, most infants acquired the infection indirectly from family members who traveled to the Hajj, highlighting this group's susceptibility to IMD. The number of MenW cases in infants began increasing again from 4 cases in 2012–13 to 12 in 2013–14 and 21 in 2014–15. During 2014–15, these 21 MenW cases represented 16.5% of 127 total IMD cases among infants, 12% of 176 total MenW cases, and 3% of 724 total IMD cases in England. All infants with MenW IMD resided in England and had not traveled abroad. The number of MenW cases increased from birth among infants, peaking at 4 months of age and remaining high until the first birthday. Most (123 [70%]) of the 176 MenW cases confirmed during (44/66 [67%]) and after (79/110 [72%]) the Hajj outbreak were in persons ≥5
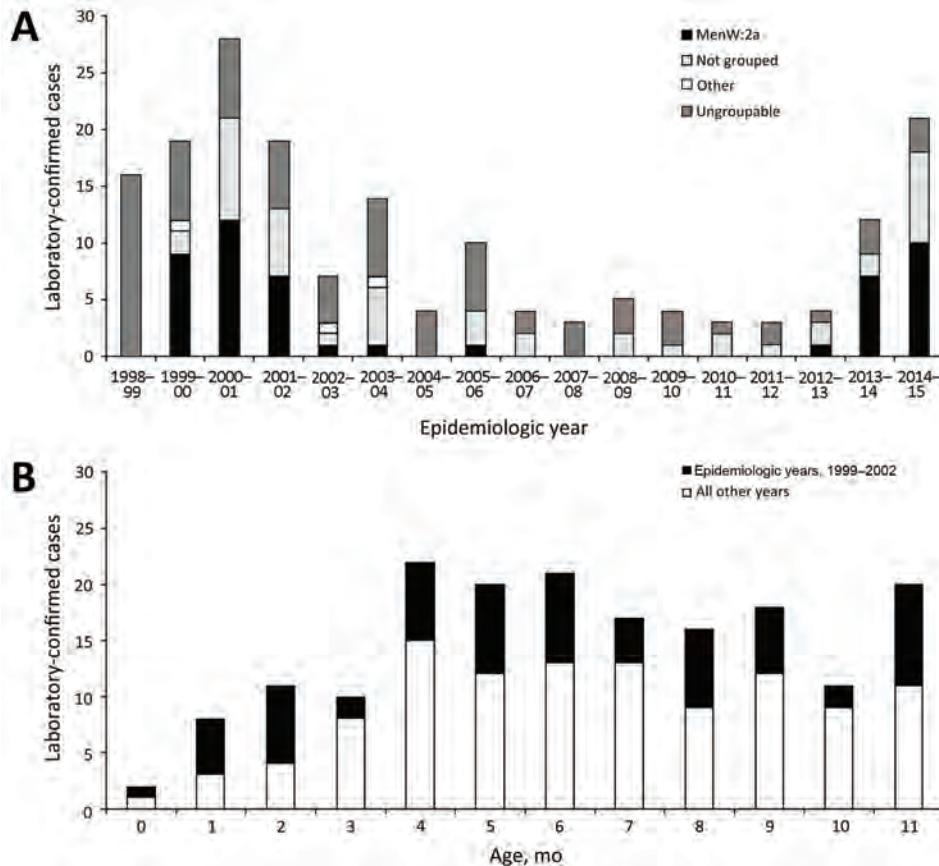
Figure. Incidence of invasive meningococcal disease (IMD) in infants <1 year of age in England during the epidemiologic years 1998–99 through 2014–15. A) Incidence of IMD and phenotypic characterization of laboratory-confirmed meningococcal group W strains in infants <1 year of age. B) Total laboratory-confirmed meningococcal group W cases in infants <1 year of age by month of age. Cases related to the Hajj outbreak occurred during 1999–00 through 2001–02.

months of age and were potentially preventable by MenB vaccine vaccination.

During 2012–13 through 2014–15, a total of 25 (67.5%) of 37 MenW cases in infants were confirmed by culture; 18 (49%) of these cases were phenotypically characterized as MenW:2a, a surrogate phenotypic marker for the hypervirulent ST11 MenW strain. Ten (48%) of the 21 isolates from infants during 2014–15 were MenW:2a, compared with 1 (25%) of 4 during 2012–13 (Figure, panel B). Final diagnoses reported for 20 infants included meningitis (n = 10 [50%]), septicemia (n = 3 [15%]), both meningitis and septicemia (n = 5 [10%]), and septic arthritis (n = 1 [2%]). From 1998–99 through 2014–15, six infants died of MenW IMD (case-fatality rate 3.4%). Four of those deaths occurred during the Hajj outbreak; only 1 death attributed to MenW occurred during the 3 most recent epidemiologic years.

The rapid increase in MenW cases among infants, particularly most recently (2014–15), is cause for concern, and the contemporaneous introduction of MenB vaccine into the national immunization schedule is timely. Although this vaccine is licensed for prevention of MenB disease, the antigens are not specific to this capsular group and could protect against other meningococcal capsular groups that share the same antigens as those in the vaccine. Infants and toddlers immunized with MenB vaccine are expected to develop bactericidal antibodies against ST11 MenW. Data on age distribution suggest that ≈70% of MenW cases in infants could be prevented by MenB vaccination at 2 and 4 months of age. Beginning in mid-2016, the MenB vaccine booster for children 1 year of age is also expected to protect toddlers, for whom MenW cases have also rapidly increased (3).

Acknowledgments

References

1. Ladhani SN, Giuliani MM, Biolchi A, Pizza M, Beebeejaun K, Lucidarme J, et al. Effectiveness of meningococcal B vaccine against endemic hypervirulent *Neisseria meningitidis* W strain, England. Emerg Infect Dis. 2016;22:309–11. http://dx.doi.org/10.3201/eid2202.150369
2. Ladhani SN, Beebeejaun K, Lucidarme J, Campbell H, Gray S, Kaczmarski E, et al. Increase in endemic *Neisseria meningitidis* capsular group W sequence type 11 complex associated with severe invasive disease in England and Wales. Clin Infect Dis. 2015;60:578–85. http://dx.doi.org/10.1093/cid/ciu881
3. Campbell H, Saliba V, Borrow R, Ramsay M, Ladhani SN. Targeted vaccination of teenagers following continued rapid endemic expansion of a single meningococcal group W clone (sequence type 11 clonal complex), United Kingdom 2015. Euro Surveill. 2015;20:21188. http://dx.doi.org/10.2807/1560-7917.ES2015.20.28.21188
4. Ramsay ME, Andrews NJ, Trotter CL, Kaczmarski EB, Miller E. Herd immunity from meningococcal serogroup C conjugate vaccination in England: database analysis. BMJ. 2003;326:365–6. http://dx.doi.org/10.1136/bmj.326.7385.365
5. Trotter CL, McVernon J, Ramsay ME, Whitney CG, Mulholland EK, Goldblatt D, et al.; SAGE subgroup. Optimising the use of conjugate vaccines to prevent disease caused by *Haemophilus influenzae* type b, *Neisseria meningitidis* and *Streptococcus pneumoniae*. Vaccine. 2008;26:4434–45. http://dx.doi.org/10.1016/j.vaccine.2008.05.073
6. Ladhani SN, Christensen H, Trotter C, Ramsay ME. Indirect impact of an adolescent meningococcal ACWY conjugate vaccine programme in England with and without catch-up: a transmission dynamic model. Presented at: 13th Congress EMGM, European Meningococcal Disease Society; 2015 September 14–17; Amsterdam, the Netherlands. Abstract 5.01. http://emgm.eu/meetings/emgm2015/EMGM2015_programme.pdf
7. Public Health England. Infection report. Invasive meningococcal disease (laboratory reports in England): 2014/2015 annual data by epidemiological year. Health Protection Report. 2015;9(38) [cited 2016 Mar 23]. https://www.gov.uk/government/uploads/system/uploads/attachment_data/file/498057/hpr3815_imd-crrctd.pdf

Address for correspondence: Shamez Ladhani, Public Health England, Immunisation, Hepatitis and Blood Safety Department, 61 Colindale Ave, London NW9 5EQ, UK; email: shamez.ladhani@phe.gov.uk

Novel Reassortant Avian Influenza A(H5N6) Viruses in Humans, Guangdong, China, 2015

Yong-Yi Shen,[1] Chang-Wen Ke,[1] Qian Li,[1] Run-Yu Yuan, Dan Xiang, Wei-Xin Jia, Yun-Di Yu, Lu Liu, Can Huang, Wen-Bao Qi, Reina Sikkema, Jie Wu, Marion Koopmans, Ming Liao

Author affiliations: Key Laboratory of Zoonosis Prevention and Control of Guangdong Province, Guangzhou (Y.-Y. Shen); College of Veterinary Medicine, South China Agricultural University, Guangzhou, China (Y.-Y. Shen, Q. Li, W.-X. Jia, Y.-D. Yu, W.-B. Qi, M. Liao); Guangdong Provincial Center for Disease Control and Prevention, Guangzhou (C.-W. Ke, R.-Y. Yuan, J. Wu); Shantou University Medical College, Shantou, China (D. Xiang, L. Liu, C. Huang); Key Laboratory of Veterinary Vaccine Innovation of the Ministry of Agriculture, Guangzhou (W.-B. Qi); National Institute of Public Health and the Environment, Bilthoven, the Netherlands (R. Sikkema, M. Koopmans); National and Regional Joint Engineering Laboratory for Medicament of Zoonosis Prevention and Control, Guangzhou (M. Liao)

[1]These authors contributed equally to this article.

To the Editor: Avian influenza A(H5N6) influenza viruses have circulated among poultry in southern (Jiangxi, Guangdong) and western (Sichuan) provinces of China since 2013 (*1,2*). In 2014, outbreaks of H5N6 virus infection occurred among poultry in China, Laos, and Vietnam (*1*). In April 2014, the first case of highly pathogenic H5N6 infection among humans was detected in Sichuan Province (*3*); the second case was detected on December 3, 2014, in Guangdong Province (*4*). In December 2015, 4 humans in Guangdong Province were infected with H5N6 influenza (*5,6*).

To study the genetic basis of continuing human infections with this avian influenza subtype, we sequenced the complete genomes of 2 of the 4 human H5N6 isolates obtained in December 2015 in Guangdong Province. We compared these sequences with those of 1 H6N6 and 8 H5N6 influenza viruses isolated from birds in live poultry markets in this region during 2013–2015 (online Technical Appendix, http://wwwnc.cdc.gov/EID/article/22/8/16-0146-TechApp1.pdf) and other published genomes of H5, H6N6, and H9N2 avian influenza viruses (online Technical Appendix Table). Phylogenetic analyses of the hemagglutinin (HA) genes showed that all human H5N6 isolates belonged to clade 2.3.4.4 (online Technical Appendix Figure 1, panel A). HA and neuraminidase (NA) genes of some H5N6 viruses isolated in Guangdong Province during 2013–2014 were in the Sichuan-like lineage, but all of those from 2015 were in the Jiangxi-like lineage (online Technical Appendix Figure 1, panels A, B).

Despite the similarities of the HA and NA genes, the 6 internal genes from the 2 human isolates from 2015, A/Guangdong/ZQ874/2015 (H5N6) and A/Guangdong/SZ872/2015 (H5N6) were different from 2 human H5N6 isolates from 2014, A/Sichuan/26221/2014 (H5N6) and A/Guangzhou/39715/2014 (H5N6). The polymerase basic (PB) 2 gene from isolate A/Guangdong/ZQ874/2015 (H5N6) appears to have derived from an H6N6 virus isolated from a duck; all other genes in this isolate were derived from H5N6 viruses that have been circulating among poultry since 2013 (online Technical Appendix Figure 1, panel C; online Technical Appendix Figure 2). This isolate showed high nucleotide identity to 6 of the 8 genes (HA, 96.5%; NA, 98.2%; nucleoprotein (NP), 98.5%; polymerase acidic (PA), 98.3%; PB1, 98.1%; PB2, 98.4%) of the isolate A/chicken/Guandong/FG594/2015 (H5N6); the identities of the matrix (M) and nonstructural protein (NSP) genes were 76.2% and 79.8% similar, respectively. This finding suggests that undetected reassortants of H5N6 may exist. The other human isolate, A/Guangdong/SZ872/2015 (H5N6), showed high nucleotide identity with A/Yunnan/0127/2015 (H5N6), an isolate collected from a person in Yunnan Province (GenBank accession nos. KT963053–60; online Technical Appendix Table), for all 8 genes (HA, 97.2%; M, 97.7%; NA, 96.8%; NP, 98.3%; NSP, 93.2%; PA, 95.9%; PB1, 96.9%; PB2, 94.0%). The 6 internal genes of A/Guangdong/SZ872/2015 (H5N6) appear to have come from the enzootic H9N2 (ZJ-HJ/07) virus lineage (online Technical Appendix Figure 1, panel C). These

Table. Molecular analyses of 5 influenza A(H5N6) virus isolates from humans in China, 2014 and 2015*

Phenotypic consequences	Mutations	A/Sichuan/ 26221/2014	A/Guangzhou/ 39715/2014	A/Yunan/ 0127/2015	A/Guangdong/ SZ872/2015	A/Guangdong/ ZQ874/2015
HA gene						
Altered receptor specificity	S128P	T	P	P	P	P
Increased α2,6-SA recognition	S137A	A	A	A	A	A
Removal of the 158N	T160A	A	T	A	A	A
glycosylation	Q226L	Q	Q	Q	Q	Q
Cleavage site sequence	Not applicable	REKRRKR↓G	REKRRKR↓G	REKRRKR↓G	REKRRKR↓G	REKRRKR↓G
NA gene						
59–69 del	TIINNHPQNNF	No	Yes	Yes	Yes	Yes
Oseltamivir resistance	H274Y	H	H	H	H	H
	N294S	N	N	N	N	N
PB2						
Increased pathogenicity in	L89V	V	V	V	V	V
mice	E627K	E	K	K	E	E
Increased virulence and	G309D, T339K	DMGV	DTGV	DKGV	DKGV	DKGV
replication in mice	R477G, I495V					
Enhanced transmission	D701N	N	D	D	D	N
NS1						
Increased virulence in mice	D92E	E	E	D	D	E
and pigs						
PDZ-motif	Not applicable	ESEV	ESEV	KPEV	KPEV	ESEV
Increased virulence in mice	P42S	S	S	S	S	S
M2						
Antiviral resistance	S31N	S	S	N	N	S
(amantadine)						

*HA, hemagglutinin; M2, matrix protein 2; NA, neuraminidase; NS1, nonstructural protein 1; PB2, polymerase basic 2 amino acid.

findings show that the circulating H5N6 virus in southern China has reassorted with enzootic H6N6 and H9N2 viruses, resulting in new H5N6 viruses that are capable of infecting humans.

We compared the 2 newly sequenced genomes with 3 available genomes of human influenza virus strains in public databases to determine if they had attained key molecular features associated with increased virulence in mammals, mammalian transmissibility, and antiviral resistance (Table). The HA gene cleavage site encoded by all 5 isolates from humans showed a multiple basic amino acid motif (REKRRKR↓G), which indicates high pathogenicity in poultry. The viruses isolated from humans in 2014 had no mutations associated with reduced sensitivity to adamantine antiviral drugs, but 2 of the 3 viruses isolated in 2015 have the 31N amino acid in M2, suggesting that those 2 viruses have acquired resistance. Thus, this virus lineage could be a great threat to public health.

Although H9N2 is not highly pathogenic in poultry, it provides internal genes for the recent emergence of many novel avian influenza viruses that infect humans, such as the H5N6 virus in this study, as well as the H7N9 (*7,8*) and H10N8 (*9*) viruses. Infection with H6 subtype viruses results in no clinically significant signs of disease in poultry (*10*), but co-circulation of these viruses with other subtypes among poultry results in transfer of internal genes. This reassortment has resulted in a major increase in genetic diversity among the H5N6 viruses that cause human infections; therefore, low-pathogenicity viruses in poultry should also be controlled in poultry.

In summary, we isolated 2 novel reassortant H5N6 viruses from 2 patients in Guangdong Province, China. The internal genes of these strains are different from those found in the first wave of H5N6 infections in 2014. The PB2 of 2 human isolate A/Guangdong/ZQ874/2015 (H5N6) appears to have been derived from a duck H6N6 virus, and all other genes of this virus originated in circulating H5N6 viruses. In contrast, the 6 internal genes of the other human isolate, A/Guangdong/SZ872/2015 (H5N6), were derived from enzootic H9N2 viruses. Although human infection has been sporadic, the co-circulation and reassortment of this virus with other enzootic low pathogenicity influenza viruses has resulted in new reassortant viruses. Further surveillance of birds is needed to monitor the spread of this novel virus.

References

1. Shen H, Wu B, Chen Y, Bi Y, Xie Q, Influenza A (H5N6) virus reassortant, Southern China, 2014. Emerg Infect Dis. 2015;21:1261–2.http://dx.doi.org/10.3201/eid2107.140838
2. Qi X, Cui L, Yu H, Ge Y, Tang F. Whole-genome sequence of a reassortant H5N6 avian influenza virus isolated from a live poultry market in China, 2013. Genome Announc. 2014;2:e00706–14. http://dx.doi.org/10.1128/genomeA.00706-14
3. World Health Organization. WHO China statement on H5N6. 7 May 2014 [cited 2016 Mar 28]. http://www.wpro.who.int/china/mediacentre/releases/2014/20140507/en/
4. Mok CKP, Da Guan W, Liu XQ, Lamers MM, Li XB, Wang M, et al. Genetic characterization of highly pathogenic avian influenza A(H5N6) virus, Guangdong, China. Emerg Infect Dis. 2015;21:2268–71. http://dx.doi.org/10.3201/eid2112.150809
5. World Health Organization. Human infection with avian influenza A(H5N6) virus—China. 04 Jan 2016 [cited 2016 Mar 28]. http://www.who.int/csr/don/4-january-2016-avian-influenza-china/en/
6. World Health Organization. Human infection with avian influenza A(H5N6) virus—China. 11 Jan 2016 [cited 2016 Mar 28]. http://www.who.int/csr/don/11-january-2016-avian-influenza-china/en/
7. Lam TT, Zhou B, Wang J, Chai Y, Shen Y, Chen X, et al. Dissemination, divergence and establishment of H7N9 influenza viruses in China. Nature. 2015;522:102–5. http://dx.doi.org/10.1038/nature14348
8. Lam TT-Y, Wang J, Shen Y, Zhou B, Duan L, Cheung C-L, et al. The genesis and source of the H7N9 influenza viruses causing human infections in China. Nature. 2013;502:241–4. http://dx.doi.org/10.1038/nature12515
9. Chen H, Yuan H, Gao R, Zhang J, Wang D, Xiong Y, et al. Clinical and epidemiological characteristics of a fatal case of avian influenza A H10N8 virus infection: a descriptive study. Lancet. 2014;383:714–21.http://dx.doi.org/10.1016/S0140-6736(14)60111-2
10. Zhao G, Lu X, Gu X, Zhao K, Song Q, Pan J, et al. Molecular evolution of the H6 subtype influenza a viruses from poultry in eastern China from 2002 to 2010.Virol J. 2011;8:470. http://dx.doi.org/10.1186/1743-422X-8-470

Address for correspondence: Ming Liao, College of Veterinary Medicine, South China Agricultural University, Guangzhou, China; email: mliao@scau.edu.cn

Rare Human Infection with Pacific Broad Tapeworm *Adenocephalus pacificus*, Australia

Casey V. Moore, R.C. Andrew Thompson, Abdul Jabbar, John Williams, Kavita Rasiah, Louise Pallant, Ann P. Koehler, Caitlin Graham, Gerhard F. Weldhagen

Author affiliations: SA Pathology, Adelaide, South Australia, Australia (C.V. Moore, G.F. Weldhagen); Murdoch University, Murdoch, Western Australia, Australia (R.C.A. Thompson, L. Pallant); University of Melbourne, Melbourne, Victoria, Australia (A. Jabbar); Investigator Clinic, Port Lincoln, South Australia (J. Williams); Women's and Children's Hospital, Adelaide (K. Rasiah); SA Health Communicable Disease Control Branch, Adelaide (A.P. Koehler, C. Graham)

To the Editor: Human diphyllobothriosis associated with the Pacific broad tapeworm *Adenocephalus pacificus* (syn. *Diphyllobothrium pacificum*) is a reemerging, global parasitic disease (*1*). Infection with the adult tapeworm occurs widely in piscivorous mammals, including humans, with various species of marine fish acting as intermediate hosts (*1,2*). In the Southern Hemisphere, the organism is well described in the coastal waters of South America, southern Africa, and Oceania (*2*). *A. pacificus* tapeworms have been recorded in pinnipeds in Australian territory as far back as 1923 (*3*). To our knowledge, no human case has been reported from this region to date.

A 3-year-old boy from a coastal town in South Australia's Eyre Peninsula was brought to a medical clinic on July 29, 2015, with a 1-month history of poor appetite and loose bowel movements. His parents had noticed tapeworm-like organisms in his feces over a period of 2 days; the organisms had been discarded and were not available for examination. The child regularly ate raw marine fish, caught by his father in the Spencer Gulf during recreational fishing. The types of fish he consumed included southern bluefin tuna (*Thunnus maccoyii*), spotted sillago (*Sillaginodes punctatus*), and southern goatfish (*Upeneichthys vlamingii*). The child had never traveled outside Australia. Fecal and blood samples were collected for further analysis at SA Pathology (Adelaide, South Australia, Australia).

Macroscopic examination of a single, 6-cm portion of unfixed strobila without scolex, obtained from feces, revealed individual proglottids, wider than they were long, and a central rosette-shaped uterus in each proglottid. Further morphologic features could not be clearly visualized from the available clinical specimen. Microscopic examination of fecal sediment revealed unembryonated ellipsoidal eggs with an operculum and abopercular knob at opposite ends (*2*). The patient had been given a preliminary clinical diagnosis of diphyllobothriosis and received oral praziquantel (10 mg/kg) on 2 occasions, 12 days apart, without any complications. Blood test results, including hemoglobin level, erythrocyte volume, and vitamin B12 levels, were all within reference ranges. A follow-up stool sample collected 1 week after the first dose of praziquantel still exhibited operculated eggs; samples collected 3 weeks later did not contain any eggs.

We identified the tapeworm more specifically through molecular methods. Genomic DNA from segments preserved in 80% ethanol were extracted using a DNeasy Blood and Tissue Kit (QIAGEN, Valencia, CA, USA) following the manufacturer's protocol. Four loci were PCR-amplified separately from the genomic DNA as described (*4–6*). The first locus (designated *cox1*) targeted the complete cytochrome *c* oxidase subunit 1 gene; the second locus (designated Dp*cox*1), located within the *cox1* gene, was amplified by using species-specific (*D. pacificum*) primers (*4*); the third locus (designated SSU) targeted the small subunit gene of RNA; and the fourth locus (designated ITS) targeted the first to second internal transcribed spacer regions. For each locus, automated DNA sequencing (Big-Dye Terminator v3.1 Kit; Applied Biosystems, Foster City, CA, USA) was performed by using the primers for PCR amplification (*4–6*) in separate reactions. We identified *cox*1 and Dp*cox*1 sequences by local alignment comparison (6 reading frames) using amino acid sequences conceptually translated online (http://www.ebi.ac.uk/Tools/st/emboss_transeq/) from respective genes of the reference sequences of *Diphyllobothrium* spp. available from Gen-Bank. DNA sequencing results identified the tapeworm as *A. pacificus*.

Sequence data from this study have been submitted to GenBank (accession nos. KU519704–6). Morphologic voucher material is archived in the Australian Helmintological Collection, South Australian Museum (accession nos. AHC47709 and AHC36233).

Data obtained from *cox1* gene analysis (Figure, panel A) suggest that this isolate is indistinguishable from an *A. pacificus* tapeworm previously obtained from an Australian sea lion, *Neophoca cinerea* (GenBank accession no. KR269744), from Kangaroo Island and an Australian fur seal, *Arctocephalus pusillus* (GenBank accession no. KR269745), from Cape Woolamai in 1993 (*2*). Similarly, the human isolate we identified is indistinguishable from isolates previously obtained from fish and humans in Chile, Peru, and Spain (Figure, panel A). However, the human isolates from Spain (GenBank accession nos. HF969327 and KM520151) have been linked with fresh
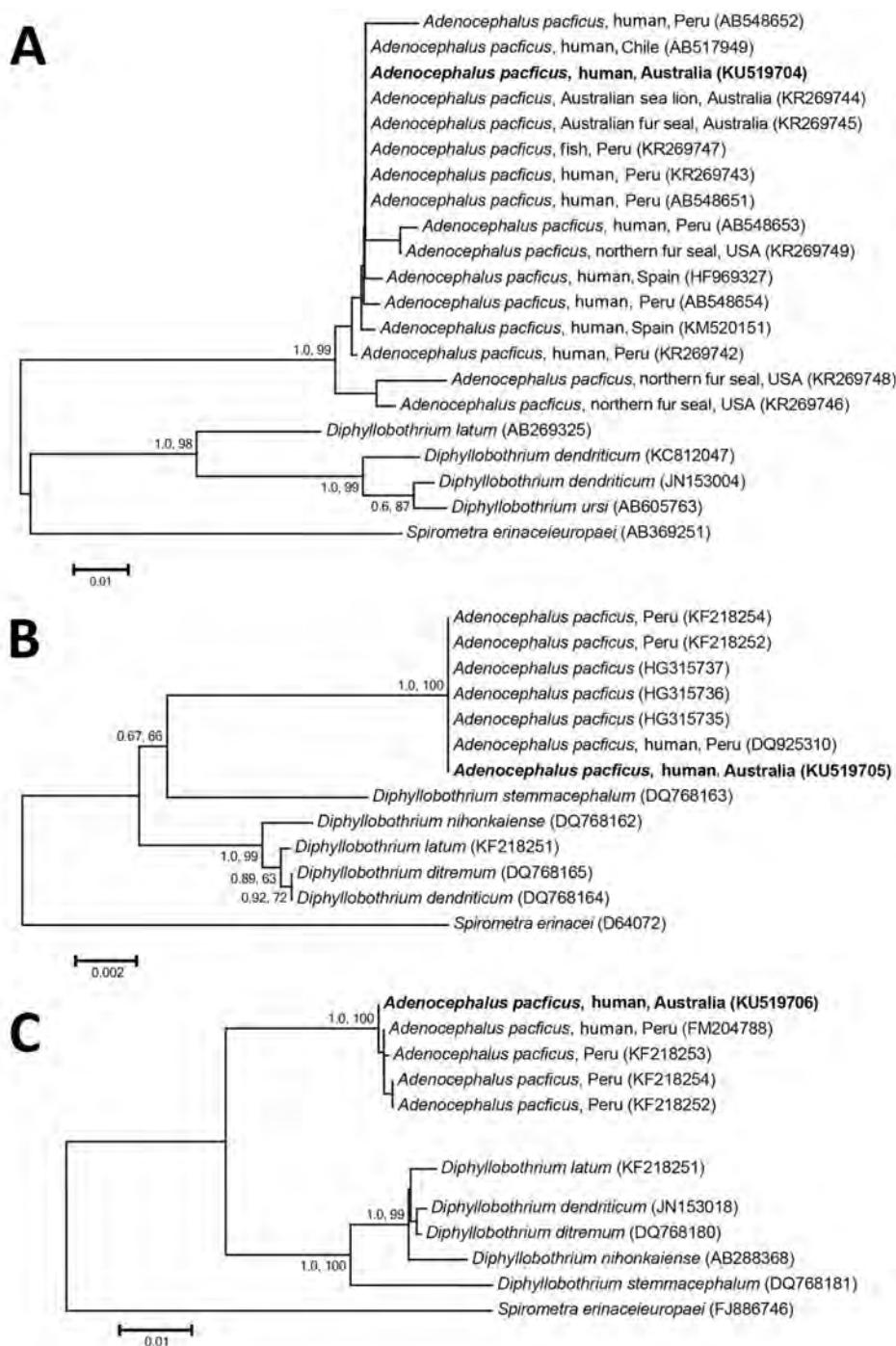
Figure. Phylogenetic relationship of genetic sequences from an *Adenocephalus pacificus* tapeworm obtained from a human in Australia (bold) and selected reference sequences. The relationship was inferred on the basis of DNA sequence analyses of cytochrome *c* oxidase 1 (A), small subunit RNA (B), and internal transcribed spacer (C) regions, using Bayesian inference and neighbor-joining phylogenetic methods. Topologies of trees generated by both methods were similar; thus, only neighbor-joining trees are shown here. *Spirometra* spp. were used as the outgroup. Nodal support is shown as posterior probability value (first) and bootstrap value (second) on the basis of 2 million generations for Bayesian inference and 10,000 replicates for neighbor joining, respectively. GenBank accession numbers are shown in parentheses. Scale bars indicate nucleotide substitutions per site.

fish imported from South America (*7,8*). Small subunit and internal transcribed spacer sequence analysis showed that the human isolate was identical or closely related to isolates from Peru (Figure, panels B, C). This finding is in keeping with this species' current predominant geographic distribution (*2*).

Two recent food risk assessments in Australia did not recognize *A. pacificus* tapeworms as a potential zoonotic threat in marine finfish (*9,10*). Although our patient only consumed raw locally caught marine fish, thus acquiring a patent infection after accidental ingestion of plerocercoids, the fish species concerned have yet to be confirmed as suitable intermediate hosts of *A. pacificus* tapeworms (*1*). These findings, and reports spanning >90 years, suggest that *A. pacificus* tapeworms are endemic in piscivorous mammals off the Australian coast, and more human

cases can be expected as pressure on marine fish stocks and consumption of uncooked fish increase. As a protective measure against this emerging foodborne zoonotic threat, the public should be made aware of risks associated with consumption of fresh, raw marine fish.

References

1. Kuchta R, Serrano-Martínez ME, Scholz T. Pacific broad tapeworm *Adenocephalus pacificus* as a causative agent of globally reemerging diphyllobothriosis. Emerg Infect Dis. 2015;21:1697–703. http://dx.doi.org/10.3201/eid2110.150516
2. Hernández-Orts JS, Scholz T, Brabec J, Kuzmina T, Kuchta R. High morphological plasticity and global geographical distribution of the Pacific broad tapeworm *Adenocephalus pacificus* (syn. *Diphyllobothrium pacificum*): molecular and morphological survey. Acta Trop. 2015;149:168–78. http://dx.doi.org/10.1016/j.actatropica.2015.05.017
3. Johnston TH. Entozoa from the Australian hair seal. Proc Linn Soc N S W. 1937. [cited 2016 Jan 20]. http://www.biodiversitylibrary.org/page/34903721#page/59/mode/1up
4. Wicht B, Yanagida T, Scholz T, Ito A, Jiménez JA, Brabec J. Multiplex PCR for differential identification of broad tapeworms (Cestoda: *Diphyllobothrium*) infecting humans. J Clin Microbiol. 2010;48:3111–6. http://dx.doi.org/10.1128/JCM.00445-10
5. Mariaux J. A molecular phylogeny of the Eucestoda. J Parasitol. 1998;84:114–24. http://dx.doi.org/10.2307/3284540
6. Luton K, Walker D, Blair D. Comparisons of ribosomal internal transcribed spacers from two congeneric species of flukes (Platyhelminthes: Trematoda: Digenea). Mol Biochem Parasitol. 1992;56:323–7. http://dx.doi.org/10.1016/0166-6851(92)90181-I
7. Pastor-Valle J, González LM, Martín-Clemente JP, Merino FJ, Gottstein B, Gárate T. Molecular diagnosis of diphyllobothriasis in Spain, most presumably acquired via imported fish, or sojourn abroad. New Microbes New Infect. 2014;2:1–6. http://dx.doi.org/10.1002/2052-2975.28
8. Kuchta R, Esteban JG, Brabec J, Scholz T. Misidentification of *Diphyllobothrium* species related to global fish trade, Europe. Emerg Infect Dis. 2014;20:1955–7. http://dx.doi.org/10.3201/eid2011.140996
9. Anantanawat S, Kiermeier A, McLeod C, Sumner J. South Australian Research and Development Institute. A semi-quantitative risk assessment of harmful parasites in Australian finfish. April 2012 [cited 2016 Jan 20]. http://safefish.com.au/wp-content/uploads/2013/03/Semi-quantitative-risk-assessment-of-Harmful-Parasites.pdf
10. New South Wales Food Authority. Seafood safety scheme—periodic review of the risk assessment. 2012. [cited 2016 Jan 20]. http://foodauthority.nsw.gov.au/_Documents/scienceandtechnical/seafood_safety_scheme.pdf

Address for correspondence: Gerhard F. Weldhagen, Microbiology and Infectious Diseases Laboratory, SA Pathology, PO Box 14, Rundle Mall, Adelaide, SA5000, Australia; email: gerhard.weldhagen@sa.gov.au

Influenza A(H7N7) Virus among Poultry Workers, Italy, 2013

Simona Puzelli,[1] Caterina Rizzo,[1] Concetta Fabiani, Marzia Facchini, Paolo Gaibani, Maria P. Landini, Carlo Gagliotti, Maria L. Moro, Roberto Rangoni, Luisa Loli Piccolomini, Alba C. Finarelli, Marco Tamba, Giovanni Rezza, Silvia Declich, Isabella Donatelli, Maria R. Castrucci

Author affiliations: Istituto Superiore Sanità, Rome, Italy (S. Puzelli, C. Rizzo, C. Fabiani, M. Facchini, G. Rezza, S. Declich, I. Donatelli, M.R. Castrucci); St. Orsola University Hospital, Bologna, Italy (P. Gaibani, M.P. Landini); Agenzia Sanitaria Regionale Emilia-Romagna Region, Bologna (C. Gagliotti, M.L. Moro, R. Rangoni, L.L. Piccolomini, A.C. Finarelli); Istituto Zooprofilattico Sperimentale della Lombardia e dell'Emilia Romagna, Brescia, Italy (M. Tamba)

To the Editor: In August 2013, an outbreak of infection with highly pathogenic influenza A(H7N7) virus occurred in Emilia-Romagna, Italy, and >1 million birds were culled (*1*). Prevention measures were immediately applied, and all workers involved in culling activities wore personal protective equipment (PPE), including face masks with eye protection. These workers were monitored for clinical symptoms, and 3 workers with laboratory-confirmed cases of conjunctivitis caused by infection with influenza A(H7N7) virus were reported during the 3-week outbreak (*2*). Workers did not receive chemoprophylaxis.

A serologic study was conducted in December 2013 to identify potential asymptomatic infections following exposure to influenza A(H7N7) virus. This study was approved by the ethics committee of the Istituto Superiore di Sanità (protocol no. PRE787/13CE13/401).

A total of 93 of 140 workers directly involved in culling activities, including the 3 confirmed case-patients with conjunctivitis, participated in the study. All participants completed a questionnaire that obtained information for demographics, poultry exposure, and use of PPE.

Paired acute-phase and convalescent-phase serum samples were available only for the 3 H7 subtype–positive persons with conjunctivitis. We tested these paired serum samples and single serum samples obtained from virus-exposed workers for antibodies against influenza A(H7N7) virus strain A/Italy/3/2013 (*2*) by using hemagglutination inhibition (HI) and microneutralization (MN) assays (*3,4*).

---

[1]These authors contributed equally to this article.

Table. HI and MN antibody titers for influenza A(H7N7) virus and other H7 subtype viruses in serum samples of 5 men, Italy, 2013*

Person ID and phase type†	Age, y	Activity of person	Date of sample collection	A/It/3/2013 (H7N7)		A/Tk/It/3889/ 1999 (H7N1)		A/Tk/It/214845/ 2002 (H7N3)		A/Ck/It/2837- 54/2007 (H7N3)	
				HI	MN	HI	MN	HI	MN	HI	MN
1											
Acute	51	PW, culling	Sep 6	10	<10	<10	<10	<10	<10	<10	<10
Convalescent			Dec 6	**20**	**35**	<10	<10	<10	<10	<10	<10
2											
Acute	46	Culling	Sep 6	10	<10	<10	<10	<10	<10	<10	<10
Convalescent			Dec 11	**20**	**62**	<10	<10	<10	<10	<10	<10
3											
Acute	49	Culling	Sep 7	<10	<10	<10	NT	<10	NT	<10	NT
Convalescent			Dec 23	**10**	**87**	<10	<10	<10	<10	<10	<10
FO10‡	34	Culling	Dec 23	**20**	**72**	<10	<10	<10	<10	<10	<10
RA32‡	55	PW, culling	Dec 11	**20**	**33**	<10	<10	<10	<10	<10	<10

*Bold indicates titers of seropositive persons (HI positive results confirmed 3 times by MN). Values for 1 of 3 MN assays that showed similar results are reported. Seropositive persons were selected from 93 persons who participated in the study among 140 persons involved in culling activities.
HI, hemagglutination inhibition; ID, identification; MN, microneutralization; NT, not tested; PW, poultry worker.
†Persons 1, 2, and 3 had laboratory-confirmed cases of conjunctivitis caused by infection with influenza A(H7N7) virus.
‡Asymptomatic person.

Other H7 subtype viruses previously circulating in Italy were included in the analysis to rule out potential cross-reactivity with influenza A(H7N7) virus (5). HI titers ≥10 and MN titers ≥20 were considered positive; only HI-positive serum samples confirmed 3 times by MN assay were considered positive results for influenza A(H7N7) virus.

We detected antibodies against influenza A(H7N7) virus in convalescent-phase serum samples from the 3 H7 subtype-positive patients and 2 asymptomatic persons but found no seropositivity against other H7 subtype viruses (Table). Because of lack of acute-phase serum samples, we could not assess whether seropositivity for the 2 asymptomatic persons, 1 (RA32) of whom worked with poultry before the outbreak, was caused by infection acquired during the outbreak. All workers were trained and most participants, including the 2 asymptomatic influenza A(H7N7) virus–seropositive persons, reported that PPE was commonly used during culling on infected premises. Nevertheless, it is likely that worker compliance with PPE was not always 100% during the 3-week outbreak because of poor knowledge and real perception of biologic risks among workers.

Future efforts should ensure timely collection of paired serum samples from all workers involved in avian influenza outbreaks, especially when infections occur in humans. Strict compliance with recommended preventive control measures and serologic surveillance programs are crucial to avoid and eventually assess risk for infections with avian influenza viruses in persons exposed to infected poultry.

References

1. Bonfanti L, Monne I, Tamba M, Santucci U, Massi P, Patregnani T, et al. Highly pathogenic H7N7 avian influenza in Italy. Vet Rec. 2014;174:382. http://dx.doi.org/10.1136/vr.102202
2. Puzelli S, Rossini G, Facchini M, Vaccari G, Di Trani L, Di Martino A, et al. Human infection with highly pathogenic A(H7N7) avian influenza virus, Italy, 2013. Emerg Infect Dis. 2014;20:1745–9. http://dx.doi.org/10.3201/eid2010.140512
3. Centers for Disease Control and Prevention. Modified hemagglutination-inhibition (HI) assay using horse RBCs for serologic detection of antibodies to H7 subtype avian influenza virus in human sera. Version 1 [cited 2016 April 8]. https://consise.tghn.org/site_media/media/articles/160713_Modified_Hemagglutination_Inhibition_Assay_Using_Horse_RBCs.pdf
4. World Health Organization. Serological detection of avian influenza A(H7N9) infections by microneutralization assay. Version 23, May 2013 [cited 2016 April 8]. http://www.who.int/influenza/gisrs_laboratory/cnic_serological_diagnosis_microneutralization_a_h7n9.pdf?ua=1
5. Puzelli S, Di Trani L, Fabiani C, Campitelli L, De Marco MA, Capua I, et al. Serological analysis of serum samples from humans exposed to avian H7 influenza viruses in Italy between 1999 and 2003. J Infect Dis. 2005;192:1318–22. http://dx.doi.org/10.1086/444390

Increase in Eyeworm Infections in Eastern Europe

Vito Colella, Zvezdelina Kirkova, Éva Fok, Andrei D. Mihalca, Suzana Tasić-Otašević, Adnan Hodžić, Filipe Dantas-Torres, Domenico Otranto

Author affiliations: Università Degli Studi di Bari, Bari, Italy (V. Colella, F. Dantas-Torres, D. Otranto); Trakia University, Stara Zagora, Bulgaria (Z. Kirkova); Szent István University, Budapest, Hungary (É. Fok); University of Agricultural Sciences and

Veterinary Medicine, Cluj Napoca, Romania (A.D. Mihalca); University of Niš, Niš, Serbia (S. Tasić-Otašević); University of Veterinary Medicine Vienna, Vienna, Austria (A. Hodžić); Centro de Pesquisas Aggeu Magalhães, Recife, Brazil (F. Dantas-Torres)

To the Editor: In the past 30 years, war in the Balkans, the fall of Communist regimes, and economic recession in Europe have undermined the economic stability of countries in eastern Europe and eventually favored occurrence of so-called neglected infections of poverty (*1*). Parasitic infections causing eye disease in persons living in areas with low socioeconomic standards might be caused by parasites not well known by healthcare providers.

A good example is *Thelazia callipaeda* (Spirurida, Thelaziidae) nematode infections in children and elderly persons living in rural and poor communities in countries in Europe and Asia (*2*). In Europe, vectors for this nematode are male *Phortica variegata* drosophilids, which feed on ocular secretions of hosts and transmit infective stage larvae to domestic and wild carnivores, lagomorphs, and humans (*3*). Possible outcomes of this infection include conjunctivitis, lacrimation, corneal ulcers, perforation, and blindness (*3*), but differentiating *T. callipaeda* infection from other ocular conditions, such as conjunctivitis-causing pathogens and allergies, can be difficult because signs and symptoms might be similar.

T. callipaeda was previously known as the oriental eyeworm because of its original description in countries in eastern Asia (e.g., China, Japan, and Thailand), where it has caused >1,000 cases of human infections in the past 2 decades (*2*). Since 1989, this nematode has also been detected in many countries in Europe, including Italy, France, Spain, Portugal, Switzerland, Germany, and Greece, as an agent of animal and human ocular infection (*3*). However, data on the occurrence of this parasite in countries in eastern Europe were not available until 2014.

Over the past 2 years, several autochthonous cases of ocular thelaziosis in dogs and cats (Romania, Croatia, Serbia, Bosnia and Herzegovina, Bulgaria) and foxes (Bosnia and Herzegovina) were reported (*4–7*) (Table). In 2016, the zoonotic potential of this parasite in those regions was further confirmed by 2 human cases of thelaziosis, one in a 36-year-old man living in Serbia (*7*) and one in an 82-year-old man living in Croatia (*8*) (Table).

We report 10 new cases of ocular infection by *T. callipaeda* in dogs living in Bulgaria (n = 9) and Hungary (n = 1). All animals had no history of travel outside their native countries and were brought to the Department of Parasitology (Stara Zagora, Bulgaria) and to a veterinary practitioner (Pécs, Hungary) with various ocular disorders (i.e., epiphora, conjunctivitis). Nematodes detected in the conjunctival sac were collected by flushing the sac with saline

Table. Cases of thelaziosis reported in animals and humans in eastern Europe

Country	Host	No. infected hosts	Reference
Bosnia and Herzegovina	Fox	51	(*5*)
Bosnia and Herzegovina	Dog	4	(*5*)
Bosnia and Herzegovina	Cat	1	(*5*)
Croatia	Dog	2	(*5*)
Croatia	Human	1	(*8*)
Romania	Dog	1	(*6*)
Serbia	Dog	6	(*4,7*)
Serbia	Cat	2	(*4*)
Serbia	Human	1	(*7*)
Hungary	Dog	1	This study
Bulgaria	Dog	9	This study

solution. These nematodes were then stored in 70% ethanol and morphologically identified according to the procedure of Otranto et al. (*9*).

Molecular characterization by using PCR amplification and sequencing of a partial region of the cytochrome oxidase subunit 1 gene were performed as described (*10*). Nucleotide sequences were identical to those of *T. callipaeda* nematode haplotype-1 (GenBank accession no. AM042549), which is the only haplotype circulating in animals and humans in Europe.

Our confirmed autochthonous cases of thelaziosis in Hungary and Bulgaria have extended the geographic distribution of *T. callipaeda* nematodes from neighboring countries (e.g., Bosnia and Herzegovina, Croatia, Romania and, Greece), where occurrence of the parasite in humans and animals was already documented. Cases of human thelaziosis are reported in areas where the infection is highly prevalent in animals (*3*). Although no large-scale prevalence study has been conducted in countries in eastern Europe, 51 (27.7%) of 184 foxes in Bosnia and Herzegovina were infected with *T. callipaeda* nematodes (*5*). Isolation of *T. callipaeda* eyeworms from dogs in Bulgaria and Hungary should increases awareness of medical and veterinary communities in countries in eastern Europe for this zoonotic parasitosis. Use of a One Health approach is imperative for preventing additional eyeworm infections in persons living in eastern Europe.

References

1. Hotez PJ, Gurwith M. Europe's neglected infections of poverty. Int J Infect Dis. 2011;15:e611–9. http://dx.doi.org/10.1016/j.ijid.2011.05.006
2. Máca J, Otranto D. Drosophilidae feeding on animals and the inherent mystery of their parasitism. Parasit Vectors. 2014;7:516. http://dx.doi.org/10.1186/s13071-014-0516-4
3. Otranto D, Cantacessi C, Dantas-Torres F, Brianti E, Pfeffer M, Genchi C, et al. The role of wild canids and felids in spreading parasites to dogs and cats in Europe. Part II: helminths and arthropods. Vet Parasitol. 2015;213:24–37. http://dx.doi.org/10.1016/j.vetpar.2015.04.020
4. Gajić B, Bogunović D, Stevanović J, Kulišić Z, Simeunović P, Stanimirović Z. Canine and feline thelaziosis caused by *Thelazia callipaeda* in Serbia. Acta Vet (Beogr). 2014;64:447–55.

5. Hodžić A, Latrofa MS, Annoscia G, Alić A, Beck R, Lia RP, et al. The spread of zoonotic *Thelazia callipaeda* in the Balkan area. Parasit Vectors. 2014;7:352. http://dx.doi.org/10.1186/1756-3305-7-352

6. Mihalca AD, D'Amico G, Scurtu I, Chirilă R, Matei IA, Ionică AM. Further spreading of canine oriental eyeworm in Europe: first report of *Thelazia callipaeda* in Romania. Parasit Vectors. 2015;8:48. http://dx.doi.org/10.1186/s13071-015-0663-2

7. Tasić-Otašević S, Gabrielli S, Trenkić-Božinović M, Petrović A, Gajić B, Colella V, et al. Eyeworm infections in dogs and in a human patient in Serbia: a One Health approach is needed. Comp Immunol Microbiol Infect Dis. 2016;45:20–2. http://dx.doi.org/10.1016/j.cimid.2016.01.003

8. Paradžik MT, Samardžić K, Živičnjak T, Martinković F, Janjetović Ž, Miletić-Medved M. *Thelazia callipaeda*: first human case of thelaziosis in Croatia. Wien Klin Wochenschr. 2016;128:221–3. http://dx.doi.org/10.1007/s00508-015-0889-1

9. Otranto D, Lia RP, Traversa D, Giannetto S. *Thelazia callipaeda* (Spirurida, Thelaziidae) of carnivores and humans: morphological study by light and scanning electron microscopy. Parassitologia. 2003;45:125–33.

10. Otranto D, Testini G, Deluca F, Hu M, Shamsi S, Gasser RB. Analysis of genetic variability within *Thelazia callipaeda* (Nematoda: Thelazioidea) from Europe and Asia by sequencing and mutation scanning of mitochondrial cytochrome c oxidase subunit 1. Mol Cell Probes. 2005;19:306–13. http://dx.doi.org/10.1016/j.mcp.2005.05.001

Febrile or Exanthematous Illness Associated with Zika, Dengue, and Chikungunya Viruses, Panama

Dimelza Araúz,[1] Luis De Urriola,[1] José Jones, Marlene Castillo, Alexander Martínez, Edison Murillo, Leonidas Troncoso, María Chen, Leyda Abrego, Blas Armién, Juan M. Pascale, Néstor Sosa, Sandra López-Verges, Brechla Moreno

Author affiliations: Gorgas Memorial Institute for Health Studies, Panama City, Panama (D. Araúz, M. Castillo, M. Chen, L. Abrego, S. López-Verges, B. Moreno, A. Martinez, B. Armién, J.M. Pascale, N. Sosa); Panama Ministry of Health Department of Epidemiology, Guna Yala, Panama (L. De Urriola); Health Center Guna Yala, Guna Yala (J. Jones, E. Murillo, L. Troncoso)

To the Editor: The earliest clinical cases of Zika virus infection were reported from continental South America in 2015 (*1*), after which the virus spread rapidly through the Americas (*2*). Here we describe an investigation of febrile or exanthematous illnesses for possible association with Zika, dengue, or chikungunya virus; these illnesses occurred in the Guna Yala region of eastern Panama, which borders northern Colombia (Figure).

We collected and analyzed a convenience sample of 276 serum samples and 26 paired urine samples from 276 patients who sought care at clinics in Guna Yala during November 27, 2015–January 22, 2016, for reported fever or rash of <5 days' duration in addition to 1 of the following: headache, malaise, arthralgia, myalgia, or conjunctivitis. We also collected data on clinical signs and symptoms, date of illness onset, age, sex, residence, and self-reported status of pregnancy.

At first, we performed real-time reverse transcription PCR (rRT-PCR) tests specific for dengue (*3*) and chikungunya (*4*) viruses. However, because all the samples received during the week of November 27 were negative for those viruses and Zika virus was being reported in Colombia as of October 2015, we also tested the samples with a flavivirus-specific rRT-PCR (*5*), followed by amplicon sequencing; or with an rRT-PCR specific for Zika virus (*6*).

Of the 276 patients whose samples were tested, 164 (60%) were female. A total of 22 (8%) samples were positive for dengue; 2 were positive for chikungunya. Of the remaining 252 patients, 50 (20%) had ≥1 sample that tested positive for Zika virus (50/252 serum samples, 4/26 paired urine samples). Of these 50 patients, 30 (60%) were female. Most of these patients reported illness onset during December 9–27, 2015 (online Technical Appendix Figure 1, http://wwwnc.cdc.gov/EID/article/22/8/16-0292-Techapp1.pdf). Zika virus infection affected all age groups (median age 35 y, range 0.1–80 y).

The most commonly reported signs and symptoms were fever (86%), exanthema (72%), and headache (62%). The clinical characteristics of these infections showed no statistically significant difference with those associated with dengue and chikungunya virus infections and with cases found to be negative for all 3 viruses, suggesting that the negative cases could represent Zika virus infections (online Technical Appendix Table). One of the patients with confirmed Zika virus infection reported being in her second trimester of pregnancy; she underwent a fetal ultrasound at 36 weeks' gestation, which was interpreted as normal, and the infant was found to have no neurologic defects at birth.

By using Vero E6 cells (American Type Culture Collection), we isolated Zika virus from 9 samples (8 serum, 1 urine). Phylogenetic analysis of 5 Zika virus sequences (a 428-nucleotide fragment encompassing a conserved region of the nonstructural protein 5 gene) placed these isolated (GenBank accession nos. KU724096–100)
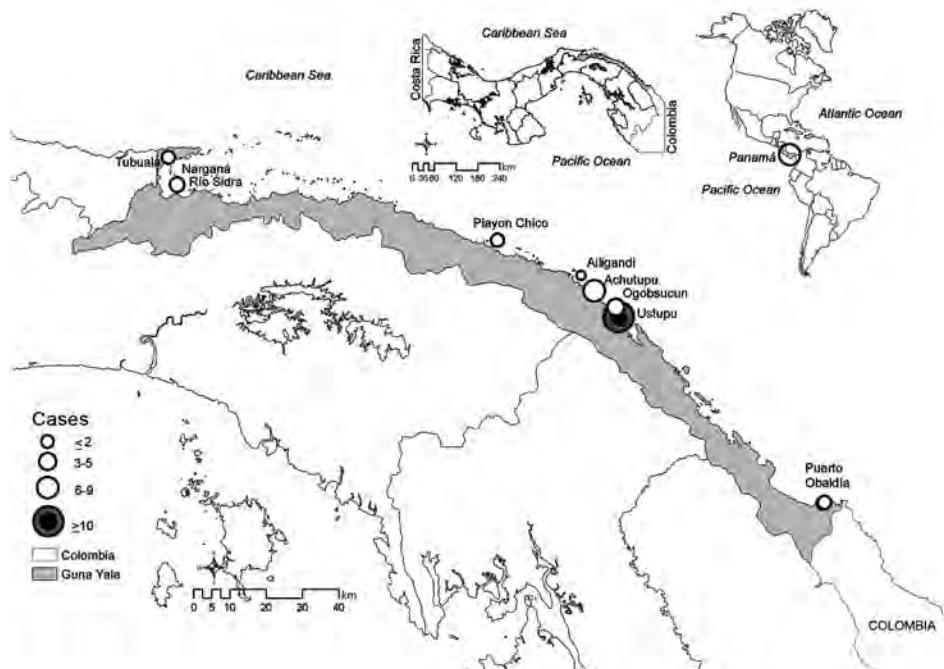
Figure. Locations in the Guna Yala region of eastern Panama with confirmed cases of Zika virus infection during November 27, 2015–January 22, 2016. Inset maps show locations of Guna Yala in Panama and of Panama in the Americas.

within the Asian lineage, the lineage involved in the spread of Zika virus in the Americas (online Technical Appendix Figure 2) (*2,7*).

By using molecular methods, we confirmed diagnoses in 27% of patients during this outbreak. The distribution of positive results suggests that Zika virus was the predominant etiologic virus in this cohort, but we cannot firmly conclude this because most specimens tested negative for Zika, dengue, and chikungunya viruses.

Although results from patient sampling and laboratory testing are not comparable, an assessment in Puerto Rico was able to detect Zika virus RNA by rRT-PCR or IgM by ELISA in 19% of 155 patients with suspected Zika virus infection (*8*). Despite the addition of IgM testing, most of the patients whose specimens were tested by rRT-PCR were negative for dengue and Zika viruses.

Several reasons might exist for the high proportion of specimens testing negative for Zika virus. Viremia is often low and short-lived in persons infected with Zika virus (*7*); the PCR test might not be sensitive enough; some patients with Zika virus infection may have sought care after the virus had been cleared from the blood and urine; our diagnostic capacity was limited by the lack of reliable serologic tests for Zika virus; and we did not test for other viral, bacterial, or parasitic causes of fever or rash illness.

The Panama Ministry of Health is following up with known pregnant women of the Guna Yala region who report Zika virus infection symptoms and is testing urine samples by using Zika virus–specific rRT-PCR within 14 days of symptom onset. Pregnant women confirmed to have Zika virus infection will receive ultrasound monitoring;

however, the test has relatively low positive predictive value for detecting microcephaly (*9*). In Guna Yala, no symptoms of Guillain-Barré syndrome or other neurologic conditions have been detected; however, since January 2016, Zika virus has spread to other regions of Panama, and at least 1 case of Guillain-Barré syndrome has been reported (*10*). Our experience shows the challenge of diagnosing the causes of fever or rash by using only molecular methods, underscoring the need for diagnostic tools that are rapid and inexpensive but more sensitive and specific.

Acknowledgments

References

1. Zanluca C, Melo VC, Mosimann ALP, Santos GI, Santos CN, Luz K. First report of autochthonous transmission of Zika virus in Brazil. Mem Inst Oswaldo Cruz. 2015;110:569–72. http://dx.doi.org/10.1590/0074-02760150192

2. Hennessey M, Fischer M, Staples JE. Zika virus spreads to new areas—region of the Americas, May 2015–January 2016. MMWR Morb Mortal Wkly Rep. 2016;65:55–8. http://dx.doi.org/10.15585/mmwr.mm6503e1

3. Lanciotti RS, Calisher CH, Gubler DJ, Chang GJ, Vorndam AV. Rapid detection and typing of dengue viruses from clinical samples by using reverse transcriptase-polymerase chain reaction. J Clin Microbiol. 1992;30:545–51.

4. Lanciotti RS, Kosoy OL, Laven JJ, Panella AJ, Velez JO, Lambert AJ, et al. Chikungunya virus in US travelers returning from India, 2006. Emerg Infect Dis. 2007;13:764–7. http://dx.doi.org/10.3201/eid1305.070015

5. Ayers M, Adachi D, Johnson G, Andonova M, Drebot M, Tellier R. A single tube RT-PCR assay for the detection of mosquito-borne flaviviruses. J Virol Methods. 2006;135:235–9. http://dx.doi.org/10.1016/j.jviromet.2006.03.009

6. Lanciotti RS, Kosoy OL, Laven JJ, Velez JO, Lambert AJ, Johnson AJ, et al. Genetic and serologic properties of Zika virus associated with an epidemic, Yap State, Micronesia, 2007. Emerg Infect Dis. 2008;14:1232–9. http://dx.doi.org/10.3201/eid1408.080287

7. Lanciotti RS, Lambert AJ, Holodniy M, Saavedra S, Signor LD. Phylogeny of Zika virus in Western Hemisphere, 2015. Emerg Infect Dis. 2016;22:933–5. http://dx.doi.org/10.3201/eid2205.160065

8. Thomas DL, Sharp TM, Torres J, Armstrong PA, Munoz-Jordan J, Ryff KR, et al. Local transmission of Zika virus—Puerto Rico, November 23, 2015–January 28, 2016. MMWR Morb Mortal Wkly Rep. 2016;65:154–8. http://dx.doi.org/10.15585/mmwr.mm6506e2

9. Leibovitz Z, Daniel-Spiegel E, Malinger G, Haratz K, Tamarkin M, Gindes L, et al. Microcephaly at birth—the accuracy of three references for fetal head circumference. How can we improve prediction? Ultrasound Obstet Gynecol. 2015;2:23. http://dx.doi.org/10.1002/uog.15801

10. World Health Organization. Guillain-Barré syndrome—Panama [cited 2016 Mar 29]. http://www.who.int/csr/don/29-march-2016-gbs-panama/en/

Address for correspondence: Brechla Moreno, Instituto Conmemorativo Gorgas de Estudios de la Salud, Ave Justo Arosemena calle 35 y 36, Panama City 0816-02593, Panama; email: bmoreno@gorgas.gob.pa

Influenza D Virus Infection in Herd of Cattle, Japan

Shin Murakami, Maiko Endoh, Tomoya Kobayashi, Akiko Takenaka-Uema, James K. Chambers, Kazuyuki Uchida, Masugi Nishihara, Benjamin Hause, Taisuke Horimoto

Author affiliations: University of Tokyo, Tokyo, Japan (S. Murakami, M. Endoh, T. Kobayashi, A. Takenaka-Uema, J.K. Chambers, K. Uchida, M. Nishihara, T. Horimoto); Kansas State University, Manhattan, Kansas, USA (B. Hause)

To the Editor: Although the provisionally named influenza D virus was first isolated as an influenza C–like virus from pigs with respiratory illness in Oklahoma in 2011 (*1,2*), epidemiologic analyses suggested that cattle are major reservoirs of this virus (*3*) and the virus is potentially involved in the bovine respiratory disease complex. The high rates of illness and death related to this disease in feedlot cattle are caused by multiple factors, including several viral and bacterial co-infections. Influenza D viruses were detected in cattle and pigs with respiratory diseases (and in some healthy cattle) in China (*4*), France (*5*), Italy (*6*), among other countries, indicating their wide global geographic distribution. Although the influenza D virus, like the human influenza C virus, is known to use 9-O-acetylated sialic acids as the cell receptor (*2,7*), its zoonotic potential is undefined because of limited research (*1,8*). We report influenza D virus infection in a herd of cattle in Japan.

To determine the presence of influenza D virus, on January 8, 2016, we used hemagglutination inhibition (HI) to test a convenience sample of 28 serum samples from healthy animals in a herd of female cattle in the Ibaraki Prefecture in central Japan. Two viruses with heterologous antigenicities, D/swine/Oklahoma/1334/2011 (D/OK) and D/bovine/Nebraska/9–5/2012 (D/NE) (*9*), were used for the assay with receptor-destroying enzyme (Denka: RDE II)–treated samples. Eight samples were positive for antibodies against both viruses, with HI titers of 1:80–1:640 for D/OK and with 2-fold or 4-fold lower HI titers (1:40–1:160) for D/NE in each sample, indicating previous infections in these cows, which ranged in age from ≈2 to 9 years. We also detected HI antibodies in serum samples from other cattle herds in several regions of Japan, although positivity rates varied (T. Horimoto, unpub. data). These data demonstrate the circulation of influenza D virus in Japan, as reported in other countries (*3–6*), emphasizing that the virus could be distributed worldwide.

Because 4 of the tested cows showed mild respiratory illness in January, we collected serum samples from the same 28 cows on February 3. At that time, only 1 cow still showed clinical signs; we collected a nasal swab sample from this cow. HI testing revealed that, of the 20 cows that had negative results in the first round of testing, 19 were positive for both D/OK and D/NE on the second test, which strongly confirms that influenza D virus infection had occurred and readily spread in this herd during January. However, most cows seemed to be subclinically infected with the virus. We cannot exclude the possibility of influenza D virus being a co-factor in causing respiratory illness because we did not evaluate the role of other viruses and bacteria in disease progression. HI titers (range 1:40–1:320) for D/NE were the same as or only 2 times lower than those for D/OK in all seroconversion samples, unlike the results for the seropositive samples in the first testing (online Technical Appendix, http://wwwnc.cdc.gov/
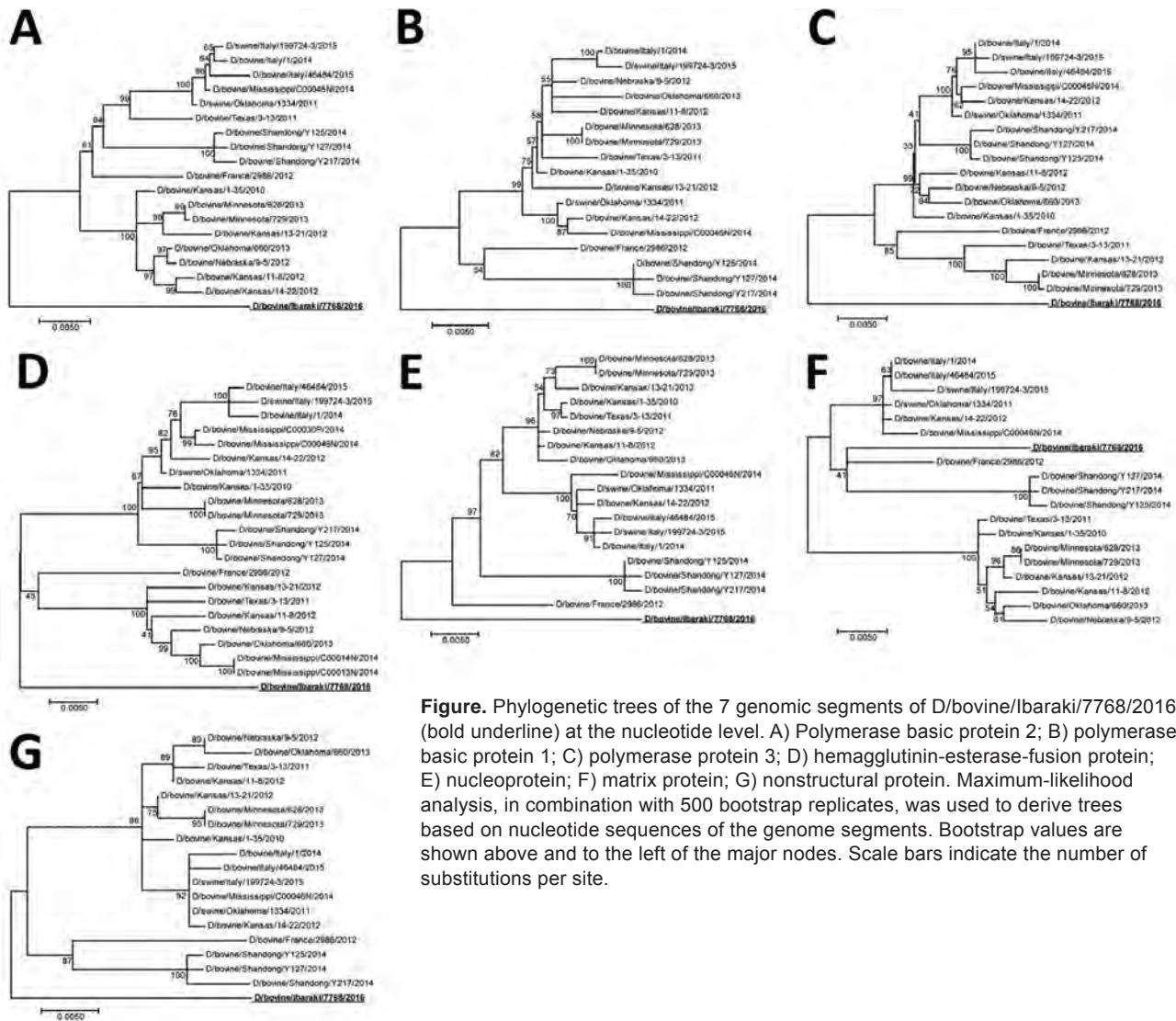
Figure. Phylogenetic trees of the 7 genomic segments of D/bovine/Ibaraki/7768/2016 (bold underline) at the nucleotide level. A) Polymerase basic protein 2; B) polymerase basic protein 1; C) polymerase protein 3; D) hemagglutinin-esterase-fusion protein; E) nucleoprotein; F) matrix protein; G) nonstructural protein. Maximum-likelihood analysis, in combination with 500 bootstrap replicates, was used to derive trees based on nucleotide sequences of the genome segments. Bootstrap values are shown above and to the left of the major nodes. Scale bars indicate the number of substitutions per site.

EID/article/22/8/16-0362-Techapp1.pdf). This result indicates that the virus that spread in this herd in January might be different from the one that infected some cows before the second testing, which suggests the presence of multiple strains with different antigenicities in this area of Japan. No increase in HI titers was observed in the second testing of samples from the 8 cows that were antibody-positive in the first testing.

We used the nasal swab sample from the 1 cow with clinical signs for virus detection, although this cow possessed the HI antibody. Reverse transcription PCR that used specific primers (available from the authors by request) successfully amplified the full genome sequence (GenBank accession nos. LC128433–9 for D/bovine/Ibaraki/7768/2016), which was aligned to the influenza D virus sequence. However, we could not isolate infectious virus by using sensitive cells (2), which might be attributable to the delayed swab sample collection.

Phylogenetic trees generated by using nucleotide sequences of individual segments from the Japan strain (95%–97% nucleotide identities with other strains) by maximum-likelihood analysis with ClustalW (http://www.clustal.org) and MEGA version 6.0 (10) indicated that this strain forms independent positions from strains isolated in other countries, although only the matrix segment was included in the same cluster as isolates from France and China (Figure). Although several unique amino acids of each protein exist in the strain from Japan, different from other isolates, their biologic characters are unknown. Among such residues, an amino acid at position 212 of hemagglutinin-esterase-fusion protein determined hemagglutinin antigenicity of the virus; lysine or arginine at this position resulted in heterologous antigenicities (9). The strain from Japan possessed serine at this position, identical to a strain from France (5), likely forming the third group of hemagglutinin antigenicity. Additionally, 1

putative N-glycosylation sequon was missing at positions 249–251 in hemagglutinin-esterase-fusion protein.

In summary, a cattle herd in Japan had influenza D virus infection. Although this study is a case report with a small number of samples, the observation shows a potential role for influenza D virus in the bovine respiratory disease complex.

References

1. Hause BM, Ducatez M, Collin EA, Ran Z, Liu R, Sheng Z, et al. Isolation of a novel swine influenza virus from Oklahoma in 2011 which is distantly related to human influenza C viruses. PLoS Pathog. 2013;9:e1003176. http://dx.doi.org/10.1371/journal.ppat.1003176
2. Hause BM, Collin EA, Liu R, Huang B, Sheng Z, Lu W, et al. Characterization of a novel influenza virus in cattle and Swine: proposal for a new genus in the *Orthomyxoviridae* family. MBio. 2014;5:e00031–14. http://dx.doi.org/10.1128/mBio.00031-14
3. Ferguson L, Eckard L, Epperson WB, Long LP, Smith D, Huston C, et al. Influenza D virus infection in Mississippi beef cattle. Virology. 2015;486:28–34. http://dx.doi.org/10.1016/j.virol.2015.08.030
4. Jiang WM, Wang SC, Peng C, Yu JM, Zhuang QY, Hou GY, et al. Identification of a potential novel type of influenza virus in bovine in China. Virus Genes. 2014;49:493–6. http://dx.doi.org/10.1007/s11262-014-1107-3
5. Ducatez MF, Pelletier C, Meyer G. Influenza D virus in cattle, France, 2011–2014. Emerg Infect Dis. 2015;21:368–71. http://dx.doi.org/10.3201/eid2102.141449
6. Chiapponi C, Faccini S, De Mattia A, Baioni L, Barbieri I, Rosignoli C, et al. Detection of influenza D virus among swine and cattle, Italy. Emerg Infect Dis. 2016;22:352–4. http://dx.doi.org/10.3201/eid2202.151439
7. Song H, Qi J, Khedri Z, Diaz S, Yu H, Chen X, et al. An open receptor-binding cavity of hemagglutinin-esterase-fusion glycoprotein from newly-identified influenza D virus: basis for its broad cell tropism. PLoS Pathog. 2016;12:e1005411. http://dx.doi.org/10.1371/journal.ppat.1005411
8. Smith DB, Gaunt ER, Digard P, Templeton K, Simmonds P. Detection of influenza C virus but not influenza D virus in Scottish respiratory samples. J Clin Virol. 2016;74:50–3. http://dx.doi.org/10.1016/j.jcv.2015.11.036
9. Collin EA, Sheng Z, Lang Y, Ma W, Hause BM, Li F. Cocirculation of two distinct genetic and antigenic lineages of proposed influenza D virus in cattle. J Virol. 2015;89:1036–42. http://dx.doi.org/10.1128/JVI.02718-14
10. Tamura K, Stecher G, Peterson D, Filipski A, Kumar S. MEGA6: molecular evolutionary genetics analysis version 6.0. Mol Biol Evol. 2013;30:2725–9. http://dx.doi.org/10.1093/molbev/mst197

Address for correspondence: Taisuke Horimoto, Laboratory of Veterinary Microbiology, Graduate School of Agricultural and Life Sciences, University of Tokyo, Yayoi 1-1-1, Bunkyo-ku, Tokyo 113-8657, Japan; email: ahorimo@mail.ecc.u-tokyo.ac.jp

Fatal Septic Meningitis in Child Caused by *Streptococcus suis* Serotype 24

Anusak Kerdsin, Marcelo Gottschalk, Rujirat Hatrongjit, Shigeyuki Hamada, Yukihiro Akeda, Kazunori Oishi

Author affiliations: Kasetsart University Chalermphrakiat Sakon Nakhon Province Campus, Sakon Nakhon, Thailand (A. Kerdsin, R. Hatrongjit); University of Montreal, Montreal, Quebec, Canada (M. Gottschalk); Osaka University, Osaka, Japan (S. Hamada, Y. Akeda); National Institute of Infectious Diseases, Tokyo, Japan (K. Oishi)

To the Editor: *Streptococcus suis* is a zoonotic bacterium that causes invasive infections in humans and pigs (*1*). Of the 29 described serotypes, serotype 2 is the most prevalent in humans, almost exclusively affecting adults (*1*). Other serotypes occurring sporadically in humans have been reported (*1*). Here we report a rare case of *S. suis* serotype 24 infection in a child.

A 2-year-old girl with Down syndrome was admitted to a hospital in Rayong Province, eastern Thailand, in May 2015. She had a high fever of 3 days' duration, vomiting, stiff neck, rash, and purpura on her right leg and hip. The initial diagnosis was cellulitis and suspected meningococcal meningitis. Physical examination revealed a temperature of 39.5°C, pulse rate of 160 beats/min, respiratory rate of 80 breaths/min, and blood pressure of 94/55 mm Hg. Oxygen saturation was 80%, which is indicative of severe respiratory failure. An analysis of the complete blood count showed a leukocyte count of 21,460 cells/mL (83% neutrophils, 13% lymphocytes, 1% eosinophils, 3% monocytes) and platelet count of 155,000 cells/μL. A comprehensive metabolic panel test was not performed.

Bacteria were isolated from the patient›s cerebrospinal fluid culture; however, hemoculture did not show any growth. Traditional biochemical tests and an API20Strep system assay (BioMérieux, Marcy l'Etoile, France) suggested that the organism was *S. suis*. The samples tested positive for *S. suis* serotype 24 by multiplex PCR and coagglutination testing (*2,3*). On the basis of these results, the condition was diagnosed as septic meningitis. Unfortunately, the patient died the day after admission, even though she had been treated with ceftriaxone on the day of admission.

The isolate from the child was susceptible to penicillin (MIC ≤0.12 μg/mL), ceftriaxone (MIC ≤1 μg/mL), erythromycin (MIC ≤0.25 μg/mL), levofloxacin (MIC ≤2.0 μg/mL), clindamycin (MIC ≤0.25 μg/mL), and vancomycin (MIC ≤1.0 μg/mL). Because breakpoints for *S. suis* are not

Table. Demographic and clinical characteristics for the 2 known reported *Streptococcus suis* infections in children

Characteristic	2015 case (this study)	2002 case (9)
Sex	F	F
Age	2 y	1 mo
Temperature, °C	39.5	38.0
Pulse rate, beats/min	160	No data
Respiratory rate, breaths/min	80	No data
Blood pressure, mm Hg	94/55	No data
Leukocyte count, cells/mL	21,460	12,000
Diagnosis	Septic meningitis	Meningitis
Hearing loss	No data	No
Underlying disease	Down syndrome	No data
Outcome	Died	Survived
S. suis serotype	24	No data
Sequence type	221	No data

defined in the 2015 Clinical and Laboratory Standards Institute guidelines, breakpoints for viridans streptococci were used instead (*4*). Multilocus sequence typing determined that the isolate was sequence type 221, which belongs to clonal complex (CC) 221/234. The previously described virulence markers (*epf, mrp,* and *sly* genes) were absent (*1*). These markers are mostly present in serotype 2 strains from Europe and Asia (*1*). We have shown that CC221/234 is a newly emerging, human infectious clone that includes serotypes 24 and 31, but not serotype 2, strains (*5,6*). Therefore, the presence of this CC should be monitored, and characterization of virulence factors of strains belonging to this CC should be further investigated.

The routes of *S. suis* infection include occupational exposure, recent contact with pigs or raw pork products, and recent consumption of raw pork products (*1*). This patient had no history of contact with pigs or pork products nor consumption of raw pig's blood soup or any other source of undercooked meals before the onset of illness. *S. suis* may affect various other animal species (*7*), but the patient did not have any close contact with other animal species. Close family members of the patient did not report having consumed raw pork products, although they did report having close contact with pork meat for cooking. However, so far, no human cases have been confirmed to be the consequence of close contact with or consumption of undercooked meat from animal species other than pigs. In addition, human-to-human transmission of *S. suis* has not been reported (*8*). As reported in other similar cases, the route of the infection could not be confirmed in this case. A previous case of *S. suis* infection in a child was reported in a 1-month-old girl with meningitis in Thailand; however, certain details of that case, including the causative bacterial serotype, were not reported (Table) (*9*).

Although the isolation rate for *S. suis* serotype 24 strains remains low, increased awareness among clinicians treating patients with predisposing conditions is required given the emergence of *S. suis* infections caused by uncommon serotypes. Such awareness will be important for development of enhanced surveillance, epidemiologic control, and prevention strategies for public health.

References

1. Goyette-Desjardins G, Auger JP, Xu J, Segura M, Gottschalk M. *Streptococcus suis*, an important pig pathogen and emerging zoonotic agent-an update on the worldwide distribution based on serotyping and sequence typing. Emerg Microbes Infect. 2014;3:e45. http://dx.doi.org/10.1038/emi.2014.45
2. Kerdsin A, Akeda Y, Hatrongjit R, Detchawna U, Sekizaki T, Hamada S, et al. *Streptococcus suis* serotyping by a new multiplex PCR. J Med Microbiol. 2014;63:824–30. http://dx.doi.org/10.1099/jmm.0.069757-0
3. Gottschalk M, Higgins R, Boudreau M. Use of polyvalent coagglutination reagents for serotyping of *Streptococcus suis.* J Clin Microbiol. 1993;31:2192–4.
4. Clinical and Laboratory Standards Institute. Performance standards for antimicrobial susceptibility testing; 25th informational supplement (M100-S25). Wayne (PA): The Institute; 2015. p. 94–6.
5. Hatrongjit R, Kerdsin A, Gottschalk M, Takeuchi D, Hamada S, Oishi K, et al. First human case report of sepsis due to infection with *Streptococcus suis* serotype 31 in Thailand. BMC Infect Dis. 2015;15:392. http://dx.doi.org/10.1186/s12879-015-1136-0
6. Kerdsin A, Dejsirilert S, Sawanpanyalert P, Boonnark A, Noithachang W, Sriyakum D, et al. Sepsis and spontaneous bacterial peritonitis in Thailand. Lancet. 2011;378:960. http://dx.doi.org/10.1016/S0140-6736(11)60923-9
7. Gottschalk M, Xu J, Calzas C, Segura M. *Streptococcus suis*: a new emerging or an old neglected zoonotic pathogen? Future Microbiol. 2010;5:371–91. http://dx.doi.org/10.2217/fmb.10.2
8. Yu H, Jing H, Chen Z, Zheng H, Zhu X, Wang H, et al.; Streptococcus suis study groups. Human *Streptococcus suis* outbreak, Sichuan, China. Emerg Infect Dis. 2006;12:914–20. http://dx.doi.org/10.3201/eid1206.051194
9. Vilaichone RK, Vilaichone W, Nunthapisud P, Wilde H. *Streptococcus suis* infection in Thailand. J Med Assoc Thai. 2002;85(Suppl 1):S109–17.

Address for correspondence: Anusak Kerdsin, Faculty of Public Health, Kasetsart University Chalermphrakiat Sakon Nakhon Province Campus, Sakon Nakhon 47000, Thailand; email: noksak99@gmail.com; and Kazunori Oishi, Infectious Disease Surveillance Center, National Institute of Infectious Diseases, 1-23-1 Toyama, Shinjyuku, Tokyo, Japan; email: oishik@nih.go.jp

Zika Virus Disease in Traveler Returning from Vietnam to Israel

Eyal Meltzer,[1] Yaniv Lustig,[1] Eyal Leshem, Ran Levy, Giora Gottesman, Rotem Weissmann, Duha Hejleh Rabi, Musa Hindiyeh, Ravit Koren, Ella Mendelson, Eli Schwartz

Author affiliations: Sheba Medical Center, Tel Hashomer, Israel (E. Meltzer, Y. Lustig, E. Leshem, M. Hindiyeh, R. Koren, E. Mendelson, E. Schwartz); Tel Aviv University, Tel Aviv, Israel (E. Meltzer, E. Leshem, G. Gottesman, M. Hindiyeh, E. Mendelson, E. Schwartz); Maccabi Health Services, Kfar-Yona, Israel (R. Levy); Meir Medical Center, Kfar Saba, Israel (G. Gottesman, R. Weissmann, D. Hejleh Rabi)

To the Editor: On February 1, 2016, the World Health Organization designated the Zika virus disease outbreak in Latin America as a Public Health Emergency of International Concern (*1*). Genetic and epidemiological data suggest that Zika virus had been present in Southeast Asia since the 1940s (*2*); however, the disease burden and geographic extent of Zika virus disease in Asia are not clear. Occasional cases in some Asian countries, mostly in returning travelers, have recently been documented (*3–5*); however, as of February 2016, none were in Vietnam.

During December 2015–February 2016, the National Center for Zoonotic Viruses (Tel Hashomer, Israel), diagnosed 8 cases of Zika virus disease in travelers returning to Israel. The Center is part of the Central Virology Laboratory of the Israel Ministry of Health and is the reference laboratory for the diagnosis of Zika, dengue, and chikungunya virus infections in Israel. During the same period, 4 cases of dengue and 1 of chikungunya were also diagnosed. Of the 8 cases of Zika virus disease, 7 were in patients returning from South and Central America and the Caribbean (online Technical Appendix, http://wwwnc.cdc.gov/EID/article/22/8/16-0480-Techapp1.pdf) and 1 was in a patient returning from Vietnam via Hong Kong. We report the patient returning from Vietnam.

The patient was a 61-year-old man from Israel who spent 10 days in Vietnam during December 2015: 3 days in Hội-An, 3 in Hue, and 4 in Ho Chi Minh City. After spending 2 more days in Hong Kong, he returned to Israel. On the third day after his return, he experienced fever, malaise, and headache; he had no rash or conjunctivitis. Laboratory studies showed only lymphopenia and mildly elevated liver enzymes. Symptoms continued for 8 days and then resolved completely. His illness was initially suspected to be dengue; however, test results for dengue (NS1 early antigen, dengue capture IgM, and dengue IgG indirect; all 3 from Panbio, Brisbane, Queensland, Australia) and chikungunya (Anti-Chikungunya Virus IIFT; Euroimmun AG, Lübeck, Germany) viruses were negative.

In Israel, Zika virus diagnostic tests were introduced in December 2015 and are available only through the National Center for Zoonotic Viruses. Serologic testing for Zika virus is performed by using an ELISA IgM and IgG kit (Euroimmun AG), which detects antibodies against the Zika nonstructural protein NS1 and is therefore considered very specific for Zika virus infection (*6*). Zika real-time reverse transcriptase PCR (rRT-PCR) against part of the envelope gene (1086–1162 bp) was adopted from the method established during the Zika virus outbreak in Micronesia (*7*).

In the traveler to Vietnam, rRT-PCR and serologic results were positive for Zika virus RNA and antibodies, respectively. For sequencing of Zika virus RNA, we amplified a 327-fragment from the prM and envelope genes by rRT-PCR, using primers Zika virus 835 (5′-TTGGT-CATGATACTGCTGATTGC-3′) and Zika virus 1162c (5′-CCACTAACGTTCTTTTGCAGACAT-3′) and an ABI 3500 Genetic Analyzer (Applied Biosystems, Foster City, CA, USA). A Bayesian maximum clade credibility time-scaled phylogenetic tree (BEAST, http://beast.bio.ed.ac.uk/Main_Page) of the 231-nt fragment obtained from this patient and from 3 other patients from Israel who acquired their infection in South and Central America (online Technical Appendix Table) was performed with 19 reference Zika virus strains. To infer the evolutionary relationships and the most recent common ancestor for the Zika virus fragment of the envelope gene, we applied the Bayesian Markov chain Monte Carlo method by using a relaxed molecular clock, as implemented in BEAST version 1.7.5. Trees were visualized and edited with FigTree version 1.4.2 (included in BEAST software). Altogether, the analysis showed that the virus belonged to the Asia Zika virus lineage and seems to be highly similar to strains currently circulating in Latin America (Figure). However, sequencing of a larger segment would be needed for a more accurate phylogeny.

This case illustrates the role of returning travelers as potential disease sentinels and the inadequacy of information about Zika virus circulation in Asia. During December 2015–January 2016, when this patient was evaluated and followed up, no cases of Zika virus disease had yet been reported from Vietnam. Since then, a case in a traveler from Australia has been reported (*8*). In addition, in late March 2016, health authorities in Vietnam reported 2 autochthonous Zika virus cases in women from Nha-Trang and Ho Chi Minh City (*9*). Because

---

[1]These co–first authors contributed equally to this article.
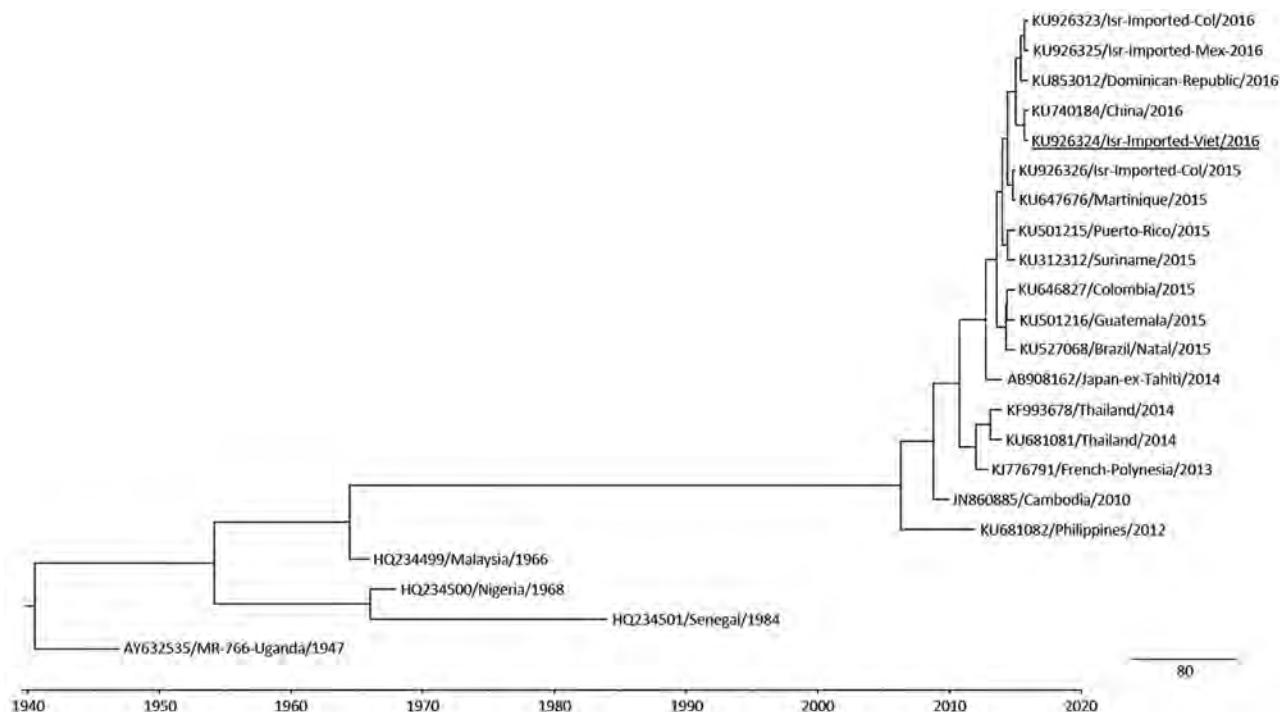
Figure. Phylogenetic tree of Zika virus RNA isolated from travelers returning to Israel. Bayesian maximum clade credibility time-scaled phylogenetic tree (BEAST, http://beast.bio.ed.ac.uk/Main_Page) was generated by using 4 partially sequenced Zika virus envelope genes (231 bp) detected from 4 samples obtained from patients in Israel during 2015–2016 and 19 reference strains belonging to the lineages from Asia and Africa. Isr, Israel; Viet, Vietnam; Col, Colombia; Mex, Mexico. Underlining indicates Zika virus imported from Vietnam. Scale bars indicate units in time (years).

the incubation period for Zika virus is not clearly defined, we are unable to definitely rule out Hong Kong as the source of infection. However, to our knowledge, Zika virus circulation in Hong Kong has not yet been reported. Assuming the most probable incubation period to be 5–8 days, we believe that the patient who visited Vietnam most likely became infected with Zika virus in Ho Chi Minh City.

Until more thorough epidemiologic data from Asia become available, testing all travelers returning from Southeast Asia with exanthema, fever, or other signs or symptoms suggestive of Zika virus disease is justified. In addition, because during this period Zika virus had become the most frequent arbovirus isolated from travelers returning to Israel, Zika virus now seems to be a substantial cause of febrile illness in travelers returning from Zika virus–endemic regions.

References

1. World Health Organization. WHO statement on the first meeting of the International Health Regulations (2005) (IHR 2005) Emergency Committee on Zika virus and observed increase in neurological disorders and neonatal malformations [cited 2016 Feb 13]. http://www.who.int/mediacentre/news/statements/2016/1st-emergency-committee-zika/en/
2. Faye O, Freire CC, Iamarino A, Faye O, de Oliveira JV, Diallo M, et al. Molecular evolution of Zika virus during its emergence in the 20(th) century. PLoS Negl Trop Dis. 2014;8:e2636. http://dx.doi.org/10.1371/journal.pntd.0002636
3. Fonseca K, Meatherall B, Zarra D, Drebot M, MacDonald J, Pabbaraju K, et al. First case of Zika virus infection in a returning Canadian traveler. Am J Trop Med Hyg. 2014;91:1035–8. http://dx.doi.org/10.4269/ajtmh.14-0151
4. Kwong JC, Druce JD, Leder K. Zika virus infection acquired during brief travel to Indonesia. Am J Trop Med Hyg. 2013;89:516–7. http://dx.doi.org/10.4269/ajtmh.13-0029
5. Heang V, Yasuda CY, Sovann L, Haddow AD, Travassos da Rosa AP, Tesh RB, et al. Zika virus infection, Cambodia, 2010. Emerg Infect Dis. 2012;18:349–51. http://dx.doi.org/10.3201/eid1802.111224
6. Huzly D, Hanselmann I, Schmidt-Chanasit J, Panning M. High specificity of a novel Zika virus ELISA in European patients after exposure to different flaviviruses. Euro Surveill. 2016;21. http://dx.doi.org/10.2807/1560-7917.ES.2016.21.16.30203
7. Lanciotti RS, Kosoy OL, Laven JJ, Velez JO, Lambert AJ, Johnson AJ, et al. Genetic and serologic properties of Zika virus associated with an epidemic, Yap State, Micronesia, 2007. Emerg Infect Dis. 2008;14:1232–9. http://dx.doi.org/10.3201/eid1408.080287
8. ProMED-mail. Zika virus—Australia ex Viet Nam NAM. 2016 March 23 [cited 2016 May 1]. http://www.promedmail.org, archive no. 20160323.4114786
9. Reuters. Vietnam reports first Zika infections, raises alarm [cited 2016 May 1]. http://www.reuters.com/article/us-health-zika-vietnam-idUSKCN0X2066

Address for correspondence: Eyal Meltzer or Eli Schwartz, The Center for Geographic Medicine and Department of Medicine C, The Chaim Sheba Medical Center, Tel Hashomer, 52621 Israel; email: meltzere@zahav.net.il or elischwa@post.tau.ac.il

Adventures of a Female Medical Detective: In Pursuit of Smallpox and AIDS

Light-hearted and easy to read, Mary Guinan's account of her career as an epidemiologist accomplishes its goal, "To help readers better understand and value the public health system that exists for the protection of the nation's health and for the prevention of disease and injury." From the early definition of the "hole in the sole," the epidemiologist's trademark, to the description of the Sherlock Holmes method, the epidemiologist's approach to public health puzzles, Guinan's stories embody the modesty and humor inherent in the culture of epidemiology as practiced by the Epidemiologic Intelligence Service (EIS) of the Centers for Disease Control and Prevention.

Young readers will be surprised, indeed as Guinan herself was surprised, at the challenges posed each day in public health, and in the end, they too may "find something to believe in," as she did during her days in the Smallpox Eradication Program. Her colleagues, EIS alumni and those now in the EIS Program, will see themselves in her description of the demands for instant, on the spot, expertise on complicated health emergencies or unknown sexually transmitted infections. They will recognize the unlikely developments so much a part of human interaction during epidemiologic investigations: pink elephants, unplanned media presentations, expert witnesses, hostile refugee camps, veiled women, seedy hotels, life-threatening needlestick injuries, famous movies featuring you, a challenging milk industry.

Investigation surprises abound in Dr. Guinan's account. Some involve the investigator herself. "I don't think anyone grows up wanting to be a physician who specializes in sexually transmitted diseases." "I was never the most important leader. A medical detective has a small part in a team effort, usually a very large team….the medical detectives who collect clues, analyze data, investigate suspected cases, and carry out their public health mission."

Some surprises involve the context of the investigation: for example, the Mujahideen in an Afghan refugee camp asking Dr. Guinan for weapons to fight in the Haj in 1980. She worked in the cramped quarters of a hotel in the Tenderloin District of San Francisco, identifying what would eventually be called the first AIDS cases. She later had to explain to the public that "nice" women can get AIDS.

Guinan and Mather wrote a book that is readable and free of technical jargon. The book is a woman's account because it reflects the experiences of a woman traveling the paths women have not traditionally traveled. During Guinan's first outbreak investigation, "I walked up to the uniformed four men and one woman and identified myself. The men were clearly shocked that 'Dr. Guinan' was a woman, and they were apologetic. They had not known that CDC was sending a woman."

Polyxeni Potter

Author affiliation: Founding Managing Editor, Emerging Infectious Diseases Journal, Atlanta, Georgia, USA

Address for correspondence: Polyxeni Potter, 3730 Bloxham Court, Atlanta, GA 30341, USA; polyxeni@bellsouth.net

Correction: Vol. 22, No. 4

An affiliation for Mitsuru Toda was missing from the article Effectiveness of a Mobile Short-Message-Service–Based Disease Outbreak Alert System in Kenya (M. Toda et al.). The article has been corrected online (http://wwwnc.cdc.gov/eid/article/22/4/15-1459_article).

Correction: Vol. 22, No. 5

Misspellings were corrected and the term "prevalence" has been replaced by "case counts" in the Table 1 title in Increased Rotavirus Prevalence in Diarrheal Outbreak Precipitated by Localized Flooding, Solomon Islands, 2014 (F.K. Jones et al.). The article has been corrected online (http://wwwnc.cdc.gov/eid/article/22/5/15-1743_article).

Cândido Portinari (1903–1962). Hill (Variant titles: Brazilian Hillside, Morro), 1933. Oil on canvas, 44 7/8 × 57 3/8 in/114 × 145.7 cm. Metropolitan Museum of Art, New York, New York; Digital image and permission courtesy of Projeto Portinari, Rio de Janeiro.

"I Am a Son of the Red Earth"

Byron Breedlove and Frank J. Sorvillo

Cândido Portinari, one of Brazil's most significant artists, was born on the Fazenda Santa Rosa coffee plantation in Brodowski in upstate São Paulo in 1903, the second of 12 children from Italian immigrants from the Veneto region of Italy. Because of his family's poverty, he did not complete his primary education.

His skill and interest in painting and drawing, evident from an early age, led Portinari to begin his formal training in painting and composition at the National School of Art in Rio de Janeiro in 1919. At the age of 15, he was among the first Brazilian artists to incorporate Modernist elements into his painting, and these elements defined his subsequent works. In 1928, Portinari won a prize at the National Salon of Brazil, which provided funds that enabled him to spend 3 years

Author affiliations: Centers for Disease Control and Prevention, Atlanta, Georgia, USA (B. Breedlove); UCLA School of Public Health, Los Angeles, California, USA (F.J. Sorvillo)

in Europe, where he traveled extensively, studied European art, visited museums, and met other artists. He continued exploring Modernism and was particularly drawn to Cubism and Surrealism. While in Europe, Portinari also met a young Uruguayan women, Maria Martinelli, his future wife.

After Portinari returned to Brazil in 1931, the artist began, according to journalist Warren Hoge, depicting scenes and themes "covering the country's earliest history, its slave trade, small-town life, gold prospectors, farming, construction, religious processions, circuses, jungle wildlife, urban slums, racial mixture and backlands bandits." Early in his life, Portinari had witnessed and experienced poverty and inequity, which not only influenced his art but also spurred him to enter politics as well. Tellingly, as noted in a *New York Times* article announcing his death, Portinari once said, "I am a son of the red earth. I decided to paint the Brazilian reality, naked and crude as it is."

Portinari's impressive career was marked by his vast output of nearly 5,000 works of art and a lengthy list of

prestigious awards and international exhibitions. Although Portinari is considered to be the greatest Brazilian artist, only a small number of his paintings are actually on public display. Portinari died on February 6, 1962, of the toxic effects of the lead-based paints he used when he was preparing an exhibit with about 200 works invited by Milan City Hall (Italy).

This month's cover image, *Hill*, portrays common people living in a favela in Rio de Janeiro by the sea. Portinari depicts the scene on coffee-colored ground, devoid of most greenery. The worn houses have open doors and windows, a few have small fences. The women trudge up and down the hill, balancing the water they have fetched for the households, their bright pastel dresses belying the severity of their lives. Several young children wander about them. No other children are scampering up the hill, and no other people are seen working. In the lower right of the painting, a woman rests her arms on the window and stares straight at the viewer, conveying through her empty expression the world-weary existence of life in the margins, her visage in contrast with the carefree posture of the man in the tilted hat leaning against a doorway.

It's likely many such villagers worked in menial occupations in the neighboring city. Portinari's painting emphasizes the poverty and marginalization by revealing a tantalizing glimpse of the city. Its monolithic buildings jut skyward near blue water surrounded by mountains but physically separated from the dwellings on the hill by a deep trench that gives way to grass that clearly is greener on the other side. Modern buildings, a passenger ship, and an airplane indicate commerce, bustle, and travel.

During the 1930s, health and healthcare would also be concerns among the people of this shantytown. Residents of resource-poor communities anywhere in the world, whether in a peri-urban area or a rural village, often suffer from inadequate housing, lack of education, poor nutrition, impaired immunity, and limited access to healthcare.

Those factors can promote the spread and amplify the global burden of key parasitic diseases, including malaria and lymphatic filariasis, as well as the neglected parasitic diseases, including Chagas disease, cysticercosis, and toxoplasmosis in resource-poor settings. Parasites capable of spreading zoonotic disease, including *Adenocephalus pacificus*, *Baylisascaris procyonis*, *Onchocerca lupi,* and pentostomes, continue to routinely emerge. Other emerging and reemerging infections, including neglected parasitic diseases, exact a staggering human and economic toll and are often linked to poverty and desperate living conditions.

Nearly 9 decades since Portinari painted this shantytown overlooking the city of Rio de Janeiro, economic development, social policies, and public health efforts have vastly reduced deaths from infectious diseases, including those from neglected parasitic diseases, in Brazil, where the average life expectancy is now 75 years. Successes there and in other parts of the world have brought many countries to the point where some parasitic infections—including Guinea worm disease, cysticercosis, and lymphatic filariasis—may be potentially controlled, eliminated, or eradicated through public health interventions. Other parasitic infections may not be eliminated, but their impact on health may be lessened through public health control and prevention efforts. With sufficient resources and resolve, stark human landscapes portrayed in works for art—such as the one illuminated in Portinari's painting of the *Hill*—and parasitic diseases, may become more rare.

Bibliography

1. Brazilian Institute of Geography and Statistics. Notices: life expectancy at birth was 74.9 years in 2013 [cited 2016 Jun 20]. http://censo2010.ibge.gov.br/en/noticias-censo.html?view=noticia&id=1&idnoticia=2773&busca=1&t=life-expectancy-at-birth-was-74-9-years-in-2013
2. Casa de Portinari Museum. A vida: Candido Portinari [cited 2016 Jun 8]. http://museucasadeportinari.org.br/candido-portinari/a-vida
3. Centers for Disease Control and Prevention. Parasites–American trypanosomiasis (also known as Chagas disease) [cited 2016 Jun 13]. http://www.cdc.gov/parasites/chagas/epi.html
4. Centers for Disease Control and Prevention. Recommendations of the international task force for disease eradication. MMWR Recomm Rep. 1993;42:1–38.
5. Freyre G. The African heritage. The Courier. p. 17 [cited 2016 Jun 10]. http://unesdoc.unesco.org/images/0007/000716/071641eo.pdf
6. Hoge W. Brazil gathers archive on its painter, Portinari. New York Times. May 30, 1983 [cited 2016 Jun 12]. http://www.nytimes.com/1983/05/30/arts/brazil-gathers-archive-on-its-painter-portinari.html
7. McKiernan M. Candido Portinari o lavrador de café (the coffee worker); 1939. Occup Med (Lond). 2011;61:383–4. http://dx.doi.org/10.1093/occmed/kqr097
8. New York Times. Candido Portinari dies at 58; outstanding Brazilian painter. February 8, 1962. 29, p. 1 [cited 2016 Jun 24]. http://query.nytimes.com/gst/abstract.html?res=9C02E5DE163AE13BBC4053DFB4668389679EDE&legacy=true
9. Projeto Portinari. Cândido Portinari [cited 2016 Jun 5]. http://www.portinari.org.br/#/pagina/candido-portinari/apresentacao
10. Southgate MT. Candido Portinari, coffee. The art of JAMA: one hundred covers and essays from the Journal of the American Medical Association. St. Louis: American Medical Association Press; 1997. p. 162.
11. Valente S. How Candido Portinari combined Brazilian politics and post-war art [cited 2016 Jun 8]. http://theculturetrip.com/south-america/brazil/articles/how-candido-portinari-combined-brazilian-politics-and-post-war-art/

Address for correspondence: Byron Breedlove, EID Journal, Centers for Disease Control and Prevention, 1600 Clifton Rd NE, Mailstop C19, Atlanta, GA 30329-4027, USA; email: wbb1@cdc.gov

EMERGING INFECTIOUS DISEASES®

Upcoming Issue

- Treatment Outcomes for Patients with Extensively Drug-Resistant Tuberculosis, KwaZulu-Natal and Eastern Cape Provinces, South Africa
- Clinical Features of and Risk Factors for Fatal Ebola Virus Disease, Moyamba District, Sierra Leone, December 2014–February 2015
- *Staphylococcus aureus* Regulatory RNAs as Potential Biomarkers for Bloodstream Infections
- Use of Testing for West Nile Virus and Other Arboviruses
- Protection against Asian Enterovirus 71 Outbreak Strains Predicted by Cross-neutralizing Capacity of Serum Samples from Dutch Donors
- Emergence of Enterohemorrhagic *Escherichia coli* Hybrid Pathotype O80:H2 as a New Therapeutic Challenge
- Persistent *Bacillus cereus* Bacteremia in 3 Persons who Inject Drugs, San Diego, California, USA
- Secondary Infections with Ebola Virus in Rural Communities, Liberia and Guinea, 2014–2015
- Large-Scale Survey for Tickborne Bacteria, Khammouan Province, Laos
- Changing Diagnostic Methods and Increased Detection of Verotoxigenic *Escherichia coli*, Ireland
- Mutation in West Nile Virus Structural Protein prM during Human Infection
- Human-Associated *Trypanosoma cruzi* Hybrid Strains, Colombia
- Multidrug-Resistant *Escherichia coli* in Bovine Animals, Europe
- Possible Transmission of *mcr-1*–Harboring *Escherichia coli* between Companion Animals and Human
- *Bifidobacterium longum* Subspecies *infantis* Bacteremia in 3 Extremely Preterm Infants Receiving Probiotics
- Multidrug-Resistant *Staphylococcus aureus*, India, 2013–2015
- Local Persistence of Novel MRSA Lineage after Hospital Ward Outbreak, Cambridge, UK, 2011–2013
- Autochthonous Chikungunya Fever in Traveler Returning to Japan from Cuba
- Carbapenem-Resistant *Enterobacter* spp. in Retail Seafood Imported from Southeast Asia to Canada
- Chromosomal Locations of *mcr-1* and *bla* in Fluoroquinolone-Resistant *Escherichia coli* ST410
- Community-Acquired *Clostridium difficile* Infections, Queensland, Australia
- *Cryptococcus gattii* Meningitis Complicated by *Listeria monocytogenes* Infection
- Melioidosis in Travelers Returning from Vietnam
- ESBL-Producing Strain of K2 Hypervirulent *Klebsiella pneumoniae*, France
- Specificity of Dengue NS1 Antigen in Differential Diagnosis of Dengue and Zika Virus Infection

Complete list of articles in the September issue at
http://www.cdc.gov/eid/upcoming.htm

Upcoming Infectious Disease Activities

August 24–28, 2016
Options IX for the Control of Influenza
Chicago, IL, USA
http://2016.isirv.org/

October 9–13, 2016
6th Annual Calicivirus Conference
Savannah, GA, USA
https://www.faingroup.com/Calicivirus/

October 28–30, 2016
ID Week
New Orleans, LA, USA
http://www.idweek.org/

October 29–November 2, 2016
American Public Health Association
Denver, CO, USA
https://www.apha.org/

November 4–7, 2016
IMED
International Meeting on Emerging Diseases and Surveillance
Vienna, Austria
http://imed.isid.org/

November 13–17, 2016
ASTMH
American Society of Tropical Medicine and Hygiene
Atlanta, GA, USA
https://www.astmh.org/

November 29–December 2, 2016
Institut Pasteur International Network Scientific Symposium
Paris, France
http://www.pasteur-network-meeting2016.org/

December 3–8, 2016
ASLM
African Society for Laboratory Medicine
Cape Town, South Africa
http://aslm2016.org/

Announcements

To submit an announcement, send an email message to EIDEditor (eideditor@cdc.gov). Include the date of the event, the location, the sponsoring organization(s), and a website that readers may visit or a telephone number or email address that readers may contact for more information.

Announcements may be posted on the journal Web page only, depending on the event date.

Earning CME Credit

To obtain credit, you should first read the journal article. After reading the article, you should be able to answer the following, related, multiple-choice questions. To complete the questions (with a minimum 75% passing score) and earn continuing medical education (CME) credit, please go to http://www.medscape.org/journal/eid. Credit cannot be obtained for tests completed on paper, although you may use the worksheet below to keep a record of your answers. You must be a registered user on Medscape.org. If you are not registered on Medscape.org, please click on the "Register" link on the right hand side of the website to register. Only one answer is correct for each question. Once you successfully answer all post-test questions you will be able to view and/or print your certificate. For questions regarding the content of this activity, contact the accredited provider, CME@medscape.net. For technical assistance, contact CME@webmd.net. American Medical Association's Physician's Recognition Award (AMA PRA) credits are accepted in the US as evidence of participation in CME activities. For further information on this award, please refer to http://www.ama-assn.org/ama/pub/about-ama/awards/ama-physicians-recognition-award.page. The AMA has determined that physicians not licensed in the US who participate in this CME activity are eligible for AMA PRA Category 1 Credits™. Through agreements that the AMA has made with agencies in some countries, AMA PRA credit may be acceptable as evidence of participation in CME activities. If you are not licensed in the US, please complete the questions online, print the certificate and present it to your national medical association for review.

Article Title

Cutaneous Melioidosis Cluster Caused by Contaminated Wound Irrigation Fluid

1. You are evaluating a 20-year-old woman with a complaint of increasing leg pain after a bicycle accident 10 days ago. She sustained a large abrasion below her knee and was seen 2 days later. She was judged to have a wound infection and was treated with debridement and a prescription for cephalexin. She has taken the antibiotic but has noticed more pain and purulent drainage from her wound. Melioidosis is possible in this case. In general, what should you consider regarding a melioidosis infection?

A.   It is associated with cutaneous infections only
B.   It has heretofore not been associated with any fatal cases
C.   Natural infection has not been described away from Asia
D.   It usually occurs after exposure to contaminated soil or water

2. Which of the following statements should you bear in mind as you evaluate this patient?

A.   A travel history is generally not important
B.   No cases of healthcare-associated melioidosis have been reported in the United States

C.   Exposure to *Burkholderia pseudomallei* may have occurred many years ago
D.   *B. pseudomallei* can exist in water but not in other liquids

3. What common medical condition or procedure did all patients with melioidosis in the current study share?

A.   Cough with upper lobe infiltrates
B.   Screening colonoscopy
C.   Minor wounds
D.   Dental surgery

4. What was the probable cause of melioidosis among patients evaluated in the current study?

A.   An infected healthcare worker
B.   Contaminated soil around the healthcare facility
C.   An opened saline fluid irrigation bottle
D.   Infected petrolatum gauze

CME Questions

Activity Evaluation

1. The activity supported the learning objectives.				
Strongly Disagree				Strongly Agree
1	2	3	4	5

2. The material was organized clearly for learning to occur.				
Strongly Disagree				Strongly Agree
1	2	3	4	5

3. The content learned from this activity will impact my practice.				
Strongly Disagree				Strongly Agree
1	2	3	4	5

4. The activity was presented objectively and free of commercial bias.				
Strongly Disagree				Strongly Agree
1	2	3	4	5

Looking for trusted information about vaccinating your child?

Visit www.cdc.gov/vaccines/parents. Learn about the vaccines your baby needs from a reliable source. The CDC's website explains the 14 diseases vaccines prevent, CDC's recommended schedule, possible side effects, how to comfort your baby during vaccine visits and more. Talk to your child's doctor, and visit our website to get the facts about vaccines.

U.S. Department of Health and Human Services
Centers for Disease Control and Prevention

Immunization. Power to Protect.

Summary of Authors' Instructions

Author's Instructions. For a complete list of EID's manuscript guidelines, see the author resource page: http://wwwnc.cdc.gov/eid/page/author-resource-center.

Manuscript Submission. To submit a manuscript, access Manuscript Central from the Emerging Infectious Diseases web page (www.cdc.gov/eid). Include a cover letter indicating the proposed category of the article (e.g., Research, Dispatch), verifying the word and reference counts, and confirming that the final manuscript has been seen and approved by all authors. Complete provided Authors Checklist.

Manuscript Preparation. For word processing, use MS Word. Set the document to show continuous line numbers. List the following information in this order: title page, article summary line, keywords, abstract, text, acknowledgments, biographical sketch, references, tables, and figure legends. Appendix materials and figures should be in separate files.

Title Page. Give complete information about each author (i.e., full name, graduate degree(s), affiliation, and the name of the institution in which the work was done). Clearly identify the corresponding author and provide that author's mailing address (include phone number, fax number, and email address). Include separate word counts for abstract and text.

Keywords. Use terms as listed in the National Library of Medicine Medical Subject Headings index (www.ncbi.nlm.nih.gov/mesh).

Text. Double-space everything, including the title page, abstract, references, tables, and figure legends. Indent paragraphs; leave no extra space between paragraphs. After a period, leave only one space before beginning the next sentence. Use 12-point Times New Roman font and format with ragged right margins (left align). Italicize (rather than underline) scientific names when needed.

Biographical Sketch. Include a short biographical sketch of the first author—both authors if only two. Include affiliations and the author's primary research interests.

References. Follow Uniform Requirements (www.icmje.org/index.html). Do not use endnotes for references. Place reference numbers in parentheses, not superscripts. Number citations in order of appearance (including in text, figures, and tables). Cite personal communications, unpublished data, and manuscripts in preparation or submitted for publication in parentheses in text. Consult List of Journals Indexed in Index Medicus for accepted journal abbreviations; if a journal is not listed, spell out the journal title. List the first six authors followed by "et al." Do not cite references in the abstract.

Tables. Provide tables within the manuscript file, not as separate files. Use the MS Word table tool, no columns, tabs, spaces, or other programs. Footnote any use of boldface. Tables should be no wider than 17 cm. Condense or divide larger tables. Extensive tables may be made available online only.

Figures. Submit editable figures as separate files (e.g., Microsoft Excel, PowerPoint). Photographs should be submitted as high-resolution (600 dpi) .tif or .jpeg files. Do not embed figures in the manuscript file. Use Arial 10 pt. or 12 pt. font for lettering so that figures, symbols, lettering, and numbering can remain legible when reduced to print size. Place figure keys within the figure. Figure legends should be placed at the end of the manuscript file.

Videos. Submit as AVI, MOV, MPG, MPEG, or WMV. Videos should not exceed 5 minutes and should include an audio description and complete captioning. If audio is not available, provide a description of the action in the video as a separate Word file. Published or copyrighted material (e.g., music) is discouraged and must be accompanied by written release. If video is part of a manuscript, files must be uploaded with manuscript submission. When uploading, choose "Video" file. Include a brief video legend in the manuscript file.

Types of Articles

Perspectives. Articles should not exceed 3,500 words and 50 references. Use of subheadings in the main body of the text is recommended. Photographs and illustrations are encouraged. Provide a short abstract (150 words), a 1-sentence summary, and biographical sketch. Articles should provide insightful analysis and commentary about new and reemerging infectious diseases and related issues. Perspectives may address factors known to influence the emergence of diseases, including microbial adaptation and change, human demographics and behavior, technology and industry, economic development and land use, international travel and commerce, and the breakdown of public health measures.

Synopses. Articles should not exceed 3,500 words in the main body of the text or include more than 50 references. Use of subheadings in the main body of the text is recommended. Photographs and illustrations are encouraged. Provide a short abstract (not to exceed 150 words), a 1-line summary of the conclusions, and a brief biographical sketch of first author or of both authors if only 2 authors. This section comprises case series papers and concise reviews of infectious diseases or closely related topics. Preference is given to reviews of new and emerging diseases; however, timely updates of other diseases or topics are also welcome. If detailed methods are included, a separate section on experimental procedures should immediately follow the body of the text.

Research. Articles should not exceed 3,500 words and 50 references. Use of subheadings in the main body of the text is recommended. Photographs and illustrations are encouraged. Provide a short abstract (150 words), 1-sentence summary, and biographical sketch. Report laboratory and epidemiologic results within a public health perspective. Explain the value of the research in public health terms and place the findings in a larger perspective (i.e., "Here is what we found, and here is what the findings mean").

Policy and Historical Reviews. Articles should not exceed 3,500 words and 50 references. Use of subheadings in the main body of the text is recommended. Photographs and illustrations are encouraged. Provide a short abstract (150 words), 1-sentence summary, and biographical sketch. Articles in this section include public health policy or historical reports that are based on research and analysis of emerging disease issues.

Dispatches. Articles should be no more than 1,200 words and need not be divided into sections. If subheadings are used, they should be general, e.g., "The Study" and "Conclusions." Provide a brief abstract (50 words); references (not to exceed 15); figures or illustrations (not to exceed 2); tables (not to exceed 2); and biographical sketch. Dispatches are updates on infectious disease trends and research that include descriptions of new methods for detecting, characterizing, or subtyping new or reemerging pathogens. Developments in antimicrobial drugs, vaccines, or infectious disease prevention or elimination programs are appropriate. Case reports are also welcome.

Another Dimension. Thoughtful essays, short stories, or poems on philosophical issues related to science, medical practice, and human health. Topics may include science and the human condition, the unanticipated side of epidemic investigations, or how people perceive and cope with infection and illness. This section is intended to evoke compassion for human suffering and to expand the science reader's literary scope. Manuscripts are selected for publication as much for their content (the experiences they describe) as for their literary merit. Include biographical sketch.

Research Letters Reporting Cases, Outbreaks, or Original Research. Starting with the January 2017 volume, EID will publish letters that report cases, outbreaks, or original research as Research Letters. Authors should provide a short abstract (50-word maximum), references (not to exceed 10), and a short biographical sketch. These letters should contain no more than 850 words (including the abstract) and may include either 1 figure or 1 table. Do not divide Research Letters into sections.

Letters Commenting on Articles. Letters commenting on articles should contain a maximum of 300 words and 5 references; they are more likely to be published if submitted within 4 weeks of the original article's publication.

Commentaries. Thoughtful discussions (500–1,000 words) of current topics. Commentaries may contain references (not to exceed 15) but no abstract, figures, or tables. Include biographical sketch.

Books, Other Media. Reviews (250–500 words) of new books or other media on emerging disease issues are welcome. Title, author(s), publisher, number of pages, and other pertinent details should be included.

Conference Summaries. Summaries of emerging infectious disease conference activities (500–1,000 words) are published online only. They should be submitted no later than 6 months after the conference and focus on content rather than process. Provide illustrations, references, and links to full reports of conference activities.

Online Reports. Reports on consensus group meetings, workshops, and other activities in which suggestions for diagnostic, treatment, or reporting methods related to infectious disease topics are formulated may be published online only. These should not exceed 3,500 words and should be authored by the group. We do not publish official guidelines or policy recommendations.

Photo Quiz. The photo quiz (1,200 words) highlights a person who made notable contributions to public health and medicine. Provide a photo of the subject, a brief clue to the person's identity, and five possible answers, followed by an essay describing the person's life and his or her significance to public health, science, and infectious disease.

Etymologia. Etymologia (100 words, 5 references). We welcome thoroughly researched derivations of emerging disease terms. Historical and other context could be included.

Announcements. We welcome brief announcements of timely events of interest to our readers. Announcements may be posted online only, depending on the event date. Email to eideditor@cdc.gov.